Ciesielski, P. F., Kristoffersen, Y., et al., 1988
Proceedings of the Ocean Drilling Program, Scientific Results, Vol. 114

11. SITE 704[1]

Shipboard Scientific Party[2]

HOLE 704A

Date occupied: 25 April 1987

Date departed: 27 April 1987

Time on hole: 1 day, 18 hr

Position: 46°52.757′S, 7°25.250′E

Bottom felt (rig floor; m; drill pipe measurement): 2542.8

Distance between rig floor and sea level (m): 10.50

Water depth (drill pipe measurement from sea level; corrected m): 2532.3

Total depth (rig floor; corrected m): 2825.5

Penetration: 282.7

Number of cores: 30

Total length of cored section (m): 282.7

Total core recovered (m): 224.55

Core recovery (%): 79

Oldest sediment cored:
Depth sub-bottom (m): 273.37
Nature: nannofossil ooze
Age: late Miocene
Measured velocity (km/s): 1.578 at 233.7 mbsf

HOLE 704B

Date occupied: 27 April 1987

Date departed: 3 May 1987

Time on hole: 6 days, 4 hr

Position: 46°52.785′S, 07°25.231′E

Bottom felt (rig floor; m; drill pipe measurement): 2542.8

Distance between rig floor and sea level (m): 10.50

Water depth (drill pipe measurement from sea level; corrected m): 2532.3

Total depth (rig floor; corrected m): 2825.5

Penetration: 671.7

Number of cores: 72

Total length of cored section (m): 671.7

Total core recovered (m): 502.75

Core recovery (%): 74

Oldest sediment cored:
Depth sub-bottom (m): 671.7
Nature: limestone
Age: early Oligocene
Measured velocity (km/s): 4.071

Principal results: Site 704 is located on the southern part of the Meteor Rise (46°52.757′S, 07°25.250′E; water depth of 2532.3 m), an aseismic ridge formed by extensive Paleocene-Eocene volcanism at a propagating extension of the Mid-Atlantic Ridge. The Leg 114 major objectives of determining the age, nature, and early subsidence history of Meteor Rise and its conjugate feature, the Islas Orcadas Rise, were largely met by drilling at Sites 702 and 703. For this reason, Site 704 was located on a region of the Meteor Rise where a maximum thickness of Neogene and upper Paleogene sediment could be obtained in order to provide a high-resolution paleoceanographic-paleoclimatic record of an interval not well represented at the preceding Leg 114 sites.

Two holes were drilled at Site 704 using the advanced hydraulic piston corer (APC) and extended core barrel (XCB) coring systems. Hole 704A was cored continuously (16 APC cores, 14 XCB cores) through an upper Miocene to Quaternary sequence to a depth of 282.7 m below seafloor (mbsf), with a recovery of 224.55 m (79.4%). After offsetting, Hole 704B was cored continuously (15 APC cores, 57 XCB cores), penetrating 671.7 m of lower Oligocene to Quaternary sediments, for a recovery of 502.75 m (74.8%). The composite section of both holes recovered more than 99% of the upper Miocene to Quaternary sequence above 282.7 mbsf. Coring operations were suspended to allow 2 days for logging and a half day for testing of the Navidrill system prior to departure from this last leg site to Mauritius. Three logging runs were made using the seismic-stratigraphic, lithodensity, and geochemical combinations. Site 704 was occupied between 25 April and 3 May in generally high seas.

Site 704 was a fitting end to Leg 114. After our recovery of thick Paleogene carbonate sequences at the preceding sites, a thick, mixed carbonate and biosiliceous sequence of Quaternary–early Oligocene age was obtained at Site 704. This recovery in conjunction with the previous sites constitutes a remarkably complete representation of the Upper Cretaceous-Quaternary, most of it carbonate bearing. Site 704 is potentially a very important reference section for the interpretation of the Neogene southern high-latitude paleoenvironment. The Neogene sequence at this site is the thickest (~576 m) and most complete section at high southern latitudes that is characterized by (1) the presence of carbonate throughout, which offers an extended stable isotopic record of planktonic and benthic environments; (2) little or no terrigenous component; (3) the continuous presence of all calcareous and siliceous microfossil groups; and (4) a relatively complete paleomagnetic record.

The two units and six subunits recovered at this site dramatically reflect the major stages of Neogene paleoclimatic evolution. The characteristics and ages of these subunits are as follows:

0–101.7 mbsf: a wide range of biogenic lithologies between diatom ooze and calcareous ooze, with large variations in carbonate content, of latest Pliocene to Quaternary age (Subunit IA);
101.7–175.7 mbsf: dominantly calcareous ooze with a biosiliceous component and large variations in carbonate content, of late Pliocene age (Subunit IB);
175.7–251.7 mbsf: diatom-bearing calcareous ooze, which becomes more siliceous between 219 and 251.7 mbsf, of late Miocene-late Pliocene age (Subunit IC);
251.7–451.2 mbsf: uniform nannofossil ooze with a minor biosiliceous component, of latest early Miocene to latest Miocene age (Subunit ID);
451.2–491.2 mbsf: micrite-bearing nannofossil chalk with a minor biosiliceous component, of early to latest early Miocene age (Subunit IIA);
491.2–671.7 mbsf: micritic nannofossil chalk with a minor biosiliceous component, of early Oligocene to early Miocene age.

---

[1] Ciesielski, P. F., Kristoffersen, Y., et al., 1988. *Proc. ODP, Init. Repts.*, 114: College Station, TX (Ocean Drilling Program).

[2] Shipboard Scientific Party is as given in the list of Participants preceding the contents.

Sedimentation rates for the Oligocene portion of Hole 704B (32/34 Ma to 23.7 Ma) were about 8-10 m/m.y. Early Miocene (23.7-16.5 Ma) sedimentation rates were also high (~20 m/m.y.) but dropped to ~11 m/m.y. during the early middle Miocene (~16.5-14.5 Ma). A hiatus of 5 to 6 m.y. separates early middle Miocene sediments (14.5 Ma) from overlying early late Miocene sediments (~9-10 Ma). After formation of this hiatus, there was an extremly high sedimentation rate of as high as 100 m/m.y. during a brief span of the early late Miocene (~10-8.5 Ma). Sedimentation was again interrupted during the late Miocene, forming a second hiatus with bracketing ages of ~8.5 and 6.5 Ma. With the resumption of sedimentation, there were not further apparent interruptions in sedimentation throughout the remainder of the late Miocene (~6.5-5.3 Ma) with an average sedimentation rate of 45 m/m.y. The early to early late Pliocene (5.3-2.8 Ma) sedimentation rate declined from that of the late Miocene but was still relatively high at 22 m/m.y. A third but brief hiatus occurs in the late Pliocene between sediments with an age of ~2.9 or 2.8 Ma to 2.5 Ma. Above this youngest hiatus, high sedimentation rates of ~82 m/m.y. were recorded for the middle late Pliocene-late Quaternary (~2.5-0.4 Ma). A precipitous drop in sedimentation rate (to ~9.0 m/m.y.) ocurred by 400 k.y. ago, resulting in the deposition of only 3.5 m of sediment since that time.

In contrast to the other Leg 114 sites, Site 704 remained north of the Antarctic Convergence Zone (ACZ) throughout most of the Miocene without experiencing major periods of nondeposition or erosion associated with the opening of the Drake Passage. The Oligocene to middle Miocene was a period of environmental stability with nearly continuous productivity dominated by calcareous microfossil groups. Little change in sedimentation occurred during the middle Miocene; however, cooler water assemblages of calcareous nannofossils began appearing by 13 Ma. A more pronounced cooling trend began during the late Miocene (~9.0 Ma), after which there is a strong cyclicity in the sediment record, as seen in carbonate fluctuations and in the geochemical logs. A severe cooling episode occurred during the latest Miocene (~6.5 Ma to earliest Pliocene), which was followed by the last, brief period of climatic stability during the early to mid-Gilbert chron.

During the late Pliocene (~2.9 Ma) the ACZ moved closer to Site 704, leading to an increase in the deposition of biogenic silica and the advent of strong cyclic sedimentation. Late Pliocene-Quaternary cyclic deposition was controlled primarily by glacial-interglacial fluctuations in calcareous and biosiliceous productivity. Logging results and detailed carbonate analyses confirm the presence of a strong, high-resolution climatic signal with cycles on the scale of tens of thousands to hundreds of thousands of years. The isotopic stratigraphy, paleontology, sedimentology, and logs of this site should provide an unequaled southern high-latitude reference section of late Neogene climatic history.

BACKGROUND AND OBJECTIVES

Site 704 is located on the central southern part of the Meteor Rise, an aseismic ridge that abuts the Agulhas Fracture Zone and extends for over 350 km southeastward, widening from about 100 to 170 km. The rise has a rugged topography and a general relief of 1-2 km, with several seamounts that reach 1100 m below sea level (mbsl) or shallower. The Meteor Rise was not recognized as a major bathymetric feature, at least in the published literature, until recently, but it forms the western boundary of the Agulhas Basin (LaBrecque and Hayes, 1979) and determines the pattern of Antarctic Bottom Water (AABW) flow within the basin (Tucholke and Embley, 1984). LaBrecque and Hayes (1979) also pointed out a possible dual tectonic relationship with the Islas Orcadas Rise.

During the Maestrichtian, the spreading axis in the Agulhas Basin shifted westward and reduced the offset in the Falkland-Agulhas Fracture Zone from over 1000 km to near the present distance of about 240 km (LaBrecque and Hayes, 1979). The Meteor Rise and Islas Orcadas Rise were formed by excessive volcanism at the new spreading center, becoming conjugate ridges as seafloor spreading progressed (Fig. 1). The presence of the rises at the ridge crest represented a major shallowing of the Mid-Atlantic Ridge segment abutting the Falkland-Agulhas Fracture Zone and constituted major obstacles to deep and intermediate oceanic circulation, particularly during the early Paleogene. Subsequent seafloor spreading and thermal relaxation of the oceanic crust opened a gateway for deep oceanic communication between antarctic water masses and the South Atlantic (Fig. 1).

The rugged basement relief (~1 km) and depositional environment on the Meteor Rise contrast strongly with the relatively smooth topography and conformable sediments of the Islas Orcadas Rise. On the highest part of the Meteor Rise, pelagic sediments deposited under strong bottom-current control have smoothed the volcanic relief and formed large sediment drifts on the lee side of the major seamounts.

Site 704 is located at 46°52.758′S and 07°25.231′E in a water depth of 2532.3 m (Figs. 2 and 3). The acoustic stratigraphy is characterized by a 0.1-0.3-s-thick (two-way traveltime—TWT) highly reflective upper unit that overlies a thick, more weakly stratified section, which locally may reach a thickness of 0.5-1.0 s (Fig. 4). In some places strong basal reflections are present about 0.2 s above basement. Gentle folding, increasing in amplitude downsection, is observed across the whole site survey area. The presence of folds above areas of relatively flat basement suggest that they may have resulted from differential compaction and tectonic movements, rather than from large-scale sliding. We note that although the syncline is flanked to the east by seamounts that extend up to 1000 m above the plain, the thickness of the individual seismic units appears remarkably symmetric with respect to its axis. Therefore, sediment transport by mass flows into the syncline from the east must have been of minor importance. The objectives of this site focused on the Neogene part of the sediment section and aimed at stratigraphic overlap with the Eocene and Oligocene sediments drilled at the companion Sites 703 and 702 on the conjugate Islas Orcadas Rise.

The location of Site 704 is between the present Subtropical Convergence and the ACZ, but still within Subantarctic Surface Water (SSW) entrained within the Antarctic Circumpolar Current (ACC). The northern edge of the ACZ is at a latitude about 2.5° south of Site 704 and is characterized in this region by a drop in surface temperature of 1.5°-2.0°C over a distance of 126 km (Lutjeharms and Valentine, 1984). Approximately 5° to the north (42°S) is the Subtropical Convergence, the region where SSW subducts northward beneath Subtropical Surface Water to form the South Atlantic Central Water. Site 704 is positioned near the mean position of the subantarctic front, which is expressed as a subsurface temperature gradient between 3° and 5°C. Sea surface temperatures over the Meteor Rise today average 6° to 7°C; we measured sea surface temperatures on site of 6.3°C.

Site 704 is in a region of the southern South Atlantic where sea surface temperature anomalies for today vs. the last glacial maximum are 2° to 3°C. Based upon studies of piston cores from the region, the Meteor Rise remained immediately to the north of the maximum extent of sea ice during glacial episodes, where pelagic carbonate sedimentation most likely persisted through glacial-interglacial cycles (Hays et al., 1976). The closer proximity of the ACZ during glacial episodes probably caused a decline in microfossil diversity and an increase in the accumulation of biogenic silica at this site.

This region of the eastern South Atlantic is north of where North Atlantic Deep Water (NADW) converges with Circumpolar Deep Water (CPDW). The influx of NADW into this region is clearly seen as a deep salinity maximum east of the Mid-Atlantic Ridge (Gordon and Goldberg, 1970). Bottom-water temperatures of 2.0° to 2.5°C were measured by a heat flow thermistor at Site 704 and are in close agreement with expected temperatures of NADW. Because the seafloor is overlain by NADW and SSW, the stable isotopic record of Site 704 may provide a

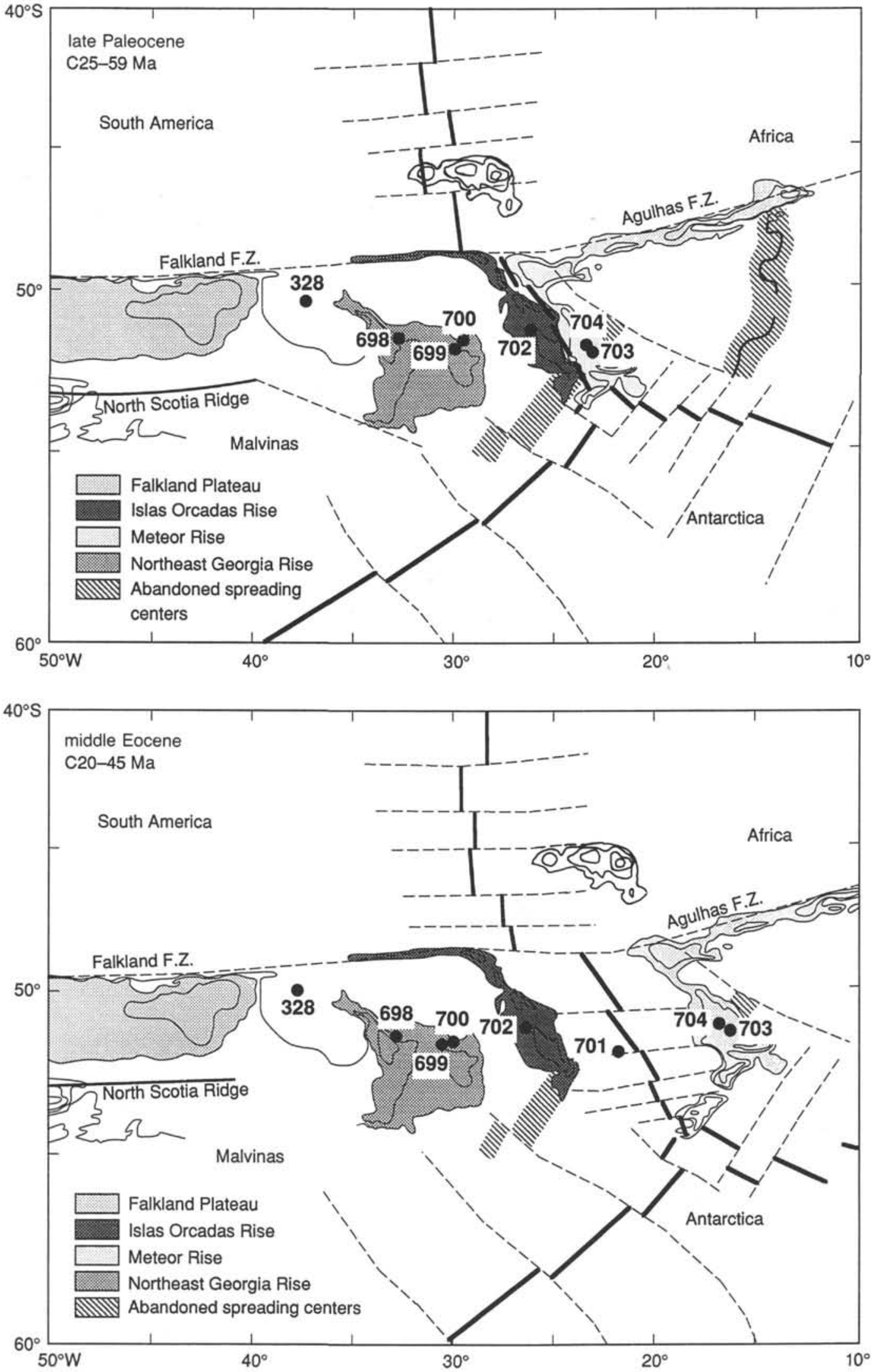

Figure 1. Reconstruction of the subantarctic sites of Leg 114 for the late Paleocene and middle Eocene. Spreading center location based on magnetic anomaly locations. Supporting data from OMD Region 13 Synthesis (LaBrecque, 1986). Bathymetry in meters.

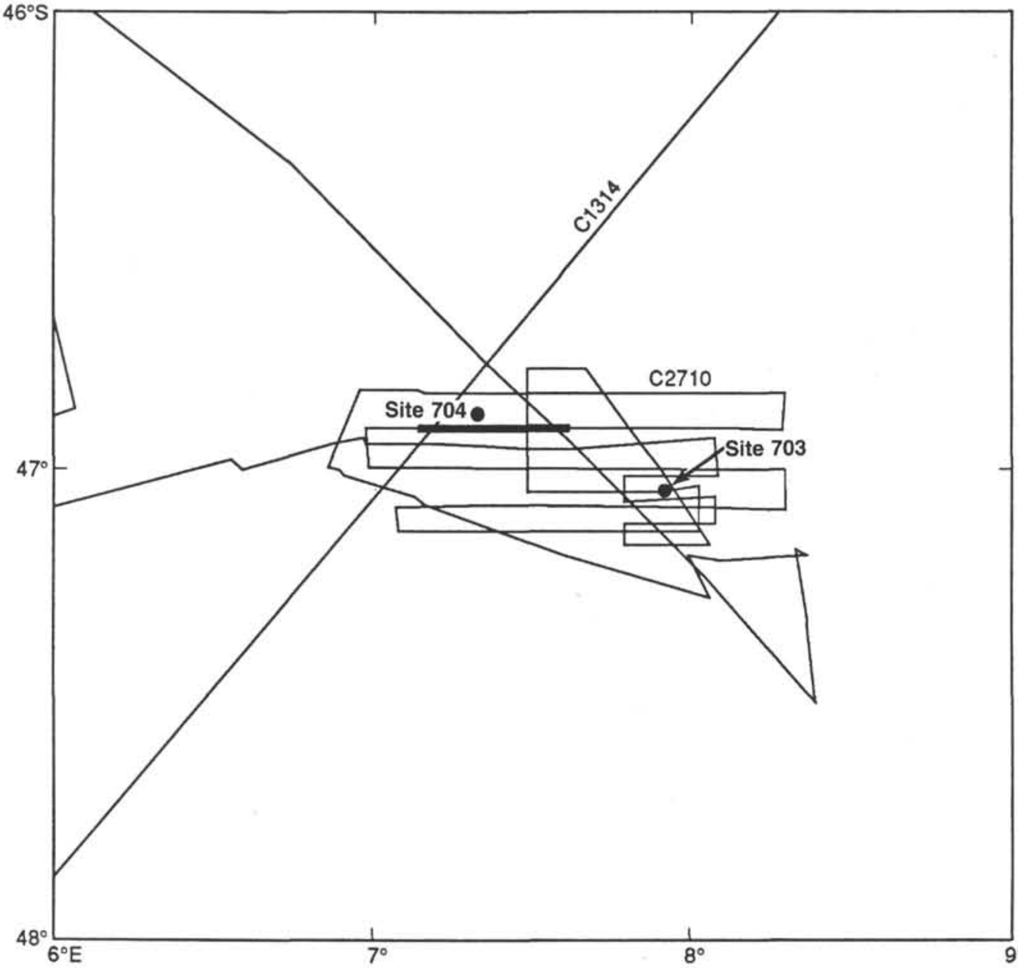

Figure 2. Site survey data base for drilling on Meteor Rise, with location of Sites 703 and 704. Bold line indicates seismic-reflection line shown in Figure 4.

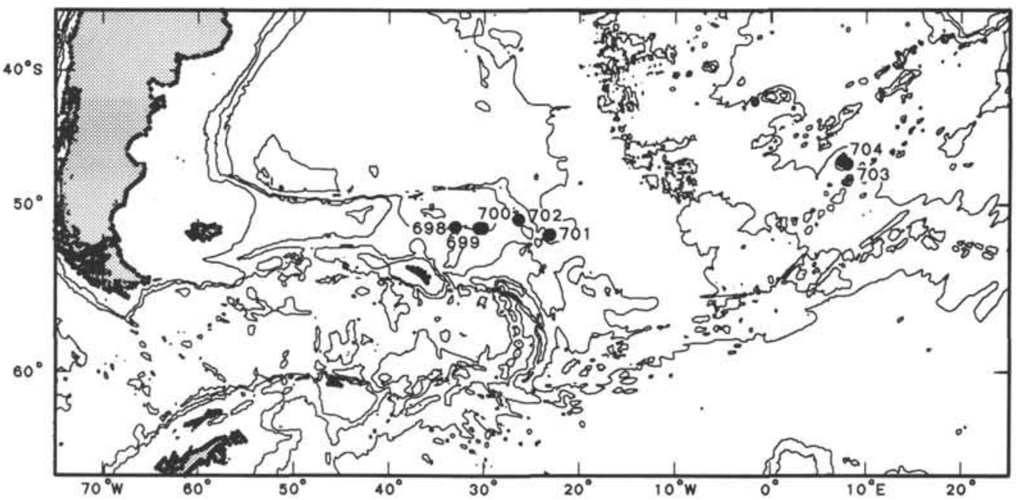

Figure 3. Bathymetric chart of the subantarctic South Atlantic showing the location of Site 704 and other Leg 114 sites. Contour interval 1500 m.

means of evaluating the temporal relationship of glacial-interglacial fluctuations of the Northern and Southern hemispheres.

Piston cores taken to the south and southeast of the site indicate that while CPDW is scouring the crest of the Southwest Indian Ridge, deposition is taking place on its north flank (Ledbetter and Ciesielski, 1982). No apparent disconformities exist below the high productivity zone near the polar front. Fracture zones breaching the Southwest Indian Ridge between 20° and 30°E allow AABW to enter the West Agulhas Basin, from where it flows to the northwest along the eastern side of Meteor

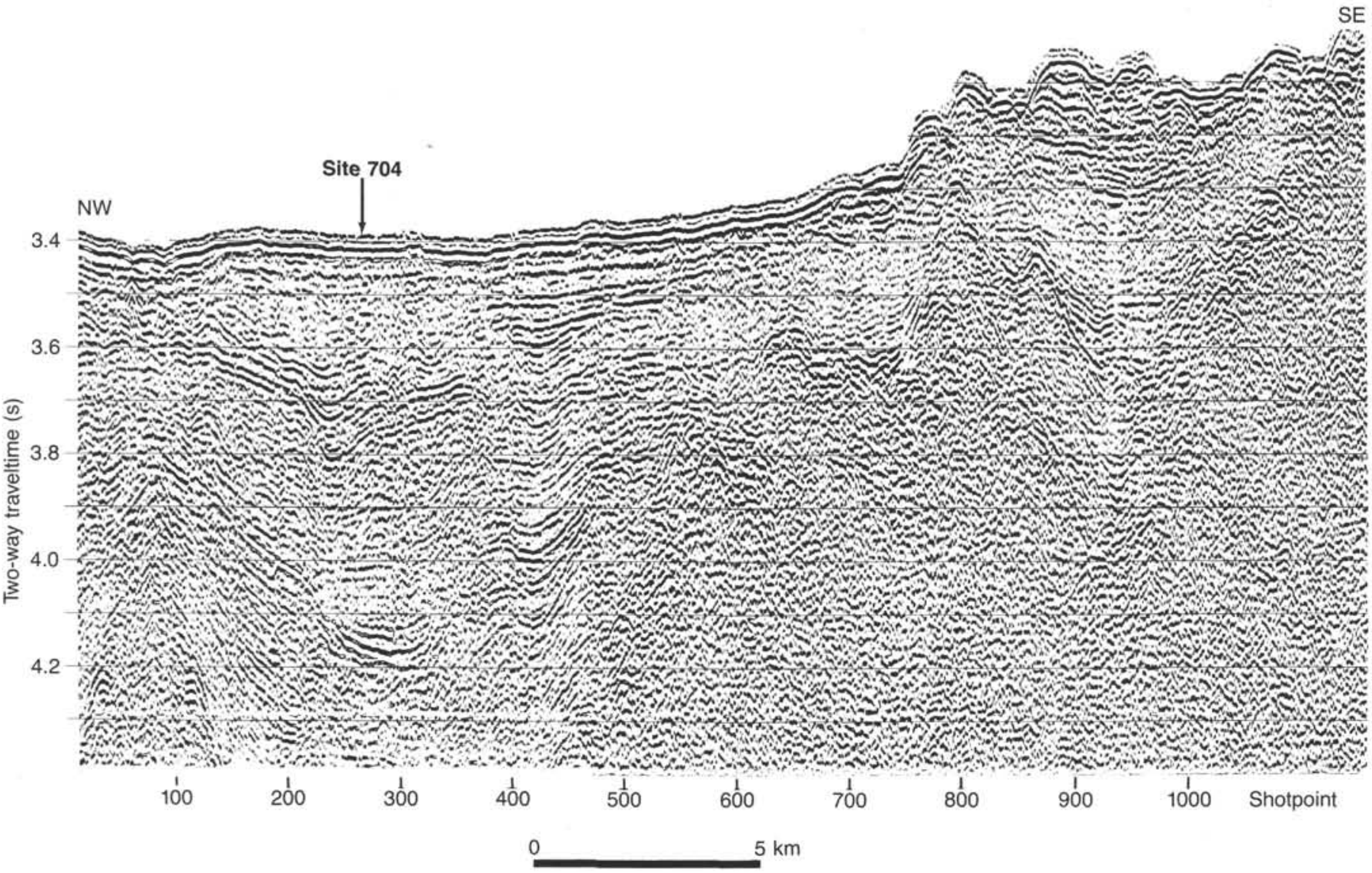

Figure 4. *JOIDES Resolution* single-channel seismic-reflection profile (*Conrad* cruise 2710) with the general location of Site 704. Location of line is shown in Figure 3.

Rise (Fig. 5). The clockwise gyre creates a scour zone along the basin perimeter (Tucholke and Embley, 1984).

The rationale for drilling on the Meteor Rise was to test models for its origin in a plate tectonic framework (Site 703) and to investigate its influence on paleocirculation (Sites 703 and 704). The specific objectives of Site 704 were

1. to interpret the influence of the shallow Paleogene Meteor Rise, Islas Orcadas Rise, and the adjacent fracture zones on oceanic communication between the high and temperate latitudes of the South Atlantic;
2. to document the development of the ACC and the history of major northward excursions of the polar front during the Neogene;
3. to interpret the vertical temperature structure of Paleogene water masses;
4. to obtain a lengthy Neogene carbonate record reflecting simultaneous fluctuations of the characteristics of SSW and NADW, thereby allowing a comparison of glacial-interglacial fluctuations in both hemispheres;
5. to integrate biostratigraphic zonal schemes of high and temperate latitudes;
6. to calibrate subantarctic biostratigraphy to the geomagnetic polarity time scale (GPTS);
7. to document the evolutionary history of high-latitude biota.

OPERATIONS

The transit from Sites 703 to 704 was to be relatively uneventful because Site 704 was just a few miles away, going from the upper slope of a seamount to an adjacent plain on the Meteor Rise. The site location was distinctive and covered a relatively large area, and seismic data were acquired underway to tie the two sites together. With Site 703 successfully completed, the deeper objectives at Meteor Rise had been met, and our investigations at Site 704 focused on the younger part of the section. All went according to plan as the vessel passed over the location, and the beacon was dropped at 1100 hr on 25 April 1987. The vessel continued past the site for another 2 nmi. The sediments, however, continued dipping westward; therefore, the upper part of the section continued to increase in thickness. The co-chiefs requested continued surveying on the same course to locate the maximum thickness of the upper sediment sequence. We decided to move the site to a new location where the sedimentary section of interest was twice as thick, and the seismic gear was retrieved after 1.5 hr. The vessel returned, and a new beacon was dropped at 1245 hr to initiate the final site of the leg.

After dropping the second beacon, the thruster pods and hydrophones were lowered. In less than an hour the vessel was operating in dynamic positioning mode, and the rig crew began to pick up the outer core barrel (OCB) assembly. A nonmagnetic drill collar was used because we planned to orient cores from at least one hole. Because the lockable float-valve assembly had sanded up on both previous deployments of this leg, a mechanical bit release (MBR) was run below the OCB assembly.

Again, prior to running in the hole, a Navidrill test was conducted on deck. This test was required to ensure that the mud motor had not been damaged pumping past the stator while the bearing sub was jammed and unable to rotate. The test demon-

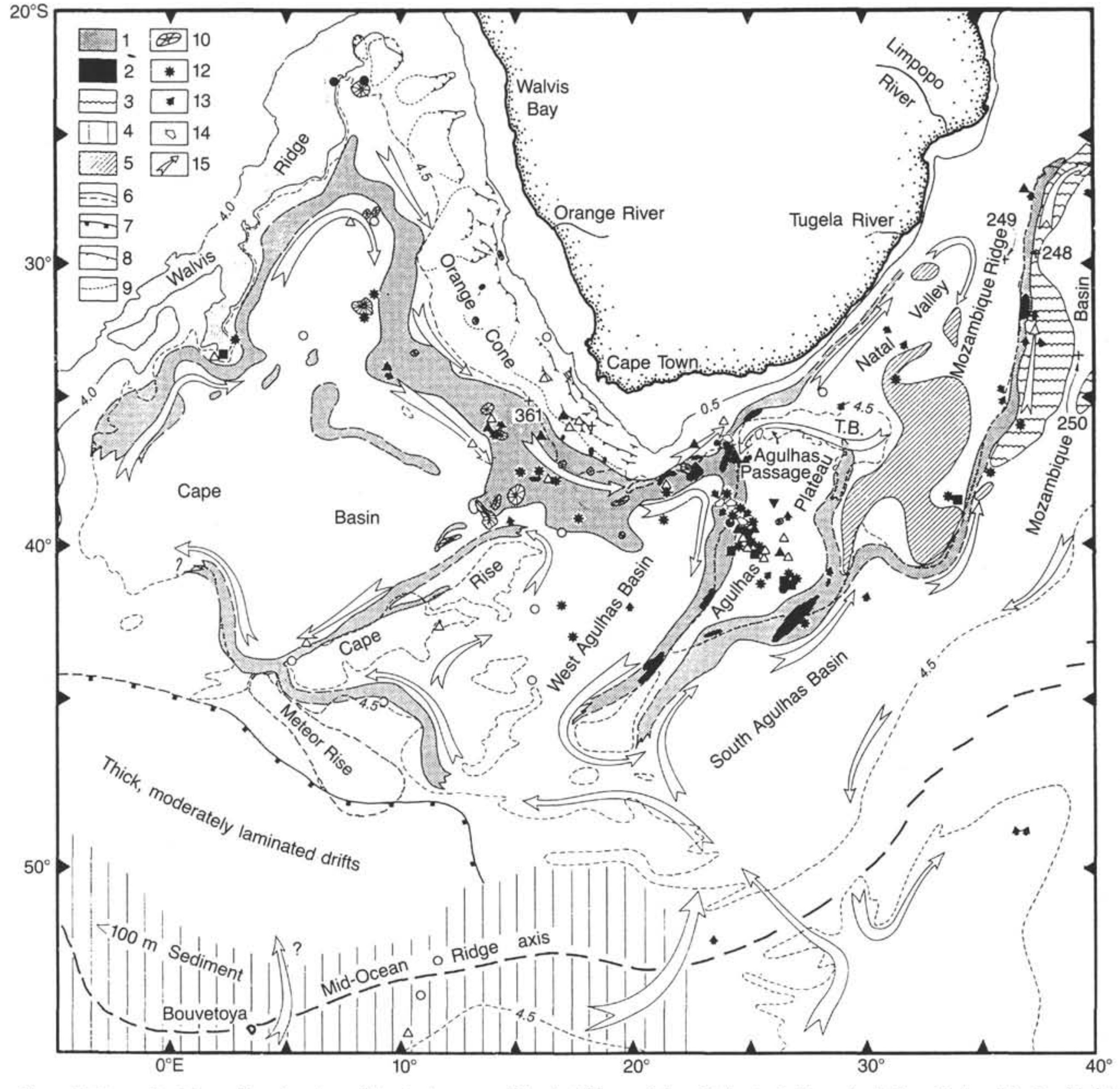

Figure 5. Generalized depositional regime of the basins around South Africa and the relation to bottom circulation. Meteor Rise is added to this representation because its existence was not known at the time of study by Tucholke and Embley (1984). 1 = core of circum-basin erosional zone; 2 = basement exposed by current erosion; 3 = sediment wave field; 4 = zone of thin sediment along the mid-oceanic ridge axis and beneath ACC; 5 = thick sediment drifts with weak acoustic laminae; 6 = generalized bathymetric contours as labeled (4500 m is a dashed line); 7 = limit of thick, moderately laminated drifts of diatomaceous sediment extending north of the polar front; 8 = glide plane scars at the head of slumps and slides; 9 = approximate seaward limit of slumps and slides; 10 = seamounts; 11 = piston cores of pre-Quaternary outcrops (from L to R, top to bottom: Pliocene, Miocene, Oligocene, Eocene, Paleocene, and Cretaceous); 12 = manganese nodules/pavement observed in bottom photographs; 13 = current direction from bottom photographs; 14 = direct current measurements; 15 = flow of AABW inferred from bottom-water potential temperature.

strated that the coring system was indeed functioning sufficiently to core through the steel cover plate on the rotary table. Operating pressures were still somewhat below normal but not as much as was experienced downhole on the earlier deployments. Assured that the tool was performing correctly, we laid down the hardware and picked up the rest of the bottom-hole assembly (BHA).

At 0155 hr on April 26, Hole 704A was spudded in a water depth of 2532.3 m (Table 1). Continuous, oriented cores were recovered with the APC system through Core 114-704A-16H, when an overpull of 80,000 lb was recorded. The coring operation was switched over to XCB mode, following a core recovery of 99% with the APC. Hole 704A was terminated at 2815 m (282.7 mbsf) after five consecutive cores (114-704A-26X to 114-

Table 1. Site 704 coring summary.

Core	Date (Apr. 1987)	Local time (hr)	Depths (mbsf)	Cored (m)	Recovered (m)	Recovery (%)
Hole 704A:						
1H	26	0210	0.0–7.2	7.2	7.28	101.0
2H	26	0310	7.2–16.7	9.5	9.66	101.0
3H	26	0400	16.7–26.2	9.5	10.00	105.2
4H	26	0510	26.2–35.7	9.5	8.29	87.2
5H	26	0620	35.7–45.2	9.5	9.43	99.2
6H	26	0720	45.2–54.7	9.5	10.00	105.2
7H	26	0825	54.7–64.2	9.5	8.85	93.1
8H	26	0910	64.2–73.7	9.5	9.02	94.9
9H	26	1000	73.7–83.2	9.5	9.60	101.0
10H	26	1100	83.2–92.7	9.5	10.06	105.9
11H	26	1140	92.7–102.2	9.5	9.81	103.0
12H	26	1245	102.2–111.7	9.5	9.16	96.4
13H	26	1415	111.7–121.2	9.5	9.78	103.0
14H	26	1507	121.2–130.7	9.5	8.58	90.3
15H	26	1635	130.7–140.2	9.5	9.78	103.0
16H	26	1810	140.2–149.7	9.5	8.70	91.6
17X	26	1930	149.7–159.2	9.5	9.21	96.9
18X	26	2010	159.2–168.7	9.5	8.84	93.0
19X	26	2045	168.7–178.2	9.5	9.59	101.0
20X	26	2125	178.2–187.7	9.5	9.68	102.0
21X	26	2203	187.7–197.2	9.5	5.67	59.7
22X	26	2245	197.2–206.7	9.5	8.13	85.6
23X	26	2345	206.7–216.2	9.5	8.10	85.2
24X	27	0030	216.2–225.7	9.5	8.11	85.3
25X	27	0110	225.7–235.2	9.5	8.78	92.4
26X	27	0145	235.2–244.7	9.5	0.00	0.0
27X	27	0220	244.7–254.2	9.5	0.06	0.6
28X	27	0315	254.2–263.7	9.5	0.00	0.0
29X	27	0400	263.7–273.2	9.5	0.21	2.2
30X	27	0445	273.2–282.7	9.5	0.17	1.8
				282.7	224.55	
Hole 704B:						
1H	27	0825	0.0–6.7	6.7	6.75	101.0
2H	27	0855	6.7–16.2	9.5	8.04	84.6
3H	27	0925	16.2–25.7	9.5	10.03	105.6
4H	27	1000	25.7–35.2	9.5	8.72	91.8
5H	27	1030	35.2–44.7	9.5	9.62	101.0
6H	27	1100	44.7–54.2	9.5	10.10	106.3
7H	27	1135	54.2–63.7	9.5	9.68	102.0
8H	27	1216	63.7–73.2	9.5	4.96	52.2
9H	27	1330	73.2–82.7	9.5	9.96	105.0
10H	27	1425	82.7–92.2	9.5	9.78	103.0
11H	27	1500	92.2–101.7	9.5	9.98	105.0
12H	27	1540	101.7–111.2	9.5	9.38	98.7
13H	27	1618	111.2–120.7	9.5	9.83	103.0
14H	27	1700	120.7–130.2	9.5	9.75	102.0
15H	27	1750	130.2–139.7	9.5	10.31	108.5
16X	27	1920	139.7–147.2	7.5	0.12	1.6
17X	27	2007	147.2–156.7	9.5	8.62	90.7
18X	27	2055	156.7–166.2	9.5	9.18	96.6
19X	27	2140	166.2–175.7	9.5	4.66	49.0
20X	27	2225	175.7–185.2	9.5	0.00	0.0
21X	27	2255	185.2–194.7	9.5	0.00	0.0
22X	27	2335	194.7–204.2	9.5	1.37	14.4
23X	28	0020	204.2–213.7	9.5	9.70	102.0
24X	28	0100	213.7–223.2	9.5	9.84	103.0
25X	28	0145	223.2–232.7	9.5	9.91	104.0
26X	28	0220	232.7–242.2	9.5	6.98	73.5
27X	28	0305	242.2–251.7	9.5	9.94	104.0
28X	28	0345	251.6–261.2	9.5	9.82	103.0
29X	28	0415	261.2–270.7	9.5	9.72	102.0
30X	28	0500	270.7–280.2	9.5	10.42	109.7
31X	28	0540	280.2–289.7	9.5	9.72	102.0
32X	28	0605	289.7–299.2	9.5	10.01	105.3
33X	28	0645	299.2–308.7	9.5	9.89	104.0
34X	28	0750	308.7–318.2	9.5	9.95	105.0
35X	28	0830	318.2–327.7	9.5	9.98	105.0
36X	28	0910	327.7–337.2	9.5	4.06	42.7
37X	28	0540	337.2–346.7	9.5	9.51	100.0
38X	28	1030	346.7–356.2	9.5	0.46	4.8
39X	28	1115	356.2–365.7	9.5	9.99	105.0
40X	28	1150	365.7–375.2	9.5	10.01	105.3
41X	28	1235	375.2–384.7	9.5	10.05	105.8
42X	28	1320	384.7–394.2	9.5	10.21	107.5
43X	28	1435	394.2–403.7	9.5	9.09	95.7
44X	28	1650	403.7–413.2	9.5	2.43	25.6
45X	28	1735	413.2–422.7	9.5	3.10	32.6
46X	28	1830	422.7–432.2	9.5	7.84	82.5
47X	28	2030	432.2–441.7	9.5	9.53	100.0
Hole 704A (cont.):						
48X	28	2115	441.7–451.2	9.5	4.57	48.1
49X	28	2150	451.2–460.7	9.5	8.00	84.2
50X	28	2320	460.7–462.7	2.0	1.23	61.5
51X	29	0045	462.7–472.2	9.5	1.69	17.8
52X	29	0115	472.2–481.7	9.5	7.69	80.9
53X	29	0415	481.7–491.2	9.5	4.90	51.6
54X	29	0510	491.2–500.7	9.5	9.81	103.0
55X	29	0550	500.7–510.2	9.5	9.44	99.3
56X	29	0630	510.2–519.7	9.5	6.39	67.2
57X	29	0735	519.7–529.2	9.5	4.32	45.5
58X	29	0920	529.2–538.7	9.5	9.02	94.9
59X	29	1010	538.7–548.2	9.5	6.70	70.5
60X	29	1100	548.2–557.7	9.5	8.52	89.7
61X	29	1230	557.7–567.2	9.5	3.03	31.9
62X	29	1345	567.2–576.7	9.5	8.59	90.4
63X	29	1500	576.7–586.2	9.5	8.13	85.6
64X	29	1615	586.2–595.7	9.5	4.61	48.5
65X	29	1730	595.7–605.2	9.5	4.51	47.5
66X	29	1910	605.2–614.7	9.5	1.01	10.6
67X	29	2015	614.7–624.2	9.5	1.58	16.6
68X	29	2145	624.2–633.7	9.5	3.65	38.4
69X	30	1710	633.7–643.2	9.5	1.20	12.6
70X	30	1930	643.2–652.7	9.5	2.60	27.3
71X	30	2100	652.7–662.2	9.5	3.95	41.6
72X	30	2245	662.2–671.7	9.5	4.61	48.5
				671.7	502.75	

704A-30X) recovered a total of only 0.44 m of core. This hole has the same type of lithology as Hole 703A, where similar recovery problems were experienced. The hole was displaced with heavy mud and the pipe pulled out of the hole. At 0645 hr the bit cleared the seafloor to end Hole 704A.

After offsetting the vessel 10 m to the east, Hole 704B was spudded at 0810 hr on 27 April. The water depth was determined to be 2532.3 m. Continuous coring with the APC, this time without orientation, continued through Core 114-704B-15H. Recovery was a very respectable 98%. To be on the safe side, we switched to coring with the XCB system one core short of the APC-recovered depth in Hole 704A. The XCB system also performed with admirable core recovery until the recovery of Cores 114-704B-19X to 114-704B-22X. This interval was 50 m above the low-recovery zone in the previous hole, and the cause of the almost total lack of recovery was not immediately known. Weather conditions had been deteriorating for most of the afternoon, and excessive vessel heave may have been partially responsible for low recovery because low bit weights were required to core the reasonably soft formation. It was apparent that drastic measures were required if any recovery was to be had at all in this interval. Because the formation appeared to be extremely water soluble, a 9³/₄-in. inner barrel sub was used to extend the XCB cutting shoe farther ahead of the main XCB jets. This was an extremely risky proposition, and we kept a close eye on the breakout torque of the cutting shoes, as well as for any significant wear. The drillers were alerted to stop coring and pull a barrel early at the first sign of a hard or penetration-resistant layer. This technique worked well, and a total recovery of 102.5% was achieved using the long extension sub. We tried drilling with the previous sub configuration to see if the formation could be cored without the extension, but recovery dropped dramatically. After Core 114-704B-45X was recovered the 9³/₄-in. sub was replaced with a 4-in. version that was somewhat safer to use. We continued to maintain a close watch as coring continued. Recovery was not quite as good as with the longer sub—only 80.8%—but was still appreciably more than the 62.6% recovery achieved without the use of any extension sub.

Three heat flow measurements were taken in Hole 704B using the Uyeda system, which was spaced out on an extra 15-ft core barrel to help decouple the heave motion of the drill string from the temperature probe. Two of the measurements were successful; one run failed to collect usable data. The last heat flow measurement was taken at 481.7 mbsf. Upon attempting to recover the tool, we found that it was stuck inside the smoothbore OCB. Apparently, an influx of sand caused the tool to become stuck, because after a few minutes of heavy circulation the tool dislodged, and we were able to recover it without any sign of damage.

Coring continued with the XCB system until Core 114-704B-68X at 633.7 mbsf. The weather began to deteriorate rapidly at this time. The barometer fell 21 mbar in 6 hr. The seas were building again, a condition that we had learned to put up with most of the leg. This time, however, the storm was projected to be worse than those experienced earlier during Leg 114, and we decided to cease coring, pull up closer to the mud line, and conduct a wiper trip that had been planned for hole conditioning. The pipe was pulled to 2684 mbsl, and a stand of wear-knotted drill pipe was picked up, placing the bit at 2713 mbsl. Conditions remained bad, and 3 hr were spent waiting on weather in a force 10 storm before the second half of the wiper trip could be continued. Upon running the pipe to bottom, the hole was swept with a mud pill to prepare for another Navidrill coring test. Two runs were made with the Navidrill, both unsuccessful. Operating pressures were significantly below normal again, and on neither run was there any indication that rotation occurred or that the diamond bit contacted the formation. Navidrill testing was terminated, and the remaining available coring time was spent with the XCB system. At 2245 hr on 30 April 1987, Core 114-704B-72X from 3202.5 mbsl (671.7 mbsf) was recovered, and coring operations for Leg 114 were terminated to provide ample time for three complete logging runs before abandoning the hole. The hole was swept with a high-viscosity mud pill, and the shifting tool for the MBR was run in the hole. At the critical moment, the sleeve shifted effortlessly and the bit released without resistance. Back flow was encountered almost immediately, indicating that the pipe was now open ended.

Four logging runs were made before abandoning the hole. The first run made with the DIT-D, SGT, BHC, and MCD tools was remarkably successful, reaching to within 4 m of the bottom of the hole. The second run, made using the LDT, CNT-G, NGT, and GPIT tools, also reached to within 4 m of bottom and was also successful, except for a few short-duration failures of the Masscomp computer. This problem precipitated some serious errors in running the logging cable, which caused an overrun of 22 m of cable after the tools had set down. Upon recovering the cable, we found a knot approximately 420 m from bottom, resulting in our having to cut off 520 m of cable. When running the third suite of tools (GST, ACT, CNT-G, and NGT) into the hole, a bridge was encountered directly below the open-ended pipe. The tools were recovered, and the drill string was periodically lowered to bottom to pick up the circulating head during the trip. After reaching bottom, a 25-bbl mud pill was circulated. Because of the windows in the MBR and a high probability of the pipe being plugged after the trip, we decided to leave the pipe in the hole and log through it for the final suite of logs. This strategy was successful, and by 0015 hr on 3 May 3 the logging tools were rigged down and the hole was filled with mud. The pipe was pulled clear of the mud line, and a final test of the Navidrill system was conducted. The HWD4 core barrel was removed to allow higher flow rates without the risk of extending below the pipe and rotating at high rpm. Our intention was to try and determine once and for all why the operating pressures were so much lower than the design and test pressures. The test was unsuccessful, as pressures remained low despite repeated attempts at seating and the use of ultra-high flow rates. The tool was recovered and again run in the hole, this time without the mud motor in an attempt to verify if the motor itself, because of tight tolerances in the seal-bore OCB, was preventing the proper landing and sealing of the external seals. The test was inconclusive in that the only pressure difference was lost by not having the pressure drop through the motor. The test was abandoned and the pipe pulled out of the hole until the top of the BHA was just below the rig floor. Here the abbreviated Navidrill assembly was dropped into the pipe, where it remained until recovery with the BHA. When the tools reached the rig floor, the Navidrill was found resting on the proper landing shoulder, the seals in place and torque segments latched. The mystery of downhole pressure loss remained unsolved. Evidence was found upon disassembly of the tool that indicated that the profile seals on the hex male spline had rotated out of position. This would have been responsible for at least some of the pressure loss, but just how much remains to be determined. The bit cleared the rotary table at 1015 hr on 3 May 1987, the rig floor was secured, and the vessel was underway at 1100 hr.

Because the seismic records upon arrival at Site 703 were poor (rough following seas), a 7-hr post-site survey was conducted over Site 703, prior to setting a course for Mauritius. At 1800 hr on 3 May 1987, the vessel finally took a heading toward Mauritius.

LITHOSTRATIGRAPHY

Two holes were drilled with the APC and XCB systems at Site 704, on the western flank of the Meteor Rise in a water depth of 2532.3 m. Hole 704A penetrated late Miocene to late Pleistocene age sediments to a depth of 282.7 mbsf, with an average recovery rate of 79.4%. Seventy-two cores were recovered in Hole 704B to a depth of 671.7 mbsf. Sediments of early Oligocene to late Pleistocene age were penetrated, with an average recovery of 74.8%.

The cored sediments consist of varying admixtures of two end-member components: (1) calcareous oozes and chalks consisting of foraminifers and calcareous nannofossils and (2) siliceous oozes composed of diatoms with minor radiolarians and silicoflagellates. The various lithologies include calcareous-bearing diatom ooze, calcareous diatom ooze, calcareous siliceous ooze, diatom-bearing calcareous ooze, siliceous-bearing calcareous ooze, siliceous-bearing nannofossil ooze, nannofossil ooze, micrite-bearing nannofossil chalk, and micritic indurated nannofossil chalk (Table 2).

Site 704 is subdivided into two units based on compositional variations and color changes (Table 2 and Figs. 6 and 7), percent calcium carbonate (Fig. 8), and diagenetic maturity (Figs. 6 and 7).

Unit I (to the base of Hole 704A and to 451.2 mbsf in Hole 704B) consists of oozes of varying siliceous and calcareous composition; middle Miocene to Pleistocene in age.

Subunit IA is marked by distinct color and lithology changes, corresponding to various admixtures of carbonate and silica. Diatoms are an important component of Subunit IA, which has lithologies ranging from diatom ooze to calcareous-bearing diatom ooze, calcareous diatom ooze, nannofossil ooze, diatom-bearing calcareous ooze, and diatom calcareous ooze. The age of this subunit is latest Pliocene to Pleistocene.

Subunit IB is dominantly a calcareous ooze with an important biosiliceous component. It is lighter in color than Subunit IA, and color changes are less sharp but still evident; late Pliocene age.

Subunit IC is composed of diatom-bearing calcareous ooze. Color variations are much less pronounced than in the overlying subunit, with the exception of Cores 114-704A-24X and 114-704A-25X. This subunit is further divided

Table 2. Major lithologies, lithostratigraphic units, age, and depth below seafloor of Site 704 cores.

Lithostratigraphic unit	Depth (mbsf)	Age	Core	Major lithology
Hole 704A:				
			1H	Calcareous-bearing diatom ooze, calcareous diatom ooze, and nannofossil ooze
			2H	Nannofossil ooze, calcareous diatom ooze, calcareous-bearing diatom ooze, and diatom ooze
			3H	Diatom ooze, calcareous-bearing diatom ooze, and diatom calcareous ooze
IA (Calcareous-bearing diatom ooze)	0–102.2	latest Pliocene–Pleistocene	4H	Diatom-bearing calcareous ooze, diatom calcareous-bearing diatom ooze
			5H	Diatom-bearing calcareous ooze, calcareous ooze, and calcareous diatom ooze
			6H	Calcareous ooze, diatom-bearing calcareous ooze, calcareous diatom ooze, and diatom ooze
			7H	Foraminifer-bearing diatom ooze
			8H	Calcareous diatom ooze
			9H	Calcareous diatom ooze
			10H	Calcareous diatom ooze
			11H	Calcareous diatom ooze
			12H	Siliceous calcareous ooze
			13H	Siliceous calcareous ooze and calcareous-bearing diatom ooze
			14H	Siliceous calcareous ooze and calcareous siliceous ooze
IB (Siliceous calcareous ooze)	102.2–178.2	late Pliocene	15H	Siliceous calcareous ooze
			16H	Calcareous siliceous ooze and siliceous-bearing calcareous ooze
			17H	Siliceous-bearing to siliceous calcareous ooze
			18X	Siliceous calcareous ooze to calcareous siliceous ooze
			19X	Calcareous siliceous ooze, siliceous-bearing nannofossil ooze, and siliceous calcareous ooze
			20X	Diatom-bearing calcareous ooze
			21X	Diatom-bearing calcareous ooze
			22X	Diatom calcareous ooze
IC (Diatom-bearing calcareous ooze)	178.2–254.2	late Miocene to late Pliocene	23X	Diatom-bearing calcareous ooze
			24X	Siliceous calcareous ooze
			25X	Diatom-bearing nannofossil ooze and siliceous calcareous ooze
			26X	No recovery
			27X	Diatom-bearing nannofossil ooze
			28X	No recovery
ID (Diatom-bearing nannofossil ooze)	254.2–282.7	late Miocene	29X	Diatom-bearing nannofossil ooze
			30X	Diatom-bearing nannofossil ooze
Hole 704B:				
			1H	Diatom-foraminifer ooze
			2H	Calcareous diatom ooze
			3H	Calcareous diatom ooze
			4H	Siliceous calcareous to Calcareous siliceous ooze
IA	0–101.7	latest Pliocene–Pleistocene	5H	Siliceous-bearing calcareous ooze, and calcareous-bearing siliceous ooze
			6H	Siliceous-bearing to siliceous calcareous ooze and diatom ooze
(Calcareous siliceous and siliceous calcareous ooze)			7H	Calcareous-bearing diatom/siliceous ooze and siliceous calcareous ooze
			8H	Siliceous-bearing calcareous ooze and diatom ooze
			9H	Siliceous calcareous ooze and calcareous siliceous ooze
			10H	Calcareous siliceous ooze and siliceous calcareous ooze
			11H	Calcareous-bearing to calcareous siliceous ooze
			12H	Siliceous-bearing calcareous ooze
			13H	Siliceous-bearing to siliceous calcareous ooze
			14H	Siliceous calcareous ooze

into Subunits IC_1 and IC_2. Subunit IC ranges from late Miocene to late Pliocene in age.

Subunit ID is a uniform, featureless white nannofossil ooze with little to no color variation and of middle to late Miocene age.

Unit II (only in Hole 704B) consists of white chalks of early Oligocene to latest early Miocene age. Subunits are defined by the degree of induration and micritization.

Subunit IIA is a white, micrite-bearing nannofossil chalk; early to late early Miocene in age.

Table 2 (continued).

Lithostratigraphic unit	Depth (mbsf)	Age	Core	Major lithology
Hole 704B:				
IB	101.7–175.7	late Pliocene	15H	Siliceous-bearing calcareous ooze
(Siliceous-bearing calcareous ooze)			16X	Siliceous calcareous ooze
			17X	Siliceous-bearing calcareous ooze
			18X	Siliceous-bearing nannofossil ooze
			19X	Siliceous calcareous ooze
			20X	No recovery
			21X	No recovery
IC	175.7–251.7	late Miocene to late Pliocene	22X	Siliceous-bearing calcareous ooze
			23X	Siliceous calcareous ooze
(Siliceous-bearing calcareous ooze)			24X	Siliceous-bearing calcareous ooze
			25X	Siliceous calcareous ooze
			26X	Siliceous calcareous ooze
			27X	Siliceous-bearing to siliceous calcareous ooze
			28X	Nannofossil ooze
			29X	Nannofossil ooze
			30X	Nannofossil ooze
			31X	Nannofossil ooze
ID	251.7–451.2	middle Miocene to late Miocene	32X	Nannofossil ooze
			33X	Nannofossil ooze
(Nannofossil ooze)			34X	Nannofossil ooze
			35X	Nannofossil ooze and diatom-bearing nannofossil ooze
			36X	Nannofossil ooze
			37X	Nannofossil ooze
			38X	Nannofossil ooze
			39X	Nannofossil ooze
			40X	Nannofossil ooze
			41X	Nannofossil ooze
			42X	Nannofossil ooze
			43X	Nannofossil ooze
			44X	Nannofossil ooze
			45X	Nannofossil ooze
			46X	Nannofossil ooze
			47X	Nannofossil ooze
			48X	Nannofossil ooze
			49X	Nannofossil chalk
IIA	451.2–491.2	early to middle Miocene	50X	Micrite-bearing nannofossil chalk
			51X	Micrite-bearing nannofossil chalk
(Micrite-bearing nannofossil chalk)			52X	Micrite-bearing nannofossil chalk
			53X	Micrite-bearing nannofossil chalk
			54X	Micritic nannofossil chalk (indurated)
			55X	Micritic nannofossil chalk (indurated)
			56X	Micritic nannofossil chalk (indurated)
			57X	Micritic nannofossil chalk (indurated)
IIB	491.2–671.7	early Oligocene to early Miocene	58X	Micritic nannofossil chalk (indurated)
			59X	Micritic nannofossil chalk (indurated)
(Micritic indurated nannofossil chalk)			60X	Micritic nannofossil chalk (indurated)
			61X	Micritic nannofossil chalk (indurated)
			62X	Micritic nannofossil chalk (indurated)
Miocene/Oligocene boundary			63X	Micritic nannofossil chalk (indurated)
			64X	Micritic nannofossil chalk (indurated)
			65X	Micritic nannofossil chalk (indurated)
			66X	Micritic nannofossil chalk (indurated)
			67X	Micritic nannofossil chalk (indurated)
			68X	Micritic nannofossil chalk (indurated)
			69X	Micritic nannofossil chalk (indurated)
			70X	Micritic nannofossil chalk (indurated)
			71X	Micritic nannofossil chalk (indurated)
			72X	Micritic nannofossil chalk (indurated)

Subunit IIB is a uniform white, indurated micritic nannofossil chalk; early Oligocene to late early Miocene.

Hole 704A

Hole 704A penetrated Subunits IA through IC, but only the uppermost part of Subunit IC is represented because of poor recovery from the basal five cores of the hole.

Unit I: Core 114-704A-1H to Section 114-704A-30X, CC; Depth: 0–282.7 mbsf; Age: late Miocene to Pleistocene.

The subdivision of Unit I in Hole 704A into three subunits is based on the relative importance of the siliceous and calcareous biogenic components (Fig. 6). This is reflected by color variations and first-order changes in the mean carbonate content of the sediment (Fig. 8). Superimposed upon these first-order changes is a high degree of variability in color and lithological character within the individual subunits.

Subunit IA: Core 114-704A-1H to Section 114-704A-11H, CC; Depth: 0–102.2 mbsf; Age: latest Pliocene to Pleistocene.

Subunit IA contains alternations of olive (5Y 5/4) diatom ooze, pale yellow (2.5Y 8/4) to light yellowish brown (2.5Y 6/4) calcareous-bearing diatom ooze, olive (5Y 5/3), pale olive (5Y 6/3), light greenish gray (5GY 7/1), and gray (5Y 6/1) to white

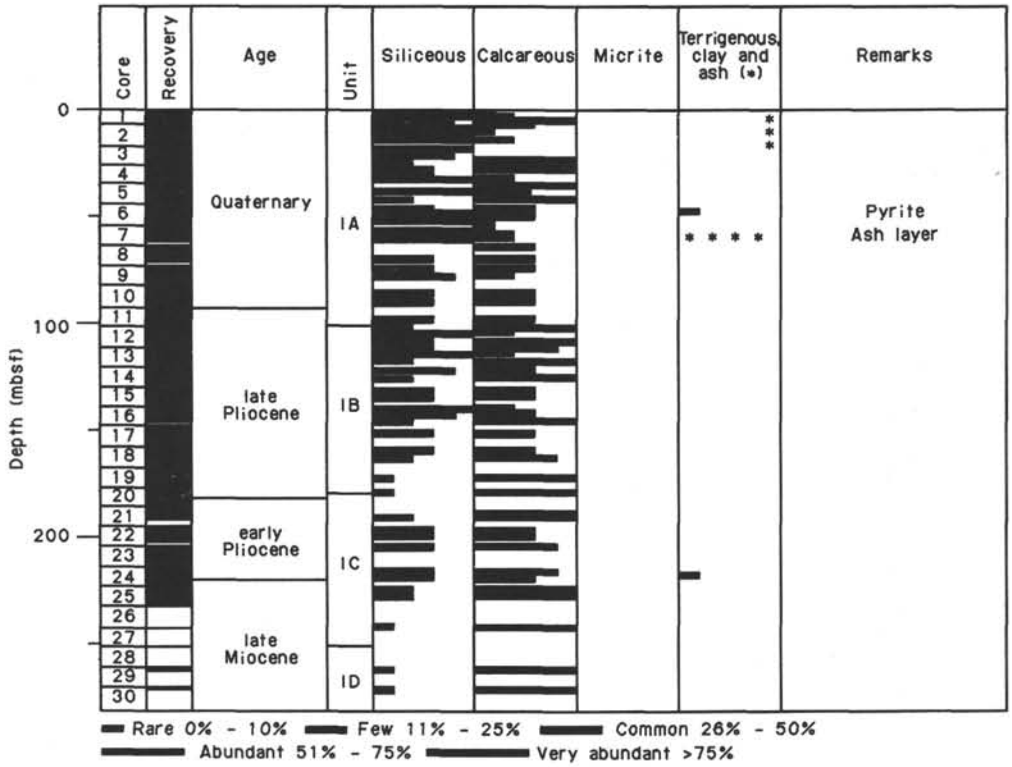

Figure 6. Relative smear slide composition of Hole 704A.

(no color code) calcareous diatom ooze, light gray (5Y 7/1) diatom calcareous ooze, light yellow (5Y 7/3) to white (no color code) calcareous ooze, and white (no color code) nannofossil ooze.

Subunit IA is highly variable in color and lithology at intervals of about 20 to 100 cm. Generally, the lighter color intervals (light yellow and light gray to white) correspond to high carbonate content, whereas the darker colors (olive and pale olive) correspond to diatom-rich intervals and low carbonate values (Fig. 8). The contacts between the lithologic and color boundaries are sharp, except where drilling disturbance has blurred the record.

In comparison to other subunits, Subunit IA exhibits strikingly sharp color variations and higher amplitude carbonate fluctuations. This reflects a greater importance in the relative contribution of biogenic silica in Subunit IA.

Pebbles first occur at 33 and 107 cm in Section 114-704A-5H-1. Soupy drilling disturbance in this section casts doubt as to whether these lithic fragments are in place. All sections of Core 114-704A-4H and the first three sections of Core 114-704A-5H are highly disturbed in Hole 704A, resulting in an homogenization of the sediment. Fine, dispersed lithic fragments (ice-rafted detritus?) were found throughout Core 114-704A-7H, and from 85 to 95 cm in Section 114-704A-8H-1.

The occurrence of pyrite-coated microfossils in Sample 114-704A-6H-2, 129 cm, and traces of pyrite and opaques in Cores 114-704A-7H to 114-704A-9H suggest localized oxygen-deficient conditions and degradation of organic carbon within the sulfate reduction zone.

Subunit IB: Core 114-704A-12H to Section 114-704A-19X, CC; Depth: 102.2–178.2 mbsf; Age: late Pliocene.

Subunit IB also consists of mixed carbonate and siliceous lithologies, but the average carbonate content is slightly higher than in Subunit IA (Fig. 8). The dominant lithology of Subunit IB is calcareous ooze, including siliceous calcareous ooze, siliceous-bearing calcareous ooze, and siliceous-bearing nannofossil ooze. The color contrasts are less distinct than those in Subunit IA but are still pronounced. Color variations include white (no color code, 2.5Y 8/0, 7.5YR 8/0), olive (5Y 5/3), light olive (5Y 6/2), light olive gray (5Y 6/2), light gray (5Y 7/2), gray (5Y 7/2), greenish gray (5G 7/1), light greenish gray (5GY 7/1), and light blue gray (5GY 7/1).

Lithic fragments and small pebbles occur sporadically, particularly in the top part of the first section of core. Pyrite occurs in small dark blebs, indicative of local anoxic microenvironments.

Subunit IC: Core 114-704A-20X to Section 114-704A-27X, CC; Depth: 178.2–254.2 mbsf; Age: late Miocene to late Pliocene.

Subunit IC is divided into Subunits IC_1 and IC_2. Core 114-704A-20X through Section 114-704A-24X-5 (178.2–222.2 mbsf) comprising Subunit IC_1 exhibit little color variation, with higher carbonate content and lower variability than Subunit IC_2. The lithology consists of uniform, diatom-bearing calcareous ooze, mostly white (no color code or 2.5Y 8/0) with subtle hues of light greenish gray (5GY 7/1) and light gray (5G 7/1). Convolute bedding from 107 to 135 cm in Section 114-704A-23X-1 may indicate slumping and sediment redeposition. Subunit IC is early to early late Pliocene in age.

Subunit IC_2 is composed of Section 114-704A-24X-5 through Core 114-704A-25X (222.2–254.2 mbsf). This interval is similar to Subunits IA and IB in that it contains distinct color variations, a lower mean carbonate content, and a greater biogenic silica component. Lithologies range from siliceous calcareous ooze to diatom-bearing nannofossil ooze. The siliceous calcareous ooze contains sharp variations in color, including light

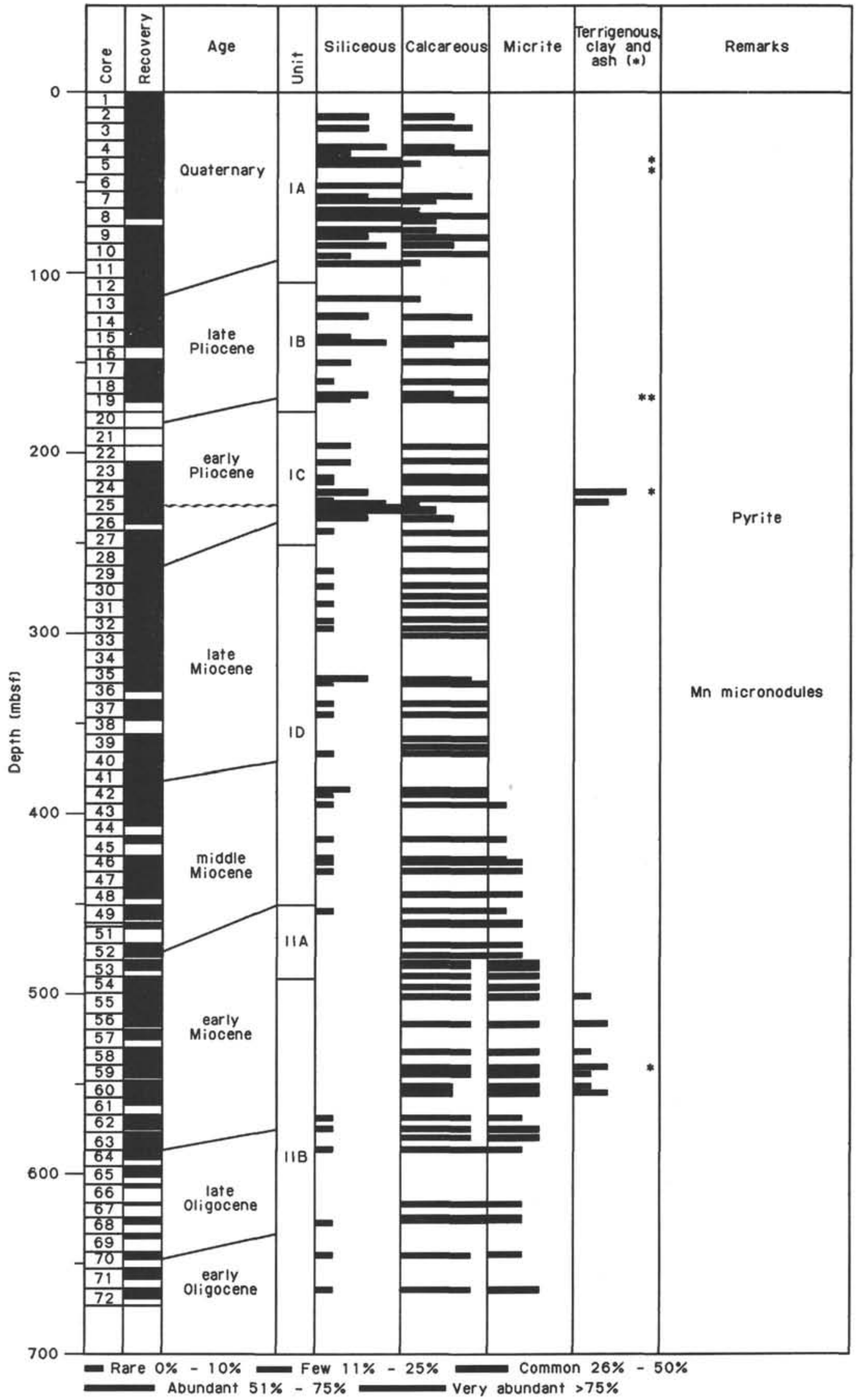

Figure 7. Relative smear slide composition of Hole 704B.

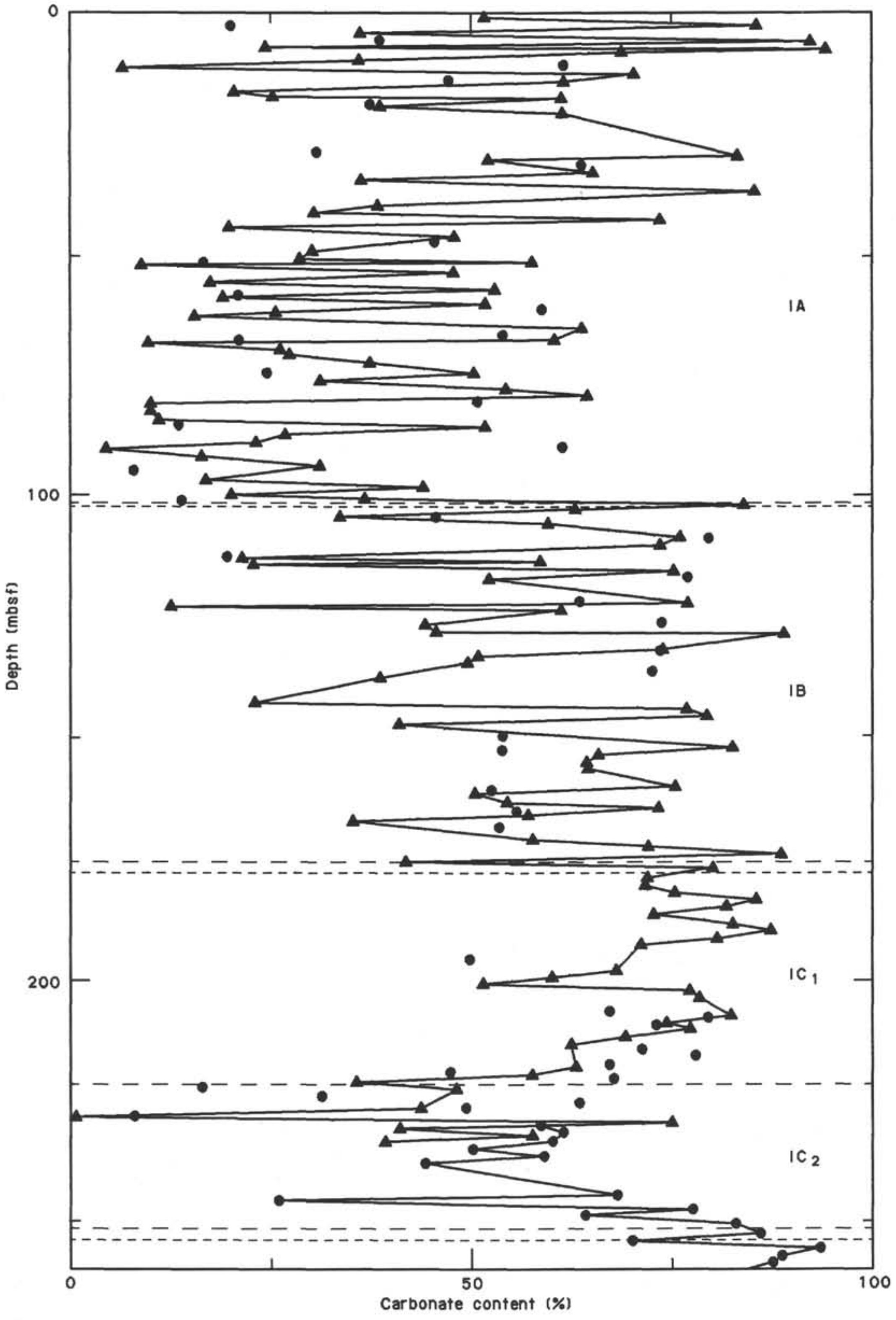

Figure 8. Carbonate content of Hole 704A.

greenish gray (5G 7/1), greenish gray (5G 6/1), light gray (2.5Y 7/2), white (5Y 8/1), and grayish brown (2.5Y 5/2). Diatom-bearing nannofossil ooze is white (no color code) to light gray (5Y 7/1). Subunit IC_2 is early Pliocene to late Miocene in age.

Below Core 114-704A-26X, recovery was extremely poor and consists of diatom-bearing nannofossil ooze, light greenish gray (5G 7/1) in color.

Hole 704B

Unit I: Core 114-704B-1H to Section 114-704B-48X, CC; Depth: 0–451.2 mbsf; Age: latest early Miocene to Pleistocene.

Unit I in Hole 704B is subdivided into four subunits based on the relative components in smear slide estimates (Fig. 7) and percent calcium carbonate (Fig. 9). Variations in the carbonate content mainly reflect the relative abundance of carbonate and biogenic silica.

Subunit IA: Core 114-704B-1H to Section 114-704B-11H, CC; Depth: 0–101.7 mbsf; Age: latest Pliocene to Pleistocene.

Subunit IA is characterized by common alternations of light gray (2.5Y 7/2), pale yellow (5Y 7/3) to white (no color code) diatom-foraminifer ooze, pale olive (5Y 6/3), light gray (5Y 7/1) to white (5Y 8/1) calcareous diatom ooze, pale olive (5Y 6/4), olive (5Y 5/4) to light gray (5Y 7/1) calcareous siliceous ooze, greenish gray (5GY 6/1), olive (5Y 5/4) to light gray (5Y 7/2) calcareous siliceous ooze, and olive (5Y 5/4) diatom ooze. Minor lithologies include white (no color code) nannofossil ooze and spots of pure diatom ooze (i.e., "diatom cotton"). These high-frequency lithologic changes are expressed in the variability of the carbonate record (Fig. 9). Ash- and ice-rafted-detritus–bearing horizons first appear in Sections 114-704B-2H-6 and 114-704B-2H-7. Disseminated lithic fragments (ice-rafted detritus?) are common in Core 114-704B-5H. Staining of the sediment by opaque minerals (pyrite?) occurs in Section 114-704B-4H-5 and is common through Core 114-704B-10H.

Bioturbation is minor to moderate, causing mottling of the oozes, which is especially evident in the darker colored sediments.

Soupy drilling disturbance occurs in a few cores (114-704B-2H and 114-704B-3H), but Subunit IA is much less disturbed in Hole 704B than in Hole 704A.

Subunit IB: Core 114-704B-12H to Section 114-704B-19X, CC; Depth: 101.7–175.7 mbsf; Age: late Pliocene.

Subunit IB is dominated by light gray (5Y 7/1), light olive gray (5Y 6/2), to white (5Y 8/1 to no color code) siliceous-bearing calcareous ooze, olive gray (5Y 5/2) to white (no color code) siliceous calcareous ooze, and greenish gray (5GY 6/1) to white (no color code) siliceous-bearing nannofossil ooze. The subunit is marked by a higher mean carbonate value than Subunit IA (Fig. 9), and a decrease in the abundance of biogenic silica is evident from smear slide estimates (Fig. 7). The boundary between Subunits IA and IB coincides with a marked change to lighter colors in the lower subunit. The lower (older) boundary of Subunit IB was extrapolated from Hole 704A because of poor recovery in Cores 114-704B-20X and 114-704B-21X.

Disseminated lithic fragments (ice-rafted detritus?) are found in Cores 114-704B-12H, 114-704B-13H, 114-704B-17X, and 114-704B-19X, and a larger pebble occurs at 102 cm in Section 114-704B-17X-4. A gray (5Y 6/1) ash-bearing horizon appears at 20–25 cm in Section 114-704B-19X-1.

Staining of the sediment by opaque minerals (pyrite?) is common in Cores 114-704B-13H, 114-704B-14H, 114-704B-17X, and 114-704B-18X.

Minor bioturbation in Cores 114-704B-14H, and 114-704B-15H is reflected by sediment mottling. *Planolites* burrows are filled with light gray (5Y 7/1) ooze.

Drilling disturbance is soupy to moderate in the very first centimeters of Cores 114-704B-1H to 114-704B-15H. Sections 114-704B-14H-2 and 114-704B-14H-3, 114-704B-15H-2 to 114-704B-15H-4, and 114-704B-15H-6 are highly disturbed.

Subunit IC: Core 114-704B-20X to Section 114-704B-27X, CC; Depth: 175.7–251.7 mbsf; Age: late Miocene to late Pliocene.

The major lithologies of Subunit IC are light bluish gray (5B 7/1) to white (2.5Y 8/1 to 7.5YR 8/1) siliceous-bearing calcareous ooze and light greenish gray (5GY 7/1) to bluish gray (5B 6/1) siliceous calcareous ooze. Minor lithologies are pinkish gray (7.YR 6/2) to greenish gray (5GY 6/1) calcareous siliceous ooze, greenish gray (5GY 6/1) ash-bearing clayey diatom ooze, and dark greenish gray (5GY 4/1) pyritic nannofossil ooze. The occurrence of the minor lithologies intercalated in the calcareous ooze is evidenced by a strong decrease in carbonate content (Fig. 9) and the dominance of siliceous biogenic material, as estimated from smear slides (Fig. 7). Minor staining of the sediment by opaque (pyrite?) minerals occurs in Core 114-704B-22X and is common to abundant in Cores 114-704B-25X to 114-704B-27X. These pyritic(?) black (7.5YR 2.5/0) spots cause sediment mottling.

Bioturbation is minor to moderate. *Zoophycos* is well developed at 99 and 105 cm in Section 114-704B-24X-6, and *Planolites* occurs from 125 to 133 cm in Section 114-704B-24X-6.

Drilling disturbance is moderate to minor in the topmost parts of Sections 114-704B-26X-1 (from 1 to 40 cm) and 114-704B-27X-1.

Subunit IC is further divided into Subunits IC_1 and IC_2.

Subunit IC_1: Core 114-704B-20X to Sample 114-704B-24X-4, 80 cm; Depth: 175.7–219.0 mbsf; Age: early Pliocene to early late Pliocene.

Subunit IC_1 consists of siliceous-bearing to siliceous calcareous ooze. This subunit is characterized by a mean carbonate content of about 60% with low variability. Color changes in this interval are extremely subtle to absent, and biogenic silica is low.

Subunit IC_2: Sample 114-704B-24X-4, 80 cm, to Section 114-704B-27X, CC; Depth: 219.0–251.7 mbsf; Age: latest Miocene to early late Pliocene.

The lower (older) boundary of this subunit is marked by a sharp decrease in carbonate content at 222.2 mbsf. This corresponds to a greenish gray (5GY 6/1) ash-bearing clayey diatom ooze from 102 to 113 cm in Section 114-704B-27X-4. Color variations are distinct in Subunit IC_2, and the siliceous biogenic component is high. The contact between Subunits IC and ID is marked by an increase in carbonate content from 25% to 77%. Siliceous biogenic components decrease markedly at this boundary (Figs. 7 and 9).

Subunit ID: Core 114-704B-28X to Section 114-704B-48X, CC; Depth: 251.7.7–451.2 mbsf; latest early Miocene to latest Miocene.

This subunit consists of light greenish gray (5GY 7/1) to white (2.5Y 8/1 to no color code) uniform nannofossil ooze. The siliceous biogenic components are rare, except for abundant diatoms in Core 114-704B-35X (Fig. 7). The mean carbonate content is about 80% and shows minor fluctuations. With increasing micrite the sediments become stiffer, and the first chalk occurs in Core 114-704B-46X. A small, normally graded turbiditic(?) layer containing ash particles occurs in Sample 114-704B-28X-1, 15 cm, and fine, dispersed ash was noted in Sample 114-704B-28X-4, 78 cm.

Spots and thin horizons of concentrated opaque particles (pyrite?) stain the ooze light blue gray (5B 7/1). They are common in Cores 114-704B-29X to 114-704B-31X, 114-704B-36X, and 114-704B-40X to 114-704B-44X and abundant in Core 114-704B-35X.

The interval between Samples 114-704B-35X-3, 40 cm, and 114-704B-35X-5, 140 cm, documents a short paleoenvironmental change in the late Miocene. Carbonate content decreases to 40% (322 mbsf in Fig. 9), and an increase in diatoms produces a yellowish mottling of the ooze. The second carbonate content low (60% at 404 mbsf) occurs just above a sand-bearing nannofossil ooze in Section 114-704B-44X-1. The sand is composed of pumice, quartz, benthic foraminifers, and pyrite, indicating a possible slump deposit or downhole contamination resulting from a heat flow measurement made prior to recovering Core 114-704B-44X.

Bioturbation is minor, resulting in faint sediment mottling. *Planolites* was found in Section 114-704B-30X-1.

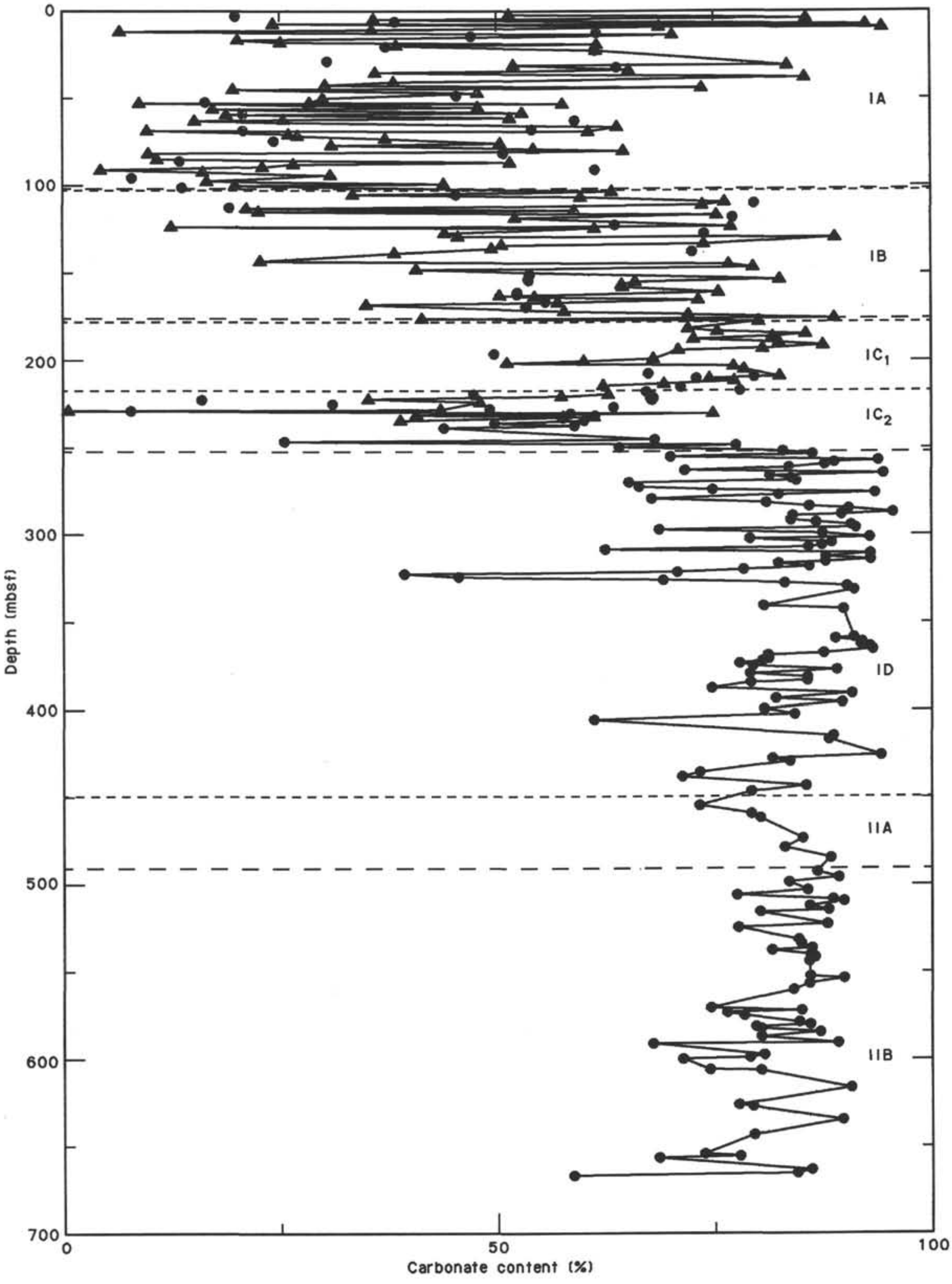

Figure 9. Carbonate content of Hole 704B.

Most of the drilling disturbance is represented by biscuiting of the sediment.

Unit II: Core 114-704B-49X to Section 114-704B-72X, CC; Depth: 451.2–671.7 mbsf; early Oligocene to late early Oligocene.

Unit II is differentiated on the basis of the increasing diagenetic maturity of the sediment.

Subunit IIA: Core 114-704B-49X to Section 114-704B-53X, CC; Depth: 451.2–491.2 mbsf; Age: late early Miocene.

The dominant lithology is light greenish gray (5GY 7/1) nannofossil chalk and white (no color code) micrite-bearing nannofossil chalk. Nannofossil ooze occurs as a minor lithology in Section 114-704B-49X-1. Calcareous biogenic components and micrite are abundant to very abundant (Fig. 7), and the carbonate content increases to 90% (Fig. 9).

Bioturbation is minor. *Zoophycos* occurs at 98 and 116 cm in Section 114-704B-49X-2, and *Planolites* is common from 105 to 150 cm in Section 114-704B-49X-4 and 140 to 150 cm in Section 114-704B-49X-5.

Drilling disturbance has resulted in biscuiting and moderate fracturing.

Subunit IIB: Core 114-704B-53X to Section 114-704B-72X, CC; Depth: 451.2–671.7 mbsf; Age: early Oligocene to late early Miocene.

Increased micritization of the carbonate results in an indurated micritic nannofossil chalk in Subunit IIB. The color of the chalk varies from gray (N6), light gray (5Y 7/1 and 10YR 7/1), to white (5Y 8/1 and 10YR 8/1 to no color code). A light gray (5Y 7/1) fine-grained, laminated turbidite with high clay content occurs from 37 to 68 cm in Section 114-704B-56X-4 (Fig. 10). The upper and lower contacts are sharp, and bioturbation is absent within the turbidite.

A volcanic breccia was found in Sample 114-704B-59X-1, 10–15 cm. Pebbles in Sections 114-704B-59X-1, 114-704B-70X-1, and 114-704B-72X-1 are interpreted as downhole contamination.

Minor to strong bioturbation is visible in most sections between Cores 114-704B-54X and 114-704B-66X. The ichnofacies is dominated by *Zoophycos* and *Planolites*. *Zoophycos* occurs in Cores 114-704B-54X and 114-704B-56X, Section 114-704B-61X-2, and Cores 114-704B-62X, 114-704B-63X, 114-704B-65X, and 114-704B-66X. *Planolites* occurs in Core 114-704B-56X, Section 114-704B-61X-2, and Cores 114-704B-62X, 114-704B-63X, 114-704B-65X, and 114-704B-66X. *Chondrites* occurs in Core 114-704B-62X.

Drilling disturbance is present throughout Subunit IIB in the form of drilling biscuits. Core 114-704B-55X is highly fractured and brecciated.

Paleoenvironment

The paleoenvironmental interpretation in Site 704 is based largely on lithologic changes recorded in both sediment color and carbonate content. The upper 250 m of sediment contains very numerous fluctuations in carbonate and biogenic silica. The shipboard carbonate analyses have captured the first-order changes in sediment composition, but the data are clearly biased. That is, the sampling spacing for carbonate analyses is greater than the natural period of variation. As a result, the character of the record is likely to change as more data become available.

The sediments at Site 704 record major paleoclimatic events that occurred during the late Cenozoic. From the base of the section to 251.7 mbsf, the sequence is dominated by pelagic carbonate sedimentation (nannofossil ooze and chalk) with little variation in color or lithology. This suggests uniform carbonate deposition above the carbonate compensation depth (CCD) between the early Oligocene and late Miocene. An interval of low carbonate content and increased diatom abundance occurs at 324 mbsf (Fig. 9) in Subunit ID, but this depositional event was

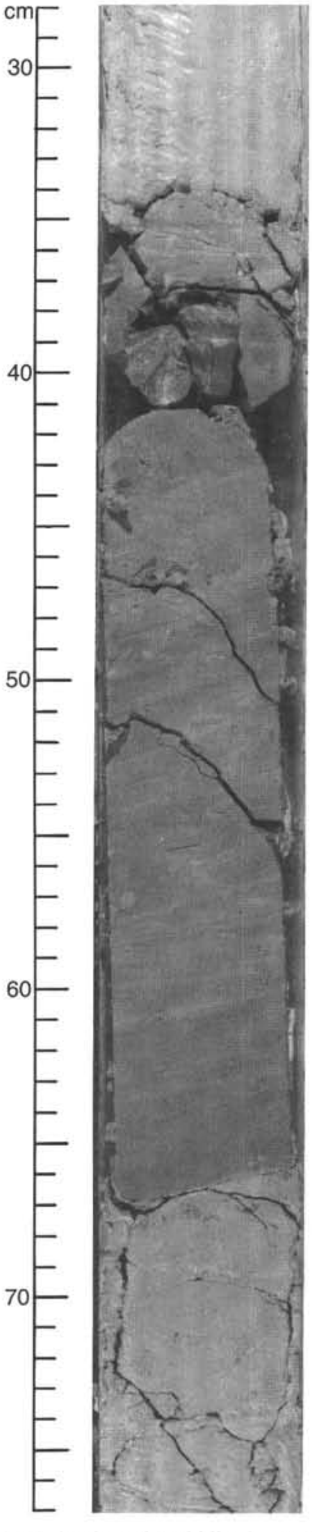

Figure 10. Fine-grained, laminated turbidite layer (Sample 114-704B-56X-4, 28–77 cm).

short lived. The dominant trend below 251.7 mbsf is a progressive increase in the diagenetic maturity of the sediment, with the ooze/chalk transition occurring at about 451.2 mbsf.

A major change in sedimentation occurred in the latest Miocene at about 251.7 mbsf, corresponding to the base of Subunit IC_2. This event is marked by a decrease in $CaCO_3$ by about 50% (Fig. 9), an increase in biogenic silica (Fig. 7), and the onset of strong color variations in the sediment. Preliminary magnetobiostratigraphic results suggest that these changes occurred in Chron C3AR.6 ($\sim$6.5–6.37 Ma) and are undoubtedly linked to other documented paleoceanographic events in the Southern Ocean at this time (Shackleton and Kennett, 1975; Ciesielski et al., 1982; Hodell and Kennett, 1986). The decrease in carbonate and increase in biogenic silica at Site 704 are related to a combined effect of increased siliceous productivity and carbonate dissolution associated with climate change during the latest Miocene. This lithologic change at Site 704 documents the northward migration of the polar front to $\sim$47°S. The amplitude and variance of the carbonate signal during the latest Miocene–earliest Pliocene (6.5 to 4.7 Ma) is comparable to the Pleistocene record, suggesting that the intensity of paleoceanographic change in the Southern Ocean was comparable during the late Miocene and Pleistocene.

Above Subunit IC_2, from 219 to 101.7 mbsf, the lithology returns to relatively high carbonate values (Fig. 8). The amplitude of the carbonate signal appears to progressively increase through Subunits IC_1 and IB. The age of this interval extends from the early Pliocene to the late Pliocene, spanning much of the Gilbert, Gauss, and lower Matuyama Chrons.

A marked change in sedimentation occurs at $\sim$101.7 mbsf, at the base of Core 114-704A-11X, and represents a significant increase in the biogenic silica component (diatoms) of the sediment. The color changes above this level are strikingly intense and more common than lower in the section. The average carbonate content is slightly lower in Subunit IA and is characterized by higher variability (Figs. 8 and 9). According to diatom biostratigraphy (see "Biostratigraphy" section, this chapter) and the magnetostratigraphic record, the Subunit IA/Subunit IB boundary occurs just below the top of the Olduvai Subchron, which has been placed at a depth of 93.7 mbsf.

The top 175 m of sediment at Site 704, including Subunits IA and IB, contains cyclic alternations of carbonate and silica components. These cycles are reflected in color variations, with the lighter shades generally correlating with higher carbonate values. These lithologic changes are probably related to glacial-interglacial cycles of the Pliocene-Pleistocene. In the Atlantic, glacial episodes usually correspond to low carbonate values, whereas interglacial episodes are marked by carbonate highs (Gardner, 1975). Post-cruise oxygen isotopic analyses confirm an Atlantic-type carbonate pattern at Site 704.

Late Pliocene–early Pleistocene deposition at Site 704 was controlled by a complex interplay of three climatically controlled processes: (1) siliceous and carbonate productivity, (2) carbonate dissolution, and (3) dilution of silica by carbonate and vice versa. Climatically induced changes in these variables on time scales of tens of thousands to hundreds of thousands of years resulted in the complex changes in sediment deposition observed in Subunits IA and IB. One explanation of the carbonate/silica variations is cyclic migration of the polar front across Site 704 in response to glacial-interglacial forcing. The excellent recovery by double APC/XCB methods over this interval coupled with detailed magnetobiostratigraphy will permit high-resolution paleoceanographic studies.

BIOSTRATIGRAPHY

Holes 704A and 704B were drilled in a water depth of 2532.3 m on the Meteor Rise. Hole 704A penetrated 282.7 m of diatom and nannofossil oozes. Hole 704B penetrated 671.7 m of diatom and nannofossil oozes overlying a nannofossil chalk.

Nannofossil preservation is moderately good throughout the Pleistocene to Miocene section, but poor in the Oligocene strata. Diatoms are abundant and well preserved throughout most of the section, with two intervals of reduced abundance in the middle Miocene and upper Miocene. Planktonic foraminifer preservation is good in the Pleistocene, moderate in the Pleistocene to lower Miocene, and poor in the lower Miocene to Oligocene. Benthic foraminifers and radiolarians are generally well preserved throughout the section.

Biostratigraphy

The following biostratigraphic divisions are drawn in a composite section of Holes 704A and 704B:

late Pleistocene	114-704A-1H-2, 110 cm, to 114-704A-1H-1, 0 cm
middle–early Pleistocene	114-704A-1H-2, 100 cm, to 114-704A-11H-1, 16 cm
late Pliocene	114-704A-11H-2, 34 cm, to 114-704A-20X-6, 85 cm
early Pliocene	114-704A-20X-6, 95 cm, to 114-704A-25X-1, 135 cm
late Miocene	114-704B-25X-1, 145 cm, to 114-704B-46X-2, 82 cm
middle Miocene	114-704B-47X-5, 79 cm, to 114-704B-48X-3, 81 cm
early Miocene	114-704B-48X, CC, to 114-704B-62X-2, 92 cm, or CC
late Oligocene	114-704B-64X, CC, to 114-704B-69X, CC
early Oligocene	114-704B-70X, CC, to 114-704B-72X, CC

The biostratigraphic results together with zonal assignments are graphically summarized in Figures 11A and 11B. A list of microfossil datums identified at this site is given in Table 3 and plotted in the age vs. depth diagram of Figure 12. Table 3 reveals that the majority of microfossil datums are based upon diatoms; however, this should not be interpreted as indicative of the lack of stratigraphic utility of other microfossil groups. At the time of this writing, other fossil groups have not been examined in detail, whereas a more detailed (though incomplete) diatom stratigraphy of the Neogene has been provided by Fenner and Ciesielski. No detailed biostratigraphic studies have been made of the Oligocene at this time.

The Pliocene/Pleistocene, early/late Pliocene, and Miocene/Pliocene boundaries are placed at the top of the Olduvai subchron, Gauss/Gilbert boundary, and Gilbert/C3AN boundaries, respectively. On the basis of foraminifer zonation, the middle/late Miocene boundary is placed at the first appearance datum (FAD) of *Neogloboquadrina acostaensis*, between Sections 114-704B-40X, CC, and 114-704B-41X, CC. Diatoms are indicative of a late/middle Miocene boundary lower in the section, between Sample 114-704B-46X-2, 82 cm, and Section 114-704B-46X, CC ($\sim$425.02 to 432.20 mbsf). The diatom stratigraphy suggests that this boundary occurs at a hiatus between the lower middle Miocene and upper Miocene, which is marked by a pile up of last appearance datums (LADs) of diatoms and calcareous nannofossils (datums 32–37; Table 3). The younger apparent age for the *N. acostaensis* datum may be attributed to a younger first occurrence in the subantarctic ($\sim$8.5 to 9.0 Ma) or a mistaken correlation of this datum to the base of Chron C5N (Berggren et al., 1985).

The early/middle Miocene boundary is tentatively placed between the FAD of *Sphenolithus heteromorphus*, between 451.2 and 460.7 mbsf (between Sections 114-704B-48X, CC, and 114-

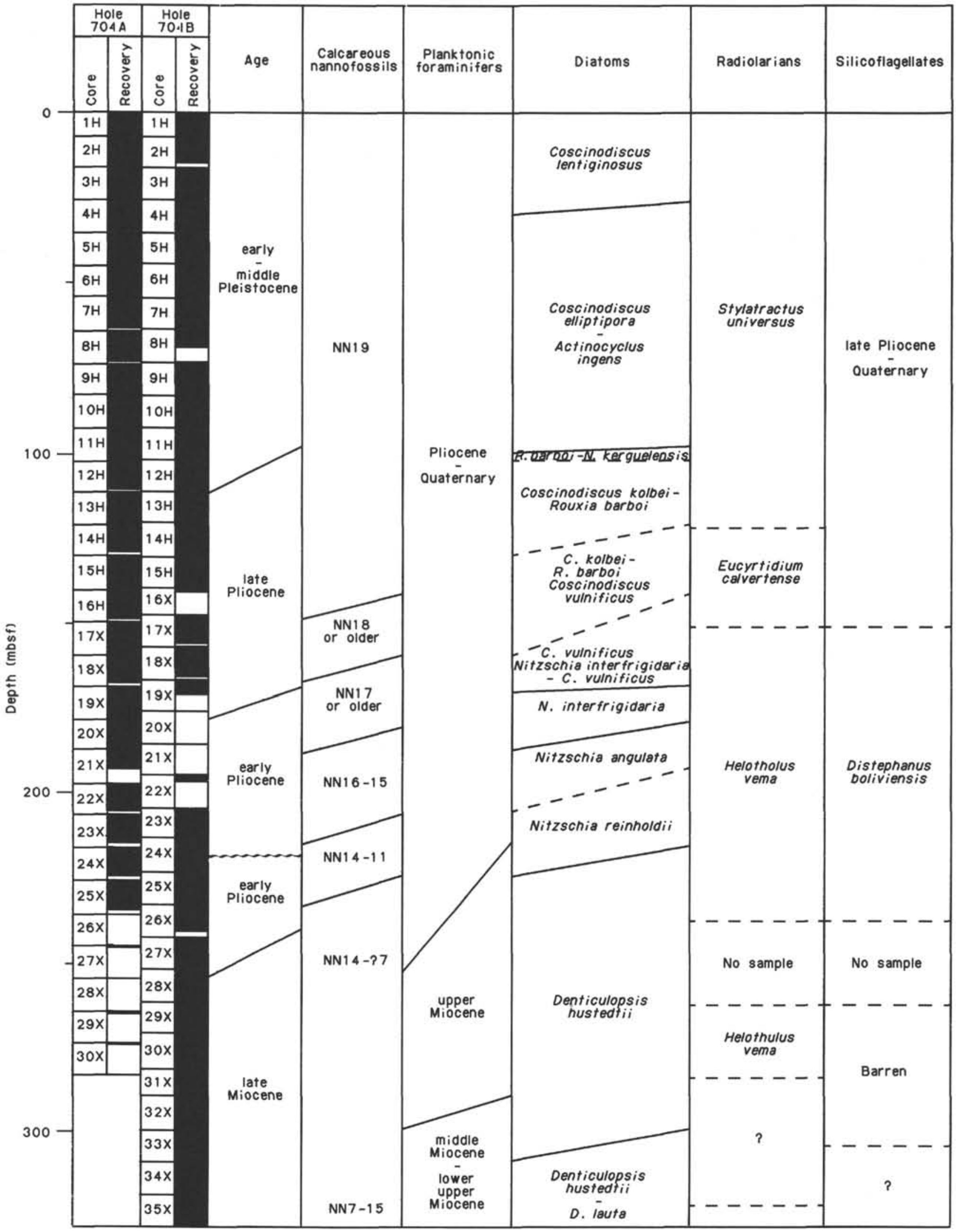

Figure 11. Summary of microfossil data from Holes 704A and 704B.

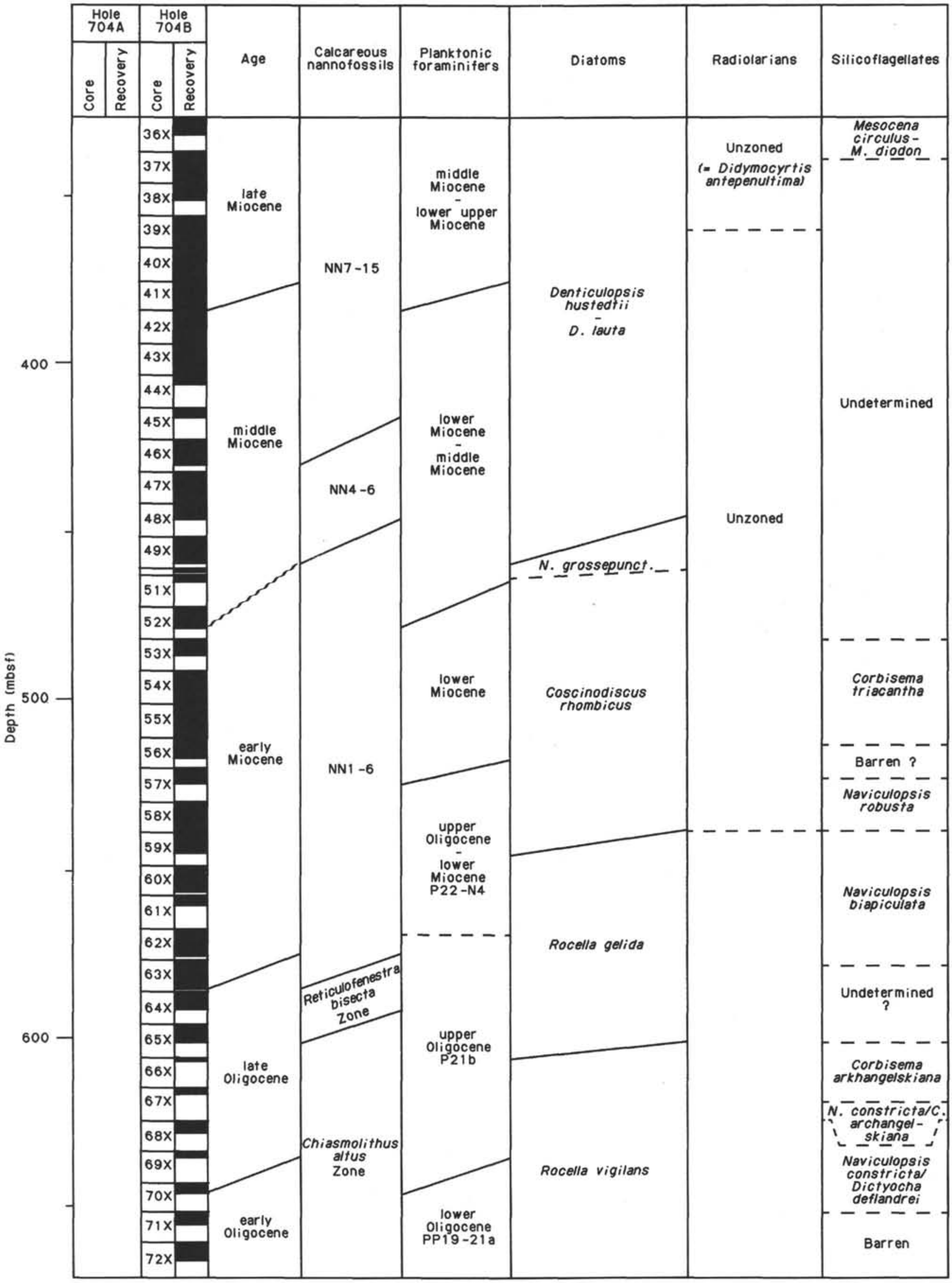

Figure 11 (continued).

Table 3. Microfossil and paleomagnetic datums in Hole 704A and 704B, with ages, bracketing sample intervals, and depths below seafloor.

Hole 704A

Microfossil and paleomagnetic datums[a]	Age (Ma)	Reference[b]	Interval in Hole 704A	Depth range (mbsf)	Mean position (mbsf)
1. LAD *Pseudoemiliana lacunosa* (N)	+0.474 (30, 37), +0.40	(29)	1H-1, 0 cm, to 1H-1, 100 cm	0.00–2.50	1.25
2. LAD *Stylatractus universus* (R)	+0.41	19	1H-1, 0 cm, to 1H, CC	0.00–7.20	3.60
3. LAD *Hemidiscus karstenii* (D)	0.195	36	1H-2, 100 cm, to 1H-3, 76 cm	2.50–5.26	3.88
4. LAD *Actinocyclus ingens* (D)	+0.62	10	2H-5, 120 cm, to 2H-5, 120 cm	14.40–15.90	15.15
5. Brunhes/Matuyama boundary	0.73	4	3H-5, 99 cm, to 5H-7, 16 cm	23.69–45.20	33.10
6. Top Olduvai subchron	1.66	4	11H-1, 16 cm, to 11H-2, 34 cm	92.86–94.54	93.70
7. LAD *Rhizosolenia barboi* (D)	+1.50	10	11H-4, 70 cm, to 11H-4, 80 cm	97.90–98.00	97.95
8. LAD *Coscinodiscus kolbei* (D)	+1.89	10	11H-6, 35 cm, to 11H-6, 80 cm	100.45–101.00	100.73
9. Top *Helicosphaera sellii* (N)	+1.37	28	13H, CC, to 14H-5, 33 cm	120.53–121.20	124.37
10. LAD *E. calvertense*	+1.90	11	13H, CC, to 14H, CC	121.20–130.70	125.95
11. LAD *Nitzschia interfrigidaria* (D)	+2.81	10	16H-2, 80 cm, to 16H-4, 70 cm	142.50–145.40	143.95
12. LAD *Coscinodiscus vulnificus* (D)	+2.20	10	16H-4, 80 cm, to 16H-2, 82 cm	145.50–142.52	144.01
13. LAD *Discoaster brouweri* (N)	+1.88	29	15H, CC, to 16H, CC	249.70–140.20	144.95
14. LAD *Helotholus vema* (R)	+2.47	11	16H, CC, to 17X, CC	149.70–159.20	154.45
15. LAD *Desmospyris spongiosa* (R)	+2.47	11	16H, CC, to 17X, CC	149.70–159.20	154.45
16. Top NN17 Zone (N)	+2.35	28	17X, CC, to 18X, CC	168.70–159.20	163.95
17. Matuyama/Gauss boundary	2.47	4	18X-6, 145 cm, to 19X-1, 5 cm	168.15–168.75	168.45
18. *LAD *Coscinodiscus insignis* (D)	+2.49	10	18X-6, 76 cm, to 19X-2, 60 cm	167.46–170.80	169.13
19. *LAD *Nitzschia weaveri* (D)	+2.64	10	18X-6, 78 cm, to 19X-2, 60 cm	167.48–170.80	169.14
20. *FAD concurrent *C. insignus* and *C. vulnificus* (D)	+3.10	10	18X, CC, to 19X-1, 77 cm	168.70–169.47	169.09
Hiatus ~2.8 or 2.9 to ~2.5 Ma				~169–171	
21. Top Kaena subchron	2.92	4	19X-5, 135 cm, to 19X-6, 5 cm	176.05–176.25	176.15
22. Base Kaena subchron	2.99	4	19X-7, 5 cm, to 19X-7, 15 cm	178.20–178.20	178.20
23. Top Mammoth subchron	3.08	4	20X-1, 85 cm, to 20X-1, 95 cm	179.05–179.15	179.10
24. FAD *N. weaveri* (D)	+3.88	10	19X, CC, to 20X-2, 70 cm	178.20–180.40	179.30
25. Base Mammoth subchron	3.18	4	20X-3, 25 cm, to 20X-3, 45 cm	181.45–181.65	181.55
26. Top NN16 Zone (N)	+2.41	4	19X, CC, to 20X, CC	187.70–178.20	182.95
27. Gauss/Gilbert boundary	3.40	4	20X-6, 85 cm, to 20X-6, 95 cm	186.55–186.65	186.60
28. FAD *Nitzschia angulata* (D)	+4.22	10	21X-3, 82 cm, to 21X-4, 5 cm	191.52–192.25	191.89
29. Top Cochiti subchron	3.88	4	22X-1, 115 cm, to 22X-1, 135 cm	198.35–198.55	198.45
30. LAD *Reticulofenestra pseudoumbilica* (N)	+3.56 (28), 3.50	(4)	21X, CC, to 22X, CC	197.20–206.70	201.95
31. Base Cochiti subchron	3.97	4	22X-4, 15 cm, to 22X-4, 75 cm	201.85–202.45	202.15
32. Top Nunivak subchron	4.10	4	22X-5, 95 cm, to 22X-5, 104 cm	204.15–204.24	204.20
33. Base Nunivak subchron	4.24	4	23X-3, 65 cm, to 23X-3, 75 cm	210,35–210.45	210.45
34. FAD *Gephrocapsa* spp. (N)	3.70–3.56	34	22X, CC, to 23X, CC	206.70–216.20	211.45
35. Top Sidufjall subchron	4.40	4	23X-4, 75 cm, to 23X-4, 85 cm	211.95–212.05	212.00
36. Base Sidufjall subchron	4.47	4	23X-5, 55 cm, to 23X-5, 65 cm	213.25–213.35	213.30
37. Top Thvera subchron	4.57	4	24X-1, 55 cm, to 24X-2, 5 cm	216.75–217.75	217.25
38. Base Thvera subchron	4.77	4	24X-3, 15 cm, to 24X-3, 35 cm	219.35–219.55	219.45
39. LAD *Triceraspyris coronata* (R)	+4.25	12	23X, CC, to 24X, CC	216.20–225.70	220.95
40. LAD *Denticulopsis hustedtii* (D)	+4.48	10	23X, CC, to 24X, CC	216.20–225.70	220.95
41. LAD *Amphymenium challengerae* (R)	+4.35–4.45	12	24X, CC, to 25X, CC	225.70–235.20	230.45
42. LAD *Stichocorys peregrina* (R)	+4.6–4.4	12	24X, CC, to 25X, CC	225.70–235.20	230.45
43. LAD *Coscinodiscus insignis* v. *triangula* (D)	~4.8–5.0	15	26X, CC, to 27X, CC	244.70–254.20	249.45
44. LAD *Lamprocyclas aegles* group (R)	+5.50	12	28X, CC, to 29X, CC	263.70–273.20	268.45
45. FAD *C. insignis* v. *triangula* (D)	+6.40	10	29X, CC, to 30X, CC	272.20–282.70	277.95
46. FAD *Nitzschia reinholdii* (D)	+6.40–6.50	38	>30X, CC	>282.70	

Hole 704B

Microfossil and paleomagnetic datums[a]	Age (Ma)	Reference[b]	Interval in Hole 704B	Depth range (mbsf)	Mean position (mbsf)
1. LAD *Hemidiscus karstenii* (D)	+0.195	36	1H-1, 0 cm, to 1H-2, 150 cm	0.00–3.00	(1.50)
2. LAD *Pseudoemiliana lacunosa* (N)	+0.474 (30, 37), +0.40	(29)	1H, 0 cm, to 1H, CC	0.00–6.70	(3.35)
3. LAD *Actinocyclus ingens* (D)	+0.62	10	3H, CC, to 4H-2, 95 cm	25.70–28.15	(26.93)
4. LAD *Rhizosolenia barboi* (D)	+1.50	10	11H, CC, to 12H, CC	101.70–111.20	(106.45)
5. LAD *Coscinodiscus kolbei* (D)	+1.89	10	12H, CC, to 13H-2, 125 cm	111.20–113.95	(112.58)
6. LAD? *Helicosphaera sellii* (N)	+1.37	28	13H, CC, to 14H, CC	120.70–130.20	(125.45)
7. LAD? *Calcidiscus macintyrei* (N)	+1.45	28	16X, CC, to 17X, CC	147.20–156.70	(151.95)
8. LAD? *Discoaster brouweri* (N)	+1.88	28	16X, CC, to 17X, CC	147.20–156.70	151.95)
9. LAD *Coscinodiscus vulnificus* (D)	+2.22	10	17X-2, 100 cm, to 17X, CC	149.70–156.70	(153.20)
Hiatus ~2.8 or 2.9 to ~2.5 Ma (position inferred from Hole 704A)				~171–169 in Hole 704A ~160–165 in Hole 704B	
10. FAD *C. vulnificus* (D)	+3.1	10	19X-1, 21 cm, to 19X-1, 75 cm	166.41–166.95	(166.68)
11. FAD *Nitzschia weaveri* (D)	+3.88	10	19X, CC, to 20X, CC	175.70–185.20	(180.45)
12. LAD *Amaurolithus triconiculatus* (N)	+4.40	31	21X, CC, to 22X, CC	194.70–204.20	(199.45)
13. LAD *Reticulofenestra pseudoumbilica* (N)	+3.56	28	21X, CC, to 22X, CC	194.70–204.20	(199.45)
14. FAD *Nitzschia angulata* (D)	+4.22	10	23X-2, 70 cm, 23, CC	206.40–213.70	(210.05)
15. LAD *Denticulopsis hustedtii* (D)	+4.88	10	23X, CC, to 24X, CC	213.70–223.20	(218.45)
16. Gilbert/C3AN boundary	5.35	4	25X-1, 135 cm, to 25X-1, 145 cm	224.55–224.65	(224.60)
17. LAD LAD *Amphymenium challengerae* (R)	+4.35–4.45	12	24X, CC, to 25X, CC	223.20–232.70	(227.95)
18. LAD *Stichocorys peregrina* (R)	+4.6–4.4	12	24X, CC, to 25X, CC	223.20–232.70	(227.95)
19. C3AN/C3AR boundary	5.89	4	26X-5, 45 cm, to 27X-2, 25 cm	239.15–243.95	(241.55)

Table 3 (continued).

Hole 704B (cont.)

Microfossil and paleomagnetic datums[a]	Age (Ma)	Reference[b]	Interval in Hole 704B	Depth range (mbsf)	Mean position (mbsf)
20. LAD *Lamprocyclas aegles* group (R)	5.5	12	26X, CC, to 27X, CC	242.20–251.70	(246.95)
21. FAD *L. aegles* group (R)	6.0–5.8	12	29X, CC, to 30X, CC	270.70–280.20	(275.45)
22. FAD *Nitzschia reinholdii* (D)	+6.5	38	30X-1, 82 cm, to 31X, CC	271.52–289.70	(280.61)
23. FAD *S. peregrina* (R)	+6.3	32	30X, CC, to 31X, CC	280.20–289.70	(284.95)
24. *FAD *Nitzschia miocenica* (D)	+6.8	9	31X-5, 82 cm, to 31, CC	287.02–289.70	(288.36)
Hiatus Maximum duration = 2.5 m.y. (8.5 to 6.5 Ma)				~287–308	
25. *LAD *Denticulopsis lauta* (D)	#8.7	10	32X, CC, to 33X, CC	299.20–308.70	(303.95)
26. LAD *Diartus hughesi* (R)	+9.0 (22)–#8.6	(10)	34X, CC, to 35X, CC	318.20–327.70	(322.95)
27. FAD *Hemidiscus cuneiformis* (D)	#8.7–8.9	39	39X-5, 82 cm, to 40X-2, 80 cm	363.02–368.00	(365.51)
28. LAD *Denticulopsis dimorpha* (D)	8.4	33	40X-5, 82 cm, to 41X-5, 80 cm	375.52–382.00	(377.26)
29. FAD *Neogloboquadrina acostaensis* (F)	10.4	4	41X, CC, to 40X, CC	384.70–375.20	(379.95)
30. LAD *Cyrtocapsella japonica* (R)	#8.7 (10), 9.1	(22)	43X, CC, to 44X, CC	403.70–415.20	(409.45)
31. FAD *D. dimorpha* (D)	8.9	33	46X-2, 82 cm, to 46X-5, 80 cm	425.02–429.50	(427.26)
Hiatus Maximum duration = ~6.0 m.y. (~9.0–15.0 Ma)				~425.02–432.20	
32. *LAD *Denticulopsis maccollumii* (D)	~10.7?	40	47X-2, 81 cm, to 47X-5, 79 cm	434.51–438.99	(436.75)
33. * LAD *Denticula nicobarica* (D)	12.6	21	46X-5, 82 cm, to 47X-2, 81 cm	438.99–434.51	(436.75)
34. *LAD *Coscinodiscus lewisianus* (D)	12.9	9, 21	47X-2, 81 cm, to 47X-5, 79 cm	434.51–438.99	(436.75)
35. *LAD *Coscinodiscus pulchellus* (D)	13.6–13.5	20	46X-2, 82 cm, to 46X-5, 80 cm	425.02–429.50	(427.26)
36. *LAD *Actinocyclus ingens* f. *nodus* (D)	~13.8	33	46X-2, 82 cm, to 46X-5, 80 cm	425.02–429.50	(427.26)
37. *LAD *Sphenolithus heteromorphus* (N)	14.4	4	45X, CC, to 46X, CC	422.70–432.20	(427.45)
38. FAD *A. ingens* f. *nodus* (D)	~15.2	33	47X-5, 79 cm, to 47X-2, 81 cm	438.99–434.51	(436.75)
39. FAD *Nitzschia denticuloides* (D)	~14.4	18	47X-5, 81 cm, to 48X-1, 79 cm	439.01–442.49	(440.75)
40. LAD *Nitzschia maleinterpretaria* (D)	15.6	20	48X-1, 79 cm, to 48X-3, 81 cm	442.49–445.51	(444.00)
41. LAD *Coscinodiscus lewisianus* v. *similis* (D)	15.7	20	48X-1, 79 cm, to 48X-3, 81 cm	442.49–445.51	(444.00)
42. FAD *D. hustedtii*? (D)	14.2	20	48X-3, 81 cm, to 49X-1, 47 cm	445.51–451.67	(448.59)
43. FAD *D. lauta* (D)	16.1	21	48X-3, 81 cm, to 49X-1, 47 cm	445.51–451.67	(448.59)
44. FAD *Cestodiscus peplum* (D)	16.4	25	48X-3, 81 cm, to 49X-1, 47 cm	445.51–451.67	(448.59)
45. FAD *A. ingens* (D)	16.8	20	48X-3, 81 cm, to 49X-1, 47 cm	445.51–451.67	(448.59)
46. FAD *Rouxia marylandica* (D)	+16.7	20	49X-4, 49 cm, to 49X-1, 49 cm	456.19–451.69	(453.94)
47. FAD? *C. macintyrei* (N)	16.2	4	48X, CC, to 49X, CC	451.20–460.70	(455.95)
48. FAD *S. heteromorphus* (N)	17.1	4	48X, CC, to 49X, CC	451.20–460.70	(455.95)
49. FAD *D. maccollumii* (D)	—	—	49X-4, 49 cm, to 50X-1, 45 cm	456.19–461.15	(458.67)
50. FAD *Denticula* cf. *kanayae* (D)	+16.9	20	49X-4, 49 cm, to 50X-1, 45 cm	456.19–461.15	(458.67)
51. FAD *C. lewisianus* v. *similis* (D)	+17.4	20	49X-4, 49 cm, to 50X-1, 45 cm	456.19–461.15	(458.67)
52. FAD *Nitzschia grossepunctata* (D)	—	—	50X-1, 45 cm, to 51X-1, 45 cm	461.15–463.15	(462.15)
53. LAD *Catapsydrax dissimilis* (F)	17.6	21, 4	51X, CC, to 52X, CC	472.20–481.70	(476.95)
54. LAD *Coscinodiscus rhombicus* (D)	17.5–17.6	41	52X-4, 42 cm, to 52X, CC	477.12–481.70	(479.41)
55. LAD *Naviculopsis* (S)	+17.5	25	53X-3, 42 cm, to 54X-2, 40 cm	485.12–493.10	(489.11)
56. LAD *Triceratium pileus* (D)	+17.6	20	53X-3, 42 cm, to 54X-2, 40 cm	485.12–493.10	(489.11)
57. FAD *Denticula nicobarica* (D)	+17.8	20	54X-2, 42 cm, to 54X-5, 40 cm	493.10–494.40	(493.75)
58. LAD *R. symmetrica* (D)	18.7	42	55X-1, 40 cm, to 56X-1, 85 cm	501.10–511.05	(506.08)
59. FAD *N.* maleinterpretaria (D)	18.8	20	56X-1, 87 cm, 57X-2, 82 cm	511.07–522.02	(516.55)
60. LAD *Rocella schraderi* (D)	~18.8	43	56X-1, 87 cm, to 57X-2, 82 cm	511.07–522.02	(516.55)
61. LAD *Rocella vigilans* (D)	—	—	56X-1, 87 cm, to 57X-2, 82 cm	511.07–522.02	(516.55)
62. LAD *Rocella gelida* (D)	22.7	21	56X-1, 87 cm, to 57X-2, 82 cm	511.07–522.02	(516.55)
63. FAD *Cyrtocapsella tetrapera* (R)	22.1	21	58X, CC, to 59X, CC	538.70–548.20	(543.45)
64. FAD *Thalassiosira fraga* (D)	19.9	21	59X-2, 82 cm, 60X-2, 80 cm	541.02–550.50	(545.76)
65. LAD *Triceratium groningensis* (D)	—	—	59X-2, 82 cm, to 60X-2, 80 cm	541.02–550.50	(545.76)
66. LAD *Bogorovia veniamini* (D)	+19.9	44	59X-2, 82 cm, to 60X-2, 80 cm	541.02–550.50	(545.76)
67. LAD *C. lewisianus* v. *rhomboides* (D)	22.5	21	59X-2, 82 cm, to 60X-2, 80 cm	541.02–550.50	(545.76)
68. LAD *Thalassiosira primalabiata* (D)	21.7	21	59X-2, 82 cm, to 60X-2, 80 cm	541.02–550.50	(545.76)
69. FAD *R. marylandicus* (D)	—	—	61X-2, 82 cm, to 62X-2, 40 cm	560.02–569.10	(564.56)
70. Top P21b Zone (F)	28.1	4	62X-2, 92 cm, to 62X-3, 90 cm	569.62–570.90	(570.26)
71. Top *Reticulofenestra bisecta* Zone (N)	23.7	1, 4	63X, CC, to 64X, CC	586.20–595.70	(590.95)
72. Top *Chiasmolithus altus* (N)	23.7–28.1	2	64X, CC, to 65X, CC	595.70–605.20	(600.45)
73. FAD *R. gelida* (D)	24.0 (21), 23.8–24.0	(25)	65X, CC, to 66X, CC	605.20–614.70	(609.95)
Possible Hiatus					
74. Base P21B Zone (F)	30.0	4	69X, CC, to 70X, CC	643.20–652.70	(647.95)
75. Base P19/20 Zone (F)	34.0	4	>72X, CC	>671.70	
76. FAD *R. vigilans* (D)	~33.0	20	>72X, CC	>671.70	

1. Wise (1983); 2. Martini and Müller (1986); 3. Perch-Nielsen (1985); 4. Berggren et al. (1985); 5. Kent and Gradstein (1985); 6. Jenkins (1985); 7. McGowran (1986); 9. Burckle et al. (1978); 10. Ciesielski (1983); 11. Chen (1975); 12. Weaver (1983); 13. L.H. Burckle pers. comm. (1980) to Barron (1985); 14. Barron et al. (1985), Ciesielski (1985); 15. Ciesielski (1985); 16. Gombos (1983); 17. Fenner (1984); 18. Weaver and Gombos (1981); 19. Hays and Shackleton (1976); 20. Barron (1985); 21. Barron et al. (1985); 22. Johnson and Wick (1982); 23. Barron (1983); 24. radiometric age by Hausback (1984) in Kim and Barron (1986); 25. Barron et al. (1985b); 26. inferred from Gombos and Ciesielski (1983); 27. inferred from Shaw and Ciesielski (1983); 28. Backman and Shackleton (1983); 29. Mijajima (1974); 30. Thierstein (1977); 31. Haq and Takayama (1984); 32. Theyer et al. (1978); 33. Barron (1986); 34. Samtleben (1980); 35. Ryan et al. (1974); 36. Burckle et al. (1978); 37. Thierstein et al. (1977); 38. Ciesielski (unpub. data); 39. inferred from (10) and (15); 40. based on correlation with LAD of *Coscinodiscus*; 41. corrected age from Weaver and Gombos (1981) based upon ages of bracketing calcareous nannofossils; 42. age based on relative position to nannofossils datum at Site 278; 43. based upon coincidence of datum with the FAD of *N. maleinterpretaria* in Site 513, as cited by Gombos and Ciesielski (1983); 44. L.H. Burckle (pers. comm) to Barron (1982).

[a] D = diatom; F = planktonic foraminifer; N = calcareous nannofossil; S = silicoflagellage; + = direct correlation to paleomagnetic stratigraphy; # = absolute age data.

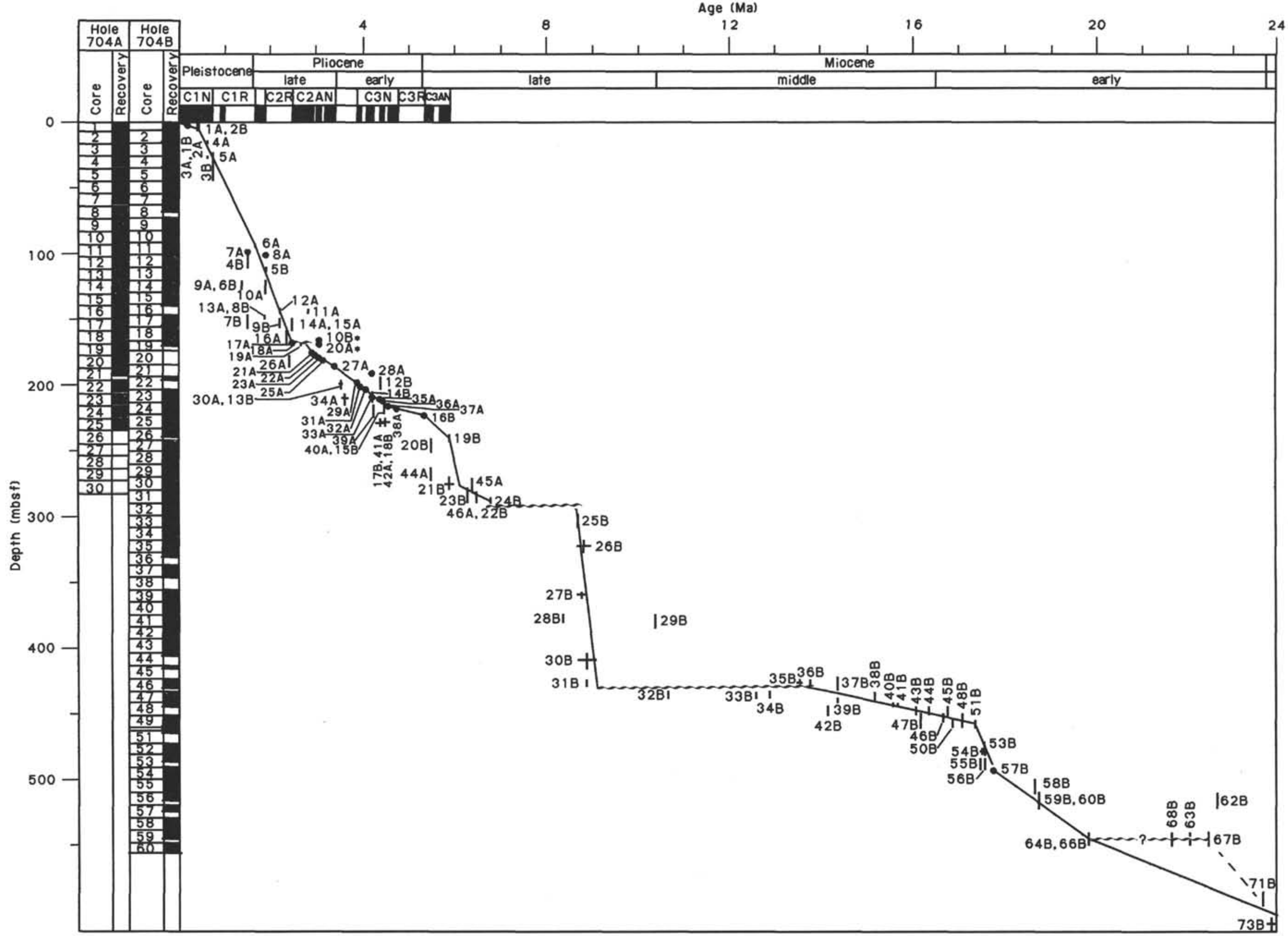

Figure 12. Age vs. depth relationship and average sedimentation rates for the Neogene of Site 704. Sparse biostratigraphic data from the lower part of Hole 704B (below Core 114-704B-63X) at this time prevents high resolution age vs. depth determinations. Numbered datums correspond to biostratigraphic and magnetostratigraphic datums identified in Table 3. The sub-bottom depth ranges of individual datums that occur in both holes are plotted separately if their ranges do not overlap; if they overlap, the plotted depth represents the interval of overlap.

704B-49X, CC) and the occurrence of several datums bracketing the boundary in Sample 114-704B-48X-3, 81 cm (Table 3). The Oligocene/Miocene boundary is placed between Sections 114-704B-64X, CC, and 114-704B-63X, CC, at the top of the *Reticulofenestra bisecta* Zone. The early/late Oligocene boundary is tentatively placed at the base of foraminifer Zone P21b, between Sections 114-704B-69X, CC, and 114-704B-70X, CC.

Strong reworking was observed in all microfossil groups in the Pleistocene. In the Oligocene and Neogene sediments, only sporadic reworked specimens were encountered.

Paleoenvironment

Radiolarian assemblages indicate warm surface waters in the early to middle Miocene, and similar conditions persisted into the late Miocene. Warmer waters characterized the early Pliocene. Radiolarians deposited after the early Pliocene show the occurrence of a general cooling trend. Ratios of the silicoflagellate genera *Dictyocha/Distephanus* in the Pleistocene show warm-water conditions prevailed during the deposition of Section 114-704A-7H, CC.

The nannofossils have a major change in assemblages between Sections 114-704B-48X, CC, and 114-704B-47X, CC, representing a drop in surface water temperature. Dramatic changes in the abundance of different nannofossil species in the uppermost three cores (114-704A-1H through 114-704A-3H) possibly reflect a rapidly changing environment of deposition.

The stratigraphic ranges of some diatom species in the Neogene seem to be determined predominantly by paleoenvironmental changes. Diatom abundance through time indicates three periods of increased productivity. These were during the late Oligocene, the middle to early late Miocene, and the latest Miocene to Pleistocene.

Deposition at Site 704 was above the foraminiferal lysocline from the Oligocene to Pleistocene, with deposition near the lysocline during the late Oligocene and late Pliocene. The benthic foraminifers indicate a paleowater depth of >1000 m.

Calcareous Nannofossils

Hole 704A

Eight core samples and all of the core-catcher samples were examined from Hole 704A. All samples examined contain nannofossils. The nannofossil floras are assigned to Martini's (1971) zones, as described in the "Explanatory Notes" chapter, this volume.

Biostratigraphy

Sample 114-704A-1H-2, 100–101 cm, to Section 114-704A-13X, CC, contain *Pseudoemiliana lacunosa* and are assigned to NN19 (middle Pleistocene–upper Pliocene). Samples in the interval between Sample 114-704A-14H-5, 33–34 cm, and Section 114-704A-15H, CC, additionally contain *Helicosphaera sellii*, a species with a LAD within NN19; thus, these samples can be assigned to the lower part of NN19 (lower Pleistocene–upper Pliocene).

The very rare occurrence of *Discoaster brouweri* and the presence of *Calcidiscus macintyrei* in Section 114-704A-16H, CC, indicate the presence of NN18 or older strata. The very rare occurrence of *Discoaster pentaradiatus* in Section 114-704A-18X, CC, indicates the presence of NN17 or older strata, whereas the presence of very rare *Discoaster surculus* in Section 114-704A-20X, CC, indicates the presence of NN16 or older strata. These fossils are all very rare, and their last occurrences, which are used to zone the upper Pliocene, are not necessarily their extinctions. The continued occurrence of *Gephyrocapsa* spp. down to Section 114-704A-22X, CC, indicates the presence of NN15 or younger strata. Rare specimens of *Reticulofenestra pseudoumbilica* possibly restrict this sample to NN15, but these may be reworked.

A stratigraphic break may occur between Sections 114-704A-22X, CC, and 114-704A-23X, CC. This is reflected in the nannofossil flora by an abrupt change in the assemblages from those dominated by *Coccolithus pelagicus* to those dominated by *R. pseudoumbilica*.

Sections 114-704A-23X, CC, and 114-704A-24X, CC, are assigned to NN15–11 on the basis of the presence of *R. pseudoumbilica* in both samples and *Amaurolithus delicatus* in the lower sample. Below Section 114-704A-25X, CC, the strata are assigned to NN15–?7. The nannofossil floras are of low diversity and are dominated by *R. pseudoumbilica*, *Reticulofenestra perplexa*, and *C. pelagicus*.

Hole 704B

The core-catcher samples from Hole 704B were examined for nannofossils. The samples all contain abundant nannofossil floras that are assigned to the zones of Martini (1971) and Wise (1983).

Biostratigraphy

Sections 114-704B-1H, CC, to 114-704B-13H, CC, contain *P. lacunosa* and are assigned to NN19 (middle Pleistocene–upper Pliocene). Samples between Sections 114-704B-14H, CC, and 114-704B-16X, CC, additionally contain *H. sellii*, a species with a LAD within NN19. These samples are thus assigned to the lower part of NN19 (lower Pleistocene–upper Pliocene).

The very rare occurrence of *D. brouweri* and the presence of *C. macintyrei* in Section 114-704B-17X, CC, indicate the presence of NN18 or older strata. No older Pliocene zones were recognized in the interval between Sections 114-704B-17X, CC, to 114-704B-21X, CC, although comparisons with Hole 704A would suggest that they are probably present.

A stratigraphic break may occur between Sections 114-704B-21X, CC, and 114-704B-22X, CC. This is reflected in the nannofossil floras by an abrupt change from assemblages dominated by *C. pelagicus* to those dominated by *R. pseudoumbilica*.

Sections 114-704B-22X, CC, to 114-704B-24X, CC, are assigned to NN14–9 (lower Pliocene–middle Miocene) on the basis of the presence of *Amaurolithus triconiculatus* (NN14–11) in the highest sample and *D. pentaradiatus* in the lowest sample. The underlying samples between Sections 114-704B-25X, CC, and 114-704B-45X, CC, are assigned to NN14–?7. They contain abundant nannofossil floras of low diversity that lack age-diagnostic species. The dominance of these floras by *R. pseudoumbilica* and *R. perplexa*, together with their stratigraphic position, confirms this age assignment.

An abrupt change in the nannofossil flora between Sections 114-704B-45X, CC, and 114-704B-46X, CC, indicates a stratigraphic break. The co-occurrence of *Sphenolithus heteromorphus* and *C. macintyrei* in the latter section indicate assignment to NN5–4. The nannofossil floras from this interval are dominated by *Cyclicargolithus floridanus* and *C. pelagicus*.

Samples below the FAD of *C. macintyrei* are assigned to between NN4 and the *Cyclicargolithus abisectus* Zone, between Sections 114-704B-50X, CC, and 114-704B-63X, CC. No zonal index taxa are present, with the exception of *C. abisectus*. This species appears to range as high as NN5 in this area, or it is reworked. Whichever case, the top of the *C. abisectus* Zone, the top of which is defined by the LAD, cannot be accurately picked in Hole 704B. The *Reticulofenestra bisecta* Zone is recognized in Section 114-704B-64X, CC, by the occurrence of the nominate taxon. The top of the *Chiasmolitus altus* Zone is recognized in Section 114-704B-65X, CC, by the consistent and significant occurrence (1%–3% of nannofossil flora) of the nominate taxon. This zone is present down to the lowest sample examined, from Section 114-704B-72X, CC.

Paleoenvironment

The uppermost three cores of Hole 704A are characterized by abundant alternations of the different species dominating the nannofossil floras. These species are *Gephyrocapsa* spp., *Calcidiscus leptoporus*, and *C. pelagicus*. The environmental significance of these changes is unknown, but they probably reflect rapidly changing surface waters. The lower Pliocene to Miocene nannofossil floras are of low diversity and are dominated by placoliths. These assemblages are typical of cold-water, high-latitude areas.

Preservation

The nannofossil floras from the upper part of Hole 704B (above Core 114-704B-10H) consist of slightly etched coccoliths. Below this, they become increasingly overgrown with secondary calcite deposition.

Planktonic Foraminifers

Samples from Sections 114-704A-1H, CC, to 114-704A-25X, CC, and 114-704B-26X, CC, to 114-704B-72X, CC, were examined. Core recovery at Hole 704A below Core 114-704A-25X was poor and, therefore, samples from Hole 704B were studied, commencing with Core 114-704B-26X, which has a sub-bottom depth 2.5 m below that of Core 114-704A-26X.

Biostratigraphy

The sediment age ranges from Quaternary to early Oligocene, without any evidence of large unconformities. The low diversity during the Quaternary-Pliocene, the almost total absence of the marker species of both standard and Jenkins' (1985) zonations and of Kennett's (1973) zonation in the Southwest Pacific during the Miocene do not allow the application of any zonal scheme. Within the Oligocene the scheme of Berggren et al. (1985) has been tentatively applied.

The age of the examined samples is summarized as follows:

Hole 704A

1H, CC	Quaternary–late Pliocene
2H, CC, to 23X, CC	Quaternary-Pliocene
24X, CC, and 25X, CC	Quaternary–late Miocene
27X, CC	Miocene

Hole 704B

26X, CC	Quaternary–late Miocene
28X, CC, to 31X, CC	late Miocene
32X, CC, to 40X, CC	early late Miocene–middle Miocene
41X, CC, to 51X, CC	middle Miocene–early Miocene
52X, CC, to 56X, CC	early Miocene
57X, CC, to 62X-2, 90–92 cm	early Miocene–late Oligocene (N4–P21b)
62X-3, 90–92 cm, to 69X, CC	late Oligocene (P21b)
70X, CC, to 72X-3, 20–22 cm	early Oligocene (P21a–20)
72X, CC	early Oligocene (?P19–20)

The Pliocene/Miocene boundary can be defined on the basis of planktonic foraminifers because the assemblages of Sections 114-704A-24X, CC, 114-704A-25X, CC, and 114-704B-26X, CC, contain only *Neogloboquadrina pachyderma*, which ranges from Quaternary to late Miocene in age.

The Miocene/Oligocene boundary is based on the FAD of *Globoquadrina dehiscens*. This event, however, is not very reliable due to the poor fossil preservation in this hole.

The late Oligocene/early Oligocene boundary is placed at the level of the LAD of chiloguembelinids.

In the Quaternary-upper Miocene stratigraphic interval, sinistral *N. pachyderma* is the most abundant foraminifer. It is associated with common to abundant specimens of the *Globorotalia crassaformis* group, *Globigerina quinqueloba*, *Globigerina bulloides*, *Globigerina umbilicata*, and *Globigerina uvula*. *Globigerina inflata* is present only in Section 114-704A-1H, CC. *Globorotalia scitula* is common in Section 114-704A-21X, CC. The planktonic foraminifer assemblage is almost monospecific in Sections 114-704A-23X, CC, to 114-704A-25X, CC, and 114-704B-26X, CC, represented only by *N. pachyderma*, although a few *G. crassaformis* appear in Section 114-704A-23X, CC. It is possible that sediments in Section 114-704B-26X, CC, were deposited below the foraminifer lysocline. *N. pachyderma* is absent below Sample 114-704B-26X, CC.

The subdivision of the Miocene stratigraphic interval into stages is difficult because the planktonic foraminifer ranges are completely unknown in this area. The upper Miocene interval is based on the presence of rare *Neogloboquadrina acostaensis*, the FAD of which is a standard event of the N16 lower boundary. This form is associated with *G. continuosa* and *Globorotalia panda*. These latter two forms, however, show a range from middle Miocene to early late Miocene in New Zealand and in the Southwest Pacific. Therefore, a hiatus may be present in the upper Miocene. Sample 114-704B-28X, CC, contains abundant reworked early Miocene age fossils, such as *Catapsydrax dissimilis* and *Globorotalia zealandica*, without excluding middle Miocene reworked fossils, such as *Globigerina druryi*.

The early late Miocene–middle Miocene age is based on the absence of *N. acostaensis* and the presence of *G. continuosa* and *G. panda*, which are associated with *G. scitula*, *G. bulloides*, and *Globigerina juvenilis*. Because *N. acostaensis* was very rare in the overlying interval, it is not possible to exclude an early late Miocene age for this stratigraphic interval.

The middle Miocene-lower Miocene stratigraphic interval is characterized by the abundance of *G. scitula*; *G. panda* does not occur below Section 114-704B-40X, CC. The assemblages of this age include *G. bulloides*, *Globigerina woodi woodi*, *G. woodi connecta*, and rare *Globorotalia miozea*.

The lower Miocene is well defined by the LAD of *C. dissimilis*, which is the second standard event in this hole and indicates the upper boundary of N5. *Globigerina brazieri*, *G. woodi woodi*, *G. woodi connecta*, *G. scitula*, and rare *G. dehiscens*, and *Globoquadrina praedehiscens*, and *Globorotalia acrostoma* are the planktonic foraminifers characteristic of this age. Some forms similar to *Globigerinoides trilobus* occur without secondary apertures.

Within the upper Oligocene, the upper boundary of the P21b Zone is placed at the last occurrence of *Globorotalia opima opima*, but the range of this marker species could be shorter at high latitude.

Paleoenvironment

From the Quaternary to the early Oligocene, deposition was above foraminiferal lysocline but appears to have oscillated close to it during some stratigraphic intervals, such as the lower Pliocene and upper Oligocene.

The lack of the *Globigerinoides* lineage during the whole Neogene is a characteristic feature of this area that can be linked to the low temperature of the surface water. The abundance of *Globorotalia*, although the species diversity is low, in the different stratigraphic intervals is confusing because the *Globorotalia* are generally considered subtropical-temperate species (Kennett and Srinivasan, 1983).

Figure 13 is a preliminary relative abundance diagram of angular or slightly keeled *Globorotalia* vs. planktonic foraminifers and of planktonic foraminifers vs. radiolarians and large diatoms. This diagram has been correlated with the percent $CaCO_3$ curve. It appears that within the late Oligocene a strong decrease of planktonic foraminifers (*Globorotalia* are absent dur-

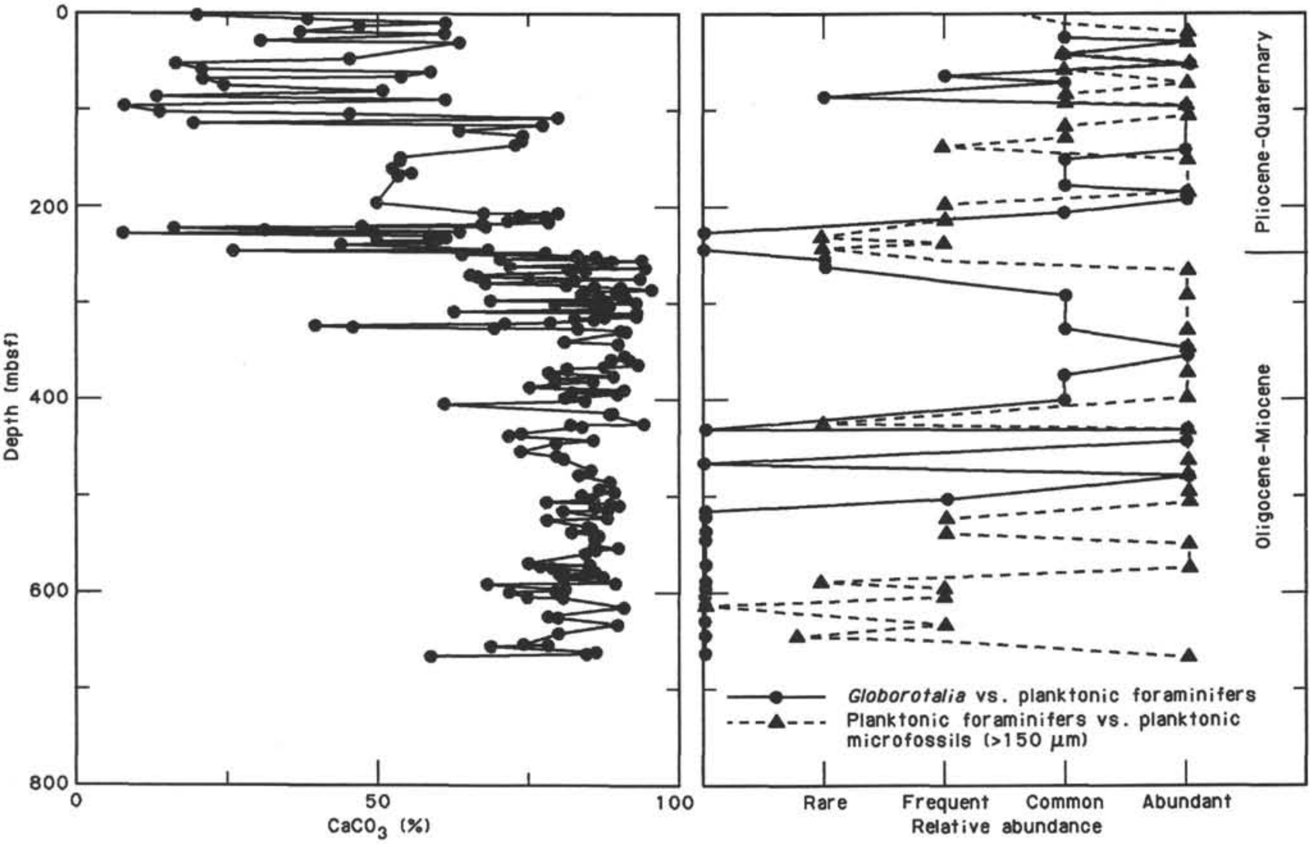

Figure 13. Relative abundances of *Globorotalia* vs. planktonic foraminifers and planktonic foraminifers vs. planktonic microfossils (>150 µm).

ing the Oligocene) did not influence the CaCO$_3$ content in the sediments. The depth of deposition may have been such that dissolution could destroy foraminifers tests but not those of calcareous nannoplankton. During the Miocene the *Globorotalia* fluctuations follow the planktonic foraminifers fluctuations, irrelative of the CaCO$_3$ variations. Close to the Pliocene/Quaternary boundary, *Globorotalia*, planktonic foraminifers, and CaCO$_3$ show a strong decrease that is probably the result of a carbonate dissolution episode. Within the late Pliocene-Quaternary the abundance of *Globorotalia* fluctuations seems to be linked more to CaCO$_3$ fluctuations than to the total planktonic abundance.

Preservation

Planktonic foraminifers are generally abundant in every stratigraphic interval, and they are associated with radiolarians and diatoms. Their preservation is good down to Section 114-704A-5H, CC, moderate from Sections 114-704A-6H, CC, to 114-704B-53X, CC, with recrystallized tests, and very poor from Sections 114-704B-54X, CC, to 114-704B-72X, CC, with some intervals of almost complete dissolution (Sections 114-704B-66X, CC, to 114-704B-69X, CC).

Benthic Foraminifers

Core-catcher samples from Holes 704A (Cores 114-704A-1H to 114-704A-30X) and 704B (Cores 114-704B-30X to 114-704B-72X) yielded generally well-preserved, moderately diverse benthic foraminifer assemblages. Preservation is deteriorated below Section 114-704B-65X, CC. Core-catcher samples were barren in Cores 114-704B-63X and 114-704B-66X. The species composition of the benthic foraminifer fauna remained fairly consistent, with few significant changes observed within the section recovered at Site 704. The most notable occurrence is the range of *Planulina wuellerstorfi* in samples from Sections 114-704B-48X, CC, to 114-704A-7H, CC. *P. wuellerstorfi* is a cosmopolitan, deep-water taxon that ranges in other localities worldwide from the middle Miocene (N9) through the Pleistocene (N23).

The benthic foraminifer fauna at Site 704 is dominated by *Cibicidoides mundulus*, *Cibicidoides cicatricosus*, *P. wuellerstorfi*, *Globocassidulina subglobosa*, *Gyroidinoides* spp., *Laticarinina pauperata*, *Melonis barleeanus*, *Melonis pompilioides*, *Oridorsalis* spp., *Pullenia bulloides*, *Pullenia eocaenica*, *Pullenia quinqueloba*, and *Stilostomella* spp. Other common species include *Astrononion pusillum*, *Cassidulina crassa*, *Cibicidoides bradyi*, *Cibicidoides robertsonianus*, *Ehrenbergina gibbera*, *Eggerella bradyi*, *Karreriella subglabra*, *Martinottiella* sp., *Nonion* sp., *Nuttallides umbonifera*, miliolids, *Uvigerina peregrina*, and *Uvigerina* sp.

There is some evidence of reworking at Site 704. Section 114-704A-12X, CC, contains common shallow-water *Hanzawaia* sp. Section 114-704A-23X, CC, contains several older, reworked specimens, including *Cibicidoides eocaenus* (Eocene to Oligocene) and *Nuttallides truempyi* (Campanian to Eocene). Sections 114-704A-30X, CC, and 114-704B-30X, CC, include several specimens of the older form *C. eocaenus*.

The benthic foraminifer faunas indicate a lower bathyal to abyssal paleodepth (>1000 m) at Site 704 for the section recovered (based on van Morkhoven et al., 1986).

Diatoms

At Site 704, which is in a basinlike structure on the Meteor Rise, two holes were drilled to recover a 585-m-thick Neogene sequence overlying 87 m of upper Oligocene sediments.

Diatoms are abundant and well preserved throughout most of the recovered section except for two intervals, where their abundance is reduced and preservation is relatively poor. One interval covers the lower to lower middle Miocene, and the other falls in the upper Miocene (Fig. 16).

Most Southern Ocean marker species are present in Site 704 Oligocene and Neogene sediments. The absence or rarity of some index species (e.g., *Nitzschia denticuloides*, *Denticulopsis hyalina*, and *Denticulopsis lauta*) is a result of the principal portion of their ranges missing because of erosion or nondeposition. The additional occurrence of lower latitude index species will provide extra stratigraphic resolution and a means of correlating high- and low-latitude zonal schemes.

Using the most probable paleomagnetic interpretation, some of the late Neogene stratigraphic marker species, which were more consistently present at this site, showed a later FAD than reported for the subantarctic region by former workers (e.g., FAD *Nitzschia weaveri*) or a LAD later than at other subantarctic sites (e.g., *Nitzschia interfrigidaria*). In single cases reworking might not have been recognized as such because the reworked material is of just slightly older age. But, in general, the shift of the LADs as well as FADs in sediments of late Pliocene and Quaternary to younger age means that these datums are diachronous toward the northern margin of the subantarctic zone. For this reason some of the middle Miocene to Quaternary diatom zones identified for Holes 704A and 704B and listed below are not time equivalent with those established at sites fully under the subantarctic influence.

The following zones were identified:

Zone	Hole 704A	Depth (mbsf)
Coscinodiscus lentiginosus	1H-1, 2 cm, to 2H-5, 120 cm, and CC	0.02–14.4
Coscinodiscus elliptipora–Actinocyclus ingens	2H-6, 120 cm, to 11H-4, 70 cm	15.9–97.9
Rhizosolenia barboi–Nitzschia kerguelensis	11H-4, 80 cm, to 11H-6, 35 cm	98.0–100.45
Coscinodiscus kolbei–R. barboi to N. weaveri	11H-6, 80 cm, to 16H-2, 80 cm	101.00–142.5
N. interfrigidaria–Coscinodiscus vulnificus	16H-4, 70 cm, to 18H, CC	145.50–168.7
Hiatus—~2.8 or 2.9 to 2.5 Ma		~171–169
N. interfrigidaria	18H, CC, 19H, CC	168.70–178.20
Nitzschia praeinterfrigidaria	20H-2, 70 cm, 21H-4, 5 cm	180.40–192.25
Nitzschia angulata	20H, CC, to 21X-3, 82 cm	187.70–191.52
Nitzschia reinholdii	21X-4, 5 cm, to 23X, CC	192.25–216.20
Denticulopsis hustedtii	24X, CC, to 30X, CC	225.70–282.70
	Hole 704B	
C. lentiginosus	1H-1, 24 cm, to 3H, CC	0.2–25.70
C. elliptipora–A. ingens	4H-2, 95 cm, to 11H, CC	28.15–101.70
R. barboi–N. kerguelensis	12H, CC	111.20
C. kolbei–R. barboi	13H-2, 125 cm, to 17H-2, 100 cm	113.95–149.70
C. vulnificus to *N. interfrigidaria–C. vulnificus*	17H, CC, to 19H-1, 21 cm	156.70–166.41
Hiatus—~2.8 or 2.9 to 2.5 Ma		~160–165
N. interfrigidaria	19H-1, 75 cm, to 19H, CC	166.95–175.70
N. angulata	22X, CC, to 23X-2, 70 cm	185.20–204.20
N. reinholdii	23X-2, 70 cm, to 23X, CC	213.70–206.40
D. hustedtii	24X, CC, to 26X, CC	223.20–242.20
?	27X, CC, to 32X, CC	252.70–299.20
D. hustedtii	24X, CC, to 31X-5, 82 cm	223.20–287.02
Zone	Hole 704A	Depth (mbsf)
Hiatus—Maximum duration = ~2.5 m.y. (~8.5–6.5 Ma)		~287–308
D. hustedtii–D. lauta	33X, CC, to 46X-2, 82 cm	308.70–425.02
Hiatus—Maximum duration = ~6.0 m.y. (~9.0–~15.0 Ma)		~425.02–432.20
lower *Coscinodiscus lewisianus*	47X-5, 79 cm, to 48X-1, 79 cm	438.99–442.49
Coscinodiscus rhombicus	52X, CC, to 55X-1, 40 cm	481.70–501.10
Rocella gelida	56X-1, 85 cm, to 65X, CC	511.05–605.20
Rocella vigilans	66X, CC, to 72X, CC	614.70–671.70

Within the Quaternary the LAD of *Rouxia* spp. occurs in Section 114-704A-1H, CC. The rarity of species of the genus *Rouxia* at this site prevents this occurrence from providing a reliable datum. *Hemidiscus karstenii* has its last abundant occurrence at approximately 3 m core depth (Sample 114-704B-1H-2, 150 cm).

Three possible hiatuses can be identified (Fig. 12). The youngest of these occurs in the upper Pliocene and may represent an interval of the late Gauss Chron between 2.9 or 2.8 Ma and ~2.5 Ma. A second hiatus occurs in the upper Miocene and probably represents a 2.0- to 2.5-m.y. period between ~8.5 and 6.5 Ma. The third hiatus encompasses most of the middle Miocene and lowermost upper Miocene, between ~15.0 and 9.0 to 10.0 Ma. An additional hiatus may occur in the Oligocene section; however, biostratigraphic resolution of this interval is currently inadequate to make such a determination.

Reworked diatoms are abundant in the Quaternary and common in the late Quaternary sediments (the first four cores in both holes). In Pliocene and middle Miocene sediments, only sporadic single, reworked diatom valves were encountered (e.g., Sections 114-704B-13X, CC, 114-704B-22X, CC, 114-704B-48X, CC, and 114-704B-49X, CC).

Radiolarians

Most core-catcher samples from Site 704 generally yielded common to abundant and moderately well-preserved radiolarians. From the biostratigraphic zonations of Hays and Opdyke (1967) and Chen (1975) from the antarctic and Weaver (1983) from the subantarctic regions, the following zones were recognized:

Hole 704A

1H, CC, to 13H, CC	*Stylatractus universus* and the remaining Quaternary section (0.49–1.9 Ma)
14H, CC, to 16H, CC	*Eucyrtidium calvertense* (late Pliocene: 1.7–2.47 Ma: Φ Zone, Matuyama, Chron C2N–C2R)
17X, CC, to 25X, CC	*Helotholus vema* (early Pliocene: 2.47–5.10 Ma; α and τ Zone; Gauss-Gilbert, Chron C2AN–C3R)
26X, CC, to 28X, CC	No sample
29X, CC, to 30X, CC	Unzoned (late Miocene)

Hole 704B

25X, CC, to 30X, CC	*H. vema* (early Pliocene: 2.47–5.10 Ma; α and τ Zone; Gauss-Gilbert, Chron C2AN–C3R) to late Miocene

31X, CC, to 34X, CC	Undetermined
35X, CC, to 38X, CC	Unzoned (coeval to the low-latitude *Didymocyrtis antepenultima* Zone; late Miocene)
39X, CC, to 58X, CC	Unzoned (middle–early Miocene)
9X, CC, to 72H, CC	Unzoned (late–early Oligocene)

Section 114-704A-1H, CC, is identified as belonging to *S. universus* Zone; therefore, the modern *Antarctissa denticulata* Zone is likely within Core 114-704A-1H. However, the absence of *Saturnalis circularis* in the Quaternary section prevents definition of the base of the *S. universus* Zone and the underlying *S. circularis* Zone.

The overlying *H. vema* Zone of both Holes 704A and 704B can also be assigned to Weaver's (1983) *Stichocorys peregrina* Zone by the occurrence of the named species.

A part of upper Miocene unzoned interval was considered as correlative to the low-latitude *Didymocyrtis antepenultima* Zone because of the occurrence of *Diartus hughesi* in the Site 704 samples. This species has the same geological range as *D. antepenultima* (Sanfilippo et al., 1985).

For the unzoned middle to lower Miocene section, neither the antarctic zonal schemes of Hays and Opdyke (1967) and Chen (1975) nor the low-latitude zonation of Sanfilippo et al. (1985) is generally applicable to Site 704 sediments, apparently because of temperate depositional conditions.

Furthermore, as already indicated at previous sites, no zonation has ever been proposed for the Paleogene section from the high- to midlatitude South Atlantic region.

We attempted to evaluate the synchronology of radiolarian events between western and eastern subantarctic regions. Some of the biostratigraphically important datums calibrated against paleomagnetic data presented by Weaver (1983) from DSDP Leg 71 are listed with those observed from Site 704. Tm refers to the top (last), or youngest, geological occurrence; Bm is for the basal (initial), or oldest, occurrence.

Tm *Triceraspyris coronata*	114-704A-24X, CC ~4.25 Ma; just below Nunivak Subchron
Tm *Amphymenium challengerae*	114-704A-25X, CC, and 114-704B-25X, CC 4.35–4.45 Ma; above or within the Sidufjall Subchron
Tm *Stichocorys peregrina*	114-704A-25X, CC, and 114-704B-25X, CC 4.6-4.4 Ma; within the lower Gilbert Chron
Tm *Lamprocyclas aegles* group	114-704A-29X, CC, and 114-704B-27X, CC 5.5 Ma
Bm *L. aegles* group	114-704B-29X, CC 6.0–5.8 Ma
Bm *S. peregrina*	114-704B-30X, CC ~6.3 Ma
Tm *Diartus hughesi*	114-704B-35X, CC ~8.6 Ma
Tm *Cyrtocapsella japonica*	114-704B-44X, CC 8.7–9.1 Ma

To this list, a new biostratigraphic datum of the basal appearance of *Cyrtocapsella tetrapera* can be added for the region. In many parts of the world, this datum signals the base of Miocene Epoch.

Silicoflagellates

Although silicoflagellate specimens were moderately well preserved, their occurrence was sporadic in core-catcher samples from Site 704. Utilizing the biostratigraphic zonations of Ciesielski (1975) and Shaw and Ciesielski (1983), silicoflagellate-bearing sediments were assigned as follows:

Hole 704A

1H, CC, to 16H, CC	Unzoned (Quaternary–late Pliocene)
17X, CC to 25X, CC	*Distephanus boliviensis* (early Pliocene)

Hole 704B

25X, CC	*D. boliviensis* (early Pliocene)
34X, CC, to 36X, CC	*Mesocena circulus/Mesocena diodon* (late Miocene)
37X, CC, to 52X, CC	Undetermined
53X, CC, to 55X, CC	*Corbisema triacantha* (early Miocene)
58X, CC	*Naviculopsis robusta* (early Miocene)
59X, CC, to 62X, CC	*Naviculopsis biapiculata* (early Miocene)
63X, CC, to 65X, CC	Undetermined
66X, CC, to 67X, CC	*Corbisema archangelskiana* (late Oligocene)
68X, CC	*"Naviculopsis constricta/C. archangelskiana"*
69X, CC, to 70X, CC	*"N. constricta/Dictyocha deflandrei"*

Regarding the last two zones, which have names in quotation marks, their assignment is provisional at present because of the complete absence of an index species, *Dictyocha deflandrei*, in the examined sediments.

Ebridians

Aside from the rare occurrence of *Ammodochium rectangulare* in numerous samples, the only ebridian species observed in core-catcher samples of Site 704 is *Ebriopsis antiqua antiqua*, occurring consistently in the lower Pliocene section from Sections 114-704A-17X, CC, through 114-704A-25X, CC.

Paleoenvironment

The presence of *Cyrtocapsella tetrapera* (radiolarian) in most of sediments of early to middle Miocene age suggests a warm-water environment during deposition. Similar conditions seem to have persisted during the late Miocene, as evidenced by the presence of *Didymocyrtis didymus*, a temperate counterpart of tropical *Didymocyrtis antepenultima* (radiolarian), and more warmer to near-tropical conditions are suggested by the occurrence of the tropical *Stichocorys peregrina* (radiolarian) in the lower Pliocene. From that time to the present, a general cooling trend has continued.

An attempt was made to interpret the Quaternary paleoceanographic depositional environment by means of the *Dictyocha/Distephanus* ratio based on the modern distributional pattern of *Dictyocha* (limited to the warm water), and *Distephanus* (exclusively in a colder environment).

Core catcher from section	1	2	3	4	5	6	7	8–13
depth (mbsl)	16.7	26.2	36.7	45.2	54.7	64.2	73.7	83.2–121.2
ratio (%)	6	6	0	0	0	0	35	0

The only distinguished warmer conditions (probably a result of the southward migration of the polar front) other than those from the present time throughout the Quaternary at Site 704 were during the deposition of Section 114-704A-7H, CC, at about 64 mbsf.

GEOCHEMISTRY

Pore-water samples were collected from nine intervals in Hole 704A (0–232 mbsf) and 15 intervals in Hole 704B (249–665 mbsf). Pore-water chemistry at this site reflects alteration reactions with volcanic silicic ash present in the upper sediment column and most likely present below the recovered section. Unit I (0–451.2 mbsf) consists of middle Miocene to upper Pleistocene biogenic oozes dominated by alternating siliceous-rich (diatomaceous) and calcareous-rich (nannofossils and foraminifers) intervals. Disseminated ash is observed throughout Unit I and is common in the upper 40 m, whereas discrete ash-bearing horizons occur at about 80, 174, 220, 254, 265 and 542 mbsf (see "Lithostratigraphy" section, this chapter). Below about 178 mbsf, the abundance of both the siliceous-rich intervals and diatoms in the calcareous oozes decrease abruptly. This lower interval is predominantly nannofossil ooze with scattered carbonate-poor diatom-bearing intervals.

Unit II (451.2-671.7 mbsf) consists of a lower Oligocene to middle Miocene micritic nannofossil chalk that is indurated below 491.2 mbsf. Pore-water chemistry reflects carbonate recrystallization reactions within this deeper sediment column, and there is some evidence for microbial sulfate reduction. There is no evidence from pore-water chemistry for formation of diagenetic silica phases. No zeolites were observed, and the section contains no chert.

Headspace samples were also analyzed for volatile hydrocarbons in both Holes 704A and 704B.

Sediment organic carbon was determined at irregular intervals throughout Hole 704A (0-234 mbsf). Sediment carbonate contents were determined at closely spaced intervals (3 to 5 per section) throughout Hole 704A and in those intervals of Hole 704B where core disturbance was thought to be severe in Hole 704A (16 to 35 mbsf) and where we needed a high-resolution stratigraphic interval at the bottom of both holes (below 215 mbsf).

Interstitial-Water Chemistry

Pore waters were squeezed from either 5- or 10-cm^3 whole-round samples taken at about 30-m intervals. Squeezers were maintained in a refrigerator at near-bottom-water temperatures (0°-2.2°C) in order to duplicate the observations at Site 702. Samples to be squeezed were placed immediately into these refrigerated squeezers and the water expressed through a 0.4-μm filter into a syringe. The same filter and syringe were used for all of our investigations at Site 704 in an attempt to minimize, characterize, and identify potential contamination artifacts in the planned shore-based determinations. About 20 drops (1 mL) of pore solution was expressed through each filter step (to waste) to minimize carry-over dilution by adjacent samples.

Measurement of the final temperature of the squeezer outlet port at the end of each squeeze confirmed that the temperature rise was less than 2°C over the 10-15-min squeezing period. The pore water was then postfiltered again from the syringe into sample vials, using the same filter (0.4 μm) throughout the procedure, again filtering 20 drops to waste. Vials containing samples with noticeable hydrogen sulfide were left uncapped until the H_2S odor had disappeared, but no attempt was made to actively purge the gas from solution. Based on the intensity of the odor, the sulfide levels in these interstitial fluids probably did not exceed 100 μmol/L, so the potential error in the sulfate data due to H_2S reoxidation artifacts is negligible (0.1 mmol/L compared to 29 mmol/L).

The results of the pore-water chemistry are reported in Table 4 and presented in Figure 14.

Salinity and Chloride

Salinity and chloride values at the top of the sediment column reflect the salinity of the overlying bottom water. Salinities and chloride values increase slightly to a maximum at about 50 mbsf, from which depth they decrease again with depth. This cyclic, small-amplitude, downward-damped salinity signal is due probably to downward diffusion of glacial-interglacial fluctuations in oceanic salinity into the sediment column from the sediment/water interface (McDuff, 1985). Other pore-water constituents displaying maxima at about 50 mbsf (Ca^{2+}, Mg^{2+}, and SO_4^{2-}) are due to this salinity maximum. These ion/Cl^- ratios are virtually constant in the upper 50 m (conservative behavior).

Calcium and Magnesium

Calcium concentrations increase in the upper 25 m from bottom-water values (10.6 mmol/L) to about 11.4 mmol/L, and then remain remarkably constant between 25 and 138 mbsf at concentrations of 11.5 mmol/L ± 0.1 mmol/L (Fig. 14). Below 138 mbsf, calcium concentrations begin increasing smoothly but nonlinearly, reaching concentration levels of about 27 mmol/L, almost three times that of seawater in the bottommost sample (665 mbsf). Magnesium concentrations likewise increase slightly down to 25 mbsf, and then remain fairly constant at concentrations within 5% of seawater until a depth of 80 mbsf. Below this level, magnesium concentrations decrease rapidly, reaching concentrations of 15 mmol/L at the bottom of the hole (665 mbsf). The $\Delta Mg/\Delta Ca$ ratio decreases slightly in the upper 138 m, from where it decreases sharply to the bottom of the hole, reaching minimum values of about 0.6.

A plot of calcium vs. magnesium demonstrates that the relative changes are not linear, particularly in the upper 200 m (Mg > 37 mmol/L; Fig. 15). Above 200 m, the slope of the line is less (more negative) than -2. Below 200 mbsf, the $\Delta Mg/\Delta Ca$ relationship is fairly linear (ignoring the bottommost points), with a slope of about -1.9. These values are diagnostic of alteration with silicic volcanic material (Gieskes and Lawrence, 1981; Gieskes, 1983; Baker, 1986).

The nonlinear shapes of these vertical calcium and magnesium profiles require reactions within the sediment column. The nonconservative nature of the $\Delta Mg/\Delta Ca$ plot and the high slopes suggest that the magnesium and calcium profiles are controlled by alteration of dispersed silicic ash within the upper several hundred meters of the sediment column, below which the $\Delta Mg/\Delta Ca$ plot is nearly linear. These downward-diffusion profiles may be controlled by reaction with nonbasaltic basement, or, more likely, with silicic volcanic ash horizons buried below the depth of recovery.

Alkalinity

Alkalinity at the top of the hole is about 3.1 mmol/L, above bottom-water concentrations (about 2.6 mmol/L). Alkalinity increases downhole to a maximum value of about 4.4 mmol/L ± 0.3 mmol/L between 150 and 400 mbsf. Below 400 mbsf, alkalinity decreases erratically downhole to minimum values of about 2.0 mmol/L at the bottom of the hole (665 mbsf). Values of pH decrease erratically from about 7.7 at the top of the hole to about 7.4 below 400 mbsf.

These profiles are consistent with regeneration of organic matter and dissolution of carbonates in the upper 150 m of the sediment column. Below about 350 m, the downward-decreasing alkalinities suggest carbonate precipitation/recrystallization reactions, consistent with the presence of micritic calcite below 450 mbsf.

Fluoride, Silica, and Sulfate

Fluoride concentrations at the top of the hole are identical to seawater values (70 μmol/L) and decrease slightly downhole to 80 mbsf, with a minimum value of 63 μmol/L at 50 mbsf. From 80 mbsf, fluoride increases dramatically downhole to maximum values of about 180 μmol/L in the interval between 305 and 364 mbsf, below which it decreases again to minimum values of 97 μmol/L at 556 mbsf. Below this, fluoride increases again to about 147 μmol/L in the bottommost sample (665 mbsf). As discussed in the "Geochemistry" section in the "Site 702" chapter, this volume, this profile is probably not the result of temperature-of-squeezing artifacts. The shape of the fluoride profile requires the following interpretations:

Table 4. Interstitial-water chemistry data from Holes 704A and 704B.

Sample (cm)	Depth (mbsf)	Volume (mL)	pH	Alkalinity (mmol/L)	Salinity (g/kg)	Magnesium (mmol/L)	Calcium (mmol/L)	Chloride (mmol/L)	Sulfate (mmol/L)	Fluoride (mmol/L)	Silica (mmol/L)	Mg/Ca (mmol/L)
Hole 704A:												
1H-4, 145-150	5.95	48	7.75	3.14	34.5	54.82	10.63	567.00	28.42	70.20	840	5.16
3H-5, 145-150	24.15	49	7.70	3.46	34.9	56.15	11.38	582.00	30.02	72.20	1009	4.83
6H-3, 145-150	49.65	48	7.64	3.90	35.2	55.95	11.58	583.00	29.94	62.80		4.83
9H-4, 145-150	79.65	51	7.66	4.05	34.9	55.19	11.46	582.00	29.31	64.10		4.82
12H-5, 145-150	109.65	39	7.59	3.99	35.0	52.90	11.35	576.00	28.05	68.30	963	4.66
15H-5, 145-150	138.15	46	7.57	4.30	34.8	49.66	12.11	573.00	26.80	78.20	1096	4.10
18X-4, 145-150	165.15	39	7.41	4.37	34.8	45.72	13.73	569.00	24.95	98.10	1080	3.33
21X-3, 145-150	192.15	25	7.49	4.20	34.5	41.30	15.11	567.00	23.12	112.70	1037	2.73
25X-4, 145-150	231.60	72	7.58	3.97	34.4	36.43	16.94	566.00	21.19	127.50	1092	2.15
Hole 704B:												
27X-5, 145-150	249.60	53	7.57	4.16	34.4	35.68	17.46	569.00	20.55	137.60	1073	2.04
30X-2, 145-150	273.60	52	7.54	4.23	34.4	33.20	18.98	569.00	19.21	158.10	1064	2.04
33X-4, 145-150	305.10	39	7.48	4.70	34.1	29.93	20.26	563.00	18.57	179.60	1154	1.48
36X-2, 145-150	330.60	50	7.41	4.38	34.0	28.77	21.11	575.00	18.35	182.50	1189	1.36
39X-5, 145-150	363.60	33	7.41	4.34	34.0	27.27	21.97	565.00	17.25	178.90	1217	1.24
42X-5, 97-107	391.67	45	7.29	4.53	34.0	25.68	22.76	565.00	17.31	161.90	1249	1.13
46X-4, 140-150	428.60	23	7.36	3.37	34.0	25.06	22.59	566.00	17.19	131.10	1164	1.11
48X-2, 140-150	444.60	20	7.35	3.23	34.0	24.26	23.31	566.00	16.35	123.00	1117	1.04
52X-4, 140-150	478.10	26	7.36	3.90	34.1	22.84	24.25	567.00	15.71	113.60	1260	0.94
54X-5, 140-150	498.60	28	7.41	3.43	34.0	23.37	24.02	566.00	16.66	108.30	1216	0.97
58X-5, 140-150	536.60	12	7.46	3.35	34.1	23.28	24.33	563.00	16.63	98.90	1133	0.96
60X-5, 140-150	555.60	23	7.44	3.50	33.9	19.67	25.47	571.00	15.51	96.90	1139	0.77
63X-4, 140-150	582.60	20	7.36	2.54	34.0	20.45	25.81	571.00	15.15	110.50	1134	0.79
70X-1, 140-150	644.60	12	7.42	2.89	33.9	15.91	27.13	566.00	13.48	124.50	1240	0.59
72X-2, 140-150	665.10	12	7.48	1.91	33.6	15.26	26.83	564.00	13.70	146.60	1247	0.57

1. Fluoride production (dissolution of some fluoride-containing solid phase) is occurring in the intervals displaying fluoride maxima (305–364 mbsf and below 665 mbsf).

2. Fluoride consumption (precipitation of some solid phase incorporating fluoride) is occurring in the intervals displaying fluoride minima (50–305 mbsf and 400–665 mbsf).

3. Fluoride is diffusing down the gradients, away from the maxima toward the minima.

The simplest explanation for these inferred reactions that is consistent with the other data is carbonate recrystallization. Biogenic calcite contains about 200 ppm fluoride, apparently inadvertently incorporated during rapid growth of calcitic tests from seawater (Froelich et al., 1983). Upon near-equilibrium dissolution and reprecipitation, inorganic calcite apparently excludes fluoride, partitioning it into the interstitial solution. Thus, fluoride gradients may be sensitive indicators of contemporaneous carbonate recrystallization reactions in calcareous sediments. This interpretation would imply that the initial micritization of carbonate skeletons starts just below 300 mbsf at this site. The phases and reactions inferred to be consuming fluoride are less clear, but may involve either precipitation of finely disseminated carbonate fluorapatite or adsorption onto clays.

Dissolved silica concentrations at the top of the section are about 840 μmol/L, far above bottom-water concentrations. Silica concentrations increase slightly downhole to about 1100 to 1250 μmol/L. This profile is consistent with the ubiquitous presence of diatoms at this site and the absence of zeolites or chert (Fig. 16).

Sulfate concentrations at the top of the hole are near seawater values and increase slightly through the upper 50 m, from where they begin a downhole decrease to minimum values of about 13.5 mmol/L in the bottommost samples. Hydrogen sulfide was noticeable by its odor in the sediments and interstitial waters from core intervals between 24 and 110 mbsf, signifying the presence of sulfate reduction in the virtual absence of reactive iron, which would otherwise precipitate the free sulfide as FeS. The shape of the sulfate pore-water profile suggests that most of the sulfate reduction is occurring in the upper 200 m, consistent with the presence of horizons with significant organic carbon in the uppermost sediment column (Fig. 17). Organic carbon is effectively zero below about 150 mbsf (see the following).

Volatile Hydrocarbon Gases

Headspace analyses for volatile hydrocarbon gases in Holes 704A and 704B are tabulated in Table 5. The very low methane values reflect the presence of sulfate throughout the sediment and thus, the virtual absence of methanogenesis, except in microenvironments. The large increase in headspace methane at the bottom of the hole (below 600 mbsf) may reflect upward diffusion of biogenic methane from the sulfate reduction zone below the recovered section.

Sedimentary Organic and Inorganic Carbon

Over 750 carbonate determinations were completed aboard ship for Holes 704A and 704B to provide a first-order high-resolution stratigraphic basis for correlating the two holes and to ensure a good paleoceanographic record of the carbonate and opal fluctuations at this site for subsequent work. Calcium carbonate and organic carbon data for Hole 704A are tabulated in Table 6. Calcium carbonate data for Hole 704B are tabulated in Table 7. The percent organic carbon profile for Hole 704A is plotted in Figure 17. The percent calcium carbonate profile for Site 704 is plotted in Figure 18.

The organic carbon data in Hole 704A clearly display an indirect correlation with %$CaCO_3$ variations in the upper 140 m, below which the organic carbon content is indistinguishable from zero. The organic-rich intervals correspond to siliceous horizons (see "Lithostratigraphy" chapter). The depth interval in which hydrogen sulfide was detected (24 to 110 mbsf) corresponds to the depth interval with the highest organic carbon contents. This carbonate cyclicity presumably reflects climatically driven shifts from calcareous to opal-rich regimes, perhaps

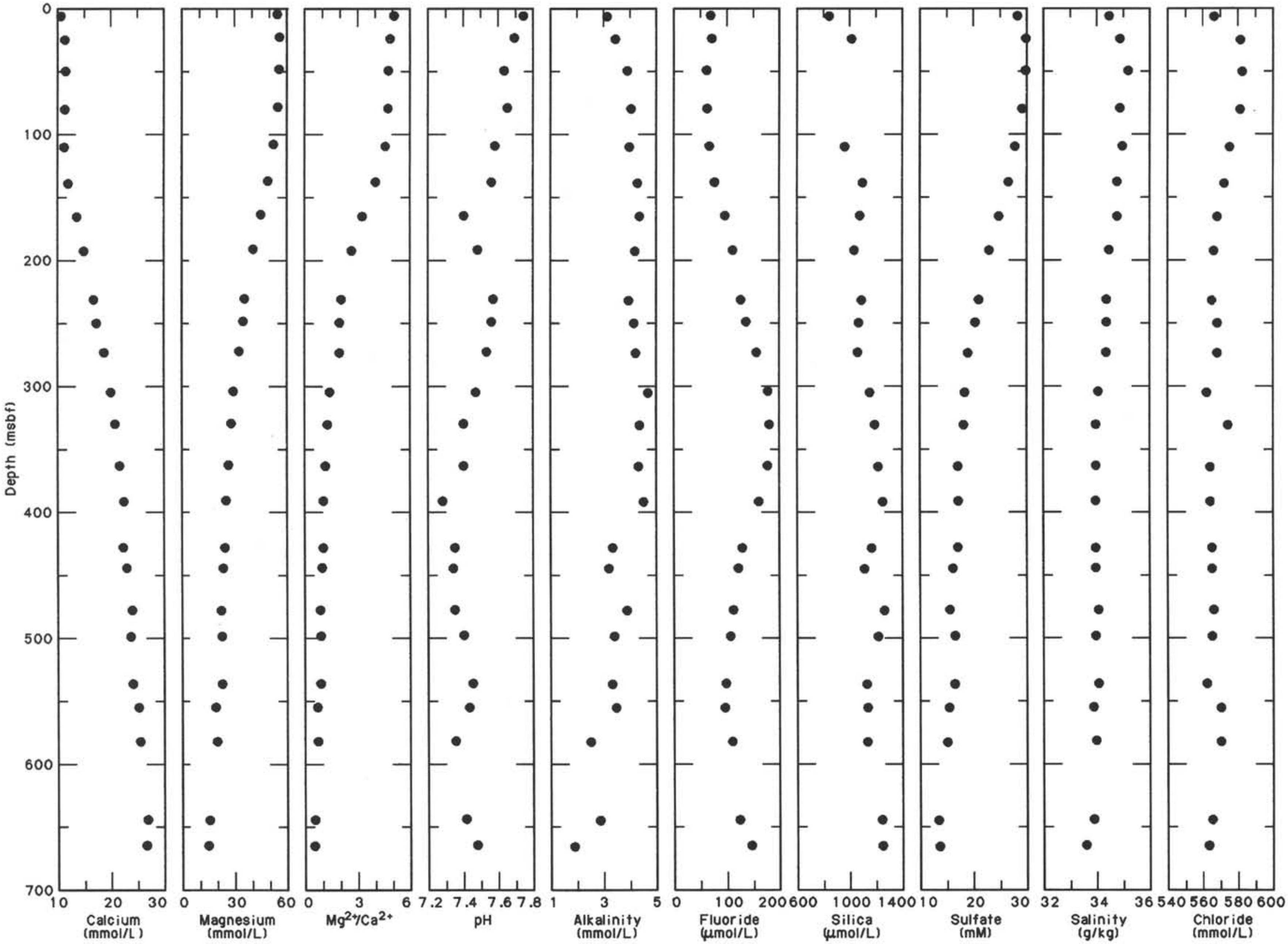

Figure 14. Pore-water calcium, magnesium, Mg/Ca ratio, pH, titration alkalinity, fluoride, dissolved silica, sulfate, salinity, and chloride profiles, Site 704.

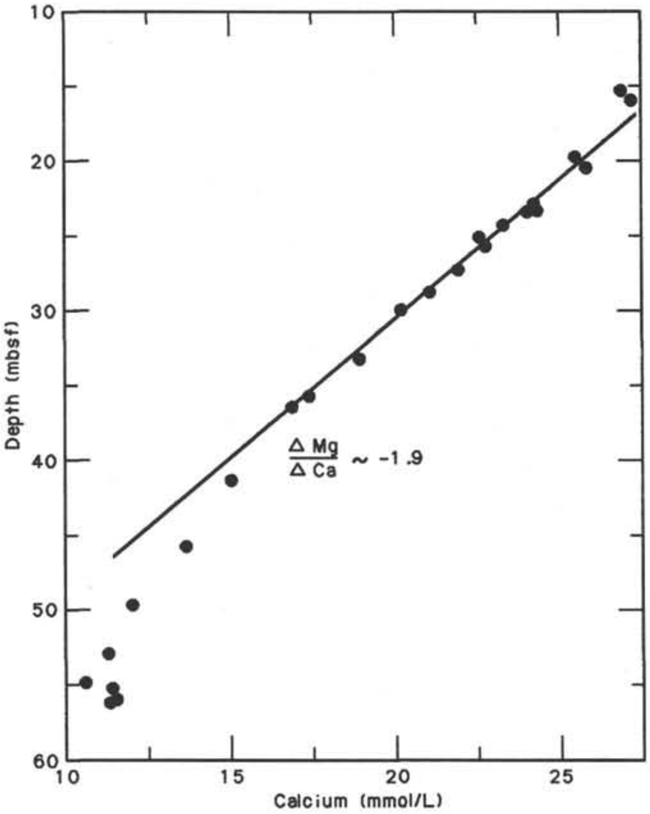

Figure 15. Pore-water calcium vs. magnesium in Holes 704A and 704B. The line through the data is an eyeball fit of the linear portion of the data trend below 200 mbsf. The Δ Mg/Δ Ca covariation over this depth interval is about -1.9, characteristic of diffusive exchange below the recovered interval with silicic volcanic ash alteration. The nonlinear portion of the curve shallower than 200 mbsf requires reaction within the sediment column in this depth interval, probably also by alteration of silicic volcanic ash.

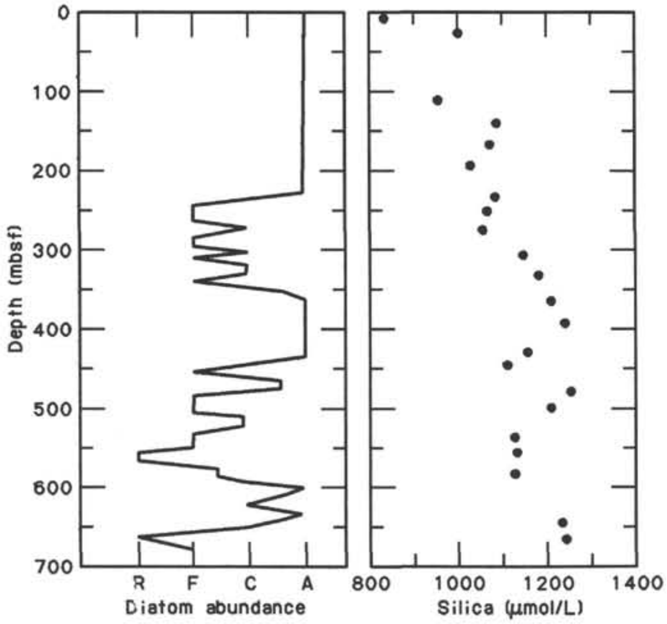

Figure 16. Abundance of diatoms and pore-water dissolved silica concentration profiles in Holes 704A and 704B (R = rare, F = few, C = common, A = abundant).

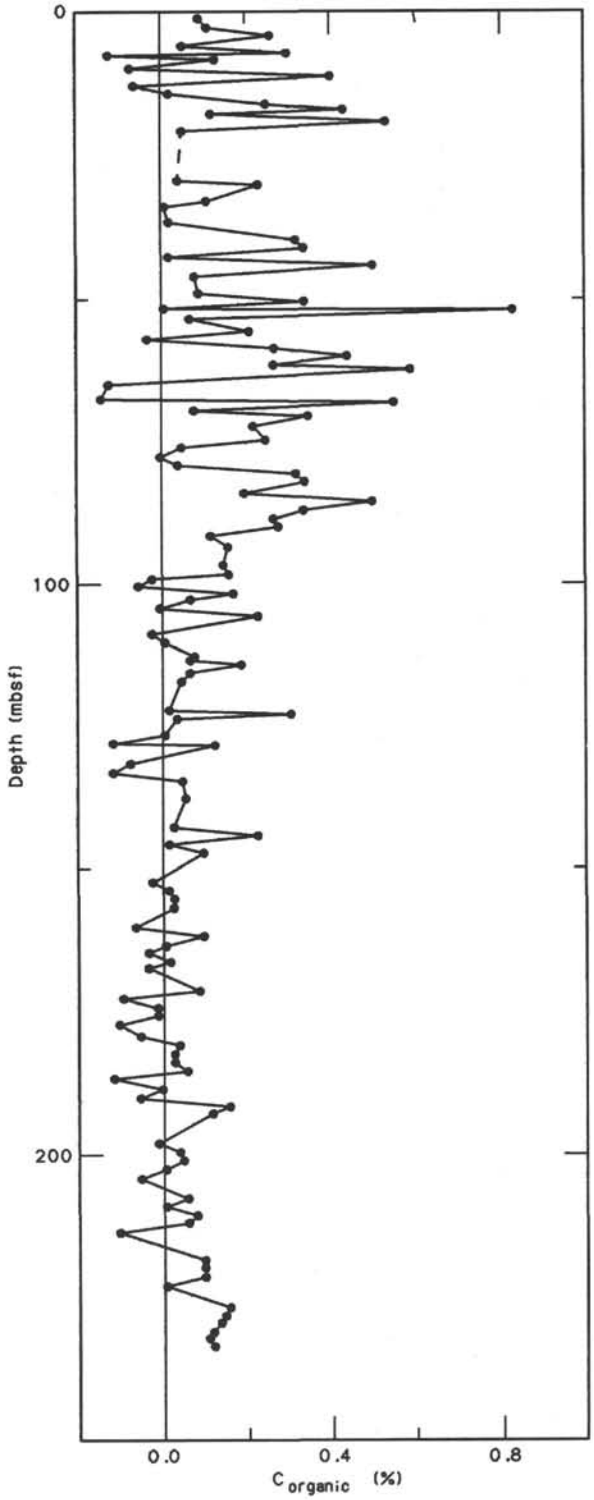

Figure 17. Percent organic carbon profile for Hole 704A. The values for organic carbon between -0.1% and +0.1% have no significance other than reflecting a statistical uncertainty in the data set of about ±0.1% C_{org} around 0.0% C_{org}.

Table 5. Volatile hydrocarbon gases (methane and ethane) from headspace analysis of Site 704 samples.

Sample (cm)	Depth (mbsf)	C_1 (ppm)	C_2 (ppm)
Hole 704A:			
1H-3, 0–5	3.00	1.7	0.0
2H-3, 0–5	10.20	1.9	0.0
3H-3, 0–5	19.70	3.4	0.0
4H-3, 0–5	29.20	0.5	0.0
6H-3, 0–5	48.20	2.7	0.0
7H-3, 0–5	57.70	2.7	0.0
8H-3, 0–5	67.20	0.7	0.0
9H-3, 0–5	76.70	3.6	0.8
11H-5, 0–5	98.70	6.3	0.0
12H-6, 0–5	109.70	6.9	2.5
13H-5, 0–5	117.70	9.0	0.0
14H-4, 145–150	127.15	9.1	0.0
15H-6, 0–5	138.20	10.1	1.2
16H-4, 0–5	144.70	7.8	0.0
17X-5, 0–5	155.70	11.4	0.8
18X-5, 0–5	165.20	12.7	0.6
19X-5, 0–5	174.70	13.0	0.0
20X-5, 0–5	184.20	11.1	0.5
21X-4, 0–5	192.20	13.8	1.4
22X-5, 0–5	203.20	14.1	0.0
23X-3, 0–5	209.70	6.9	0.0
24X-2, 121–126	218.91	6.2	0.0
25X-4, 0–5	230.20	9.6	0.0
Hole 704B:			
27X-6, 0–5	249.70	8.1	0.0
28X-3, 0–5	254.70	17.1	6.0
29X-3, 0–5	264.20	9.6	0.3
30X-3, 0–5	273.70	12.6	0.0
31X-3, 0–5	283.20	16.6	0.0
33X-5, 0–5	305.20	14.9	0.0
34X-3, 0–5	311.70	15.8	0.9
35X-5, 0–5	324.20	16.0	0.0
36X-3, 0–5	330.70	14.4	0.0
37X-3, 0–5	340.20	14.0	0.0
39X-6, 0–5	363.70	13.3	0.0
40X-5, 145–150	373.15	11.6	0.3
41X-5, 0–5	381.20	17.8	0.6
42X-5, 67–72	391.37	16.6	0.0
44X-2, 0–5	405.20	10.4	0.5
45X-2, 0–5	414.70	14.2	0.0
46X-5, 0–5	428.70	7.0	0.0
47X-4, 0–5	436.70	7.0	0.0
48X-3, 0–5	444.70	7.3	0.0
52X-5, 0–5	478.20	1.4	0.0
53X-3, 0–5	484.70	2.9	0.0
54X-6, 0–5	498.70	3.5	0.0
55X-5, 0–5	506.70	4.8	0.0
58X-6, 0–5	536.70	7.2	0.3
59X-2, 0–5	540.20	14.4	0.0
60X-6, 0–5	555.70	3.2	0.0
63X-5, 0–5	582.70	11.7	0.0
68X-2, 0–5	625.70	10.9	0.5
70X-2, 0–5	644.70	32.2	1.3
72X-3, 0–5	665.20	27.6	1.3

driven by changes in the location of the polar front over the Meteor Rise or in local carbonate dissolution.

PALEOMAGNETICS

Paleomagnetic study of sediments recovered at Site 704 included whole-core magnetic susceptibility determinations and measurements of the remanence of the archive halves of the cores using the cryogenic magnetometer. Both Holes 704A and 704B were cored using the APC and XCB systems. Sediments from the upper 140 m (Quaternary) of the section recovered at this site are characterized by high water content and were easily disturbed by normal handling procedures on deck. These sediments exhibited extremely low magnetization intensities. The magnetic susceptibility values from this interval are near the noise level of the susceptibility meter and are not considered in this report. Below 140 mbsf, relatively undisturbed cores and nearly continuous core recovery allow the recognition of magnetic polarity zones. However, the magnetizations remain near the instrument noise level, and below 330 mbsf, intervals exist that are difficult to interpret in terms of a polarity zonation.

Magnetic Susceptibility

The variation of magnetic susceptibility with depth in Hole 704B is shown with the boundaries of the major lithostratigraphic units ("Lithostratigraphy" section) indicated in Figure 19. The susceptibility variations are marked by what appear to be cyclic changes with depth. The amplitudes of the variations range up to 2.5–5.0 ($\times 4\pi$ SI), and the wavelengths vary from about 1.5 to 5 m. No notable changes in the susceptibility record are observed across lithostratigraphic unit boundaries, with the exception of the boundary between Subunits IC and ID. Subunit IC is characterized by changes in susceptibility that are two to three times those observed in the lower units.

Magnetic Polarity Stratigraphy

Because of the high sedimentation rates throughout much of the Miocene to Quaternary at Site 704, it should be possible to obtain a high-resolution magnetostratigraphic and biostratigraphic record from this interval. The high sedimentation rate, however, adversely affects the paleomagnetic record in two ways. First, the high water content and the low shear strength of these sediments (particularly above 140 mbsf) cause the cores to be easily disturbed by normal handling procedures. Second, the high accumulation rate of biogenic material appears to have diluted the magnetic carrier, resulting in extremely weak magnetizations (typically less than 0.1 mA/m) that are near the noise level of the shipboard cryogenic magnetometer.

Paleomagnetic data obtained from the interval below 140 mbsf from both Holes 704A and 704B exhibit slightly stronger magnetizations (~0.5 mA/m). All cores from this interval were drilled using the XCB system and therefore, azimuthal orientation is not maintained either within or between cores. For this reason, only the inclination records were used to interpret the magnetic polarity.

The majority of the core archive halves were measured using the pass-through cryogenic magnetometer, both before and after partial alternating-field (AF) demagnetization at 5 to 9 mT. In general, the demagnetization treatment resulted in a small decrease of intensity and a reduction of scatter in the data, but in virtually all sections, the polarity of the remanent magnetization remained unchanged. We conclude that, although the magnetization of these sediments is very weak, it appears to be stable and only minor secondary magnetic overprints are present.

A well-defined sequence of normal and reverse polarity magnetozones is identified in the depth interval 140 to 233 mbsf in Hole 704A from the half-core paleomagnetic data (Fig. 20). The paleomagnetic record for Hole 704B is poorly defined above 218 mbsf because of coring/sampling disturbance and weak magnetization intensities, but a reliable record was obtained below this depth. There is good agreement between the half-core polarity log for the two holes in the 15 m of stratigraphic overlap (Fig. 20). The combined record from the two holes provides a fairly continuous magnetostratigraphic sequence to a depth of 330 m. Below this depth the polarity record becomes more discontinuous because of a combination of coring gaps and intervals of extremely low magnetization intensities, for which a reliable polarity assignment cannot be made (e.g., 383–400 mbsf).

The half-core cryogenic magnetometer data have been supplemented by incremental AF demagnetization analyses on 82

Table 6. Sedimentary organic carbon and calcium carbonate data, Hole 704A.

Sample (cm)	Depth (mbsf)	C_{org} (%)	$CaCO_3$ (%)
1H-1, 10–14	0.10		82.42
1H-1, 100–102	1.00	0.09	51.62
1H-1, 108–112	1.08		62.75
1H-2, 70–74	2.20		68.50
1H-2, 100–102	2.50	0.11	85.74
1H-2, 108–112	2.58		79.25
1H-3, 10–14	3.10		29.58
1H-3, 100–102	4.00	0.26	36.20
1H-3, 108–112	4.08		39.83
1H-4, 70–74	5.20		60.17
1H-4, 108–112	5.58		94.25
1H-4, 130–132	5.80	0.05	92.32
1H-5, 10–14	6.10		93.08
1H-5, 108–112	7.08		43.42
1H-5, 111–113	7.11	0.30	24.52
2H-1, 30–32	7.50	−0.12	94.24
2H-1, 64–68	7.84		93.42
2H-1, 80–84	8.00		90.33
2H-1, 100–102	8.20	0.13	68.89
2H-2, 30–34	9.00		48.67
2H-2, 80–84	9.50		56.83
2H-2, 100–102	9.70	−0.07	36.03
2H-3, 80–84	11.00		7.92
2H-3, 100–102	11.20	0.40	6.76
2H-3, 140–144	11.60		14.67
2H-4, 80–84	12.50		79.75
2H-4, 100–102	12.70	−0.06	70.39
2H-4, 140–144	13.10		46.83
2H-5, 30–34	13.50		62.50
2H-5, 80–84	14.00		52.58
2H-5, 100–102	14.20	0.02	61.80
2H-6, 64–68	15.34		57.42
2H-6, 130–132	16.00	0.25	20.60
3H-1, 30–32	17.00	0.43	25.44
3H-1, 80–84	17.50		62.83
3H-1, 100–102	17.70	0.12	61.38
3H-1, 130–134	18.00		55.92
3H-2, 80–84	19.00		39.50
3H-2, 100–102	19.20	0.53	38.78
3H-2, 130–134	19.50		52.08
3H-3, 80–84	20.50		50.25
3H-3, 110–112	20.80	0.05	61.55
3H-3, 130–134	21.00		57.67
3H-4, 40–44	21.60		46.25
3H-4, 80–84	22.00		67.25
3H-5, 80–84	23.50		64.92
3H-5, 96–100	23.66		61.67
3H-6, 80–84	25.00		73.03
3H-6, 96–100	25.16		77.25
4H-3, 20–22	29.40	0.04	83.40
4H-3, 100–102	30.20	0.23	52.21
4H-5, 80–82	33.00	0.11	65.39
4H-6, 35–37	34.05	0.01	36.36
4H-6, 38–42	34.08		44.17
5H-1, 80–82	36.50		79.33
5H-1, 100–102	36.70	0.02	85.57
5H-1, 130–134	37.00		42.50
5H-2, 80–82	38.00		68.50
5H-3, 29–33	38.99		36.50
5H-3, 100–102	39.70	0.32	38.53
5H-4, 80–82	41.00		34.17
5H-4, 100–102	41.20	0.34	30.61
5H-5, 50–52	42.20		67.67
5H-5, 100–102	42.70	0.02	73.73
5H-5, 133–137	43.03		22.25
5H-5, 140–142	43.10		54.33
5H-6, 29–33	43.49		18.42
5H-6, 50–52	43.70		17.50
5H-6, 100–102	44.20	0.50	20.10
5H-6, 133–137	44.53		47.17
5H-6, 140–142	44.60		22.83
6H-1, 54–56	45.74		44.08
6H-1, 68–72	45.88		56.17
6H-1, 100–102	46.20	0.08	48.04
6H-2, 54–56	47.24		82.00
6H-2, 120–124	47.90		46.33
6H-2, 140–142	48.10		65.67
6H-3, 28–32	48.48		65.92
6H-3, 54–56	48.74		51.75
6H-3, 80–82	49.00		38.75
6H-3, 100–102	49.20	0.09	30.36
6H-4, 54–56	50.24		27.58
6H-4, 100–102	50.70	0.34	28.77
6H-4, 120–124	50.90		40.75
6H-4, 140–142	51.10		34.92
6H-5, 50–52	51.70	0.01	57.71
6H-5, 54–56	51.74		58.42
6H-5, 100–102	52.20	0.83	9.09
6H-5, 120–124	52.40		19.58
6H-5, 140–142	52.60		29.33
6H-6, 54–56	53.24		36.25
6H-6, 100–102	53.70	0.07	47.96
6H-6, 140–142	54.10		45.08
6H-7, 54–56	54.74		55.58
7H-1, 108–110	55.78	0.21	17.68
7H-1, 119–121	55.89		20.92
7H-2, 10–12	56.30		35.42
7H-2, 70–74	56.90		51.83
7H-2, 102–104	57.22	−0.03	53.04
7H-2, 119–121	57.39		20.33
7H-3, 10–12	57.80		67.17
7H-3, 102–104	58.72	0.27	19.27
7H-3, 109–113	58.79		25.58
7H-3, 119–121	58.89		19.25
7H-4, 10–12	59.30		48.83
7H-4, 66–68	59.86		40.50
7H-4, 102–104	60.22	0.44	51.79
7H-4, 119–121	60.39		43.67
7H-5, 10–12	60.80		42.75
7H-5, 18–22	60.88		45.25
7H-5, 18–22	50.88		53.83
7H-5, 102–104	61.72	0.27	25.85
7H-5, 119–121	61.89		29.00
7H-6, 10–12	62.30		35.83
7H-6, 40–42	62.60	0.59	15.60
7H-6, 67–69	62.87		20.00
8H-1, 9–13	64.29		51.67
8H-1, 100–102	65.20	−0.12	64.05
8H-1, 139–141	65.59		8.25
8H-2, 50–52	66.20		13.17
8H-2, 69–73	66.39		21.08
8H-2, 139–141	67.09		41.92
8H-3, 47–49	67.67		61.08
8H-3, 52–54	67.72	−0.14	60.72
8H-3, 69–73	67.89		7.42
8H-3, 100–102	68.20	0.55	10.01
8H-3, 139–141	68.59		32.75
8H-4, 9–13	68.79		9.58
8H-4, 50–52	69.20		36.92
8H-4, 90–92	69.60	0.08	26.44
8H-4, 139–141	70.09		18.75
8H-5, 40–42	70.60	0.35	27.36
8H-5, 50–52	70.70		23.08
8H-5, 69–73	70.89		22.67
8H-5, 139–141	71.59		24.67
8H-6, 50–52	72.20		36.50
8H-6, 60–62	72.30	0.22	37.53
8H-6, 69–73	72.39		44.92
9H-1, 50–52	74.20		55.00
9H-1, 68–72	74.38		42.75
9H-1, 100–102	74.70	0.25	50.54
9H-1, 140–142	75.10		44.25
9H-2, 8–12	75.28		40.75
9H-2, 50-52	75.70		55.58
9H-2, 100–102	76.20	0.05	31.36
9H-2, 118–122	76.38		33.67
9H-2, 140–142	76.60		31.75
9H-3, 50–52	77.20		44.50
9H-3, 100–102	77.70	0.00	54.54
9H-3, 140–142	78.10		44.70
9H-4, 8–12	78.28		45.30
9H-4, 50–52	78.70		45.92
9H-4, 100–102	79.20	0.04	64.80
9H-5, 8–12	79.78		39.30
9H-5, 50–52	80.20		37.50
9H-5, 100–102	80.70	0.32	10.26
9H-5, 140–142	81.10		19.92
9H-6, 50–52	81.70		13.83
9H-6, 100–102	82.20	0.34	10.17
9H-6, 118–122	92.38		13.60
9H-6, 140–142	82.60		11.67
10H-1, 50–52	93.70		10.40
10H-1, 99–102	84.19	0.20	11.18
10H-2, 50–52	85.20		54.67
10H-2, 99–101	85.69	0.50	51.79
10H-2, 118–122	85.88		28.80
10H-3, 50–52	86.70		16.67
10H-3, 99–101	87.19	0.34	26.94
10H-3, 118–122	87.38		25.50
10H-4, 50–52	88.20		26.00
10H-4, 105–107	88.75	0.27	23.44
10H-5, 50–52	89.70		7.83
10H-5, 99–101	90.19	0.28	4.67
10H-6, 50–52	91.20		10.80
10H-6, 99–101	91.69	0.12	16.51
10H-7, 10–14	92.30		21.70
10H-7, 45–47	92.65		10.50
11H-1, 50–52	93.20		26.25
11H-1, 70-74	93.40		30.00
11H-1, 100–102	93.70	0.16	31.19
11H-1, 140–142	94.10		30.33
11H-2, 50–52	94.70		26.90
11H-2, 120–124	95.40		11.80
11H-2, 140–142	95.60		11.67
11H-3, 10–14	95.80		14.20
11H-3, 50–52	96.20		17.60
11H-3, 100–102	96.70	0.15	17.10
11H-3, 140–142	97.10		17.08
11H-4, 50–52	97.70		24.08
11H-4, 110–112	98.30	0.16	44.28
11H-4, 140–142	98.60		43.17
11H-5, 10–14	98.80		43.40
11H-5, 50–52	99.20		22.33
11H-5, 70-72	99.40	−0.02	20.27
11H-5, 140–142	100.10		50.00
11H-6, 30–32	100.50	−0.05	36.86
11H-6, 50–52	100.70		42.83
11H-6, 70–74	100.90		49.60
11H-6, 140–142	101.60		53.83
11H-7, 10–14	101.80		83.90
11H-7, 20–22	101.90	0.17	84.32
12H-1, 50–52	102.70		67.25
12H-1, 58–60	102.78	0.07	63.22
12H-1, 70–74	102.90		72.90
12H-1, 140–142	103.60		75.67
12H-2, 10–14	103.80		79.30
12H-2, 50–52	104.20		33.08
12H-2, 58–60	104.28	0.00	33.86
12H-2, 140–142	105.10		69.42
12H-3, 10–14	105.30		65.90
12H-3, 50–52	105.70		67.17
12H-3, 58–60	105.78	0.23	59.70
12H-3, 140–142	106.60		74.20
12H-4, 50–52	107.20		81.00
12H-4, 70–74	107.40		70.40
12H-4, 140–142	108.10		77.83
12H-5, 50–52	108.70		67.58
12H-5, 58–60	108.78	−0.02	76.48
12H-5, 70–74	108.90		71.60
12H-6, 10–14	109.80		75.80
12H-6, 50–52	110.20		78.58
12H-6, 58–60	110.28	0.01	73.89
12H-6, 140–142	111.10		77.00
13H-1, 50–52	112.20		51.92
13H-1, 70–74	112.40		17.20
13H-1, 100–102	112.70	0.08	21.68
13H-1, 140–142	113.10		20.10
13H-2, 10–14	113.30		49.40
13H-2, 30–32	113.50	0.07	58.96
13H-2, 50–52	113.70		72.08
13H-2, 100–102	114.20	0.19	23.10
13H-2, 140–142	114.60		34.50
13H-3, 10–14	114.80		57.60
13H-3, 50–52	115.20		69.25

Table 6 (continued).

Sample (cm)	Depth (mbsf)	C_{org} (%)	$CaCO_3$ (%)
13H-3, 100–102	115.70	0.07	75.64
13H-3, 140–142	116.10		65.00
13H-4, 10–14	116.30		64.50
13H-4, 50–52	116.70		47.17
13H-4, 100–102	117.20	0.05	52.54
13H-4, 140–142	117.60		65.92
13H-5, 10–14	117.80		70.30
13H-5, 50–52	118.20		50.33
13H-5, 140–142	119.10		83.33
13H-6, 50–52	119.70		75.58
13H-6, 117–121	120.37		77.20
13H-6, 140–142	120.60		79.00
13H-7, 10–14	120.80		72.08
13H-7, 50–52	121.20		70.58
14H-1, 50–52	121.70		70.67
14H-1, 70–74	121.90		69.90
14H-1, 100–102	122.20	0.02	77.40
14H-1, 139–141	122.59		69.00
14H-2, 30–32	123.00	0.31	14.01
14H-2, 50–52	123.20		72.08
14H-2, 70–74	123.40		63.50
14H-2, 100–102	123.70	0.04	61.47
14H-2, 139–141	124.09		76.17
14H-3, 10–14	124.30		78.90
14H-3, 50–52	124.70		61.25
14H-3, 139–141	125.59		63.17
14H-4, 50–52	126.20		73.33
14H-4, 70–74	126.40		69.30
14H-4, 100–102	126.70	0.01	44.45
14H-4, 139–141	127.09		57.67
14H-5, 10–14	127.30		69.90
14H-5, 50–52	127.70		44.70
14H-5, 100–102	128.20	−0.11	45.87
14H-5, 130–132	128.50	0.13	89.24
14H-5, 139–141	128.59		63.10
14H-6, 50–52	129.20		51.90
14H-6, 70–74	129.40		25.10
15H-1, 10–14	130.80		32.10
15H-1, 50–52	131.20		46.00
15H-1, 100–102	131.70	−0.07	74.56
15H-2, 10–14	132.20		56.90
15H-2, 50–52	132.70		60.50
15H-2, 100–102	133.20	−0.11	50.96
15H-2, 140–142	133.60		46.92
15H-3, 50–52	134.20		51.42
15H-3, 70–74	134.40		50.30
15H-3, 100–102	134.70	0.05	49.87
15-3, 140–142	135.10		32.83
15H-4, 10–14	135.30		57.25
15H-4, 50–52	135.70		52.25
15H-4, 140–142	136.60		73.75
15H-5, 10–14	136.80		49.25
15H-5, 50–52	137.20		55.20
15H-5, 100–102	137.70	0.06	38.79
15H-6, 10–14	138.30		40.42
15H-6, 50–52	138.70		42.17
15H-6, 140–142	139.60		38.25
15H-7, 50–52	140.20		52.83
16H-1, 10–14	140.30		19.25
16H-1, 50–52	140.70		24.50
16H-1, 144–146	141.64		18.83
16H-2, 50–52	142.20		31.75
16H-2, 100–102	142.70	0.03	23.35
16H-2, 120–124	142.90		27.83
16H-2, 144–146	143.14		26.92
16H-3, 50–52	143.70		28.83
16H-3, 70–74	143.90		62.83
16H-3, 100–102	144.20	0.23	77.22
16H-3, 144–146	144.64		77.70
16H-4, 50–52	145.20		78.33
16H-4, 100–102	145.70	0.02	79.81
16H-4, 120–124	145.90		67.83
16H-4, 144–146	146.14		64.75
16H-5, 50–52	146.70		52.10
16H-5, 70–74	146.90		52.25
16H-5, 70–74	146.90		53.00
16H-5, 100–102	147.20	0.10	41.28
16H-5, 144–146	147.64		49.60

Table 6 (continued).

Sample (cm)	Depth (mbsf)	C_{org} (%)	$CaCO_3$ (%)
16H-6, 50–52	148.20		70.00
16H-6, 70–74	148.40		29.42
17X-1, 50–52	150.20		19.00
17X-1, 123–127	150.93		79.58
17X-2, 10–14	151.30		55.75
17X-2, 50–52	151.70		80.42
17X-2, 100–102	152.20	−0.02	82.90
17X-2, 136–138	152.56		81.75
17X-2, 140–142	152.60		55.25
17X-3, 10–14	152.80		59.92
17X-3, 50–52	153.20		65.00
17X-3, 60–62	153.30		88.50
17X-3, 100–102	153.70	0.02	66.20
17X-3, 140–142	154.10		54.67
17X-4, 50–52	154.70		55.67
17X-4, 70–74	154.90		63.92
17X-4, 100–102	155.20	0.03	67.39
17X-4, 140–142	155.60		69.00
17X-5, 50–52	156.20		64.17
17X-5, 100–102	156.70	0.03	64.89
17X-5, 123–127	156.93		59.67
17X-5, 140–142	157.10		57.42
17X-6, 50–52	157.70		52.67
17X-6, 123–127	158.43		81.83
17X-6, 140–142	158.60		79.08
18X-1, 50–52	159.70		36.90
18X-1, 10–102	160.20	−0.06	75.89
18X-1, 120–124	160.40		45.58
18X-1, 140–142	160.60		70.25
18X-2, 50–52	161.20		78.58
18X-2, 70–74	161.40		73.42
18X-2, 100–102	161.70	0.10	49.62
18X-2, 140–142	162.10		68.83
18X-3, 50–52	162.70		68.25
18X-3, 70–74	162.90		73.92
18X-3, 125–127	163.45	0.01	54.79
18X-3, 140–142	163.60		81.25
18X-4, 10–14	163.80		73.75
18X-4, 50–52	164.20		58.50
18X-4, 100–102	164.70	−0.03	73.73
18X-5, 50–52	165.70		45.08
18X-5, 100–102	166.20	0.02	57.46
18X-5, 120–124	166.40		54.00
18X-5, 140–142	166.60		54.90
18X-6, 50–52	167.20		45.50
18X-6, 60–62	167.30	−0.03	35.44
18X-6, 70–74	167.40		50.00
19X-1, 10–14	168.80		43.32
19X-1, 50–52	169.20		64.67
19X-1, 140–142	170.10		77.75
19X-2, 50–52	170.70		64.75
19X-2, 100–102	171.20	0.09	58.05
19X-2, 120–124	171.40		55.58
19X-2, 140–142	171.60		62.42
19X-3, 50–52	172.20		55.42
19X-3, 100–102	172.70	−0.09	72.47
19X-3, 120–124	172.90		57.75
19X-3, 140–142	173.10		54.83
19X-4, 50–52	173.70		85.92
19X-4, 70–74	173.90		86.08
19X-4, 100–102	174.20	−0.01	88.99
19X-4, 140–142	174.60		73.42
19X-5, 10–14	174.80		73.67
19X-5, 50–52	175.20		76.75
19X-5, 100–102	175.70	−0.01	41.95
19X-5, 140–142	176.18		57.58
19X-6, 10–14	176.30		74.50
19X-6, 50–52	176.70		80.50
19X-6, 100–102	177.20	−0.10	80.56
19X-6, 140–142	177.60		65.33
20X-1, 46–48	178.66		71.67
20X-1, 100–102	179.20	−0.05	72.39
20X-1, 140–142	179.60		65.17
20X-2, 46–48	180.16		57.67
20X-2, 100–102	180.70	0.04	72.22
20X-2, 140–142	181.10		63.00
20X-3, 46–48	181.66		75.33
20X-3, 90–94	182.10		77.67

Table 6 (continued).

Sample (cm)	Depth (mbsf)	C_{org} (%)	$CaCO_3$ (%)
20X-3, 100–102	182.20	0.03	75.81
20X-3, 140–142	182.60		43.25
20X-4, 46–48	183.16		80.10
20X-4, 90–94	183.60		83.92
20X-4, 100–102	183.70	0.03	85.82
20X-4, 140–142	184.10		79.67
20X-5, 46–48	184.66		78.83
20X-5, 90–94	185.10		62.92
20X-5, 100–102	185.20	0.06	82.23
20X-5, 140–142	185.60		72.33
20X-6, 46–48	186.16		75.17
20X-6, 90–94	186.60		69.42
20X-6, 100–102	186.70	−0.11	77.81
20X-6, 140–142	187.10		75.67
21X-1, 100–102	188.70	0.00	83.07
21X-2, 100–102	190.20	−0.05	87.74
21X-2, 140–142	190.60		85.25
21X-3, 100–102	191.70	0.16	81.06
21X-4, 70–72	192.90	0.12	71.47
22X-1, 100–102	198.20	−0.01	68.47
22X-2, 100–102	199.70	0.04	60.46
22X-3, 100–102	201.20	0.05	51.79
22X-4, 100–102	202.70	0.01	77.81
22X-5, 100–102	204.20	−0.05	78.90
23X-1, 100–102	107.70	0.06	82.90
23X-2, 100–102	209.20	0.01	74.98
23X-3, 100–102	210.70	0.08	77.81
23X-4, 100–102	212.20	0.06	69.72
23X-5, 100–102	213.70	−0.10	62.72
24X-2, 82–84	218.52	0.10	63.22
24X-3, 82–84	220.02	0.10	57.80
24X-4, 82–84	221.52	0.10	35.78
24X-5, 82–84	223.02	0.01	50.71
25X-1, 130–132	227.00	0.16	43.95
25X-2, 130–132	228.50	0.15	1.00
25X-3, 90–92	229.60	0.14	75.39
25X-4, 90–92	231.10	0.12	41.20
25X-5, 50–52	232.20	0.11	57.88
25X-6, 50–52	233.70	0.12	39.53

Table 7. Sedimentary calcium carbonate data, Hole 704B.

Sample (cm)	Depth (mbsf)	$CaCO_3$ (%)
1H-2, 110–112	2.60	20.02
1H-4, 110–112	5.60	38.45
2H-3, 110–112	10.80	61.47
2H-5, 110–112	13.80	47.12
3H-1, 20–22	16.40	50.50
3H-1, 94–96	17.14	63.75
3H-2, 20–22	17.90	55.58
3H-2, 94–96	18.64	45.58
3H-2, 110–112	18.80	37.28
3H-3, 20–22	19.40	38.83
3H-3, 94–96	20.14	50.92
3H-4, 20–22	20.90	45.75
3H-4, 94–96	21.64	54.42
3H-4, 110–112	21.80	61.30
3H-5, 20–22	22.40	46.25
3H-5, 94–96	23.14	68.42
3H-6, 20–22	23.90	48.50
3H-6, 94–96	24.64	39.33
3H-7, 20–22	25.40	28.42
4H-1, 30–32	26.00	43.75
4H-1, 132–136	27.02	43.50
4H-1, 145–147	27.15	58.17
4H-2, 30–32	27.50	74.75
4H-2, 110–112	28.30	30.69
4H-2, 132–136	28.52	41.42
4H-2, 145–147	28.65	42.83
4H-3, 30–32	29.00	73.75
4H-3, 132–136	30.02	36.46
4H-3, 145–147	30.15	56.20
4H-4, 30–32	30.50	73.20
4H-4, 110–112	31.30	63.72
4H-4, 132–136	31.52	71.42
4H-4, 145–147	31.65	75.60
4H-5, 30–32	32.00	31.10
4H-5, 132–136	33.02	58.67
4H-5, 145–147	33.15	35.30
4H-6, 30–32	33.50	63.80
5H-1, 15–17	35.35	68.90
5H-1, 93–95	36.13	49.70
5H-1, 120–122	36.40	64.80
5H-2, 15–17	36.85	34.20
5H-2, 93–95	37.63	72.90
5H-3, 15–17	38.35	74.40
5H-3, 93–95	39.13	18.30
5H-4, 15–17	39.85	53.20
5H-4, 93–95	40.63	53.90
5H-5, 15–17	41.35	69.20
5H-5, 93–95	42.13	64.80
5H-6, 15–17	42.85	34.30
5H-6, 93–95	43.63	27.00
5H-7, 15–17	44.35	61.60
6H-2, 100–102	47.20	45.45
6H-5, 100–102	51.70	16.60
7H-3, 100–102	58.20	20.93
7H-5, 100–102	61.20	58.96
8H-3, 30–32	66.66	54.04
8H-3, 110–112	67.46	21.10
9H-1, 110–112	74.30	24.52
9H-5, 110–112	80.30	50.87
10H-2, 110–112	85.30	13.51
10H-5, 110–112	89.80	61.38
11H-2, 110–112	94.80	8.01
11H-6, 110–112	100.80	13.93
12H-2, 110–112	104.30	45.54
12H-5, 110–112	108.80	79.90
13H-1, 110–112	112.30	19.52
13H-4, 110–112	116.80	77.40
14H-1, 110–112	121.80	63.72
14H-4, 110–112	126.30	74.06
15H-2, 110–112	131.94	73.98
15H-5, 110–112	136.44	72.81
17X-2, 100–102	149.70	54.04
17X-4, 100–102	152.70	53.96
18X-3, 110–112	160.80	52.63
18X-6, 110–112	165.30	55.79
19X-2, 90–92	168.60	53.63
22X-1, 100–102	195.70	50.04
23X-2, 100–102	206.70	67.55
23X-3, 100–102	208.20	79.90
23X-4, 100–102	209.70	73.39
23X-5, 100–102	211.20	77.73
24X-1, 50–52	214.20	72.30
24X-1, 100–102	214.70	71.56
24X-1, 140–142	215.10	76.40
24X-2, 50–52	215.70	73.00
24X-2, 100–102	216.20	78.31
24X-2, 140–142	216.60	81.20
24X-3, 50–52	217.20	77.80
24X-3, 100–102	217.70	67.47
24X-3, 140–142	218.10	80.50
24X-4, 50–52	218.70	70.20
24X-4, 100–102	219.20	47.54
24X-4, 140–142	219.60	55.40
24X-5, 50–52	220.20	52.75
24X-5, 100–102	220.70	68.05
24X-5, 140–142	221.10	67.00
24X-6, 10–12	221.30	56.42
24X-6, 100–102	222.20	16.35
24X-6, 140–142	222.60	49.17
24X-7, 50–52	223.20	48.70
25X-1, 52–54	223.72	72.20
25X-1, 100–102	224.20	31.36
25X-1, 140–142	224.60	70.42
25X-2, 52–54	225.22	18.40
25X-2, 100–102	225.70	63.72
25X-2, 140–142	226.10	62.90
25X-3, 50–52	226.70	49.46
25X-3, 52–54	226.72	60.92
25X-4, 140–142	227.60	66.00
25X-4, 50–52	228.20	8.01
25X-4, 52–53	228.22	8.58
25X-4, 140–142	229.10	49.00
25X-5, 53–54	229.72	84.20
25X-5, 100–102	230.20	58.80
25X-5, 140–142	230.60	42.70
25X-6, 52–54	231.22	60.30
25X-6, 100–102	231.70	61.55
25X-6, 140–142	232.10	71.75
25X-7, 52–54	232.72	47.60
26X-1, 50–52	233.20	70.83
26X-1, 100–102	233.70	60.21
26X-1, 140–142	234.10	44.08
26X-2, 50–52	234.70	76.90
26X-2, 100–102	235.20	50.12
26X-2, 140–142	235.60	50.00
26X-3, 50–52	236.20	35.33
26X-3, 100–102	236.70	59.13
26X-3, 140–142	237.10	50.80
26X-3, 140–142	237.10	53.00
26X-4, 50–52	237.70	75.17
26X-4, 100–102	238.20	44.20
26X-5, 50–52	239.20	69.50
27X-1, 140–142	243.60	45.00
27X-2, 50–52	244.20	78.40
27X-2, 100–102	244.70	68.42
27X-2, 140–142	245.10	72.30
27X-3, 50–52	245.70	32.50
27X-3, 60–62	245.80	25.92
27X-3, 140–142	246.60	68.70
27X-4, 50–52	247.20	72.67
27X-4, 100–102	247.70	77.92
27X-4, 140–142	248.10	72.80
27X-5, 50–52	248.70	76.80
27X-5, 75–77	248.95	64.33
27X-6, 50–52	250.20	87.10
27X-6, 100–102	250.70	83.25
27X-6, 140–142	251.10	87.20
27X-7, 50–52	251.70	78.20
28X-1, 49–51	252.19	88.20
28X-1, 110–112	252.80	86.33
28X-1, 140–142	253.10	93.50
28X-2, 49–51	253.69	80.20
28X-2, 110–112	254.30	70.33
28X-3, 140–142	254.60	87.10
28X-3, 49–51	255.19	91.08
28X-3, 110–112	255.80	93.75
28X-3, 130–142	256.10	85.50
28X-4, 49–51	256.69	85.42
28X-4, 100–102	257.20	88.92
28X-4, 140–142	257.60	90.75
28X-5, 49–51	258.19	87.90
28X-5, 100–102	258.70	87.83
28X-5, 140–142	159.10	84.75
28X-6, 49–51	159.69	85.20
28X-6, 110–112	260.30	83.92
28X-6, 140–142	260.60	83.50
28X-7, 49–51	261.19	91.70
29X-1, 50–52	261.70	79.58
29X-1, 90–92	262.10	72.00
29X-1, 140–142	262.60	81.25
29X-2, 50-52	263.20	94.20
29X-2, 90–92	263.60	94.50
29X-2, 140–142	264.10	79.50
29X-3, 50–52	264.70	83.80
29X-3, 90–92	265.10	81.83
29X-3, 140–142	265.60	86.83
29X-4, 50–52	266.20	91.00
29X-4, 90–92	266.60	84.33
29X-4, 140–142	267.10	81.50
29X-5, 50–52	167.70	90.67
29X-5, 90–92	268.10	84.83
29X-5, 140–142	268.60	91.10
29X-6, 50–52	269.20	80.20
29X-6, 90–92	269.60	65.58
29X-7, 50–52	270.70	85.42
30X-1, 50–52	271.20	92.30
30X-1, 100–102	271.70	66.67
30X-1, 140–142	272.10	76.83
30X-2, 50–52	272.70	83.25
30X-2, 100–102	273.20	75.23
30X-2, 137–139	273.57	69.20
30X-3, 50–52	274.20	92.60
30X-3, 100–102	274.70	93.49
30X-3, 140–142	275.10	87.42
30X-4, 50–52	275.70	79.70
30X-4, 100–102	276.20	82.82
30X-4, 140–142	276.60	80.92
30X-5, 50–52	277.20	89.70
30X-7, 50–52	278.20	84.10
30X-7, 100–102	278.70	68.14
30X-7, 140–142	279.10	84.10
30X-8, 50–52	279.70	88.75
30X-8, 140–142	280.69	90.58
30X-8, 140–142	280.69	90.75
31X-1, 100–102	281.20	81.48
31X-2, 100–102	282.70	86.24
31X-3, 100–102	284.20	90.57
31X-4, 100–102	285.70	95.49
31X-5, 100–102	287.20	89.91
31X-6, 100–102	288.70	84.48
32X-1, 100–102	290.70	84.15
32X-2, 100–102	292.20	86.99
32X-3, 100–102	293.70	90.91
32X-4, 100–102	295.20	91.49
32X-5, 100–102	296.70	68.89
32X-6, 100–102	298.20	87.74
33X-1, 100–102	300.20	92.99
33X-2, 100–102	301.70	79.56
33X-3, 100–102	303.20	88.74
33X-4, 100–102	304.70	87.57
33X-5, 100–102	306.20	86.07
33X-6, 100–102	307.70	62.88
34X-1, 100–102	309.70	92.99
34X-2, 100–102	311.20	88.07
34X-3, 100–102	312.70	93.07
34X-4, 100–102	314.20	87.99
34X-5, 100–102	315.70	82.82
34X-6, 100–102	317.20	86.07
35X-1, 100–102	319.20	78.73
35X-2, 100–102	320.70	71.14
35X-3, 100–102	322.20	39.20
35X-4, 100–102	323.70	46.04
35X-5, 100–102	325.20	69.39
35X-6, 100–102	326.70	83.48
36X-1, 100–102	328.70	90.49
36X-2, 97–99	330.17	91.24
37X-2, 100–102	339.70	81.15
37X-3, 100–102	341.20	89.92
39X-1, 100–102	357.20	91.16
39X-2, 100–102	358.70	89.07
39X-3, 100–102	360.20	92.16
39X-4, 100–102	361.70	91.99
39X-5, 100–102	363.20	92.91
39X-6, 100–102	364.70	93.24
40X-1, 98–100	366.68	87.82
40X-2, 98–100	368.18	81.57
40X-3, 98–100	369.68	81.73
40X-4, 98–100	371.18	81.06
40X-5, 98–100	372.68	78.40
40X-6, 98–100	374.18	79.90
41X-1, 101–103	376.21	89.15
41X-2, 101–103	377.71	79.73
41X-3, 101–103	379.21	79.48
41X-4, 101–103	380.71	85.99
41X-5, 101–103	382.21	85.99
41X-6, 101–103	383.71	79.56
42X-2, 99–101	387.19	75.14
42X-4, 99–101	390.19	90.99
42X-6, 99–101	392.76	82.40
43X-1, 100–102	395.20	89.91
43X-4, 100–102	398.70	81.32
43X-7, 50–52	401.80	84.57
44X-1, 100–102	404.70	72.81
45X-1, 101–103	414.21	88.99
45X-2, 101–103	415.71	88.57
46X-2, 101–103	425.21	94.16
46X-3, 101–103	426.71	82.15
46X-4, 94–96	428.14	84.15
47X-2, 90–92	434.60	73.89
47X-4, 90–92	437.60	71.72
48X-1, 100–102	442.70	85.90
48X-3, 100–102	445.70	79.73
49X-2, 83–85	453.53	73.73
49X-5, 135–137	458.55	79.73
50X-1, 50–51	461.20	80.90
52X-1, 100–102	473.20	85.57
52X-4, 98–100	477.68	83.57
53X-2, 115–117	484.35	88.74
54X-1, 103–105	492.23	87.07
54X-3, 100–102	495.20	89.49
54X-5, 100–102	498.20	84.07
55X-2, 70–75	502.90	86.07
55X-4, 54–56	505.74	78.07
55X-5, 95–97	507.65	88.90
5X-6, 74–76	508.94	90.10
56X-2, 25–27	511.95	86.40
56X-3, 57–59	513.77	88.40
56X-4, 62–64	515.32	80.71
57X-2, 93–95	522.13	88.32
57X, CC (26–28)	523.86	78.23
58X-2, 78–80	531.48	85.07
58X-3, 102–104	533.22	85.40
58X-5, 54–56	535.74	86.57
58X-6, 42–44	537.12	82.23
59X-1, 103–105	539.73	86.32
59X-2, 123–125	541.43	86.82
59X-3, 125–127	542.95	86.32
60X-3, 40–42	551.60	86.32
60X-4, 48–50	553.18	90.07
60X-6, 10–12	555.80	86.32
61X-2, 78–80	559.98	84.57
62X-2, 122–124	569.92	75.14
62X-3, 116–118	571.36	85.49
62X-4, 109–111	572.79	76.98
62X-5, 135–137	574.55	78.98
63X-1, 130–132	578.00	85.07
63X-2, 115–117	579.35	86.40
63X-3, 136–138	581.06	80.40
63X-4, 63–65	581.83	80.98
63X-5, 100–102	583.70	87.57
64X-1, 1–3	586.21	80.90

Table 7 (continued).

Sample (cm)	Depth (mbsf)	$CaCO_3$ (%)
64X-3, 74–76	589.94	89.57
64X, CC (31–33)	590.79	68.39
65X-1, 137–139	597.07	81.23
65X-2, 134–136	598.54	79.65
65X-3, 90–92	599.60	71.81
66X-1, 5–7	605.25	74.98
66X, CC (12–14)	605.91	80.90
67X-1, 108–110	615.78	90.99
68X-1, 126–128	625.46	78.40
68X-2, 77–79	626.47	79.98
69X-1, 60–62	634.30	89.99
70X-1, 4–6	643.24	80.06
71X-1, 105–107	653.75	74.31
71X-2, 98–100	655.18	78.40
71X-3, 55–57	656.25	68.97
72X-1, 104–105	663.24	86.40
72X-2, 93–95	664.63	84.90
72X-3, 114–115	666.34	59.05

discrete samples from Hole 704A, spanning the depth range 0 to 230 mbsf, and 40 discrete samples from Hole 704B, from 190 to 360 mbsf. Each of these discrete samples has been demagnetized at 2.5 or 5 mT increments up to a maximum field of 35 mT in order to isolate the stable characteristic magnetization vectors.

The sequence of normal and reverse polarity magnetozones defined from the combined half-core and discrete sample data for the depth interval 0–360 mbsf is shown in Figure 21. The Brunhes/Matuyama chron boundary is constrained to lie between the lower part of Core 114-704A-3H and the upper part of Core 114-704A-5H. The top of the Olduvai subchron is well defined in the upper part of Core 114-704A-11H. However, the apparent extension of this normal polarity magnetozone through Cores 114-704A-13H and 114-704A-14H requires an extraordinarily high sedimentation rate on the order of 150 m/m.y., which is hard to accept for this site. This anomalously thick magnetozone may be explained by downslope movement of material from adjacent areas of higher topography on the Meteor Rise or else by the presence of a normal polarity magnetic overprint in these two cores.

Initial demagnetization analyses of samples from these cores have failed to provide evidence for such an overprint, but further, more detailed studies will form part of the post-cruise investigations. Short normal polarity zones in Cores 114-704A-16X and 114-704A-17X, identified from the half-core measurements, have yet to be confirmed by post-cruise studies of discrete samples but are tentatively correlated with the Reunion subchron.

The sequence of normal and reverse polarity magnetozones in the depth range 169 to 290 mbsf can be correlated with the Gauss to the Chron C4R part of the GPTS, as indicated in Figure 21. This correlation provides a reasonable fit with the majority of biostratigraphic datums, but a number of significant discrepancies remain. Post-cruise studies will attempt to resolve these discrepancies.

PHYSICAL PROPERTIES

High-resolution physical-property measurements of deep-sea sediments at Site 704 have two main objectives: to investigate the characteristics of physical properties where fluctuations in the position of the Southern Ocean polar front are the dominant control over the depositional environment and to investigate whether the periodicity observed in the physical-property record may correspond to climatic cycles. Furthermore, we examined whether the onset of the climatic deterioration during the middle Pliocene influenced the changes in physical-property amplitudes and thus may be detected as a characteristic change in the seismic sequence.

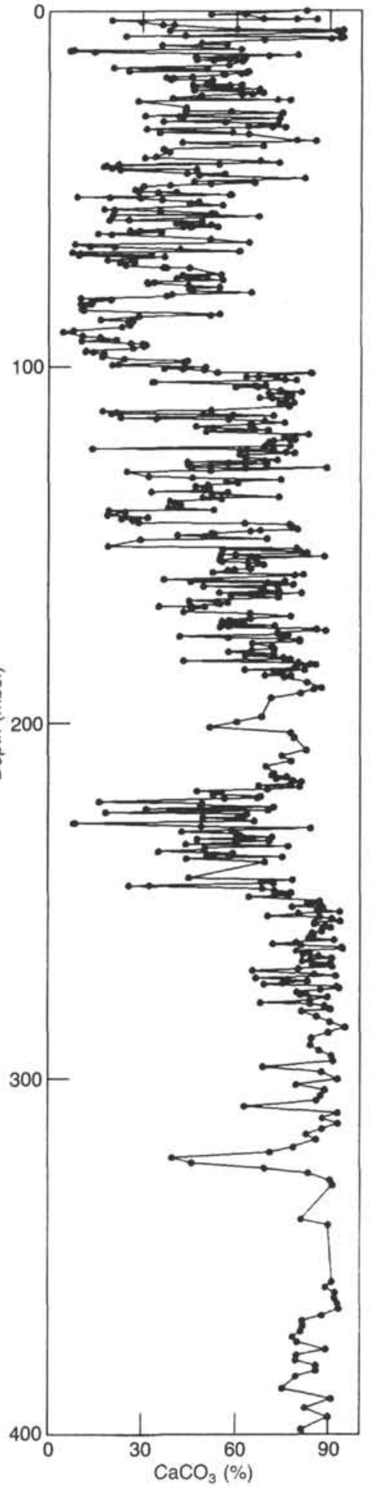

Figure 18. Percent calcium carbonate profile for Site 704. The interval between 0 and 215 mbsf is from Hole 704A, except for the interval between 25 and 35 mbsf spliced in from Hole 704B. The interval below 215 mbsf is from Hole 704B.

The techniques of physical-property measurement were described in the "Explanatory Notes" chapter. Four sets of measurements were obtained: (1) index properties (wet-bulk density, dry-bulk density, porosity, water content, and grain density), (2)

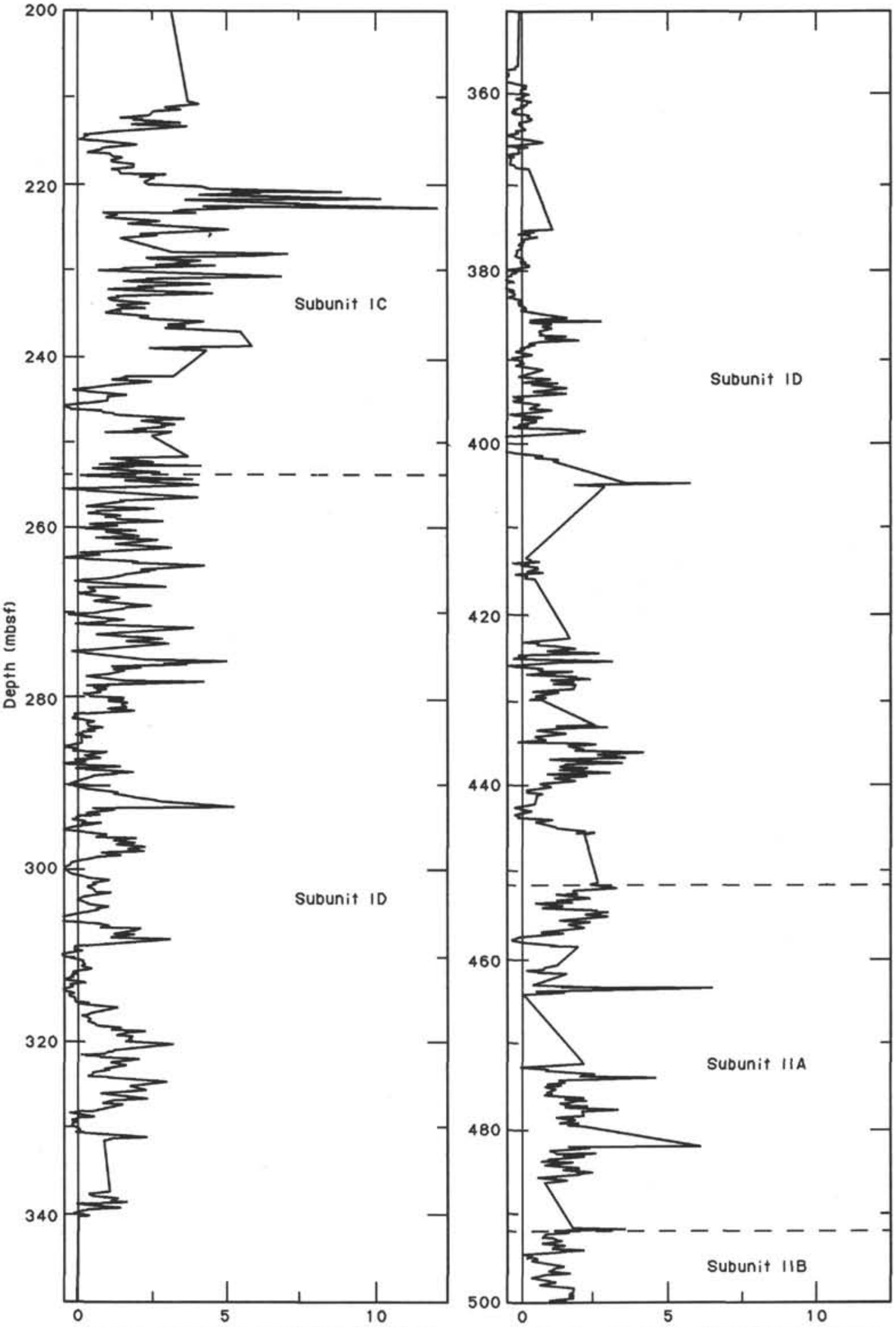

Figure 19. Variation of magnetic susceptibility with depth below seafloor in Hole 704B. Lithostratigraphic unit boundaries are shown.

compressional wave (*P*-wave) velocity, (3) vane shear strength, and (4) thermal conductivity. The carbonate content (from the "Geochemistry" section, this chapter) is shown for comparison with the physical-property data. All of the data presented are unfiltered for any bad data points.

Physical-Property Summary and Lithostratigraphic Correlation

The index properties, carbonate contents, *P*-wave velocities, thermal conductivities, and shear strengths are listed in Tables 8

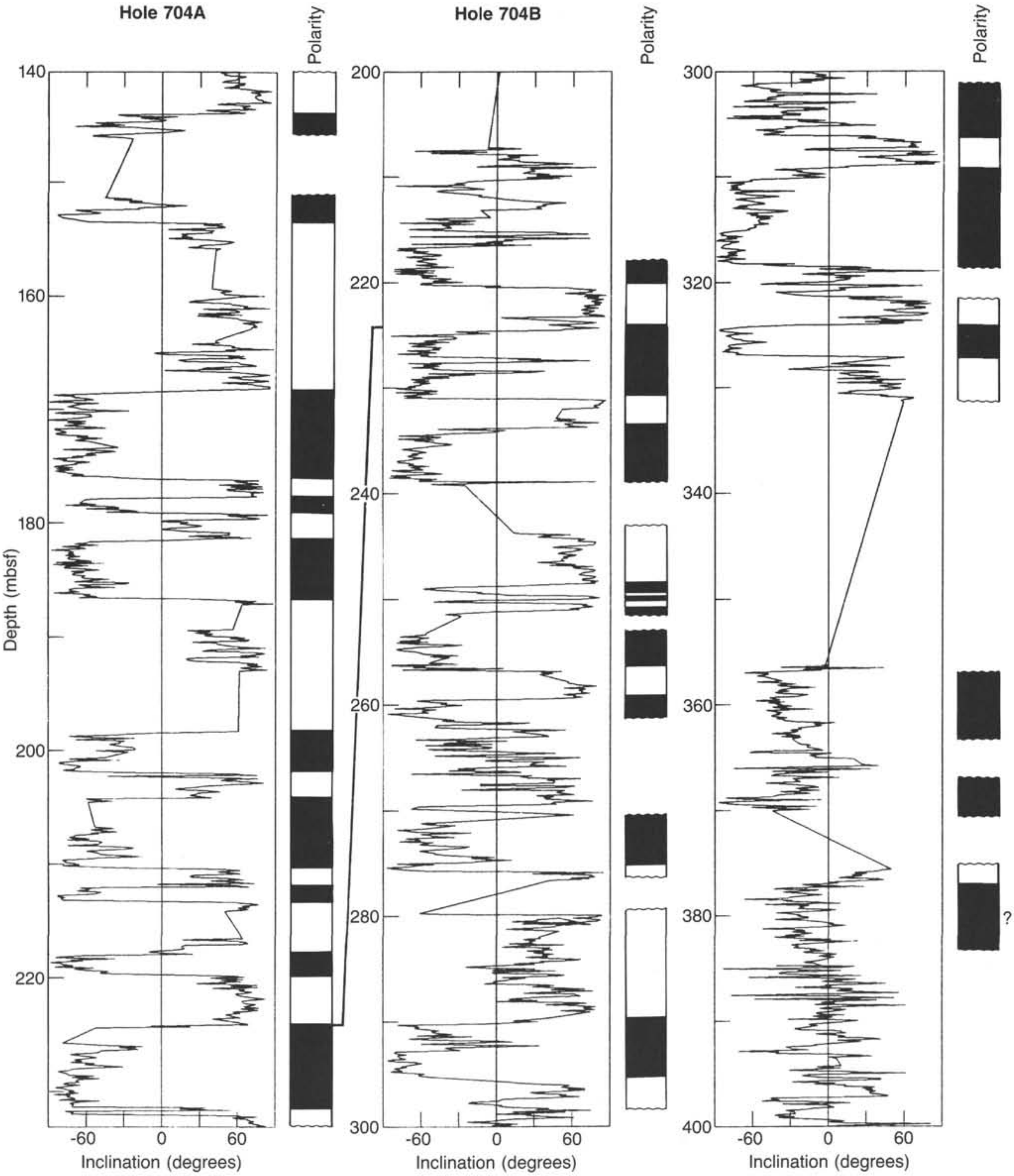

Figure 20. Variation of magnetic inclination with depth below seafloor in Holes 704A and 704B. Inferred magnetic polarity is indicated (black, normal polarity; white, reverse polarity).

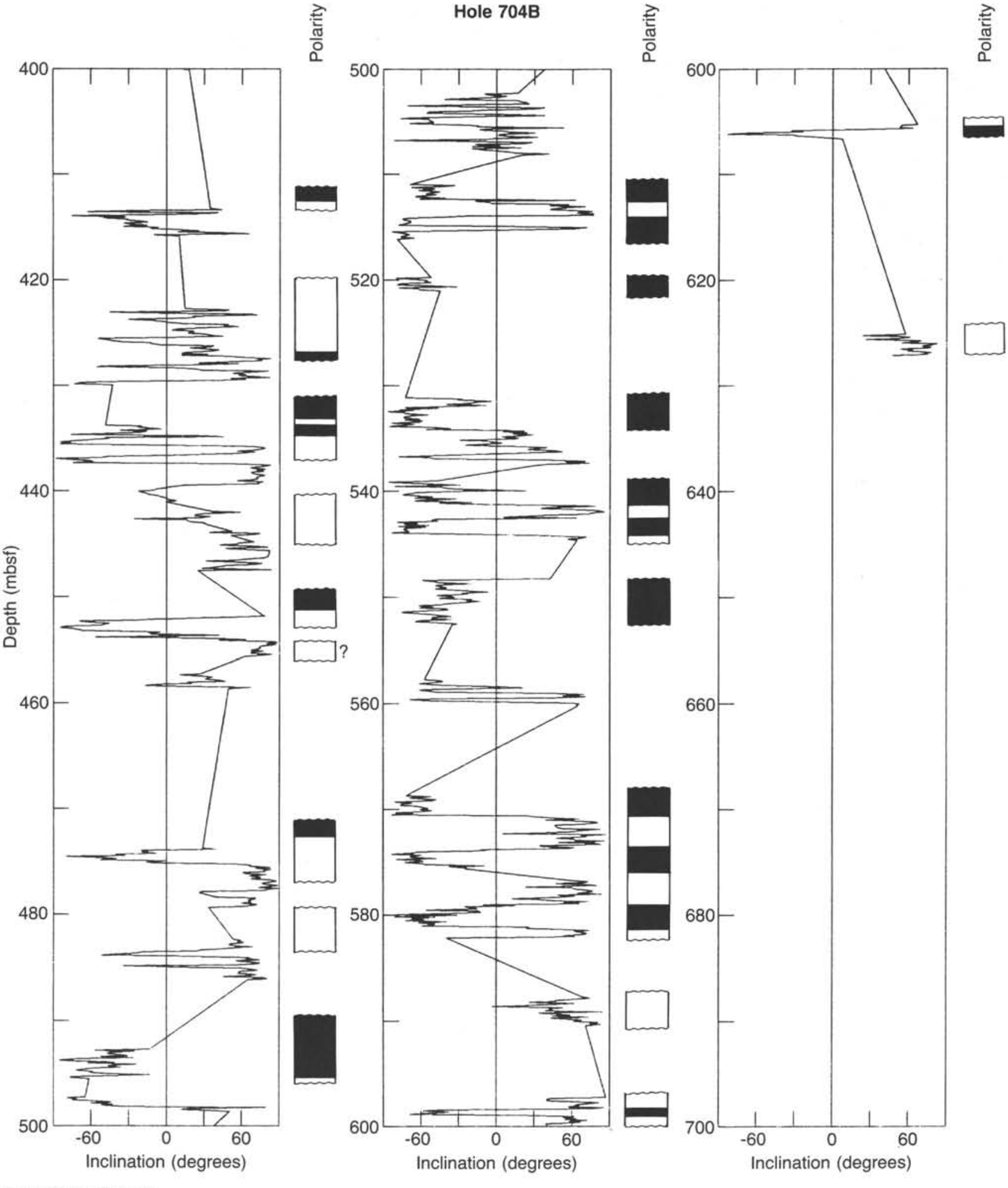

Figure 20 (continued).

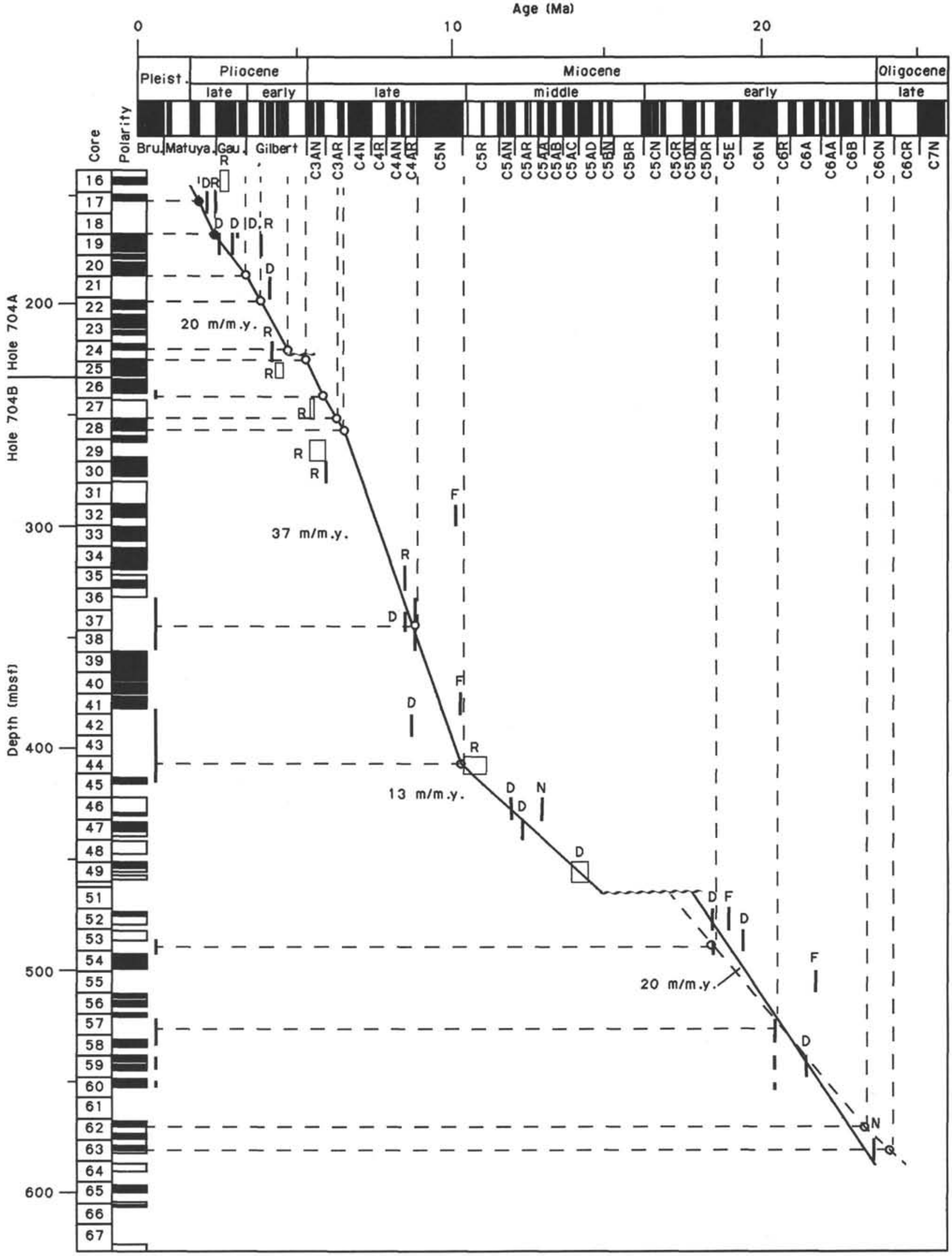

Figure 21. Tentative correlation of magnetic polarity zones in Holes 704A and 704B with the GPTS of Berggren et al. (1985). Biostratigraphic datums are shown coded by fossil group (D = diatom; F = planktonic foraminifer; R = radiolarian; and N = nannofossil).

Table 8. Index properties, Site 704.

				Densities		
Sample (cm)	Depth (mbsf)	Water content (%)	Porosity (%)	Wet bulk (g/cm^3)	Dry bulk (g/cm^3)	Grain (g/cm^3)
Hole 704A:						
1H-1, 100–102	1.00	65.65	84.13	1.40	0.48	2.78
1H-2, 100–102	2.50	47.98	70.63	1.58	0.82	2.63
1H-3, 100–102	4.00	65.25	82.64	1.34	0.47	2.54
1H-4, 130–132	5.80	43.88	68.31	1.64	0.92	2.79
1H-5, 111–113	7.11	67.86	84.47	1.30	0.42	2.58
2H-1, 30–32	7.50	45.61	70.69	1.63	0.89	2.91
2H-1, 100–102	8.20	51.57	75.10	1.53	0.74	2.86
2H-2, 100–102	9.70	66.25	83.21	1.33	0.45	2.53
2H-3, 100–102	11.20	74.76	87.33	1.24	0.31	2.31
2H-4, 100–102	12.70	57.17	76.92	1.43	0.61	2.51
2H-5, 100–102	14.20	59.16	79.47	1.40	0.57	2.69
2H-6, 130–132	16.00	73.91	87.82	1.26	0.33	2.53
3H-1, 30–32	17.00	71.54	85.28	1.26	0.36	2.29
3H-1, 100–102	17.70	63.50	81.43	1.35	0.49	2.53
3H-2, 100–102	19.20	70.34	85.50	1.27	0.38	2.48
3H-3, 110–112	20.80	60.89	80.84	1.38	0.54	2.73
4H-3, 20–22	29.40	50.36	72.61	1.53	0.76	2.64
4H-3, 100–112	30.20	56.70	76.99	1.42	0.62	2.57
4H-5, 80–82	33.00	49.65	72.54	1.53	0.77	2.71
5H-1, 100–102	36.70	42.38	67.82	1.66	0.95	2.90
5H-3, 100–102	39.70	63.49	81.32	1.34	0.49	2.51
5H-4, 100–102	41.20	65.46	81.97	1.33	0.46	2.40
5H-5, 100–102	42.70	56.57	77.66	1.44	0.63	2.69
5H-6, 100–102	44.20	72.06	86.56	1.28	0.36	2.49
6H-1, 100–102	46.20	65.88	83.39	1.33	0.45	2.61
6H-3, 100–103	49.20	70.00	84.83	1.29	0.39	2.39
6H-4, 100–102	50.70	69.75	86.01	1.29	0.39	2.66
6H-5, 50–52	51.70	62.54	81.69	1.38	0.52	2.69
6H-5, 100–102	52.20	73.19	85.36	1.24	0.33	2.12
6H-6, 100–102	53.70	65.46	83.71	1.34	0.46	2.7
7H-1, 108–110	55.78	74.25	88.12	1.23	0.32	2.56
7H-2, 102–104	57.22	62.67	81.71	1.35	0.50	2.67
7H-3, 102–104	58.72	71.38	86.26	1.27	0.36	2.51
7H-4, 100–102	60.20	65.28	83.48	1.34	0.47	2.70
7H-5, 102–104	61.72	72.48	87.27	1.26	0.35	2.59
7H-6, 40–42	62.60	66.46	83.88	1.35	0.45	2.63
8H-1, 100–102	65.20	59.76	80.00	1.41	0.57	2.71
8H-3, 52–54	67.72	57.90	77.79	1.39	0.59	2.56
8H-3, 100–102	68.20	72.43	86.51	1.23	0.34	2.43
8H-4, 90–92	69.60	70.09	84.07	1.26	0.38	2.24
8H-5, 40–42	70.60	67.37	84.98	1.32	0.43	2.75
8H-6, 60–62	72.30	66.23	83.80	1.32	0.45	2.64
9H-1, 100–102	74.70	58.53	78.53	1.43	0.59	2.61
9H-2, 100–102	76.20	70.75	85.16	1.26	0.37	2.36
9H-3, 100–102	77.70	62.57	81.67	1.34	0.50	2.68
9H-4, 100–102	79.20	57.20	78.79	1.43	0.61	2.80
9H-5, 100–102	80.70	73.11	86.34	1.24	0.33	2.31
9H-6, 100–102	82.20	73.83	85.57	1.24	0.32	2.08
10H-1, 99–101	84.19	72.62	86.28	1.25	0.34	2.36
10H-2, 99–101	85.69	62.12	80.91	1.35	0.51	2.60
10H-3, 99–101	87.19	60.60	80.73	1.39	0.55	2.74
10H-4, 105–107	88.75	55.27	74.77	1.41	0.63	2.41
10H-5, 99–101	90.19	74.82	86.48	1.23	0.31	2.13
10H-6, 99–101	91.69	72.78	86.43	1.27	0.35	2.37
11H-1, 100–102	93.70	70.11	85.17	1.29	0.39	2.44
11H-3, 100–102	96.70	66.23	82.91	1.31	0.44	2.48
11H-4, 110–112	98.30	61.12	80.50	1.40	0.54	2.64
11H-5, 70–72	99.40	78.63	86.22	1.27	0.27	1.65
11H-6, 30–32	100.50	65.89	83.56	1.34	0.46	2.64
11H-7, 20–22	101.90	50.51	74.33	1.56	0.77	2.87
12H-1, 58–60	102.78	51.18	72.42	1.51	0.74	2.53
12H-2, 58–60	104.28	62.89	81.63	1.35	0.50	2.63
12H-3, 58–60	105.78	46.56	69.23	1.56	0.83	2.61
12H-5, 58–60	108.78	43.59	66.30	1.60	0.90	2.57
12H-6, 58–60	110.28	47.18	69.75	1.55	0.82	2.61
13H-1, 100–102	112.70	67.04	83.41	1.32	0.44	2.47
13H-2, 100–102	114.20	64.46	81.64	1.33	0.47	2.46
13H-2, 30–32	113.50	57.24	78.58	1.45	0.62	2.76
13H-3, 100–102	115.70	43.67	66.87	1.62	0.91	2.63
13H-4, 100–102	117.20	54.19	75.56	1.50	0.69	2.63
14H-1, 100–102	112.20	45.32	70.13	1.64	0.90	2.86
14H-2, 30–32	123.00	59.75	78.81	1.39	0.56	2.52
14H-2, 100–102	123.7	53.46	75.14	1.49	0.69	2.65
14H-4, 100–102	126.70	61.81	80.26	1.38	0.53	2.52

Table 8 (continued).

				Densities		
Sample (cm)	Depth (mbsf)	Water content (%)	Porosity (%)	Wet bulk (g/cm^3)	Dry bulk (g/cm^3)	Grain (g/cm^3)
Hole 704A (continued):						
14H-5, 100–102	128.20	41.22	66.47	1.68	0.99	2.86
14H-5, 130–132	128.50	59.85	80.24	1.41	0.57	2.74
15H-1, 100–102	131.70	43.88	67.26	1.60	0.90	2.66
15H-2, 100–102	133.20	59.20	79.22	1.41	0.57	2.64
15H-3, 100–102	134.70	59.23	78.81	1.41	0.57	2.57
15H-5, 100–102	137.70	62.87	81.58	1.38	0.51	2.63
16H-2, 100–102	142.70	70.39	86.64	1.32	0.39	2.73
16H-3, 100–102	144.20	44.82	68.26	1.58	0.87	2.68
16H-4, 100–102	145.70	41.02	65.07	1.66	0.98	2.71
16H-5, 100–102	147.20	57.54	76.66	1.39	0.59	2.44
17X-2, 100–102	152.20	38.46	63.44	1.77	1.09	2.81
17X-3, 100–102	153.70	52.15	73.12	1.49	0.71	2.52
17X-4, 100–102	155.20	50.44	72.20	1.54	0.76	2.57
17X-5, 100–102	156.70	51.81	73.59	1.50	0.72	2.61
18X-1, 100–102	160.20	39.95	63.74	1.65	0.99	2.67
18X-2, 100–102	161.70	55.94	77.78	1.47	0.65	2.78
18X-3, 125–127	163.45	50.35	72.24	1.52	0.76	2.59
18X-4, 100–102	164.70	47.03	69.54	1.58	0.84	2.60
18X-5, 100–102	166.20	54.50	75.41	1.50	0.68	2.58
18X-6, 60–62	167.30	62.80	81.79	1.37	0.51	2.67
19X-2, 100–102	171.20	51.45	74.79	1.53	0.74	2.83
19X-3, 100–102	172.70	42.70	65.98	1.63	0.93	2.63
19X-4, 100–102	174.20	36.79	60.92	1.73	1.09	2.71
19X-5, 100–102	175.70	52.37	73.83	1.50	0.71	2.59
19X-6, 100–102	177.20	40.44	64.52	1.67	0.99	2.71
20X-1, 100–102	179.20	46.97	70.88	1.57	0.84	2.78
20X-2, 100–102	180.70	43.53	67.25	1.62	0.91	2.69
20X-3, 100–102	182.20	39.57	63.36	1.66	1.00	2.67
20X-4, 100–102	183.70	36.94	62.42	1.77	1.11	2.87
20X-5, 100–102	185.20	43.14	67.55	1.62	0.92	2.78
20X-6, 100–102	186.70	41.66	65.95	1.63	0.95	2.74
21X-1, 100–102	188.70	33.47	57.54	1.81	1.21	2.73
21X-2, 100–102	190.20	35.82	60.27	1.72	1.11	2.75
21X-3, 100–102	191.70	40.84	64.25	1.65	0.97	2.63
21X-4, 70–72	192.90	41.10	66.52	1.68	0.99	2.88
22X-1, 100–102	198.20	43.29	67.55	1.60	0.91	2.76
22X-2, 100–102	199.70	46.92	69.69	1.53	0.81	2.63
22X-3, 100–102	201.20	48.62	72.33	1.54	0.79	2.79
22X-4, 100–102	202.70	40.50	63.71	1.63	0.97	2.61
22X-5, 100–102	204.20	41.15	66.00	1.70	1.00	2.81
23X-1, 100–102	207.70	36.23	60.90	1.75	1.12	2.78
23X-2, 100–102	209.20	37.87	60.26	1.69	1.05	2.52
23X-3, 100–102	210.70	38.13	62.19	1.70	1.05	2.70
23X-4, 100–102	212.20	36.97	61.29	1.75	1.10	2.73
23X-5, 100–102	213.70	47.19	69.43	1.56	0.83	2.57
24X-2, 82–84	218.52	47.43	70.94	1.56	0.82	2.73
24X-3, 82–84	220.02	42.61	65.77	1.61	0.93	2.62
24X-4, 82–84	221.52	52.17	73.62	1.49	0.71	2.58
24X-5, 80–82	223.00	46.56	69.77	1.55	0.83	2.68
25X-1, 130–132	227.00	50.12	73.12	1.53	0.76	2.73
25X-2, 130–132	228.50	60.39	80.11	1.39	0.55	2.66
25X-3, 90–92	229.60	39.07	63.00	1.69	1.03	2.69
25X-4, 90–92	231.10	54.18	74.44	1.45	0.66	2.48
25X-5, 50–52	232.20	47.58	69.97	1.56	0.82	2.59
25X-6, 50–52	233.70	55.99	75.52	1.44	0.63	2.44
Hole 704B:						
1H-2, 110–112	2.60	65.59	84.38	1.37	0.47	2.84
1H-4, 110–112	5.60	67.44	83.31	1.38	0.45	2.41
2H-3, 110–112	10.80	62.98	81.96	1.42	0.52	2.68
2H-5, 110–112	13.80	66.80	84.13	1.33	0.44	2.64
3H-2, 110–112	18.80	63.62	81.72	1.34	0.49	2.56
3H-4, 110–112	21.80	56.50	76.34	1.41	0.61	2.50
4H-2, 110–112	28.30	67.90	83.77	1.31	0.42	2.44
4H-4, 110–112	31.30	51.54	73.18	1.49	0.72	2.59
6H-2, 100–102	47.20	61.33	81.92	1.44	0.56	2.87
6H-5, 100–102	51.70	69.61	84.28	1.27	0.39	2.34
7H-3, 100–102	58.20	68.76	85.64	1.31	0.41	2.71
7H-5, 100–102	61.20	59.16	78.44	1.40	0.57	2.53
8H-3, 30–32	66.66	61.89	80.11	1.38	0.53	2.49
8H-3, 110–112	67.46	67.89	83.23	1.33	0.43	2.34
9H-1, 110–112	74.30	68.97	84.65	1.47	0.46	2.48
9H-5, 110–112	80.30	67.09	84.24	1.31	0.43	2.63

Table 8 (continued).

				Densities		
Sample (cm)	Depth (mbsf)	Water content (%)	Porosity (%)	Wet bulk (g/cm^3)	Dry bulk (g/cm^3)	Grain (g/cm^3)
Hole 704B (continued):						
10H-2, 110–112	85.30	69.48	84.32	1.26	0.39	2.36
10H-5, 110–112	89.80	56.00	77.05	1.40	0.62	2.66
11H-2, 110–112	94.80	71.05	85.72	1.40	0.41	2.44
11H-6, 110–112	100.80	69.16	84.51	1.31	0.40	2.43
12H-2, 110–112	104.30	60.56	81.36	1.39	0.5	2.86
12H-5, 110–112	108.80	45.20	68.10	1.61	0.88	2.62
13H-1, 110–112	112.30	58.29	77.91	1.40	0.58	2.54
13H-4, 110–112	116.80	44.81	68.03	1.58	0.87	2.65
14H-1, 110–112	121.80	49.91	72.41	1.53	0.77	2.66
14H-4, 110–112	126.30	45.51	69.47	1.61	0.88	2.75
15H-2, 110–112	131.94	44.94	67.16	1.67	0.92	2.53
15H-5, 110–112	136.44	45.22	68.49	1.56	0.86	2.66
17H-2, 100–102	149.70	57.20	77.96	1.42	0.61	2.66
17H-4, 100–102	152.70	56.53	76.63	1.43	0.62	2.54
18H-3, 110–112	160.80	45.50	67.53	1.59	0.86	2.52
18H-6, 110–112	165.30	56.49	76.46	1.42	0.62	2.52
19H-2, 90–92	168.60	53.83	75.48	1.47	0.68	2.66
22H-1, 100–102	195.70	46.80	69.97	1.59	0.84	2.68
23X-2, 100–102	206.70	37.87	62.26	1.72	1.07	2.74
23X-3, 100–102	208.20	40.73	64.15	1.64	0.97	2.63
23X-4, 100–102	209.70	37.43	61.65	1.72	1.08	2.72
23X-5, 100–102	211.20	39.04	63.06	1.66	1.01	2.70
24X-1, 100–102	214.70	42.25	66.42	1.65	0.95	2.73
24X-2, 100–102	216.20	41.22	65.06	1.62	0.95	2.69
24X-3, 100–102	217.70	43.78	67.14	1.59	0.89	2.65
24X-4, 100–102	219.20	49.98	72.53	1.52	0.76	2.67
24X-5, 100–102	220.70	39.72	6.34	1.71	1.03	2.65
24X-6, 100–102	222.20	54.15	76.45	1.44	0.66	2.77
25X-1, 100–102	224.20	55.96	76.29	1.44	0.63	2.55
25X-2, 100–102	225.70	45.39	63.4	1.57	0.85	2.11
25X-3, 52–54	226.72	57.19	78.92	1.54	0.66	2.82
25X-4, 52–54	228.22	59.57	78.09	1.38	0.56	2.43
25X-5, 100–102	230.20	44.93	68.97	1.61	0.88	2.75
25X-6, 100–102	231.70	42.94	66.62	1.61	0.92	2.68
26X-1, 100–102	233.70	44.29	67.32	1.57	0.88	2.52
26X-2, 100–102	235.20	45.92	67.96	1.54	0.83	2.52
26X-3, 100–102	236.70	44.60	68.13	1.58	0.87	2.68
26X-4, 100–102	238.20	49.04	72.51	1.53	0.78	2.77
27X-2, 100–102	244.70	39.55	62.59	1.67	1.01	2.59
27X-3, 60–62	245.80	62.26	79.57	1.36	0.51	2.37
27X-4, 100–102	247.70	36.24	60.63	1.75	1.11	2.74
27X-5, 75–77	248.95	40.00	63.87	1.65	0.99	2.68
27X-6, 100–102	250.70	30.92	55.56	1.89	1.31	2.83
28X-1, 110–112	252.80	30.41	55.09	1.89	1.31	2.85
28X-2, 110–112	254.30	38.22	62.32	1.72	1.07	2.71
28X-3, 110–112	255.80	32.72	57.74	1.81	1.21	2.85
28X-4, 100–102	257.20	33.17	57.57	1.80	1.20	2.77
27X-5, 100–102	258.70	31.90	56.69	1.84	1.26	2.83
28X-6, 110–112	260.30	32.93	57.63	1.86	1.25	2.81
29X-1, 90–92	262.10	38.14	62.42	1.71	1.06	2.73
29X-2, 90–92	263.60	32.33	57.01	1.81	1.22	2.81
29X-3, 90–92	265.10	32.67	57.30	1.84	1.24	2.80
29X-4, 90–92	266.60	33.35	57.61	1.80	1.20	2.75
29X-5, 90–92	268.10	31.50	55.67	1.86	1.27	2.77
29X-6, 90–92	269.60	31.48	55.12	1.87	1.28	2.71
30X-1, 90–92	271.60	36.63	62.49	1.77	1.12	2.92
30X-2, 90–92	273.10	36.04	60.75	1.74	1.12	2.78
30X-3, 90–92	274.60	31.45	56.45	1.87	1.28	2.86
30X-4, 90–92	276.10	33.88	58.98	1.83	1.21	2.84
30X-7, 90–92	278.60	40.64	66.03	1.69	1.00	2.88
31X-1, 100–102	281.20	32.25	57.47	1.88	1.28	2.88
31X-2, 100–102	282.70	30.05	54.32	1.90	1.33	2.81
31X-3, 100–102	284.20	30.28	53.78	1.86	1.30	2.72
31X-4, 100–102	285.70	24.83	47.68	2.03	1.53	2.80
31X-5, 100–102	287.20	29.65	54.06	1.92	1.35	2.83
31X-6, 100–102	288.70	29.47	53.84	1.93	1.36	2.83
32X-1, 100–102	290.70	30.03	53.75	1.88	1.32	2.75
32X-2, 100–102	292.20	31.11	55.21	1.89	1.30	2.77
32X-3, 100–102	293.70	31.19	55.13	1.84	1.27	2.75
32X-4, 100–102	295.20	30.38	55.34	1.86	1.29	2.88
32X-5, 100–102	296.70	41.76	66.01	1.85	1.08	2.74
32X-6, 100–102	298.20	24.64	47.35	1.77	1.34	2.79
33X-1, 100–102	300.20	30.71	55.41	1.90	1.32	2.84
33X-2, 100–102	301.70	33.47	57.86	1.81	1.21	2.77

Table 8 (continued).

				Densities		
Sample (cm)	Depth (mbsf)	Water content (%)	Porosity (%)	Wet bulk (g/cm^3)	Dry bulk (g/cm^3)	Grain (g/cm^3)
Hole 704B (continued):						
33X-3, 100–102	303.20	32.46	57.28	1.85	1.25	2.83
33X-4, 100–102	304.70	31.82	55.93	1.86	1.27	2.76
33X-5, 100–102	306.20	32.12	56.81	1.86	1.26	2.82
33X-6, 100–102	307.70	38.19	61.96	1.73	1.07	2.67
34X-1, 100–102	309.70	33.95	57.90	1.80	1.19	2.71
34X-2, 100–102	311.20	29.89	53.82	1.88	1.32	2.77
34X-3, 100–102	312.70	30.00	55.48	1.92	1.35	2.95
34X-4, 100–102	314.20	28.62	52.22	1.94	1.39	2.76
34X-5, 100–102	315.70	31.79	55.95	1.84	1.26	2.76
34X-6, 100–102	317.20	31.25	56.80	1.90	1.31	2.93
35X-1, 100–102	319.20	31.55	55.78	1.85	1.27	2.77
35X-2, 100–102	320.70	35.64	60.03	1.79	1.15	2.75
35X-3, 100–102	322.20	46.89	68.79	1.56	0.83	2.52
36X-1, 100–102	328.70	30.40	53.23	1.84	1.28	2.64
36X-2, 97–99	330.17	30.28	53.95	1.86	1.30	2.73
37X-2, 100–102	339.70	33.43	56.92	1.79	1.19	2.67
37X-3, 100–102	341.20	31.28	55.83	1.89	1.30	2.82
39X-1, 100–102	357.20	31.71	56.87	1.93	1.32	2.88
39X-2, 100–102	358.70	30.27	53.89	1.87	1.30	2.73
39X-3, 100–102	360.20	29.00	53.42	1.92	1.36	2.85
39X-4, 100–102	361.70	30.06	53.68	1.90	1.33	2.73
39X-5, 100–102	363.20	29.97	54.22	1.90	1.33	2.81
39X-6, 100–102	364.70	29.56	52.97	1.88	1.32	2.72
40X-1, 98–100	366.68	29.95	53.01	1.85	1.29	2.67
40X-2, 98–100	368.18	29.82	53.57	1.86	1.31	2.75
40X-3, 98–100	369.68	30.55	54.28	1.82	1.26	2.74
40X-4, 98–100	371.18	31.00	55.20	1.86	1.28	2.78
40X-5, 98–100	372.68	30.89	54.78	1.85	1.28	2.75
40X-6, 98–100	374.18	31.56	54.44	1.84	1.26	2.63
41X-1, 101–103	376.21	29.08	52.73	1.90	1.35	2.76
41X-2, 101–103	377.71	31.75	55.21	1.81	1.24	2.69
41X-3, 101–103	379.21	31.16	55.02	1.82	1.25	2.74
41X-4, 101–103	380.71	30.25	54.81	1.89	1.32	2.83
41X-5, 101–103	382.21	31.01	54.51	1.85	1.27	2.70
41X-6, 101–103	373.71	32.23	54.64	1.81	1.22	2.57
42X-2, 99–101	387.19	32.57	56.13	1.80	1.22	2.68
42X-4, 99–101	390.19	28.61	51.55	1.87	1.33	2.69
42X-6, 99–101	392.76	28.07	50.85	1.88	1.35	2.69
43X-1, 100–102	395.20	27.51	50.40	1.95	1.42	2.72
43X-4, 100–102	398.70	27.30	50.14	1.93	1.41	2.72
43X-7, 50–52	401.80	28.04	51.39	1.91	1.38	2.75
44X-1, 100–102	404.70	34.37	58.92	1.79	1.17	2.78
45X-1, 101–103	414.21	32.56	56.74	1.85	1.25	2.75
45X-2, 101–103	415.71	31.11	54.68	1.87	1.29	2.71
46X-2, 101–103	425.21	28.26	51.39	1.90	1.37	2.72
46X-3, 101–103	426.71	61.75	81.87	1.85	0.71	2.81
47X-2, 90–92	434.60	32.54	56.33	1.81	1.22	2.71
47X-3, 90–92	436.10	28.73	52.75	1.92	137	2.81
47X-4, 90–92	437.60	33.38	56.78	1.80	1.20	2.65
47X-5, 100–102	439.20	29.74	53.11	1.86	1.31	2.71
47X-6, 90–92	440.60	32.23	56.21	1.83	1.24	2.74
48X-1, 100–102	442.70	29.91	54.82	1.88	1.32	2.88
48X-2, 100–102	444.20	31.26	54.59	1.83	1.26	2.68
48X-3, 100–102	445.70	28.08	51.74	1.91	1.37	2.78
49X-1, 99–101	452.19	30.84	55.30	1.94	1.34	2.81
49X-2, 83–85	453.53	29.40	53.69	1.88	1.32	2.82
49X-3, 84–86	455.04	30.87	55.49	1.83	1.27	2.83
49X-4, 84–86	456.54	34.33	58.81	1.65	1.09	2.77
49X-5, 135–137	458.55	30.79	55.25	1.90	1.31	2.81
50X-1, 50–51	461.20	29.12	54.74	2.02	1.43	2.99
52X-1, 100–102	473.20	31.08	55.07	1.85	1.28	2.76
52X-2, 100–102	474.70	29.31	54.26	2.00	1.41	2.90
52X-3, 100–102	476.20	27.51	51.33	2.20	1.59	2.82
52X-4, 98–100	477.68	29.44	54.83	2.02	1.42	2.95
52X-5, 98–100	479.18	28.03	52.37	2.07	1.49	2.86
53X-1, 105–107	482.75	28.00	53.45	2.14	1.54	3.00
53X-2, 115–117	484.35	32.24	57.63	1.94	1.32	2.90
54X-1, 103–105	492.23	29.67	55.91	2.20	1.55	3.05
54X-2, 100–102	493.70	33.60	57.29	1.86	1.23	2.69
54X-3, 100–102	495.20	32.04	55.81	1.86	1.26	2.71
54X-4, 100–102	496.70	30.59	57.18	1.95	1.36	3.07
54X-5, 100–102	498.20	32.55	57.63	1.97	1.33	2.86
55X-2, 70–72	502.90	30.40	52.45	2.09	1.45	2.56
55X-4, 54–56	505.74	29.04	51.41	2.04	1.45	2.62

Table 8 (continued).

Sample (cm)	Depth (mbsf)	Water content (%)	Porosity (%)	Densities Wet bulk (g/cm^3)	Dry bulk (g/cm^3)	Grain (g/cm^3)
Hole 704B (continued):						
55X-5, 95–97	507.65	33.94	59.43	1.83	1.21	2.89
55X-6, 74–76	508.94	31.83	59.73	2.07	1.41	3.22
56X-2, 25–27	511.95	28.39	58.37	2.44	1.75	3.59
56X-3, 57–59	513.77	32.57	57.41	1.86	1.25	2.83
56X-4, 62–64	515.32	21.18	42.50	2.44	1.92	2.79
57X-2, 93–95	522.13	31.29	54.94	2.19	1.50	2.71
57X-CC, 26–28	523.86	28.41	52.37	2.17	1.55	2.81
58X-2, 78–80	531.48	25.45	49.61	2.09	1.56	2.93
58X-3, 102–104	533.22	28.27	50.52	1.97	1.41	2.63
58X-5, 54–56	535.74	26.53	49.73	2.11	1.55	2.78
58X-6, 42–44	537.12	25.32	49.04	2.12	1.59	2.88
59X-1, 103–105	539.73	23.15	45.42	2.12	1.6	2.80
59X-2, 123–125	541.43	27.83	51.48	2.01	1.45	2.79
59X-3, 125–127	542.95	25.43	48.66	2.05	1.53	2.82
60X-3, 40–42	551.60	24.70	53.08	2.73	2.05	3.50
60X-4, 48–50	553.18	26.81	51.26	2.00	1.46	2.91
60X-6, 10–12	555.80	27.89	51.82	1.96	1.41	2.82
61X-2, 78–80	559.98	25.74	49.29	1.97	1.46	2.85
62X-2, 122–124	569.92	27.63	50.28	2.00	1.45	2.69
62X-3, 116–118	571.36	28.05	51.38	1.99	1.43	2.75
62X-4, 109–111	572.79	26.43	49.29	1.98	1.46	2.75
62X-5, 135–137	574.55	27.55	49.63	1.91	1.38	2.63
63X-1, 130–132	578.00	28.15	52.20	2.02	1.45	2.83
63X-2, 115–117	579.35	29.00	52.13	1.96	1.39	2.70
63X-3, 136–138	581.06	27.76	51.01	1.98	1.43	2.76
63X-4, 63–65	581.83	29.78	53.93	1.90	1.33	2.80
63X-5, 100–102	583.70	33.30	57.56	1.82	1.21	2.75
64X-1, 1–3	586.21	32.15	57.50	1.88	1.28	2.90
64X-3, 74–76	589.94	29.68	53.10	1.91	1.34	2.72
64X-CC, 31–33	590.79	31.45	54.79	1.87	1.28	2.68
65X-1, 137–139	597.07	30.87	54.87	1.95	1.35	2.76
65X-2, 134–136	598.54	29.47	53.52	1.89	1.34	2.79
65X-3, 90–92	599.60	29.66	52.10	1.89	1.33	2.61
66X-1, 5–7	605.25	28.79	52.35	1.96	1.40	2.76
66X-CC, 12–14	605.91	23.81	44.78	2.04	1.55	2.63
67X-1, 108–110	615.78	26.62	49.62	2.02	1.49	2.75
68X-1, 126–128	625.46	27.32	50.55	1.96	1.42	2.76
68X-2, 77–79	626.47	26.91	50.12	1.93	1.41	2.77
69X-1, 60–62	634.30	25.65	48.36	1.98	1.47	2.75
70X-1, 4–6	643.24	26.96	48.43	1.92	1.40	2.58
71X-1, 105–107	653.75	27.50	50.92	1.97	1.43	2.78
71X-2, 98–100	655.18	20.11	40.57	2.03	1.62	2.75
71X-3, 55–57	656.25	23.26	45.41	2.04	1.57	2.79
72X-1, 102–105	663.22	20.91	41.91	2.15	1.70	2.77
72X-2, 93–95	664.63	23.55	44.75	2.06	1.58	2.67
72X-3, 114–116	666.34	4.99	11.19	2.43	2.31	2.44

through 12. Downcore profiles of wet-bulk density, porosity, water content, grain density, carbonate content, *P*-wave velocity, thermal conductivity, and shear strength are presented in Figure 22. To illustrate how high productivity and climatic cycles affect the physical properties of sediments, a comparison between carbonate content, organic carbon, and grain density and a comparison between GRAPE density, carbonate content, and wet-bulk density are shown in Figures 23 and 24, respectively. The changes in these parameters correlate well with the climatically controlled depositional environment and the two lithostratigraphic units (see "Lithostratigraphy" section). For comparison, the properties of the two lithostratigraphic units are summarized as follows:

Lithostratigraphic Unit I (0–451.2 mbsf) is subdivided into four subunits, which are readily apparent in the physical properties:

Subunit IA (0–101.7 mbsf) consists of a mixture of calcareous siliceous and siliceous calcareous ooze, which is characterized by numerous variations in carbonate content and grain density. The other index properties and thermal conductivity show a similar pattern (Fig. 22). For example, large changes in wet-bulk density parallel distinct changes in the concentrations of carbonate. *P*-wave velocity and shear strength data (Fig. 22) have only small variations, which appear to be independent from the variations in carbonate.

Subunit IB (101.7–175.7 mbsf) is a dominantly siliceous calcareous ooze, with high variations in carbonate content. The average values for this subunit of carbonate content, wet-bulk density, grain density, thermal conductivity, and shear strength (Fig. 22) are distinctly higher than in Subunit IA. The transition between Subunits IA and IB is marked by lows in carbonate content (20.27% at 99.4 mbsf) and in grain density (1.65 g/cm^3), which correspond to a diatom layer (J. Fenner, pers. comm., 1987).

Subunit IC (175.7–251.7 mbsf) is a siliceous calcareous ooze in which the average values of carbonate content, wet-bulk density, grain density, thermal conductivity, and shear strength are higher than in the previous subunits, illustrating a stepwise increase in these properties from Subunits IA through IC to ID. The lower part of Subunit IC and the transition between Subunits IC and ID are marked by a low in carbonate content that corresponds to lows in wet-bulk density and thermal conductivity and highs in porosity and water content (Fig. 22).

Subunit ID (251.7–451.2mbsf) consists of a nannofossil ooze that shows high carbonate content values of about 80%, with small variations throughout the subunit. Only at 322.2 and 404.7 mbsf does the carbonate content drop to 39.7% and 61.47%, respectively (Table 9), which corresponds at 322.2 mbsf to an increase in wet-bulk density and grain density and a decrease in porosity, shear strength, and water content (Fig. 22). The decrease in carbonate content at 322.2 mbsf may correspond mainly to dilution by increased concentrations of siliceous material, as shown by the low grain density of 2.52 g/cm^3. However, if the dissolution of carbonate is proportional to an increased concentration of siliceous material, the same effect would be seen. Because the decrease in carbonate content at 404.7 mbsf does not accompany the distinct changes in grain density observed above, siliceous material is believed to occur in only minor proportions.

In summary, Subunits IA through IC show high-amplitude changes in the concentrations of carbonate and in the physical properties. These changes diminish quite abruptly at the top of Subunit ID. In contrast to the other physical properties, the *P*-wave velocities are consistently low throughout Unit I with two exceptions, at 186.7 mbsf (2058 m/s, hard sediment layer) and at 428.14 mbsf (1994 m/s, indurated chalk) (Fig. 22).

Lithostratigraphic Unit I (0–451.2 mbsf, middle Miocene to Pleistocene)

Subunit IA (0–101.7 mbsf, uppermost Pliocene to Pleistocene)

		Mean	Maximum	Minimum
Wet-bulk density	(g/cm^3)	1.37	1.66	1.23
Dry-bulk density	(g/cm^3)	0.50	0.92	0.27
Grain density	(g/cm^3)	2.55	2.91	1.65
Porosity	(%)	81.90	88.12	67.82
Water content	(%)	64.34	78.63	42.38
Carbonate content	(%)	39.58	94.24	4.67
Thermal conductivity	(W/m/K)	0.933	1.483	0.459
Shear strength	(kPa)	12.2	30.3	3.5
P-wave velocity	(m/s)	1568	1613	1528

Subunit IB (101.7-175.7 mbsf, upper Pliocene)

		Mean	Maximum	Minimum
Wet-bulk density	(g/cm^3)	1.51	1.77	1.32
Dry-bulk density	(g/cm^3)	0.75	1.09	0.39
Grain density	(g/cm^3)	2.64	2.86	2.44
Porosity	(%)	73.13	86.64	60.92
Water content	(%)	51.51	70.39	36.79
Carbonate content	(%)	59.05	89.24	12.84
Thermal conductivity	(W/m/K)	1.105	1.438	0.843
Shear strength	(kPa)	37.5	135.0	11.6
P-wave velocity	(m/s)	1570	1703	1526

Subunit IC (175.7–251.7 mbsf, uppermost Miocene to upper Pliocene)

		Mean	Maximum	Minimum
Wet-bulk density	(g/cm^3)	1.61	1.77	1.32
Dry-bulk density	(g/cm^3)	0.90	1.31	0.55
Grain density	(g/cm^3)	2.66	2.88	2.11
Porosity	(%)	67.49	80.11	55.56
Water content	(%)	44.63	62.26	30.92
Carbonate content	(%)	61.51	87.74	1.00
Thermal conductivity	(W/m/K)	1.232	1.550	0.838
Shear strength	(kPa)	64.4	107.0	20.9
P-wave velocity	(m/s)	1594	2059	1522

Subunit ID (251.7–451.2 mbsf, uppermost lower Miocene to uppermost Miocene)

		Mean	Maximum	Minimum
Wet-bulk density	(g/cm^3)	1.85	2.03	1.71
Dry-bulk density	(g/cm^3)	1.26	1.53	0.71
Grain density	(g/cm^3)	2.76	2.95	2.52
Porosity	(%)	56.00	81.87	47.35
Water content	(%)	32.03	61.75	24.83
Carbonate content	(%)	82.98	94.50	39.70
Thermal conductivity	(W/m/K)	1.506	1.798	1.236
Shear strength	(kPa)	74.8	238.9	11.6
P-wave velocity	(m/s)	1622	1994	1541

Lithostratigraphic Unit II (451.2–671.7 mbsf) is subdivided into Subunit IIA, a micrite-bearing nannofossil chalk (451.2–491.2 mbsf), and Subunit IIB, a micritic indurated nannofossil chalk (491.2–671.7 mbsf). The overall pattern of physical properties in Unit II illustrates a decrease in porosity and water content with depth, with one major excursion at the bottom of the sediment column that corresponds to a distinct decrease in carbonate content (Fig. 22). Wet-bulk densities and grain densities (Fig. 22) display some erratic values, especially at and below the diagenetic transition (480–550 mbsf) from nannofossil chalk to indurated nannofossil chalk. A major change is also noted in *P*-wave velocities at about 505 mbsf (Fig. 22), which marks more clearly the distinct increase in diagenesis. This is the first instance of *P*-wave velocities increasing steadily to a value of about 2000 m/s. Below 600 mbsf, velocities show more variability, in the range from 1700 to 2500 m/s, and reach a maximum of about 4071 m/s in a limestone at 666.32 mbsf. The low velocities at these depths are more likely indicative of drilling disturbance, and the higher values may be more representative.

Lithostratigraphic Unit II (451.2–671.7 mbsf, lower Oligocene to upper lower Miocene)

Subunit IIA (451.2–491.2 mbsf, upper lower Miocene to middle Miocene)

		Mean	Maximum	Minimum
Wet-bulk density	(g/cm^3)	1.96	2.20	1.65
Dry-bulk density	(g/cm^3)	1.37	1.59	1.09
Grain density	(g/cm^3)	2.86	3.00	2.76
Porosity	(%)	54.80	58.81	51.33
Water content	(%)	30.07	34.33	27.51
Carbonate content	(%)	82.04	88.74	73.73
Thermal conductivity	(W/m/K)	1.554	1.759	1.280
Shear strength	(kPa)	52.9	59.3	46.5
P-wave velocity	(m/s)	1674	1742	1577

Subunit IIB (491.2–671.7 mbsf, lower Oligocene to upper lower Miocene)

		Mean	Maximum	Minimum
Wet-bulk density	(g/cm^3)	2.03	2.73	1.82
Dry-bulk density	(g/cm^3)	1.47	2.31	1.21
Grain density	(g/cm^3)	2.80	3.59	2.44
Porosity	(%)	50.84	59.73	11.19
Water content	(%)	27.55	33.94	4.99
Carbonate content	(%)	82.51	90.99	59.05
Thermal conductivity	(W/m/K)	1.532	1.839	1.108
P-wave velocity	(m/s)	1977	4071	1655

Discussion and Conclusions

The physical properties of sediments are highly variable in an oceanic upwelling area at the polar front of the Southern Ocean. The variations in grain density (Fig. 22), in particular, are proxy indicators for the concentration of siliceous material (Mienert et al., 1988) and show an overall pattern of a stepwise increase in the concentration of siliceous material from about 6 Ma, with a distinct increase and change in the amplitude of the variability from about 2.6 Ma. The grain density and carbonate content are inversely correlated (Fig. 23), as are carbonate and organic carbon. Low grain densities (less than 2.6 g/cm^3) correspond to low carbonate content values and high values of organic carbon. Detailed investigations in upwelling areas off Northwest Africa have shown that high concentrations of organic carbon correspond to high biologic productivity in the surface waters (Thiede et al., 1982). Thus, our preliminary results may indicate a distinct increase in productivity since the middle Pliocene.

The marked changes in the amplitudes of the physical properties, however, occurred by about 6.2 Ma (approx. 246 mbsf), based on biostratigraphic and magnetostratigraphic data (see "Biostratigraphy" and "Paleomagnetics" sections, respectively, this chapter). Although *P*-wave velocities are quite uniform throughout this interval, wet-bulk densities show distinct changes that may give rise to a distinct sequence of reflectors.

The periodicity observed in the wet-bulk density and GRAPE records correlates quite well with the carbonate content record. Biostratigraphic and magnetostratigraphic data ("Biostratigraphy" and "Paleomagnetics" sections, respectively) give an age of 2.45 Ma for the depth interval at approximately 168 mbsf. The periodicity of the wet-bulk density, the GRAPE density, and the carbonate content gives an average cycle of approximately 75,000 for this period of time. Thus, the high-resolution GRAPE data are certainly valuable to explore whether Milankovitch cycles are contained in this sedimentological record, and as such, they will be analyzed in more detailed shore-based studies.

SEISMIC STRATIGRAPHY

Site 704 is located on the southern part of the Meteor Rise (46°52.758′S, 07°25.231′E) in a water depth of 2532.3 m, on a plain west of and deeper than (~1000 m) the crestal area (Fig. 25). A 0.8-s-thick (TWT) section of pelagic sediments was deposited on a 40-km-wide, level or gently westward-sloping basement surface in the southern part of the site survey area, which changes to the north into a synclinal trough about 20 km wide (Fig. 25).

JOIDES Resolution acquired seismic data on approach and departure from Site 704 (Fig. 25). The sediments at Site 704 are predominantly carbonates, with a varying biosiliceous component down to about 250 mbsf (Fig. 26). At 451 mbsf the nannofossil ooze changes into micrite-bearing chalk that is further altered to indurated chalk at 491.2 mbsf. The wet-bulk density closely reflects the downhole variation in carbonate content in the ooze and varies by as much as 50%. On the other hand, *P*-wave velocity measured on samples is nearly constant (1500–1650 m/s) down to 450 mbsf, from where it increases gradually across the chalk/indurated chalk transition to about 2000 m/s. The *in-situ* sonic log shows low velocities between 120 and 245 mbsf, except for two intervals that correlate with higher resistivities and lower values of carbonate content. At 245 mbsf, the velocity increases linearly from 1700 to 2300 m/s at the bottom of the hole. Therefore, the acoustic impedance, or reflectivity, is directly related to the CaCO$_3$ content, as documented by Mayer (1979). We note that the amplitude of fluctuations in carbonate content and wet-bulk density is particulary high above 175 mbsf, intermediate from 175–330 mbsf, and small below this depth. In

Table 9. Calcium carbonate content, Site 704.

Sample (cm)	Depth (mbsf)	Carbonate (%)
Hole 704A:		
1H-1, 100–102	1.00	51.62
1H-2, 100–102	2.50	85.74
1H-3, 100–102	4.00	36.20
1H-4, 130–132	5.80	92.32
1H-5, 111–113	7.11	24.52
2H-1, 30–32	7.50	94.24
2H-1, 100–102	8.20	68.89
2H-2, 100–102	9.70	36.03
2H-3, 100–102	11.20	6.76
2H-4, 100–102	12.70	70.39
2H-5, 100–102	14.20	61.80
2H-6, 130–132	16.00	20.60
3H-1, 30–32	17.00	25.44
3H-1, 100–102	17.70	61.38
3H-2, 100–102	19.20	38.78
3H-3, 110–112	20.80	61.55
4H-3, 20–22	29.40	83.40
4H-3, 100–102	30.20	52.21
4H-5, 80–82	33.00	65.39
4H-6, 35–37	34.05	36.36
5H-1, 100–102	36.70	85.57
5H-3, 100–102	39.70	38.53
5H-4, 100–102	41.20	30.61
5H-5, 100–102	42.70	73.73
5H-6, 100–102	44.20	20.10
6H-1, 100–102	46.20	48.04
6H-3, 100–102	49.20	30.36
6H-4, 100–102	50.70	28.77
6H-5, 50–52	51.70	57.71
6H-5, 100–102	52.20	9.09
6H-6, 100–102	53.70	47.96
7H-1, 108–110	55.78	17.68
7H-2, 102–104	57.22	53.04
7H-3, 102–104	58.72	19.27
7H-4, 102–104	60.22	51.79
7H-5, 102–104	61.72	25.85
7H-6, 40–42	62.60	15.60
8H-1, 100–102	65.20	64.05
8H-3, 53–54	67.72	60.72
8H-3, 100–102	68.20	10.01
8H-4, 90–92	69.90	26.44
8H-5, 40–42	70.60	27.36
8H-6, 60–62	72.30	37.53
9H-1, 100–102	74.70	50.54
9H-2, 100–102	76.20	31.36
9H-3, 100–102	77.70	54.54
9H-4, 100–102	79.20	64.80
9H-5, 100–102	80.70	10.26
9H-6, 100–102	82.20	10.17
10H-1, 99–101	84.19	11.18
10H-2, 99–101	85.69	51.79
10H-3, 99–101	87.19	26.94
10H-4, 105–107	88.75	23.44
10H-5, 99–101	90.19	4.67
10H-6, 99–101	91.69	16.51
11H-1, 100–102	93.70	31.19
11H-3, 100–102	96.70	17.10
11H-4, 110–112	98.30	44.28
11H-5, 70–72	99.40	20.27
11H-6, 30–32	100.50	36.86
11H-7, 20–22	101.90	84.32
12H-1, 58–60	102.78	63.22
12H-2, 58–60	104.28	33.86
12H-3, 58–60	105.78	59.80
12H-5, 58–60	108.78	76.48
12H-5, 58–60	110.28	73.89
13H-1, 100–102	112.70	21.68
13H-2, 30–32	113.50	58.96
13H-2, 100–102	114.20	23.10
13H-3, 100–102	115.70	75.64
13H-4, 100–102	117.20	52.54
14H-1, 100–102	122.28	77.40
14H-2, 30–32	123.00	12.84
14H-2, 100–102	123.70	61.47
14H-4, 100–102	126.70	44.45
Hole 704A (continued):		
14H-5, 100–102	128.20	45.87
14H-5, 130–132	128.50	89.24
15H-1, 100–102	131.70	74.56
15H-2, 100–102	133.20	50.96
15H-3, 100–102	134.70	49.87
15H-5, 100–102	137.70	38.79
16H-2, 100–102	142.70	23.35
16H-3, 100–102	144.20	77.22
16H-4, 100–102	145.70	79.81
16H-5, 100–102	147.20	41.28
17X-2, 100–102	152.20	82.90
17X-3, 100–102	153.70	66.20
17X-4, 100–102	155.20	64.80
17X-5, 100–102	156.70	64.89
18X-1, 100–102	160.20	75.89
18X-2, 100–102	161.70	50.71
18X-3, 125–127	163.45	54.79
18X-4, 100–102	164.70	73.73
18X-5, 100–102	166.20	57.46
18X-6, 60–62	167.30	35.44
19X-2, 100–102	171.20	58.05
19X-3, 100–102	172.70	72.47
19X-4, 100–102	174.20	88.99
19X-5, 100–102	175.70	41.95
19X-6, 100–102	177.20	80.56
20X-1, 100–102	179.20	72.39
20X-2, 100–102	180.70	72.22
20X-3, 100–102	182.20	75.81
20X-4, 100–102	183.70	85.82
20X-5, 100–102	185.20	82.23
20X-6, 100–102	186.70	72.23
21X-1, 100–102	188.70	83.07
21X-2, 100–102	190.20	87.74
21X-3, 100–102	191.70	81.06
21X-4, 70–72	192.90	71.47
22X-1, 100–102	198.20	68.47
22X-2, 100–102	199.70	60.46
22X-3, 100–102	201.20	51.79
22X-4, 100–102	202.70	77.81
22X-5, 100–102	204.20	78.90
23X-1, 100–102	207.70	82.90
23X-2, 100–102	209.20	74.98
23X-3, 100–102	210.70	77.81
23X-4, 100–102	212.20	69.72
23X-5, 100–102	213.70	62.72
24X-2, 82–84	218.52	63.22
24X-3, 82–84	220.02	57.80
24X-4, 82–84	221.52	35.78
24X-5, 82–84	223.02	48.46
25X-1, 130–132	227.00	43.95
25X-2, 130–132	228.50	1.00
25X-3, 90–92	229.60	75.39
25X-4, 90–92	231.10	41.20
25X-5, 50–52	232.20	57.88
25X-6, 50–52	233.70	39.53
Hole 704B:		
1H-2, 110–112	2.60	20.02
1H-4, 110–112	5.60	38.45
2H-3, 110–112	10.80	61.47
2H-5, 110–112	13.80	47.12
3H-2, 110–112	18.80	37.28
3H-4, 110–112	21.80	61.30
4H-2, 110–112	28.30	30.69
4H-4, 110–112	31.30	63.72
6H-2, 100–102	47.20	45.45
6H-5, 100–102	51.70	16.60
7H-3, 100–102	58.20	20.93
7H-5, 100–102	61.20	58.96
8H-3, 30–32	66.66	54.04
8H-3, 110–112	67.46	21.10
9H-1, 110–112	74.30	24.52
9H-5, 110–112	80.30	50.87
10H-2, 110–112	85.30	13.51
10H-5, 110–112	89.80	61.38
Hole 704B (continued):		
11H-2, 110–112	94.80	8.01
11H-6, 110–112	100.80	13.93
12H-2, 110–112	104.30	45.54
12H-5, 110–112	108.80	79.90
13H-1, 110–112	112.30	19.52
13H-4, 110–112	116.80	77.40
14H-1, 110–112	121.80	63.72
14H-4, 110–112	126.30	74.06
15H-2, 110–112	131.94	73.98
15H-5, 110–112	136.44	72.81
17X-2, 100–102	149.70	54.04
17X-4, 100–102	152.70	53.96
18X-3, 110–112	160.80	52.63
18X-6, 110–112	165.30	55.79
19X-2, 90–92	168.60	53.63
22X-1, 100–102	195.70	50.04
23X-2, 100–102	206.70	67.55
23X-3, 100–102	208.20	79.90
23X-4, 100–102	209.70	73.39
23X-5, 100–102	211.20	77.73
24X-1, 100–102	214.70	71.56
24X-2, 100–102	216.20	78.31
24X-3, 100–102	217.70	67.47
24X-4, 100–102	219.20	47.54
24X-5, 100–102	220.70	68.05
24X-6, 100–102	222.20	16.35
25X-1, 100–102	224.20	31.36
25X-2, 100–102	225.70	63.72
25X-3, 50–52	226.70	49.46
25X-4, 50–52	228.20	8.01
25X-5, 100–102	230.20	58.80
25X-6, 100–102	231.70	61.55
26X-1, 100–102	233.70	60.21
26X-2, 100–102	235.20	50.12
26X-3, 100–102	236.70	59.13
26X-4, 100–102	238.20	44.20
27X-2, 100–102	244.70	68.42
27X-3, 60–62	245.80	25.92
27X-4, 100–102	247.70	77.92
27X-5, 75–77	248.95	64.33
27X-6, 100–102	250.70	83.25
28X-1, 110–112	252.80	86.33
28X-2, 110–112	254.30	70.33
28X-3, 110–112	255.80	93.75
28X-4, 100–102	257.20	88.92
28X-5, 100–102	258.70	87.83
28X-6, 110–112	260.30	83.92
29X-1, 90–92	262.10	72.60
29X-2, 90–92	263.60	94.50
29X-3, 90–92	265.10	81.83
29X-4, 90–92	266.60	84.33
29X-5, 90–92	268.10	84.83
29X-6, 90–92	269.60	65.58
30X-1, 100–102	271.70	66.67
30X-2, 100–102	273.20	75.23
30X-3, 100–102	274.70	93.49
30X-4, 100–102	276.20	82.82
30X-7, 100–102	278.70	68.14
31X-1, 100–102	281.20	81.48
31X-2, 100–102	282.70	86.24
31X-3, 100–102	284.20	90.57
31X-4, 100–102	285.70	95.49
31X-5, 100–102	287.20	89.91
31X-6, 100–102	288.70	84.48
32X-1, 100–102	290.70	84.15
32X-2, 100–102	292.20	86.99
32X-3, 100–102	293.70	90.91
32X-4, 100–102	295.20	91.49
32X-5, 100–102	296.70	68.89
32X-6, 100–102	298.20	87.74
33X-1, 100–102	300.20	92.99
33X-2, 100–102	301.70	79.56
33X-3, 100–102	303.20	88.74
33X-4, 100–102	304.70	87.57
33X-5, 100–102	306.20	86.07

Table 9 (continued).

Sample (cm)	Depth (mbsf)	Carbonate (%)
Hole 704B (continued):		
33X-6, 100–102	307.70	62.88
34X-1, 100–102	309.70	92.99
34X-2, 100–102	311.20	88.07
34X-3, 100–102	312.70	93.07
34X-4, 100–102	314.20	87.99
34X-5, 100–102	315.70	82.82
34X-6, 100–102	317.20	86.07
35X-1, 100–102	319.20	78.73
35X-2, 100–102	320.70	71.14
35X-3, 100–102	322.20	39.70
35X-4, 100–102	323.70	46.04
35X-4, 100–102	325.20	69.39
35X-6, 100–102	326.70	83.48
36X-1, 100–102	328.70	90.49
36X-2, 97–99	330.17	91.24
37X-3, 100–102	339.70	81.15
37X-3, 100–102	341.20	89.92
39X-1, 100–102	357.20	91.16
39X-2, 100–102	358.70	89.07
39X-3, 100–102	360.20	92.16
39X-4, 100–102	361.70	91.99
39X-5, 100–102	363.20	92.91
39X-6, 100–102	364.70	93.24
40X-1, 98–100	366.68	87.82
40X-2, 98–100	368.18	81.57
40X-3, 98–100	369.68	81.73
40X-4, 98–100	371.18	81.06
40X-5, 98–100	372.68	78.40
40X-6, 98–100	374.18	79.90
41X-1, 101–103	376.21	89.15
41X-2, 101–103	377.71	79.73
41X-3, 101–103	379.21	79.48
41X-4, 101–103	380.71	85.99
41X-5, 101–103	382.21	85.99
41X-6, 101–103	383.71	79.56
42X-2, 99–101	387.19	75.14
42X-4, 99–101	390.19	90.99
42X-6, 99–101	392.76	82.40
43X-1, 100–102	395.20	89.91
43X-4, 100–102	398.70	81.32
43X-7, 50–52	401.80	84.57
44X-1, 100–102	404.78	61.47
45X-1, 101–103	414.21	88.99
45X-2, 101–103	415.71	88.57
46X-2, 101–103	425.31	94.16
46X-3, 101–103	426.71	82.15
46X-4, 94–96	428.14	84.15
47X-2, 90–92	434.60	73.89
47X-4, 90–92	437.60	71.72
48X-1, 100–102	442.70	85.90
48X-3, 100–102	445.70	79.73
49X-2, 83–85	453.53	73.73
49X-5, 135–137	458.55	79.73
50X-1, 50–51	461.20	80.90
52X-1, 100–102	473.20	85.57
52X-4, 98–100	477.68	83.57
53X-2, 115–117	484.35	88.74
54X-1, 103–105	492.23	87.07
54X-3, 100–102	495.20	89.49
54X-5, 100–102	498.20	84.07
55X-2, 70–75	502.90	86.07
55X-4, 54–56	505.74	78.07
55X-5, 95–97	507.65	88.90
55X-6, 74–76	508.94	90.10
56X-2, 25–27	511.95	86.40
56X-3, 57–59	513.77	88.40
56X-4, 62–64	515.32	80.81
57X-2, 93–95	522.13	88.32
57X, CC (26–28)	523.86	78.23
58X-2, 78–80	531.48	85.07
58X-3, 102–104	533.22	85.40
58X-5, 54–56	535.74	86.57
58X-6, 42–44	537.12	82.23
59X-1, 103–105	539.73	86.32
59X-2, 123–125	541.43	86.82
59X-3, 125–127	542.95	86.32
60X-3, 40–42	551.60	86.32
60X-4, 48–50	553.18	90.07
60X-6, 10–12	555.80	86.32
61X-2, 78–80	559.98	84.57
62X-2, 122–124	569.92	75.14
62X-3, 116–118	571.36	85.49
62X-4, 109–111	572.79	76.98
62X-5, 135–137	574.55	78.98
63X-1, 130–132	578.00	85.07
63X-2, 115–117	579.35	86.40
63X-3, 136–138	581.06	80.40
63X-4, 63–65	581.83	80.98
63X-5, 100–102	583.70	87.57
64X-1, 1–3	586.21	80.90
64X-3, 74–76	589.94	89.57
64X, CC (31–33)	590.79	68.39
65X-1, 137–139	597.07	81.23
65X-2, 134–136	598.54	79.65
65X-3, 90–92	599.60	71.81
66X-1, 5–7	605.25	74.98
66X, CC (12–14)	605.91	80.90
67X-1, 108–110	615.78	90.99
68X-1, 126–128	625.46	78.40
68X-2, 77–79	626.47	79.98
69X-1, 60–62	634.30	89.99
70X-1, 4–6	643.24	80.06
71X-1, 105–107	653.75	74.31
71X-2, 98–100	655.18	78.40
71X-3, 55–57	656.25	68.97
72X-1, 104–105	663.24	86.40
72X-2, 93–95	664.63	84.90
72X-3, 114–115	666.34	59.05

the seismic-reflection record, this corresponds to the upper 220 ms (TWT) of the section with short continuous reflections, the underlying 230–440 ms acoustically stratified interval, and the deeper, less reflective sediments, respectively. In relating traveltime to depth we use velocities derived from the sonic log (see "Logging" section).

The reflection at 220 ms, or 175 mbsf, truncates reflection events west of Site 704 and is therefore associated with a major unconformity separating units of differing reflection character and pattern of carbonate fluctuations (Fig. 26). The upper and lower boundaries of the carbonate low, between 40 and 100 mbsf, are represented by surprisingly weak reflections. A major shift in wet-bulk density occurs at the base of a low-carbonate interval at 245 mbsf. The associated reflection event shows that the stratigraphic position of this shift is related to an erosional event, rather than to a continuous change in carbonate supply, as underlying strata are truncated upslope from Site 704. The brief carbonate low at 320 mbsf corresponds to an event at 400 ms depth in the reflection record, but is about 30 m above the base of the highly reflective unit.

At depth, the change in diagenetic maturity represented by the transition from micrite-bearing chalk to indurated chalk at 491 mbsf is associated with a fluctuation of wet-bulk density over a 60 m interval. Three seismic-reflection events corresponds to this interval, with the deepest event possibly having a phase reversal. Drilling was terminated at 671.7 mbsf when the penetration rate decreased drastically in hard, lower upper Oligocene carbonate rocks that have velocities of about 4 km/s. This level corresponds to the first arrival of the train of multiple reflections at 4.2 s (Fig. 26).

The acoustic and physical properties of deep-sea carbonates and their relation to the paleoceanographic record have been

Table 10. ***P*-wave velocity, Site 704.**

Sample (cm)	Depth (mbsf)	Direction	Velocity (m/s)
Hole 704A:			
1H-2, 80–82	2.30	C	1548.9
1H-5, 20–22	6.20	C	1543.7
2H-2, 100–102	9.70	C	1555.1
2H-3, 100–102	11.20	C	1529.2
2H-4, 100–102	12.70	C	1582.5
2H-6, 100–102	15.70	C	1558.2
3H-2, 100–102	19.20	C	1563.3
4H-3, 100–102	30.20	C	1588.5
5H-3, 100–102	39.70	C	1574.0
5H-5, 100–102	42.70	C	1595.9
5H-6, 100–102	44.20	C	1587.1
6H-3, 40–42	48.60	C	1612.7
6H-4, 100–102	50.70	C	1571.8
6H-6, 100–102	53.70	C	1588.6
7H-1, 110–112	55.80	C	1584.0
7H-2, 100–102	57.20	C	1579.8
7H-3, 102–104	58.72	C	1588.8
7H-4, 100–102	60.20	C	1575.4
8H-3, 50–52	67.70	C	1590.1
8H-3, 100–102	68.20	C	1583.4
8H-5, 40–42	70.60	C	1571.1
9H-2, 100–102	76.20	C	1573.1
9H-4, 100–102	79.20	C	1553.0
9H-6, 100–102	82.20	C	1577.3
10H-2, 98–100	85.68	C	1611.2
10H-4, 106–108	88.76	C	1582.6
10H-6, 100–102	91.70	C	1588.8
11H-1, 100–102	93.70	C	1566.7
11H-4, 110–112	98.30	C	1584.7
11H-6, 30–32	100.50	C	1585.3
12H-2, 60–62	104.30	C	1582.7
12H-4, 60–62	107.30	C	1628.3
12H-6, 60–62	110.30	C	1603.4
13H-1, 100–102	112.70	C	1572.7
13H-2, 38–40	113.58	C	1574.4
13H-3, 100–102	115.70	C	1703.0
13H-4, 100–102	118.70	C	1613.8
14H-1, 100–102	122.20	C	1557.5
14H-2, 38–40	123.08	C	1576.7
14H-2, 100–102	123.70	C	1567.6
14H-4, 100–102	126.70	C	1563.6
15H-2, 100–102	133.20	C	1547.2
15H-4, 100–102	136.20	C	1526.0
16H-2, 100–102	142.70	C	1556.1
16H-4, 100–102	145.70	C	1588.5
17X-2, 100–102	152.20	C	1620.3
17X-6, 100–102	158.20	C	1635.4
18X-2, 100–102	161.70	C	1565.4
18X-5, 100–102	166.20	C	1508.0
19X-3, 100–102	172.70	C	1607.5
19X-5, 100–102	175.70	C	1575.9
20X-2, 100–102	180.70	C	1593.8
20X-4, 100–102	183.70	C	1616.9
20X-6, 100–102	186.70	C	2058.5
21X-2, 100–102	190.20	C	1671.8
21X-4, 69–71	192.89	C	1521.8
22X-2, 100–102	199.70	C	1566.4
22X-4, 100–102	202.70	C	1581.3
23X-2, 100–102	209.20	C	1610.2
23X-4, 100–102	212.20	C	1581.3
24X-2, 80–82	218.50	C	1570.3
24X-4, 80–82	221.50	C	1552.6
25X-2, 130–132	229.50	C	1583.2
25X-4, 90–92	231.10	C	1573.6
25X-6, 50–52	233.70	C	1578.3
Hole 704B:			
1H-4, 100–102	5.50	C	1562.6
2H-5, 100–102	13.70	C	1574.3
3H-4, 110–112	21.80	C	1591.8
4H-4, 110–112	31.30	C	1592.5
5H-6, 110–112	43.80	C	1554.5
6H-4, 110–112	50.30	C	1586.1
7H-3, 110–112	58.30	C	1543.5
8H-3, 110–112	67.46	C	1542.5
Hole 704B (cont):			
9H-3, 110–112	77.30	C	1530.7
10H-4, 110–112	88.30	C	1528.4
11H-4, 110–112	97.80	C	1534.3
12H-4, 110–112	106.30	C	1546.4
13H-4, 110–112	116.80	C	1530.0
14H-4, 110–112	126.30	C	1541.2
15H-5, 110–112	136.44	C	1578.5
17H-5, 110–112	154.30	C	1576.6
18H-5, 110–112	162.80	C	1553.2
19H-2, 90–92	168.60	C	1557.3
23X-2, 100–102	206.70	C	1579.9
23X-4, 100–102	209.70	C	1570.2
24X-2, 100–102	216.20	C	1577.5
24X-4, 100–102	219.20	C	1547.9
24X-6, 100–102	222.20	C	1607.9
25X-2, 100–102	225.70	C	1558.8
25X-4, 50–52	228.20	C	1569.4
25X-6, 100–102	231.70	C	1552.5
26X-2, 100–102	235.20	C	1563.7
26X-4, 100–102	238.20	C	1549.8
27X-2, 100–102	244.70	C	1552.1
27X-4, 100–102	247.70	C	1560.5
27X-6, 100–102	250.70	C	1611.6
28X-2, 110–112	254.30	C	1541.2
28X-4, 100–102	257.20	C	1577.1
28X-6, 110–112	260.30	C	1567.1
29X-2, 90–92	263.60	C	1585.9
29X-4, 90–92	266.60	C	1587.4
29X-6, 90–92	269.60	C	1625.3
30X-7, 100–102	278.70	C	1563.7
31X-2, 100–102	282.70	C	1600.5
31X-4, 100–102	285.70	C	1633.2
31X-6, 100–102	288.70	C	1625.0
32X-2, 100–102	292.20	C	1582.9
32X-4, 100–102	295.20	C	1592.0
32X-6, 100–102	298.20	C	1633.2
33X-2, 100–102	301.70	C	1578.9
33X-4, 100–102	304.70	C	1582.8
33X-6, 100–102	307.70	C	1607.1
34X-2, 100–102	311.20	C	1606.0
34X-4, 100–102	314.20	C	1602.9
34X-6, 100–102	317.20	C	1608.0
35X-2, 100–102	320.70	C	1565.2
35X-4, 100–102	323.70	C	1567.6
36X-2, 100–102	330.20	C	1615.1
37X-2, 100–102	339.70	C	1579.4
39X-2, 100–102	358.70	C	1593.3
39X-4, 100–102	361.70	C	1605.5
40X-2, 100–102	368.20	C	1599.7
40X-4, 100–102	371.20	C	1610.3
40X-6, 100–102	374.20	C	1612.1
41X-2, 100–102	377.70	C	1598.5
41X-4, 100–102	380.70	C	1582.8
41X-6, 100–102	383.70	C	1619.0
42X-2, 100–102	387.20	C	1597.0
42X-4, 100–102	390.20	C	1616.2
42X-6, 100–102	392.77	C	1631.8
43X-1, 100–102	395.20	C	1510.1
43X-1, 100–102	398.70	C	1646.5
43X-7, 50–52	401.80	C	1613.2
44X-1, 100–102	404.70	C	1610.4
45X-1, 100–102	414.20	C	1603.5
46X-2, 100–102	425.20	C	1607.7
46X-4, 94–96	428.14	A	1944.0
46X-4, 94–96	428.14	B	1945.9
46X-4, 94–96	428.14	C	1993.7
47X-2, 90–92	434.60	C	1549.2
47X-4, 90–92	437.60	C	1559.7
47X-6, 90–92	440.60	C	1633.9
48X-1, 100–102	442.70	C	1590.0
48X-3, 100–102	445.70	C	1671.2
49X-1, 100–102	452.20	C	1666.3
49X-3, 84–86	455.04	C	1702.7
49X-4, 135–137	457.05	C	1700.5
51X-1, 110–112	463.80	C	1577.4
52X-2, 110–112	474.80	C	1612.7

Table 10 (continued).

Sample (cm)	Depth (mbsf)	Direction	Velocity (m/s)
Hole 704B (cont):			
52X-4, 110–112	477.80	C	1685.4
53X-2, 120–122	484.40	C	1742.3
53X-2, 140–142	486.10	C	1708.0
54X-2, 140–142	494.10	C	1759.6
54X-4, 80–82	496.50	C	1726.6
55X-4, 60–62	505.80	C	1721.3
55X-5, 66–68	507.36	C	1894.1
55X-5, 80–82	507.50	C	1816.2
56X-2, 26–28	511.96	C	1840.5
56X-2, 142–144	513.12	C	1837.6
56X-3, 57–59	513.77	C	1866.2
56X-4, 60–62	515.30	C	2078.1
56X-4, 61–63	515.31	C	2156.9
57X-2, 90–92	522.10	C	1757.6
58X-2, 78–80	531.48	C	1896.7
58X-3, 102–104	533.22	C	1989.4
58X-5, 54–56	535.74	C	1925.7
58-6, 42–44	537.12	C	1928.6
59X-1, 103–105	539.73	C	1973.4
59X-1, 123–125	539.93	C	1853.4
59X-3, 125–127	542.95	C	1973.4
60X-3, 40–42	551.60	C	1947.4
60X-4, 48–50	553.18	C	2014.7
60X-6, 10–12	555.80	C	1897.4
61X-2, 78–80	559.98	C	2002.9
62X-2, 122–124	569.92	C	2000.0
62X-3, 116–118	571.36	C	1922.1
62X-4, 109–111	572.79	C	1892.3
62X-5, 135–137	574.55	C	2013.5
63X-1, 130–132	578.00	C	2123.7
63X-2, 115–117	579.35	C	1996.2
63X-3, 136–138	581.06	C	2097.6
63X-4, 63–65	581.83	C	2037.8
64X-1, 1–3	586.21	A	1921.1
64X-1, 1–3	586.21	B	1961.6
64X-1, 1–3	586.21	C	2017.7
64X-1, 110–112	587.30	C	1699.4
64X-3, 74–76	589.94	A	1972.1
64X-3, 74–76	589.94	B	1944.6
64X-3, 74–76	589.94	C	1892.9
64X, CC (31–33)	590.79	A	1891.5
64X, CC (31–33)	590.79	B	1996.4
65X, 137–139	597.07	A	1948.6
65X-1, 137–139	597.07	C	2005.8
65X-2, 134–136	598.54	C	1870.9
65X-3, 90–92	599.60	A	1882.9
65X-3, 90–92	599.60	B	1985.8
65X-3, 90–92	599.60	C	1939.5
66X-1, 5–7	605.25	A	1930.3
66X-1, 5–7	605.25	C	2068.6
66X, CC (12–14)	605.91	C	2220.9
67X-1, 108–110	615.78	C	1677.0
68X-1, 126–128	625.46	B	2093.0
68X-1, 126–128	625.46	C	2131.5
69X-1, 60–62	634.30	C	1655.0
70X-1, 4–6	643.24	B	1971.0
70X-1, 4–6	643.24	C	2020.2
71X-1, 105–107	653.75	C	1830.0
71X-2, 98–100	655.18	A	2134.3
71X-2, 98–100	655.18	B	2276.1
71X-2, 98–100	655.18	C	2269.2
72X-1, 102–104	663.22	C	1741.4
72X-2, 92–94	664.62	C	1725.6
72X-3, 112–114	666.32	C	4071.4

discussed by Mayer (1979) and Mayer et al. (1986). The reflection pattern is determined by the relationship between the stratigraphic thickness of individual changes in the carbonate content in relation to the seismic acquisition and processing parameters. The lower coherency of reflections in the upper 175 m at Site 704 is surprising, but may be due in part to thickness variations centered around values that essentially lead to cancellation of reflections generated by neighboring carbonate cycles. A semichaotic depositional pattern is another possibility, which is partly supported by the seismic-reflection record. We note, however, that the upper sediments have been laid down in an environment where the topographic slope has been minimal throughout the site's depositional history. The present dip of the strata at the bottom of the hole is about 1.5°. The stratigraphic level at 175 mbsf corresponds to the top of the Gauss Chron (see "Paleomagnetics" section) and may be associated with a major advance of the polar front at 2.6–2.47 Ma, as documented by Ciesielski and Grinstead (1986). The base of the highly reflective sediments at 360 mbsf is about 30 m deeper than the corresponding stratigraphic level of the first occurence of ice-rafted material at Site 513, at about 8.6 Ma (Ciesielski and Weaver, 1983). Thus, the climatic variations represented by modulation of the carbonate content of the sediments have generated a characteristic acoustic image of these deposits.

Although they were separated longitudinally by 500 km or less, there is an apparent difference in Paleogene carbonate sedimentation between the Meteor Rise and the Islas Orcadas Rise. The middle Eocene and older sediments on the Islas Orcadas Rise are 0.5–0.8 s thick and were deposited under quiet conditions with no sign of bottom current activity. Similarly, the deeper section on the Meteor Rise shows little evidence of current control, but extrapolation of the stratigraphy at Site 704 to the section above flat basement suggests that Eocene and older sediments may be only half as thick as those observed at Islas Orcadas Rise. This may indicate that at least the investigated part of Meteor Rise is a slightly younger feature or that the early Paleogene paleoceanographic regime separated the two rises into areas of different productivity. The second alternative seems less probably, considering the similarity of Eocene and Oligocene microfossil assemblages on both rises.

LOGGING

Downhole logging at Site 704 had three major objectives: (1) to obtain a continuous record of geophysical and geochemical data to tie in with the lithostratigraphy and to interpret sections with poor core recovery, (2) to obtain *in-situ* geophysical parameters (compressional-wave velocity, density, porosity, and electrical conductivity; Serra, 1984, 1987) to use in interpreting seismic-reflection data and to compare with laboratory physical-property measurements, and (3) to delineate the cyclicity between siliceous and calcareous oozes observed within the thick Miocene-Quaternary sedimentary sequence recovered at this site. Three logging runs were made, consisting of the following suite of Schlumberger logging tools:

1. Seismic-stratigraphic combination: borehole compensated sonic (BHC), natural gamma ray (GR), dual induction resistivity (SFLU, ILM, and ILD), and caliper (CALI).
2. Lithoporosity combination: lithodensity (LDT), neutron porosity (CNL), and natural gamma-ray spectrometry (NGT).
3. Geochemical combination: induced gamma-ray spectrometry (GST), aluminum clay tool (ACT), and natural gamma-ray spectrometry (NGT).

Thirty-six hr of logging time and 12 hr of rig-up and rig-down time were scheduled at this site, with all logs to be run open hole. Approximately 150 m of drill pipe and BHA was left in the top section of the hole. The geochemical combination string was run through pipe because of deteriorating hole conditions by the time this last logging run was started. Details of logging operations are discussed in the following.

Logging Operations

The condition of Hole 704B was good at the start of logging operations, and there was no need to use the side entry sub. Logging-related operations began at 0400 hr local time on 1

Table 11. Thermal conductivity, Site 704.

Sample (cm)	Depth (mbsf)	Thermal conductivity (W/m/K)
Hole 704A:		
1H-5, 65	6.65	1.4440
1H-5, 80	6.80	1.4590
2H-2, 100	9.70	0.8060
2H-4, 100	12.70	1.0230
3H-2, 100	19.20	0.8620
3H-4, 100	22.20	0.8550
5H-2, 100	38.20	1.4830
5H-4, 100	41.20	1.2090
6H-3, 100	49.20	0.9380
6H-5, 100	52.20	0.7480
7H-2, 100	57.20	1.0270
7H-4, 100	60.20	0.9210
8H-2, 100	66.70	0.8960
8H-4, 100	69.70	0.8170
9H-2, 100	76.20	0.8580
9H-5, 100	80.70	0.7930
10H-2, 100	85.70	0.9260
10H-4, 100	88.70	0.9390
11H-2, 90	95.10	0.8600
11H-4, 100	98.20	0.9050
12H-2, 100	104.70	1.1420
12H-4, 100	107.70	1.1630
12H-6, 100	110.70	1.2420
13H-1, 100	112.70	0.8570
13H-3, 100	115.70	1.2450
13H-5, 100	118.70	1.0150
14H-2, 100	123.70	1.0680
14H-4, 100	126.70	0.9280
14H-5, 100	128.20	1.3610
15H-4, 100	136.20	0.9640
15H-6, 100	139.20	0.9040
16H-2, 100	142.70	0.8430
16H-4, 100	145.70	1.2100
17X-2, 100	152.50	1.3660
17X-4, 100	155.20	1.0990
18X-2, 100	161.70	0.9770
18X-4, 100	164.70	1.0780
19X-2, 100	171.20	1.0910
19X-4, 100	174.20	1.4380
20X-2, 100	180.70	1.1770
20X-4, 100	183.70	0.8380
21X-1, 100	188.70	1.4540
21X-3, 100	191.70	1.3130
22X-2, 100	199.70	1.0590
22X-5, 100	204.20	1.3190
23X-2, 100	209.20	1.4490
23X-4, 100	212.20	1.4060
25X-2, 100	228.20	1.1450
25X-5, 100	232.70	1.1220
Hole 704B:		
1H-2, 100	2.50	0.7130
1H-4, 100	5.50	0.8830
2H-3, 100	10.70	0.6740
2H-5, 100	13.70	0.8940
3H-3, 100	20.20	0.9890
3H-5, 100	23.20	0.9800
4H-3, 100	29.70	0.9270
4H-5, 100	32.70	1.0460
5H-3, 100	39.20	0.8320
5H-5, 100	42.20	1.0240
6H-3, 100	48.70	0.8250
6H-5, 100	51.70	0.8220
7H-3, 100	58.20	0.4590
7H-5, 100	61.20	0.9690
8H-3, 100	67.36	0.9060
9H-3, 100	77.20	1.0190
9H-5, 100	80.20	0.9670
23X-2, 100	206.70	1.5500
23X-5, 100	211.20	1.3230
24X-2, 100	216.20	1.2020
24X-5, 100	220.70	1.4030
25X-2, 100	225.70	1.1700
25X-5, 100	230.20	0.9950
Hole 704B (cont.):		
26X-2, 100	235.20	1.2240
26X-4, 100	238.20	1.0900
27X-2, 100	244.70	1.2680
27X-5, 100	249.20	1.4440
28X-2, 100	254.20	1.4170
28X-5, 100	258.70	1.5410
29X-2, 100	263.70	1.5110
29X-5, 100	268.20	1.4120
31X-2, 100	282.70	1.6050
31X-5, 100	287.20	1.4780
32X-2, 100	292.20	1.6790
32X-5, 100	296.70	1.2980
33X-2, 100	301.70	1.6340
33X-5, 100	306.20	1.4950
34X-2, 100	311.20	1.7600
34X-5, 100	315.70	1.4270
35X-2, 100	320.70	1.3080
35X-5, 100	325.20	1.5620
36X-2, 100	330.20	1.4880
36X-3, 70	331.40	1.5000
37X-2, 100	339.70	1.4040
37X-5, 100	344.20	1.5320
39X-2, 100	358.70	1.4960
39X-5, 100	363.20	1.4930
40X-2, 100	368.20	1.4680
40X-5, 100	372.70	1.4050
41X-2, 100	377.70	1.3430
41X-5, 100	382.20	1.4970
42X-2, 100	387.20	1.4550
42X-4, 100	390.20	1.5790
43X-1, 100	395.20	1.5200
44X-1, 100	404.70	1.3870
45X-1, 100	414.20	1.7980
46X-2, 100	425.20	1.6220
46X-5, 100	429.70	1.6520
47X-2, 100	434.70	1.2360
47X-5, 100	439.20	1.5510
48X-1, 100	442.70	1.5360
48X-3, 100	445.70	1.6210
49X-2, 100	453.70	1.4090
49X-5, 100	458.20	1.7590
51X-1, 100	463.70	1.6550
52X-2, 100	474.70	1.2800
52X-4, 100	477.70	1.5400
53X-2, 100	484.20	1.6790
54X-2, 100	493.70	1.1080
54X-5, 100	498.20	1.5520
55X-2, 100	503.20	1.7420
55X-5, 100	507.70	1.7900
56X-2, 100	512.70	1.5140
56X-4, 100	515.70	1.3930
57X-2, 100	522.20	1.4780
58X-2, 100	531.70	1.4550
58X-5, 100	536.20	1.5190
59X-2, 100	541.20	1.4180
59X-4, 100	544.20	1.5170
60X-2, 100	550.70	1.6790
60X-5, 100	555.20	1.4260
61X-1, 100	558.70	1.4360
62X-2, 100	569.70	1.7190
62X-5, 100	574.20	1.8390
63X-2, 100	579.20	1.6350
63X-5, 100	583.70	1.3270
64X-2, 100	588.70	1.5580

May 1987 and concluded at 2100 hr on 2 May. The problems that we experienced with the heave motion compensator were possibly due to loss of pressure in the accumulator, and all of the logging runs were made without the compensator. The seas were quite rough, with heave averaging more than 3 m. Heave diminished throughout the logging operations and was greatly reduced during the third run (geochemical combination). Even

Table 12. Shear strength, Site 704.

Sample (cm)	Depth (mbsf)	Shear strength (kPa)
Hole 704A:		
1H-2, 100–102	2.50	11.6
1H-5, 50–52	6.50	9.3
2H-1, 100–102	8.20	11.6
2H-2, 100–102	9.70	9.3
2H-3, 100–102	11.20	9.3
2H-4, 100–102	12.70	7.0
2H-6, 100–102	15.70	9.3
3H-2, 100–102	19.20	9.3
4H-3, 100–102	30.20	11.6
5H-3, 100–102	39.70	4.7
5H-6, 100–102	44.20	7.0
6H-4, 100–102	50.70	4.7
6H-6, 100–102	53.70	5.8
7H-1, 110–112	55.80	8.1
7H-3, 102–104	58.72	18.6
7H-4, 100–102	60.20	27.9
8H-3, 50–52	67.70	11.6
8H-5, 40–42	70.60	16.3
9H-2, 100–102	76.20	11.6
9H-4, 100–102	79.20	11.2
9H-6, 100–102	82.20	22.1
10H-2, 98–100	85.68	14.0
10H-4, 106–108	88.76	19.8
10H-6, 100–102	91.70	3.5
11H-1, 100–102	93.70	5.8
11H-4, 110–112	98.3	30.3
11H-6, 30–32	100.50	17.5
12H-2, 60–62	104.30	17.5
12H-4, 60–62	107.30	18.6
12H-6, 60–62	110.30	32.6
13H-1, 100–102	112.70	14.0
13H-2, 100–102	114.20	18.6
13H-2, 38–40	113.58	16.3
13H-3, 100–102	115.70	14.0
13H-5, 100–102	118.70	11.6
14H-1, 100–102	122.20	41.9
14H-2, 30–32	123.00	60.5
14H-2, 100–102	123.70	32.6
14H-4, 100–102	126.70	93.1
15H-2, 100–102	133.20	46.5
15H-5, 100–102	137.70	51.2
16H-2, 100–102	142.70	32.6
16H-4, 100–102	145.70	44.2
17X-2, 100–102	152.20	18.6
17X-6, 100–102	158.20	51.2
18X-2, 100–102	161.70	23.3
18X-5, 100–102	166.20	18.6
19X-3, 95–97	172.65	41.9
19X-4, 110–112	174.30	27.9
19X-5, 100–102	175.70	135.0
20X-2, 100–102	180.70	30.3
20X-4, 100–102	183.70	20.9
20X-6, 100–102	186.70	36.1
21X-2, 100–102	190.20	44.2
21X-4, 69–71	192.89	100.1
22X-2, 100–102	199.70	23.3
22X-4, 100–102	202.70	46.5
23X-2, 100–102	209.20	75.6
23X-4, 100–102	212.20	96.6
24X-2, 80–82	218.50	55.9
24X-4, 80–82	221.50	95.4
25X-2, 130–132	228.50	104.7
25X-4, 90–92	231.10	107.0
Hole 704B:		
24X-2, 100–102	216.20	20.9
24X-4, 100–102	219.20	58.2
25X-2, 100–102	225.70	83.8
25X-4, 50–52	228.20	176.9
25X-6, 100–102	231.70	72.1
26X-2, 100–102	235.20	111.7
26X-4, 100–102	238.20	118.7
27X-2, 100–102	244.70	58.2
27X-4, 100–102	247.70	69.8
27X-6, 100–102	250.70	93.1
Hole 704B (cont.):		
28X-2, 110–112	254.30	104.7
28X-4, 100–102	257.20	69.8
28X-6, 110–112	260.30	59.3
29X-2, 90–92	263.60	11.6
29X-4, 90–92	266.60	69.8
29X-6, 90–92	269.60	93.1
30X-1, 100–102	271.70	64.0
30X-4, 100–102	276.20	72.1
30X-7, 100–102	278.70	83.8
31X-2, 100–102	282.70	86.1
31X-4, 100–102	285.70	55.9
31X-6, 100–102	288.70	90.8
32X-2, 100–102	292.20	83.8
32X-4, 100–102	295.20	55.9
32X-6, 100–102	298.20	74.5
33X-2, 100–102	301.70	51.2
33X-4, 100–102	304.70	34.9
33X-6, 100–102	307.70	111.7
34X-2, 100–102	311.20	41.9
34X-4, 100–102	314.20	23.3
34X-6, 100–102	317.20	79.1
35X-2, 100–102	320.70	86.1
35X-4, 100–102	323.70	193.2
36X-2, 100–102	330.20	72.1
37X-2, 100–102	339.70	41.9
39X-2, 100–102	358.70	74.5
39X-4, 100–102	361.70	58.2
40X-2, 100–102	368.20	54.7
40X-4, 100–102	371.20	102.4
40X-6, 100–102	374.20	126.8
41X-2, 100–102	377.70	62.8
41X-4, 100–102	380.70	48.9
41X-6, 100–102	383.70	64.0
42X-2, 100–102	387.20	41.9
42X-4, 100–102	390.20	45.4
42X-6, 100–102	392.77	64.0
43X-4, 100–102	398.70	130.3
43X-7, 50–52	401.80	81.4
44X-1, 100–102	404.70	65.2
45X-1, 100–102	414.20	48.9
46X-2, 100–102	425.20	27.9
47X-2, 90–92	434.60	65.2
47X-4, 90–92	437.60	95.4
47X-6, 90–92	440.60	48.9
48X-1, 100–102	442.70	43.1
48X-3, 100–102	445.70	283.9
49X-1, 100–102	452.20	59.3
51X-1, 100–102	463.70	46.5

with a working heave motion compensator, the heave experienced during the logging runs would have exceeded the operational limits of the compensator. The first run was the seismic-stratigraphic combination, BHC/GR/DIL/CALI, which was run up through open hole from 660 to 124 mbsf and through pipe and BHA to the mud line. The second run, with the litho-porosity combination (LDT/CNL/NGT/GPIT—data for the inclinometry (GPIT) tool are not presented here), began at 1400 hr and ended at 2030 hr on 1 May. This run was also conducted through open hole from 660 to 150 mbsf and through pipe and BHA from 150 mbsf to the mud line. A knot formed during this logging run forced us to cut approximately 520 m of cable and rehead the cable. All quality control parameters indicated the acquisition of good data; however, it appears that the bottom sections of the logs are suspect, possibly as a result of the cable coiling up to form a knot. The geochemical combination (GST/ACT/NGT) was started as soon as the cable was reheaded. A bridge was encountered just upon entering the open hole, and we decided to bring the drill string down and circulate, to be followed by logging through pipe, in consideration of the potential

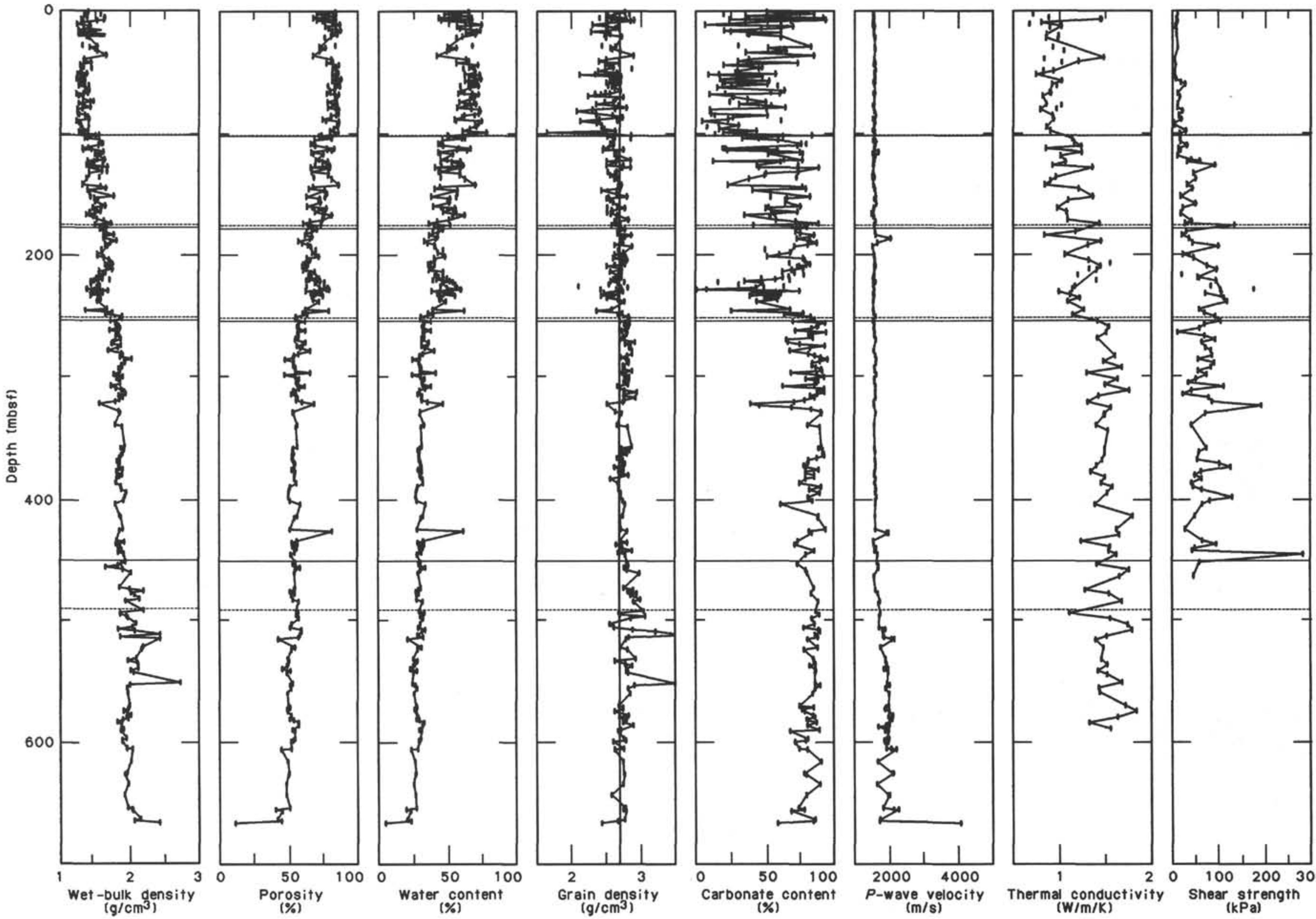

Figure 22. Wet-bulk density, porosity, water content, grain density, carbonate content, *P*-wave velocity, thermal conductivity, and shear strength profiles, Site 704. Triangles represent data from Hole 704A; dots represent data from Hole 704B. The boundaries between the lithostratigraphic units are indicated by a solid line, and the subunit divisions are shown by short dashed lines (single dashes for Hole 704A and double dashes for Hole 704B subunits).

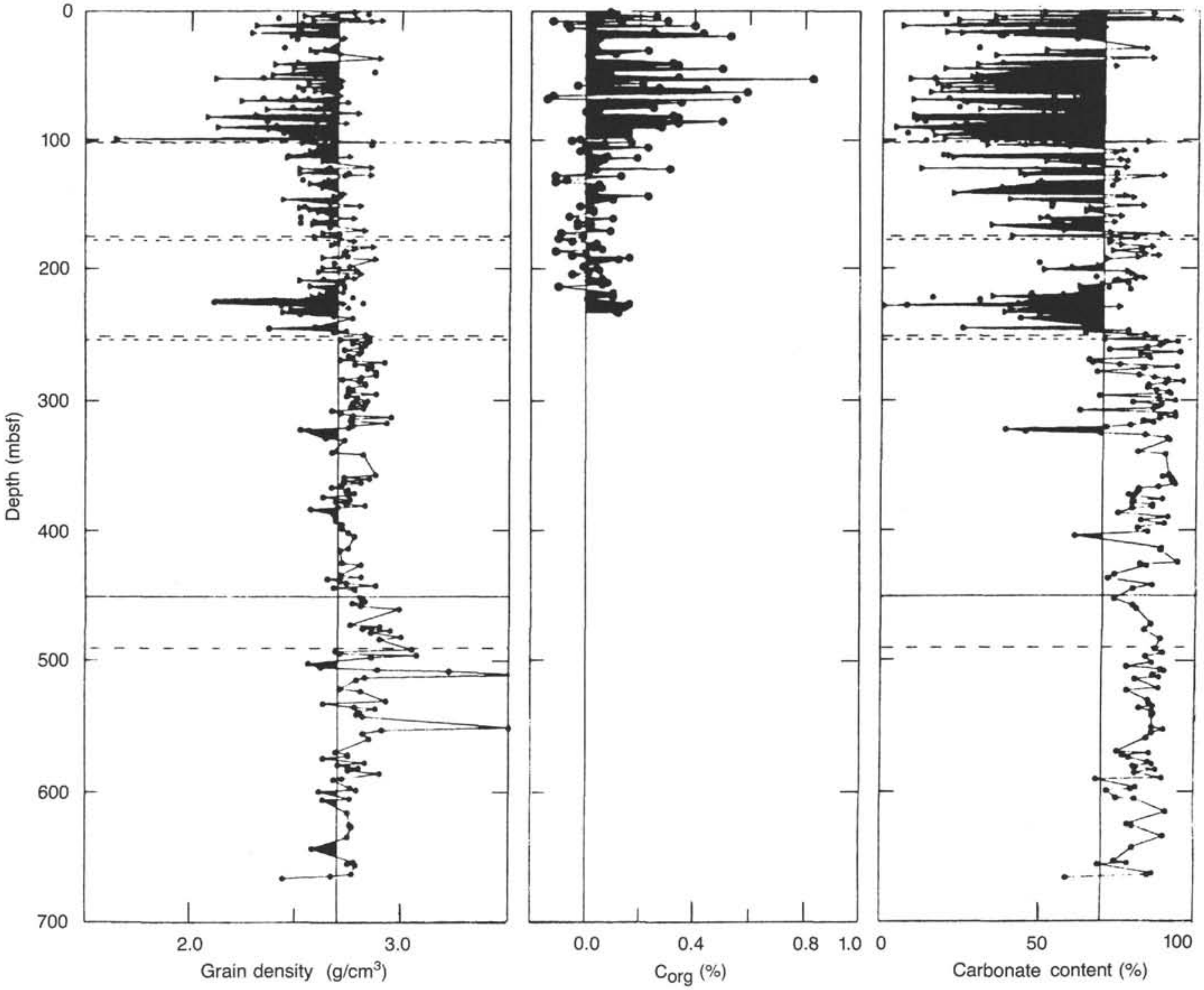

Figure 23. Comparison of grain density, organic carbon, and carbonate content (organic carbon and carbonate content from "Geochemistry" section). Lithostratigraphic unit boundaries are shown as in Figure 22. The vertical lines correspond to 2.7 g/cm^3 (grain density), 0.0 (organic carbon), and 70% (carbonate content).

of the hole plugging during the logging operations. The GST/ACT/NGT was run uphole through pipe from 640 mbsf to the mud line. This logging run started at 1100 hr and ended at 2100 hr on 2 May. Good data were obtained for a number of elemental yields, with a varying degree of effects from the thick drill pipe. The signals were significantly attenuated by the pipe, especially within the BHA, which is more than 5 cm thick.

All measurements were acquired at a sample depth interval of approximately 15 cm (0.5 ft) while logging up the hole at 10 m/min (1800 ft/hr) for the first run (BHC/DIL/GR/CALI), 5 m/min (900 ft/hr) for the second run (lithodensity), and 1.5 m/min (300 ft/hr) for the geochemical tool string. There were no repeat runs because of the time constraints. Had logging operations gone smoothly, we would have conducted a repeat run with the geochemical combination tool. Good quality data were acquired, however. The data were acquired in Schlumberger tape format and had to be edited, with the tapes copied from 800 to 1600 BPI for display and analysis with the processing facilities of the borehole logging group.

Logging Measurements

Brief descriptions of two of the tool strings and the logging parameters that they measure can be found in the "Explanatory Notes" chapter. The following is a brief description of the lithodensity and compensated neutron tools. For a detailed discussion, reference should be made to the "Explanatory Notes" and Schlumberger (1972, 1974) documentation.

The lithodensity tool (LDT; also known as the gamma-gamma tool) consists of a source of gamma rays (cesium) and two detectors (near and far). As the gamma rays or photons collide with atoms in the formation, they gradually lose their incident energy and undergo the following three interactions (in order of decreasing energy required): pair production, Compton scattering, and photoelectric effect. In the latter, the gamma ray collides with an inner layer electron (usually from the K layer) and is absorbed. The absorption of gamma rays is an exponential function of the electron density. Additionally, the photoelectric cross section is defined as the probability of a photoelectric interaction and is a function of both the atomic number and the

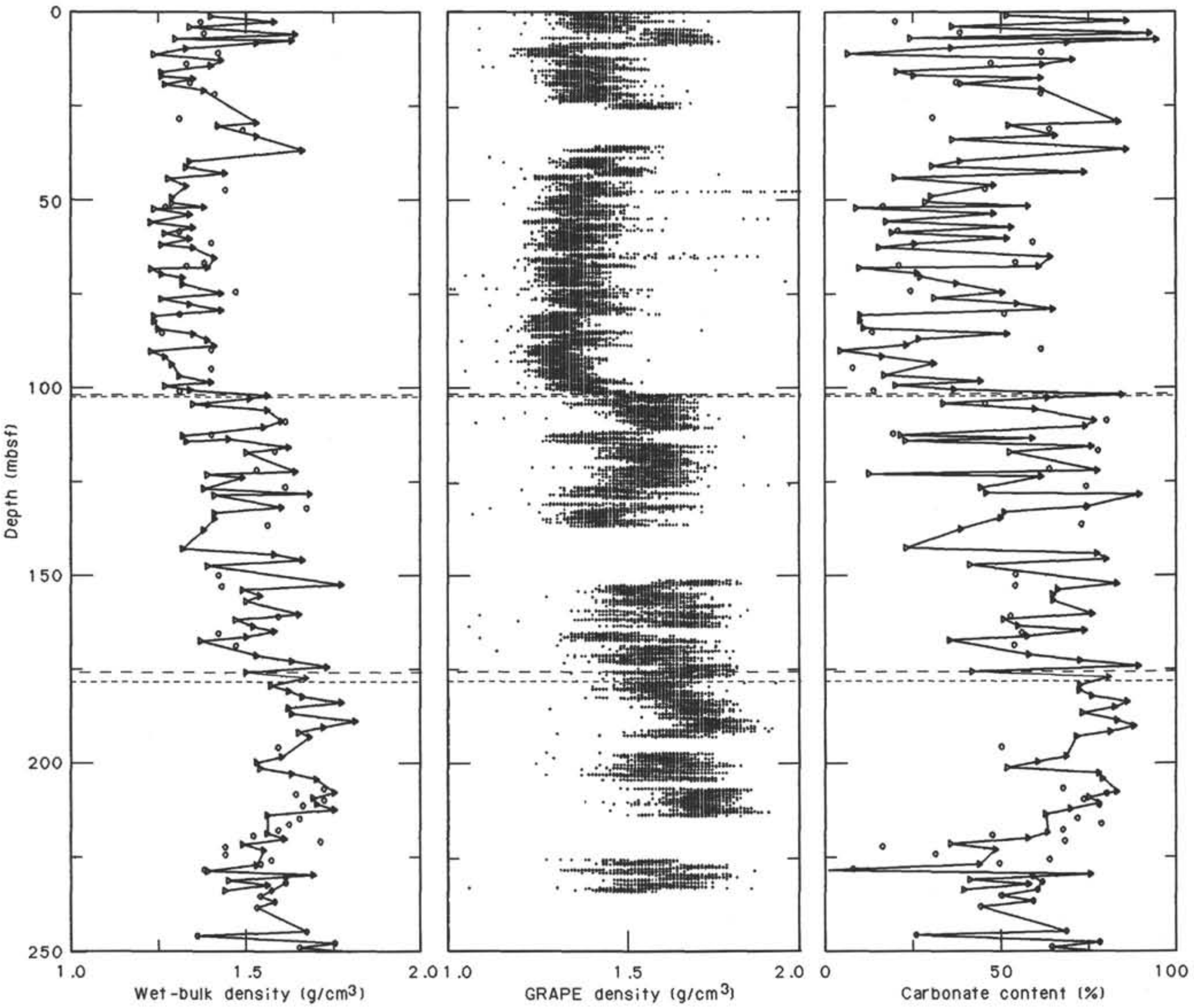

Figure 24. Comparison of wet-bulk density, GRAPE density, and carbonate content. Lithostratigraphic unit boundaries are shown as in Figure 22.

energy of the incident gamma ray. The Pe (which is not discussed here) is proportional to the "average cross section per electron." Having obtained an estimate of the electron density of a formation, we can deduce its bulk density (from the relationship between electron density and bulk density). The depth of investigation is usually less than 10 cm.

The neutron tools (CNL) measure the apparent hydrogen index of a formation. Neutrons of different energies are emitted from a chemical source, interact with formation atoms, slow down, and undergo "capture." Similar to the LDT, this tool has near and far detectors. The counts are measured in API units and can be directly related to the hydrogen index of the formation. Assuming water saturation, we can then extract the formation porosity. The depth of investigation of the tool is less than approximately 30 cm.

Discussion of Results

The data presented in Figures 27 and 28 are from the seismic-stratigraphic combination tool, from the lithodensity-neutron porosity tool in Figure 29, and from the geochemical tool combination in Figure 30. All of the logs in the preceding discussion are referenced to zero depth at the seafloor. This depth was determined from the drilling information and should coincide with the core depths. The good core recovery at this site made it easy to tie in the downhole logging measurements with some prominent changes in lithology. The downhole measurements were tied into the drill core depths by logging up to the mud line, with the gamma-ray logs used to correct for depth offsets between runs. The water depth at Site 704 was 2532.3 m, and the hole was drilled to 671.8 mbsf.

Because of the failure of the heave motion compensator, the caliper and tension logs play an important role in monitoring the quality of the data. The caliper log looks very noisy because of the heave, but it generally indicates fairly stable hole conditions. The hole diameter varied from 10 to 14 in. There are no indications of washouts or bridges (open-hole logging in run 2; Fig. 29). Large variations in the tension log (run 2 with the lithodensity tool string) indicate locations where problems occurred. The tension drop between 262 to 268 mbsf was due to the lifting of drill pipe with the knotted cable. From the tension log, data acquired below 460 mbsf (Fig. 29) are suspect, because they appear to be too low. All logs show fairly constant responses, and during the logging run, this was interpreted as indicating homogeneous lithology. However, a comparison of the

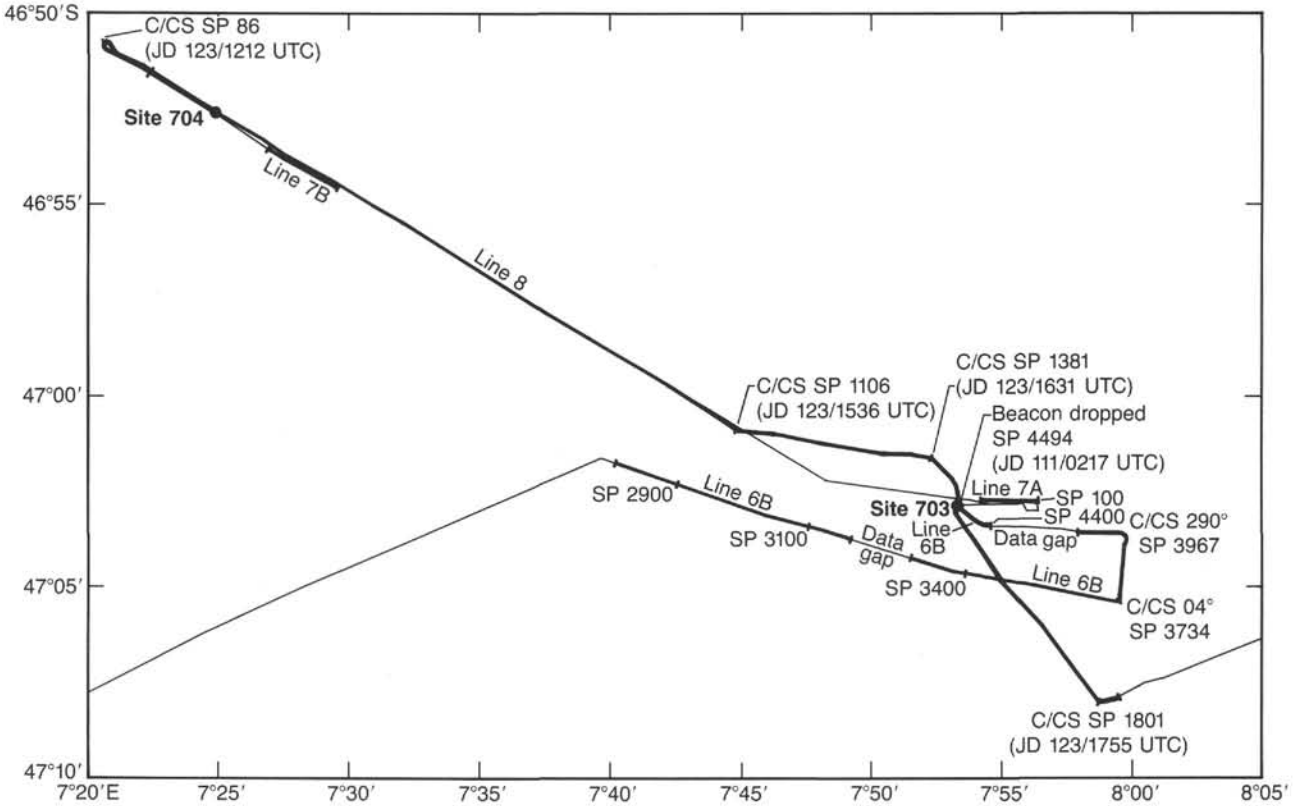

Figure 25. Track of *JOIDES Resolution* on approach and departure from Site 704. Seismic section shown in Figure 26 is indicated by bold line northwest of Hole 704.

gamma-ray data obtained with the seismic-stratigraphic combination tool (Figs. 27 and 28) indicates the discrepancy for this depth interval. This would imply that the logging cable had been damaged somewhat by knotting and pulling. The gamma-ray log is made on each logging run mainly for stratigraphic control and for depth offset corrections between different runs.

Most of the lithologic interpretations are based on the geochemical parameters. The natural gamma-ray logs also provide useful lithologic information in spite of the low radioactivity encountered in this hole. Because of the low radioactivity, and hence poor counting statistics (low signal to ratio), the spectrometry data (K, U, and Th logs) are quite unreliable, and we have deliberately ignored them, presenting only the total count gamma-ray log. The gamma-ray log shows changes in radioactivity that may be related to changes in clay content.

In-Situ Physical Properties

It is difficult to duplicate *in-situ* conditions when measuring physical properties in the laboratory, and logging data provide a more realistic way of determining the physical properties of earth materials. Logging also provides data for the missing gaps in the laboratory physical-property measurements that result from problems in core recovery (disturbed recovered core or missing core). The *in-situ* physical properties measured with the tool strings run in Hole 704B include electrical conductivity, compressional-wave velocities, density, and porosity. Conductivity variations within carbonate sediments are mainly a function of porosity and clay content, assuming a constant salinity of the pore fluids throughout the formation intersected by the borehole. Because conductivities mainly reflect change in porosities, apparent porosities can be determined from the resistivity logs using Archie's (1942) law. The porosities are only approximate, because variations in borehole diameter and clay content affect the apparent resistivities. The natural gamma-ray log indicates the presence of clay minerals (higher radioactivity) and may be used to isolate anomalous derived porosities. Porosities are also derived from density and interval traveltime data (using the Wyllie et al.'s (1956) time-average equation). The porosity derived from density data assumed a grain density of 2.71 g/cm^3 for the sediments. The neutron tool directly measures the porosity of the formation. All of the measured and derived porosities should correlate fairly well, and discrepancies may be used to interpret lithology. Differences in porosities derived from resistivity and density data, for instance, may indicate occurrences of mineral constituents with grain densities different from the assumed value of 2.71 g/cm^3 and may also indicate the presence of interstitial-water salinity anomalies. The data presented are not corrected for borehole and other effects; therefore, the physical properties are only apparent, not true, values.

Figure 28 shows the interval velocity estimates computed from the interval traveltimes of the sonic log (Fig. 27). Interval velocities above 280 mbsf are less than 1900 m/s. A low velocity zone (~ 1500 m/s) occurs between 215 and 245 mbsf. This zone correlates with low resistivity, high radioactivity, low calcium, and low density zones and is interpreted as a clay-bearing ooze. This interpretation is supported by the visual core descriptions. From approximately 280 to 350 mbsf, the velocities are fairly constant, with an average of about 1900 m/s. A steady increase in velocities from 1900 to 2500 m/s is observed between 350 and 520 mbsf. From 520 to 605 mbsf, the estimated velocities are approximately 2250 m/s and are fairly constant. Below this depth there is a slight increase in velocities. The relationship of these

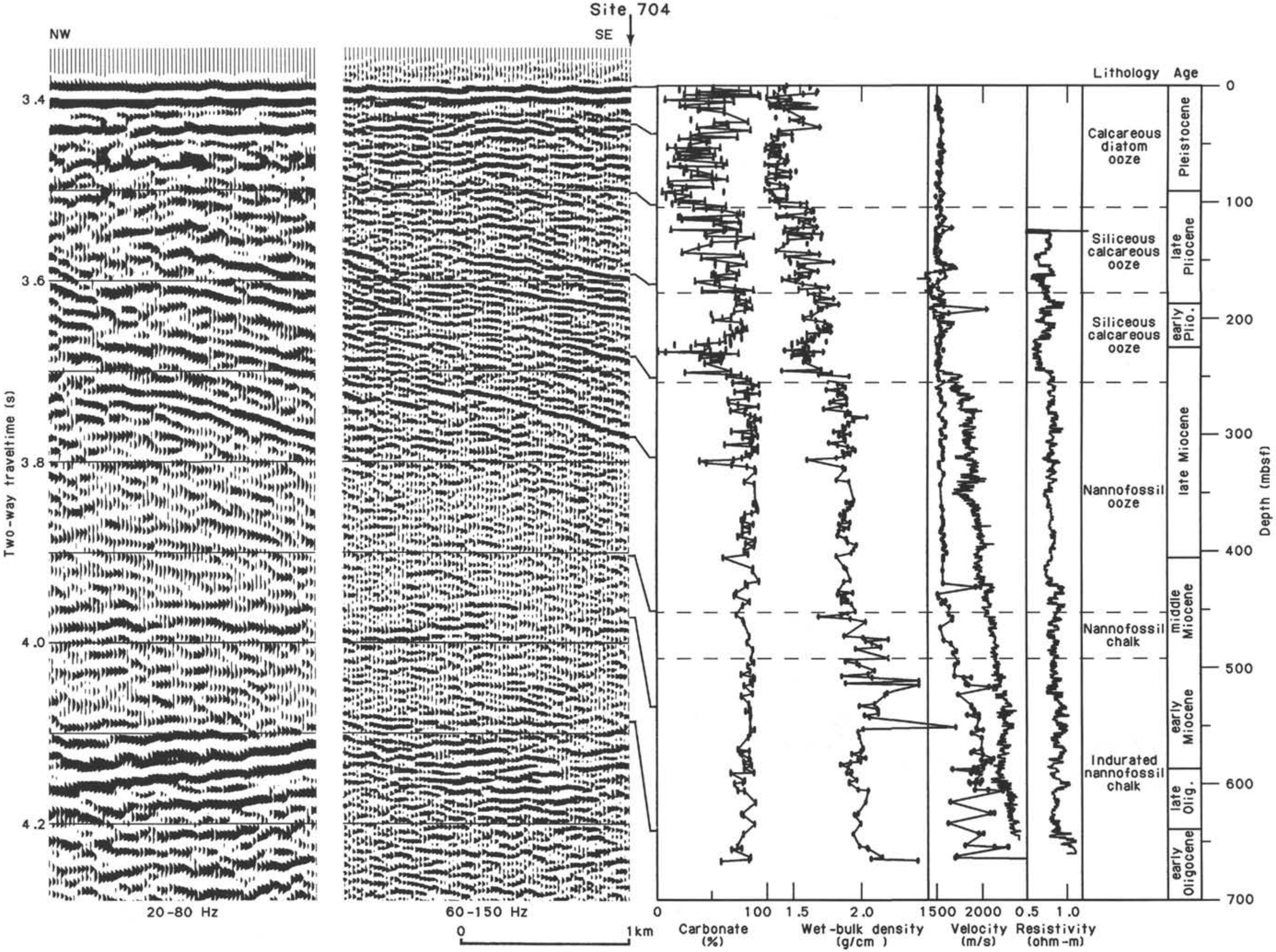

Figure 26. Summary of *P*-wave velocity, wet-bulk density, and carbonate content (from "Physical Properties" section), sonic velocity and resistivity (from "Logging" section), lithology (from "Lithostratigraphy" section), and age (from "Biostratigraphy" section) from Site 704 correlated with single-channel seismic-reflection data obtained by *JOIDES Resolution* over the site location.

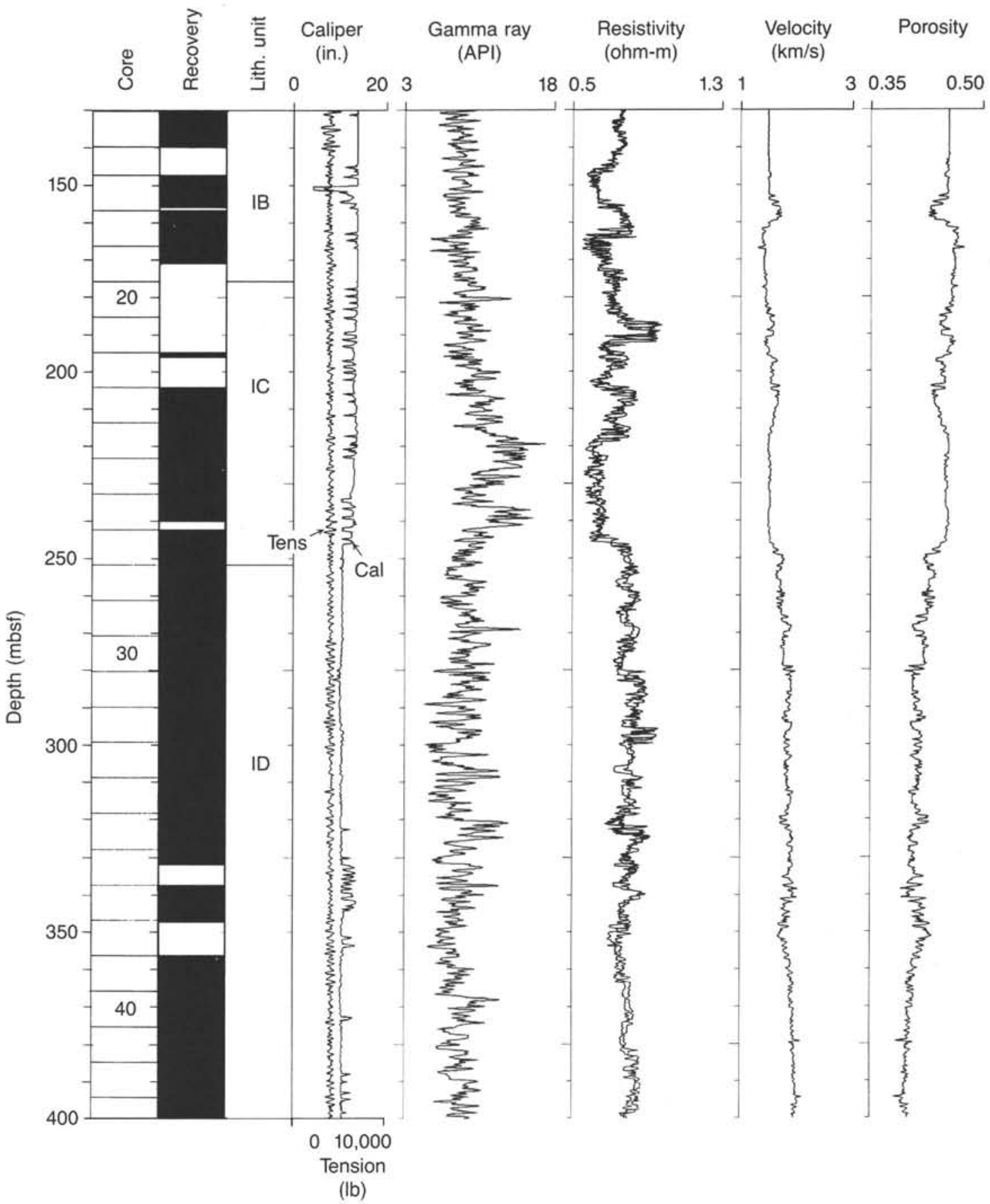

Figure 27. Caliper (CAL), tension (TENS), gamma ray, three resistivities (SFLU, ILM, and ILD), interval traveltimes, and porosity derived from the interval traveltimes recorded in Hole 704B.

velocity changes to lithology is not clear below 350 mbsf. This data correlates poorly with the lithostratigraphy. There is, however, a fairly good correlation between the velocity and resistivity logs. The general trend and amplitudes in the velocity log are consistent with the physical-property data, except for the lower depths (see "Physical Properties" section, this chapter).

The density and neutron logs below 460 mbsf are suspect for reasons discussed in the preceding "Logging Operations." The densities of the carbonate sequence at this site are approximately 1.85 g/cm^3. These density values correlate with the laboratory wet-bulk densities with the exception, again, of the lower depths. The porosity derived from the density data correlates poorly with the neutron porosities. The interpretation of these discrepancies can not be established at the moment and awaits critical examination of the quality of the data and further processing. The porosity indicator ratio (PIR) from the geochemical tool is a relative measure, but it shows good correlation with the laboratory measurements and the porosities derived from the sonic data.

Cyclicity within the Quaternary Sedimentary Sequence

Figure 31 is an expanded section of the calcium log, lithology indicator ratio (LIR), and PIR. There are distinct cycles in the amount of calcium (carbonate) that correlate with the dark

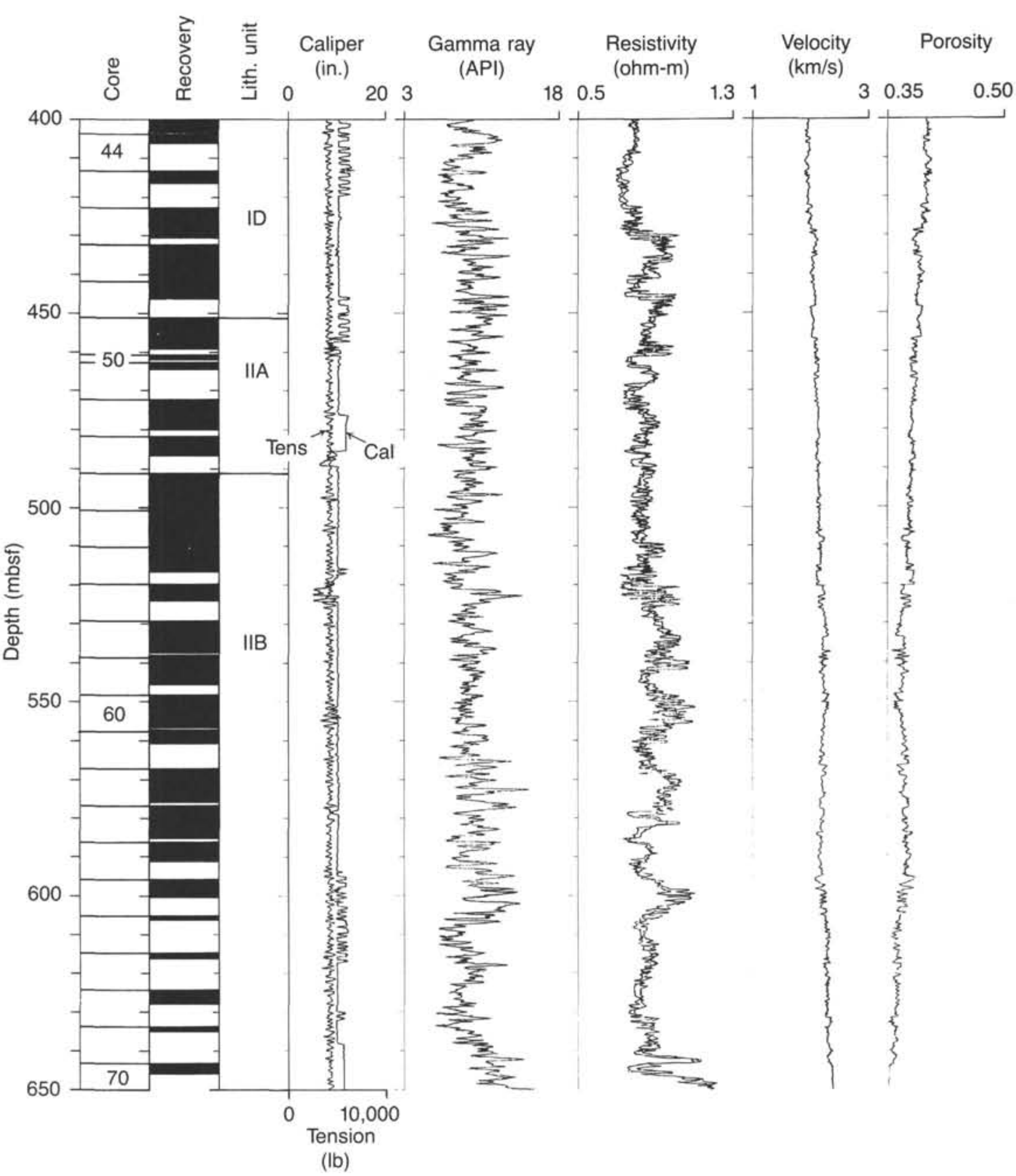

Figure 27 (continued).

and light cycles in sediment color. The calcium minima correspond to darker parts of the color cycles, and most maxima correspond to higher carbonate content. The prominent cycles are on the order of 10 m. A detailed analysis of the logs is currently being made. Spectral analysis is being applied in order to accurately determine the cyclicity in these sediments, which may show good correlation with Milankovitch cycles.

Correlation of Logging Data with Lithostratigraphy, Biostratigraphy, and Physical-Properties Measurements

Summaries of the lithology and biostratigraphy of Hole 704B are given in Table 2 and in the "Lithostratigraphy" and "Biostratigraphy" sections. The log-derived stratigraphic divisions are based mainly on the elemental calcium log, LIR, and PIR (Fig. 30). There are three major intervals based on the LIR and PIR: from 0 to 102, from 102 to 245, and from 245 mbsf to the bottom of the hole.

1. From 0 to 102 mbsf, the lithology ratio is high, indicating high silica content, and is coupled with a high porosity ratio. This interval corresponds to lithologic Subunit IA and consists of siliceous-bearing to siliceous calcareous ooze and calcareous-bearing to calcareous siliceous oozes of middle to early Pleistocene age. This interval may be further subdivided into three segments: (a) low calcium yield and porosity from 0 to 17.0 mbsf, (b) higher calcium and lower porosity from 17 to 45 mbsf, and (c) low calcium and higher lithology and porosity ratios than the overlying segment from 45 to 102 mbsf. The alternating high and low calcium yields within these segments reflect the alternations of siliceous to calcareous oozes. These cycles are clearly

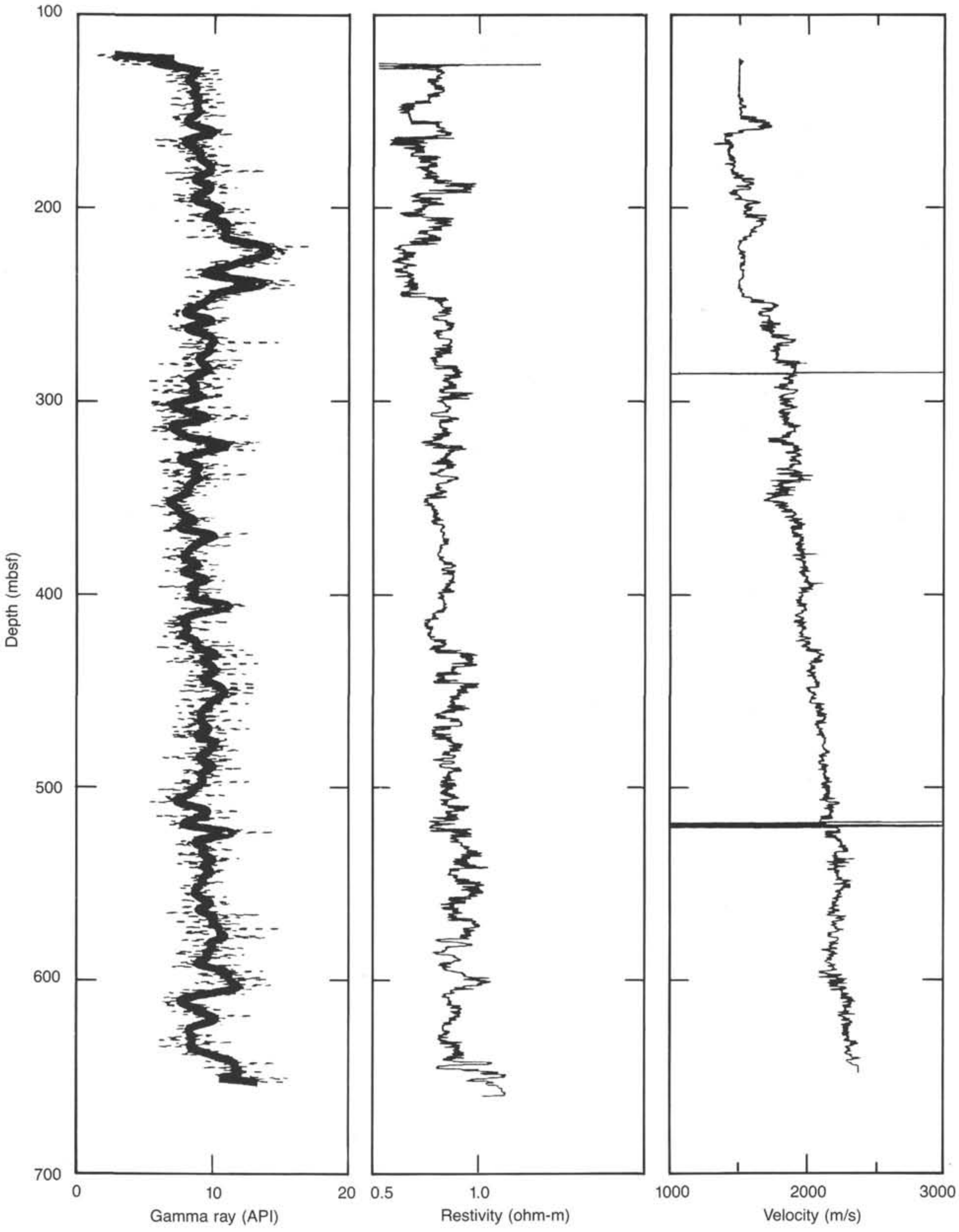

Figure 28. Total count gamma ray (GR), deep dual induction resistivity (ILD), and interval velocity computed from the interval traveltimes of the sonic data (Fig. 27) recorded in Hole 704B.

indicated in the core data by a change in sediment color. The more siliceous sections have a darker color and should correspond to low calcium. The other nuclear data acquired through the drill pipe and BHA were not interpreted aboard ship. Interpretability is questionable at this time, because of the acquisition conditions.

2. From 102 to 245 mbsf, the calcium log generally shows higher values. The LIR and PIR are lower than from 0 to 102

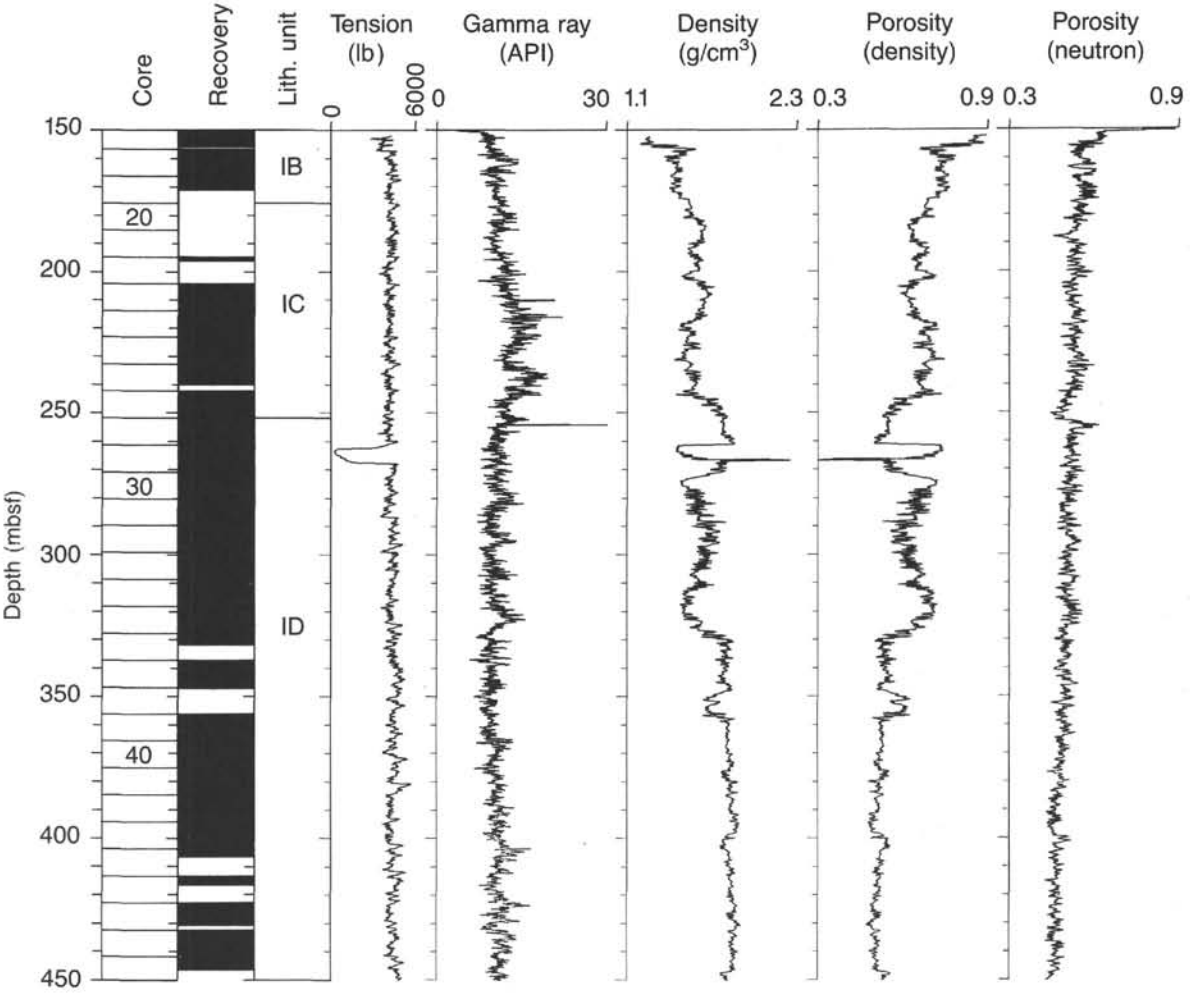

Figure 29. Tension, total gamma ray (SGR), bulk density (RHOB), porosity derived from density (DPHI), and neutron (NPHI) porosity recorded in Hole 704B.

mbsf. This interval may be further subdivided from (a) 102 to 165 mbsf, (b) 165 to 215 mbsf, and (c) 215 to 245 mbsf. The calcium values between the first two subdivisions do not vary much, and the PIR shows a subtle but distinct change with lower values from 165 to 215 mbsf. The segment from 102 to 165 mbsf is of late Pliocene age, and that from 165 to 215 mbsf is of latest Miocene to late Pliocene age. These subdivisions correlate with the lithostratigraphic subunits. The segment from 215 to 245 mbsf has distinct physical and chemical properties. The gamma-ray count is high (Fig. 28), indicating the presence of clay or ash layers. Low calcium values, density, and porosity, a high silica/calcium ratio, and low resistivities are also observed within this segment. The lithostratigraphy has two subunits from 102 to 245 mbsf. The log-defined interval from 102 to 165 mbsf roughly corresponds to Subunit IB, and the section from 165 to 245 mbsf is included in Subunit IC. From the logging data it appears that Subunit IB should be defined from 102 to 215 mbsf; the clay-bearing, siliceous-bearing to siliceous calcareous ooze should be established from 215 to 245 mbsf.

3. From 245 to 580 mbsf, the calcium elemental yields are fairly constant, except for two zones around 275 and 320 mbsf that have low calcium and high LIR and PIR values. This interval is of late Miocene to early Miocene age and is subdivided into three lithostratigraphic subunits. The lithostratigraphic subdivisions correspond to possible changes in the geochemistry of the sediments. The *in-situ* physical properties do not correlate well with these lithostratigraphic boundaries. Variations in the sonic velocities and resistivities suggest that the interval from 245 to 580 mbsf may be further subdivided; however, there is not much supporting evidence from other logging data at present.

In summary, the lithostratigraphic units are closely related to the boundaries derived from the calcium log within the upper 245 m of the sediment section. The laboratory-determined percent carbonate content has an excellent correlation with the calcium log. The sampling rate of the carbonate data is too coarse to adequately resolve the finer scale variations in carbonate content; high-resolution information is obtained from logging measurements.

A comparison between the physical properties measured on the cores and those derived from the logs is illustrated in Figure 32. In general, velocity and density log readings are higher than those measured on cores, and log porosities are lower than core porosities.

Conclusions

The high-resolution, continuous downhole geophysical and geochemical measurements enable better definition of the lithologic boundaries. Porosity data show a general decreasing trend with depth, reflecting normal diagenetic changes along the sedimentary column. Because of the high core recovery this site will

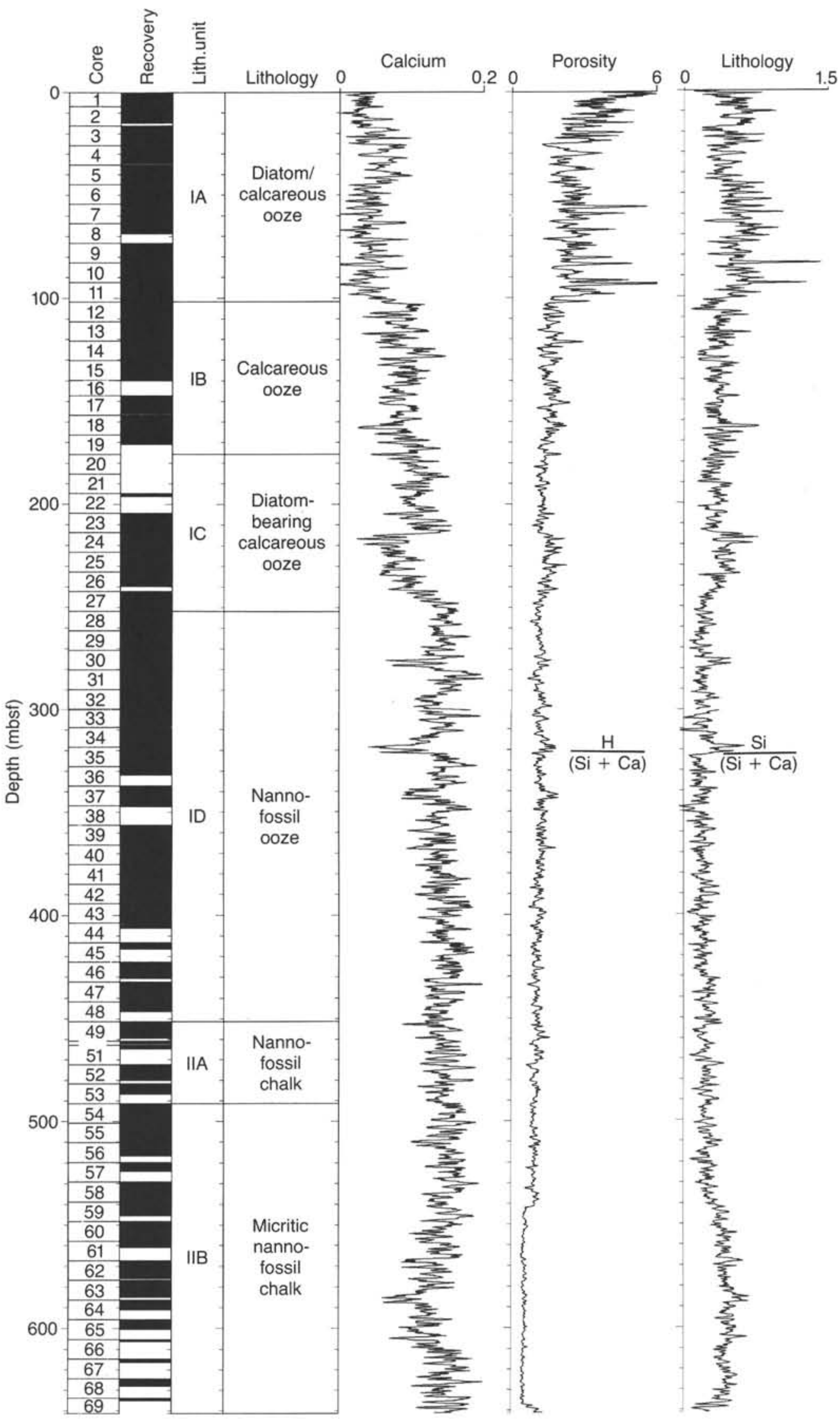

Figure 30. Elemental yield ratios from the induced gamma-ray spectrometry tool recorded in Hole 704B: elemental calcium, porosity indicator ratio, and lithology indicator ratio.

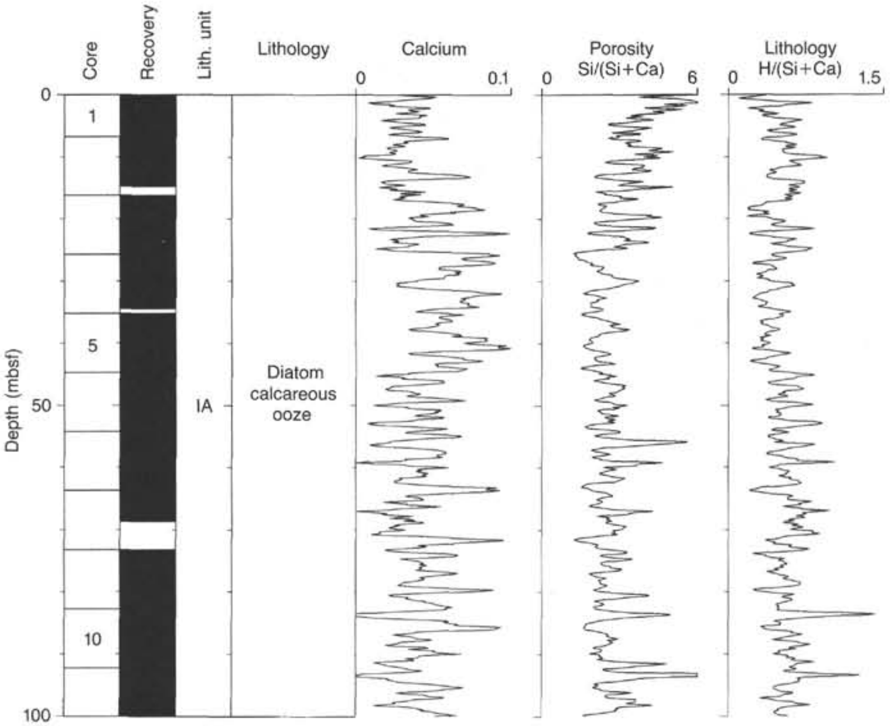

Figure 31. Expanded section of Figure 30 from 0 to 120 mbsf to clarify cyclicity in the upper part of the Quaternary sediment sequence.

be particularly useful in tying the logs to the physical-property measurements, biostratigraphy, and sedimentation cycles.

SUMMARY AND CONCLUSIONS

Summary

Site 704 is located on the southern part of the Meteor Rise (46°52.758′S, 07°5.231′E), in a water depth of 2532.5 m (Figs. 3 and 4). The site is on a plain west of and deeper than (~1000 m) the rugged basement crest of the Meteor Rise. The Meteor Rise and the Islas Orcadas Rise were formed by extensive volcanism during Paleocene-Eocene time at a propagating extension of the Mid-Atlantic Ridge. These rises formed a major shallowing of the Mid-Atlantic Ridge segment that abutted the Falkland-Agulhas Fracture Zone; together they constituted major obstacles to deep and intermediate oceanic circulation, particularly during the Paleogene (Fig. 1). A major objective of Leg 114 was to interpret the influence on oceanic circulation and environment of the formation, subsidence, and separation of the Islas Orcadas and Meteor rises. Site 702 on the Islas Orcadas Rise and Site 703 on the Meteor Rise were located where younger sedimentary sequences were greatly attenuated in order to obtain the Paleogene sedimentary history and basement of these once conjugate aseismic ridges within drilling time constraints. The objectives of determining the age, nature, and subsidence history of these aseismic ridges were successfully met at Sites 702 and 703. For this reason, Site 704 was located on a region of the Meteor Rise where a maximum thickness of Neogene and upper Paleogene sediment could be obtained in order to provide a carbonate-bearing, high-resolution paleoceanographic-paleoclimatic record of an interval not well represented at the previous Leg 114 sites. A complete listing of other major objectives at Site 704 is provided in the "Background and Objectives" section of this chapter.

The acoustic stratigraphy in the vicinity of Site 704 is characterized by an upper 0.4-s-thick (TWT) highly reflective unit overlying a more weakly stratified section that may reach a local thickness of 0.5–1.0 s (Fig. 4). In some places, strong basal reflections are present about 0.2 s above basement.

Site 704 consists of two holes, each drilled using the APC and XCB systems. An upper Miocene to Quaternary sequence was continuously cored in Hole 704A using the APC to a depth of 149.7 mbsf (Cores 114-704A-1H to 114-704A-16H), from which the XCB was employed to a total depth of 282.7 mbsf (Cores 114-704A-17X to 114-704A-30X). Lower Oligocene to Quaternary sediments were obtained from Hole 704B by employing the APC to a depth of 139.7 mbsf (Cores 114-704B-1H to 114-704B-15H) and continuing with the XCB to a total depth of 671.7 mbsf (Cores 114-704B-16X to 114-704B-72X). Recovery rates were good for both holes, 79.4% for Hole 704A and 74.8% for Hole 704B. For the interval of stratigraphic overlap between both holes, recovery was greater than 99% for the composite upper Miocene to Quaternary sequence above 282.7 mbsf. Hole 704B was terminated at 671.7 mbsf to allow sufficient time for three logging runs and a Navidrill test prior to the final transit of the leg to Mauritius.

The previous holes drilled during Leg 114 were extremely successful in obtaining thick Paleogene pelagic sediment sequences that allow for a more complete interpretation of the southern high-latitude paleoenvironment than previously possible. It was a fitting end to the drilling activities of the leg to also obtain at Site 704 a high-resolution Neogene sequence that undoubtably contains the best pelagic Neogene paleoenvironmental record yet recovered from the antarctic or subantarctic regions. This site contains the thickest Neogene high-latitude sedimentary sequence (~520 m) with carbonate throughout, thus offering a valuable record of planktonic and benthic isotopic variations for this period. High-frequency fluctuations in much of the section of carbonate content, biogenic silica, temperature affinities of microfossils, physical properties, and logging parameters all are indicative of an extremely sensitive climatic record for this site.

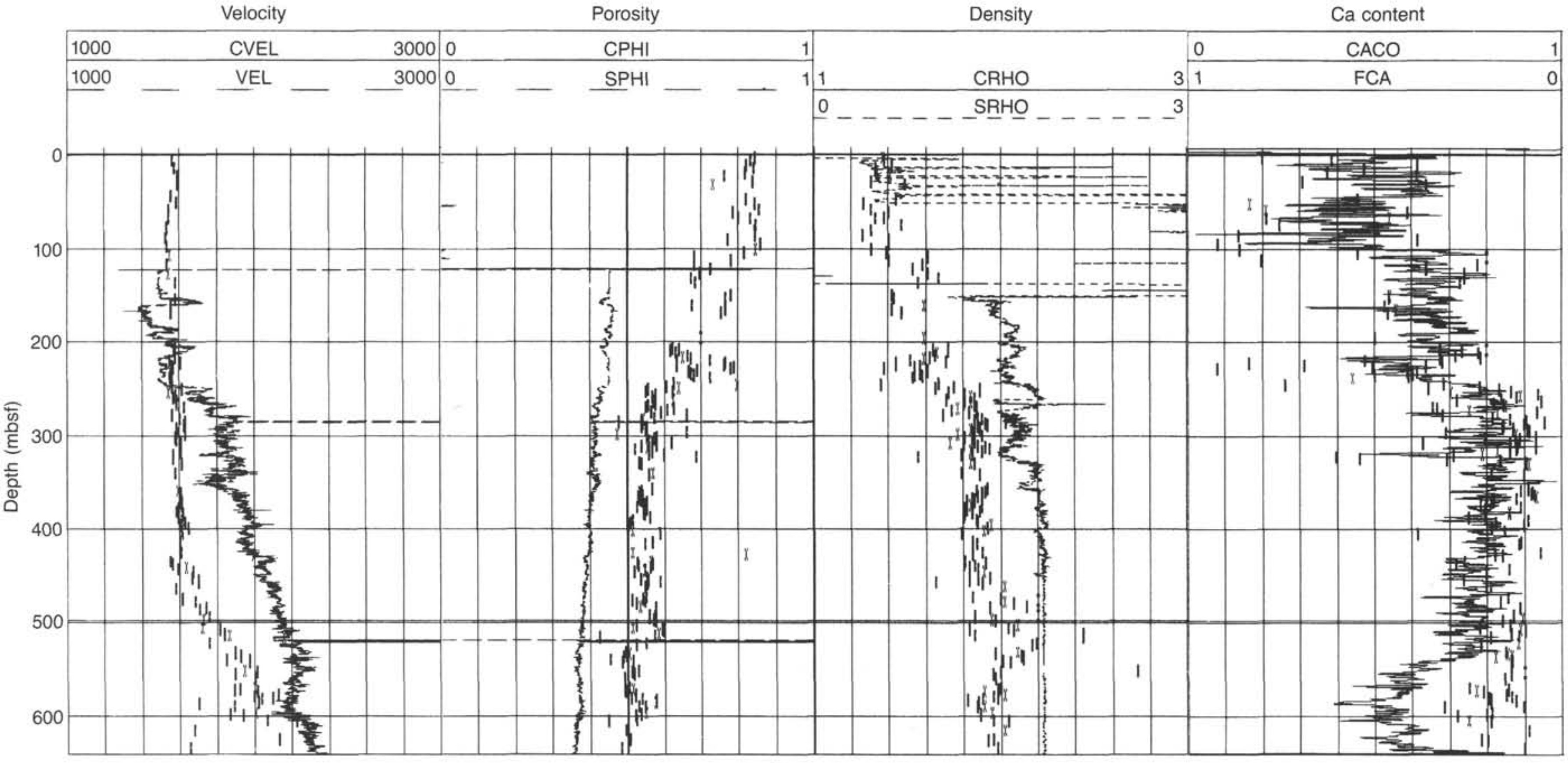

Figure 32. Comparison between core-measured properties and *in-situ* log-derived physical properties at Hole 704B. CVEL = core velocity; VEL = compressional velocity from sonic log; CPHI = core porosity; SPHI = sonic-derived porosity; CRHO = core bulk density; SRHO = density from lithodensity tool; CACO = core calcium carbonate content; FCA = lithologic index (Si/Ca + Si) after filtering through a 9-point running-average filter.

Sedimentation rates for the Oligocene portion of Hole 704B (32-34 Ma to 23.7 Ma) were about 8-10 m/m.y. Early Miocene (23.7-16.5 Ma) sedimentation rates were also high (~20 m/m.y.), but dropped to ~11 m/m.y. during the early middle Miocene (~16.5-14.5 Ma). A hiatus of 5 to 6 m.y. separates early middle Miocene sediments (14.5 Ma) from overlying early late Miocene sediments (~9-10 Ma). After formation of this hiatus, there was an extremely high sedimentation rate, as high as 100 m/m.y., during a brief span of the early late Miocene (~10-8.5 Ma). Sedimentation was again interrupted during the late Miocene, forming a second hiatus with bracketing ages of ~8.5 and 6.5 Ma. With the resumption of sedimentation, there were no further apparent interruptions in sedimentation throughout the remainder of the late Miocene (~6.5-5.3 Ma), which had an average sedimentation rate of 45 m/m.y. The early to early late Pliocene (5.3-2.8 Ma) sedimentation rate declined from that of the late Miocene, but was still relatively high at 22 m/m.y. A third, but brief, hiatus occurs in the late Pliocene between sediments with an age of ~2.9 or 2.8 Ma to 2.5 Ma. Above this youngest hiatus, high sedimentation rates of ~82 m/m.y. were recorded for the middle late Pliocene-late Quaternary (~2.5-0.4 Ma). Finally, a precipitous drop in sedimentation rate (to ~9.0 m/m.y.) occurred by 400 k.y. ago, resulting in the deposition of only 3.5 m of sediment since that time.

Sedimentation was rapid throughout most of the Neogene, except during the late Pleistocene. Sedimentation rates were 22 m/m.y. during the late Oligocene and early Miocene and 13 m/m.y. during the middle Miocene. The late Miocene brought an increase in sedimentation rates to 37 m/m.y., which dropped again to a lower rate of ~20 m/m.y. during the latest Miocene and early Pliocene. High sedimentation rates resumed during the latest Pliocene to middle Pleistocene to a remarkable ~73 m/m.y., dropping during the late Pleistocene to ~58 m/m.y. from 0.62 to 0.195 Ma and to 15 m/m.y. between 0.195 Ma and the Present.

Site 704 is within a zone that experienced mixed biosiliceous and calcareous productivity throughout the early Oligocene-Quaternary, with very little influx of terrigenous sediment by currents or ice rafting. As a consequence, the sedimentary sequence consists of varying amounts of two end-member components: (1) calcareous oozes and chalks composed mainly of foraminifers and calcareous nannofossils and (2) siliceous oozes composed mainly of diatoms with minor amounts of radiolarians and silicoflagellates. Two lithostratigraphic units were defined on the basis of compositional variations and color changes (Table 2 and Figs. 6 and 7), percent calcium carbonate (Fig. 8), and diagenetic maturity (Figs. 6 and 7), as summarized in Figure 33. A summary of these units and subunits follows, with depths in mbsf as recorded in Hole 704B.

Unit I (0-451.2 mbsf) consists of late early Miocene to Quaternary age oozes of varying siliceous and calcareous composition. The unit is subdivided into four subunits based on upon the amount and frequency of change in the carbonate and biosiliceous end-members.

Subunit IA (0-101.7 mbsf) is characterized by abundant lithologic alternations between lithologies ranging from diatom ooze to calcareous-bearing diatom ooze, calcareous diatom ooze, nannofossil ooze, diatom-bearing calcareous ooze, and diatom calcareous ooze. Common lithologic variations in this latest Pliocene to Pleistocene age subunit are reflected in numerous sharp and transitional color changes and by large amplitude fluctuations in percent carbonate content (Fig. 33).

Subunit IB (101.7-175.7 mbsf) is a dominantly calcareous ooze with a significant biosiliceous component. It has a lighter color, higher mean carbonate content, and a lower biogenic silica component than Subunit IA. Large amplitude fluctuations in carbonate content also occur in this late Pliocene age subunit.

Subunit IC (175.7-251.7 mbsf) is composed primarily of diatom-bearing calcareous ooze of latest Miocene to late Pliocene age. Color and carbonate variability are less than in the overlying subunits, except in Cores 114-704A-24X and 114-704A-25X. Subunit IC is further divided into two subunits. Subunit IC_1 (175.7-219 mbsf) exhibits very little color variation and a high carbonate content with little variability. Subunit IC_2 (219-251.7 mbsf) contains a greater color variation, a lower mean carbonate content, and a greater biogenic silica component. Lithologies in this subunit range from siliceous calcareous ooze to diatom-bearing nannofossil ooze.

Subunit ID (251.7-451.2 mbsf) consists of a uniform, featureless nannofossil ooze with a minor biosiliceous component. The mean carbonate content of this latest early Miocene to latest Miocene age subunit is ~80%, with much less variation than in the above subunits.

Unit II (451.2-671.7 mbsf) is an early Oligocene to late early Miocene age micrite-bearing nannofossil chalk and micritic indurated chalk that is divided into two subunits on the basis of increased diagenetic maturity with depth. Subunit IIA (451.2-491.2 mbsf) is a late early Miocene age nannofossil chalk and micrite-bearing nannofossil chalk with a carbonate content of ~90%. Increased micritization of the carbonate causes a noticeable increase in induration of the lower Oligocene to lower Miocene micritic nannofossil chalk, thereby defining the basal Subunit IIB (491.2-671.7 mbsf).

The upper Paleogene-Neogene sequence of Site 704 is unique among antarctic and subantarctic sites of this age by being

1. the most complete stratigraphic sequence;
2. the thickest pelagic sequence with little to no terrigenous component;
3. the only site with a continuous presence of carbonate, which offers an extended stable isotopic record of the planktonic and benthic environment;
4. the only site with a continuous presence of all major calcareous and siliceous microfossil groups;
5. a Miocene through Pliocene magnetostratigraphic record.

This exceptional section will provide a a high-quality reference section for calibration of calcareous and siliceous microfossil zonal schemes to one another and to the GPTS. In addition, the site is well situated with respect to the concurrent occurrence of middle- and high-latitude species, which may assist in the calibration of the antarctic and subantarctic stratigraphic framework to standard lower-latitude zonations.

Calcareous microfossils are abundant and well to moderately well preserved throughout the Neogene. Although they remain abundant in the Oligocene, all of the calcareous microfossils have been altered by diagenesis with recrystallization and secondary overgrowths. Calcareous nannofossils generally exhibit low diversity; planktonic foraminifer diversity is similarly low for the Pliocene-Quaternary but increases in the Oligocene and Miocene. Moderately diverse and well-preserved assemblages of benthic foraminifers occur throughout the sequence.

Diatoms are abundant and well preserved throughout most of the section, except for the lower Miocene, the lower middle Miocene, and part of the upper Miocene. The more resistant radiolarians are common to abundant and diverse in most samples. Silicoflagellates are also well preserved but occur more sporadically. There is no evidence for the diagenesis of biogenic silica, as seen at other Leg 114 sites.

Preliminary paleomagnetic results suggest a relatively complete magnetic polarity record of the upper Miocene and Pliocene (Figs. 20 and 21). Other magnetic polarity zones are recognized to a depth of 520 mbsf, but further shore-based paleomagnetic and biostratigraphic studies are needed for their interpretation.

Conclusions

Seismic and Tectonic Interpretation

Site 704 was drilled in a syncline in order to maximize the thickness of the Neogene sediments. Although the syncline is flanked to the east by seamounts extending up to 1000 m above the plain, the thickness of individual seismic units appears remarkably symmetric with respect to the syncline axis, indicating that sediment transport by gravity flows into the syncline from the east was of minor importance. This conclusion is supported by the drilling results.

The direct relationship between carbonate content and wet-bulk density determines the acoustic properties of the calcareous sediments at Site 704, which gives particular reflection characteristics dependent on the amplitude and frequency of the fluctuations in carbonate content. Changes in *P*-wave velocity are essentially linear, with few exceptions throughout the sequence. The upper sequence (0–175 mbsf), with the largest amplitude in carbonate variations (±30%), shows continuous reflections in the upper 100 m, but the discontinuous deeper reflections give a transparent appearance. This sequence was laid down following a major advance of the polar front at 2.6–2.47 Ma (Ciesielski and Grinstead, 1986). The amplitude of variations in the carbonate content is lower (±15%) in the underlying sequence (175–360 mbsf), which is characterized by high and uniform reflectivity. The base of this sequence is only slightly older than the stratigraphic level that corresponds to the first occurrence of ice-rafted material at Site 513 (Ciesielski and Weaver, 1983). Sediments below 360 mbsf show little contrast in acoustic expression.

The Meteor Rise and Islas Orcadas Rise show an apparent difference in the thickness of Paleogene carbonate sedimentation, with a thinner sequence on the Meteor Rise. This may indicate that at least the investigated part of the Meteor Rise is a slightly younger feature or that the early Paleogene paleoceanographic regime separated the two rises into areas of different productivity. Gentle folding of the sediments on Meteor Rise may be due to differential compaction and tectonic movements, rather than large scale sliding.

Paleoenvironmental History

Oligocene–Middle Miocene

Sediments at the base of Hole 704B are of late early Oligocene age, not much older than base of Zone P21b and younger than the base of P19 (<34.0–30.0 Ma). The preservational state of calcareous microfossils suggests deposition near the foraminifer lysocline. This interval of poor preservation is similar to that of the other Leg 114 sites and Deep Sea Drilling Project (DSDP) Sites 511 and 513 (Leg 71), which also reveal evidence of a "mid"-Oligocene rise in the lysocline and CCD. Deposition was above the lysocline the remainder of the Oligocene.

Interpretation of the relative surface water mass temperatures during the Oligocene is difficult because of the poor preservation of the microfossils in the micritic nannofossil chalk. Some discoasters were preserved and indicate relatively warm surface waters. In comparison to most of the Neogene, stable environmental conditions persisted throughout the Oligocene. This paleoenvironmental stability is supported by relatively constant values of calcium carbonate percentages (Fig. 33). Surface-water productivity was dominated by calcareous nannofossils and, to a lesser degree, foraminifers; siliceous productivity was relatively minor.

The logging results from the geochemical combination tool reveal that calcium elemental yields from the Oligocene are much more constant than for most of the Neogene (Fig. 30). Nevertheless, Oligocene calcium elemental yields, measured at 15-cm intervals, exhibit consistent cyclicity. The cause of the cyclicity can not be determined at the present time, nor did it have any obvious influence on sedimentation or characteristics of surface-water productivity.

Sedimentation continued uninterrupted across the Oligocene/Miocene boundary, as it also did at Sites 699 and 703. Surface-water temperatures were still relatively warm and conditions were stable, as during the Oligocene. This similarity is reflected in calcium carbonate values and calcium elemental yields recorded from the geochemical log (Figs. 35 and 37, "Site 700" chapter, this volume).

Sedimentation apparently was continous throughout the early Miocene and early middle Miocene. Although biostratigraphic data for the early Miocene is sparse and poorly constrained at the present time, the sedimentation rate was about 20 m/m.y. During the late early Miocene, at about 17–17.5 Ma, the sedimentation rate was reduced to ~11 m/m.y. Following this reduction in sedimentation rate was an erosional or nondepositional event(s) which produced the most significant hiatus in Hole 704B, encompassing the middle middle through earliest late Miocene.

In spite of the presence of one lengthy Miocene hiatus, Site 704 has the most complete Miocene record of all Leg 14 sites. Previous sites all have a major hiatus separating the Paleogene or lowermost Miocene from sediments no older than late middle to late Miocene in age. These major hiatuses at our previous sites were attributed to, at least partially, the opening of the Drake Passage and subsequent erosion by more intensified circulation of Antarctic Bottom Water (AABW) and Circumpolar Deep Water (CPDW). The complete middle middle Miocene through early Miocene record of Site 704 and the dominance of carbonate sedimentation suggest that this site was north of the influence of the Circumpolar Current as it became established during the early Neogene. Site 704 also remained north of the Antarctic Convergence through this period; whereas, the more southerly Site 699 (51°32.5′S) came under the influence of this frontal zone during the earliest Miocene.

Site 704 microfossil assemblages and the high carbonate content of the sediment suggest that Site 704 was north of the Antarctic Convergence prior to and immediately after the formation of the middle middle to earliest late Miocene hiatus. It seems unlikely, therefore, that the agent of non-deposition and/or erosion was Circumpolar Deep Water. Instead, the cause of this hiatus may have been an increase in the production of North Atlantic Deep Water (NADW) which more likely bathed the sea floor at Site 704 (see Background and Objectives). It is noteworthy that the hiatus follows shortly after the subsidence of Iceland–Faeroe Ridge below a threshold depth which allowed a rapid increase in advection of NADW into the North Atlantic between 15 and 14.6 Ma (Miller and Fairbanks, 1985).

Late Miocene

After formation of the hiatus bracketing the middle/late Miocene boundary, a period of extremely high sedimentation (as high as 100 m/m.y.) occurred during no more than 1.5 m.y. (8.5–10.0 Ma).[3] During this period, approximately 130 m of nannofossil ooze were deposited with little variation in the carbonate, which generally varies between 75 and 95%. Only in the upper portion of this early late Miocene interval does the percentage of carbonate decline appreciably, to only 40% at approximately 320 mbsf. This carbonate low, representing the first interval in which carbonate dominance was replaced by biogenic silica dominance during the Oligocene to late Miocene period, has an estimated age of 8.5 to 9.0 Ma. This first major peak in biogenic silica productivity was short-lived, and carbonate content once again increased prior to the late Miocene hiatus between 287–308 mbsf.

---

[3] Ages based upon the correlation of Anomaly 5 to Chron 11.

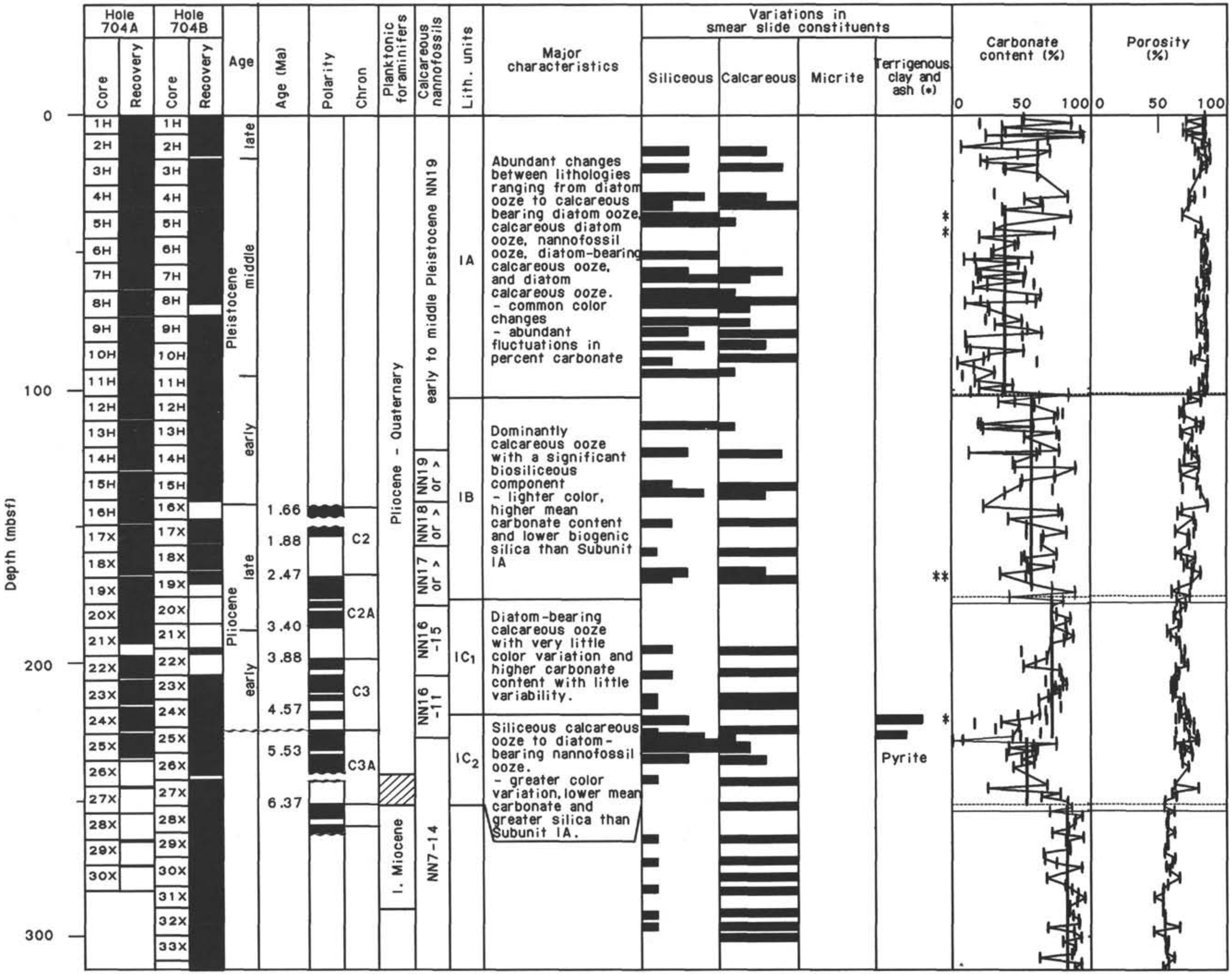

Figure 33. Summary diagram of a variety of data collected at Site 704, including depth, core recovery for Holes 704A and 704B, age, paleomagnetic polarity zones and chrons, selected paleontologic zones and ages, lithostratigraphic units and subunits and a description of their major characteristics, variation in smear slide constituents, %CaCO$_3$, and porosity.

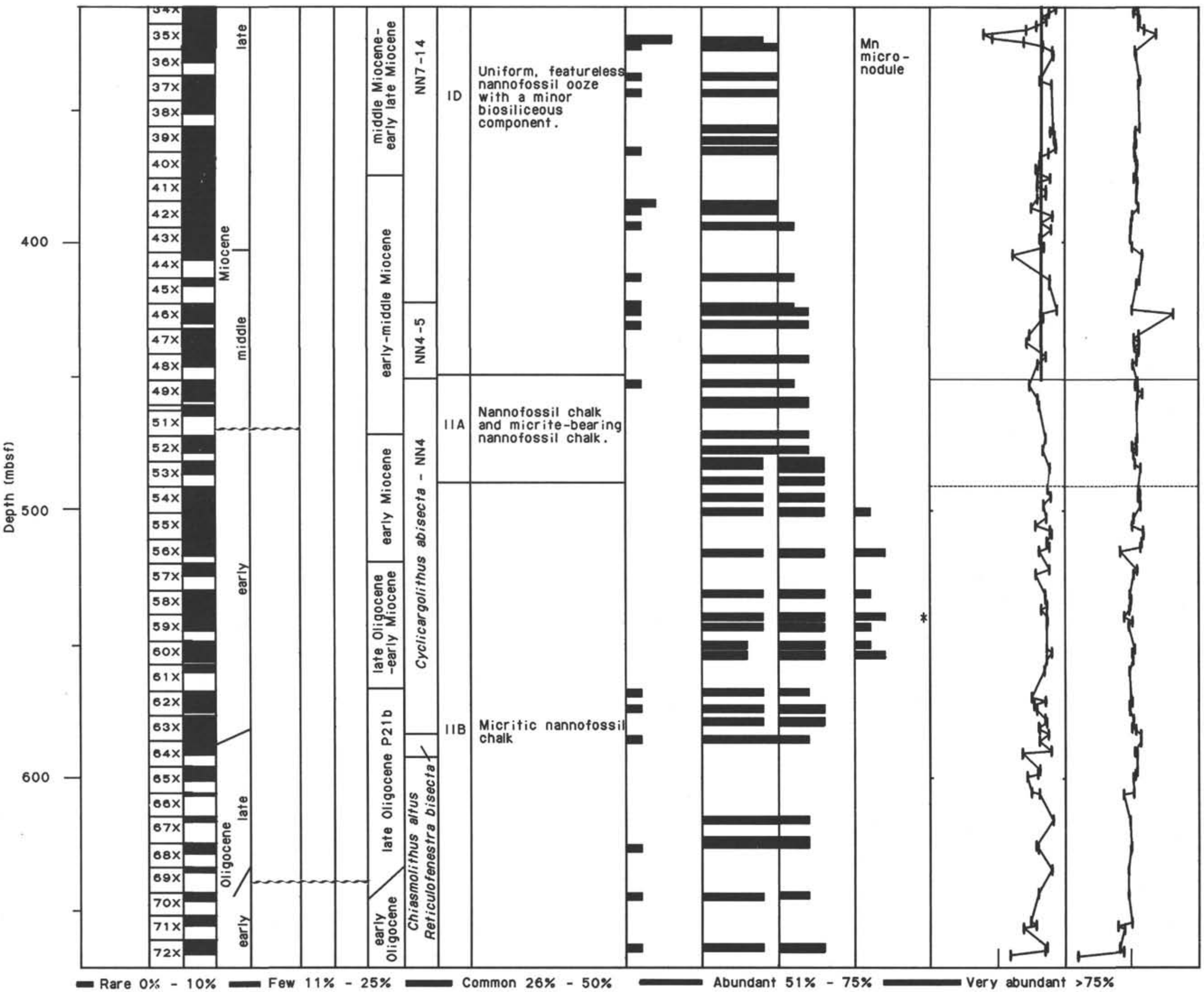

Figure 33 (continued).

The high carbonate values and microfossil assemblages for most of the early late Miocene interval (~10-8.5 Ma) are indicative of continued deposition from temperate surface waters well to the north of the Antarctic Convergence zone. The subtropical foraminifer genus *Globorotalia* was common to abundant during this period; however, it is unlikely that surface waters were warmer than cool temperate because of the dominance of low-diversity placolith calcareous nannofossils. The exceptionally high sedimentation rate of this interval clearly suggests that the site was in close proximity to upwelling. Microfossil assemblage characteristics are more consistent with a position close to the Subtropical Convergence rather than to the Antarctic Convergence.

The onset of significant long-term late Miocene cooling is inferred as beginning at ~8.5-9.0 Ma, just prior to the formation of the late Miocene hiatus. This event is manifested by the major decline in carbonate to 40% and a decline in the abundance of *Globorotalia*. Increased bottom current activity followed, resulting in the formation of the late Miocene hiatus which spans ~8.5 to 6.5 Ma.

Sedimentation once again resumed at Site 704 by ~6.5 Ma. Shortly thereafter (~6.0 Ma), and for the remainder of the late Miocene, rapid fluctuations of the paleoenvironment of the Meteor Rise occurred and persisted for most of the remainder of the Neogene. High-frequency and large-amplitude fluctuations in carbonate and biogenic silica content began at this time, as can be seen in the downhole plot of percent carbonate (Fig. 33). This permanent change in the carbonate record coincides with the lower boundary of Subunit Ic2 at 251.7 mbsf. For the remainder of the late Miocene, carbonate percentages are generally less than 63% and occasionally as low as 10%.

The late Miocene decrease in carbonate and associated increase in biogenic silica may be the consequence of increased siliceous productivity and dissolution of carbonate. Foraminifer assemblages of the latest Miocene consist almost entirely of two cold-water dissolution-resistant species, and siliceous microfossils are dominated to a greater extent by more endemic high-latitude species. It would appear that the Antarctic Convergence first migrated to within close proximitry of Site 704 during the latest Miocene (~6.0 Ma). If correct, this would most likely have required a near fully glaciated Antarctica.

From the record of Site 704 it is clear that the late Miocene interval between ~8.5 and 6.0 Ma brought a permanent end to the more temperate climatic conditions which persisted over the Meteor Rise since the Oligocene. After ~6.0 Ma, high-frequency fluctuations in surface water conditions signal the dominance of Quaternary-type glacial-interglacial variations. Coinciding closely with the late Miocene change in the paleoenvironment of the Meteor Rise region were: (a) the initial ice-rafting to Site 513 in the southeast Argentine Basin (Ciesielski and Weaver, 1983); (b) a northward expansion of the zone of ice-rafting throughout the Southern Ocean (Ciesielski et al., 1982); (c) further expansion of the Southern Ocean biosiliceous province and Antarctic Convergence Zone (Ciesielski and Weaver, 1983; Ciesielski et al., 1982); (d) an increase in Antarctic ice volume (Shackleton and Kennett, 1975; Ciesielski et al., 1982; Hodell et al., 1985); (e) increased upwelling and biogenic silica accumulation rates (Brewster, 1980); (f) a conspicuous high-latitude cooling (Kennett and Vella, 1975), and (g) a shoaling of the CCD (Hsü et al., 1984).

Pliocene

The Miocene/Pliocene boundary occurs at ~224.6 mbsf, just below the Subunit Ic1 and Ic2 boundary at 219.0 mbsf. Conditions responsible for the high-frequency fluctuations, and lower mean carbonate values of the latest Miocene, persisted into the earliest Gilbert Chron of the Pliocene. At ~4.77 Ma there was an abrupt increase in carbonate from 20% to 80%, marking the base of Subunit Ic1. From ~4.77 Ma throughout most of the remainder of the Gilbert Chron there was an apparent return to higher and more stable carbonate values. The increased carbonate values and other characteristics are inferred to represent a return to warmer conditions during the earliest Pliocene and a southward retreat of the Polar Front. This period of maximum early Pliocene warmth has been previously documented in other Southern Ocean regions (Ciesielski and Weaver, 1974, 1983; Keany, 1978).

The termination of the Gilbert Chron warming interval in the southwest Atlantic sector of the Southern Ocean began with a gradual decline in sea-surface temperatures commencing at ~3.97 to 3.86 Ma with northward movement of the Antarctic Convergence Zone toward its modern position (Ciesielski and Grinstead, 1986). Four successive major advances of the Antarctic Convergence Zone occurred at Site 514, at a similar latitude as Site 704 but in the Argentine Basin, during the Gauss Chron (at 2.86, 2.79, 2.67, and 2.58-2.47 Ma). Closely coinciding with the first of these advances was another significant change in the sedimentation at Site 704, suggesting a more northernly position of the convergence across the entire South Atlantic than during the earlier Pliocene. At Site 704 the changes in sedimentation occurred at ~3.0-2.9 Ma near the base of Subunit Ib and includes: a decrease in the mean carbonate content and an increase in the amplitude of the carbonate fluctuations (Figs. 30 and 33), and the onset of alterations in color and biogenic silica content (Fig. 30). Shortly following this change in sedimentation was the formation of a hiatus of brief duration (~2.8-2.5 Ma).

The major advance in the mean position of the Antarctic Convergence during the Gauss, as seen in the western (Site 514) and eastern (Site 704) sides of the subantarctic South Atlantic, precedes the first major Nothern Hemisphere glaciation (~2.37 Ma, Shackleton et al., 1984). Also shortly preceeding the first major Northern Hemisphere glaciation was: the closure of the Central American seaway (~3.0 Ma, Keigwin, 1982), the initial glaciation in Iceland (~3.1 Ma, McDougall and Wensink, 1966), and the first extensive sea ice in the Norwegian Sea (~2.8 Ma, Ciesielski and Case, unpublished data). Clearly the Gauss Chron was a time of global climatic change; however, the interhemispheric feedback mechanism driving these glacial and climaic changes is still poorly understood.

Quaternary

The final significant change in the pattern of sedimentation at Site 704 occurs at the base of Subunit IA (~101.7 mbsf) and approximates the base of the Quaternary. This boundary marks a significant increase in the occurrence of biogenic silica and a slightly lower carbonate content than the underlying subunit. Striking and repeated fluctuations in the carbonate and silica contents are the cause of pronounced color changes in the sediments. Variations of these two end-member components can be seen in the plot of carbonate values (Fig. 33) and in high-frequency, large-amplitude variations in calcium and silica elemental values in the geochemical log of Subunit IA (Fig. 31). The cyclic variations in lithology in Subunits IA and IB appear to be related to the glacial-interglacial cycles of the Pliocene-Pleistocene, with glacial episodes corresponding to intervals with low carbonate values.

Late Pliocene-Quaternary deposition at Site 704 was controlled by a complex interplay of three climatically controlled processes, including siliceous and carbonate productivity, carbonate dissolution, and dilution by carbonate or biogenic silica. Intervals of higher silica accumulation were probably the result of glacial advances of the biosiliceous productivity belt to Site 704, only to be followed by the dominance of carbonate productivity upon the interglacial retreat of the polar front. The logging results of Hole 704B confirm the presence of a strong high-resolution climatic signal with cycles on the scale of tens of thousands to hundreds of thousands of years. Shore-based determinations of isotopic, paleontologic, sedimentologic, and other characteristics of this site should provide an unequaled southern high-latitude reference section of late Neogene climatic history.

REFERENCES

Archie, G. E., 1942, The electrical resistivity log as an aid in determining some reservoir characteristics. *Trans. Am. Inst. Min. Metall. Pet. Eng.*, 146:54-67.

Backman, J., and Shackleton, N. J., 1983. Quantitative biochronology of Pliocene and early Pleistocene calcareous nannofossils from the Atlantic, Indian and Pacific oceans. *Mar. Micropaleontol.* 8:141-170.

Baker, P. A., 1986. Pore water chemistry of carbonate-rich sediments, Lord Howe Rise, Southwest Pacific Ocean. *In* Kennett, J. P., von der Borch, C. C., et al., *Init. Repts. DSDP*, 90: Washington (U.S. Govt. Printing Office), 1249-1256.

Barron, J. A., 1983. Latest Oligocene through early middle Miocene diatom biostratigraphy of the eastern tropical Pacific. *Mar. Micropaleontol.*, 7:487-515.

________, 1985. Miocene to Holocene planktic diatoms. *In* Bolli, H. M., Saunders, J. B., and Perch-Nielsen, K. (Eds.), *Plankton Stratigraphy*: Cambridge (Cambridge Univ. Press), 763-810.

Barron, J., Nigrini, C. A., Pujos, A., Saito, T., Thayer, F., Thomas, E., and Weinreich, N., 1985b. Synthesis of biostratigraphy, central Equatorial Pacific, Deep-Sea Drilling Project Leg 85: refinement of Oligocene to Quaternary biochronology. *Init. Repts. DSDP,* 85: Washington (U.S. Govt. Printing Office), 905-934.

Berggren, W. A., Kent, D. V., and Flynn, J. J., 1985. Paleogene geochronology and chronostratigraphy. *In* Snelling, N. J. (Ed.), *The Chronology of the Geological Record*. Geol. Soc. London Mem., 10:141-145.

Brewster, N. A., 1980. Cenozoic biogenic silica sedimentation in the Antarctic Ocean, based on two Deep Sea Drilling Sites. *Geol. Soc. Am. Bull.*, 91:337-349.

Burckle, L. H., Clarke, D. B., and Shackleton, N. J., 1978. Isochronous last-abundant-appearance datum (LAAD) of the diatom *Hemidiscus karstenii* in the sub-Antarctic. *Geology*, 6:243-246.

Chen, P. H., 1975. Antarctic radiolaria. *In* Hayes, D. E., Frakes, L. A., et al., *Init. Repts. DSDP*, 28: Washington (U.S. Govt. Printing Office), 437-513.

Ciesielski, P. F., 1975. Biostratigraphy and paleoecology of Neogene and Oligocene silicoflagellates from cores recovered during Antarctic Leg 28. *In* Hayes, D. E., Frakes, L. A., et al., *Init. Repts. DSDP*, 28: Washington (U.S. Govt. Printing Office), 625-691.

________, 1983. The Neogene and Quaternary diatom biostratigraphy of subantarctic sediments, Deep Sea Drilling Leg 71. *In* Ludwig, W. J., Krasheninnikov, V. A., et al., *Init. Repts. DSDP*, 71: Washington (U.S. Govt. Printing Office), 625-691.

________, 1985. Middle Miocene to Quaternary diatom biostratigraphy of Deep Sea Drilling Project Site 594, Chatham Rise, Southwest Pacific. *In* Kennett, J. P., von der Borch, D. D., et al., *Init. Repts. DSDP,* 90 Pt.2: Washington (U.S. Govt. Printing Office), 863-885.

Ciesielski, P. F., and Grinstead, G. P., 1986. Pliocene variations in the position of the Antarctic Convergence in the Southwest Atlantic. *Paleoceanography*, 1:197-232.

Ciesielski, P. F., Ledbetter, M. T., and Ellwood, B. B., 1982. The development of Antarctic glaciation and the Neogene paleoenvironment of the Maurice Ewing Bank. *Mar. Geol.*, 46:1-51.

Ciesielski, P. F., and Weaver, F. M., 1974. Early Pliocene climatic changes in the antarctic seas. *Geology*, 2:511-515.

________, 1983. Neogene and Quaternary paleoenvironmental history of Deep Sea Drilling Project Leg 71 sediments, southwest Atlantic Ocean. *In* Ludwig, W. J., and Krasheninnikov, V. A., et al., *Init. Repts. DSDP*, 71: Washington (U.S. Govt. Printing Office), 461-477.

Fenner, J. M., 1984. Eocene-Oligocene planktic diatom stratigraphy in the low latitudes and the high northern latitudes. *Micropaleontology*, 30:319-342.

Froelich, P. N., Kim, K. K., Jahnke, R. J., Burnett, W. R., and Deakin, M., 1983. Pore water fluoride in Peru continental margin sediments: uptake from seawater. *Geochim. Cosmochim. Acta*, 47:1605-1612.

Gardner, J. V., 1975. Late Pleistocene carbonate dissolution cycles in the eastern Equatorial Atlantic. *Spec. Publ. Cushman Found. Foraminiferal Res.*, 13:129-141.

Gartner, S., 1972. Late Pleistocene calcareous nannofossils in the Caribbean and their interoceanic correlation. *Palaeogr. Palaeoclimat. Palaeoecol.*, 12:169-191.

Gersonde, , and Schrader, H., 1984. Marine plankton correlation of lower Messinian deposits in the western Mediterranean. *Mar. Micropaleontol.*, 9:93-110.

Gieskes, J. M., 1983. The chemistry of interstitial waters of deep-sea sediments: interpretation of deep-sea drilling data. *In* Riley, J. P., and Chester, R. (Eds.), *Chemical Oceanography* (Vol. 8): London (Academic Press), 222-269.

Gieskes, J. M., and Lawrence, J. R., 1981. Alteration of volcanic matter in deep-sea sediments: evidence from the chemical composition of interstitial waters from deep-sea cores. *Geochim. Cosmochim. Acta*, 45:1687-1703.

Gombos, A. M., Jr., 1983. Middle Eocene diatoms from the North Atlantic. *In* Ludwig, W. J., Krasheninnikov, V. A., et al., *Init. Repts. DSDP*, 71: Washington (U.S. Govt. Printing Office), 565-582.

Gombos, A. M., Jr., and Ciesielski, P. F., 1983. Late Eocene to early Miocene diatoms from the southwest Atlantic. *In* Ludwig, W. J., Krasheninnikov, V. A., et al., *Init. Repts. DSDP*, 71: Washington (U.S. Govt. Printing Office), 583-634.

Gordon, A. L., and Goldberg, R. D., 1970. Circumpolar characteristics of antarctic waters. *In* Bushnell, V. (Ed.), *Antarctic Map Folio Series*: New York (Am. Geogr. Soc.), 13.

Haq, B. U., Worsley, T. R., Burckle, L. H., Douglas, R. G., et al., 1980. Late Miocene carbon-isotopic shift and synchroneity of some phytoplanktonic biostratigraphic events. *Geology*, 8:427-431.

Haq, B. U., and Takayama, T., 1984. Neogene calcareous nannoplankton datum planes and their correlation to magnetostratigraphy. *In* Ikebe and Tsuchi (Eds.) *Pacific Neogene Datum Planes*. Univ. of Tokyo Press, 27-33.

Hays, J. D., Lozano, J. A., Shackleton, N. J., and Irving, G., 1976. Reconstruction of the Atlantic and western Indian Ocean sectors of the 18,000 B.P. Antarctic Ocean. *Mem. Geol. Soc. Am.*, 145:337-372.

Hays, J. D., and Opdyke, N. D., 1967. Antarctic radiolaria, magnetic reversals, and climatic change. *Science*, 158:1001-1011.

Hays, J. D., and Shackleton, N. J., 1976. Globally synchronous extinction of the radiolarian *Stylatractus universus*. *Geology*, 4:649-652.

Hodell, D. A., Elmstrom, K. M., and Kennett, J. P., 1985. Latest Miocene $\delta^{18}O$ changes, global ice volume, sea level and the Messinian salinity crisis. *Nature*, 320:411-414.

Hodell, D. A., and Kennett, J. P., 1986. Late Miocene-early Pliocene stratigraphy and paleoceanography of the South Atlantic and southwest Pacific Oceans: a synthesis. *Paleoceanography*, 1:285-311.

Hsü, K. J., McKenzie, J. A., Oberhaensli, H., Weissert, H., and Wright, R. C., 1984. South Atlantic paleoceanography. *In* Hsü, K. J., LaBrecque, J. L., et al., *Init. Repts. DSDP*, 73, Washington (U.S. Govt. Printing Office), 771-785.

Jenkins, D. G., 1985. Southern mid-latitude Paleocene to Holocene planktic foraminifera. *In* Bolli, H. M., Saunders, J. B., and Perch-Nielsen, K. (Eds.), *Plankton Stratigraphy*: Cambridge (Cambridge Univ. Press), 263-282.

Johnson, D. A., and Wick, B. J., 1982. Precision of correlation of radiolarian datum levels in the middle Miocene equatorial Pacific: *Micropaleontology,* 28:1-30

Keany, J. 1978. Paleoclimatic trends in the early and middle Pliocene sediments of the Antarctic. *Mar. Micropaleontol.*, 3:35-49.

Keigwin, L. D., Jr., 1982. Isotopic paleoceanography of the Caribbean and East Pacific: role of the Panama uplift in the late Neogene. *Science*, 217:350-353.

Kennett, J. P., 1973. Middle and late Cenozoic planktonic foraminiferal biostratigraphy of the Southwest Pacific—DSDP Leg 21. *In* Burns, R. E., Andrews, J. E., et al., *Init. Repts. DSDP*, 21: Washington (U.S. Govt. Printing Office), 575-639.

Kennett, J. P., and Vella, P., 1975. Late Cenozoic planktonic foraminifera and paleoceanography at DSDP Site 284 in the cool subtropical South Pacific. *In* Kennett, J. P., Houtz, R. E., et al., *Init. Repts. DSDP*, 29: Washington (U.S. Govt. Printing Office), 769-799.

Kennett, J. P., and Srinivasan, M. S., 1983. *Neogene Planktonic Foraminifera: A Phylogenetic Atlas*: (Hutchinson Ross).

Kent, D. V., and Gradstein, F., 1985. A Cretaceous and Jurassic geochronology. *Geol. Soc. Am. Bull.*, 96:1419-1427.

Kim, W. H., and Barron, J. A., 1986. Diatom biostratigraphy of the upper Oligocene to lowermost Miocene San Gregorio Formation, Baja California Sur, Mexico. *Diatom Res.*, 1:169-187.

LaBrecque, J. L. (Ed.), 1986. *South Atlantic Ocean and Adjacent Continental Margin Atlas 13*: Ocean Margin Drilling Program Reg. Atlas Ser., 13.

LaBrecque, J. L., and Hayes, D. E., 1979. Seafloor spreading history of the Agulhas Basin. *Earth Planet. Sci. Lett.*, 45:411-428.

Ledbetter, M. T., and Ciesielski, P. F., 1982. Bottom-current erosion along a traverse in the South Atlantic sector of the Southern Ocean. *Mar. Geol.*, 46:329-341.

Lutjeharms, J.R.E., and Valentine, H. R., 1984. Southern Ocean thermal fronts south of Africa. *Deep Sea Res.*, 31:1461-1475.

Martini, E., 1971. Standard Tertiary and Quaternary calcareous nannoplankton zonation. *In* Farinacci, A. (Ed.), *Proc. Planktonic Conf. II Rome 1970*: Rome (Technoscienze), 2:739-785.

Mayer, L. A., 1979. Deep sea carbonates: acoustic, physical, and stratigraphic properties. *J. Sediment. Petrol.*, 49:819-836.

Mayer, L. A., Shipley, T. H., and Winterer, E. L., 1986. Equatorial Pacific seismic reflectors as indicators of global oceanographic events. *Science*, 233:761-764.

McDougall, I., and Wensink, H., 1966. Paleomagnetism and geochronology of the Pliocene-Pleistocene lavas in Iceland. *Earth Planet. Sci. Lett.*, 1:232-236.

McDuff, R. E., 1985. The chemistry of interstitial waters, Deep Sea Drilling Project Leg 86. *In* Heath, G. R., Burckle, L. H., et al., *Init. Repts. DSDP*, 86: Washington (U.S. Govt. Printing Office), 675-687.

McGowran, B., 1986. Cainozoic oceanic and climatic events: the Indo-Pacific foraminiferal biostratigraphic records. *Palaeogr. Palaeoclimat. Palaeoecol.*, 55:247-265.

Mienert, J., Stein, R., and Schultheiss, P., and Shipboard Scientific Party, 1988. Relationship between density and biogenic opal in sediments from Sites 658 and 660. *In* Ruddiman, W., Sarnthein, M., et al., *Proc. ODP, Init. Repts.*, 108: College Station, TX (Ocean Drilling Program), 1047-1053.

Mijajima, M. H., 1974. Absolute chronology of upper Pleistocene calcareous nannofossil zones of the southeast Indian Ocean. *Antarctic J. U.S.*, 9:261-263.

Miller, K. G., and Fairbanks, R. G., 1985. Oligocene to Miocene carbon isotopic cycles and abyssal circulation changes. *In The Carbon Cycle and Atmospheric CO_2: Natural Variations Archean to Present*: Am. Geophys. Union Monogr., 32:469-486.

Morkhoven, F.P.C.M. van, Berggren, W. A., and Edwards, A. S., 1986. Cenozoic cosmopolitan deep-water benthic foraminifera. *Mem. Cent. Rech. Explor. Prod. Elf Aquitaine*, 11.

Perch-Nielsen, K., 1985. Cenozoic calcareous nannofossils. *In* Bolli, H. M., Saunders, J. B., and Perch-Nielsen, K. (Eds.), *Plankton Stratigraphy*: Cambridge (Cambridge Univ. Press), 427-554.

Ryan, W. B. F., Cita, M. B., Rawson, M. D., Burckle, L. H., and Saito, T., 1974. A paleomagnetic assignment of Neogene stage boundaries and the development of isochronous datum planes between the Mediterranean, the Pacific and Indian oceans in order to investigate the response of the world ocean to the Mediterranean "salinity crisis." *Riv. Ital. Paleont.*, 80:631-688.

Samtleben, C., 1980. Die evolution Coccolithophoriden-Gattung *Gephyrocapsa* nach befunden in Atlantik. *Paläontol. Z.*, 54:91-127.

Sanfilippo, A., Westberg-Smith, M. J., and Riedel, W. R., 1985. Cenozoic radiolaria. *In* Bolli, H. M., Saunders, J. B., and Perch-Nielsen, K. (Eds.), *Plankton Stratigraphy*: Cambridge (Cambridge Univ. Press), 573-630.

Schlumberger, Inc., 1972. *Log Interpretation (Vol. 1): Principles*: New York (Schlumberger).

_______, 1974. *Log Interpretation (Vol. 2): Applications*: New York (Schlumberger).

Serra, O., 1984. *Fundamentals of Well Log Interpretation: Volume 1. The Acquisition of Logging Data*: Amsterdam (Elsevier).

_______, 1987. *Fundamentals of Well Log Interpretation: Volume 2. Interpretation*: Amsterdam (Elsevier).

Shackleton, N. J., Backman, J., Zimmerman, H., et al., 1984. Oxygen isotopic calibration of the onset of ice-rafting and history of glaciation in the North Atlantic region. *Nature*, 307:620-623.

Shackleton, N. J., and Kennett, J. P., 1975. Paleotemperature history of the Cenozoic and the initiation of Antarctic glaciation: oxygen and carbon isotope analyses in DSDP Sites 277, 279, and 281. *In* Kennett, J. P., Houtz, R. E., et al., *Init. Repts. DSDP*, 29: Washington (U.S. Govt. Printing Office), 743-755.

Shaw, C. A., and Ciesielski, P. F., 1983. Silicoflagellate biostratigraphy of middle Eocene to Holocene subantarctic sediments recovered by Deep Sea Drilling Project Leg 71. *In* Ludwig, W. J., Krasheninnikov, V. A., et al., *Init. Repts. DSDP*, 71: Washington (U.S. Govt. Printing Office), 687-737.

Theyer, F., Mato, C. Y., and Hammond, S. R., 1978. Paleomagnetic and geochronologic calibration of latest Oligocene to Pliocene radiolarian events, equatorial Pacific. *Mar. Micropaleontol.*, 3:377-395.

Thiede, J., Suess, E., and Mueller, P. J., 1982. Late Quaternary fluxes of major sediment components to the sea floor at the northwest African continental slope. *In* von Rad, U., Hinz, K., Sarnthein, M., and Seibold, E. (Eds.), *Geology of the Northwest African Continental Margin*: Berlin (Springer), 605-631.

Thierstein, H. R., Gertzenaur, K. R., and Moffino, B., 1977. Global synchroneity of Late Quaternary cocolith datum levels: validation by oxygen isotopes. *Geology*, 5:400-404.

Tucholke, B. E., and Embley, R. W., 1984. Cenozoic regional erosion of the abyssal seafloor off South Africa. *In* Schlee, J. S. (Ed.), Interregional unconformities and hydrocarbon accumulation. *AAPG Mem.*, 36:145-164.

Weaver, F. M., 1983. Cenozoic radiolarians from the southwest Atlantic, Falkland Plateau region, Deep Sea Drilling Project Leg 71. *In* Ludwig, W. J., Krasheninnikov, V. A., et al., *Init. Repts. DSDP*, 71: Washington (U.S. Govt. Printing Office), 667-686.

Weaver, F. M., and Gombos, A. M., Jr., 1981. Southern high latitude diatom biostratigraphy. *In* Warme, J. E., Douglas, R. G., and Winterer, E. L. (Eds.), *The Deep Sea Drilling Project: A Decade of Progress*: Spec. Publ. Soc. Econ. Paleontol. Mineral., 32:445-470.

Wise, S. W., 1983. Mesozoic and Cenozoic calcareous nannofossils recovered by Deep Sea Drilling Project Leg 71 in the Falkland Plateau region, southwest Atlantic Ocean. *In* Ludwig, W. J., Krasheninnikov, V. A., et al., *Init. Repts. DSDP*, 71: Washington (U.S. Govt. Printing Office), 481-550.

Wyllie, M.R.J., Gregory, A. R., and Gardner, G.H.F., 1956. Elastic wave velocities in heterogeneous and porous media. *Geophysics*, 21: 41-70.

Ms 114A-111

Summary log for Hole 704B.

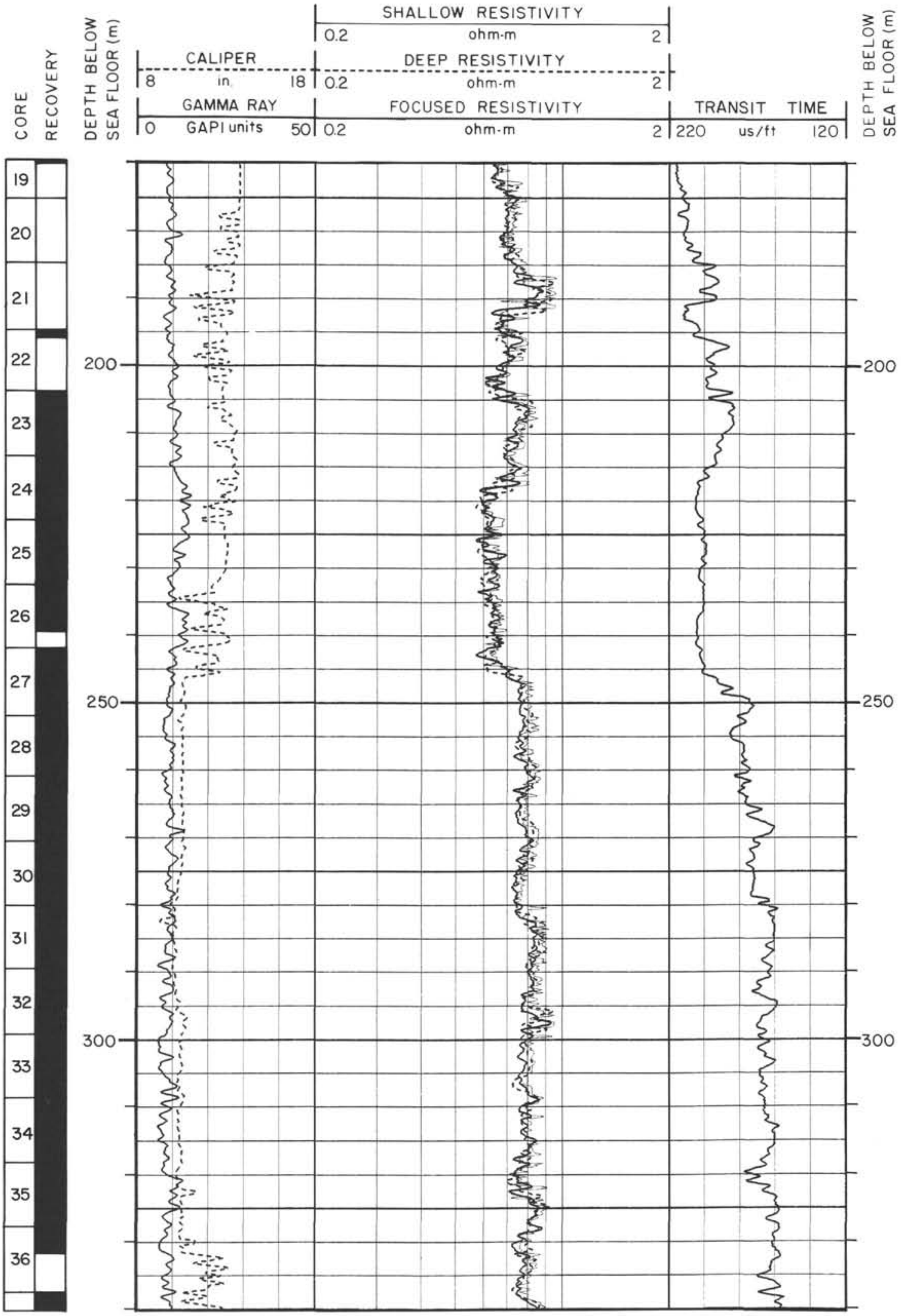

Summary log for Hole 704B (continued).

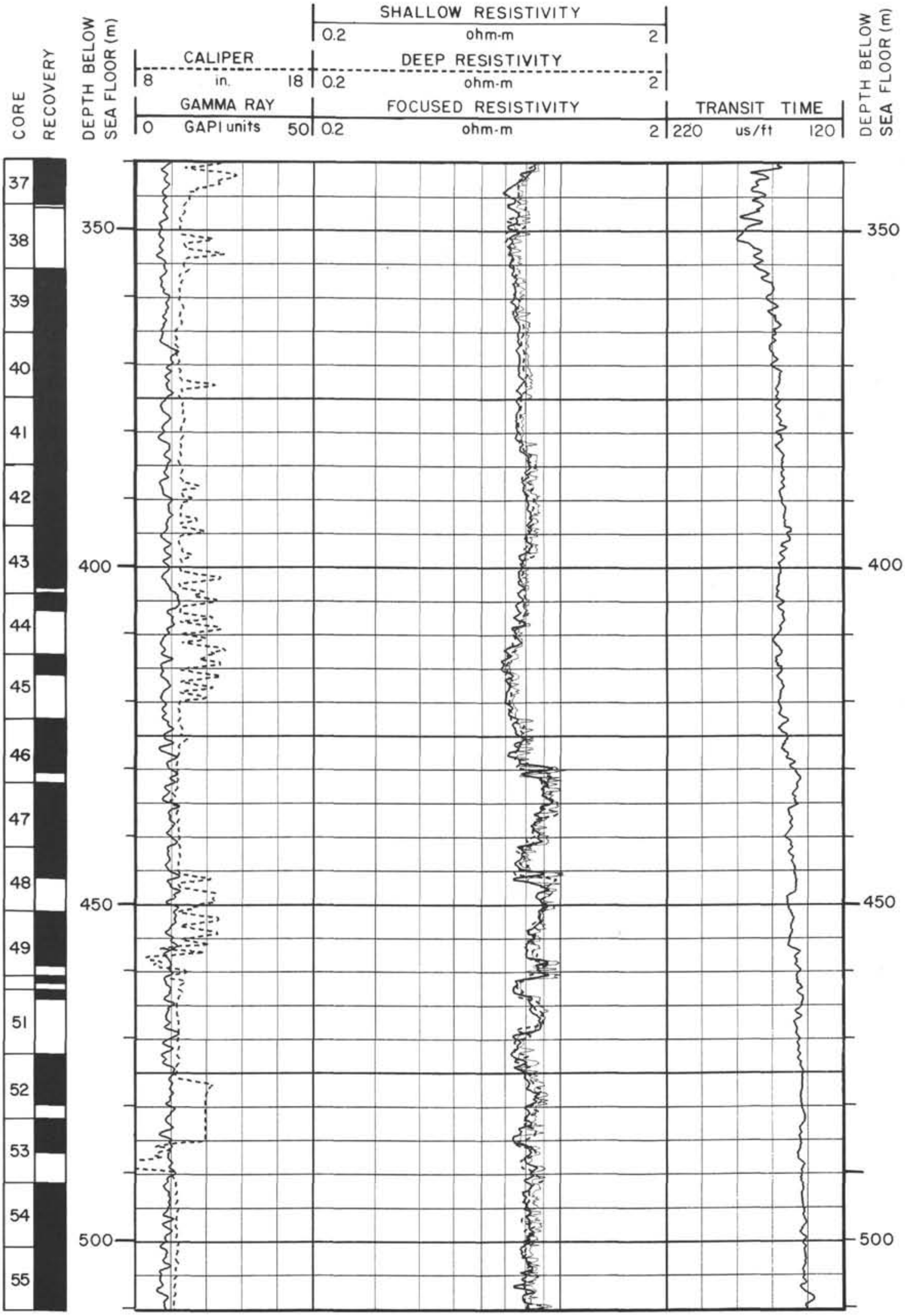

Summary log for Hole 704B (continued).

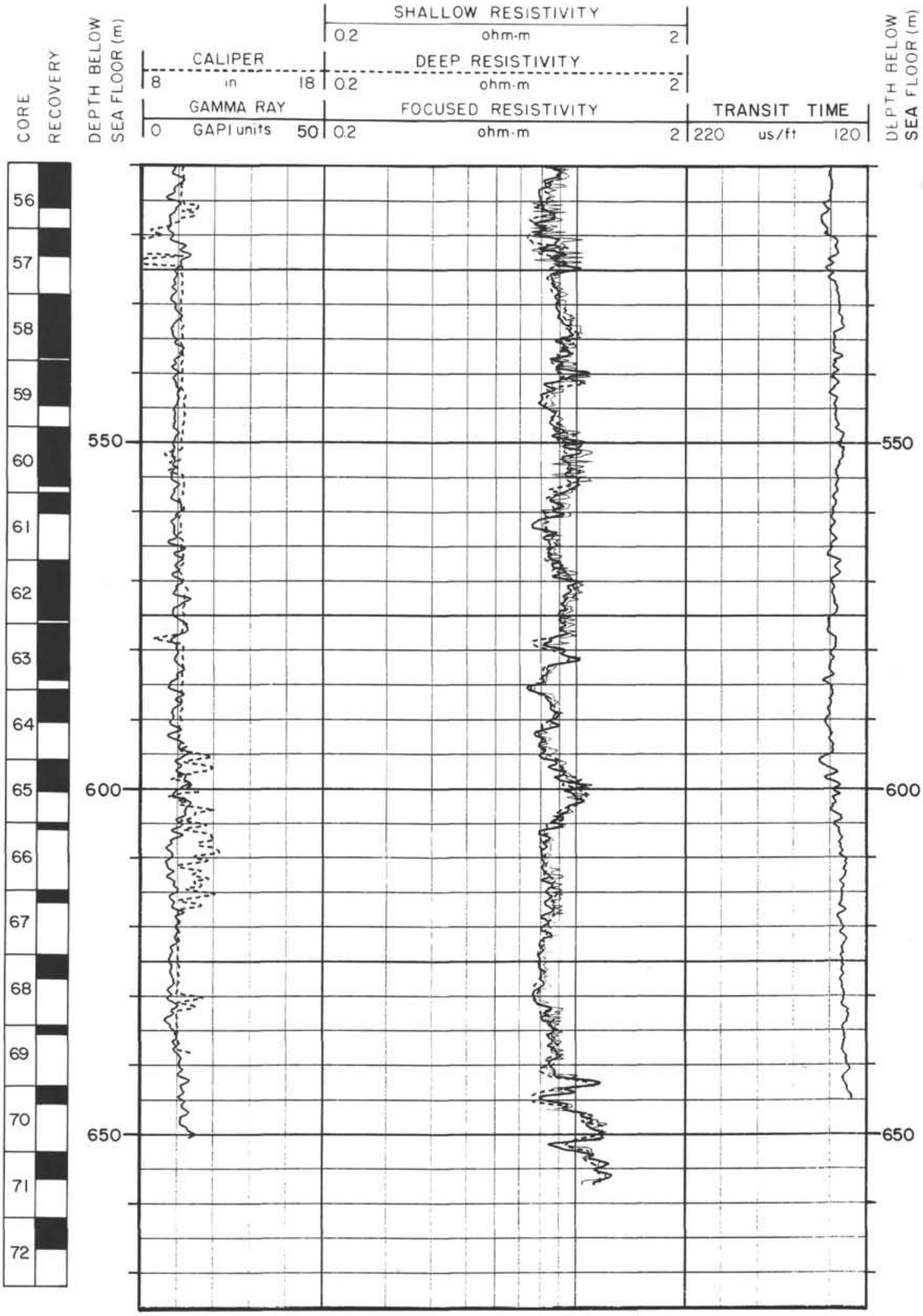

Summary log for Hole 704B (continued).

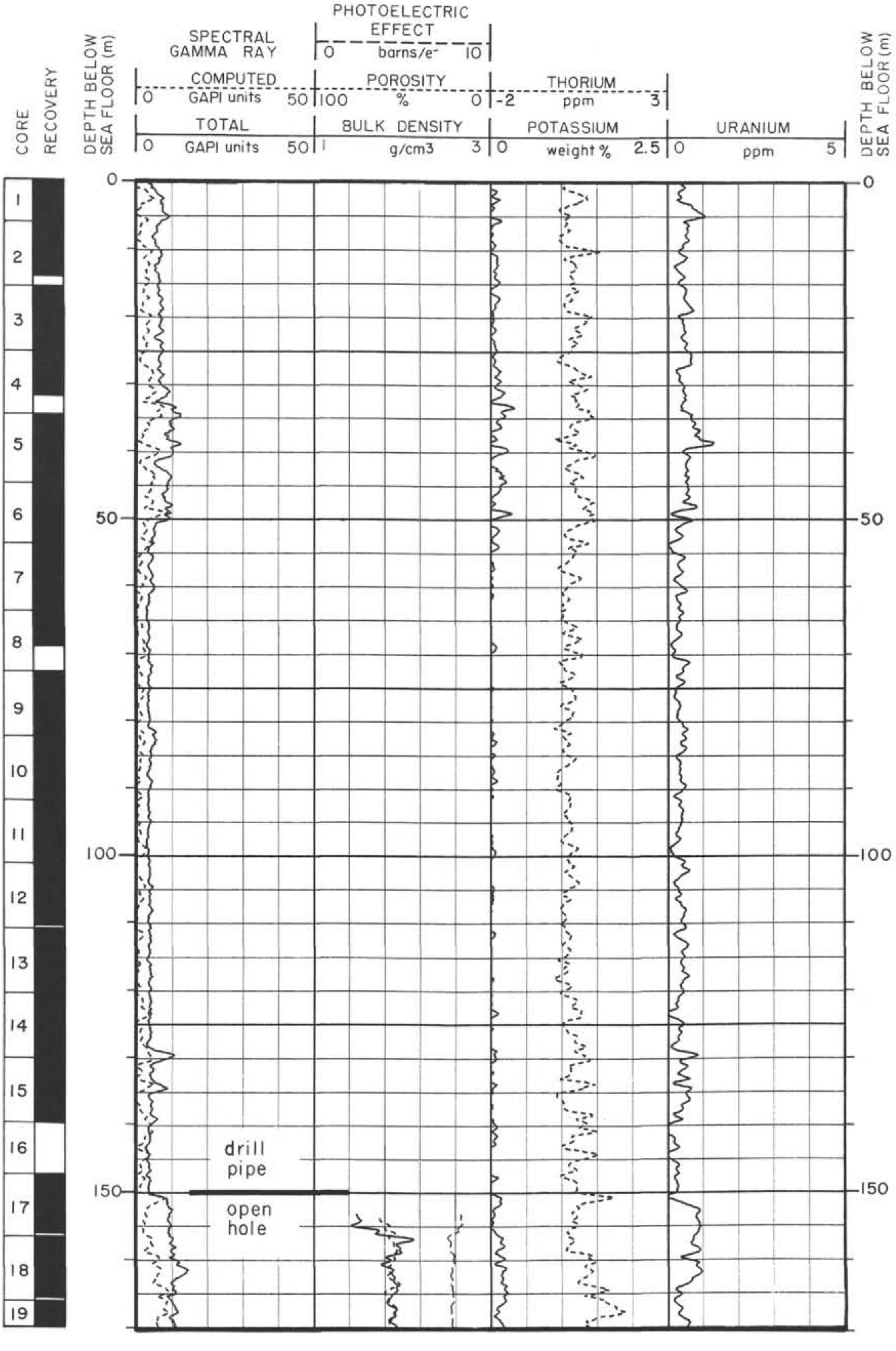

Summary log for Hole 704B (continued).

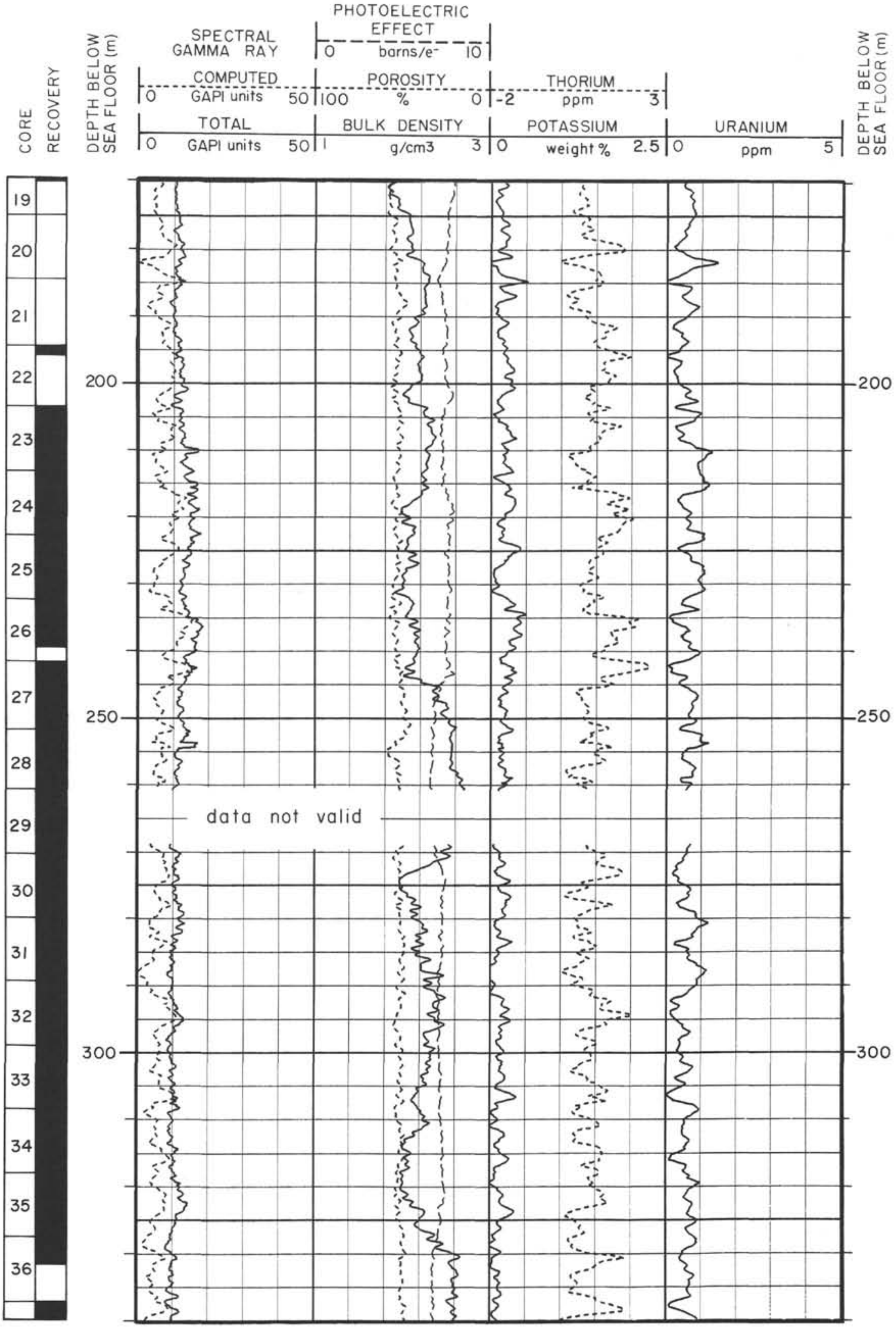

Summary log for Hole 704B (continued).

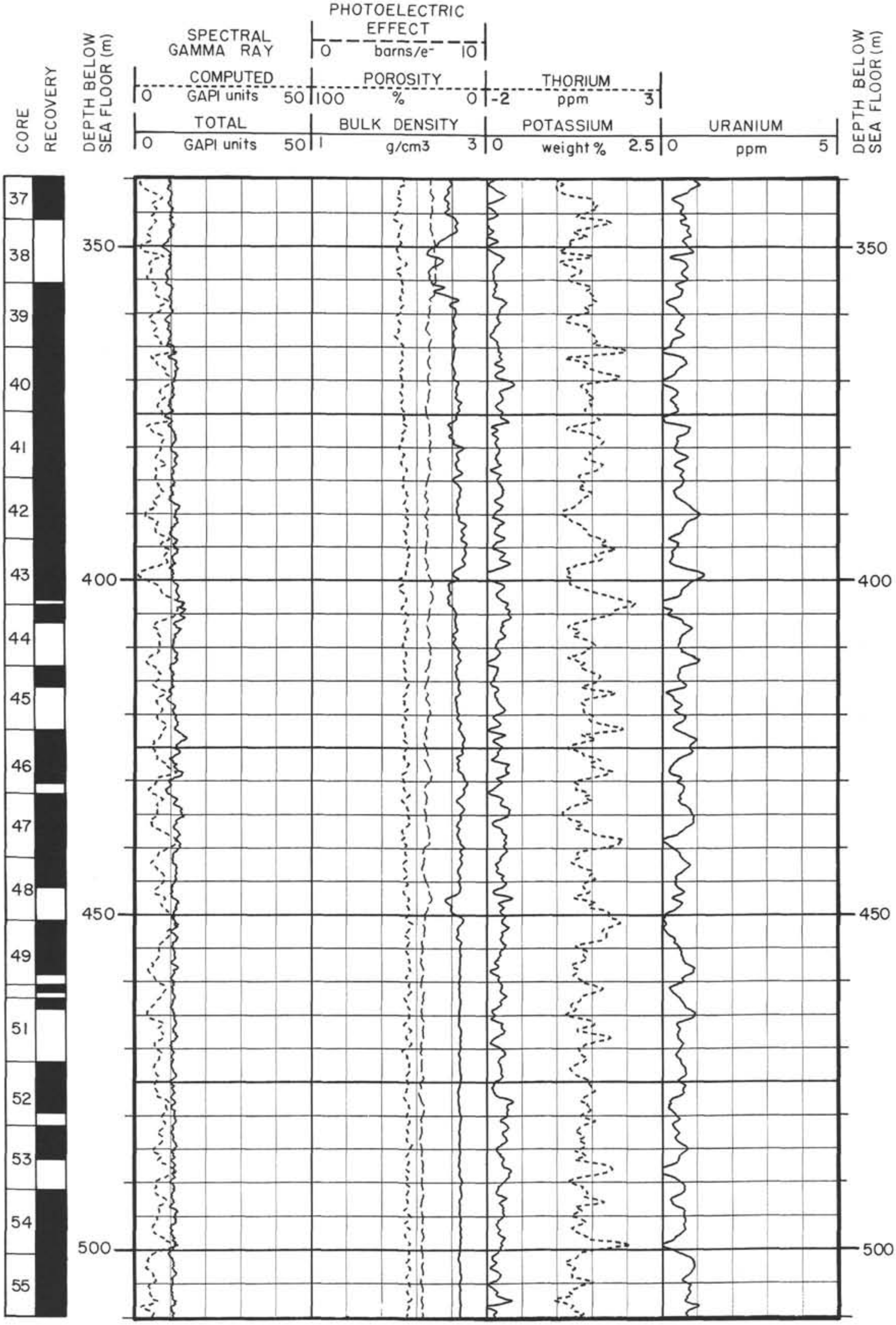

Summary log for Hole 704B (continued).

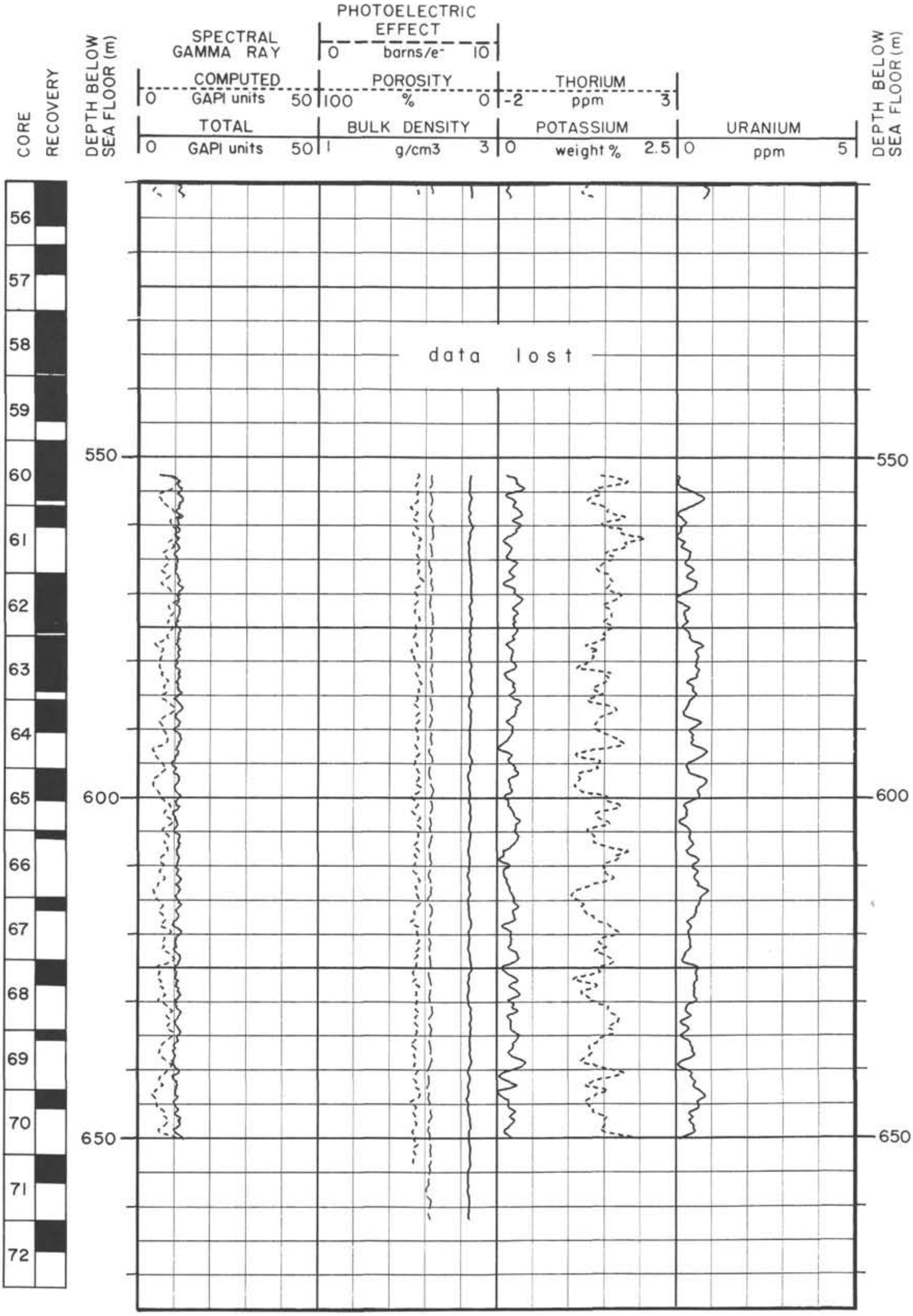

Summary log for Hole 704B (continued).

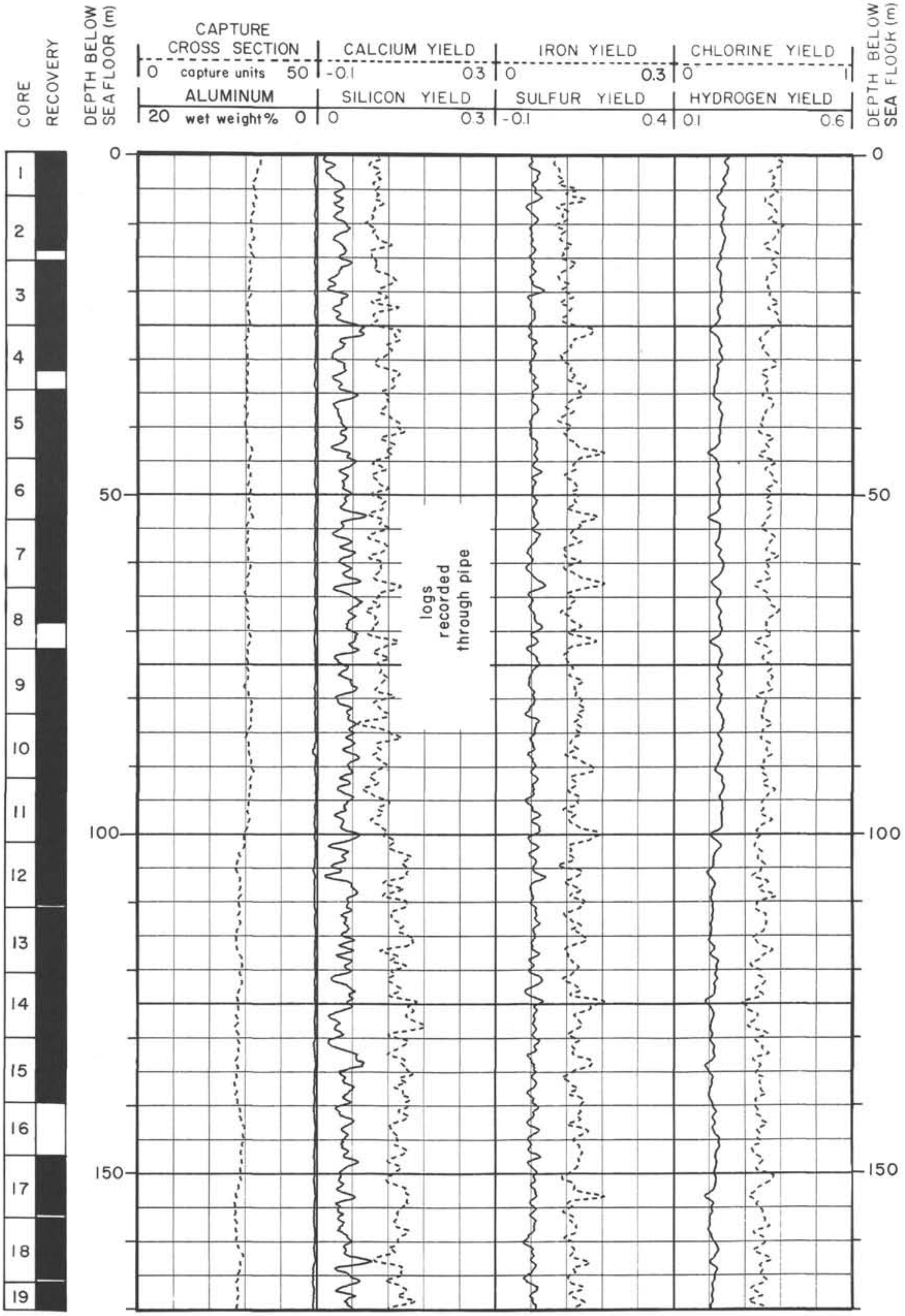

Summary log for Hole 704B (continued).

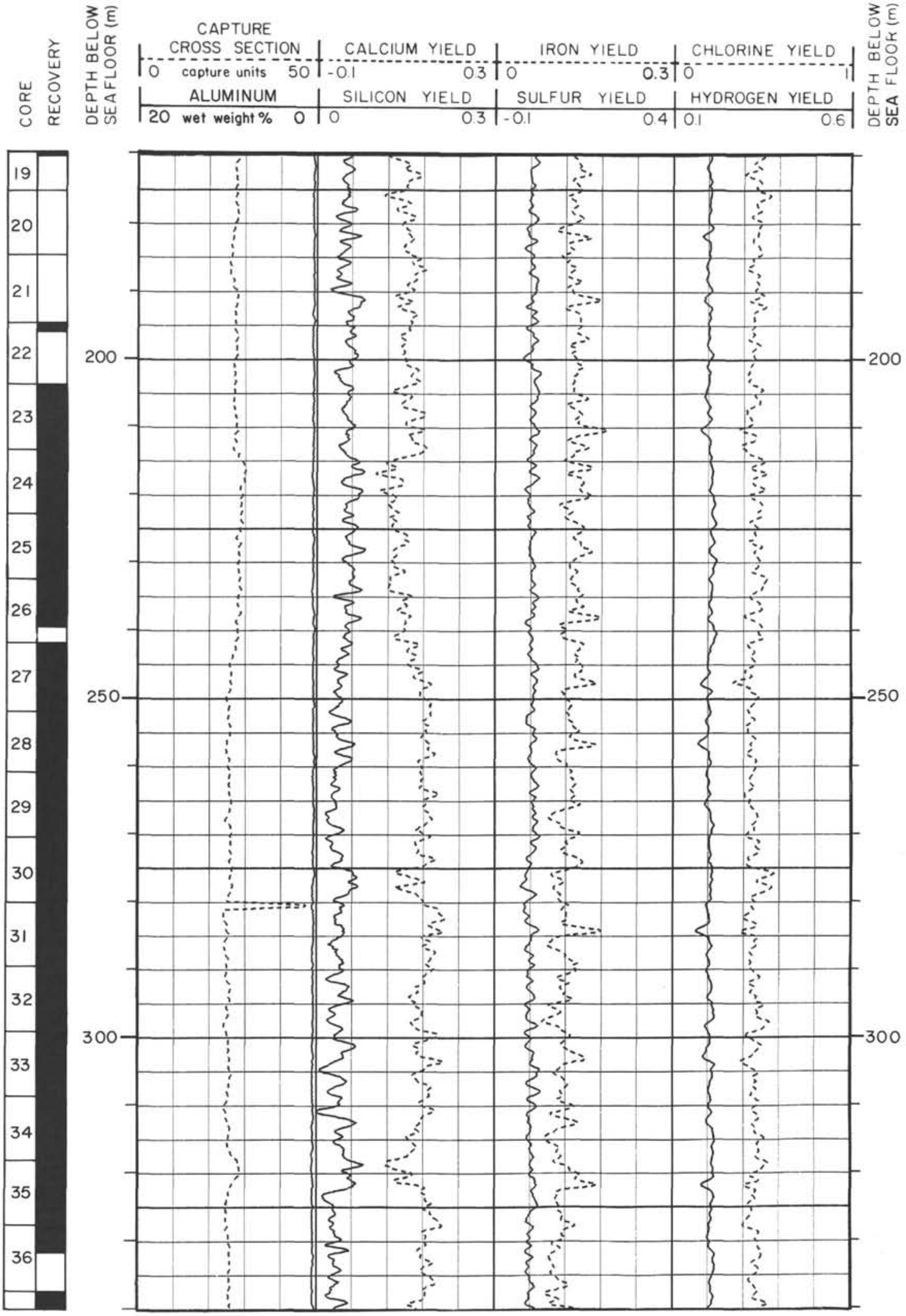

Summary log for Hole 704B (continued).

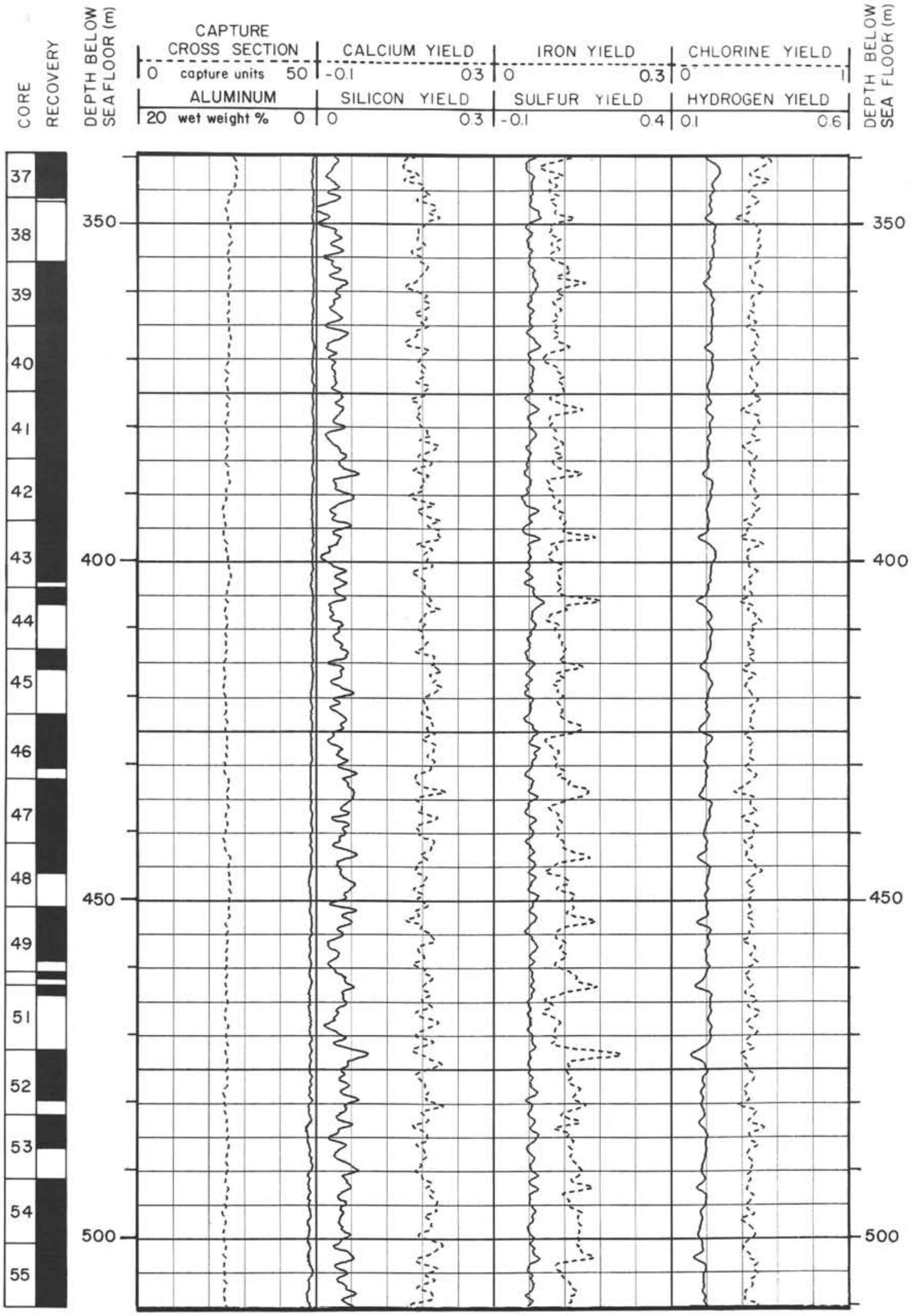

Summary log for Hole 704B (continued).

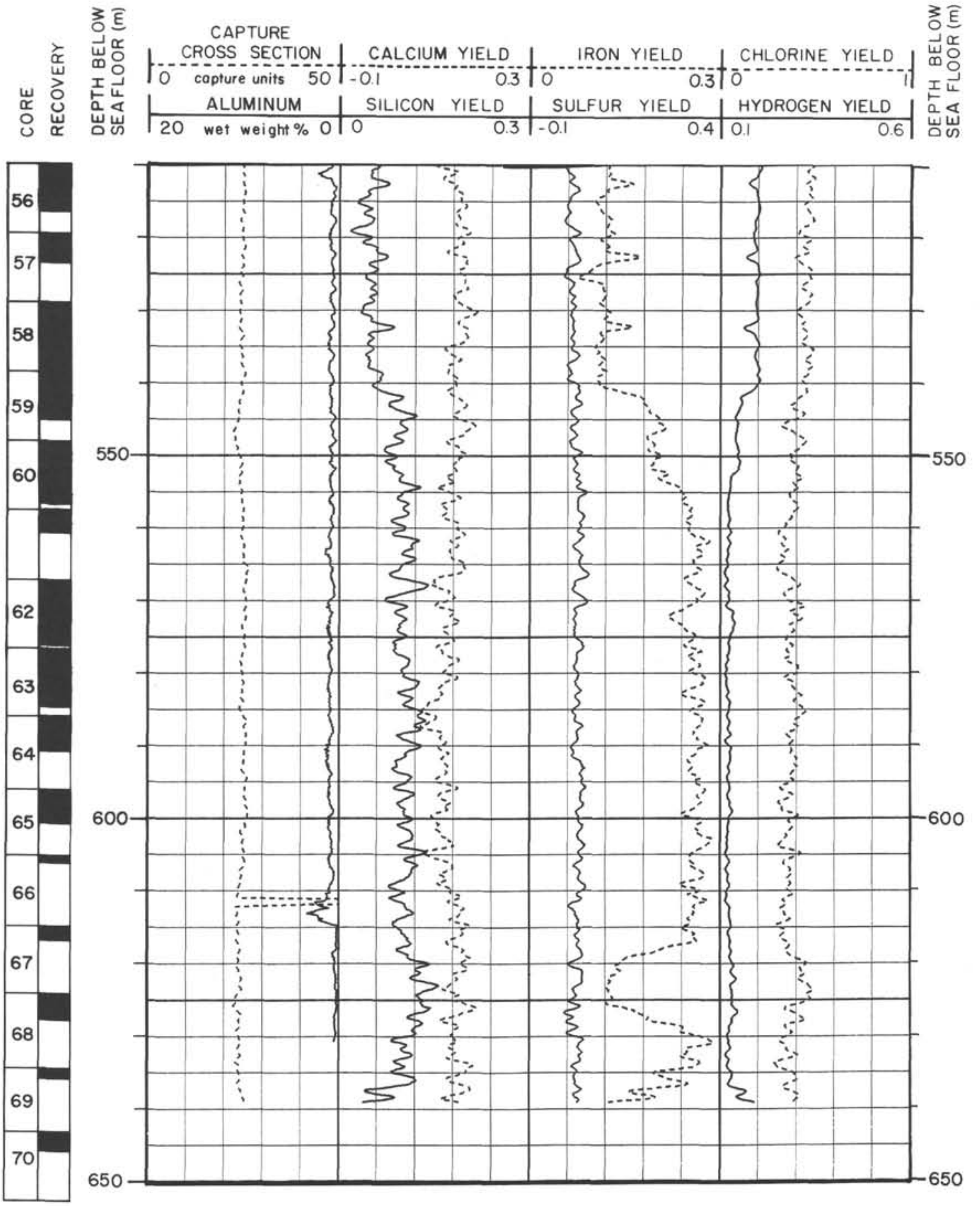

SITE 704 HOLE A CORE 1H CORED INTERVAL 2521.8-2529.0 mbsl; 0-7.2 mbsf

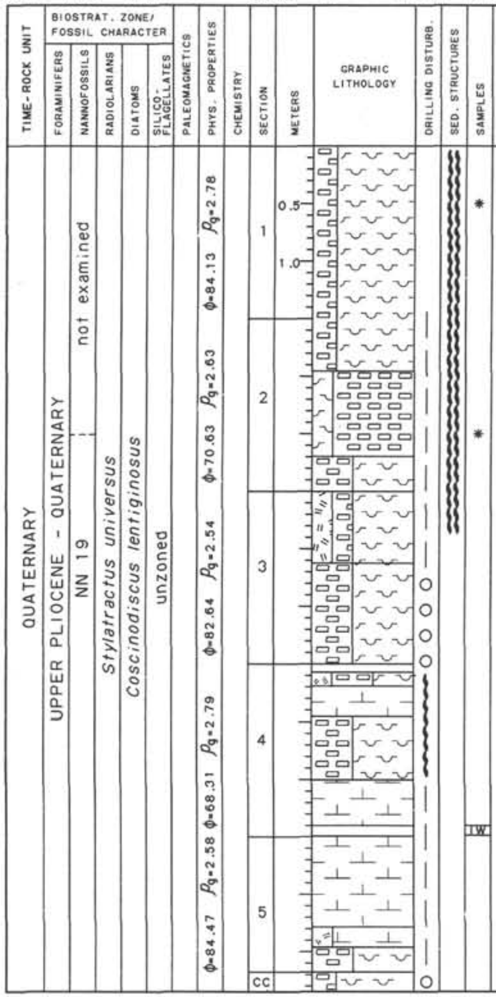

LITHOLOGIC DESCRIPTION

CALCAREOUS-BEARING DIATOM OOZE, CALCAREOUS DIATOM OOZE, and NANNOFOSSIL OOZE

Drilling disturbance: Slightly disturbed, Section 2, Section 3, 0-45 cm, Section 4, 100-150 cm; and Section 5, 0-90 cm; soupy, Section 3, 45-150 cm; highly disturbed, Section 4, 0-95 cm.

Major lithology: Alternations of calcareous-bearing diatom ooze, pale yellow (2.5Y 8/4) to light yellowish brown (2.5Y 6/4), calcareous diatom ooze, olive (5Y 5/3) to white (no color code), and nannofossil ooze, white (no color code). Color boundaries are sharp.

Minor lithology: Ash-bearing calcareous diatom ooze, very pale gray (no color code).

SMEAR SLIDE SUMMARY (%):

	1, 55 D	2, 100 D	4, 40 D	4, 70 D
COMPOSITION:				
COMPOSITION:				
Volcanic glass	5	5	Tr	Tr
Calcite	2	—	—	18
Foraminifers	2	15	5	Tr
Nannofossils	7	70	95	30
Diatoms	83	8	—	51
Radiolarians	1	2	—	1
Silicoflagellates	Tr	Tr	—	—

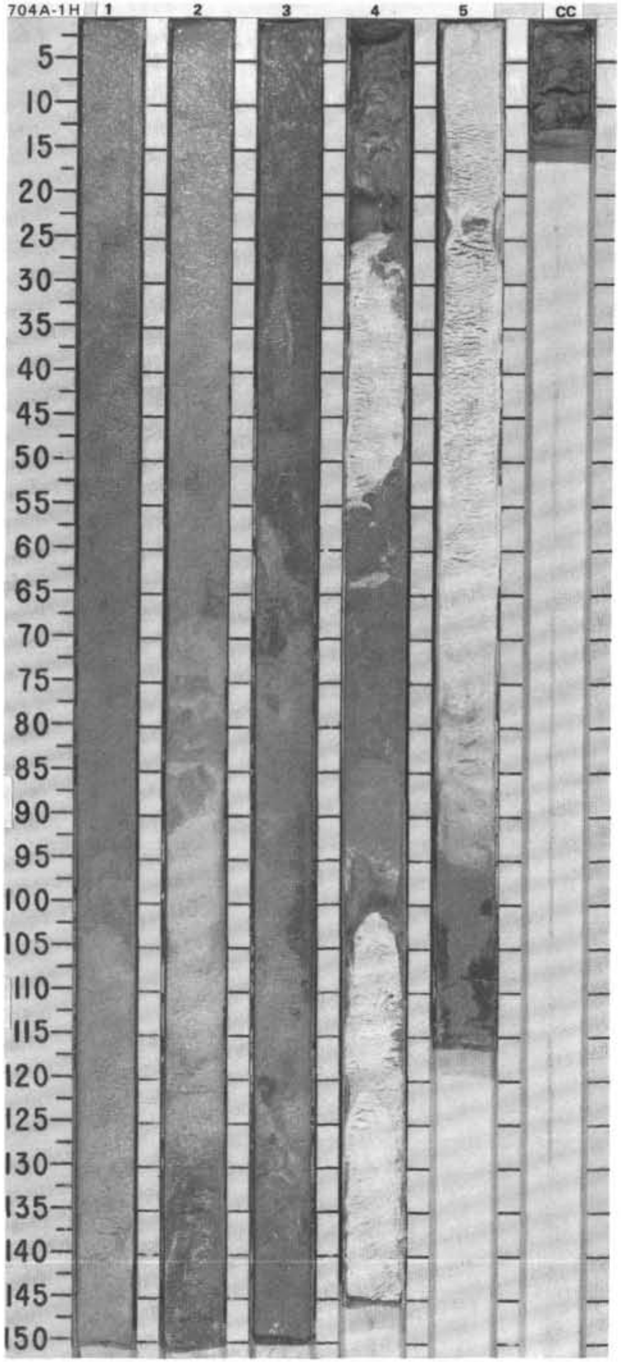

SITE 704 HOLE A CORE 2H CORED INTERVAL 2529.0-2538.5 mbsl; 7.2-16.7 mbsf

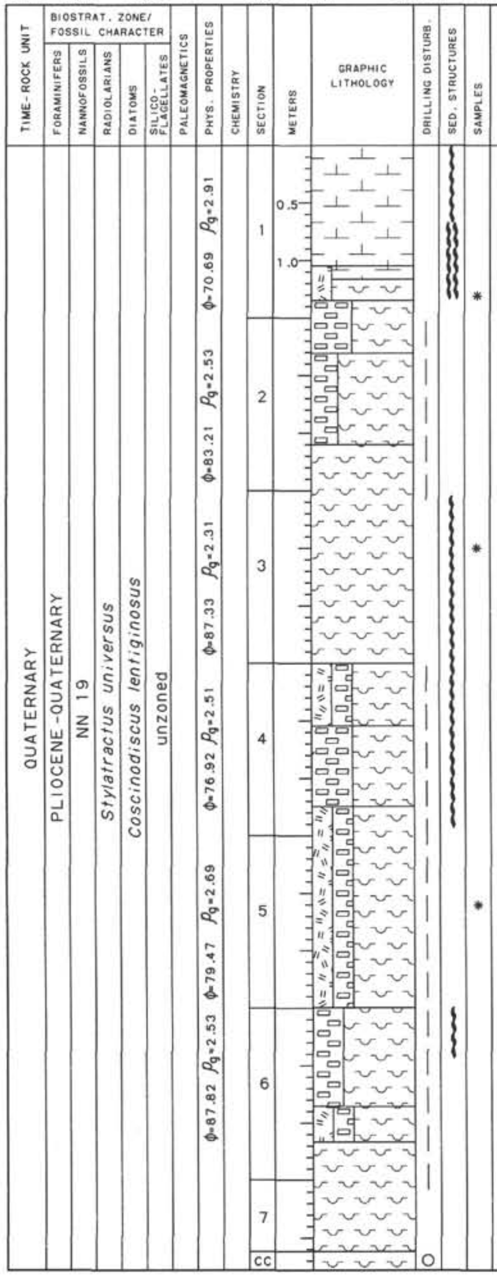

LITHOLOGIC DESCRIPTION

NANNOFOSSIL OOZE, CALCAREOUS DIATOM OOZE, CALCAREOUS-BEARING DIATOM OOZE, and DIATOM OOZE

Drilling disturbance: Slightly disturbed in Sections 2 and 4-6.

Major lithologies: Alternations of nannofossil ooze, pure white (no color code); calcareous diatom ooze, gray (5Y 6/1); calcareous-bearing diatom ooze, pale olive (5Y 6/3); and diatom ooze, olive (5Y 5/4). Boundaries between units are marked by abrupt color changes.

Minor lithology: Ash-bearing calcareous diatom ooze, white (10YR 8/2) to light gray (5Y 7/2).

SMEAR SLIDE SUMMARY (%):

	1, 120 D	3, 50 M	5, 60 D
COMPOSITION:			
Volcanic glass	10	1	—
Calcite	—	1	—
Foraminifers	Tr	10	10
Diatoms	88	87	77
Radiolarians	2	1	2
Silicoflagellates	Tr	Tr	Tr

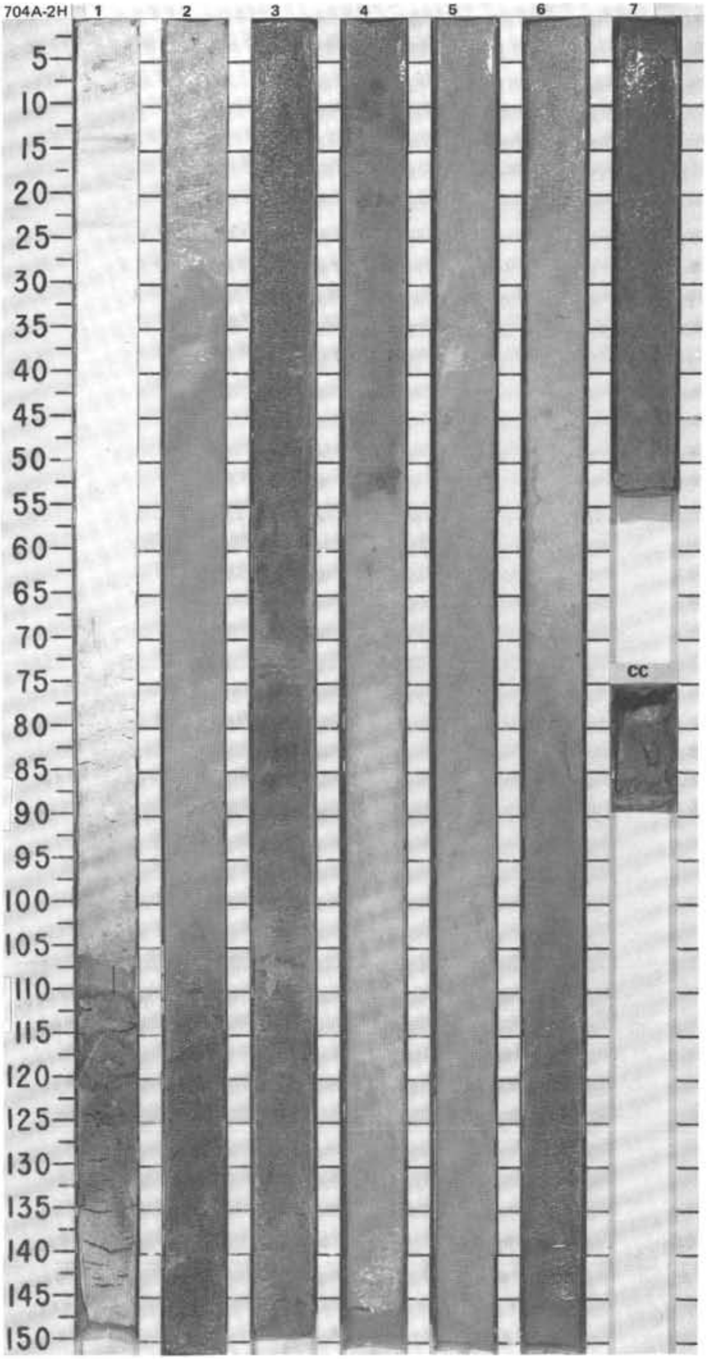

SITE 704 HOLE A CORE 3H CORED INTERVAL 2538.5-2548.0 mbsl; 16.7-26.2 mbsf

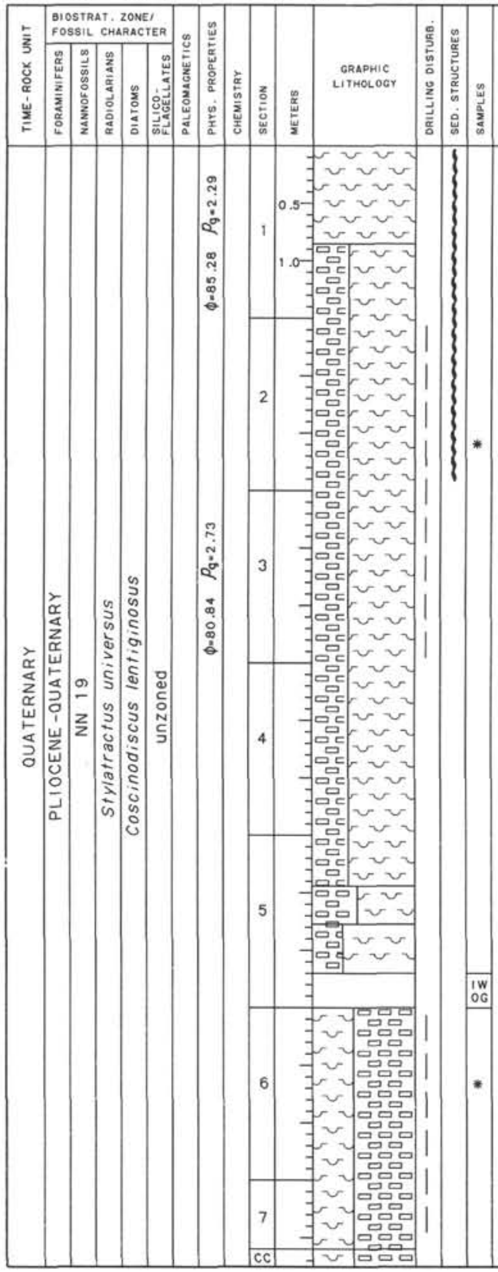

LITHOLOGIC DESCRIPTION

DIATOM OOZE, CALCAREOUS-BEARING DIATOM OOZE, and DIATOM CALCAREOUS OOZE

Drilling disturbance: Slightly disturbed, Sections 2, 3, 6, and 7.

Major lithology: Alternations of diatom ooze, olive (5Y 5/4) to pale olive (5Y 6/3); calcareous-bearing diatom ooze, white (5Y 8/1) to light gray (5Y 7/1); and diatom calcareous ooze, light gray (5Y 7/1).

SMEAR SLIDE SUMMARY (%):

COMPOSITION:	2, 110 D	6, 80 D
Volcanic glass	Tr	Tr
Calcite, broken	10	43
Foraminifers	4	30
Nannofossils	Tr	2
Diatoms	80	25
Radiolarians	5	Tr
Silicoflagellates	1	—

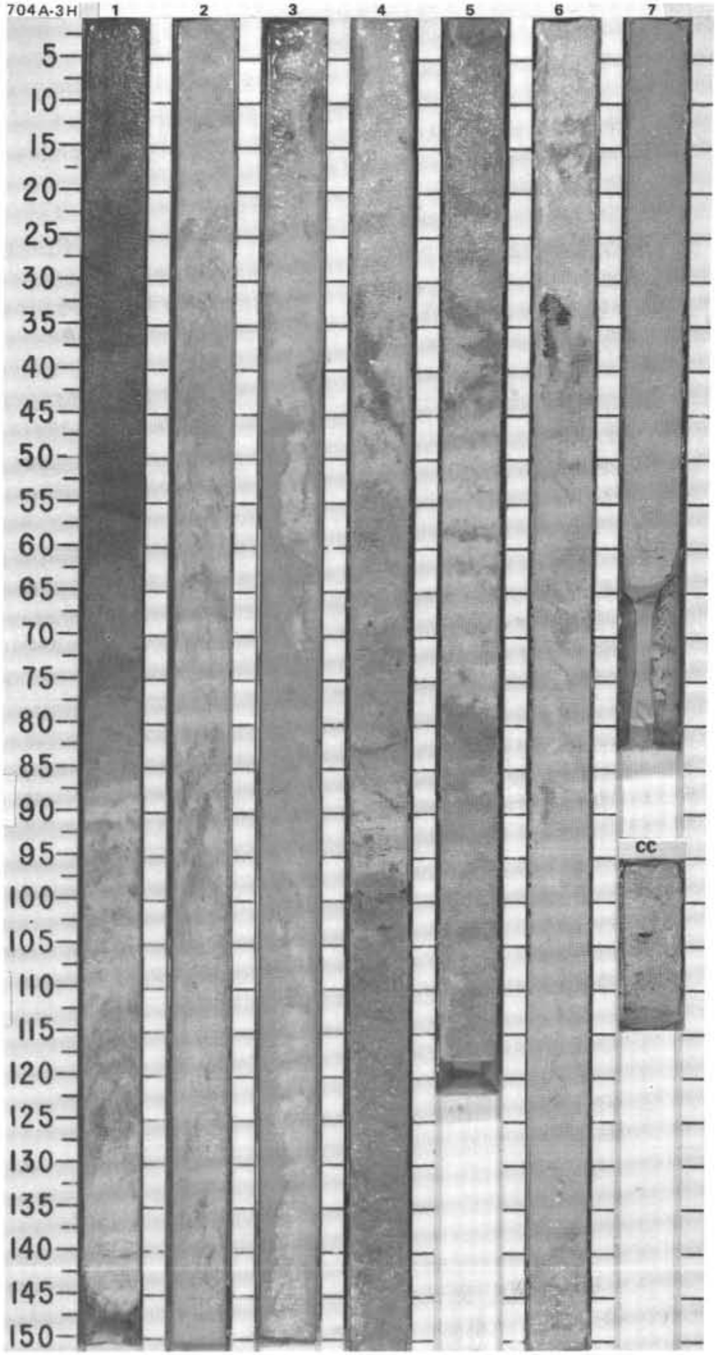

SITE 704 HOLE A CORE 4H CORED INTERVAL 2548.0-2557.5 mbsl; 26.2-35.7 mbsf

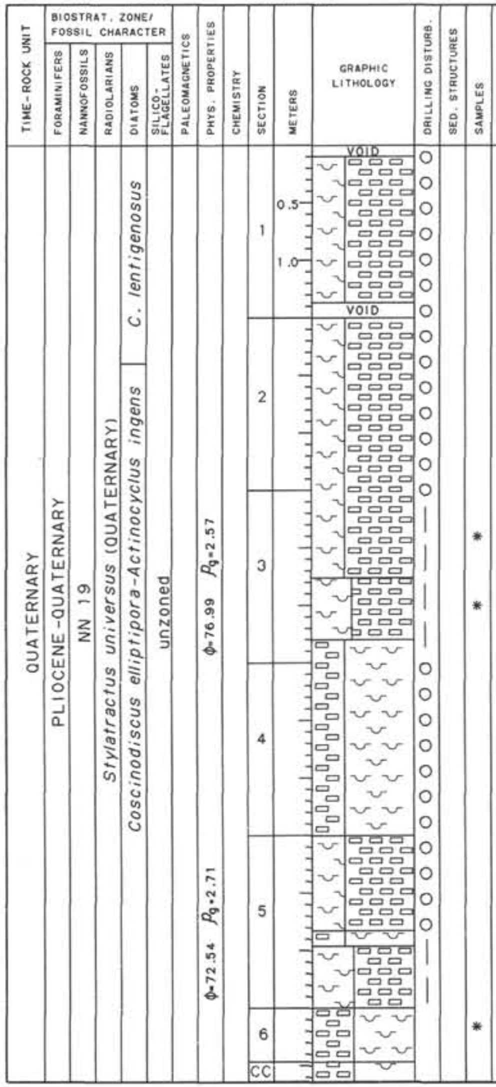

LITHOLOGIC DESCRIPTION

DIATOM-BEARING CALCAREOUS OOZE, DIATOM CALCAREOUS OOZE, and CALCAREOUS-BEARING DIATOM OOZE

Drilling disturbance: Soupy, complete homogenization of Sections 1-5.

Major lithology: Alternations of diatom-bearing calcareous ooze, white (2.5Y 8/2); diatom calcareous ooze, light gray (2.5Y 7/2); and calcareous-bearing diatom ooze, white (10YR 8/1) and olive (5Y 6/3).

SMEAR SLIDE SUMMARY (%):

	3, 40 D	*3, 100* D	*6, 20* D
COMPOSITION:			
Volcanic glass	Tr	—	—
Calcite fragments	12	20	15
Foraminifers	70	40	10
Diatoms	8	40	72
Radiolarians	2	—	2
Sponge spicules	2	—	—
Silicoflagellates	—	—	1

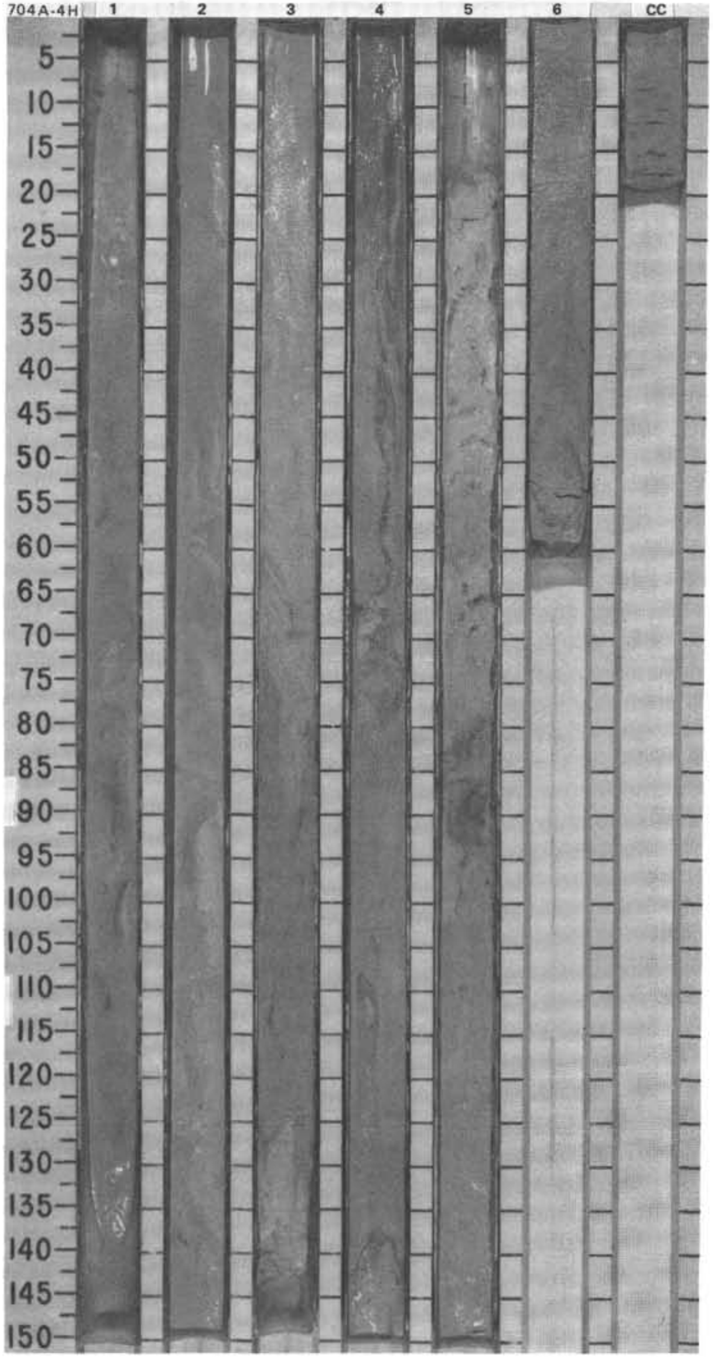

SITE 704 HOLE A CORE 5H CORED INTERVAL 2557.5-2567.0 mbsl; 35.7-45.2 mbsf

TIME-ROCK UNIT	FORAMINIFERS	NANNOFOSSILS	RADIOLARIANS	DIATOMS	SILICO-FLAGELLATES	PALEOMAGNETICS	PHYS. PROPERTIES	CHEMISTRY	SECTION	METERS	SAMPLES
QUATERNARY	PLIOCENE-QUATERNARY	NN 19	QUATERNARY	*Coscinodiscus elliptipora-Actinocyclus ingens*	unzoned		φ=67.82 ρg=2.90		1	0.5 1.0	*
									2		*
							φ=81.32 ρg=2.51		3		
									4		
							φ=77.66 ρg=2.69		5		*
									6		*
									7		
									CC		

GRAPHIC LITHOLOGY

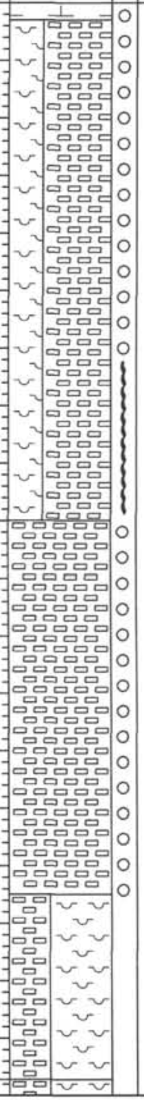

LITHOLOGIC DESCRIPTION

DIATOM-BEARING CALCAREOUS OOZE, CALCAREOUS OOZE, and CALCAREOUS DIATOM OOZE

Drilling disturbance: Soupy, highly disturbed in Sections 1-5.

Major lithology: Alternations of diatom-bearing calcareous ooze, white (no color code to 5Y 8/1) and light gray (5Y 7/1); calcareous ooze, light yellow (5Y 7/3) and white (5Y 8/2); and calcareous diatom ooze, pale olive (5Y 6/4).

Minor lithology: Large lithic fragments in Section 1, 30-33 and 105-110 cm.

SMEAR SLIDE SUMMARY (%):

	1, 4 M	2, 20 D	5, 70 D	6, 70 D
COMPOSITION:				
COMPOSITION:				
Clay	—	—	—	1
Accessory minerals	1	—	—	—
Foraminifers	3	40	20	30
Nannofossils, tricarbonate		96	30	60
Diatoms	15	—	29	20
Radiolarians	54	—	Tr	—
Silicoflagellates	Tr	1	—	—

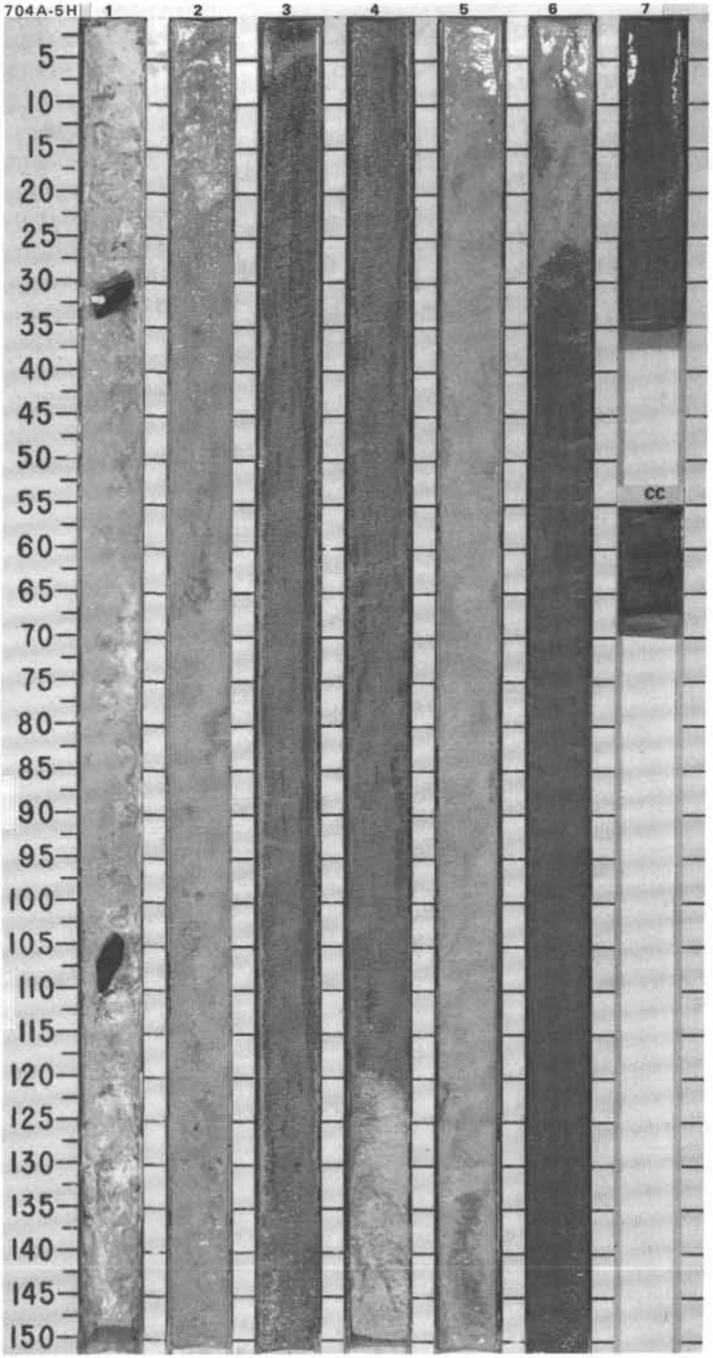

SITE 704 HOLE A CORE 6H CORED INTERVAL 2567.0-2576.5 mbsl; 45.2-54.7 mbsf

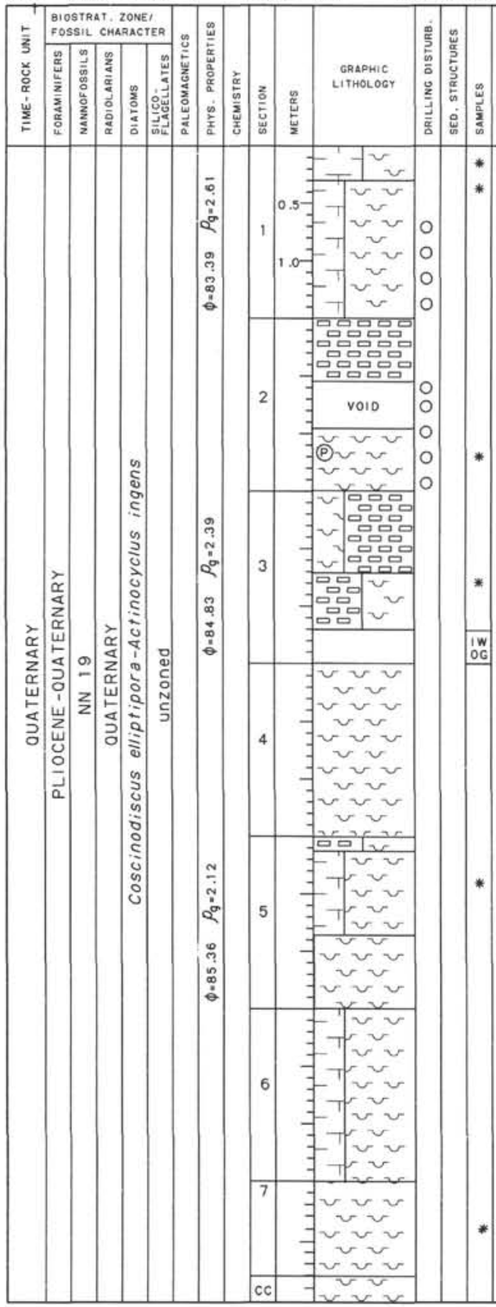

LITHOLOGIC DESCRIPTION

CALCAREOUS OOZE, DIATOM-BEARING CALCAREOUS OOZE, CALCAREOUS DIATOM OOZE, and DIATOM OOZE

Drilling disturbance: Soupy in Section 1, 75-150 cm, and Section 2, 55-150 cm.

Major lithology: Alternations of calcareous ooze, white (2.5Y 8/1); diatom-bearing calcareous ooze, white (2.5Y 8/1); and calcareous diatom ooze, pale olive (5Y 6/4) to light olive gray (5Y 6/2); and diatom ooze, white (2.5Y 8/1).

Minor lithology: Dark gray bleb containing pyrite-coated microfossils in Section 2, 129 cm.

SMEAR SLIDE SUMMARY (%):

	1, 25 M	1, 27 M	1, 75 D	2, 128 M	3, 75 D	5, 40 D	7, 50 D
COMPOSITION:							
COMPOSITION:							
Quartz/feldspar	2	5	4	1	—	—	—
Clay	4	4	—	—	—	—	5
Accessory minerals:							
Pyrite	—	—	—	10	—	—	—
Foraminifers	40	15	20	2	39	10	3
Nannofossils	Tr	—	—	—	—	1	—
Diatoms	43	75	75	88	60	83	87
Radiolarians	—	—	—	Tr	—	5	5
Silicoflagellates	1	1	1	—	—	1	Tr

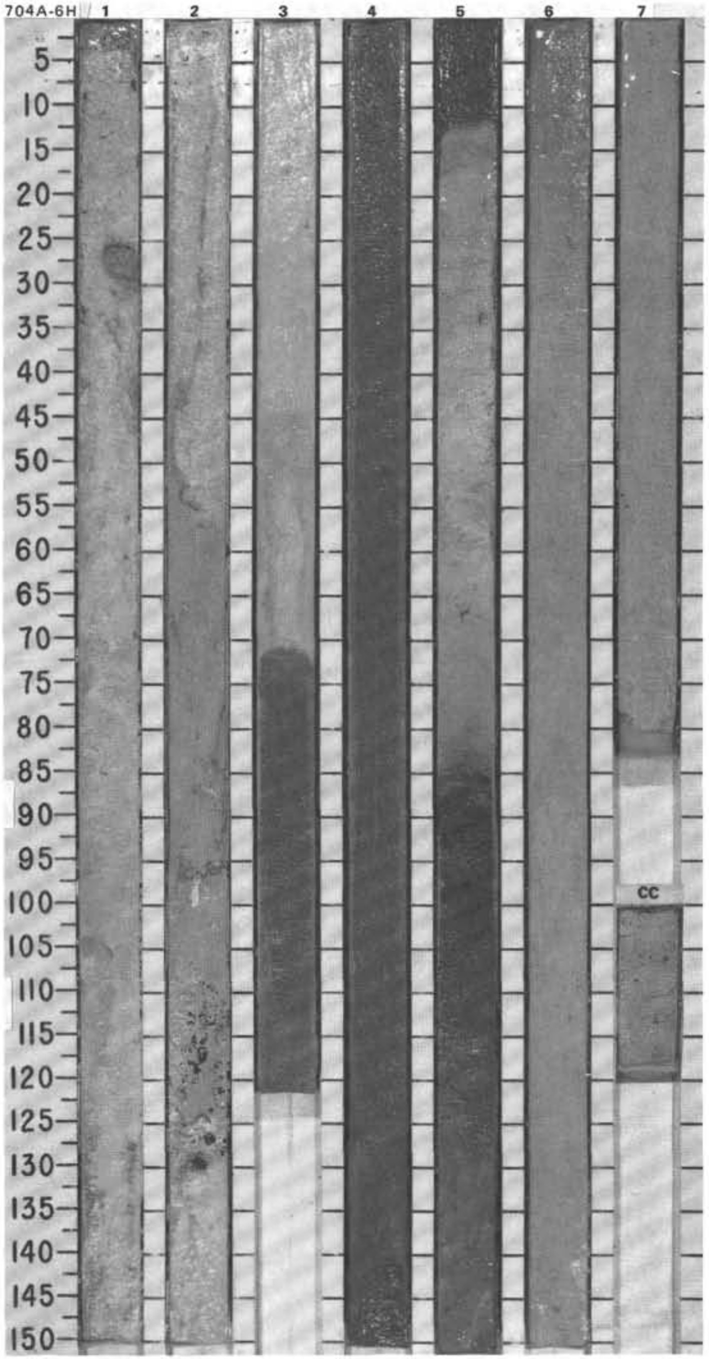

SITE 704 HOLE A CORE 7H CORED INTERVAL 2576.5-2586.0 mbsl: 54.7-64.2 mbsf

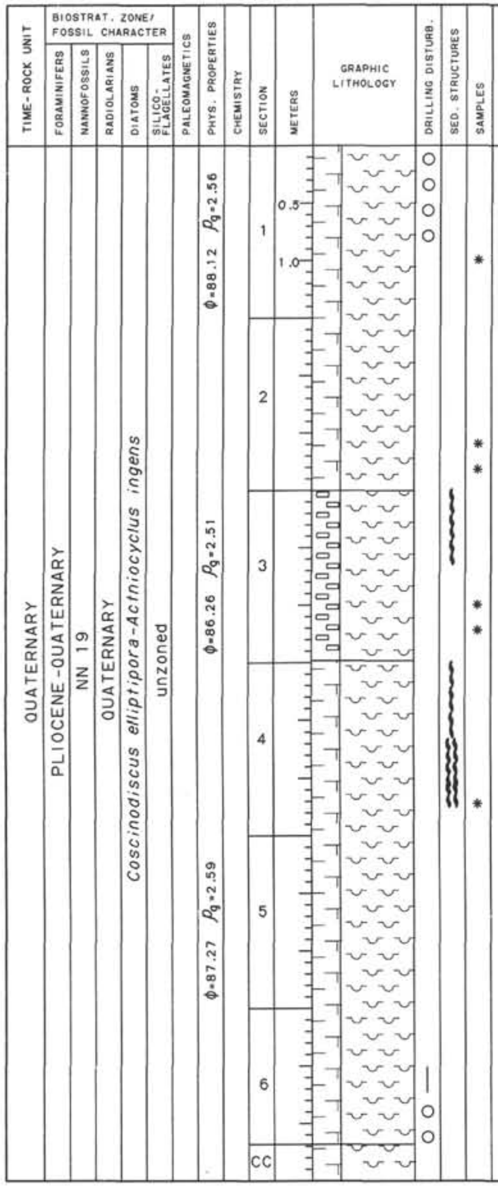

LITHOLOGIC DESCRIPTION

FORAMINIFER-BEARING DIATOM OOZE

Drilling disturbance: Soupy, Section 1, 0-60 cm.

Major lithology: Foraminifer-bearing diatom ooze with alternating color variations, including white (5Y 8/1), light yellowish brown (2.5Y 6/4), light gray (5Y 7/2), and light olive gray (5Y 6/2).

Minor lithology: Lithic fragments dispersed throughout Section 1, 21-32 cm.

SMEAR SLIDE SUMMARY (%):

	1, 100 D	2, 120 D	2, 122 M	3, 93 D	3, 120 D	4, 122 D
COMPOSITION:						
COMPOSITION:						
Quartz	—	5	10	—	—	—
Feldspar	—	—	50	—	—	—
Clay	5	—	30	—	—	—
Volcanic glass	—	—	5	—	—	—
Accessory minerals	—	—	5	—	—	—
Pyrite	—	Tr	—	—	—	—
Foraminifers	10	15	—	3	12z	15
Nannofossils	2	Tr	—	12	8	3
Diatoms	78	78	—	85	80	82
Radiolarians	5	2	—	—	—	—
Silicoflagellates	Tr	—	—	—	—	—

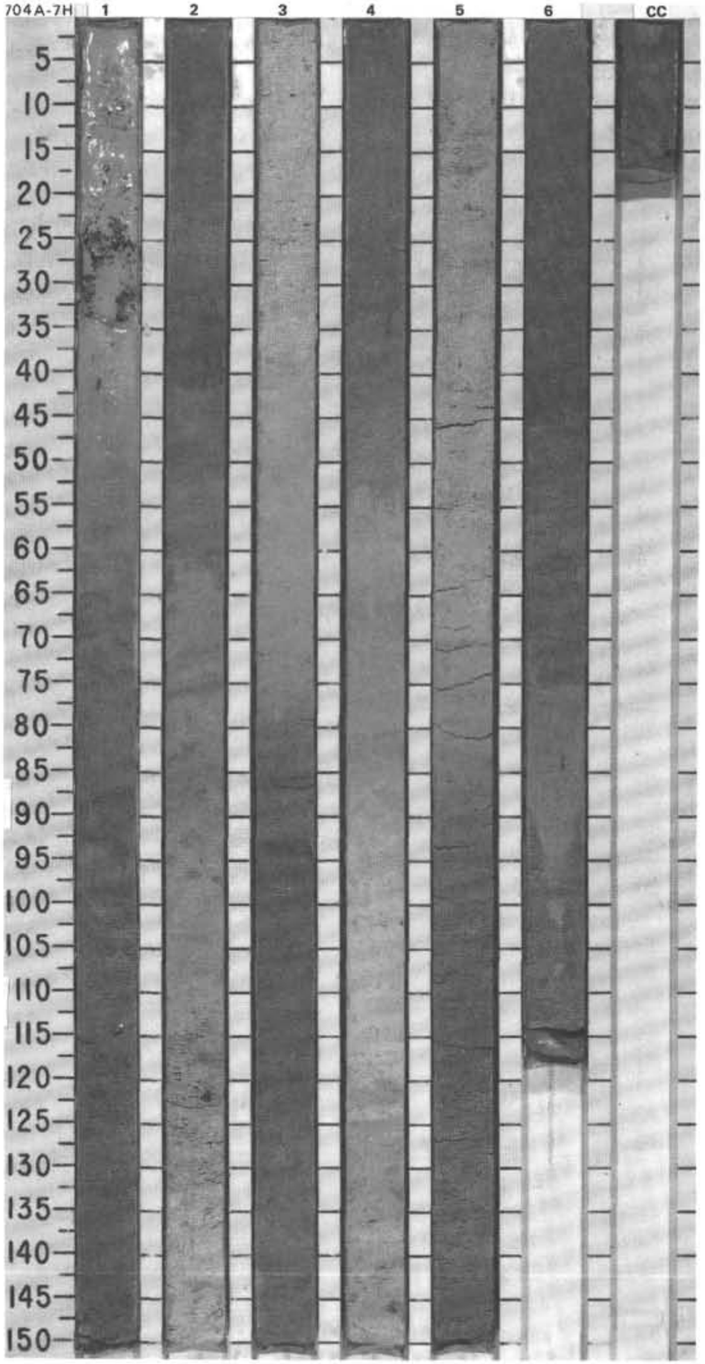

SITE 704 HOLE A CORE 8H CORED INTERVAL 2586.0-2595.5 mbsl; 64.2-73.7 mbsf

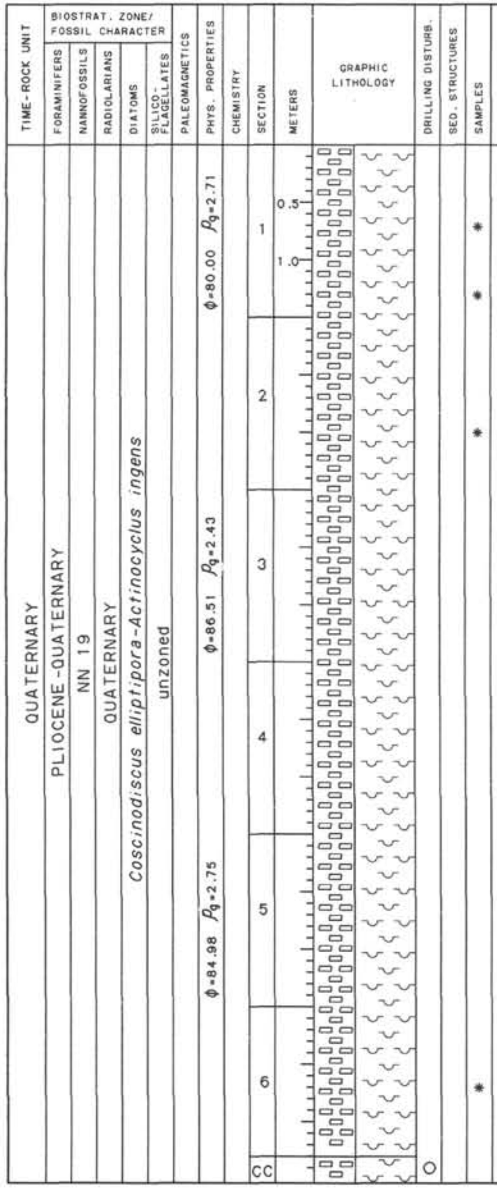

LITHOLOGIC DESCRIPTION

CALCAREOUS DIATOM OOZE

Major lithology: Calcareous diatom ooze, white (5Y 8/1) and pale olive (5Y 6/4) to light greenish gray (5Y 7/1).

Minor lithology: Lithic fragments in Section 1, 85-95 cm.

SMEAR SLIDE SUMMARY (%):

	1, 70 D	1, 140 D	2, 100 D	6, 70 D
COMPOSITION:				
COMPOSITION:				
Clay	—	—	Tr	—
Volcanic glass	Tr	—	Tr	1
Accessory minerals	—	Tr	—	—
Opaques	Tr	Tr	Tr	—
Foraminifers	30	48	20	27
Nannofossils	19	—	29	20
Diatoms	50	50	50	50
Radiolarians	—	2	1	2
Sponge spicules	1	Tr	—	Tr
Silicoflagellates	Tr	—	Tr	Tr

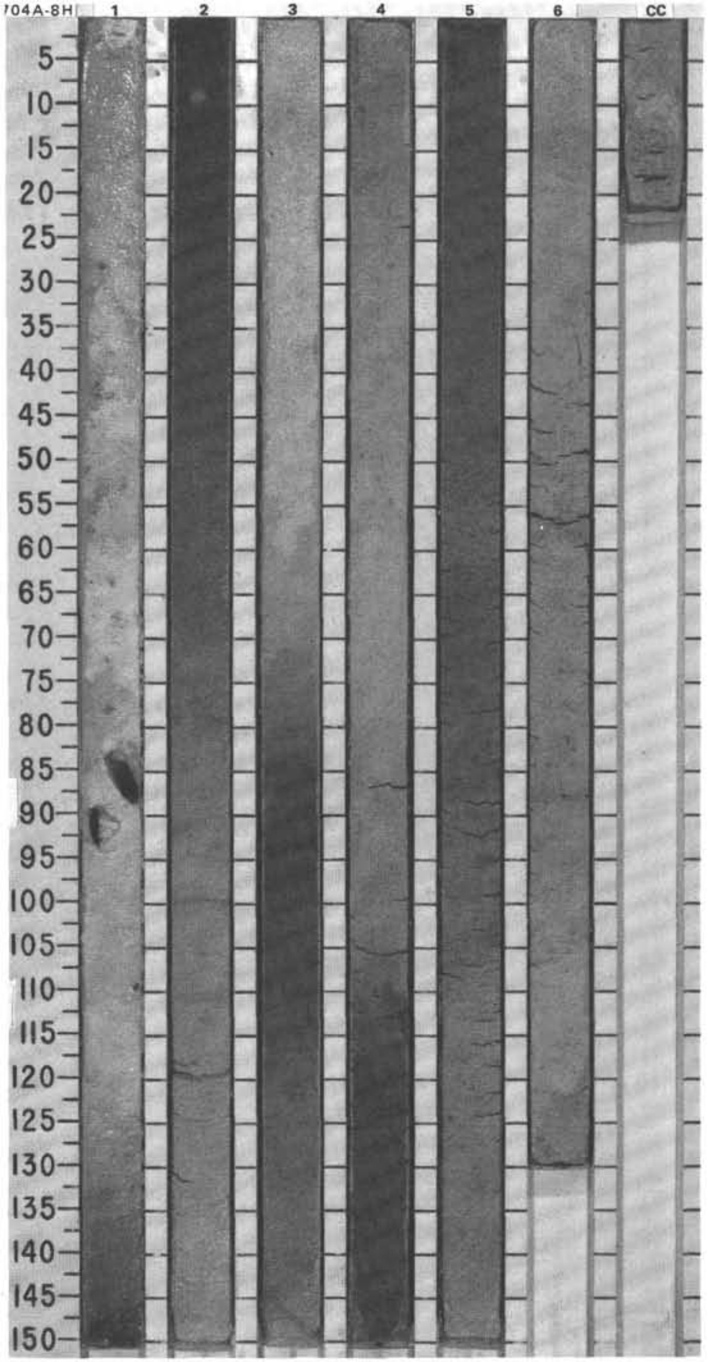

SITE 704 HOLE A CORE 9H CORED INTERVAL 2595.5-2605.0 mbsl; 73.7-83.2 mbsf

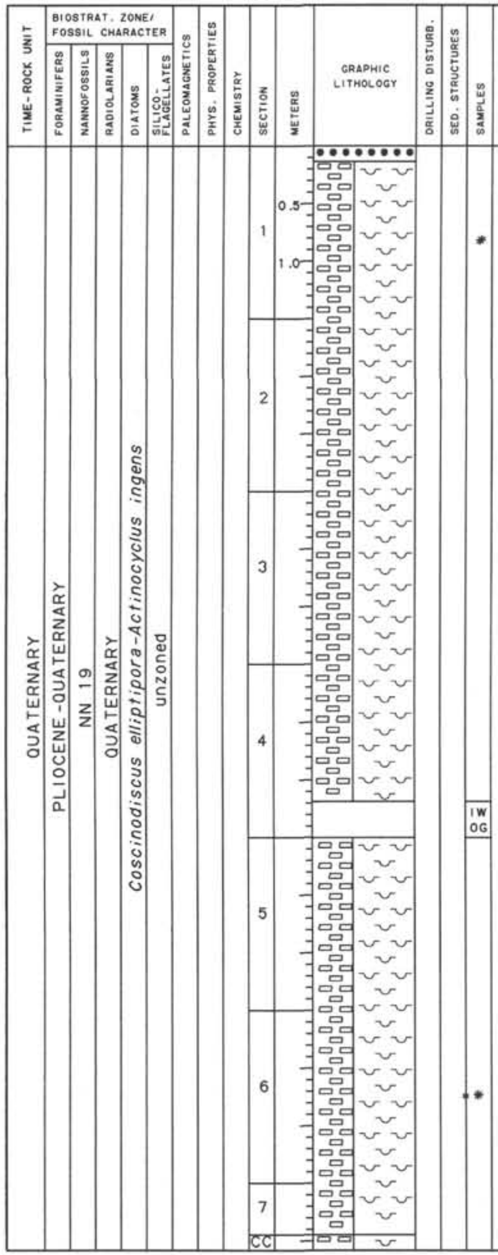

LITHOLOGIC DESCRIPTION

CALCAREOUS DIATOM OOZE

Drilling disturbance: Soupy, Section 1, 0-15 cm.

Major lithology: Calcareous diatom ooze with alternating color variations, including white (2.5Y 8/0, 5Y 8/1), light gray (2.5Y 7/2), and pale olive (5Y 6/3).

SMEAR SLIDE SUMMARY (%):

	1, 80 D	6, 77 D
COMPOSITION:		
Feldspar	—	Tr
Clay	Tr	—
Volcanic glass	1	1
Accessory minerals	Tr	—
Opaques	—	Tr
Foraminifers	10	5
Nannofossils	35	35
Diatoms	50	55
Radiolarians	1	2
Sponge spicules	1	1
Silicoflagellates	2	1

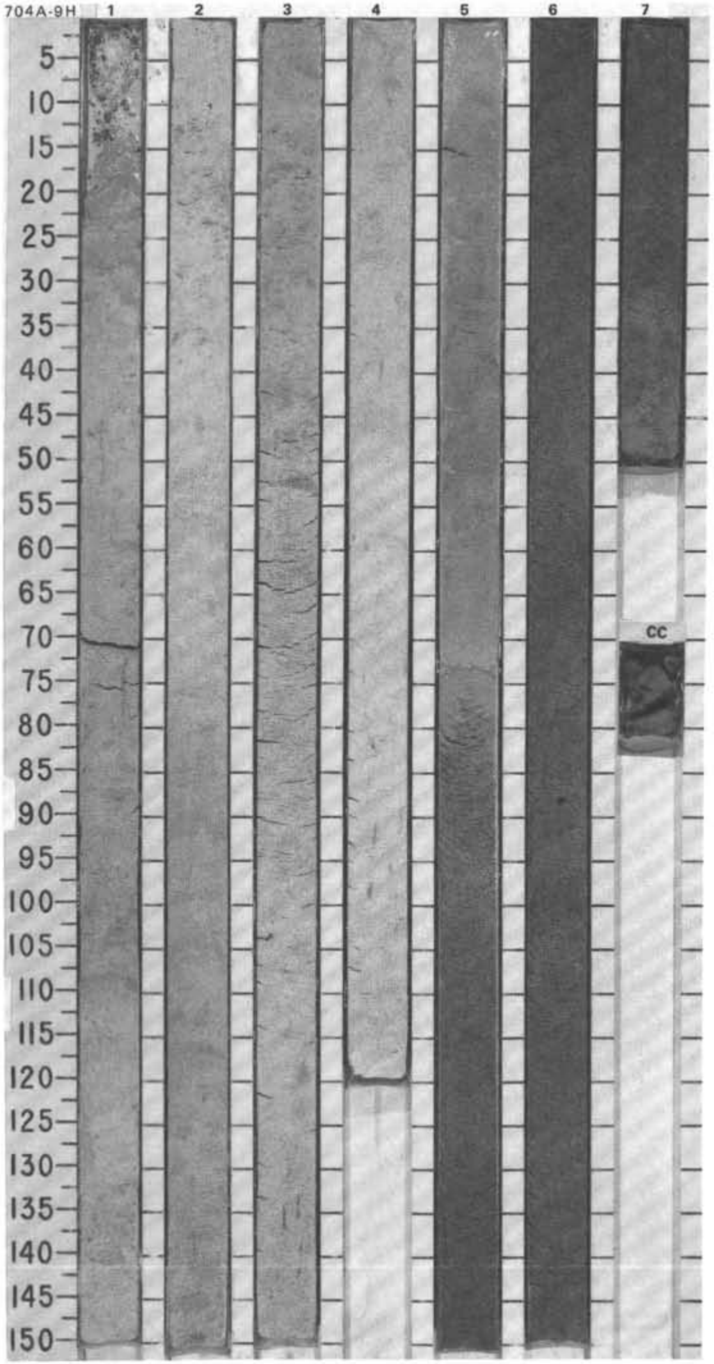

SITE 704 HOLE A CORE 10H CORED INTERVAL 2605.0-2614.5 mbsl; 83.2-92.7 mbsf

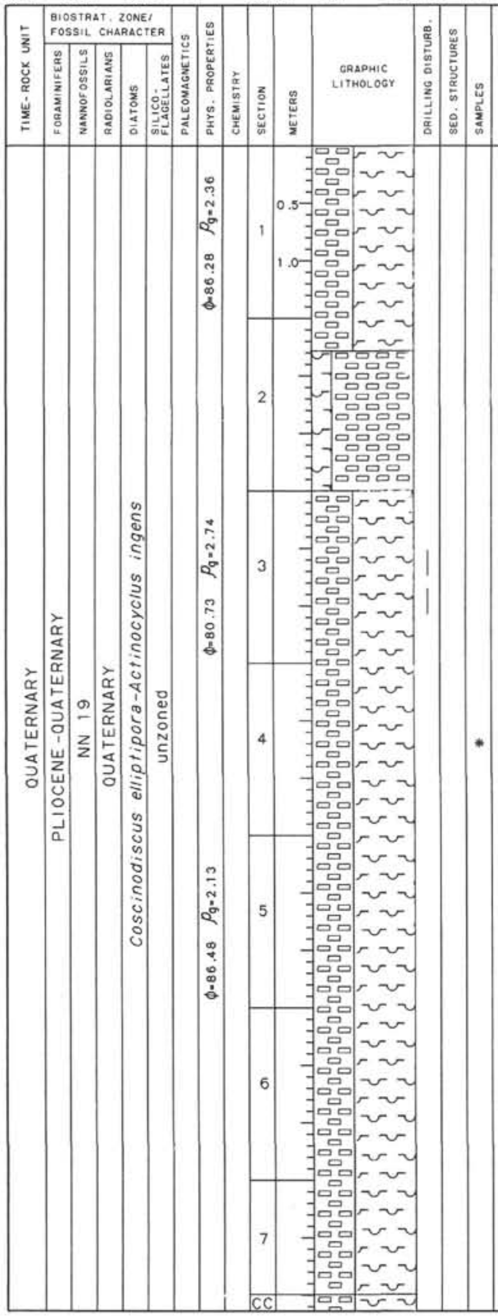

LITHOLOGIC DESCRIPTION

CALCAREOUS DIATOM OOZE

Drilling disturbance: Bowed sedimentary contacts, Section 3, 70-105 cm.

Major lithology: Calcareous diatom ooze with alternating color variations, including light gray (5Y 7/2), white (5Y 8/1), pale olive (5Y 6/3), and pale yellow (5Y 7/3).

SMEAR SLIDE SUMMARY (%):

	4, 70 D
COMPOSITION:	
Feldspar	1
Volcanic glass	1
Calcite/dolomite	5
Foraminifers	10
Nannofossils	30
Diatoms	50
Radiolarians	2
Silicoflagellates	1

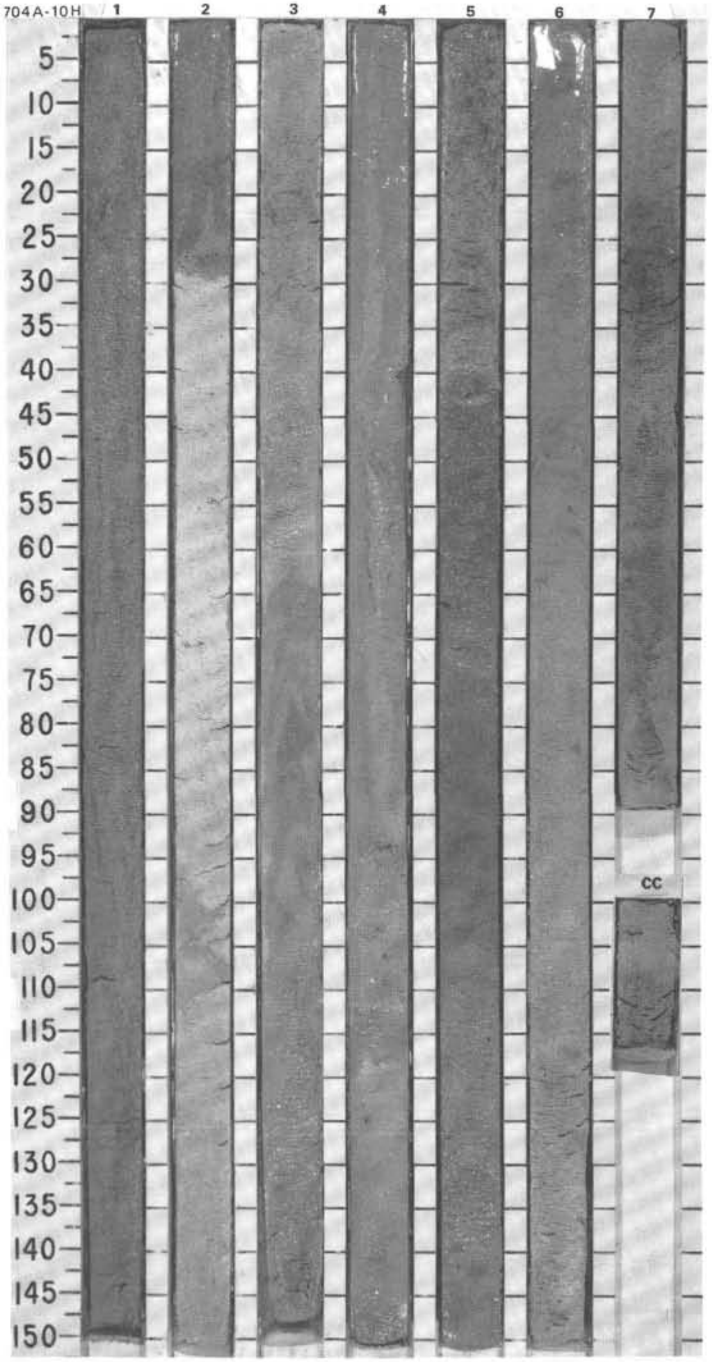

SITE 704 HOLE A CORE 11H CORED INTERVAL 2614.5-2624.0 mbsl; 92.7-102.2 mbsf

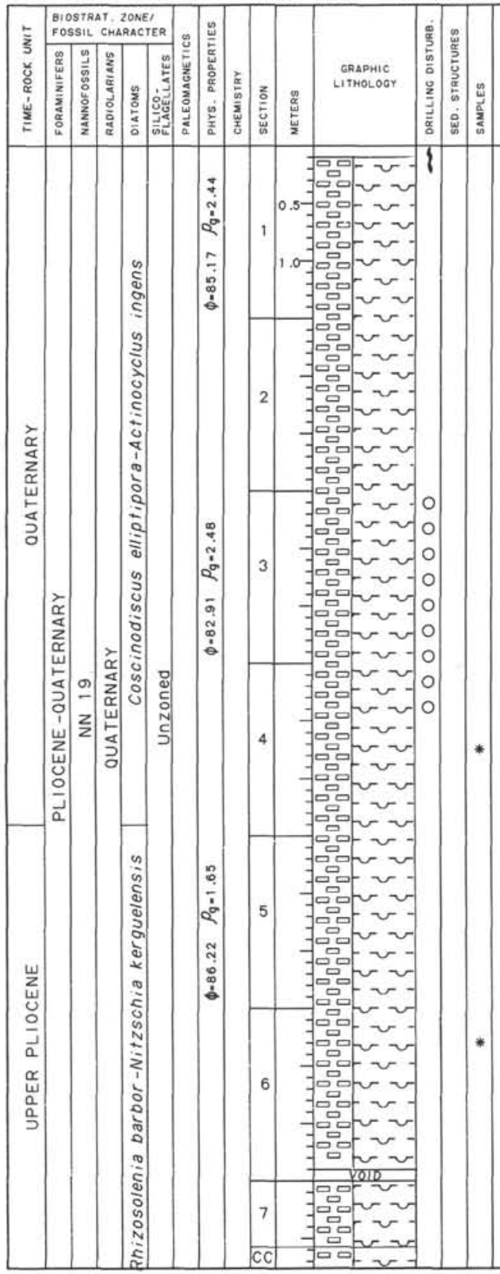

LITHOLOGIC DESCRIPTION

CALCAREOUS DIATOM OOZE

Drilling disturbance: Soupy, throughout Section 3 and Section 4, 0-45 cm.

Major lithology: Calcareous diatom ooze with alternating color variations, including light gray (5Y 7/1, 7/2) and white (5Y 8/1).

Minor lithology: Lithic fragments mixed with ooze in Section 1, 0-9 cm.

SMEAR SLIDE SUMMARY (%):

	4, 70 D	6, 35 D
COMPOSITION:		
Clay	Tr	—
Volcanic glass	1	Tr
Accessory minerals	Tr	—
Micrite	—	20
Opaques	—	Tr
Foraminifers	20	20
Nannofossils	25	5
Diatoms	47	44
Radiolarians	3	—
Sponge spicules	1	1
Silicoflagellates	3	—

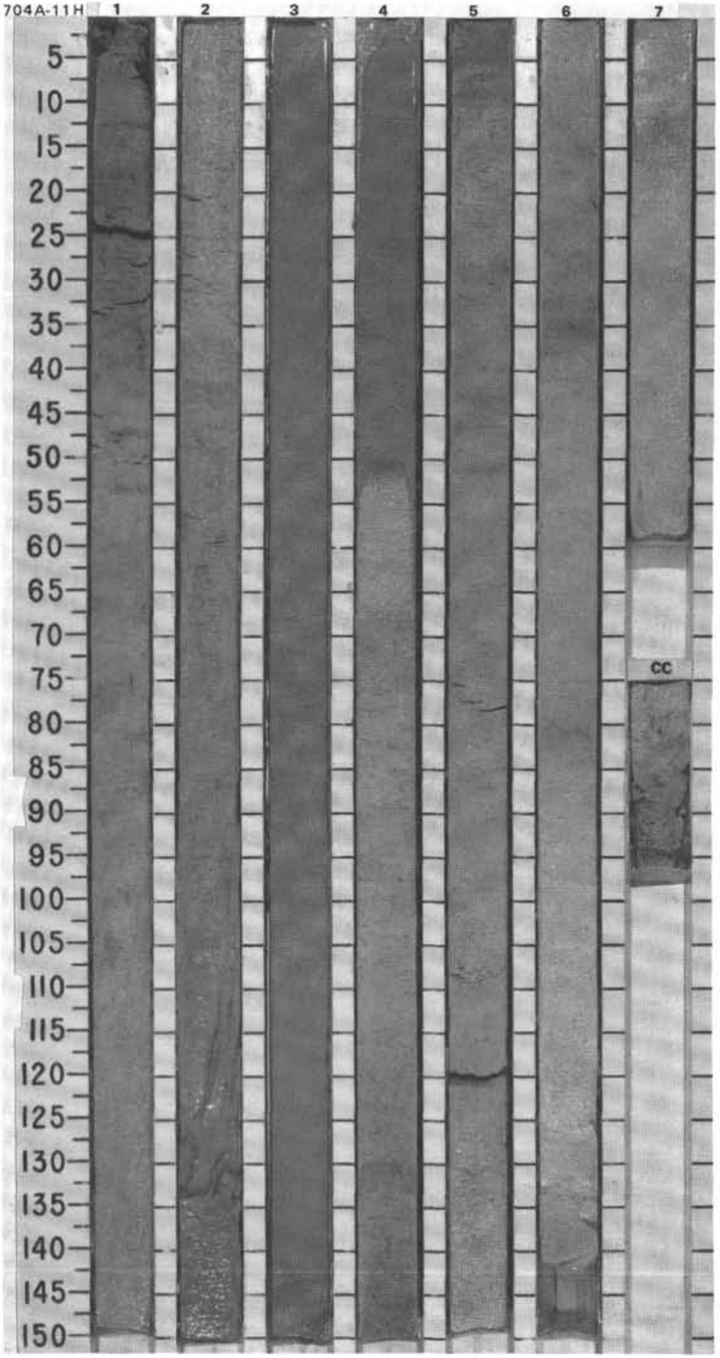

SITE 704 HOLE A CORE 12H CORED INTERVAL 2624.0-2633.5 mbsl; 102.2-111.7 mbsf

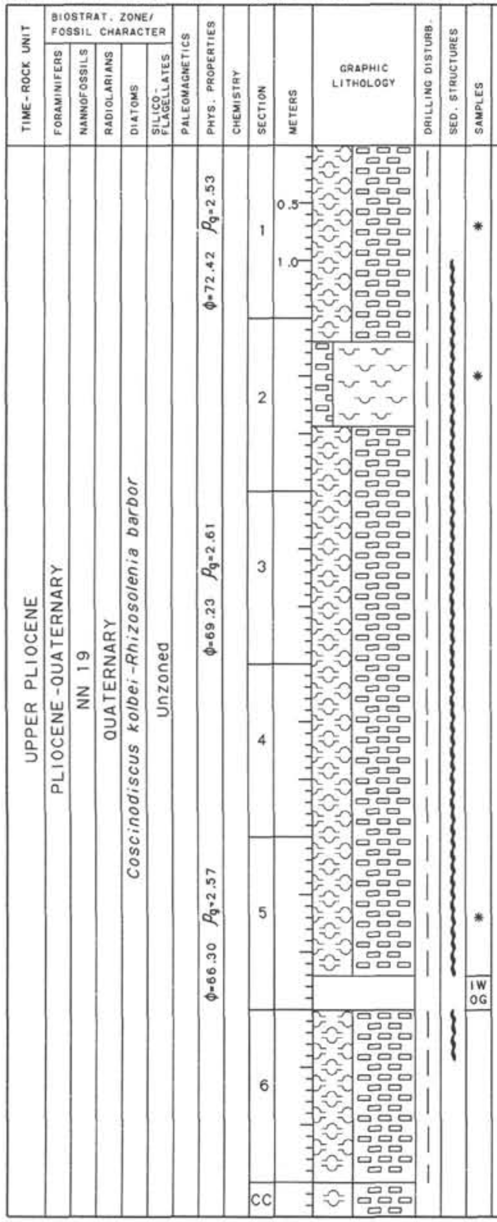

LITHOLOGIC DESCRIPTION

SILICEOUS CALCAREOUS OOZE

Drilling disturbance: Slightly disturbed, all sections, flow-in, contorted sedimentary contacts.

Major lithology: Siliceous calcareous ooze, white (2.5Y 8/0) and olive (5Y 5/3); faint bioturbation in Sections 2-6.

SMEAR SLIDE SUMMARY (%):

	1, 70 D	2, 48 M	5, 70 D
COMPOSITION:			
Accessory minerals:			
Opaques	Tr	—	—
Fragmented carbonate	50	40	—
Foraminifers	5	2	3
Nannofossils	20	Tr	73
Diatoms	20	85	10
Radiolarians	3	2	3
Sponge spicules	1	1	10
Silicoflagellates	—	—	1

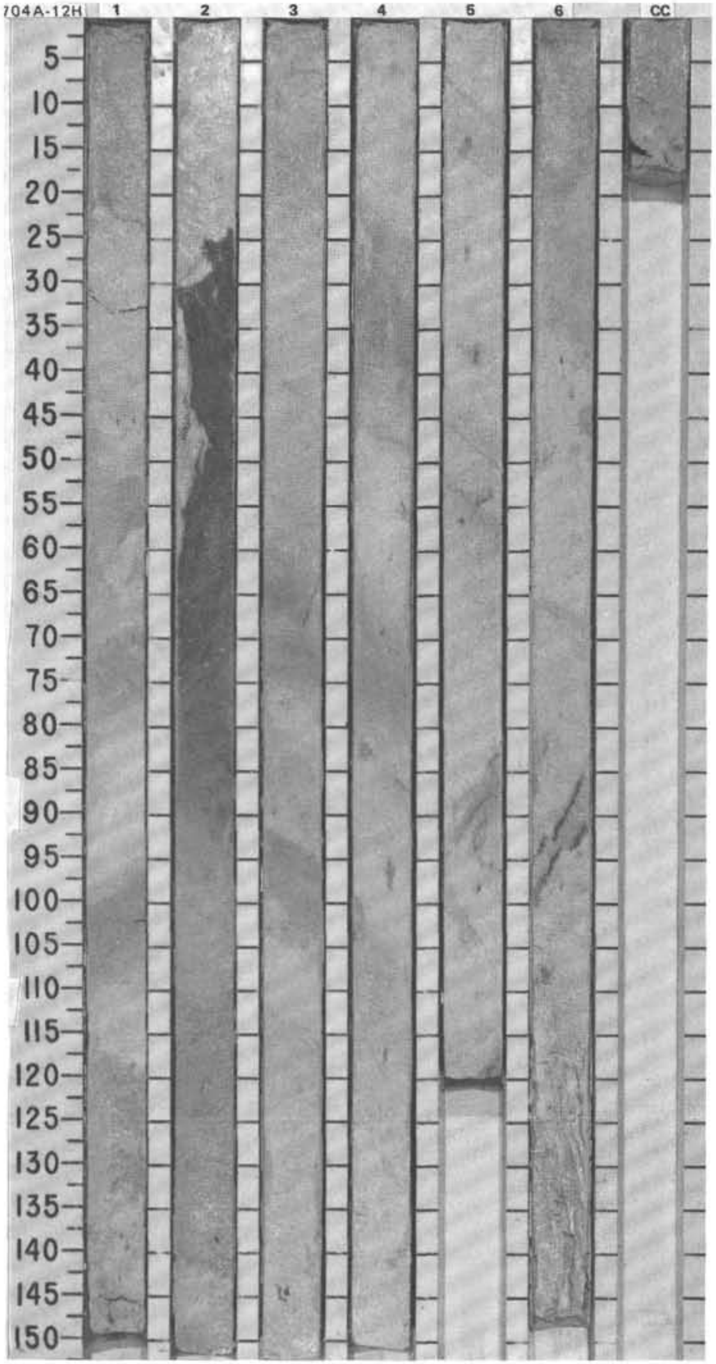

SITE 704 HOLE A CORE 13H CORED INTERVAL 2633.5-2643.0 mbsl; 111.7-121.2 mbsf

TIME-ROCK UNIT	BIOSTRAT. ZONE/ FOSSIL CHARACTER					PALEOMAGNETICS	PHYS. PROPERTIES	CHEMISTRY	SECTION	METERS	DRILLING DISTURB.	SED. STRUCTURES	SAMPLES
	FORAMINIFERS	NANNOFOSSILS	RADIOLARIANS	DIATOMS	SILICO-FLAGELLATES								
UPPER PLIOCENE	PLIOCENE-QUATERNARY	NN 19	QUATERNARY	*Coscinodiscus kolbei-Rhizosolenia barbor*	Unzoned		ϕ=83.41 ρ_g=2.47 ϕ=66.87 ρ_g=2.63		1 2 3 4 5 6 7 CC	0.5 1.0			* * *

GRAPHIC LITHOLOGY

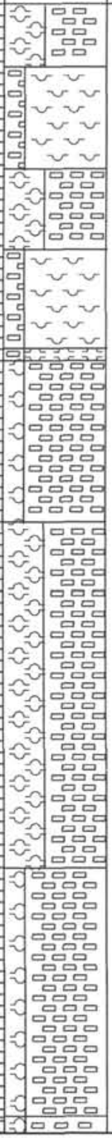

LITHOLOGIC DESCRIPTION

SILICEOUS CALCAREOUS OOZE

Major lithology: Siliceous calcareous ooze, white (2.5Y 8/0), olive (5Y 6/4), and light gray (5Y 7/1).

SMEAR SLIDE SUMMARY (%):

	1, 20 D	1, 122 M	6, 80 D
COMPOSITION:			
Volcanic glass	Tr	—	Tr
Accessory minerals:			
Carbonate fragments	60	15	15
Foraminifers	3	2	7
Nannofossils	10	—	58
Diatoms	7	80	8
Radiolarians	4	1	5
Sponge spicules	15	2	5
Silicoflagellates	1	—	2

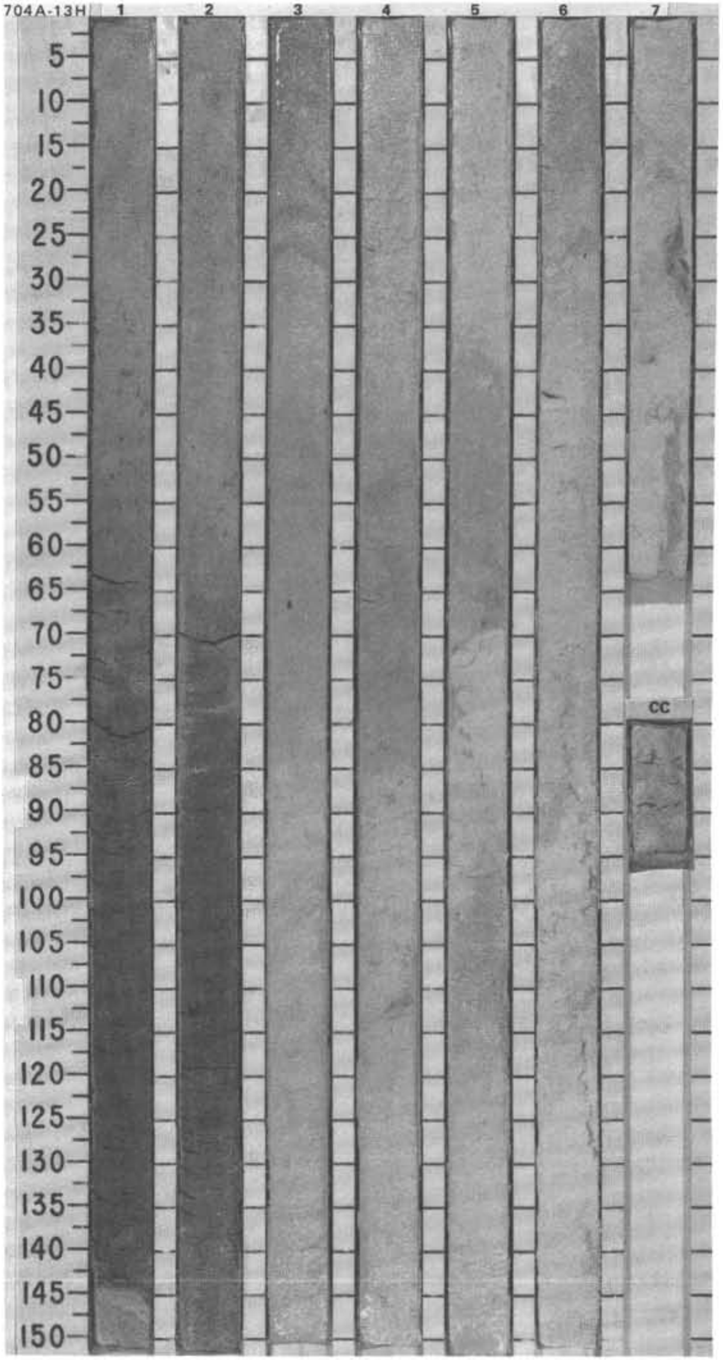

SITE 704 HOLE A CORE 14H CORED INTERVAL 2643.0-2625.5 mbsl; 121.2-130.7 mbsf

TIME-ROCK UNIT: UPPER PLIOCENE

BIOSTRAT. ZONE/ FOSSIL CHARACTER

FORAMINIFERS: PLIOCENE-QUATERNARY

NANNOFOSSILS: NN 19

RADIOLARIANS: *Eucyrtidium calvertense* (UPPER PLIOCENE)

DIATOMS: *Coscinodiscus vulnificus* to *cosmiodiscus insignis*

SILICO-FLAGELLATES: unzoned

PALEOMAGNETICS

PHYS. PROPERTIES: ϕ=70.13 ρ_g=2.86 (Section 1); ϕ=66.47 ρ_g=2.87 (Section 5)

CHEMISTRY

SECTION: 1, 2, 3, 4, 5, 6, CC

METERS: 0.5, 1.0

GRAPHIC LITHOLOGY

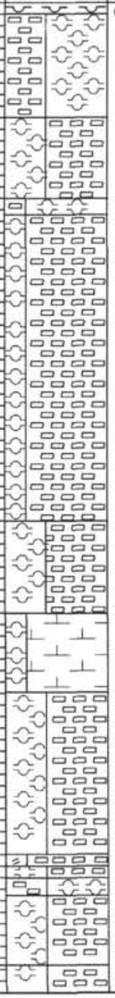

DRILLING DISTURB.

SED. STRUCTURES

SAMPLES: * (Section 1); * (Section 4)

LITHOLOGIC DESCRIPTION

CALCAREOUS SILICEOUS OOZE and SILICEOUS CALCAREOUS OOZE

Major lithology: Calcareous siliceous ooze, white (2.5Y 8/0), olive (5Y 5/3), and light gray (5Y 7/2); and siliceous calcareous ooze, white (no color code), diffusely bioturbated.

Minor lithology: Dropstone(?) in Section 4, 31-34 cm; ash horizon at Section 3, 135 cm.

SMEAR SLIDE SUMMARY (%):

	1, 90 M	4, 105 D
COMPOSITION:		
Accessory minerals:		
Fragmented carbonate	42	5
Foraminifers	5	3
Nannofossils	—	76
Diatoms	40	5
Radiolarians	3	3
Sponge spicules	10	5
Silicoflagellates	Tr	3

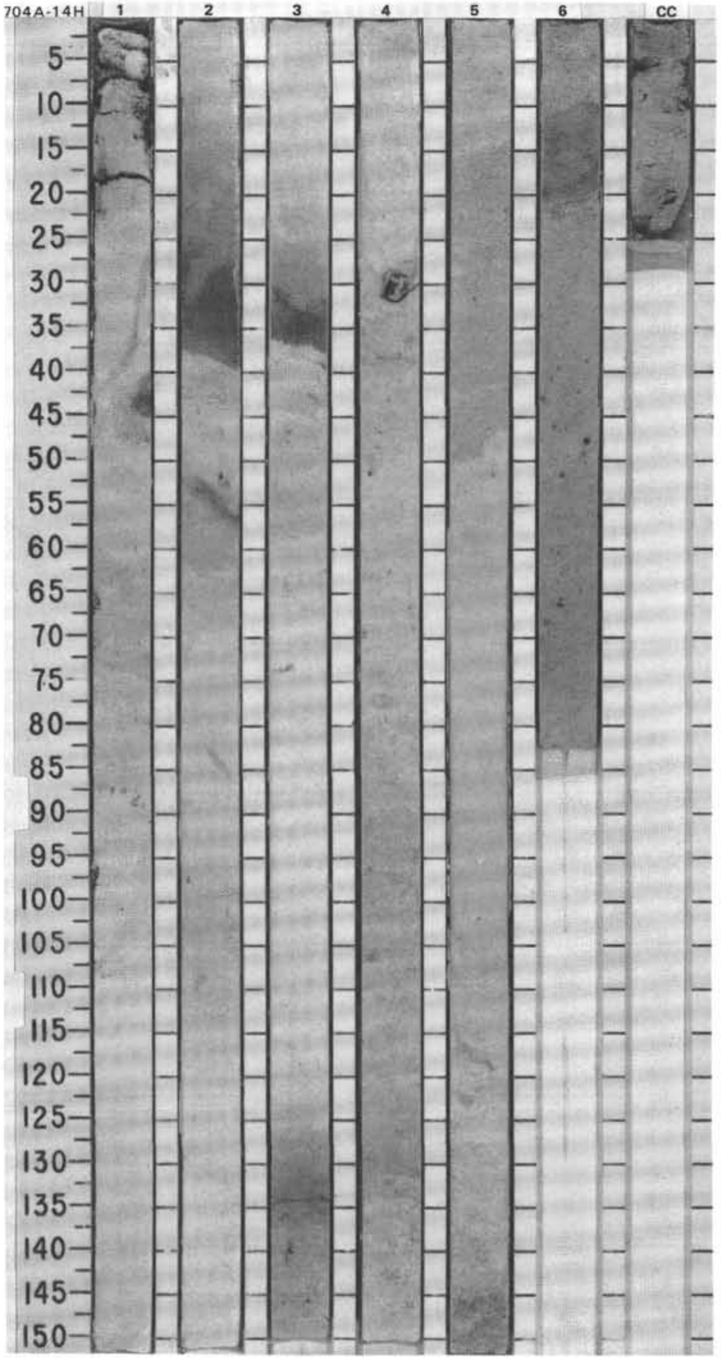

SITE 704 HOLE A CORE 15H CORED INTERVAL 2652.5-2662.0 mbsl; 130.7-140.2 mbsf

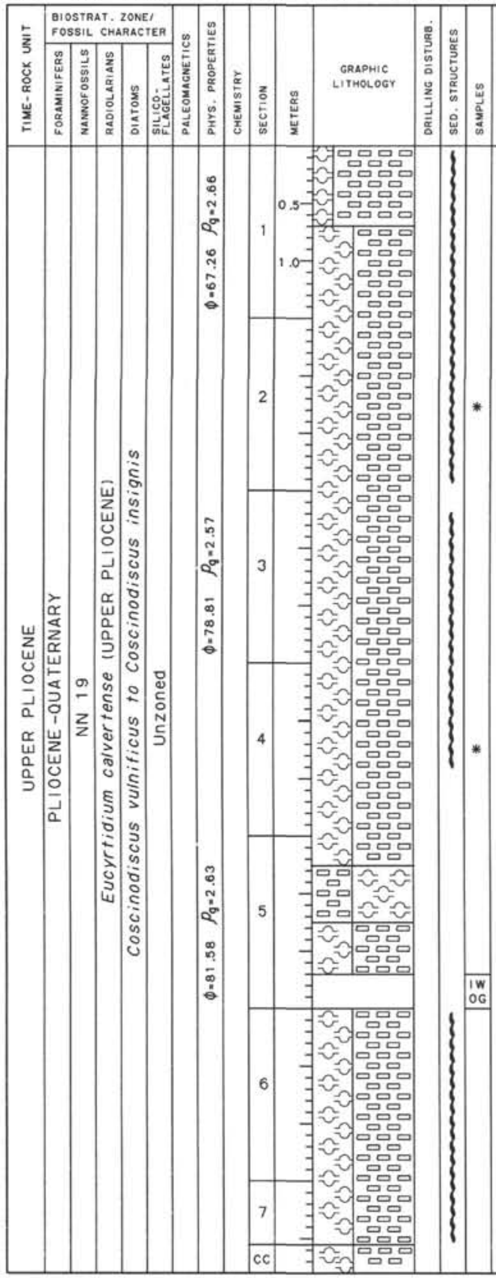

LITHOLOGIC DESCRIPTION

SILICEOUS CALCAREOUS OOZE

Major lithology: Siliceous calcareous ooze, light gray (5Y 7/1) to white (7.5YR 8/0, 2.5Y 8/0). Diffuse bioturbation in Sections 1-4, 6, and 7.

SMEAR SLIDE SUMMARY (%):

	2, 70 D	4, 72 D
COMPOSITION:		
Volcanic glass	—	1
Calcite	1	1
Foraminifers	10	10
Nannofossils	45z	41
Diatoms	41	44
Radiolarians	2	2
Sponge spicules	Tr	—
Silicoflagellates	1	1

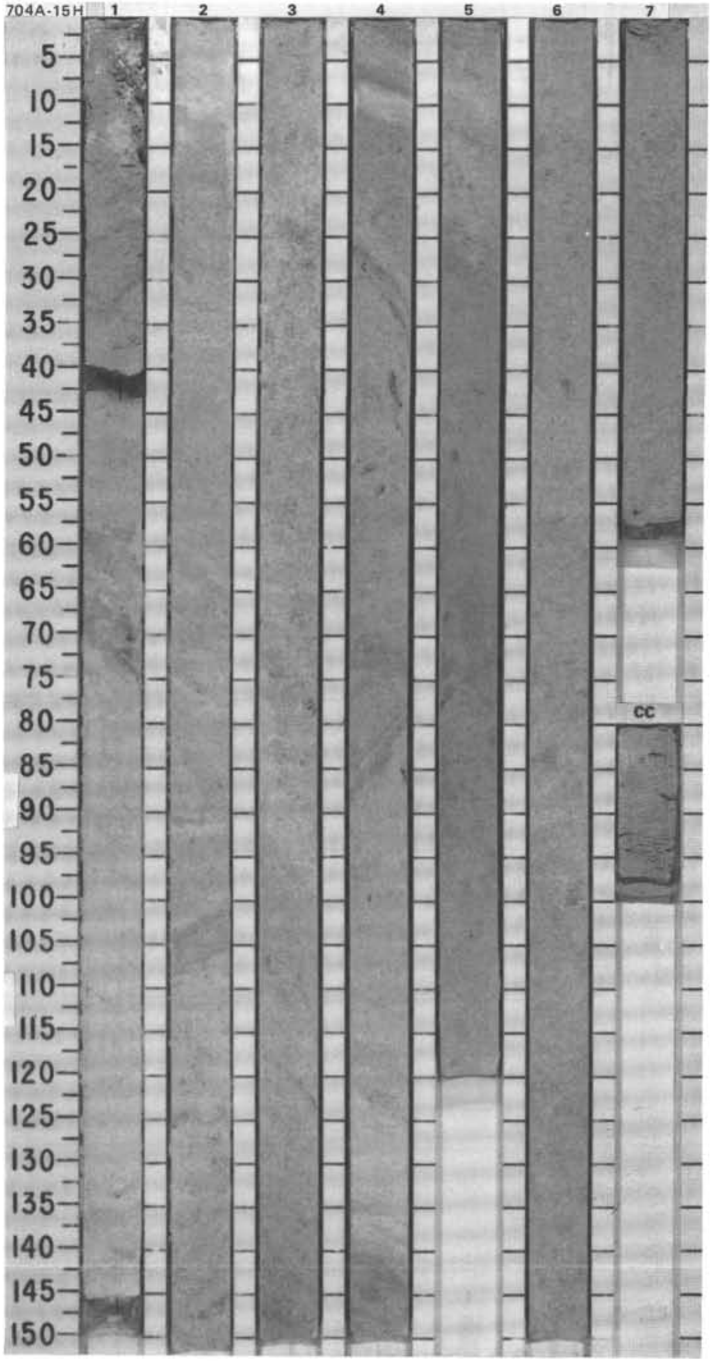

SITE 704 HOLE A CORE 16H CORED INTERVAL 2662.0-2671.5 mbsl; 140.2-149.7 mbsf

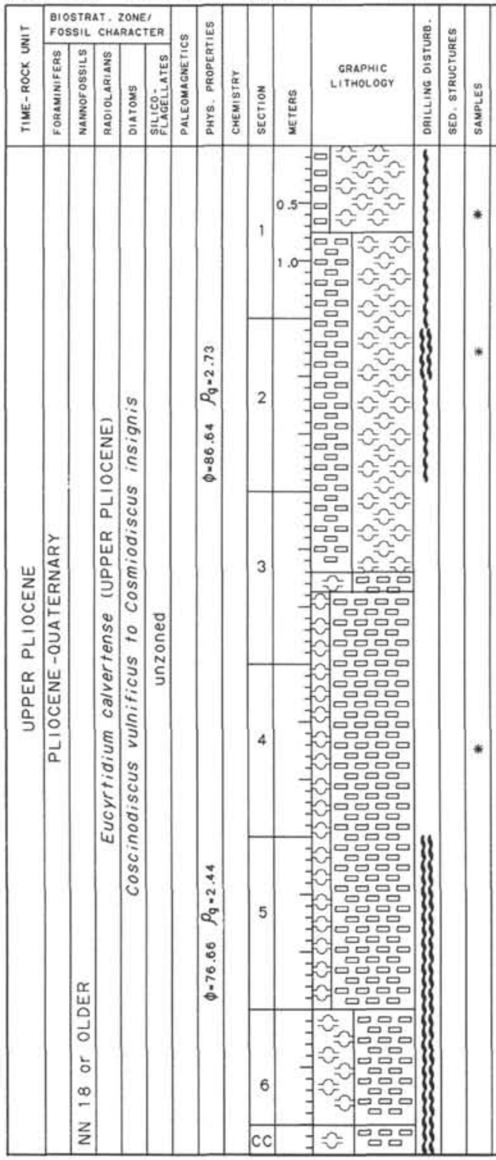

LITHOLOGIC DESCRIPTION

CALCAREOUS SILICEOUS OOZE and SILICEOUS-BEARING CALCAREOUS OOZE

Major lithology: Calcareous siliceous ooze, light gray (5Y 7/2), light olive gray (5Y 6/2), light olive (5Y 6/2), and greenish gray (5G 7/1), occurring in color bands; and siliceous-bearing calcareous ooze, light blue gray (5B 7/1) to light greenish gray (5GY 7/1). Slight to moderate bioturbation in Sections 1, 2, 5, and 6.

Minor lithology: Pebbles and lithic fragments in Section 1, 0-20 cm (contamination?).

SMEAR SLIDE SUMMARY (%):

	1, 60 D	2, 30 D	4, 70 D
COMPOSITION:			
Volcanic glass	—	—	Tr
Calcite	1	1	5
Accessory minerals:			
Mn-micronodules	—	Tr	1
Foraminifers	5	10	5
Nannofossils	10	20	79
Diatoms	82	68	8
Radiolarians	1	1	2
Sponge spicules	Tr	Tr	Tr
Silicoflagellates	1	Tr	Tr

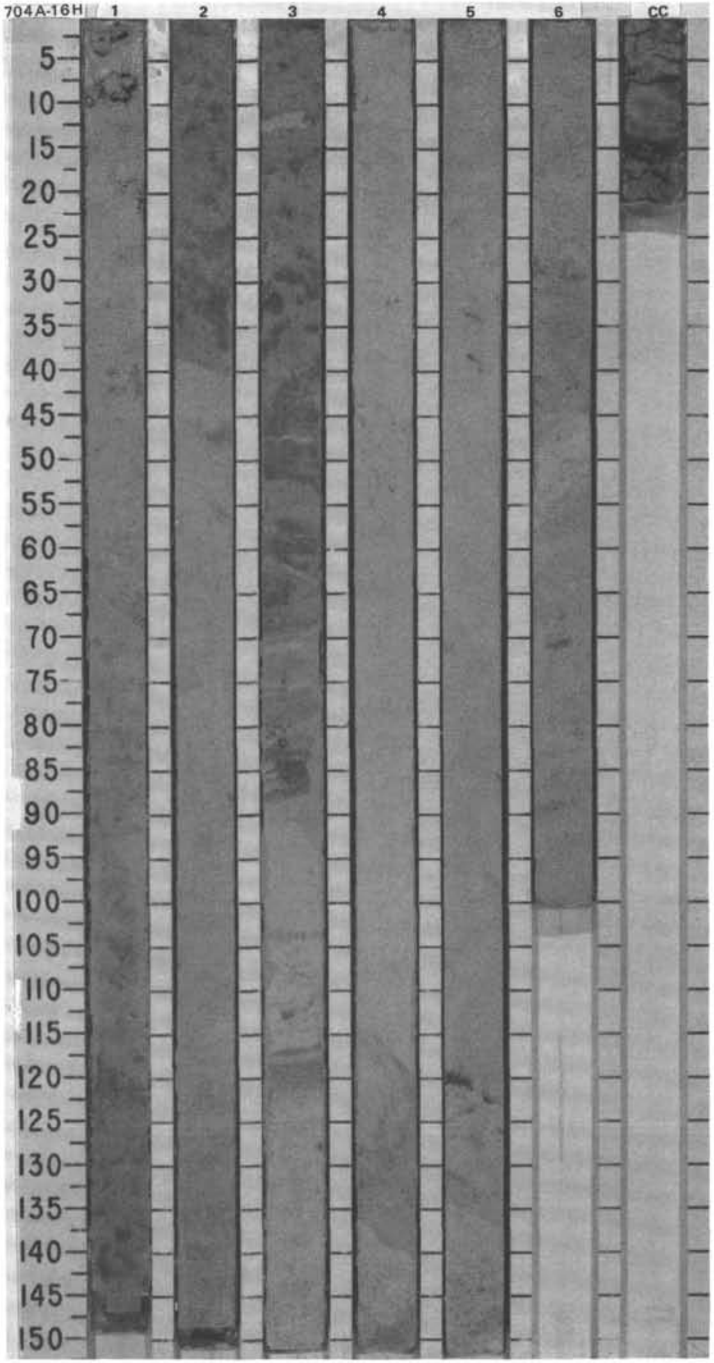

SITE 704 HOLE A CORE 17H CORED INTERVAL 2671.5-2681.0 mbsl; 149.7-159.2 mbsf

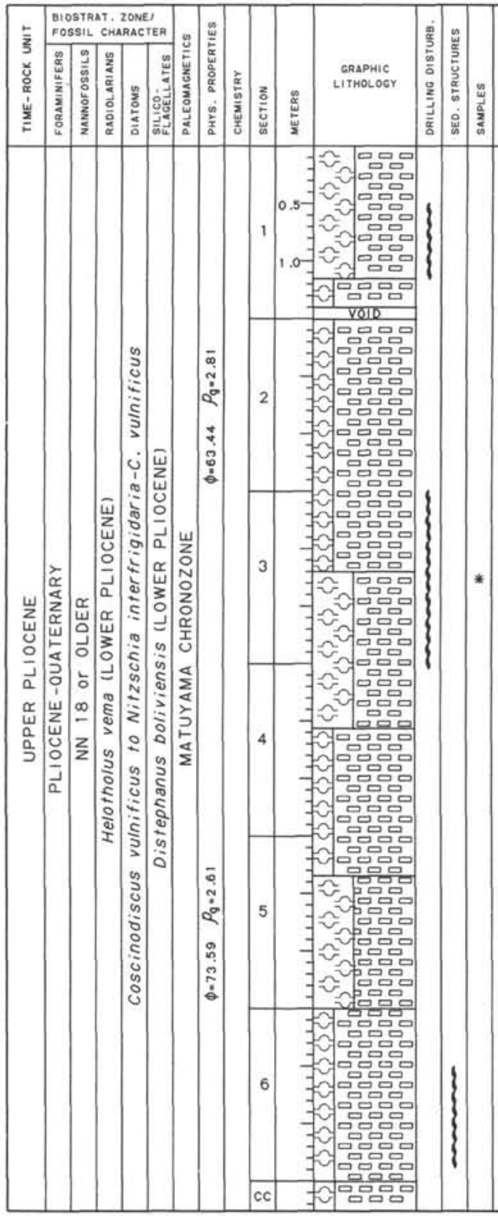

LITHOLOGIC DESCRIPTION

SILICEOUS-BEARING CALCAREOUS OOZE to SILICEOUS CALCAREOUS OOZE

Major lithology: Siliceous-bearing calcareous ooze to siliceous calcareous ooze, light gray (5Y 7/1 to 7/2), slightly bioturbated (mottled) in Sections 1, 3, and 6.

Minor lithology: Lithic fragments and small pebbles (ice-rafted debris) in Section 1, 0-90 cm; pyrite blebs in Section 3, 16 cm.

SMEAR SLIDE SUMMARY (%):

	3, 90 D
COMPOSITION:	
Volcanic glass	Tr
Calcite	1
Accessory minerals:	
Mn-micronodules	Tr
Foraminifers	25
Nannofossils	33
Diatoms	40
Radiolarians	1
Sponge spicules	Tr
Silicoflagellates	Tr

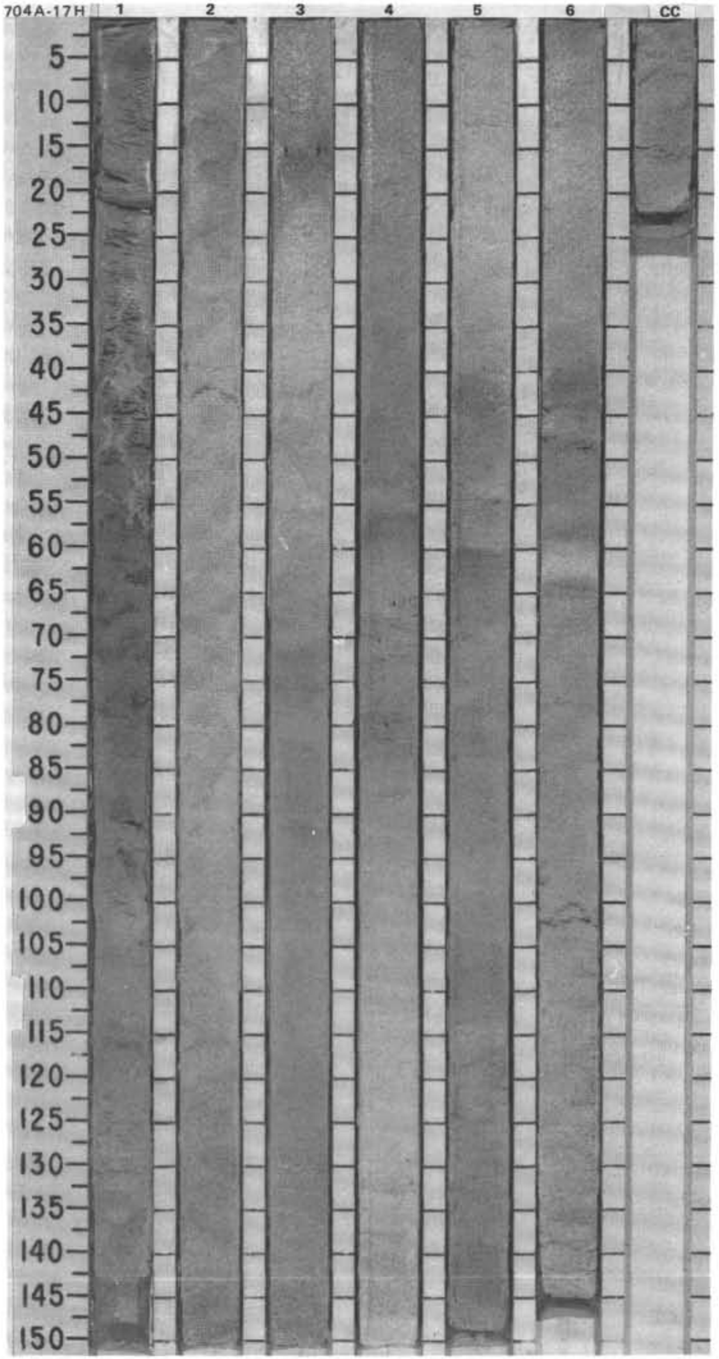

SITE 704 HOLE A CORE 18X CORED INTERVAL 2681.0-2690.5 mbsl; 159.2-168.7 mbsf

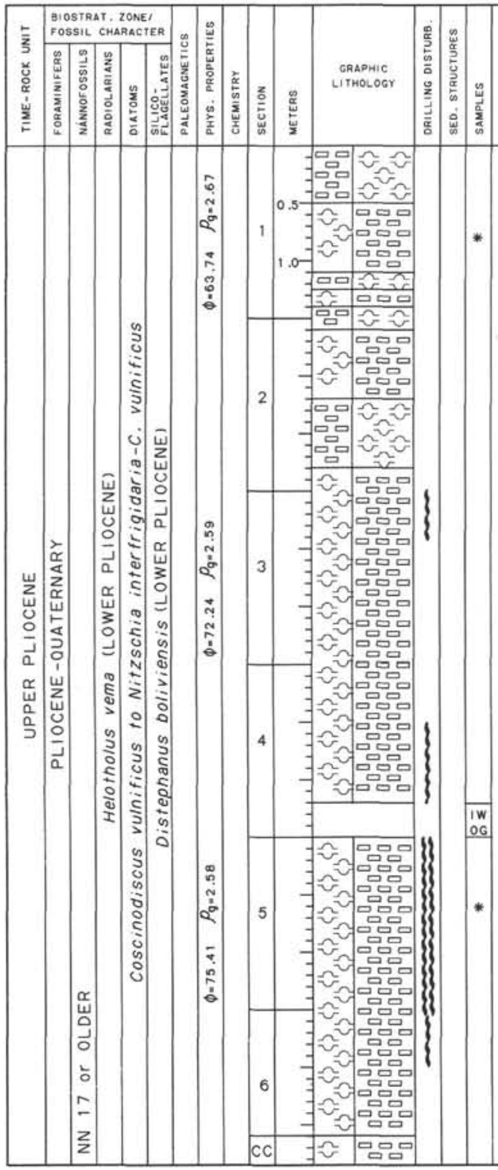

LITHOLOGIC DESCRIPTION

SILICEOUS CALCAREOUS OOZE to CALCAREOUS SILICEOUS OOZE

Major lithology: Siliceous calcareous ooze, white (no color code), light gray (5Y 7/1), and pale olive (5Y 6/3); and calcareous siliceous ooze, white (no color code) to light gray (5Y 7/1).

Minor lithology: Pebbles (contamination?) in Section 1, 0-5 cm, and Section 4, 40-120 cm; pyrite blebs in Section 4, 39-66 cm.

SMEAR SLIDE SUMMARY (%):

	1, 80 D	5, 60 D
COMPOSITION:		
Volcanic glass	—	Tr
Calcite	4	5
Accessory minerals:		
Mn-micronodules	Tr	—
Foraminifers	10	15
Nannofossils	45	45
Diatoms	40	34
Radiolarians	1	1
Sponge spicules	—	Tr
Silicoflagellates	Tr	Tr

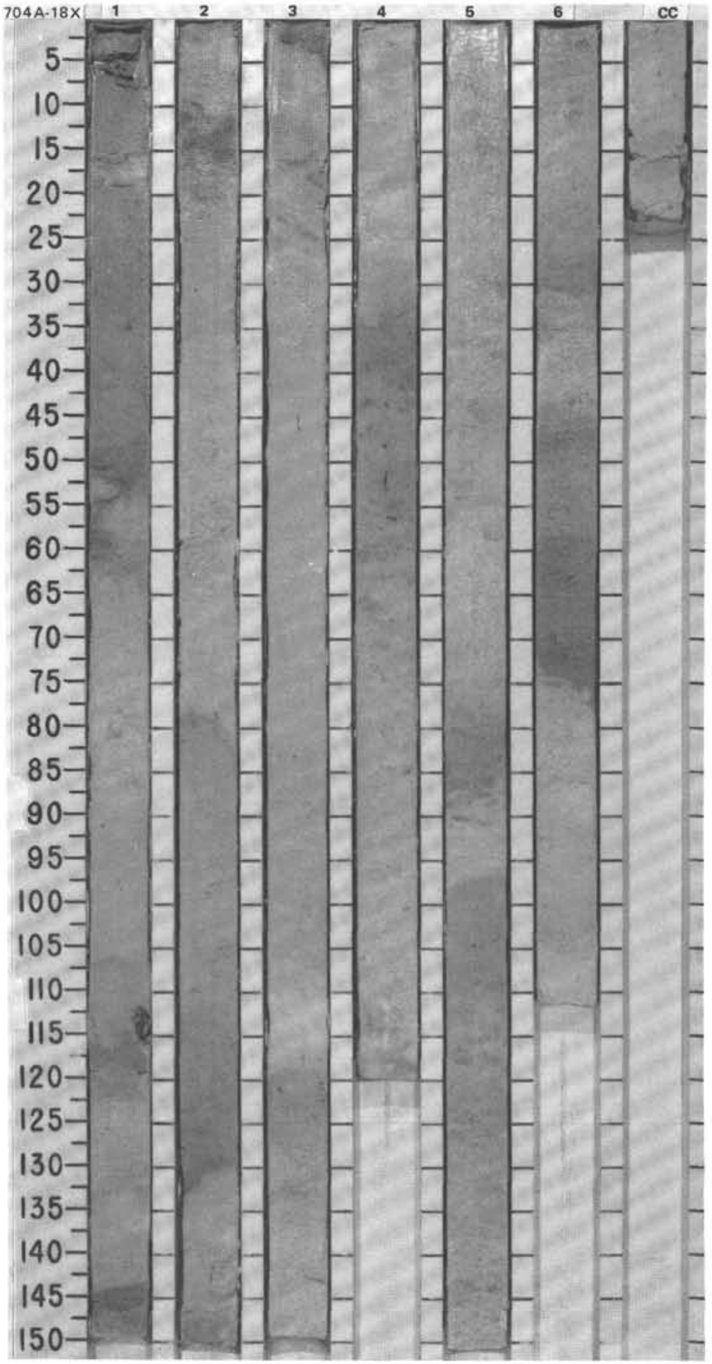

SITE 704 HOLE A CORE 19X CORED INTERVAL 2690.5-2700.0 mbsl; 168.7-178.2 mbsf

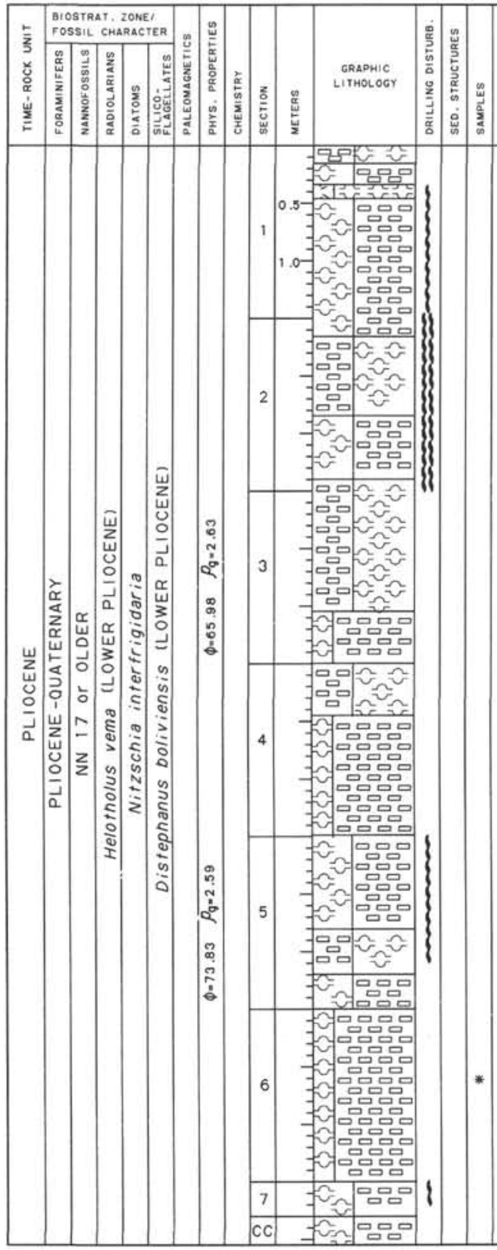

LITHOLOGIC DESCRIPTION

CALCAREOUS SILICEOUS OOZE, SILICEOUS-BEARING NANNOFOSSIL OOZE, and SILICEOUS CALCAREOUS OOZE

Major lithology: Alternating horizons of calcareous siliceous ooze, greenish gray (5GY 6/1, 7/1), light gray (5Y 7/1); siliceous-bearing nannofossil ooze, white (no color code); and siliceous calcareous ooze, light gray (5Y 7/1). Faintly bioturbated in Sections 1, 2, 5, and 7.

SMEAR SLIDE SUMMARY (%):

	6, 60 D
COMPOSITION:	
Volcanic glass	Tr
Accessory minerals:	
Fragmented carbonate	3
Foraminifers	3
Nannofossils	84
Diatoms	3
Radiolarians	2
Sponge spicules	5

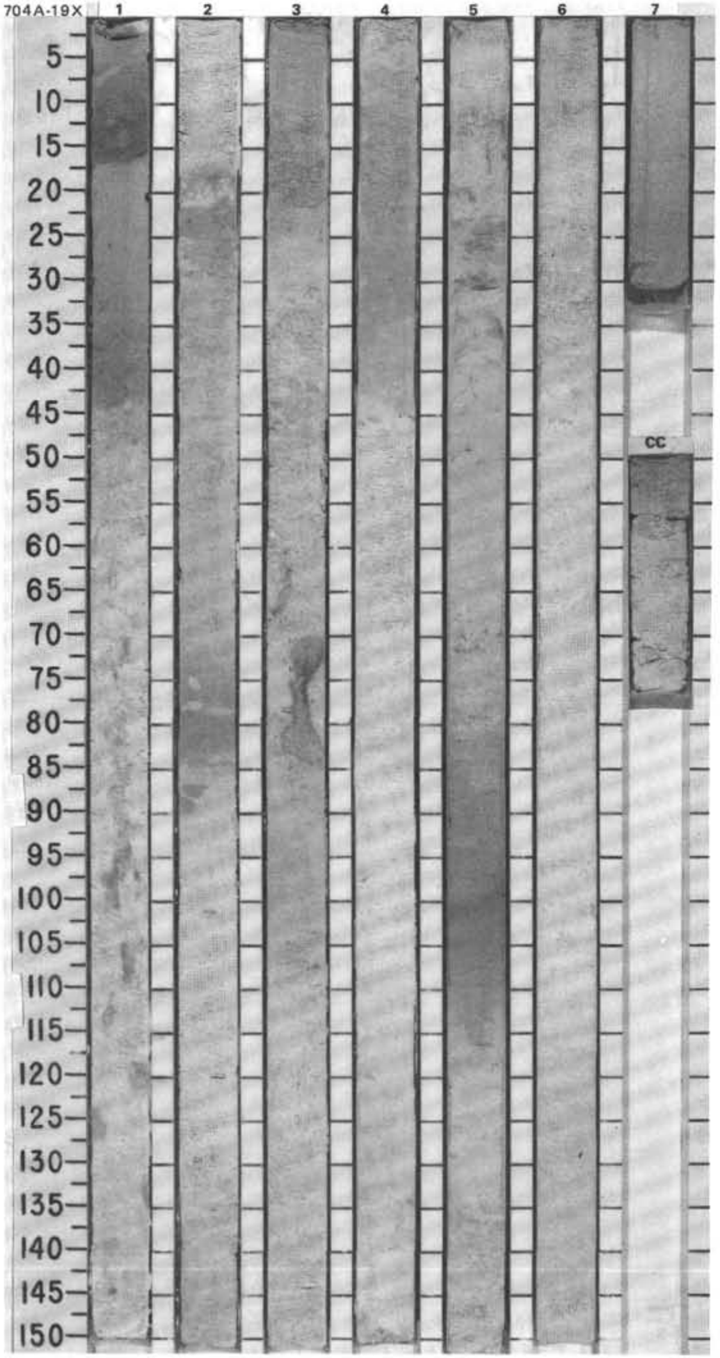

SITE 704 HOLE A CORE 20X CORED INTERVAL 2700.0-2709.5 mbsl; 178.2-187.7 mbsf

TIME-ROCK UNIT	BIOSTRAT. ZONE/ FOSSIL CHARACTER					PALEOMAGNETICS	PHYS. PROPERTIES	CHEMISTRY	SECTION	METERS	GRAPHIC LITHOLOGY	DRILLING DISTURB.	SED. STRUCTURES	SAMPLES
	FORAMINIFERS	NANNOFOSSILS	RADIOLARIANS	DIATOMS	SILICO-FLAGELLATES									
LOWER PLIOCENE	PLIOCENE-QUATERNARY	NN 15-16	*Helotholus vema* (LOWER PLIOCENE)	*Nitzschia angulata*	*Distephanus boliviensis* (LOWER PLIOCENE)		ϕ=70.88 ρ_g=2.78 ϕ=65.98 ρ_g=2.63 ϕ=67.55 ρ_g=2.78		1 2 3 4 5 6 7 CC	0.5 1.0	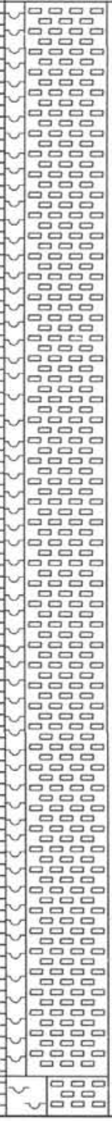			*

LITHOLOGIC DESCRIPTION

DIATOM-BEARING CALCAREOUS OOZE

Major lithology: Diatom-bearing calcareous ooze, featureless, white (no color code), light greenish gray (5GY 7/1), light gray (5G 7/1). Color variations are much subtler in this core than above.

Minor lithology: Dark fine-grained lithic fragment in Section 1, 50–55 cm.

SMEAR SLIDE SUMMARY (%):

	2, 70 D
COMPOSITION:	
Nannofossils	85
Diatoms	5
Silicoflagellates	5
Micrite	5

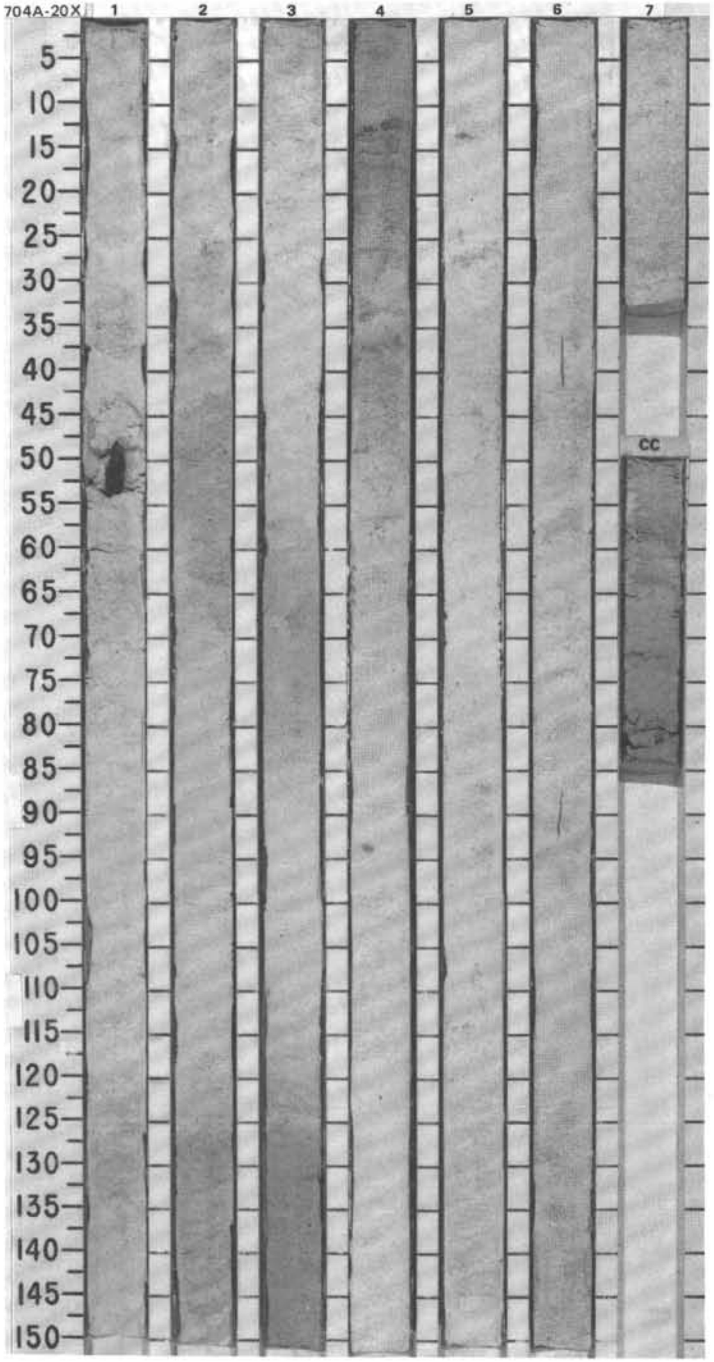

SITE 704 HOLE A CORE 21X CORED INTERVAL 2709.5-2719.0 mbsl; 187.7-197.0 mbsf

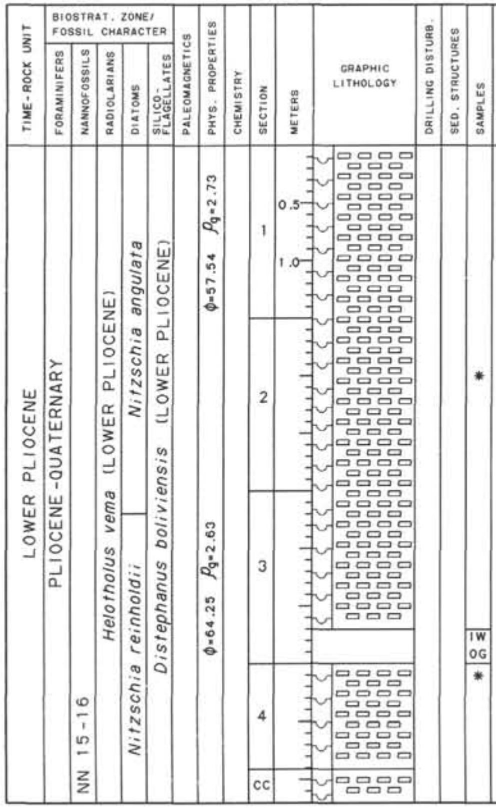

LITHOLOGIC DESCRIPTION

DIATOM-BEARING CALCAREOUS OOZE

Major lithology: Diatom-bearing calcareous ooze, featureless, white (2.5Y 8/0).

Minor lithology: Blebs containing pyrite in Section 2, 55 cm; Section 3, 95 cm; and Section 4, at 5, 15, 35, and 65 cm.

SMEAR SLIDE SUMMARY (%):

	2, 55 M	4, 5 D
COMPOSITION:		
Feldspar	1	Tr
Volcanic glass	1	1
Accessory minerals:		
Opaque (pyrite?)	12	6
Foraminifers	25	77
Nannofossils	58	—
Diatoms	2	15
Radiolarians	Tr	—
Sponge spicules	1	Tr
Silicoflagellates	—	1

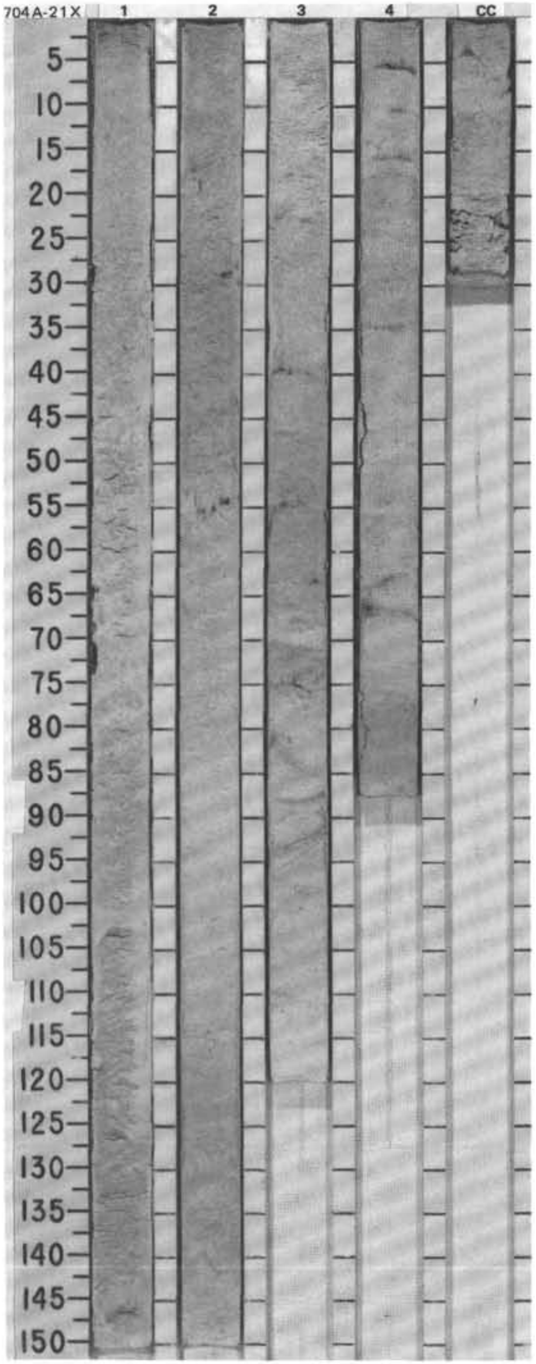

SITE 704 HOLE A CORE 22X CORED INTERVAL 2719.0-2728.5 mbsl; 197.0-206.7 mbsf

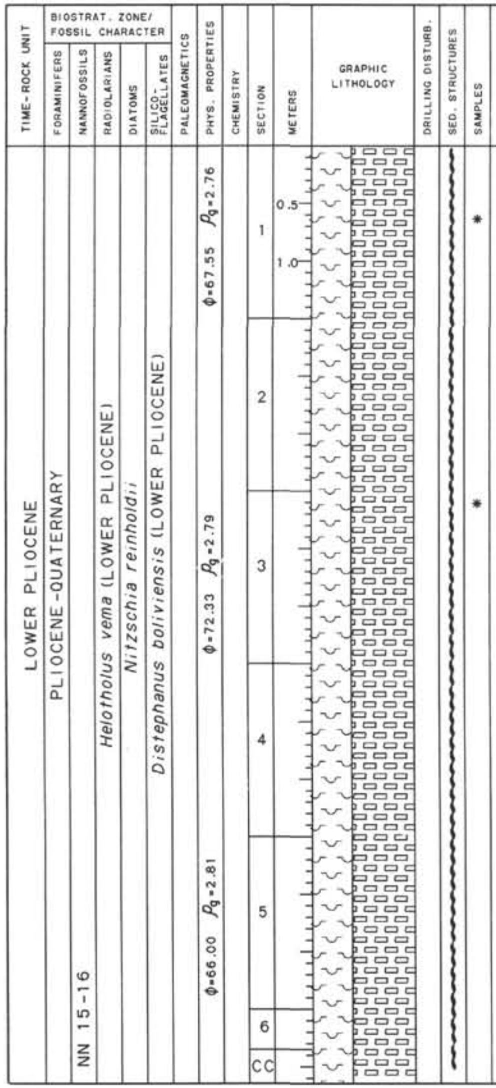

LITHOLOGIC DESCRIPTION

DIATOM CALCAREOUS OOZE

Major lithology: Diatom calcareous ooze, white (no color code) to light greenish gray (5G 7/1), diffuse bioturbation, slightly mottled.

Minor lithology: Pyrite-bearing horizon in Section 3, 14 cm.

SMEAR SLIDE SUMMARY (%):

	1, 70 D	3, 12 D
COMPOSITION:		
Feldspar	—	Tr
Volcanic glass	Tr	1
Micrite	10	10
Accessory minerals:		
Opaques	—	Tr
Foraminifers/ nannofossils	50	50
Diatoms	36	33
Radiolarians	3	5
Sponge spicules	1	1

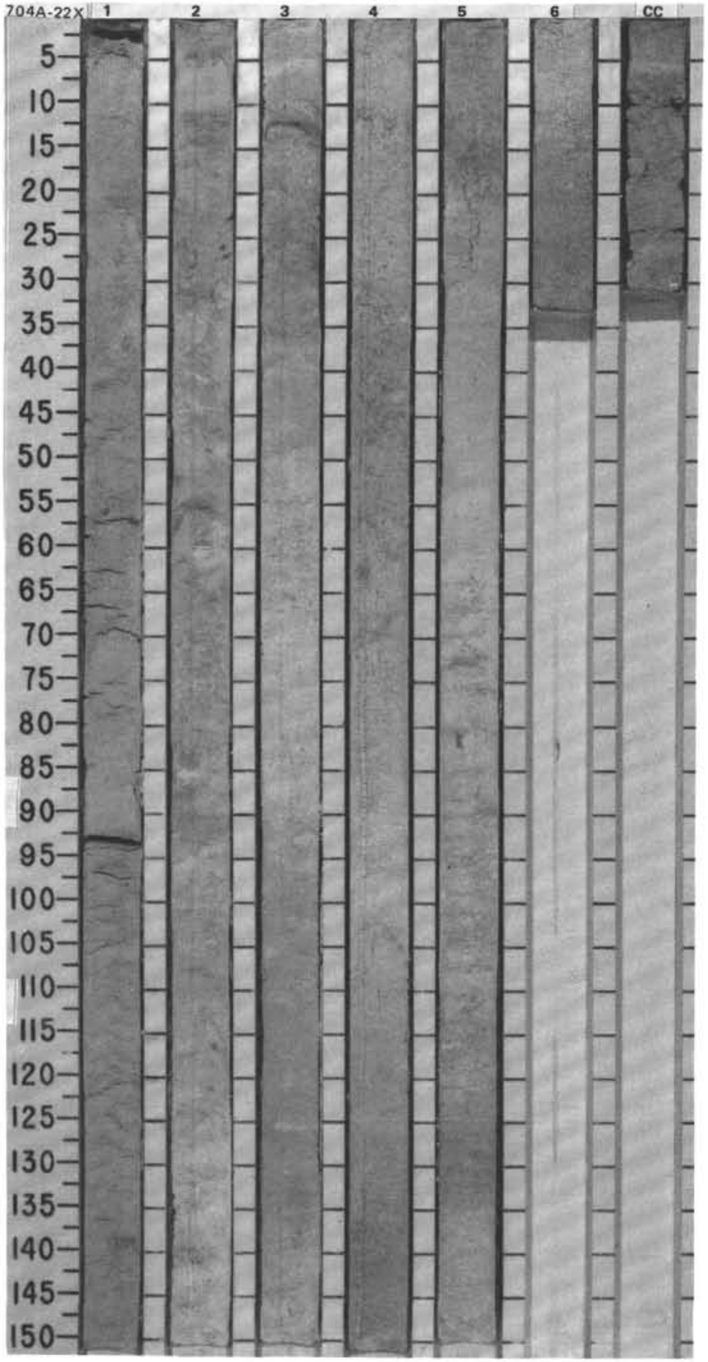

SITE 704 HOLE A CORE 23X CORED INTERVAL 2728.5-2738.0 mbsl; 206.7-216.2 mbsf

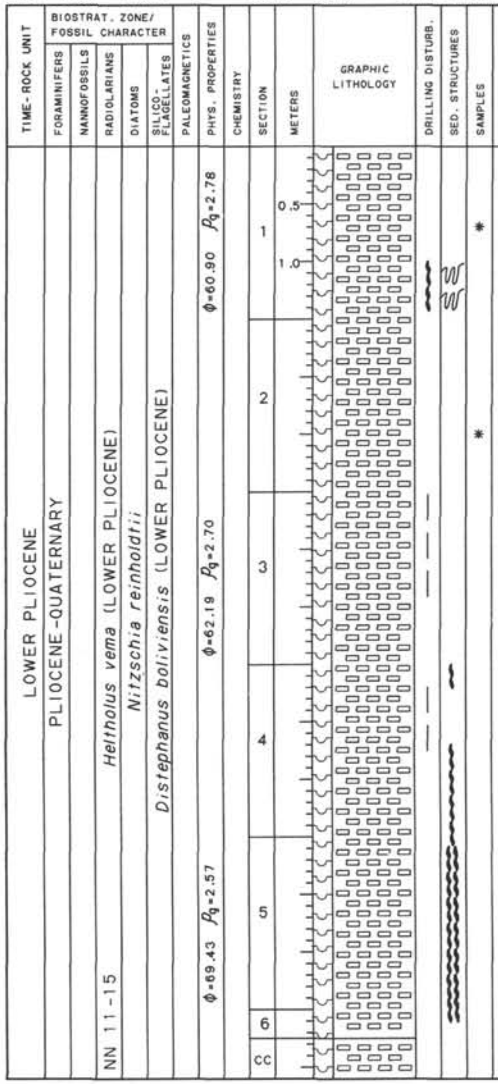

LITHOLOGIC DESCRIPTION

DIATOM-BEARING CALCAREOUS OOZE

Drilling disturbance: Slight in Section 1, 110-140 cm; Section 3, 0-60 cm; and Section 4, 25-60 cm.

Major lithology: Diatom-bearing calcareous ooze, light greenish-gray (5G 7/1). Convolute bedding possibly indicating slumping/redeposition in Section 1, 107-135 cm.

SMEAR SLIDE SUMMARY (%):

	1, 70 D	2, 100 D
COMPOSITION:		
Quartz/feldspar	—	3
Feldspar	Tr	—
Clay	—	2
Volcanic glass	1	—
Micrite	10	—
Accessory minerals:		
Opaques	Tr	—
Foraminifers	60	8
Nannofossils	—	54
Diatoms	26	20
Radiolarians	22	10
Sponge spicules	1	—
Silicoflagellates	Tr	3

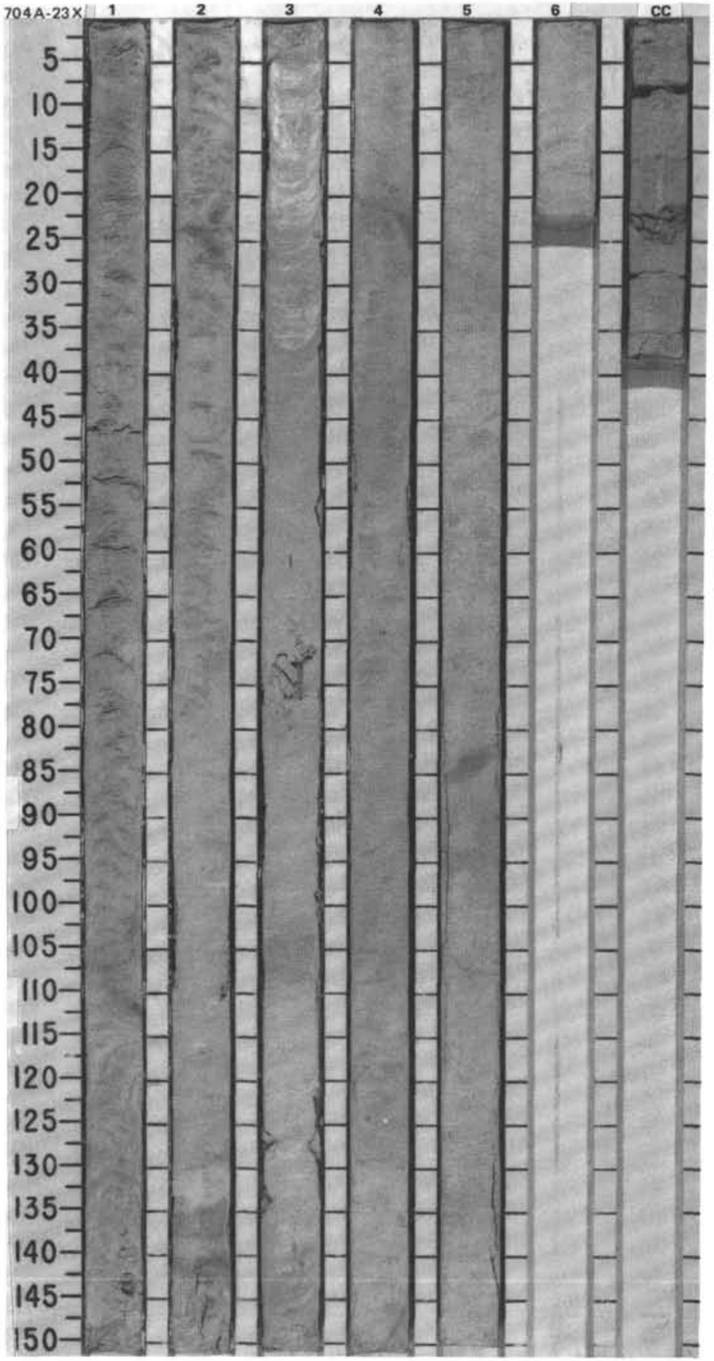

SITE 704 HOLE A CORE 24X CORED INTERVAL 2738.0-2747.5 mbsl; 216.2-225.7 mbsf

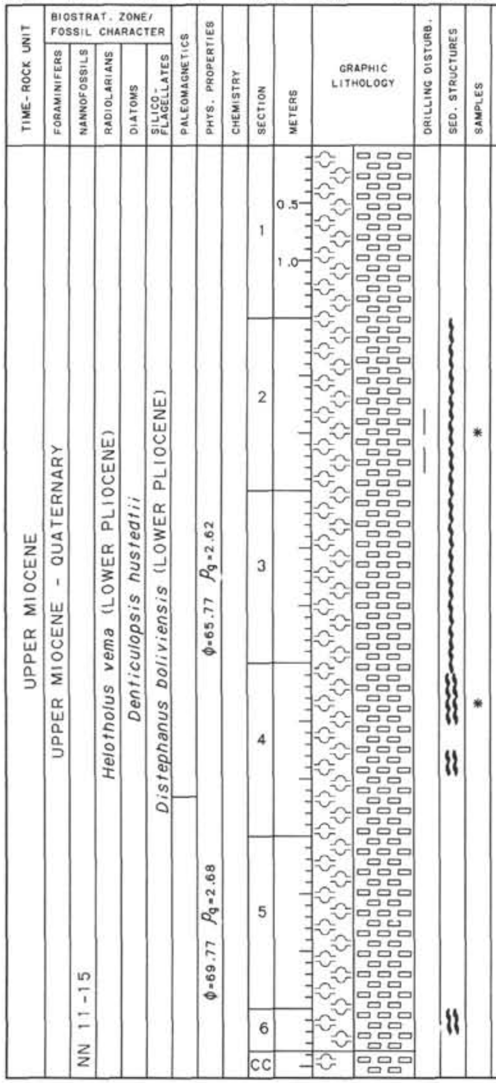

LITHOLOGIC DESCRIPTION

SILICEOUS CALCAREOUS OOZE

Drilling disturbance: Slight in Section 2, 85-150 cm.

Major lithology: Siliceous calcareous ooze, showing strong color variations from light greenish gray (5G 7/1), to greenish gray (5G 6/1), to light gray (2.5Y 7/2), to white (5Y 8/1), to grayish brown (2.5Y 5/2). Bioturbation apparent in Sections 2, 3, 4, and 6.

SMEAR SLIDE SUMMARY (%):

	2, 100 D	4, 34 D
COMPOSITION:		
Quartz/feldspar	3	—
Feldspar	—	1
Clay	2	Tr
Volcanic glass	—	1
Accessory minerals:		
Opaques	—	1
Foraminifers	8	49
Nannofossils	54	—
Diatoms	20	25
Radiolarians	10	20
Sponge spicules	—	1
Silicoflagellates	3	Tr
Pellets	—	2

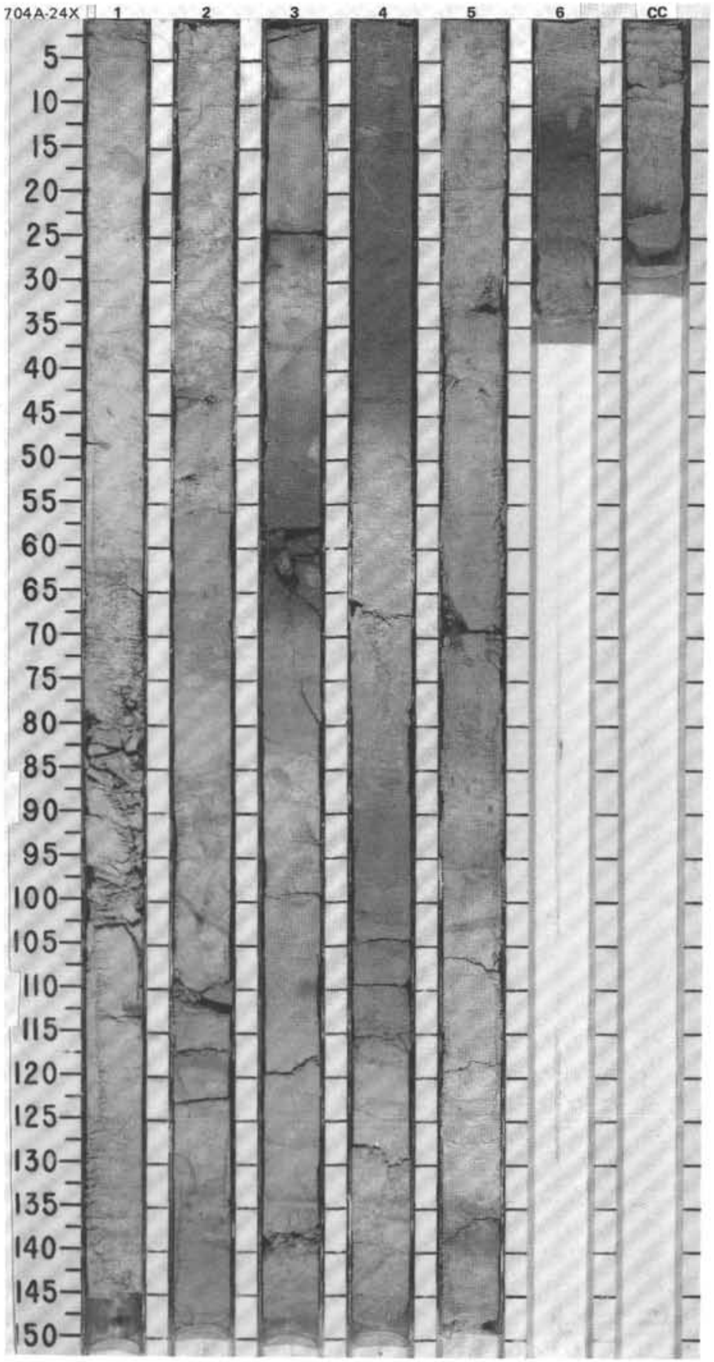

SITE 704 HOLE A CORE 25X CORED INTERVAL 2747.5-2757.0 mbsl; 225.7-235.2 mbsf

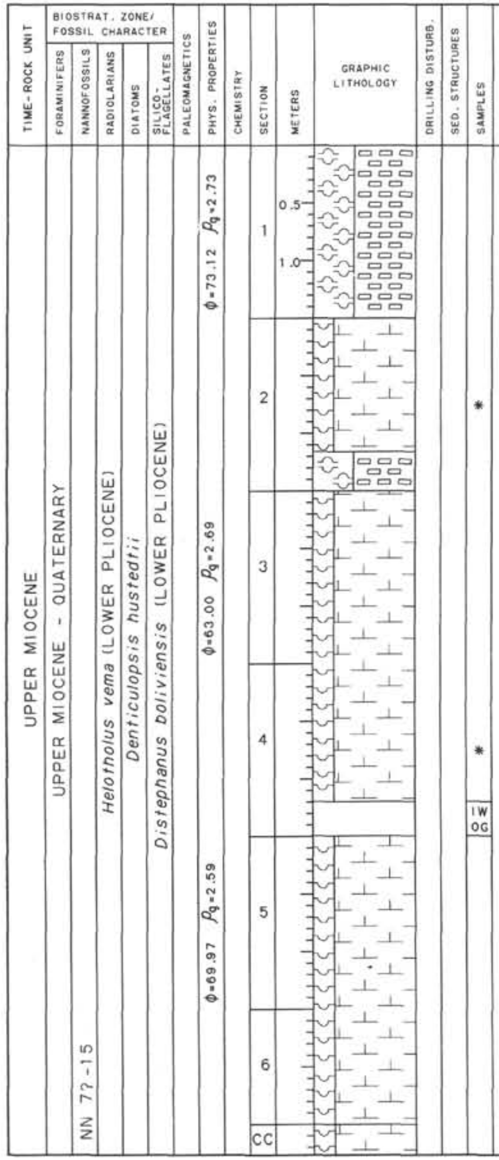

LITHOLOGIC DESCRIPTION

SILICEOUS CALCAREOUS OOZE and DIATOM-BEARING NANNOFOSSIL OOZE

Major lithology: Alternating horizons of siliceous calcareous ooze, light greenish gray (5G 7/1) and greenish gray (5G 6/1); and diatom-bearing nannofossil ooze, white (no color code) and light gray (5Y 7/1).

Minor lithology: Pyrite-bearing horizons in Section 3, 49, 61, and 79 cm; Section 4, 70 cm; Section 5, 42 cm; and Section 6, 11-12 and 63 cm.

SMEAR SLIDE SUMMARY (%):

	2, 70 D	4, 71 D
COMPOSITION:		
Clay	—	1
Volcanic glass	Tr	2
Micrite	—	10
Accessory minerals:		
Opaques (pyrite?)	Tr	5
Foraminifers	2	5
Nannofossils	71	56
Diatoms	25	20
Radiolarians	1	1
Sponge spicules	1	Tr
Silicoflagellates	—	Tr

704A-26X NO RECOVERY

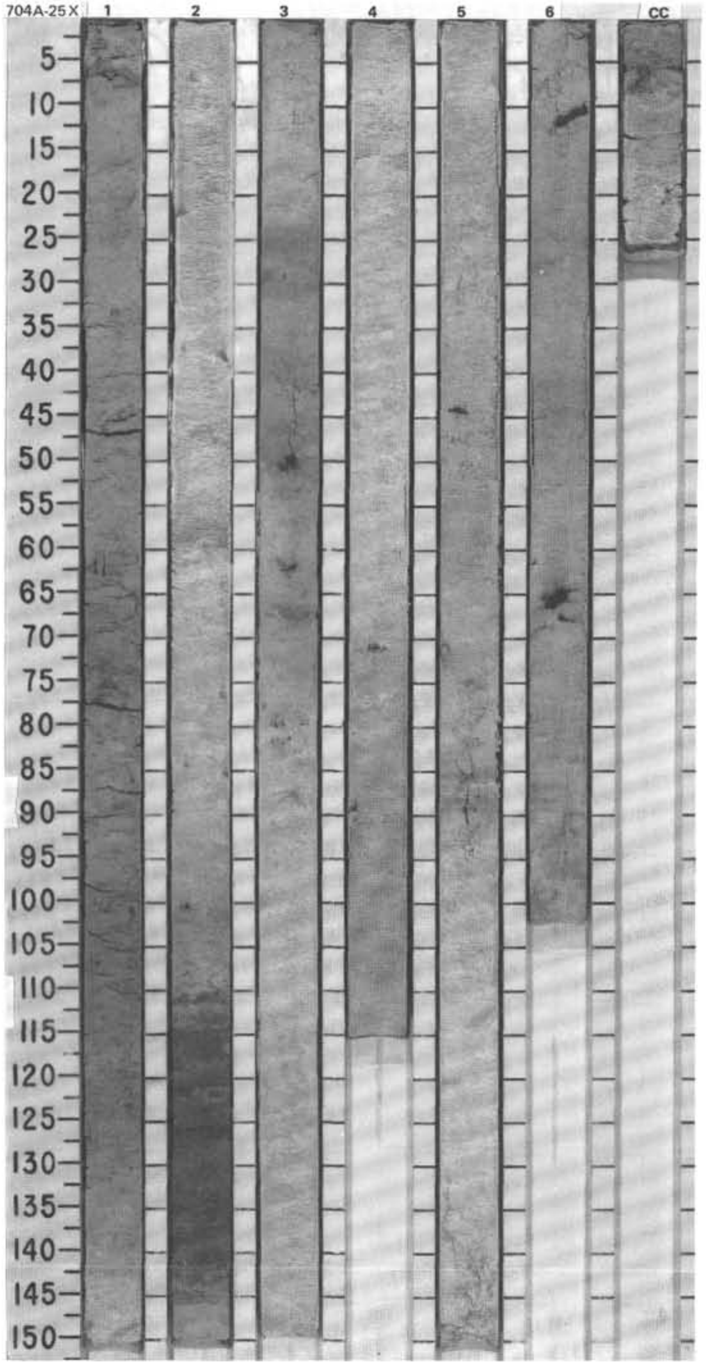

SITE 704 HOLE A CORE 27X CORED INTERVAL 2766.5-2776.0 mbsl; 244.7-254.2 mbsf

TIME-ROCK UNIT	BIOSTRAT. ZONE/ FOSSIL CHARACTER					PALEOMAGNETICS	PHYS. PROPERTIES	CHEMISTRY	SECTION	METERS	GRAPHIC LITHOLOGY	DRILLING DISTURB.	SED. STRUCTURES	SAMPLES
	FORAMINIFERS	NANNOFOSSILS	RADIOLARIANS	DIATOMS	SILICO-FLAGELLATES									
UPPER MIOCENE	MIOCENE	NN 7?-15	no sample	*Denticulopsis hustedtii*	no sample				CC					*

LITHOLOGIC DESCRIPTION

DIATOM-BEARING NANNOFOSSIL OOZE

Major lithology: No recovery except for 7 cm of diatom-bearing nannofossil ooze, light greenish gray (5G 7/1), in CC.

SMEAR SLIDE SUMMARY (%):

	CC, 4 D
COMPOSITION:	
Micrite	10
Nannofossils	80
Diatoms	10

704A-28X NO RECOVERY

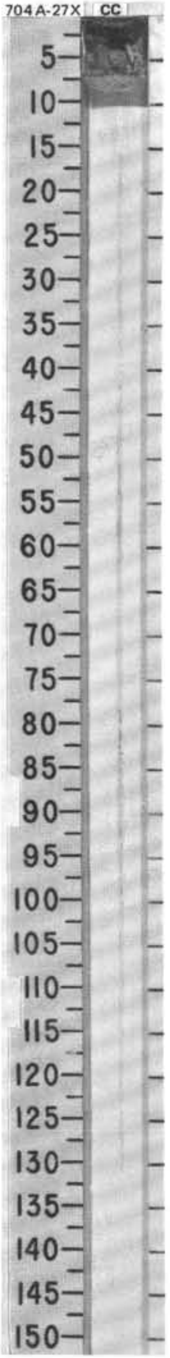

SITE 704 HOLE A CORE 29X CORED INTERVAL 2785.5-2795.0 mbsl; 263.7-273.2 mbsf

TIME-ROCK UNIT	BIOSTRAT. ZONE/ FOSSIL CHARACTER					PALEOMAGNETICS	PHYS. PROPERTIES	CHEMISTRY	SECTION	METERS	GRAPHIC LITHOLOGY	DRILLING DISTURB.	SED. STRUCTURES	SAMPLES
	FORAMINIFERS	NANNOFOSSILS	RADIOLARIANS	DIATOMS	SILICO-FLAGELLATES									
UPPER MIOCENE	not examined	NN 7?-15	unzoned	*Denticulopsis hustedtii*	Barren				CC					*

LITHOLOGIC DESCRIPTION

DIATOM-BEARING NANNOFOSSIL OOZE

Major lithology: No recovery except for 21 cm of diatom-bearing nannofossil ooze, light greenish gray (5G 7/1), in CC.

SMEAR SLIDE SUMMARY (%):

	CC, 12 D
COMPOSITION:	
Micrite	12
Foraminifers	10
Nannofossils	68
Diatoms	10

SITE 704 HOLE A CORE 30X CORED INTERVAL 2795.0-2804.5 mbsl; 273.2-282.7 mbsf

TIME-ROCK UNIT	BIOSTRAT. ZONE/ FOSSIL CHARACTER					PALEOMAGNETICS	PHYS. PROPERTIES	CHEMISTRY	SECTION	METERS	GRAPHIC LITHOLOGY	DRILLING DISTURB.	SED. STRUCTURES	SAMPLES
	FORAMINIFERS	NANNOFOSSILS	RADIOLARIANS	DIATOMS	SILICO-FLAGELLATES									
UPPER MIOCENE	not examined	NN 7?-15	unzoned	*Denticulopsis hustedtii*	Barren				CC					*

LITHOLOGIC DESCRIPTION

DIATOM-BEARING NANNOFOSSIL OOZE

Major lithology: No recovery except for 17 cm of diatom-bearing nannofossil ooze, light greenish gray (5G 7/1), in CC.

SMEAR SLIDE SUMMARY (%):

	CC, 10 D
COMPOSITION:	
Micrite	12
Foraminifers	8
Nannofossils	70
Diatoms	10

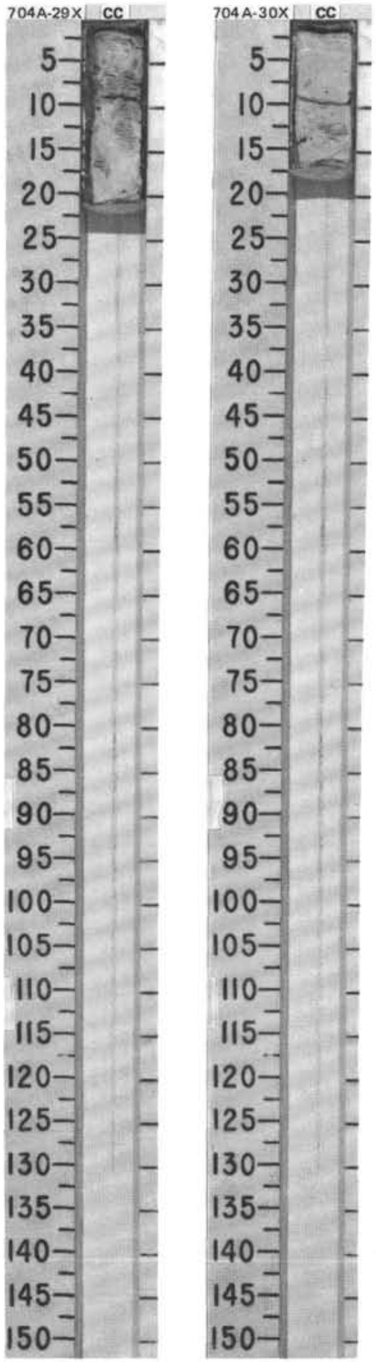

SITE 704 HOLE B CORE 1H CORED INTERVAL 2520.3-2527.0 mbsl; 0.0-6.7 mbsf

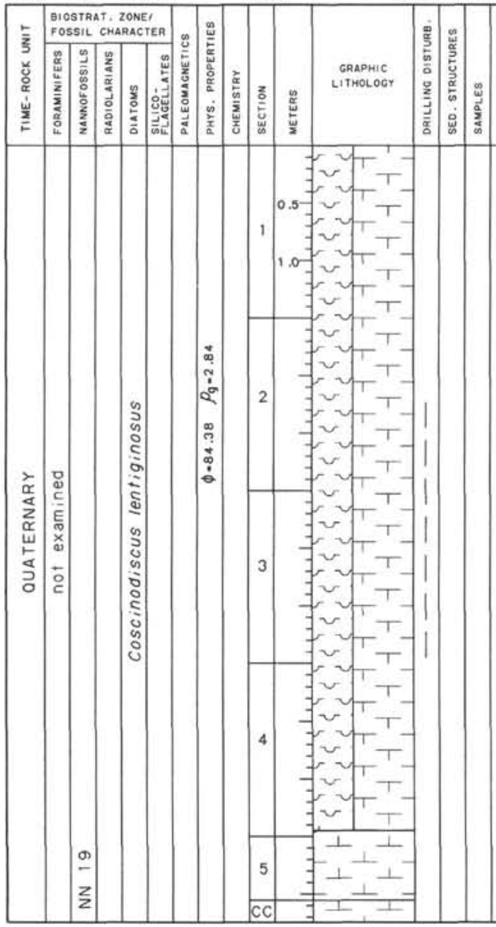

LITHOLOGIC DESCRIPTION

DIATOM-FORAMINIFER OOZE

Drilling disturbance: Slightly disturbed in Section 2, 70-150 cm, and in Section 3.

Major lithology: Diatom-foraminifer ooze, light gray (2.5Y 7/2) and pale yellow (5Y 7/3) to white (no color code), containing green altered volcanic ash in Sections 3 and 4.

Minor lithology: Nannofossil ooze, white (no color code), in Section 4, 139-150 cm; Section 5, 0-56 cm; and in the CC.

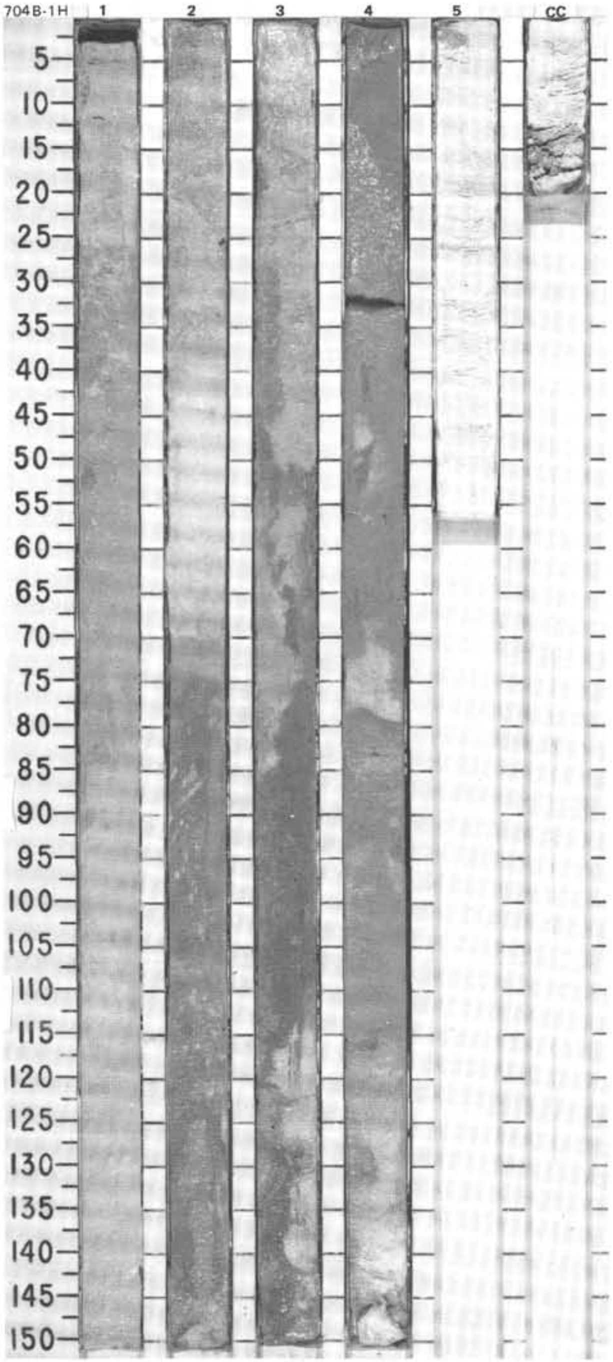

SITE 704 HOLE B CORE 2H CORED INTERVAL 2527.0-2536.5 mbsl; 6.7-16.2 mbsf

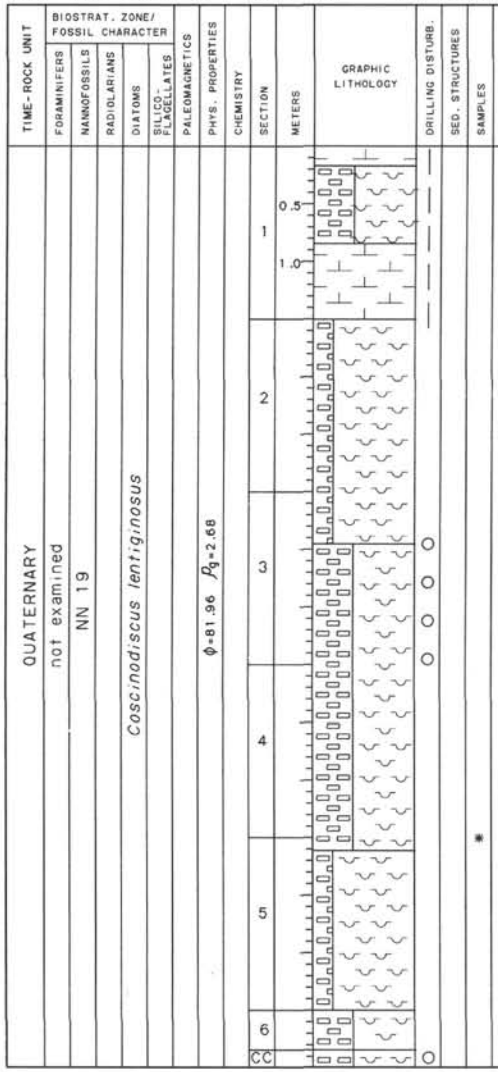

LITHOLOGIC DESCRIPTION

CALCAREOUS DIATOM OOZE

Drilling disturbance: Slightly disturbed in Section 1; soupy in Section 3, 40-150 cm.

Major lithology: Calcareous diatom ooze, pale olive (5Y 6/3) to light gray (5Y 7/1).

Minor lithologies: Calcareous-bearing diatom ooze, pale olive (5Y 6/3), in Section 2; 3 and 0-40 cm; and Section 5, 11-150 cm. Nannofossil ooze, white (no color code), in Section 1, 0-18 and 85-135 cm.

SMEAR SLIDE SUMMARY (%):

	4, 145 D
COMPOSITION:	
Feldspar	1
Volcanic glass	1
Micrite	10
Foraminifers	5
Nannofossils	35
Diatoms	49
Radiolarians	1
Silicoflagellates	Tr

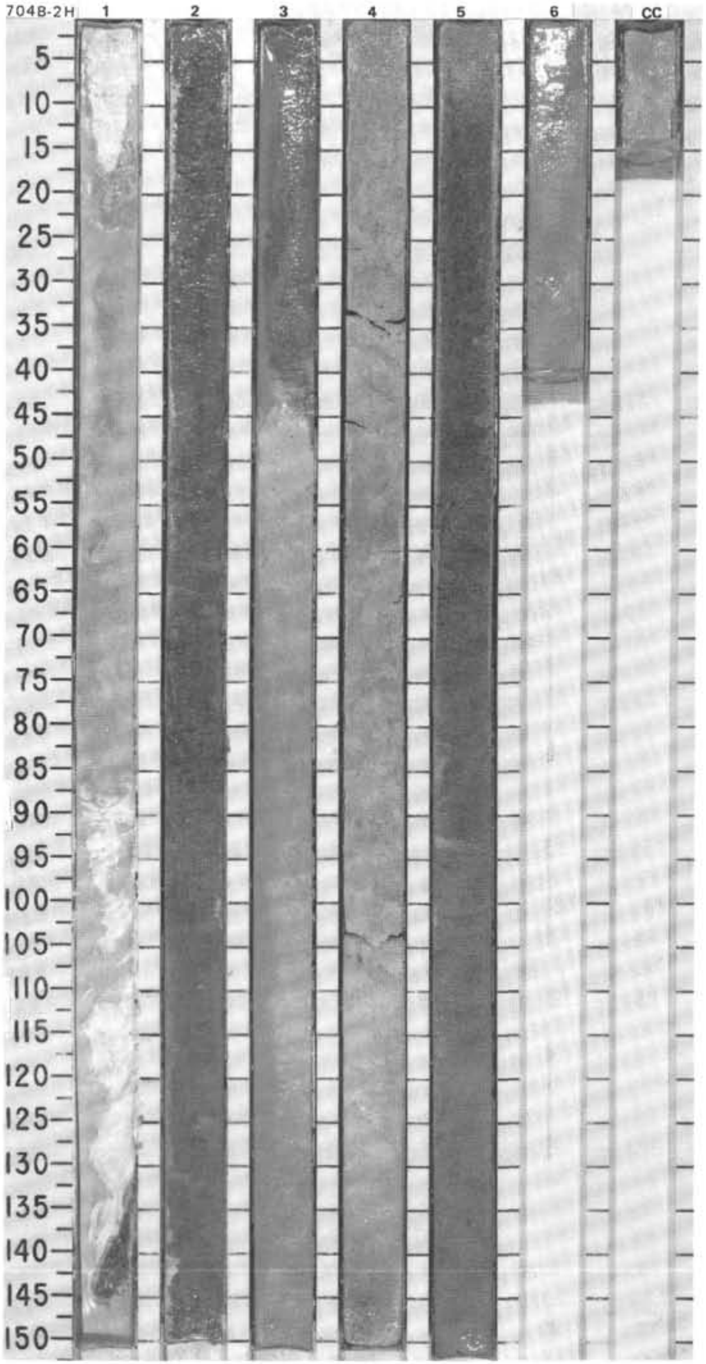

SITE 704 HOLE B CORE 3H CORED INTERVAL 2536.5-2546.0 mbsl; 16.2-25.7 mbsf

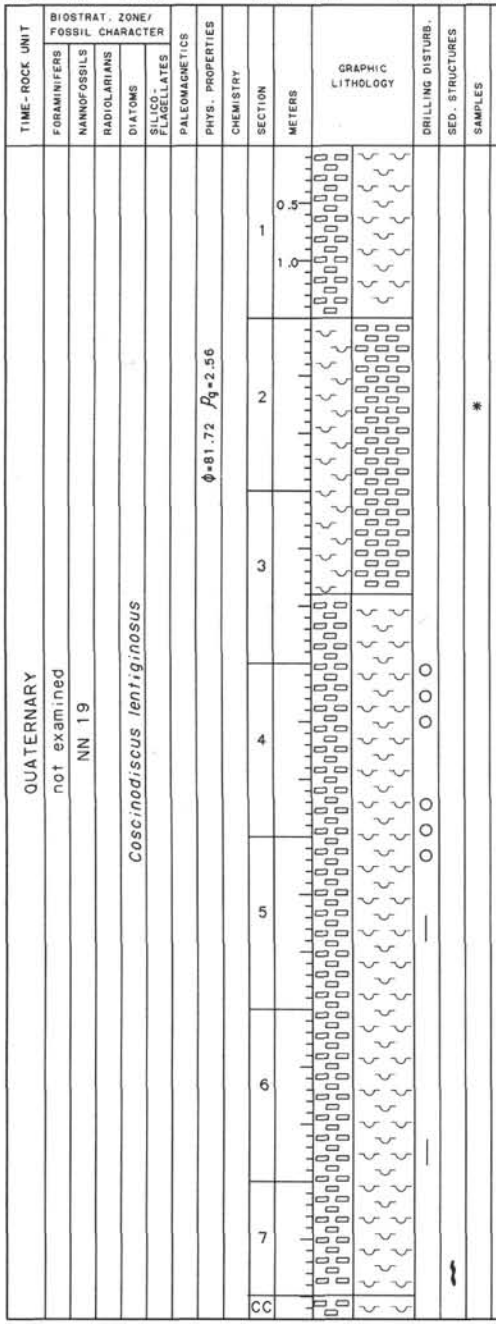

LITHOLOGIC DESCRIPTION

CALCAREOUS DIATOM OOZE

Drilling disturbance: Soupy in Section 3, 140-150 cm; Section 4, 0-40 and 120-150 cm; and Section 5, 0-20 cm.

Major lithology: Calcareous diatom ooze, light olive gray (5Y 6/2) and light gray (5Y 7/1) to white (5Y 8/1).

Minor lithology: Diatom calcareous ooze, white (5Y 8/1), in Section 2 and Section 3, 0-91 cm. Ash-bearing and ice-rafted debris-bearing silty horizons, light olive gray (5Y 6/2), occur in Section 6, 125-129 and 135-146 cm; and Section 7, 15-25 cm.

SMEAR SLIDE SUMMARY (%):

	2, 70 D
COMPOSITION:	
Feldspar	Tr
Volcanic glass	1
Foraminifers/ nannofossils	60
Diatoms	37
Radiolarians	1
Sponge spicules	1
Silicoflagellates	Tr

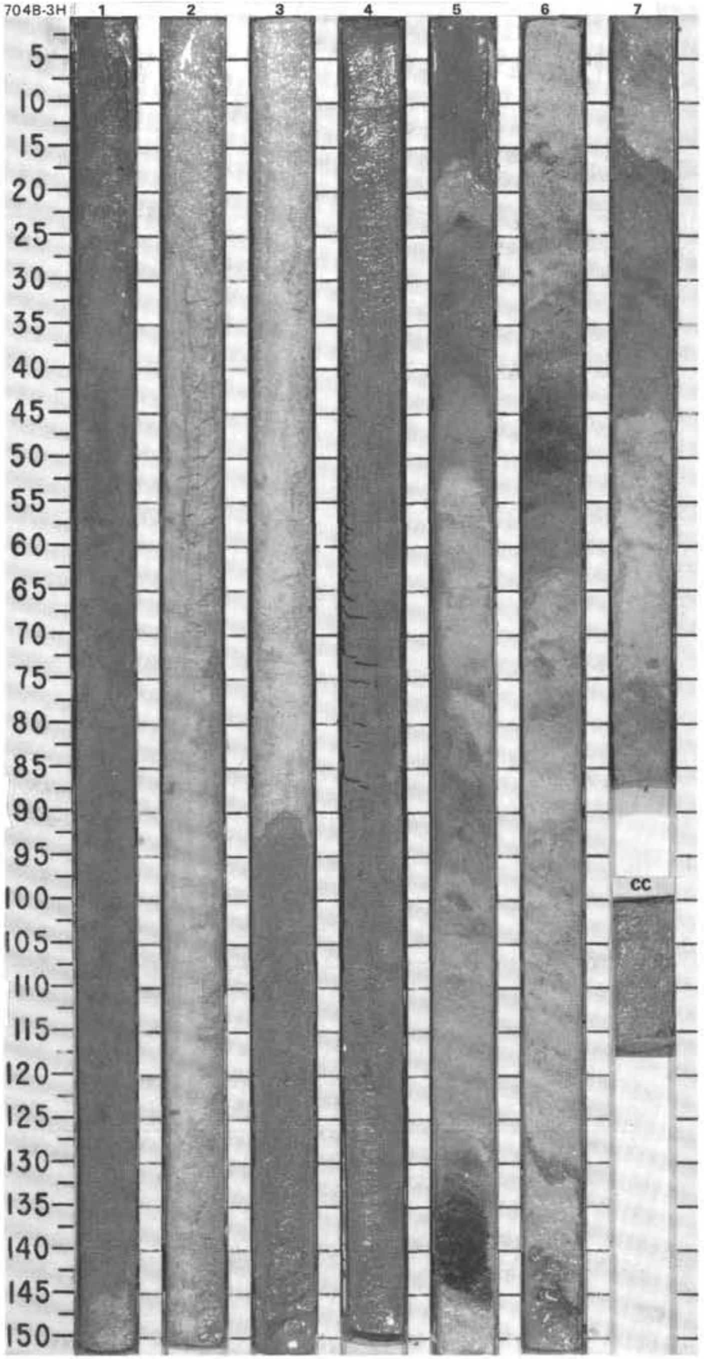

SITE 704 HOLE B CORE 4H CORED INTERVAL 2546.0-2555.5 mbsl; 25.7-35.2 mbsf

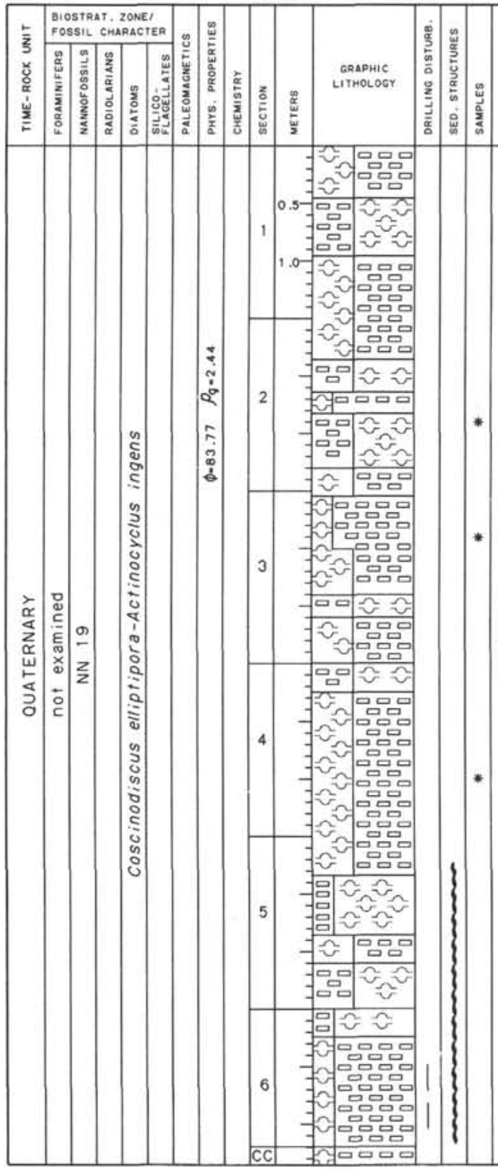

LITHOLOGIC DESCRIPTION

SILICEOUS CALCAREOUS OOZE to CALCAREOUS SILICEOUS OOZE

Drilling disturbance: Moderately to slightly disturbed in Section 1 and Section 6, 50-110 cm.

Major lithology: Siliceous calcareous ooze, light gray (5Y 7/2) and white (no color code), light yellowish brown (10YR 6/4); alternating with calcareous siliceous ooze, pale olive (5Y 6/4) and olive (5Y 5/4) to light gray (5Y 7/2). Opaque (pyrite?) staining occurs in Section 1, 44 and 67 cm; Section 5, 0-32 cm. Color changes are gradational.

Minor lithology: Siliceous-bearing calcareous ooze, white (no color code) in Section 2, 61-82 cm, Section 3, 7-50 cm, and Section 6, 27-110 cm. Accumulation of opaques (pyrite?) in Section 5, 38-44 cm.

Minor bioturbation occurs throughout Sections 5 and 6.

SMEAR SLIDE SUMMARY (%):

	2, 95 D	3, 35 D	4, 90 D
COMPOSITION:			
Accessory minerals:			
Fragmented carbonate	—	—	17
Mn-micronodules	3	15	35
Foraminifers	3	15	35
Nannofossils	25	70	30
Diatoms	64	15	15
Radiolarians	3	Tr	3
Sponge spicules	—	Tr	—
Silicoflagellates	5	Tr	—

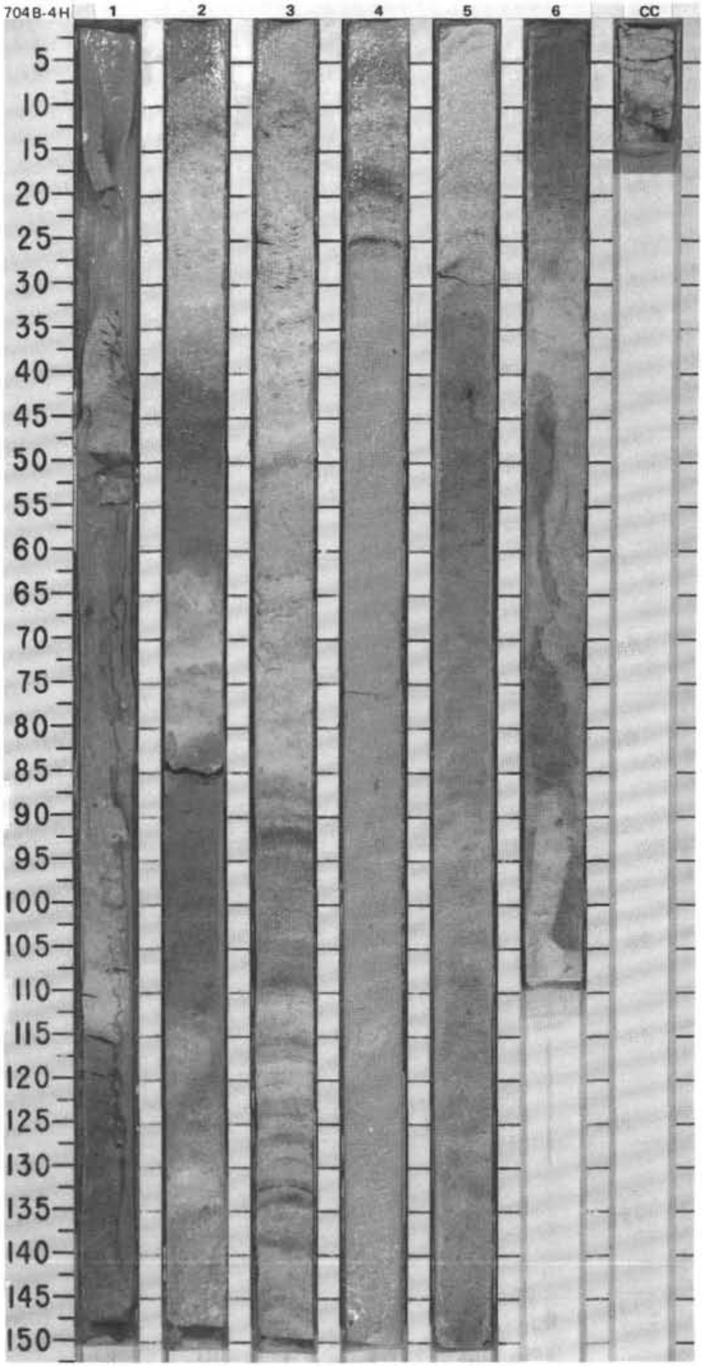

SITE 704 HOLE B CORE 5H CORED INTERVAL 2555.5-2565.0 mbsl; 35.2-44.7 mbsf

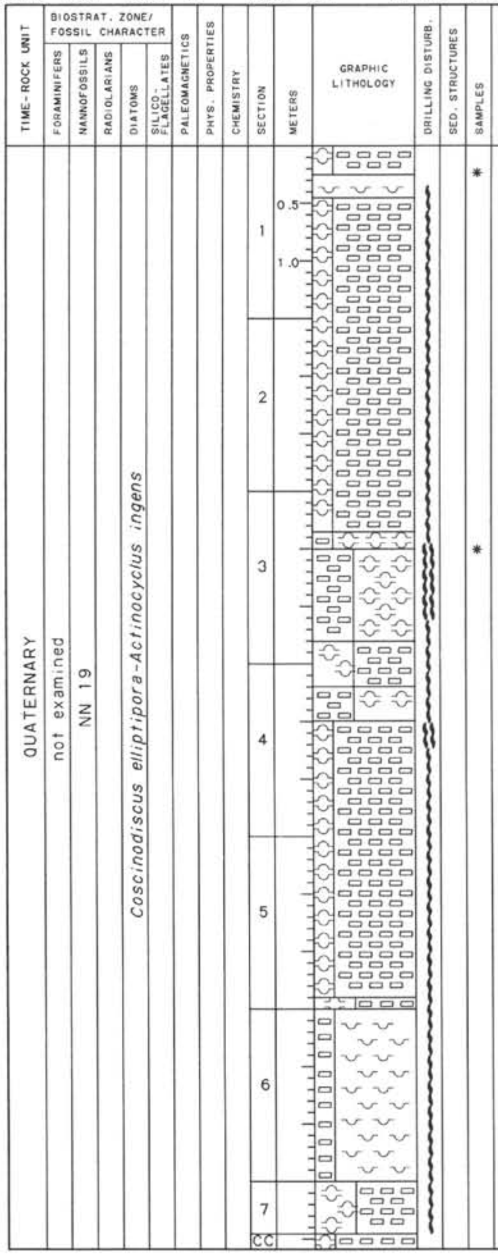

LITHOLOGIC DESCRIPTION

SILICEOUS-BEARING CALCAREOUS OOZE and CALCAREOUS-BEARING SILICEOUS OOZE

Major lithology: Siliceous-bearing calcareous ooze, white (no color code), light gray (5Y 7/2) and pale yellow (5Y 7/3); alternating with calcareous-bearing siliceous ooze, greenish gray (5GY 6/1), olive (5Y 5/4), and light gray (5Y 7/2). Spots of fine dispersed opaques (pyrite?) are common.

Minor lithology: Diatom ooze, olive (5Y 4/3), in Section 1, 27-45 cm. Calcareous siliceous ooze, light olive gray (5Y 6/2) with spots of olive (5Y 5/3) calcareous-bearing siliceous ooze in Section 3, 50-130 cm. Siliceous calcareous ooze, light gray (5Y 7/2) in Section 3, 130-150 cm, Section 4, 0-20 cm; and Section 7, 0-44 cm. Pumice piece (2 cm) in Section 6, 110 cm; disseminated lithic fragments in Section 1, 44, 81, and 94 cm; throughout Section 2; Section 3, 33-130 cm; and Section 6, 140 cm. Minor to moderate bioturbation throughout the core.

SMEAR SLIDE SUMMARY (%):

	1, 30 D	3, 48 M
COMPOSITION:		
Feldspar	Tr	—
Volcanic glass	5	2
Calcite	1	—
Accessory minerals:		
Mn-micronodules	Tr	Tr
Foraminifers	Tr	6
Nannofossils	—	4
Diatoms	93	87
Radiolarians	1	1
Sponge spicules	—	Tr
Silicoflagellates	—	Tr

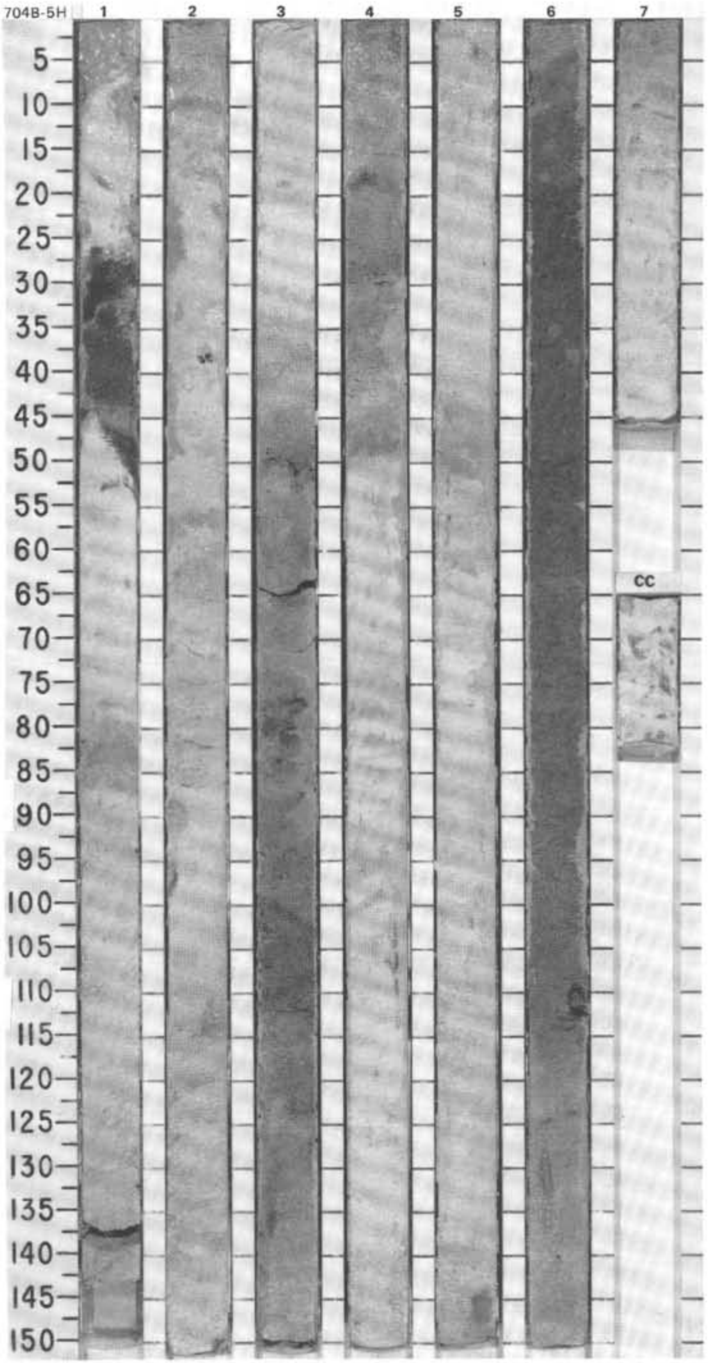

SITE 704 HOLE B CORE 6H CORED INTERVAL 2565.0-2574.5 mbsl; 44.7-54.2 mbsf

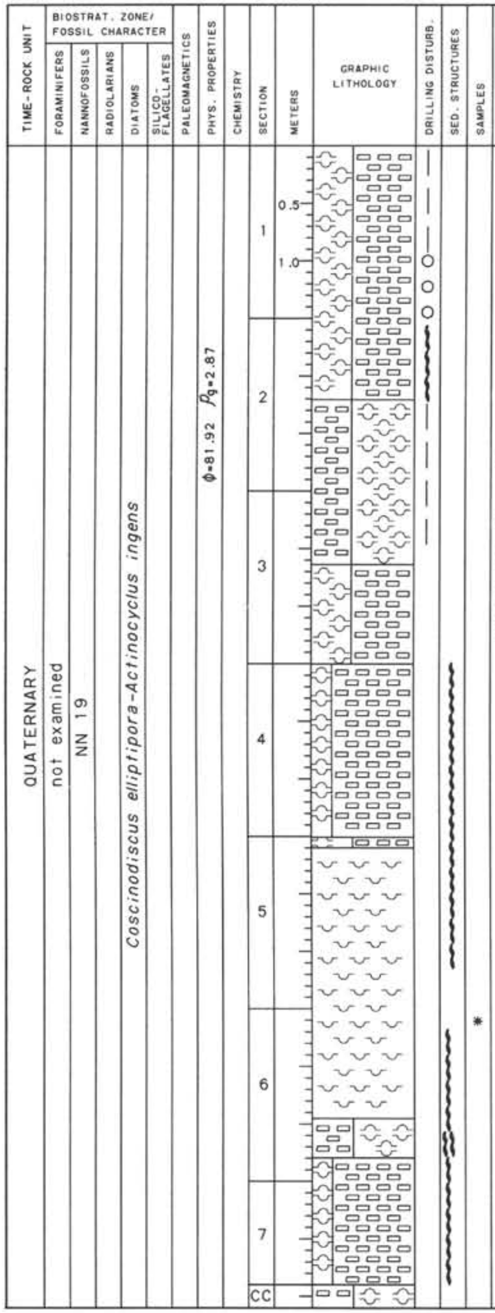

LITHOLOGIC DESCRIPTION

SILICEOUS-BEARING to SILICEOUS CALCAREOUS OOZE and DIATOM OOZE

Drilling disturbance: Moderate in Section 1, 0-85 cm; Section 2, 70-150 cm; Section 3, 0-5 cm. Soupy in Section 1, 90-150 cm.

Major lithologies: Siliceous calcareous ooze to siliceous-bearing calcareous ooze, light olive gray (5Y 6/2), light gray (5Y 7/1), gray (5Y 6/1), and white (no color code). Diatom ooze, olive (5Y 5/4).

Minor lithology: Calcareous siliceous ooze, light gray (5Y 7/2), in Section 2, 70-150 cm; Section 3, 0-66 cm; and Section 6, 94-130 cm. Calcareous-bearing siliceous ooze, light olive gray (5Y 6/2), in Section 7, 70-87 cm. Opaque (pyrite?) staining is common in Section 3, 137-142 cm; Section 4, with concentric rings at 55-70 cm; and Section 7, 0-90 cm. Minor bioturbation in Sections 4-7, causing mottling in the sediment.

SMEAR SLIDE SUMMARY (%):

	6, 10 D
COMPOSITION:	
Volcanic glass	1
Accessory minerals	1
Mn-micronodules	Tr
Diatoms	98
Radiolarians	Tr
Silicoflagellates	Tr

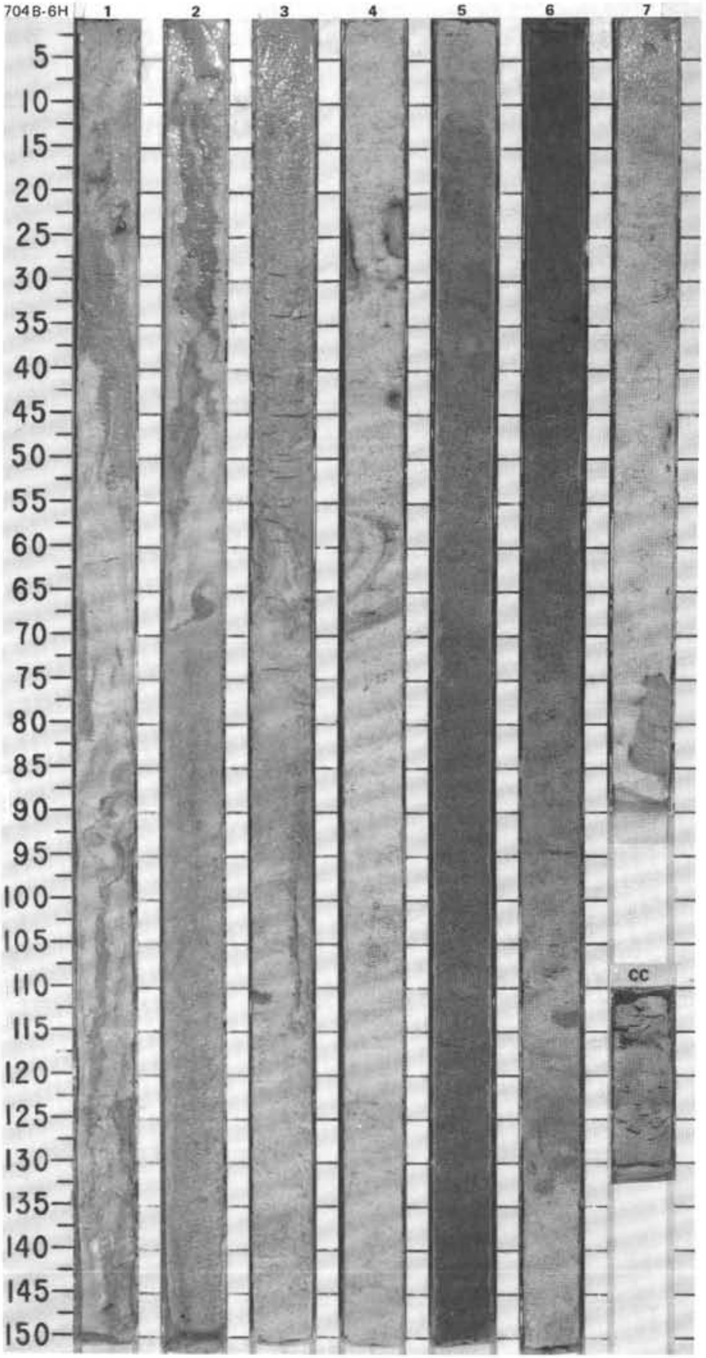

SITE 704 HOLE B CORE 7H CORED INTERVAL 2574.5-2584.0 mbsl; 54.2-63.7 mbsf

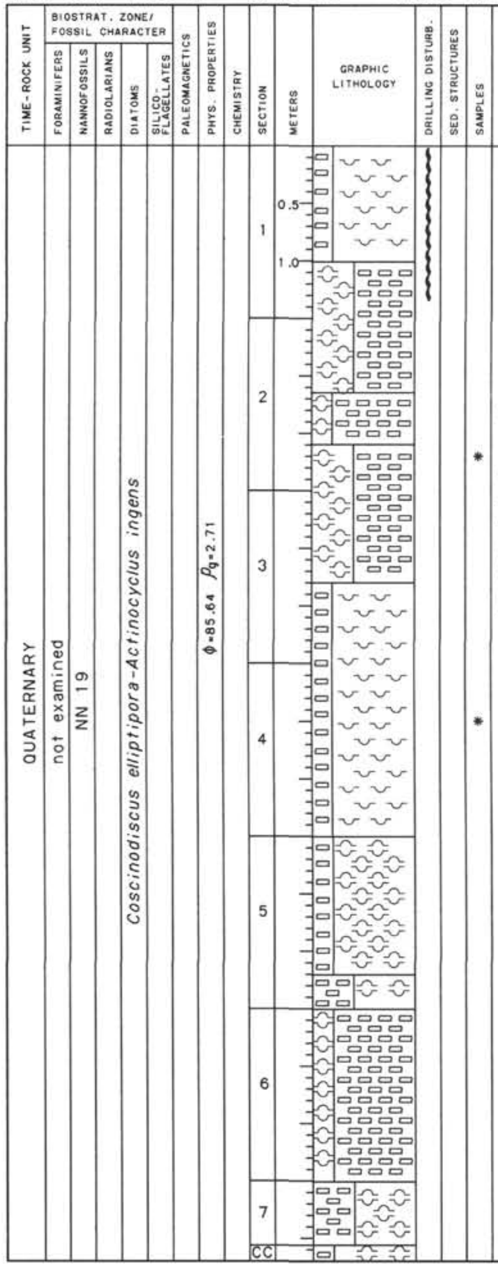

LITHOLOGIC DESCRIPTION

CALCAREOUS-BEARING DIATOM OOZE, CALCAREOUS-BEARING SILICEOUS OOZE, and SILICEOUS CALCAREOUS OOZE

Drilling disturbance: Very disturbed throughout Section 1.

Major lithology: Calcareous-bearing diatom ooze, light olive gray (5Y 6/2) and light yellowish brown (10YR 6/3). Calcareous-bearing siliceous ooze, light olive gray (5Y 6/2) to light olive brown (2.5Y 5/4). Siliceous calcareous ooze, white (5Y 8/1).

Minor lithology: Siliceous-bearing calcareous ooze, white (no color code) to light gray (5Y 7/1), in Section 2, 64-110 cm, and Section 6, 0-150 cm. Opaque staining in Section 2, 64-150 cm. All color changes are gradational.

SMEAR SLIDE SUMMARY (%):

	2, 126 D	4, 50 D
COMPOSITION:		
Volcanic glass	Tr	—
Accessory minerals:		
Mn-micronodules	Tr	—
Foraminifers	20	10
Nannofossils	40	10
Diatoms	39	79
Radiolarians	1	1
Silicoflagellates	Tr	Tr

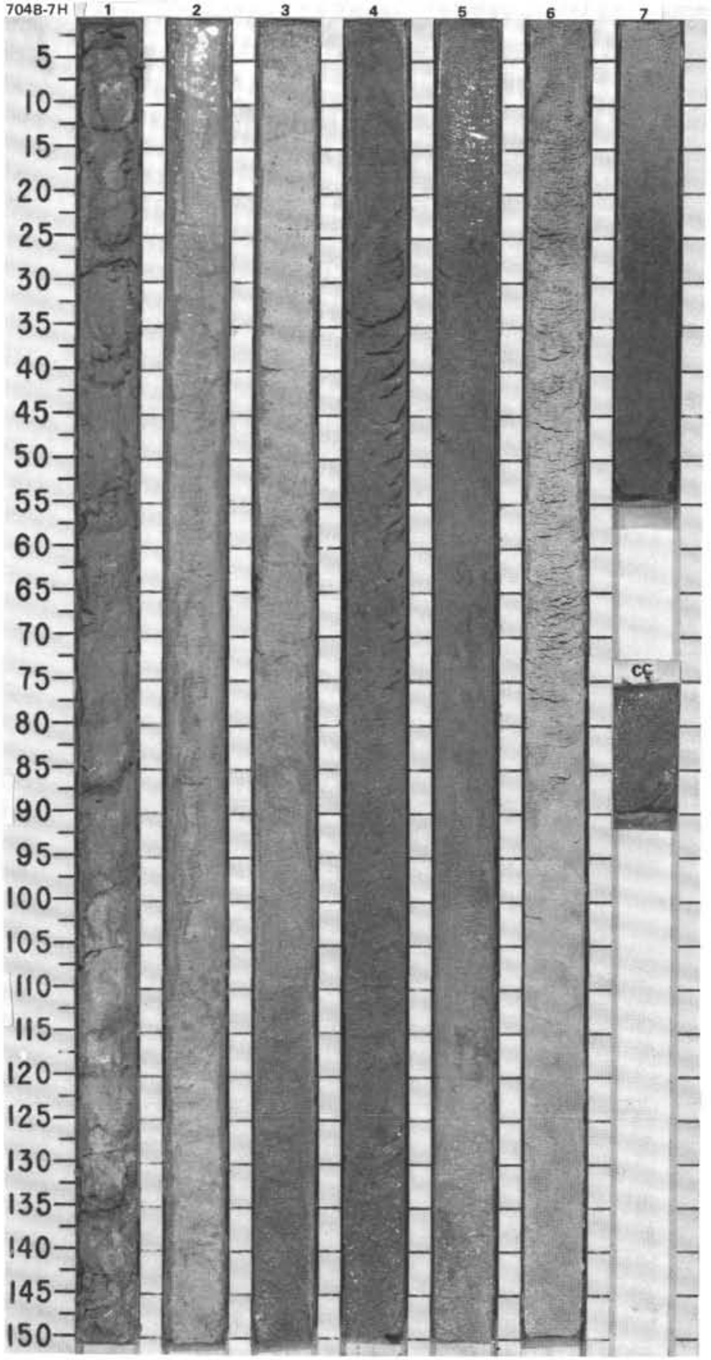

SITE 704 HOLE B CORE 8H CORED INTERVAL 2584.0-2593.5 mbsl; 63.7-73.2 mbsf

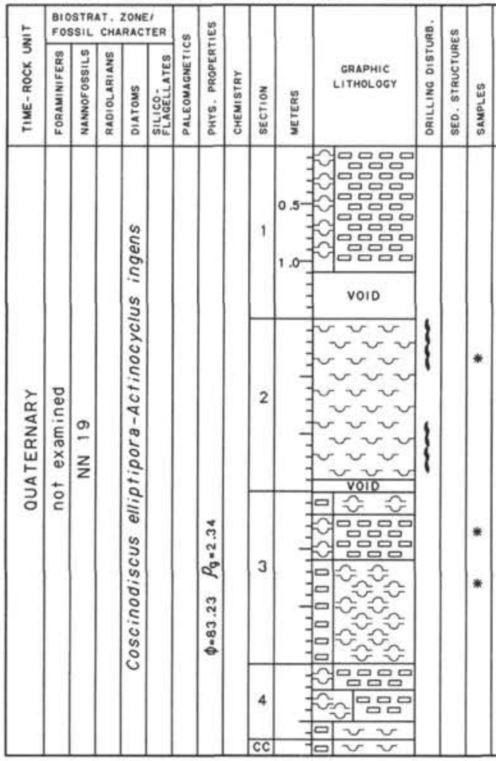

LITHOLOGIC DESCRIPTION

SILICEOUS-BEARING CALCAREOUS OOZE and DIATOM OOZE

Drilling disturbance: Very disturbed in Section 2, 0-50 and 80-140 cm.

Major lithology: Siliceous-bearing calcareous ooze, white (no color code), stained by fine dispersed opaques (pyrite?). Diatom ooze, dark yellowish brown (10YR 4/4) and light yellowish brown (10YR 6/4) to pale brown (10YR 6/3).

Minor lithology: Calcareous-bearing siliceous ooze, light yellowish brown (10YR 6/4) and very pale brown (10YR 7/3) in Section 3, 0-18 and 58-125 cm; Section 4, 0-26 cm (stained by disseminated opaque minerals); and in CC.

SMEAR SLIDE SUMMARY (%):

	2, 35 M	3, 35 D	3, 80 D
COMPOSITION:			
Volcanic glass	—	—	Tr
Accessory minerals:			
Opaques	Tr	—	—
Fragmented carbonate	8	—	15
Mn-micronodules	—	Tr	—
Foraminifers	—	25	1
Nannofossils	Tr	60	Tr
Diatoms	87	15	79
Radiolarians	3	—	3
Sponge spicules	1	—	1
Silicoflagellates	1	Tr	1

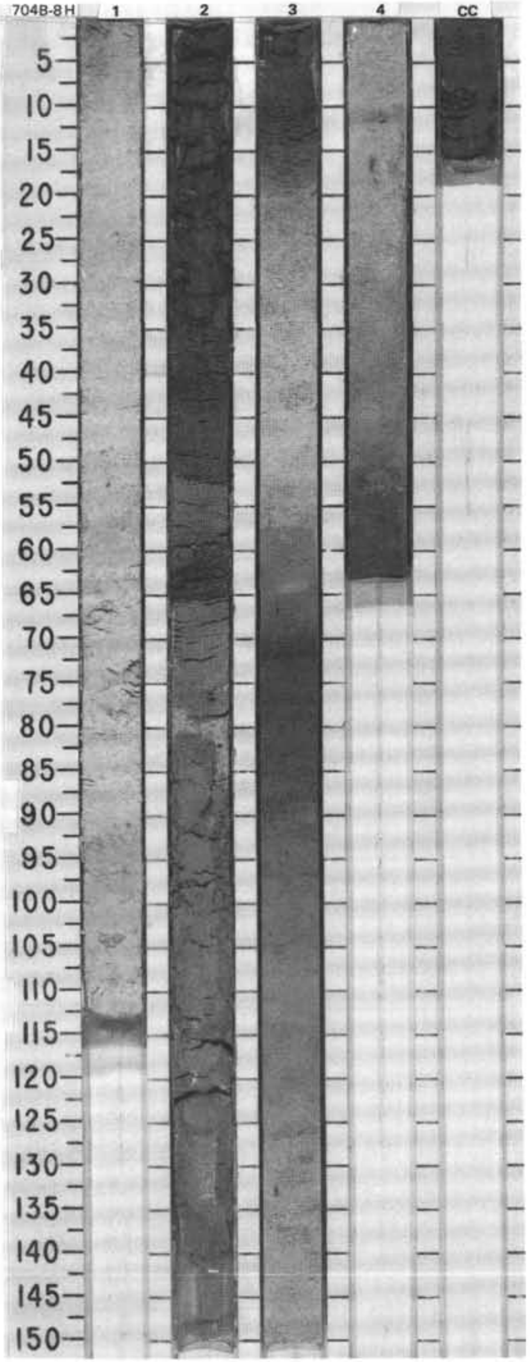

SITE 704 HOLE B CORE 9H CORED INTERVAL 2593.5-2603.0 mbsl; 73.2-82.7 mbsf

TIME-ROCK UNIT	BIOSTRAT. ZONE/ FOSSIL CHARACTER					PALEOMAGNETICS	PHYS. PROPERTIES	CHEMISTRY
	FORAMINIFERS	NANNOFOSSILS	RADIOLARIANS	DIATOMS	SILICO-FLAGELLATES			
QUATERNARY	not examined	NN 19		*Coscinodiscus elliptipora-Actinocyclus ingens*			ϕ=84.24 ρ_g=2.63	

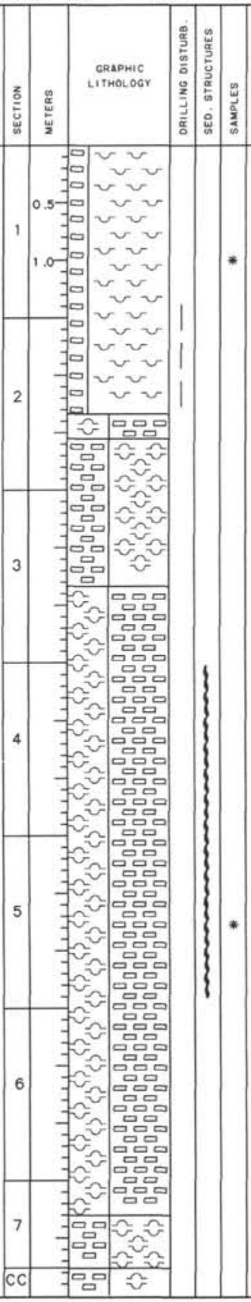

LITHOLOGIC DESCRIPTION

SILICEOUS CALCAREOUS OOZE and CALCAREOUS SILICEOUS OOZE

Drilling disturbance: Slightly in Section 2, 0-85 cm.

Major lithology: Siliceous calcareous ooze, white (no color code to 10YR 8/1)) to light gray (10YR 7/1) with common opaque staining, gray (N4/). Calcareous siliceous ooze, light olive gray (5Y 6/2) and pale olive (5Y 6/3).

Minor lithology: Calcareous-bearing diatom ooze, olive (5Y 5/4).

Minor bioturbation in Sections 4 and 5, causing mottling in the sediment.

SMEAR SLIDE SUMMARY (%):

	1, 100 D	5, 77 D
COMPOSITION:		
Volcanic glass	1	—
Calcite	2	—
Accessory minerals:		
Mn-micronodules	Tr	—
Foraminifers	5	15
Nannofossils	10	50
Diatoms	81	34
Radiolarians	1	—
Silicoflagellates	Tr	1

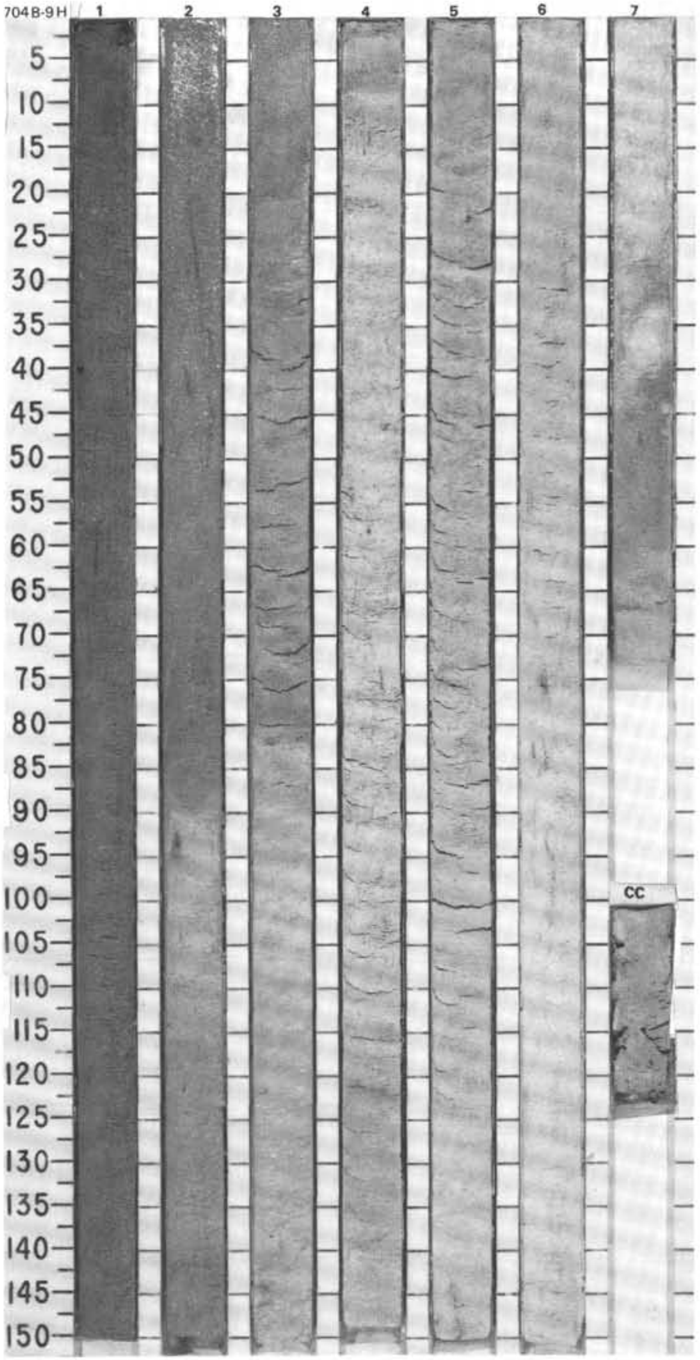

SITE 704 HOLE B CORE 10H CORED INTERVAL 2603.0-2612.5 mbsl; 82.7-92.2 mbsf

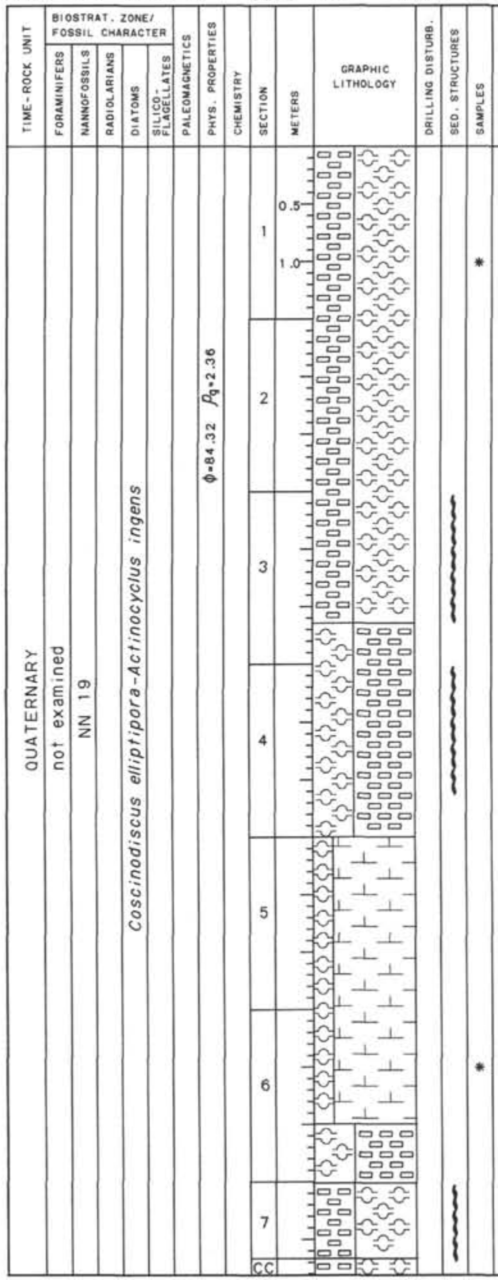

LITHOLOGIC DESCRIPTION

CALCAREOUS SILICEOUS OOZE and SILICEOUS CALCAREOUS OOZE

Major lithology: Calcareous siliceous ooze, olive (5Y 5/4) and pale olive (5Y 6/3) to light gray (5Y 7/2). Siliceous calcareous ooze, pale olive (5Y 6/3) to pale yellow (5Y 7/3).

Minor lithology: Siliceous-bearing nannofossil ooze, white (no color code), Section 5 and Section 6, 0-100 cm. Opaques (pyrite?) occur in Section 7, 17 cm.

Minor bioturbation, causing mottling.

SMEAR SLIDE SUMMARY (%):

	1, 100 D	6, 50 D
COMPOSITION:		
Volcanic glass	Tr	Tr
Accessory minerals:		
Fragmented carbonate	30	3
Foraminifers	2	2
Nannofossils	—	71
Diatoms	62	20
Radiolarians	2	—
Silicoflagellates	4	—
Calcispheres	4	—

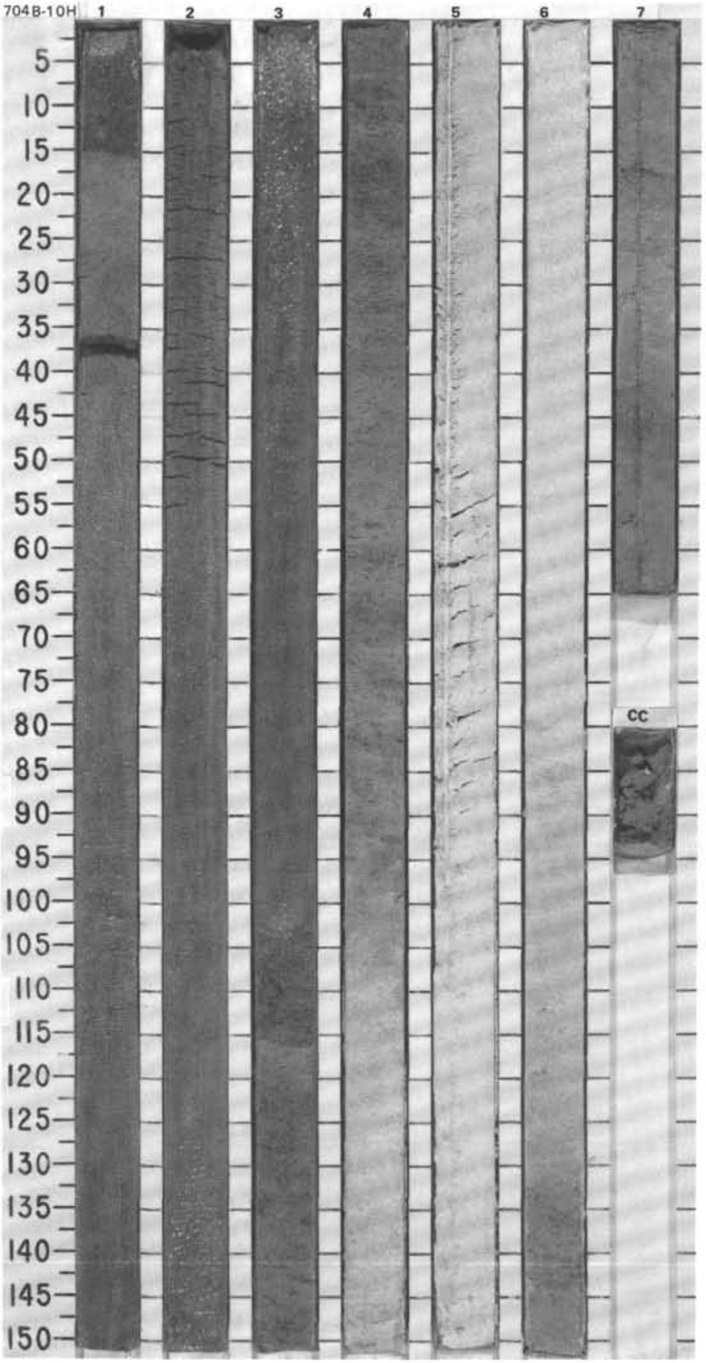

SITE 704 HOLE B CORE 11H CORED INTERVAL 2612.5-2622.0 mbsl; 92.2-101.7 mbsf

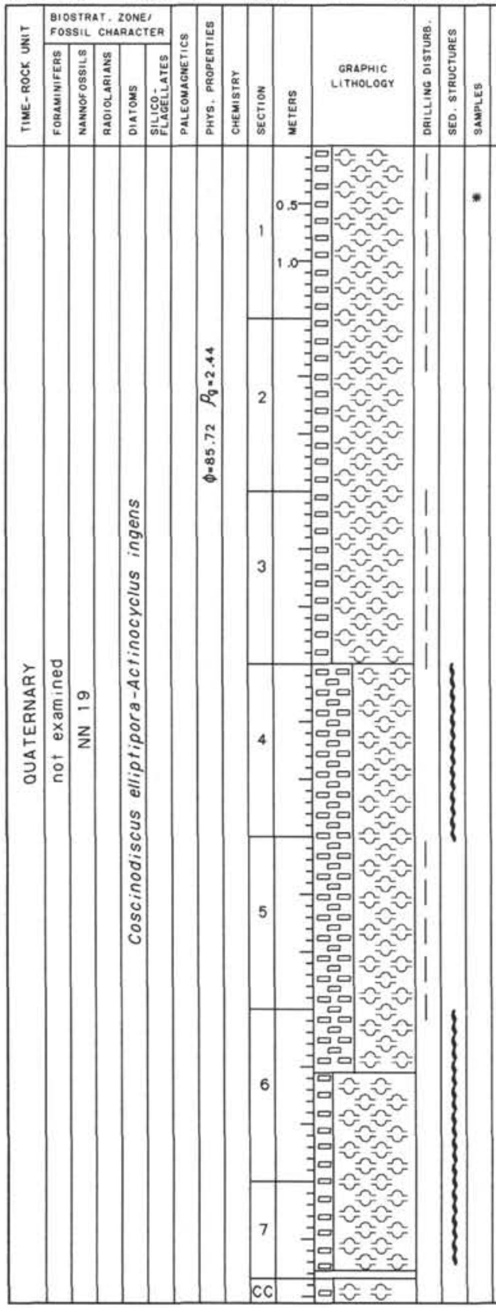

LITHOLOGIC DESCRIPTION

CALCAREOUS-BEARING OOZE to CALCAREOUS SILICEOUS OOZE

Drilling disturbance: Slight in Section 1, Section 2, 0-60 cm, Section 3, and Section 5.

Major lithology: Calcareous-bearing ooze to calcareous siliceous ooze, light yellowish brown (2.5Y 6/4) and pale olive (5Y 6/3) to light gray (5Y 7/2). Lithic fragments (ice-rafted debris) in Section 1, 7, 115, and 122 cm. Spots of opaque staining in Section 4, 64-150 cm. Minor bioturbation, causing mottling, in Sections 4, 6, and 7.

SMEAR SLIDE SUMMARY (%):

	1, 50 D
COMPOSITION:	
Calcite/dolomite fragments	10
Nannofossils	Tr
Diatoms	87
Sponge spicules	1
Silicoflagellates	2

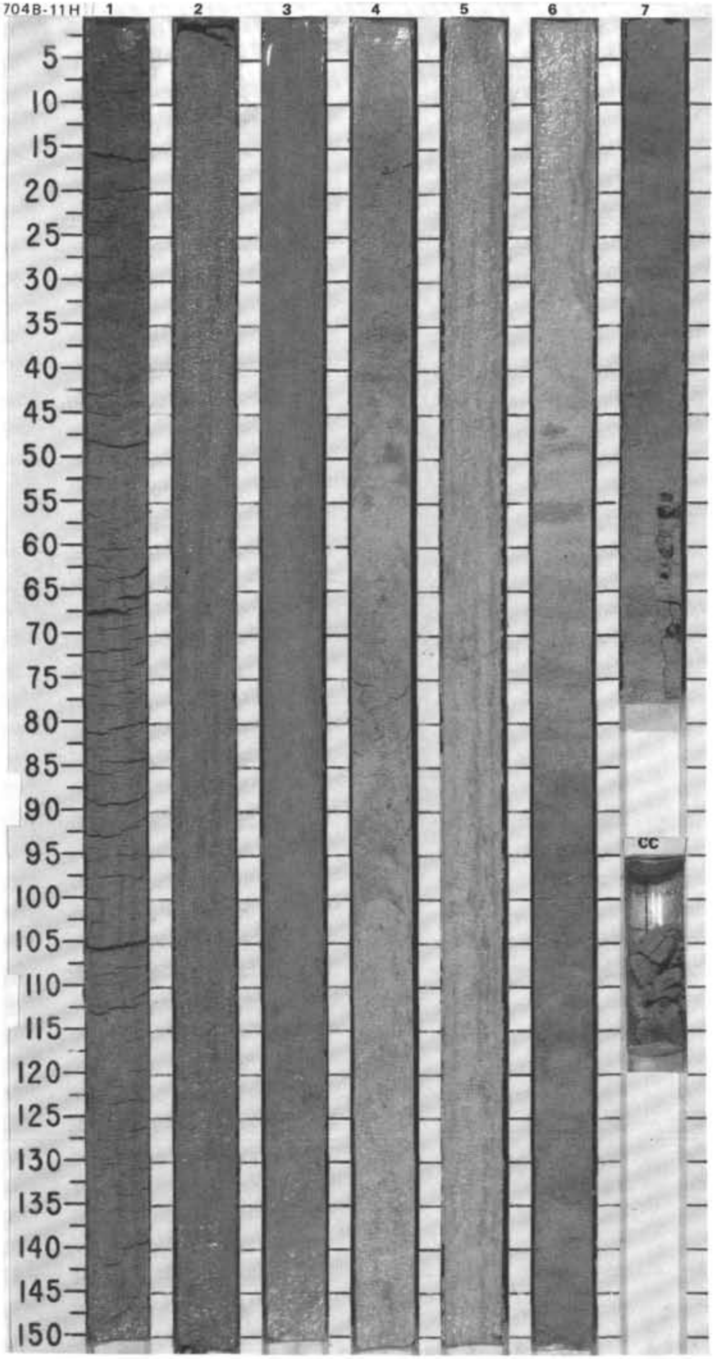

SITE 704 HOLE B CORE 12H CORED INTERVAL 2622.0-2613.5 mbsl; 101.7-111.2 mbsf

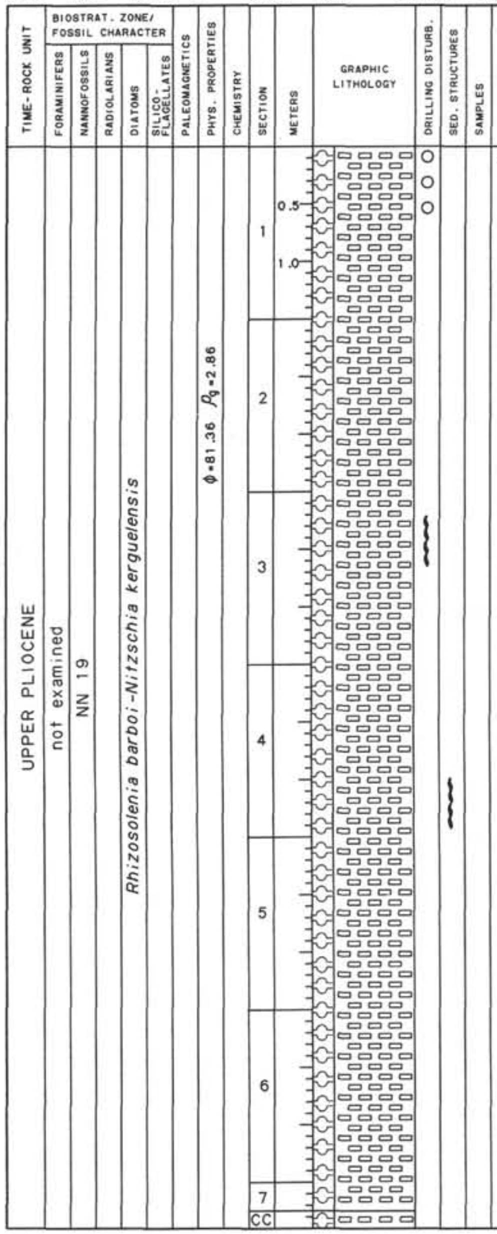

LITHOLOGIC DESCRIPTION

SILICEOUS-BEARING CALCAREOUS OOZE

Drilling disturbance: Soupy, Section 1, 0-40 cm; highly disturbed, in Section 3, 25-49 cm.

Major lithology: Siliceous-bearing calcareous ooze, light gray (5Y 7/1), light olive gray (5Y 6/2), and white (5Y 8/1) to white (no color code). Diatom cotton appears in Section 5, 21-22 cm. Lithic fragments occur disseminated in the soupy ooze, Section 1, 0-28 cm; and in Section 1, 68, 99, and 121-134 cm. Stained color bands by opaques in Section 4, 40-50 cm; and Section 6, 15, 22, 43, and 114 cm.

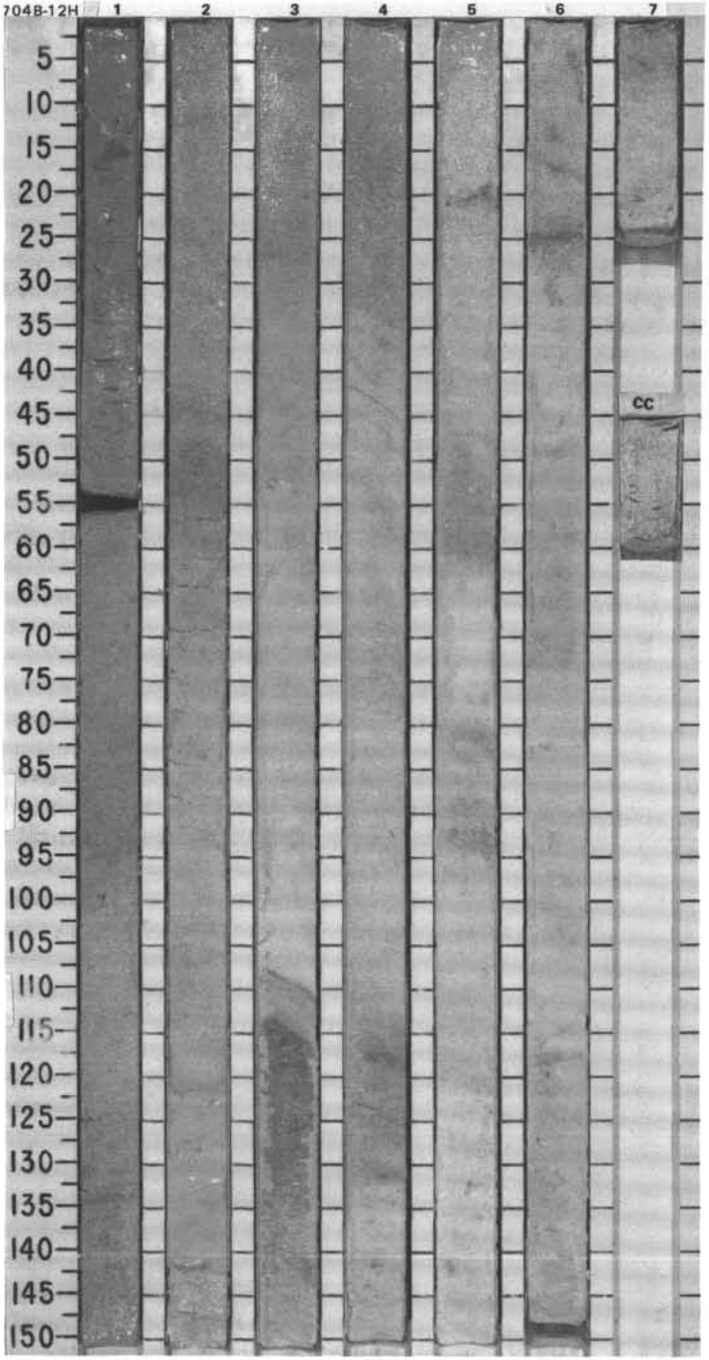

SITE 704 HOLE B CORE 13H CORED INTERVAL 2631.5-2641.0 mbsl; 111.2-120.7 mbsf

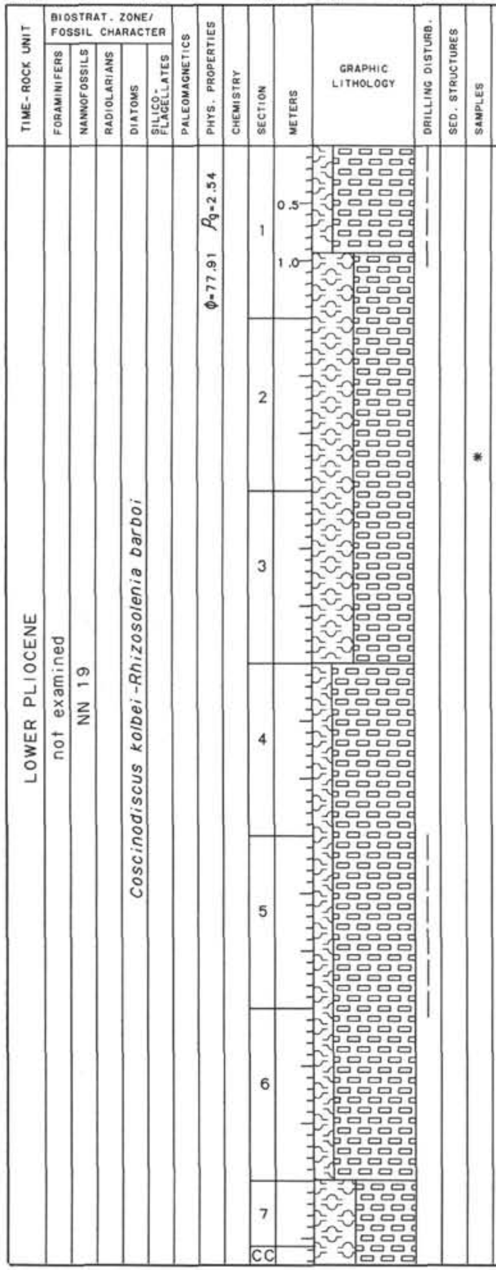

LITHOLOGIC DESCRIPTION

SILICEOUS-BEARING OOZE to SILICEOUS CALCAREOUS OOZE

Drilling disturbance: Moderate in Section 1, 0-95 cm, and Section 5.

Major lithology: Siliceous-bearing calcareous ooze, light gray (5Y 7/1) to white (no color code), and siliceous calcareous ooze, olive gray (5Y 5/2) to white (no color code). Opaques (pyrite?) occur in Section 1, 94 cm, and Section 6, 33-45 cm. Staining due to opaques occurs in Section 1, 10-75 and 94 cm; Section 3, 50-63 and 145 cm; Section 5, 8-80 cm, and Section 6, 70-95 cm.

Small disseminated lithic fragments in Section 2, 90-145 cm.

SMEAR SLIDE SUMMARY (%):

	2, 125 D
COMPOSITION:	
Volcanic glass	Tr
Calcite/dolomite fragments	10
Foraminifers	3
Diatoms	79
Radiolarians	3
Sponge spicules	2
Silicoflagellates	3

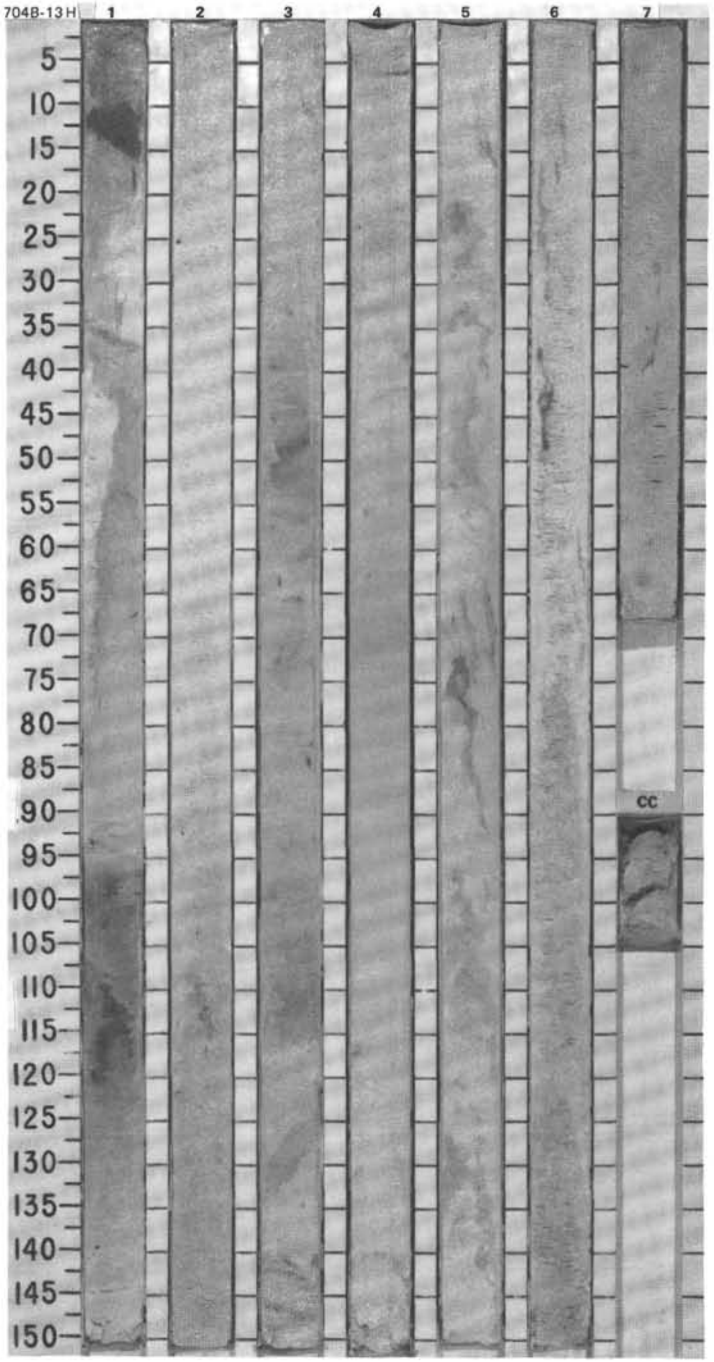

SITE 704 HOLE B CORE 14H CORED INTERVAL 2641.0-2650.5 mbsl; 120.7-130.2 mbsf

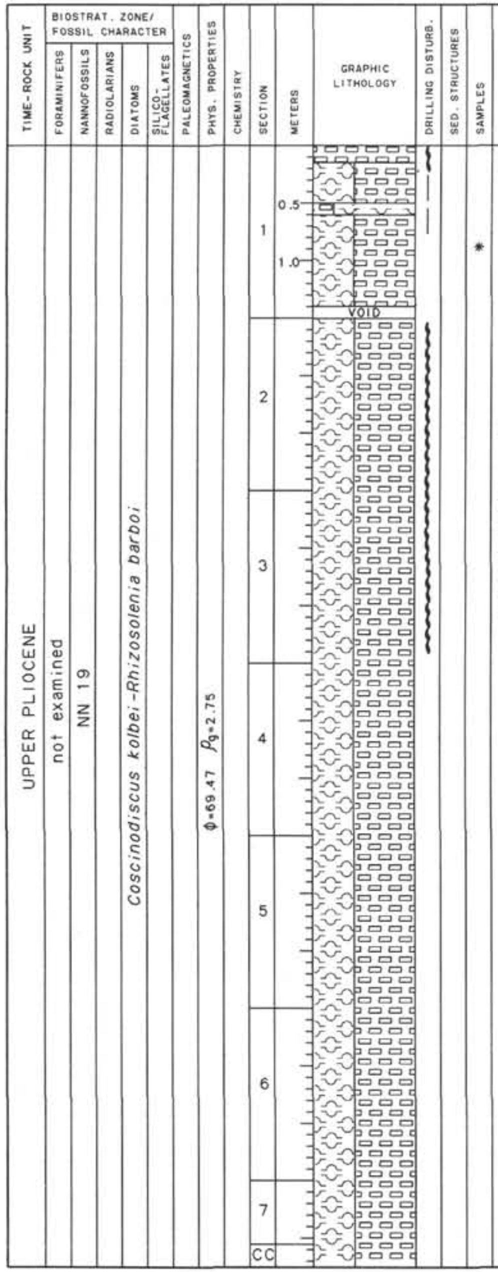

LITHOLOGIC DESCRIPTION

SILICEOUS CALCAREOUS OOZE

Drilling disturbance: Highly disturbed in Section 1, 0-35 cm; throughout Sections 2 and 3; and slightly disturbed in Section 1, 35-70 cm.

Major lithology: Siliceous calcareous ooze, light gray (5Y 7/1) to white (5Y 8/1 to no color code). Opaques (pyrite?) occur in Section 5, 12-39, 110, and 116-140 cm, and Section 7, 33-40 cm. Staining due to opaques (pyrite?) in Section 3, 87-94, 102-105, 114-120, and 137-139 cm; Section 4, 10-25 cm; and Section 6, 96-123 cm.

Minor lithology: Calcareous ooze, white (no color code), Section 1, 0-15 cm. Calcareous-bearing diatom ooze, olive (5Y 5/4), Section 1, 47-62 cm.

SMEAR SLIDE SUMMARY (%):

	1, 90 D
COMPOSITION:	
Volcanic glass	Tr
Calcite/dolomite fragments	20
Foraminifers	10
Nannofossils	38
Diatoms	39
Radiolarians	2

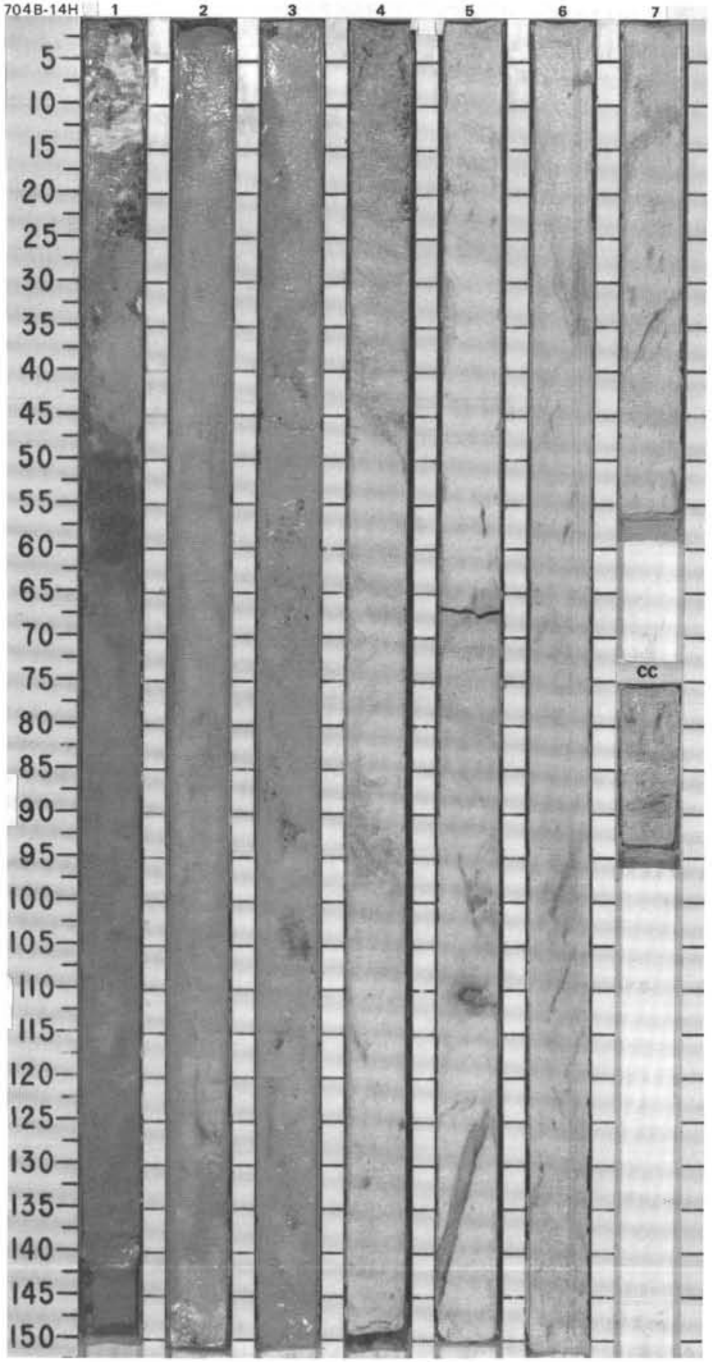

SITE 704 HOLE B CORE 15H CORED INTERVAL 2650.5-2660.0 mbsl; 130.2-139.7 mbsf

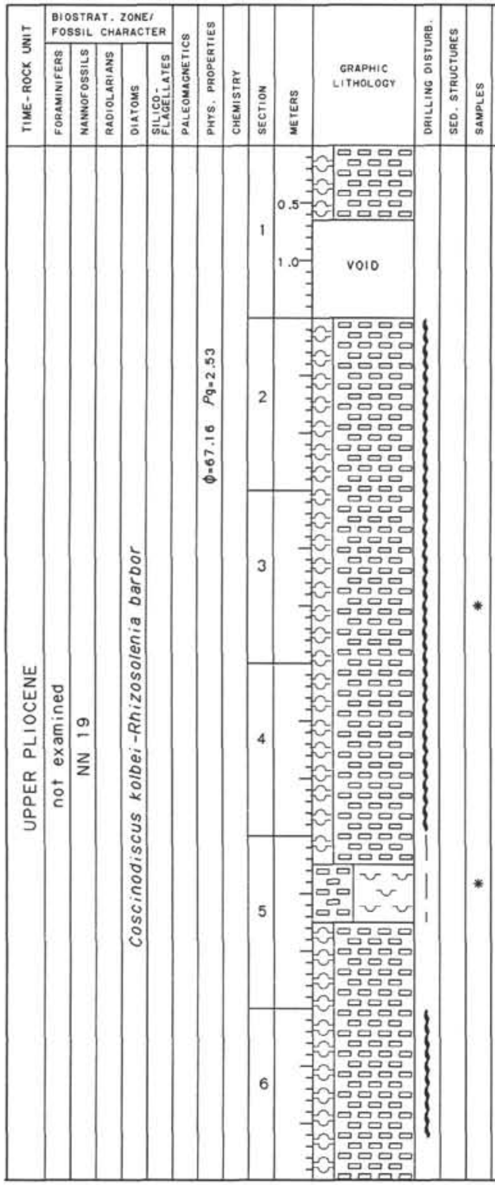

LITHOLOGIC DESCRIPTION

SILICEOUS-BEARING CALCAREOUS OOZE

Drilling disturbance: Highly disturbed in Sections 2-4 and Section 6, 0-95 cm. Vertical color banding due to flow in. Moderate disturbance in Section 5, 0-70 cm.

Major lithology: Siliceous-bearing calcareous ooze, white (5Y 8/1 to no code) to light gray (5Y 7/1). Opaque (pyrite?) spots in Section 1, 27 and 33 cm. Vertical dark discoloration in Section 4.

Minor lithology: Calcareous diatom ooze, olive (5Y 5/3), in Section 5, 25-75 cm.

Faint mottling due to bioturbation in Sections 7 and 8. *Planolites* occurs in Section 8. The burrows are light gray (5Y 7/1) to gray (N6).

SMEAR SLIDE SUMMARY (%):

	3, 100 D	5, 40 M
COMPOSITION:		
Volcanic glass	Tr	Tr
Calcite fragments	1	30
Foraminifers	10	2
Nannofossils	69	Tr
Diatoms	20	64
Radiolarians	—	4

Continued.

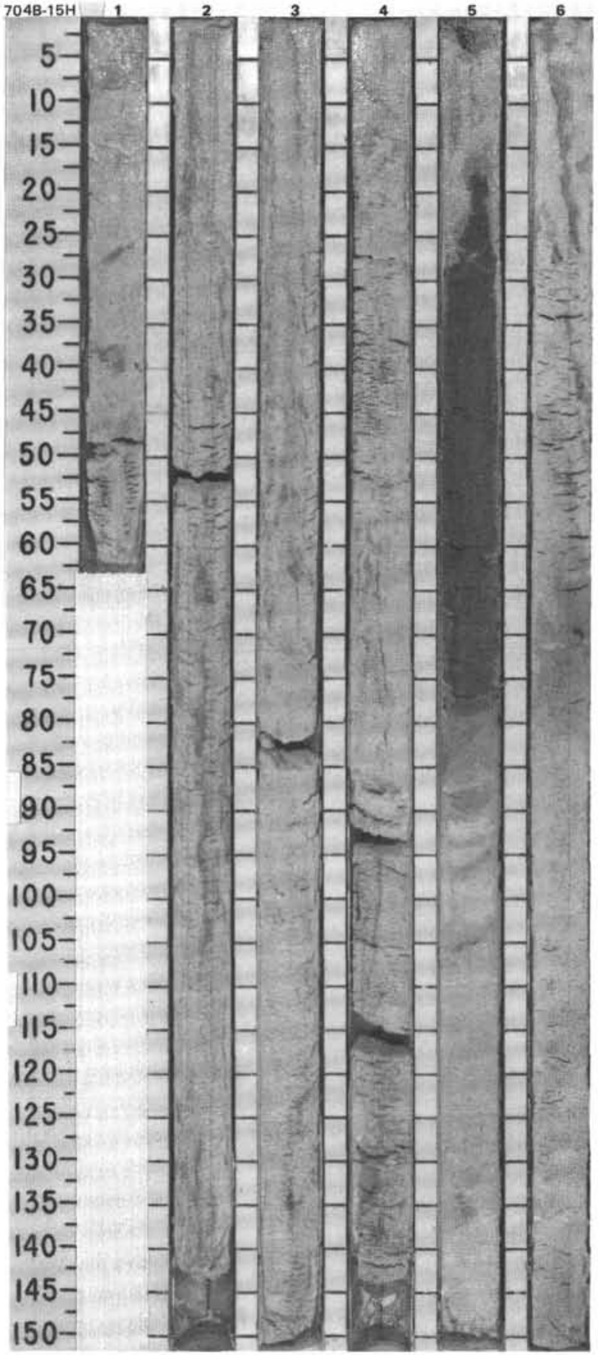

SITE 704 HOLE B CORE 15H CORED INTERVAL 2650.5-2660.0 mbsl; 130.2-139.7 mbsf

TIME-ROCK UNIT	BIOSTRAT. ZONE/ FOSSIL CHARACTER				PALEOMAGNETICS	PHYS. PROPERTIES	CHEMISTRY	SECTION	METERS	GRAPHIC LITHOLOGY	DRILLING DISTURB.	SED. STRUCTURES	SAMPLES	LITHOLOGIC DESCRIPTION
	FORAMINIFERS	NANNOFOSSILS	RADIOLARIANS	DIATOMS										
								7	0.5 1.0	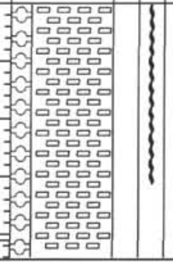				Continued.
								8						
								CC						

SITE 704 HOLE B CORE 16X CORED INTERVAL 2660.0-2667.5 mbsl; 139.7-147.2 mbsf

TIME-ROCK UNIT	BIOSTRAT. ZONE/ FOSSIL CHARACTER					PALEOMAGNETICS	PHYS. PROPERTIES	CHEMISTRY	SECTION	METERS	GRAPHIC LITHOLOGY	DRILLING DISTURB.	SED. STRUCTURES	SAMPLES	LITHOLOGIC DESCRIPTION
	FORAMINIFERS	NANNOFOSSILS	RADIOLARIANS	DIATOMS	SILICO-FLAGELLATES										
UPPER PLIOCENE	not examined	NN 19		*Coscinodiscus kolbei-Rhizosolenia barboi*					CC						SILICEOUS CALCAREOUS OOZE Major lithology: Siliceous calcareous ooze, light gray (5Y 7/1). Minor lithology: Granodiorite pebbles.

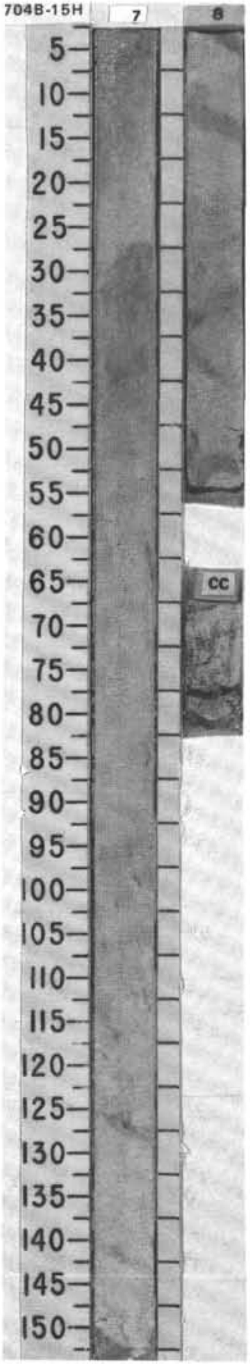

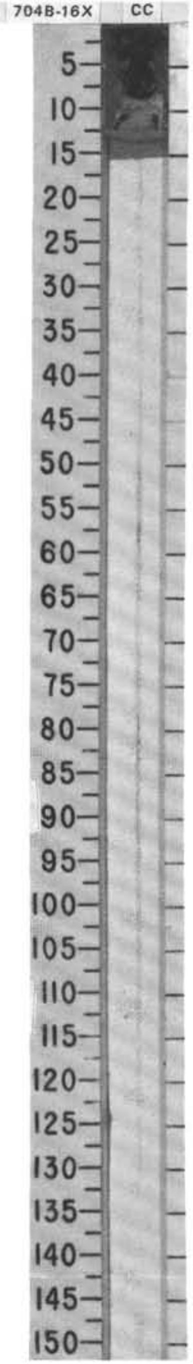

SITE 704 HOLE B CORE 17X CORED INTERVAL 2667.5-2677.0 mbsl; 147.2-156.7 mbsf

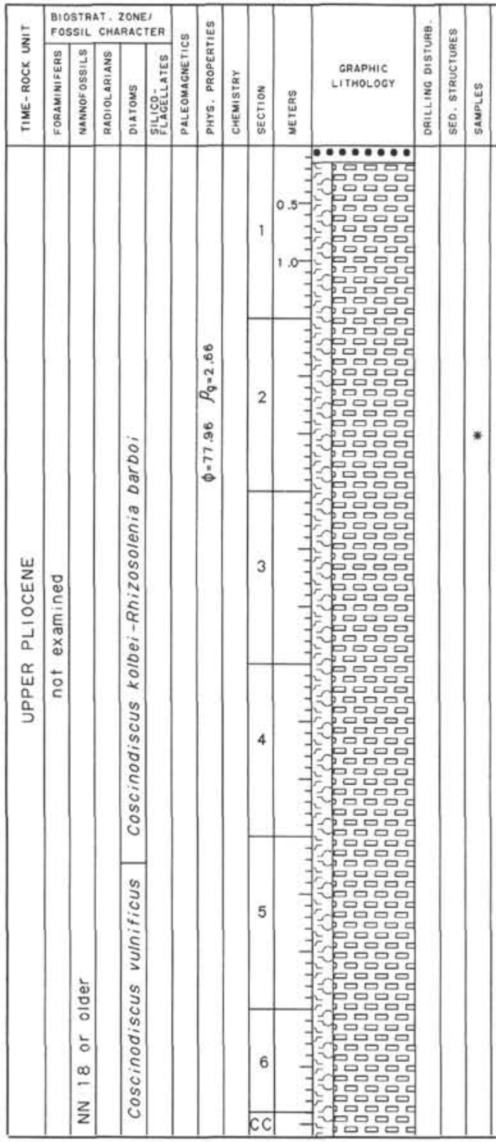

LITHOLOGIC DESCRIPTION

SILICEOUS-BEARING CALCAREOUS OOZE

Major lithology: Siliceous-bearing calcareous ooze, light gray (5Y 7/1) to white (no color code). Disseminated lithic fragments throughout Sections 2-4. Larger pebble occurs in Section 4, 102 cm. Opaque horizons in Section 5, 106-150 cm, and Section 6, 0-4 cm.

Minor lithology: Pebbles (downhole contamination) in Section 1, 0-17 cm.

Minor bioturbation in Section 6.

SMEAR SLIDE SUMMARY (%):

	2, 100 D
COMPOSITION:	
Accessory minerals:	
Opaques	Tr
Foraminifers	5
Nannofossils, broken	70
Diatoms	20
Radiolarians	3
Silicoflagellates	2

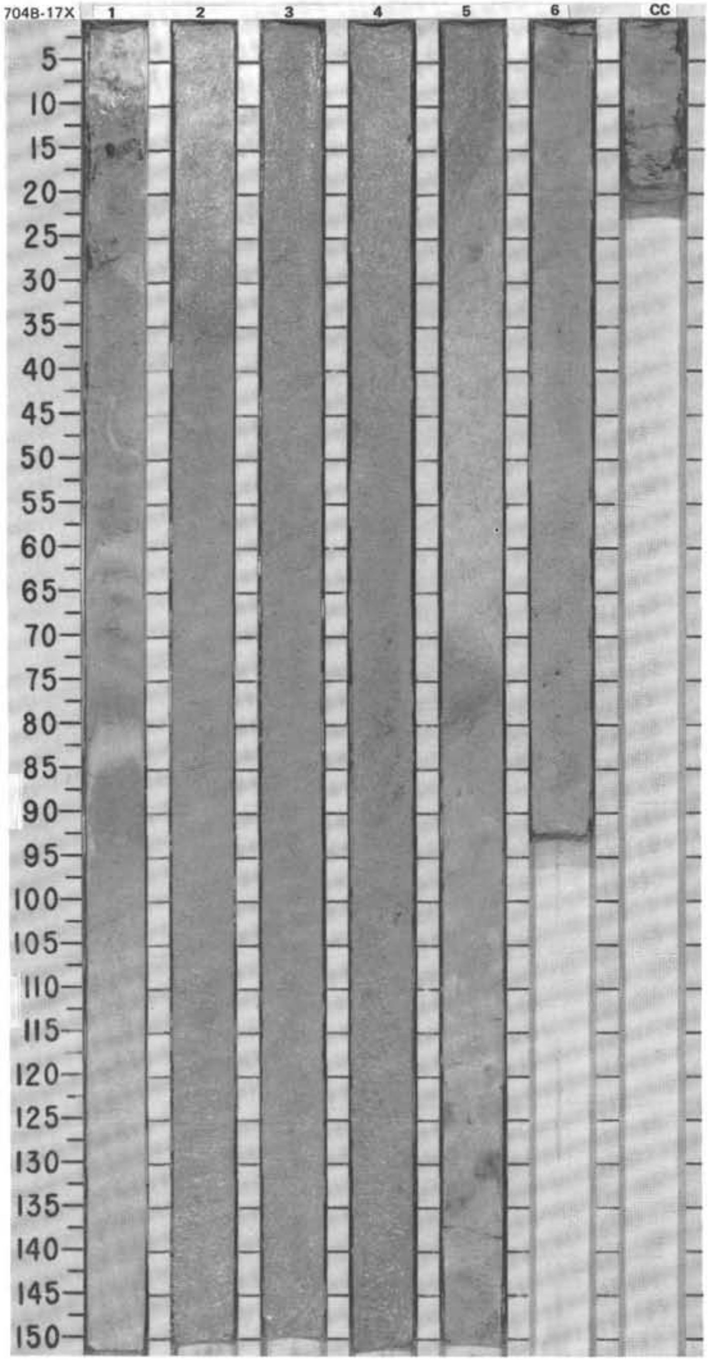

SITE 704 HOLE B CORE 18X CORED INTERVAL 2677.0-2686.5 mbsl; 156.7-166.2 mbsf

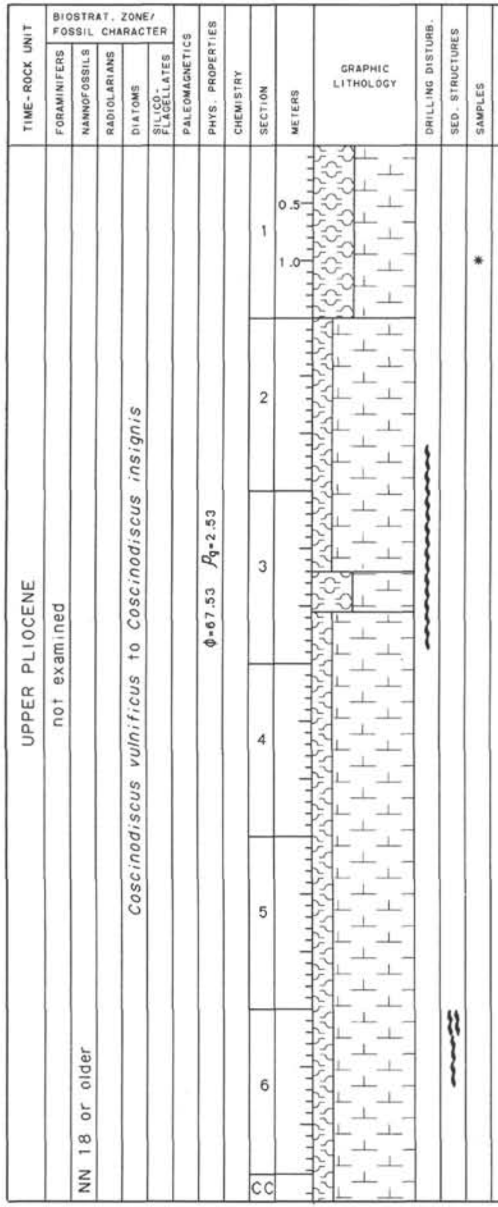

LITHOLOGIC DESCRIPTION

SILICEOUS-BEARING NANNOFOSSIL OOZE

Drilling disturbance: Highly disturbed in Section 2, 110-150 cm, and in Section 3.

Major lithology: Siliceous-bearing nannofossil ooze, white (no color code) to greenish gray (5GY 6/1). Opaque staining in Section 2, 118-150 cm.

Minor lithology: Siliceous nannofossil ooze, light gray (5Y 7/1), throughout Section 1 and in Section 3, 70-105 cm.

Minor to moderate bioturbation in Section 6.

SMEAR SLIDE SUMMARY (%):

	1, 100 D
COMPOSITION:	
Volcanic glass	Tr
Calcite/dolomite fragments	5
Nannofossils	83
Diatoms	10
Radiolarians	2
Sponge spicules	Tr

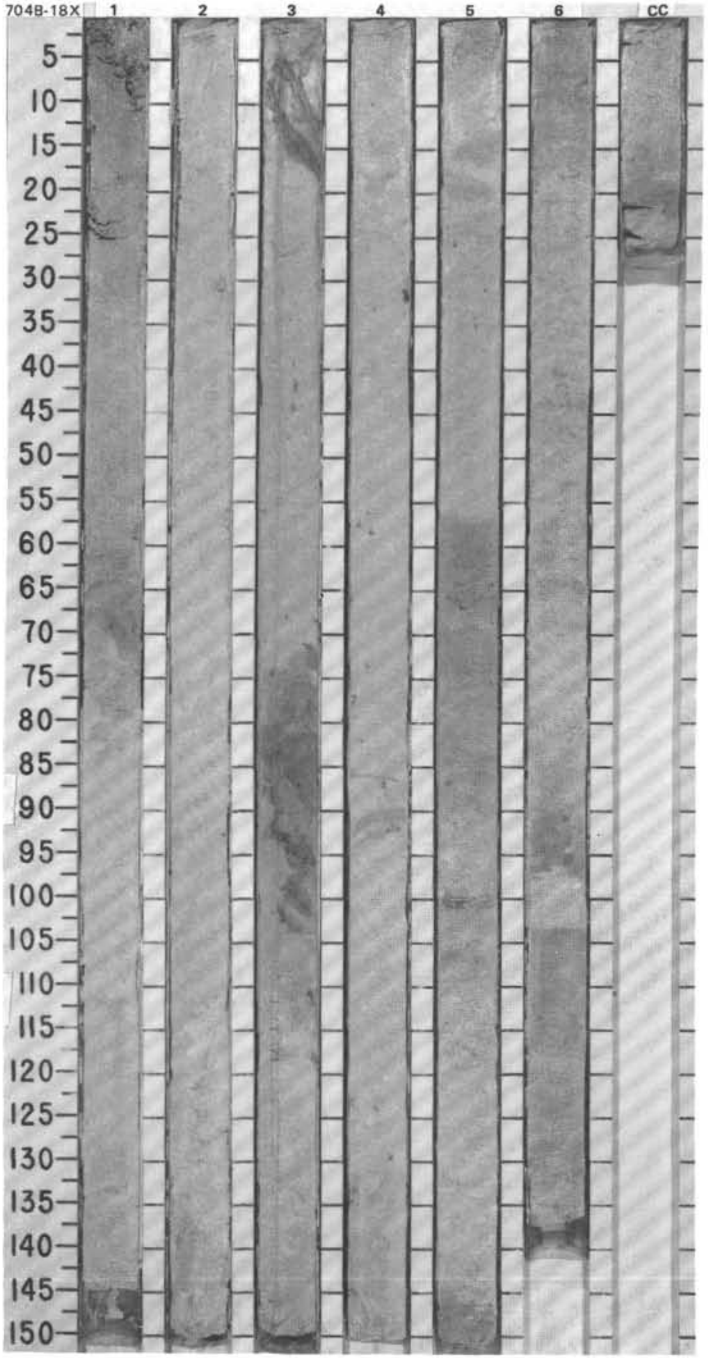

SITE 704 HOLE B CORE 19X CORED INTERVAL 2686.5-2696.0 mbsl; 166.2-175.7 mbsf

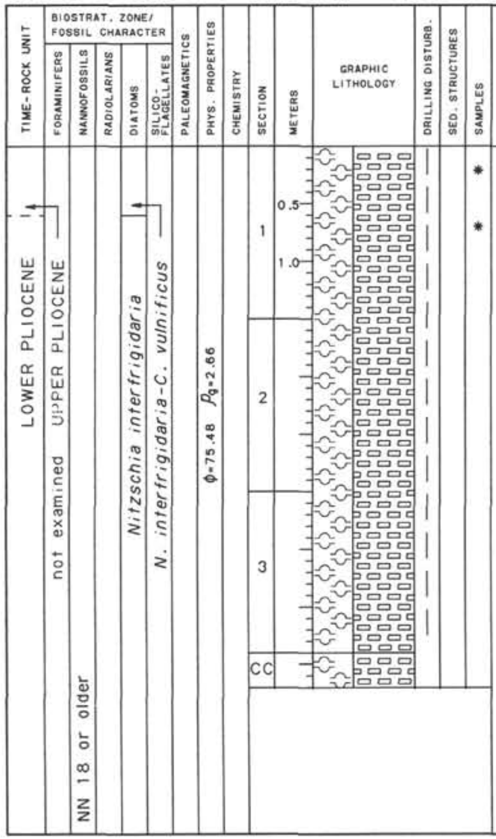

LITHOLOGIC DESCRIPTION

SILICEOUS CALCAREOUS OOZE

Drilling disturbance: Slight throughout the core.

Major lithology: Siliceous calcareous ooze, white (2.5Y 8/1), with some shades of greenish gray (5GY 6/1) in Section 2, 24-39 and 74-94 cm. Lithic fragments (ice-rafted debris) in Section 1, 11-25 cm; ash-bearing horizon, gray (5Y 6/1), in Section 1, between 20-25 cm.

SMEAR SLIDE SUMMARY (%):

	1, 21 M	1, 75 D
COMPOSITION:		
Quartz/feldspar	10	—
Clay	5	—
Volcanic glass	—	1
Micrite	—	15
Accessory minerals	Tr	1
Foraminifers	43	10
Nannofossils	—	47
Diatoms	40	24
Radiolarians	2	1
Sponge spicules	—	1

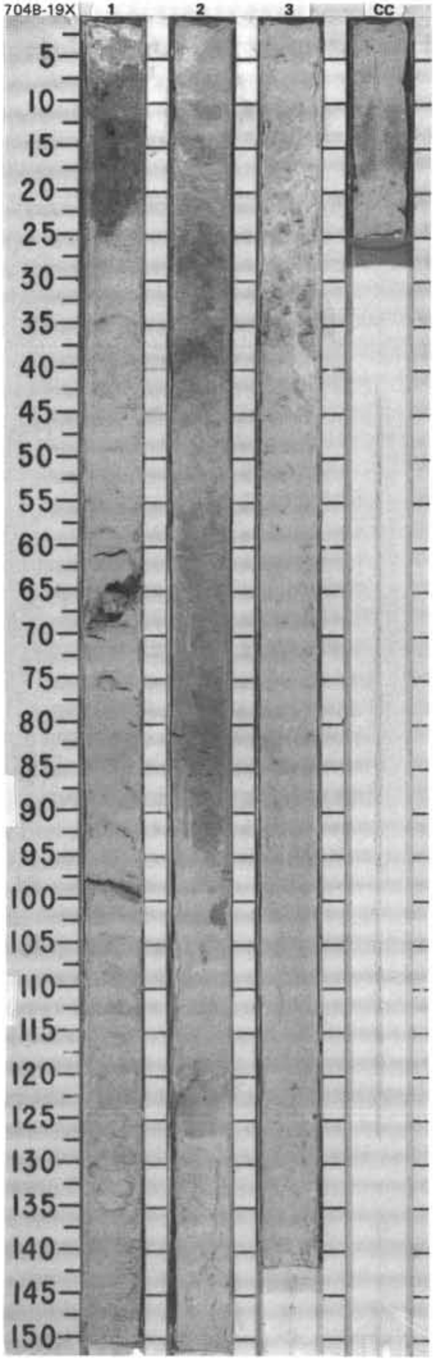

704B-20X NO RECOVERY

704B-21X NO RECOVERY

SITE 704 HOLE B CORE 22X CORED INTERVAL 2715.0-2724.5 mbsl; 194.7-204.2 mbsf

TIME-ROCK UNIT	BIOSTRAT. ZONE/ FOSSIL CHARACTER					PALEOMAGNETICS	PHYS. PROPERTIES	CHEMISTRY	SECTION	METERS	GRAPHIC LITHOLOGY	DRILLING DISTURB.	SED. STRUCTURES	SAMPLES	LITHOLOGIC DESCRIPTION
	FORAMINIFERS	NANNOFOSSILS	RADIOLARIANS	DIATOMS	SILICO-FLAGELLATES										
LOWER PLIOCENE	not examined	NN 11-14		*Nitzschia angulata*			ϕ=69.97 ρ_g=2.68		1 CC	0.5 1.0	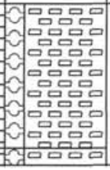				SILICEOUS-BEARING CALCAREOUS OOZE Drilling disturbance: Moderately disturbed. Major lithology: Siliceous-bearing calcareous ooze, white (2.5Y 8/1). Pyrite(?) staining in Section 1, 9-14 cm.

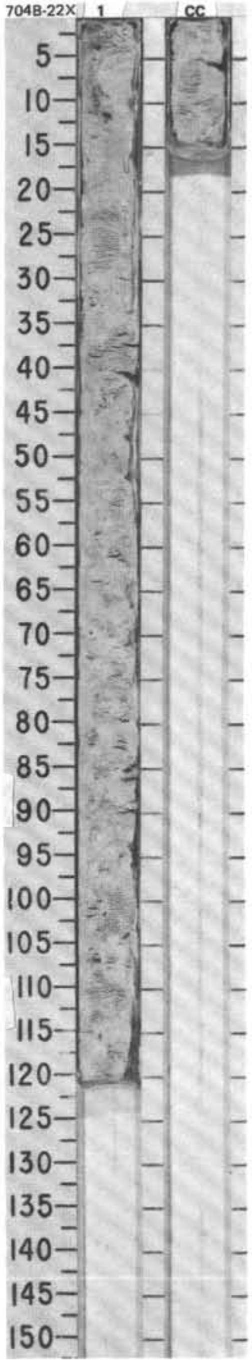

SITE 704 HOLE B CORE 23X CORED INTERVAL 2724.5-2734.0 mbsl; 204.2-213.7 mbsf

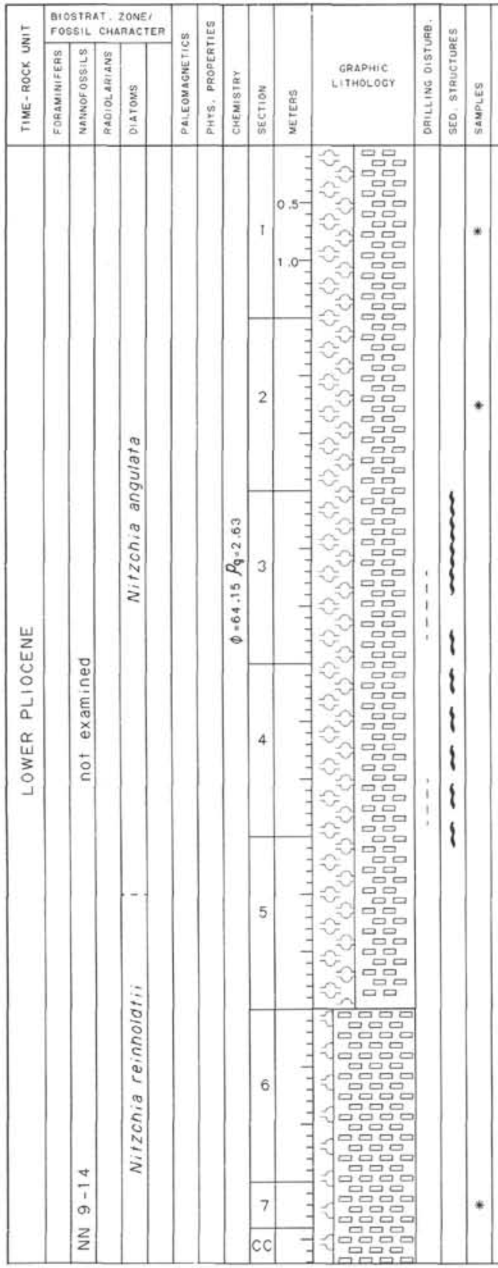

LITHOLOGIC DESCRIPTION

SILICEOUS CALCAREOUS OOZE

Drilling disturbance: Slight in Section 1, 0-10 cm; Section 3, 85-140 cm; and Section 4, 110-150 cm.

Major lithology: Siliceous calcareous ooze, light greenish gray (5GY 7/1); bluish gray (5B 6/1) in Section 2, 40-115 cm, and Section 5, 45-60 and 75 cm.

Minor lithology: Siliceous-bearing calcareous ooze, light greenish gray (5GY 7/1) and light bluish gray (5B 7/1).

Minor bioturbation causes mottling in Sections 3 and 4.

SMEAR SLIDE SUMMARY (%):

	1, 70 D	2, 70 D	7, 20 M
COMPOSITION:			
Feldspar	Tr	Tr	—
Volcanic glass	1	1	—
Micrite	20	20	—
Accessory minerals	Tr	Tr	Tr
Opaques (pyrite?)	—	Tr	—
Foraminifers/ nannofossils	53	53	69
Diatoms	25	25	10
Radiolarians	1	1	1
Sponge spicules	Tr	Tr	Tr
Silicoflagellates	Tr	Tr	Tr

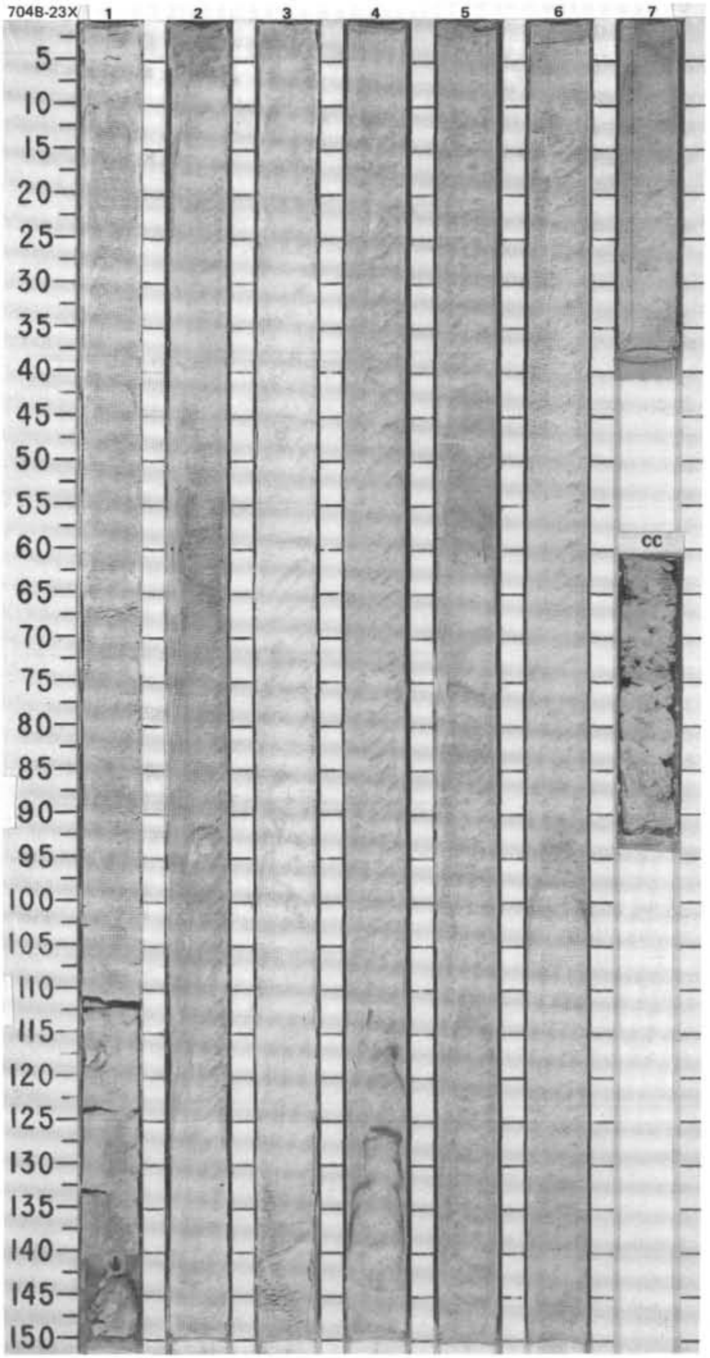

SITE 704 HOLE B CORE 24X CORED INTERVAL 2734.0-2743.5 mbsl; 213.7-223.2 mbsf

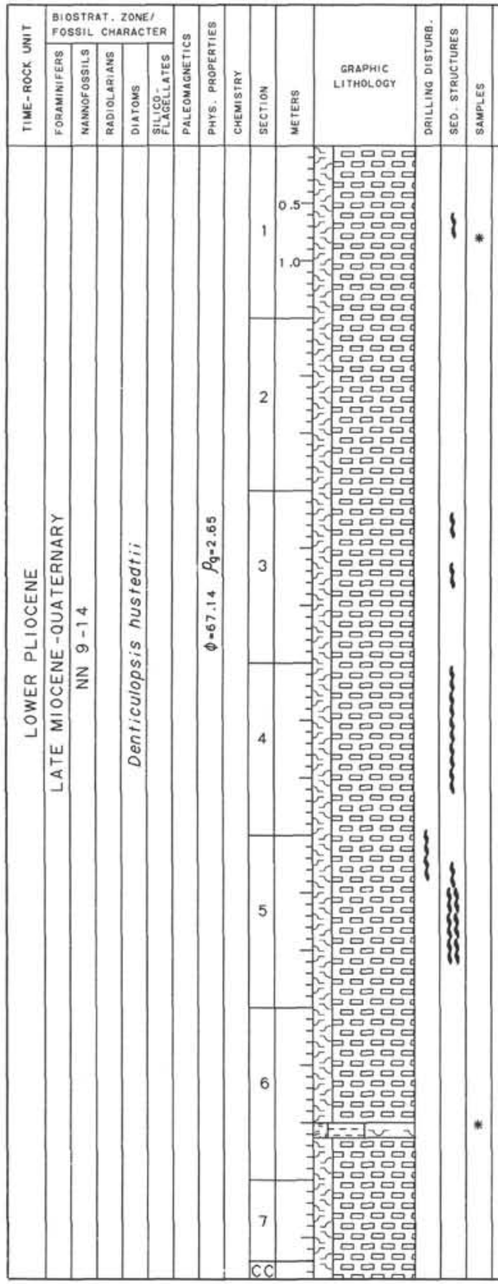

LITHOLOGIC DESCRIPTION

SILICEOUS-BEARING CALCAREOUS OOZE

Drilling disturbance: High in Section 5, 0–25 and 140–150 cm.

Major lithology: Siliceous-bearing calcareous ooze, white (7.5YR 8/1) to light gray (7.5YR 7/1). Light greenish gray (5GY 7/1) to bluish gray (5B 7/1) patches in Section 6.

Minor lithology: Ash-bearing clayey diatom ooze, greenish gray (5GY 6/1) in Section 6, 102–113 cm.

Minor to moderate bioturbation; *Zoophycos* occurs in Section 6, 99 and 105 cm, and *Planolites* in Section 6, 125–133 cm.

SMEAR SLIDE SUMMARY (%):

	1, 75 D	6, 110 M
COMPOSITION:		
Quartz/feldspar	—	20
Clay	—	30
Volcanic glass	1	—
Accessory minerals	Tr	—
Foraminifers/ nannofossils	89	—
Diatoms		45
Radiolarians	10	5
Silicoflagellates	Tr	—

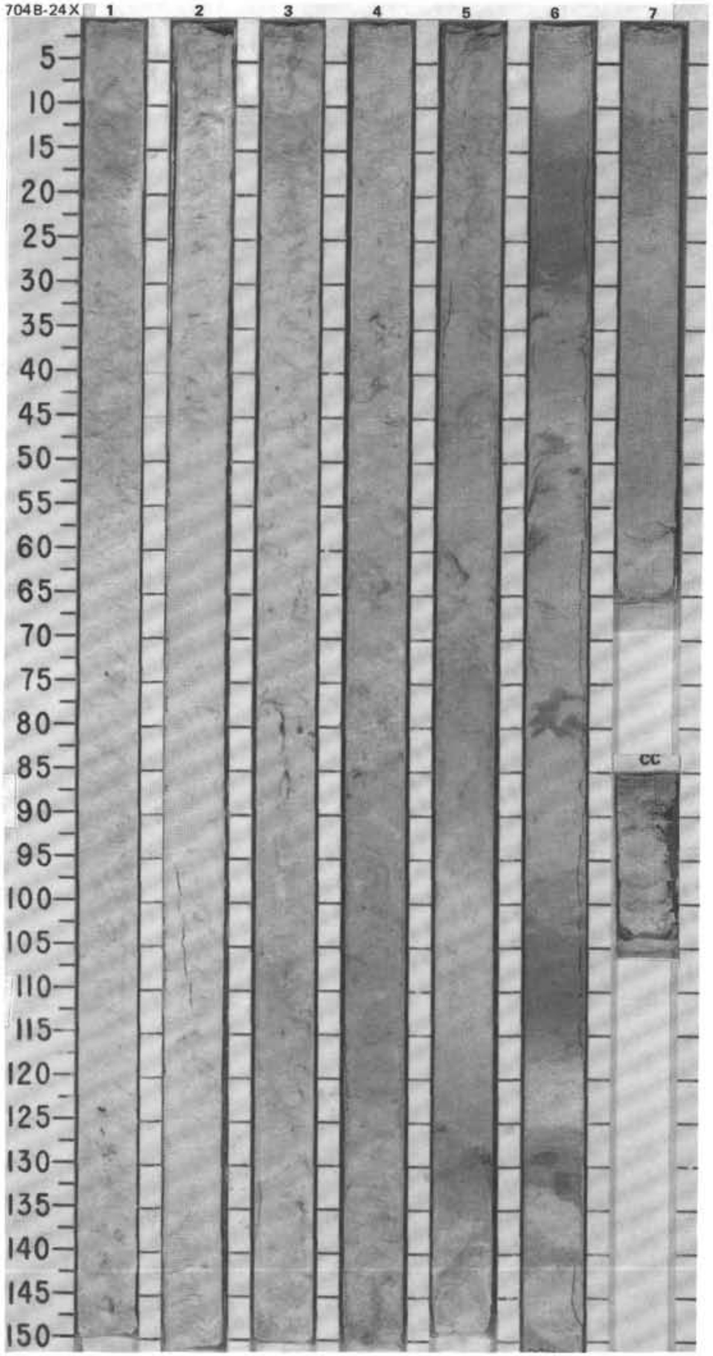

SITE 704 HOLE B CORE 25X CORED INTERVAL 2734.5-2753.0 mbsl; 223.2-232.7 mbsf

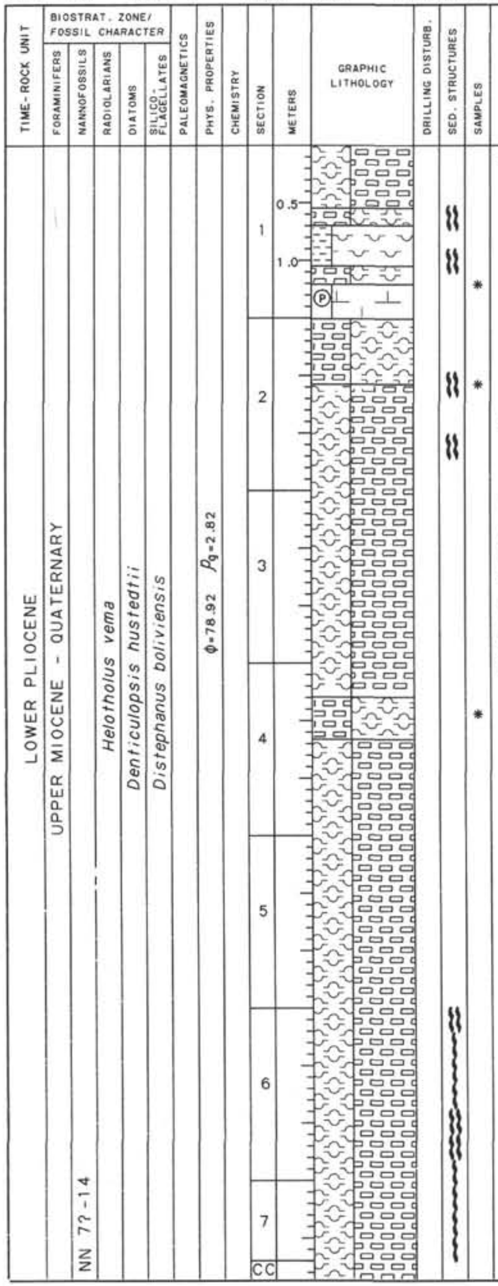

LITHOLOGIC DESCRIPTION

SILICEOUS CALCAREOUS OOZE

Major lithology: Siliceous calcareous ooze, light gray (7.5YR 7/0), white (7.5YR 8/0), and light greenish gray (5GY 7/1). Pyritic patches, black (7.5YR 2.5/0) in Section 1, 38, 56, and 105 cm; Section 2, 140 cm; and Section 6, 35 and 110 cm.

Minor lithologies: Clay-bearing diatom ooze, brown (7.5YR 5/2), Section 1, 70–105 cm. Pyritic nannofossil ooze, dark greenish gray (5GY 4/1), Section 1, 120–150 cm. Calcareous siliceous ooze, pinkish gray (7.5YR 6/2), Section 1, 55–70 and 105–120 cm; and Section 2, 0–59 cm; greenish gray (5GY 6/1) to pinkish gray (7.5YR 6/2) in Section 4, 28–64 cm.

Minor to moderate bioturbation in Sections 6 and 7.

SMEAR SLIDE SUMMARY (%):

	1, 84 D	1, 130 M	2, 55 D	4, 41 D
COMPOSITION:				
Quartz/feldspar	4	—	—	3
Clay	20	—	—	—
Calcite/dolomite	—	—	20	12
Accessory minerals:				
Pyrite	Tr	—	—	—
Nannofossils	5	90	3	10
Diatoms	65	8	66	59
Radiolarians	5	2	10	—
Sponge spicules	—	—	—	15
Silicoflagellates	1	—	1	1

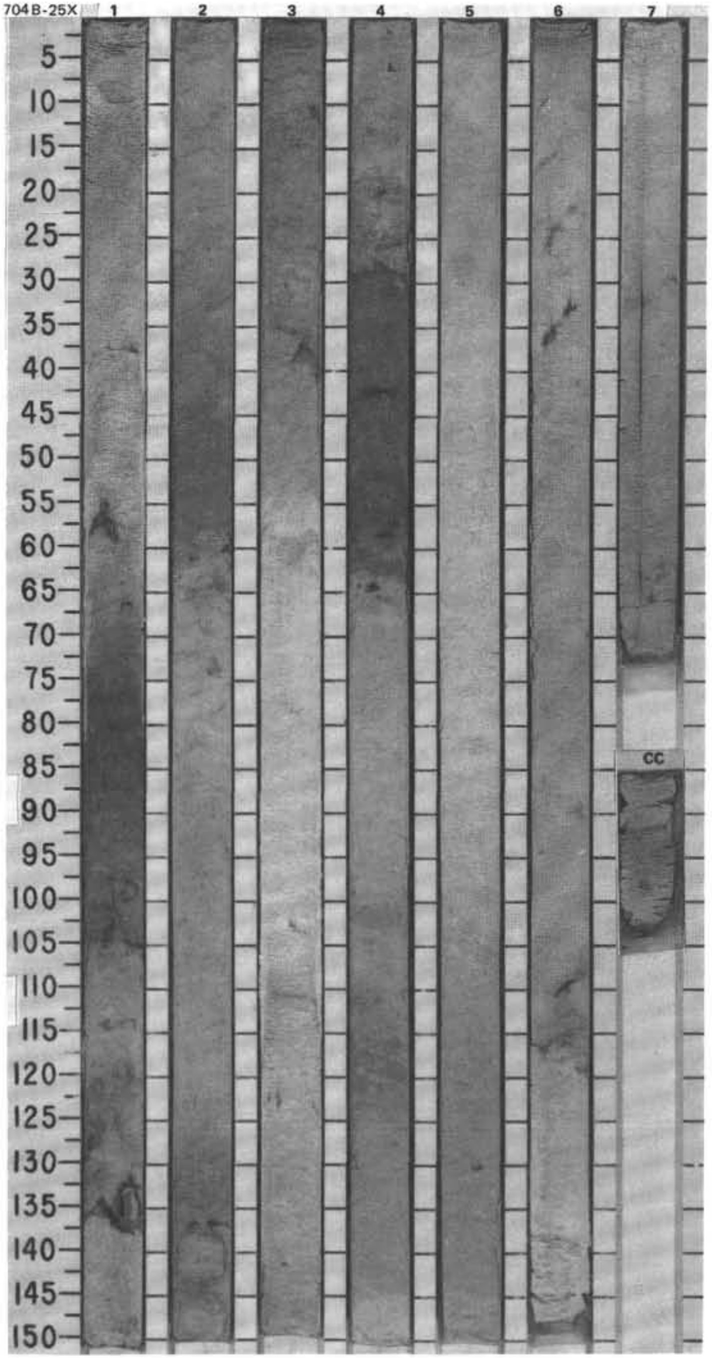

SITE 704 HOLE B CORE 26X CORED INTERVAL 2753.0-2762.5 mbsl; 232.7-242.2 mbsf

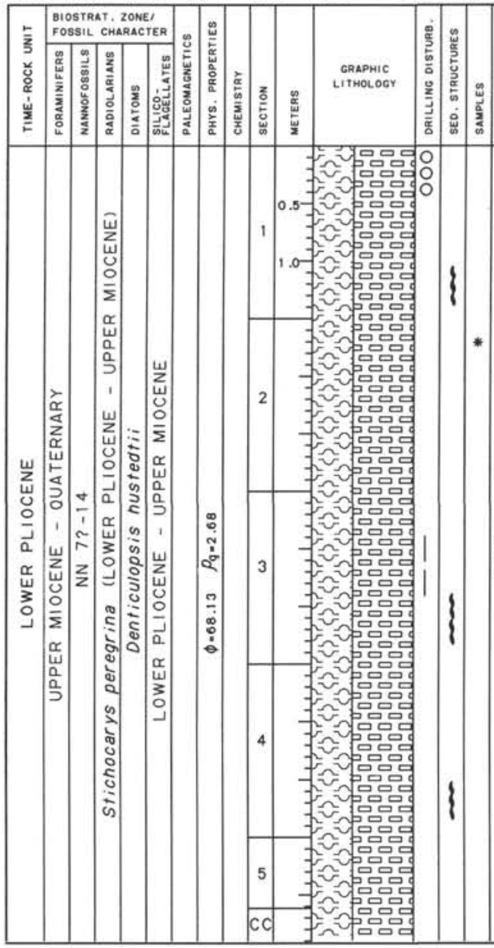

LITHOLOGIC DESCRIPTION

SILICEOUS CALCAREOUS OOZE

Drilling disturbance: Soupy in Section 1, 0-40 cm; moderate in Section 3, 50-100 cm.

Major lithology: Siliceous calcareous ooze, greenish gray (5GY 6/1), light greenish gray (5GY 7/1), light gray (5Y 7/1) to white (no color code). Pyrite-bearing spots (mottling), dark gray (N4/) in Section 1, 137 cm; Section 2, 34-38 and 63-84 cm; Section 3, 34-40, 57, and 91-98 cm; Section 4, 13, 40, and 130 cm; and Section 5, 22 and 50-58 cm.

Bioturbation: Minor, *Planolites*(?) in Section 1.

SMEAR SLIDE SUMMARY (%):

COMPOSITION:	2, 19 M
Volcanic glass	2
Accessory minerals	1
Opaques (pyrite)	35
Nannofossils	35
Diatoms	35
Radiolarians	1
Sponge spicules	1

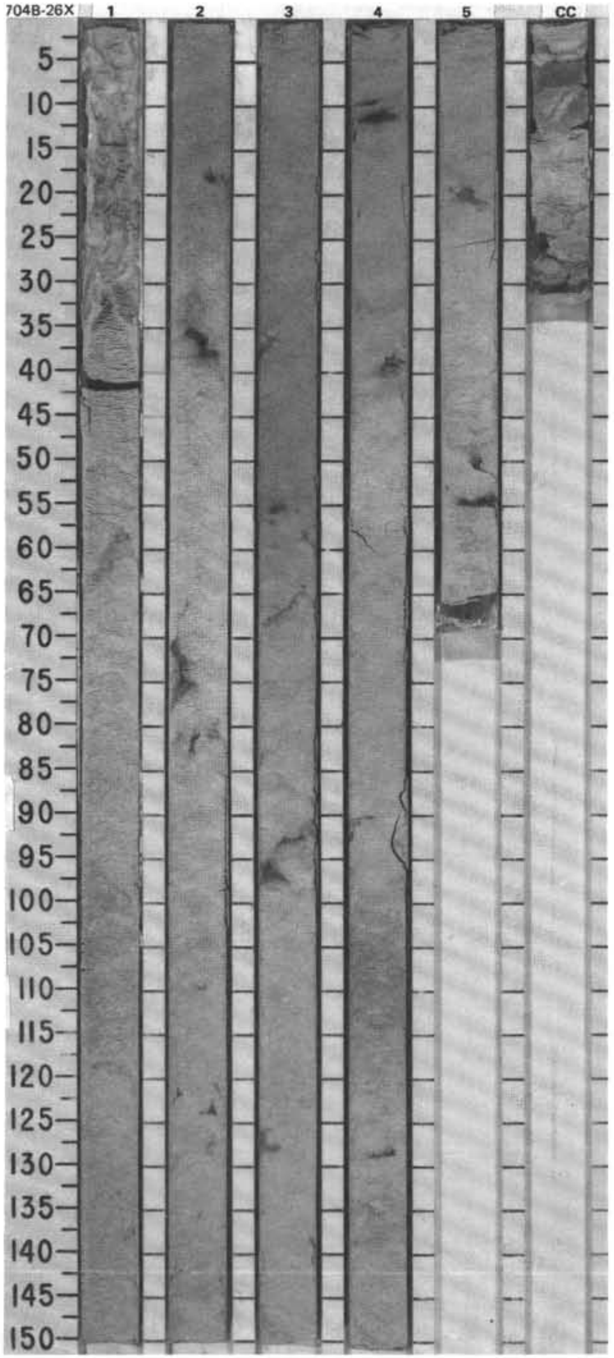

SITE 704 HOLE B CORE 27X CORED INTERVAL 2762.5-2772.0 mbsl; 242.2-251.7 mbsf

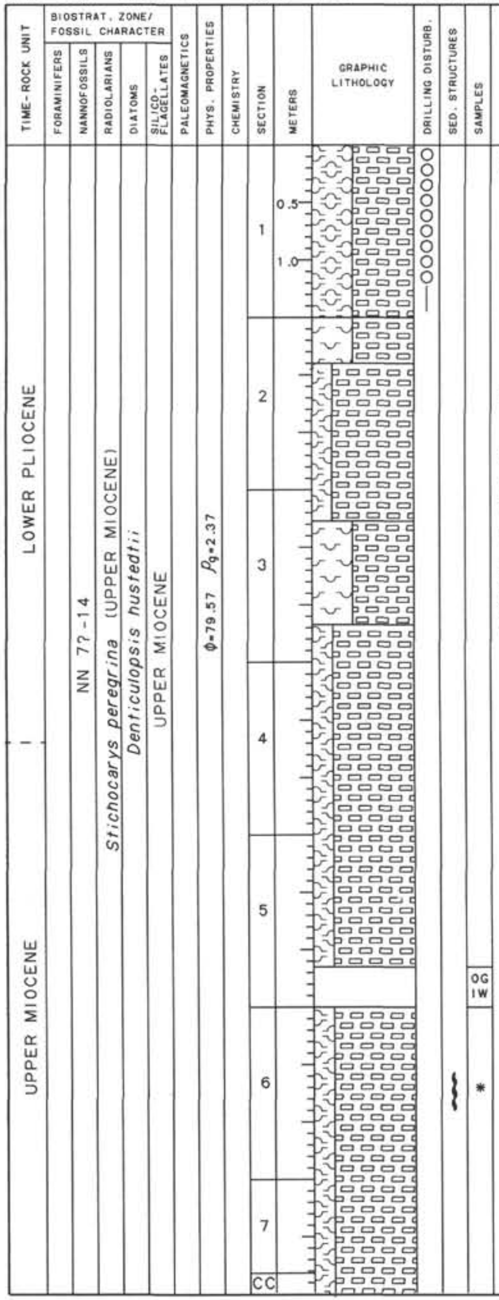

LITHOLOGIC DESCRIPTION

SILICEOUS-BEARING CALCAREOUS OOZE to SILICEOUS CALCAREOUS OOZE

Drilling disturbance: Soupy to moderate in Section 1.

Major lithology: Siliceous-bearing calcareous ooze, white (2.5Y 8/1 to no color code) to light greenish gray (5GY 7/1). Siliceous calcareous ooze, white 5Y 8/1). Both major lithologies are mottled by dark gray (5Y 3/1) pyritic(?) spots.

Minor lithology: Diatom calcareous ooze, pale brown (10YR 6/3).

Minor bioturbation in Section 6.

SMEAR SLIDE SUMMARY (%):

	6, 70 D
COMPOSITION:	
Volcanic glass	Tr
Accessory minerals:	
Opaques (pyrite)	Tr
Foraminifers/ nannofossils	85
Diatoms	9
Radiolarians	1
Sponge spicules	1
Silicoflagellates	Tr
Micrite	4

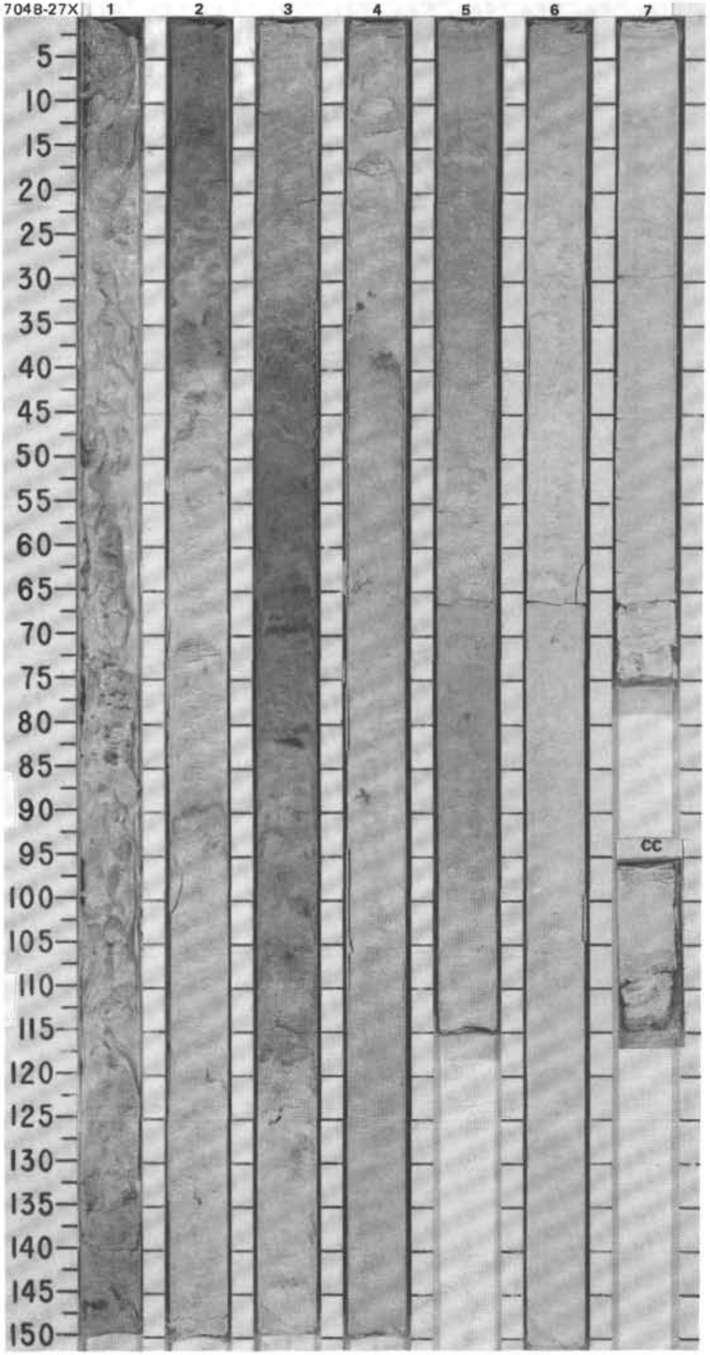

SITE 704 HOLE B CORE 28X CORED INTERVAL 2772.0-2781.5 mbsl; 251.7-261.2 mbsf

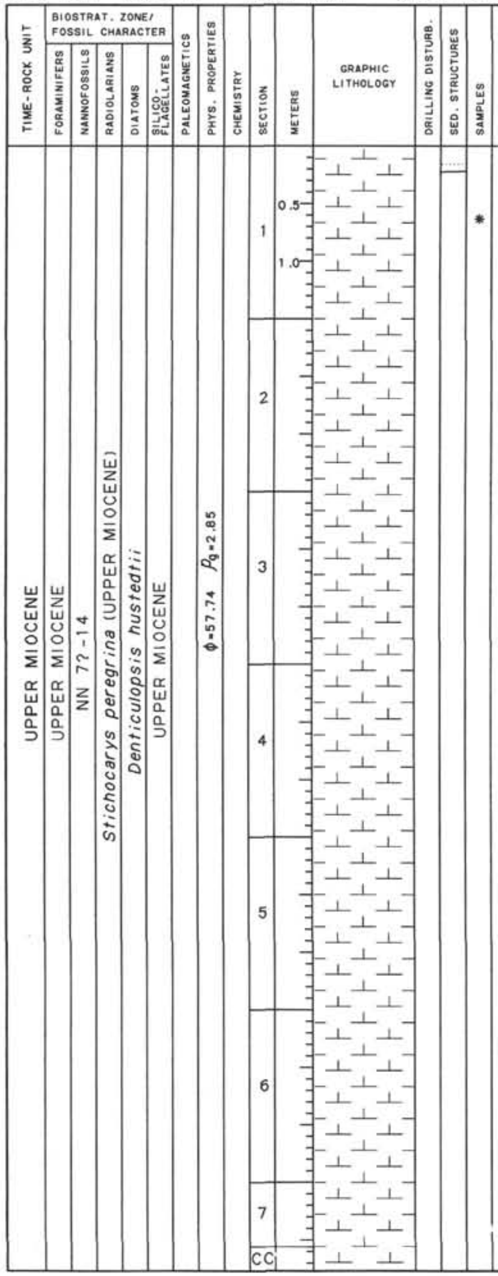

LITHOLOGIC DESCRIPTION

NANNOFOSSIL OOZE

Major lithology: Nannofossil ooze, white (2.5Y 8/1 to no color code) and light greenish gray (5GY 7/1). Dispersed ash(?) in Section 4, 78 cm.

Minor lithology: Small turbidite(?) layer, normally graded, containing ash particles.

SMEAR SLIDE SUMMARY (%):

	1, 70 D
COMPOSITION:	
Volcanic glass	1
Foraminifers	4
Nannofossils	93
Diatoms	1
Radiolarians	1
Sponge spicules	Tr

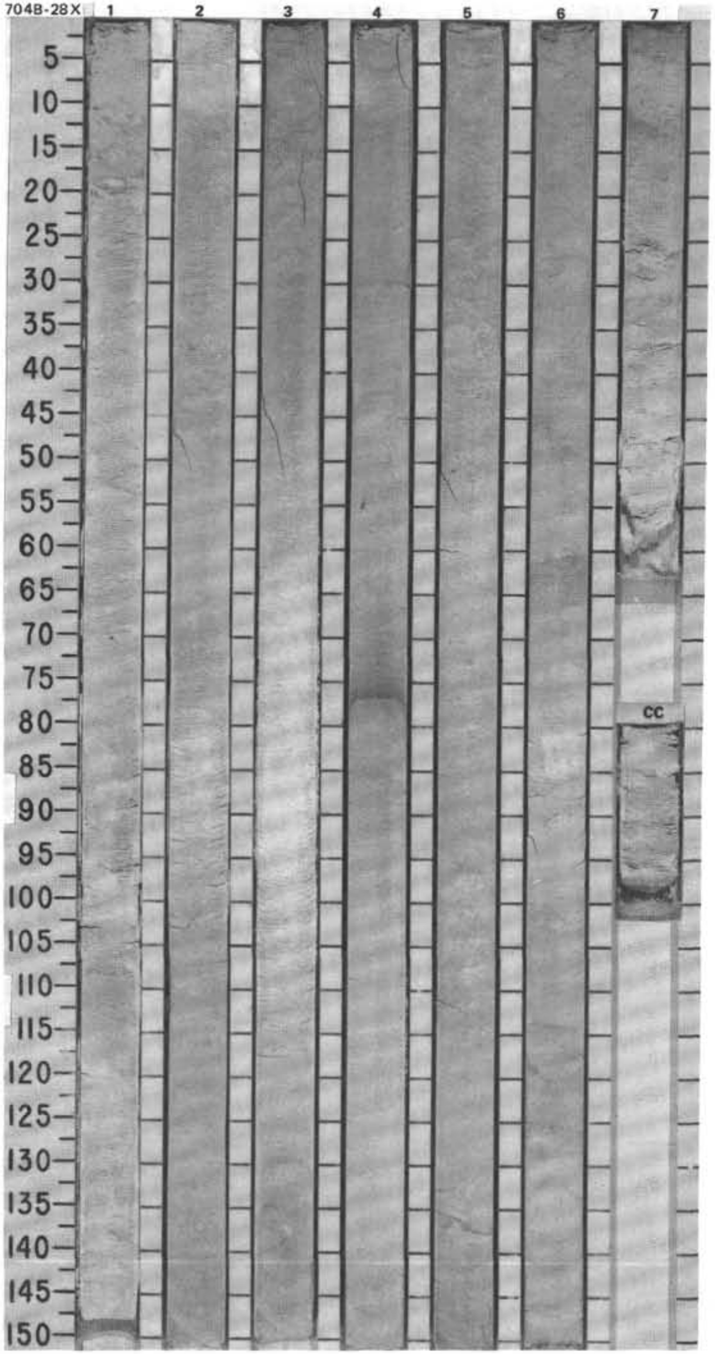

SITE 704 HOLE B CORE 29X CORED INTERVAL 2781.5-2791.0 mbsl; 261.2-270.7 mbsf

TIME-ROCK UNIT	BIOSTRAT. ZONE/ FOSSIL CHARACTER					PALEOMAGNETICS	PHYS. PROPERTIES	CHEMISTRY	SECTION	METERS	GRAPHIC LITHOLOGY	DRILLING DISTURB.	SED. STRUCTURES	SAMPLES
	FORAMINIFERS	NANNOFOSSILS	RADIOLARIANS	DIATOMS	SILICO-FLAGELLATES									
UPPER MIOCENE	UPPER MIOCENE	NN 7?-14	*Stichocorys peregrina* (UPPER MIOCENE)	*Denticulopsis hustedtii*	UPPER MIOCENE		ϕ=57.30 ρ_g=57.30		1 2 3 4 5 6 7 CC	0.5 1.0	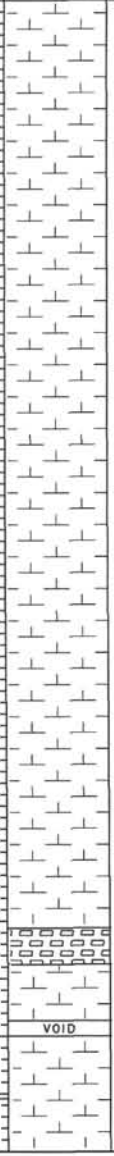			*

LITHOLOGIC DESCRIPTION

NANNOFOSSIL OOZE

Major lithology: Nannofossil ooze, light greenish gray (5GY 7/1) to white (no color code).

Minor lithology: Calcareous ooze, light blue gray (5B 7/1), Section 6, 59-89 cm. Pyrite-bearing horizon in Section 7, 9-13 cm; pyrite-bearing spots in Section 7, 40 cm.

SMEAR SLIDE SUMMARY (%):

	2, 70 D
COMPOSITION:	
Volcanic glass	Tr
Foraminifers	7
Nannofossils	90
Diatoms	1
Radiolarians	2

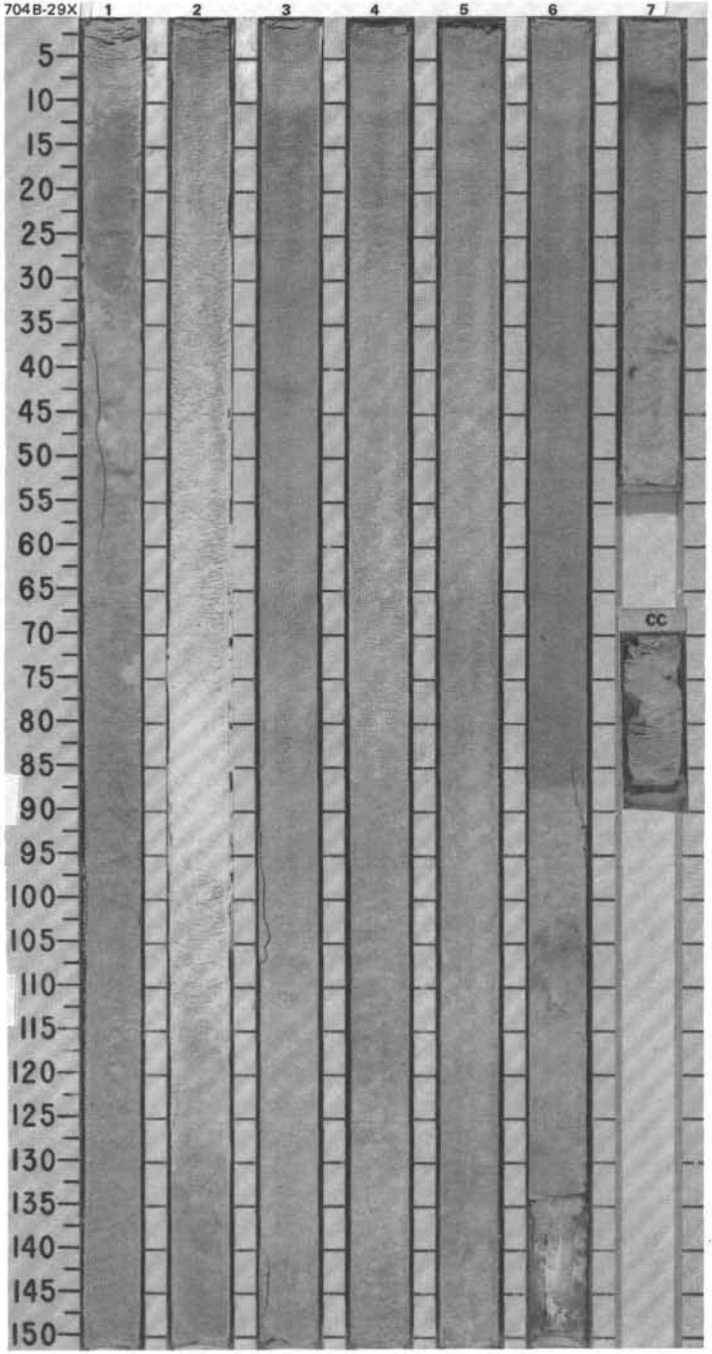

SITE 704 HOLE B CORE 30X CORED INTERVAL 2791.0-2800.5 mbsl; 270.7-280.2 mbsf

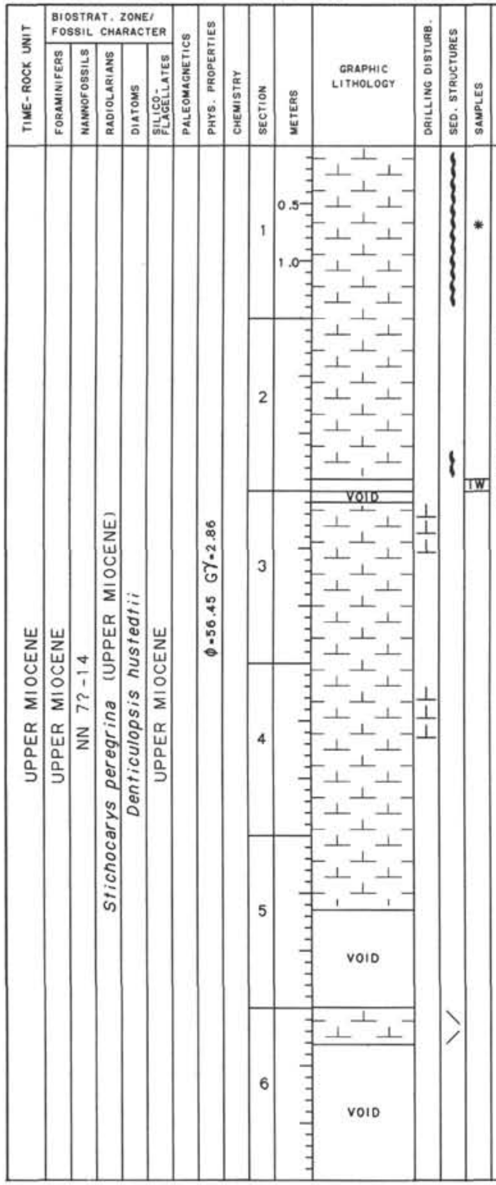

LITHOLOGIC DESCRIPTION

NANNOFOSSIL OOZE

Drilling disturbance: Biscuits.

Major lithology: Nannofossil ooze, light gray (5Y 7/1) to white (no color code). Opaques present in Section 1 and in Section 8, 56, 92, 112, 118, 130, and 139 cm. Opaque (pyrite?) layer in Section 8, 95 cm.

Bioturbation: Minor, few *Planolites* in Section 1.

SMEAR SLIDE SUMMARY (%):

	1, 70 D
COMPOSITION:	
Clay	2
Foraminifers	1
Nannofossils	93
Diatoms	3
Radiolarians	Tr
Sponge spicules	1

Cont.

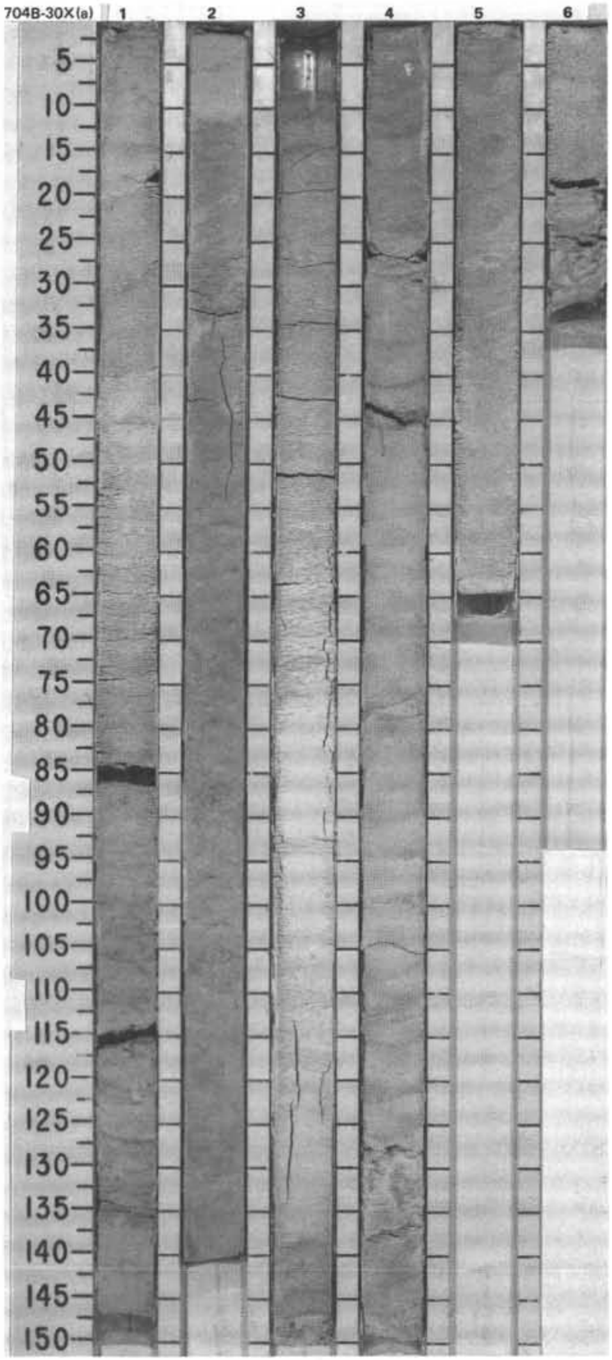

SITE 704 HOLE B CORE 30X CORED INTERVAL 2791.0-2800.5 mbsl; 270.7-280.2 mbsf

TIME-ROCK UNIT	BIOSTRAT. ZONE/ FOSSIL CHARACTER					PALEOMAGNETICS	PHYS. PROPERTIES	CHEMISTRY	SECTION	METERS	GRAPHIC LITHOLOGY	DRILLING DISTURB.	SED. STRUCTURES	SAMPLES	LITHOLOGIC DESCRIPTION
	FORAMINIFERS	NANNOFOSSILS	RADIOLARIANS	DIATOMS											
									7	0.5 1.0					Cont.
									8						
									CC						

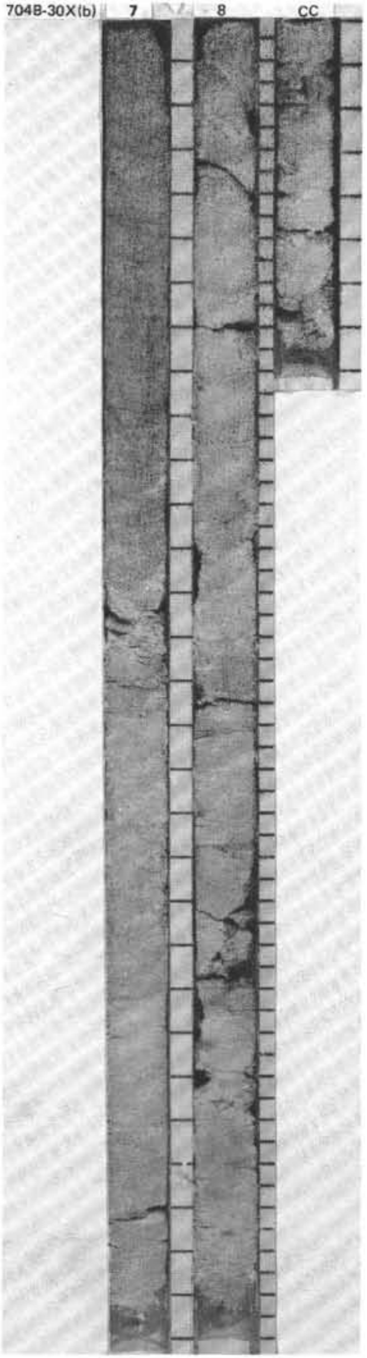

SITE 704 HOLE B CORE 31X CORED INTERVAL 2800.5-2810.0 mbsl; 280.2-289.7 mbsf

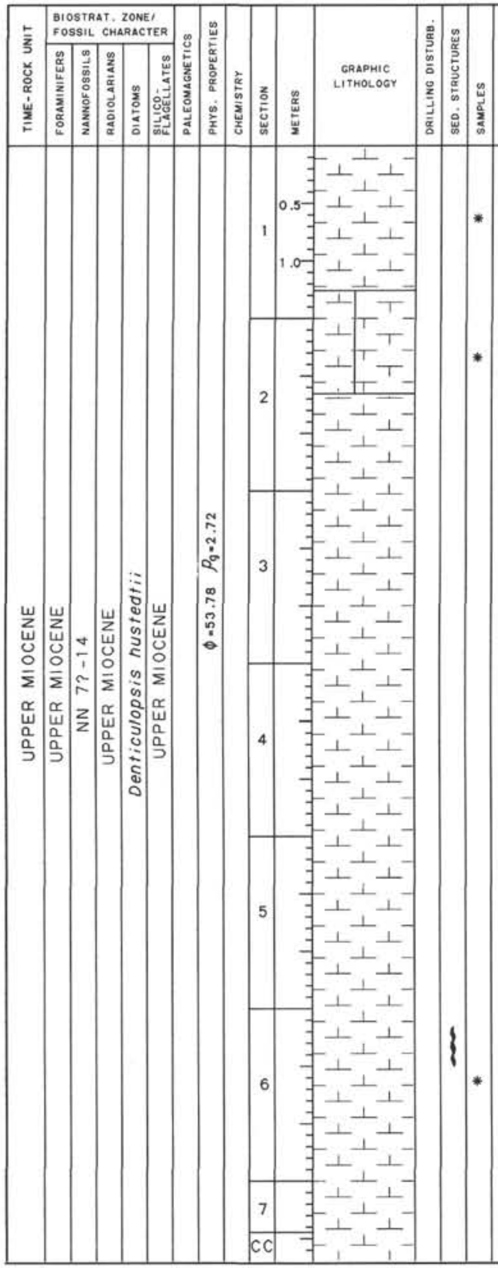

LITHOLOGIC DESCRIPTION

NANNOFOSSIL OOZE

Major lithology: Nannofossil ooze, white (no color code), with light gray (5Y 7/1) color banding in Section 6. Opaque stained nannofossil ooze, gray (N4), in Section 6, 112 cm.

Bioturbation: Minor.

SMEAR SLIDE SUMMARY (%):

	1, 70 D	2, 33 M	6, 111 D
COMPOSITION:			
Clay	2	—	—
Volcanic glass	—	—	Tr
Accessory minerals:			
Opaques	—	Tr	—
Foraminifers	1	50	1
Nannofossils	91	30	96
Diatoms	3	Tr	Tr
Radiolarians	Tr	Tr	—
Sponge spicules	—	Tr	—
Fragmented carbonate	3	20	3

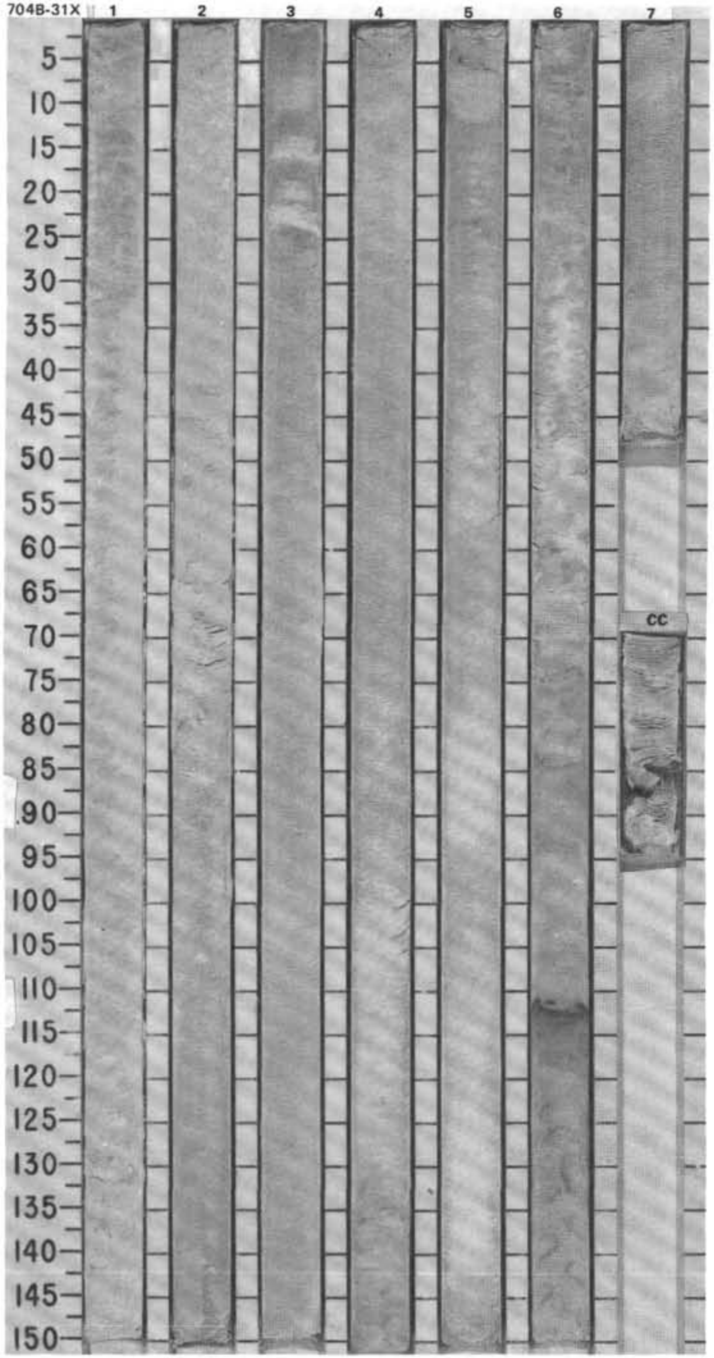

SITE 704 HOLE B CORE 32X CORED INTERVAL 2810.0-2819.5 mbsl; 289.7-299.2 mbsf

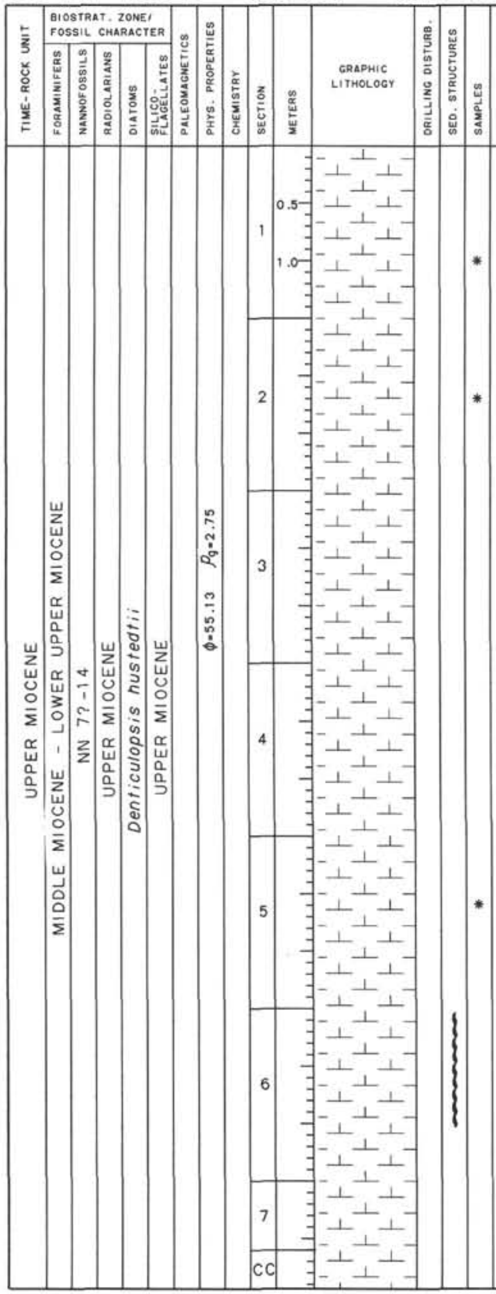

LITHOLOGIC DESCRIPTION

NANNOFOSSIL OOZE

Major lithology: Nannofossil ooze, white (no color code to 5Y 8/1). Opaque stained horizon in Section 7, 39 cm, and the CC, 10 and 17-22 cm.

Bioturbation: Faint mottling in Section 6, 0-100 cm.

SMEAR SLIDE SUMMARY (%):

	2, 70 D	5, 70 D	1, 100 D
COMPOSITION:			
Volcanic glass	—	Tr	—
Accessory minerals	Tr	—	—
Foraminifers	2	87	1
Nannofossils	88	—	99
Diatoms	3	3	Tr
Radiolarians	Tr	Tr	—
Fragmented carbonate	7	10	—

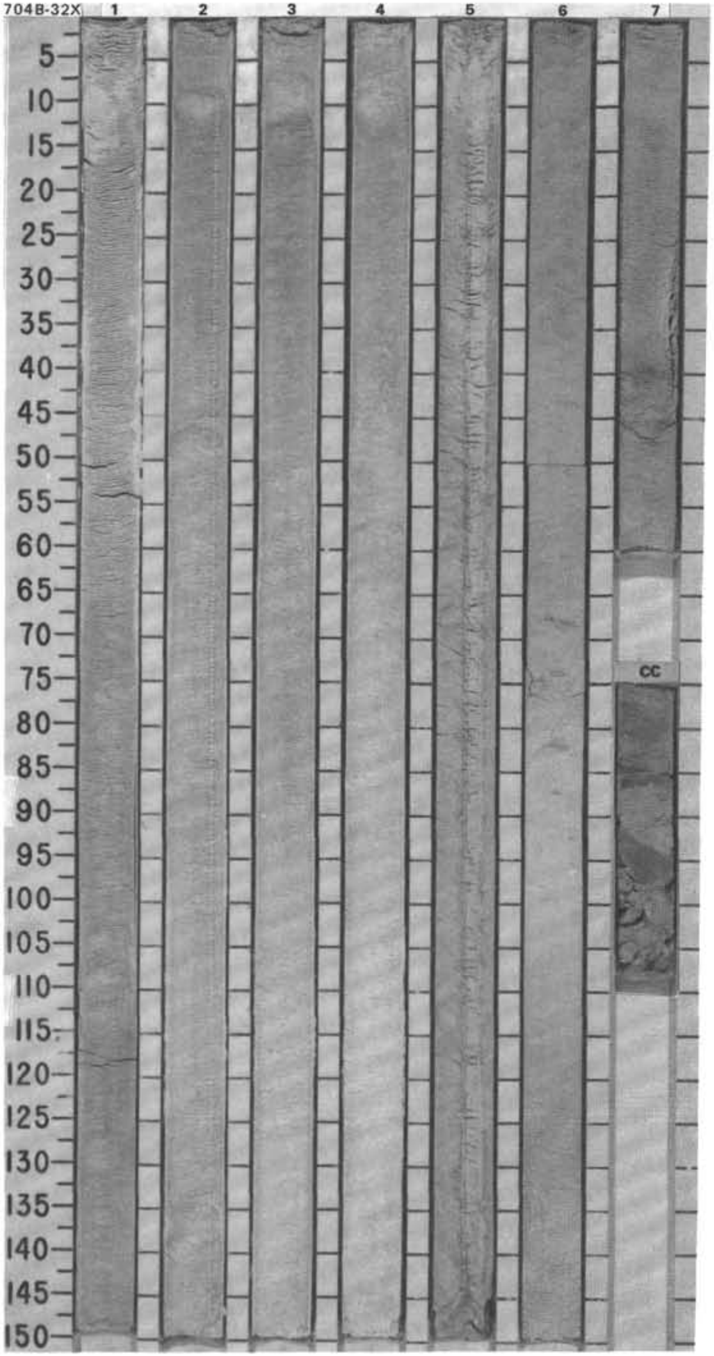

SITE 704 HOLE B CORE 33X CORED INTERVAL 2819.5-2829.0 mbsl; 299.2-308.7 mbsf

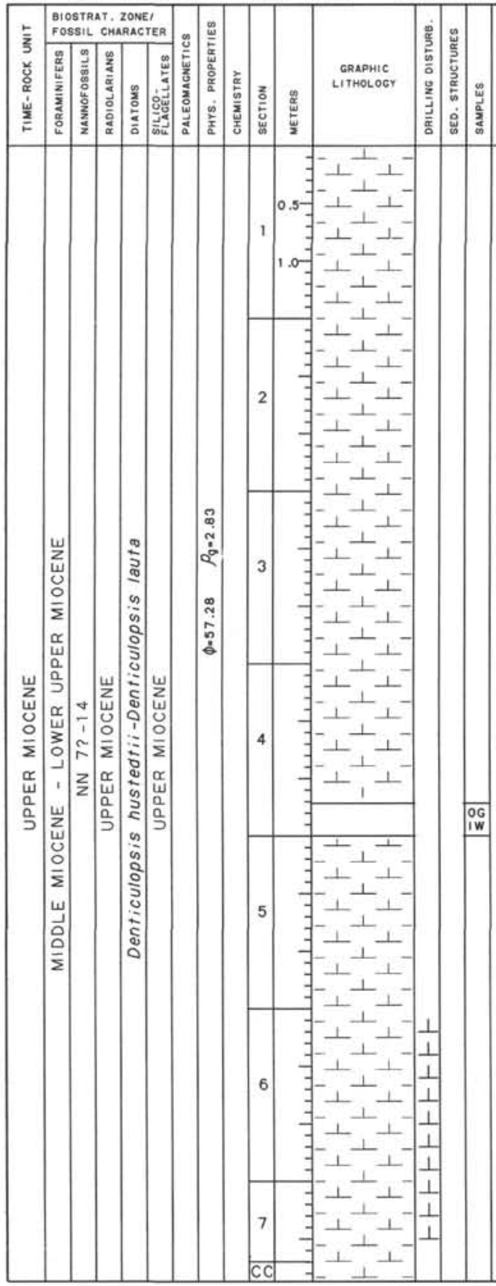

LITHOLOGIC DESCRIPTION

NANNOFOSSIL OOZE

Drilling disturbance: Biscuits in Sections 6 and 7.

Major lithology: Nannofossil ooze, white (no color code) to light greenish gray (5GY 7/1). Light blue gray (5B 7/1) due to occurrence of opaques in Section 7, 40-65 cm. Opaque (pyrite?) horizon in the CC, 6-8 cm.

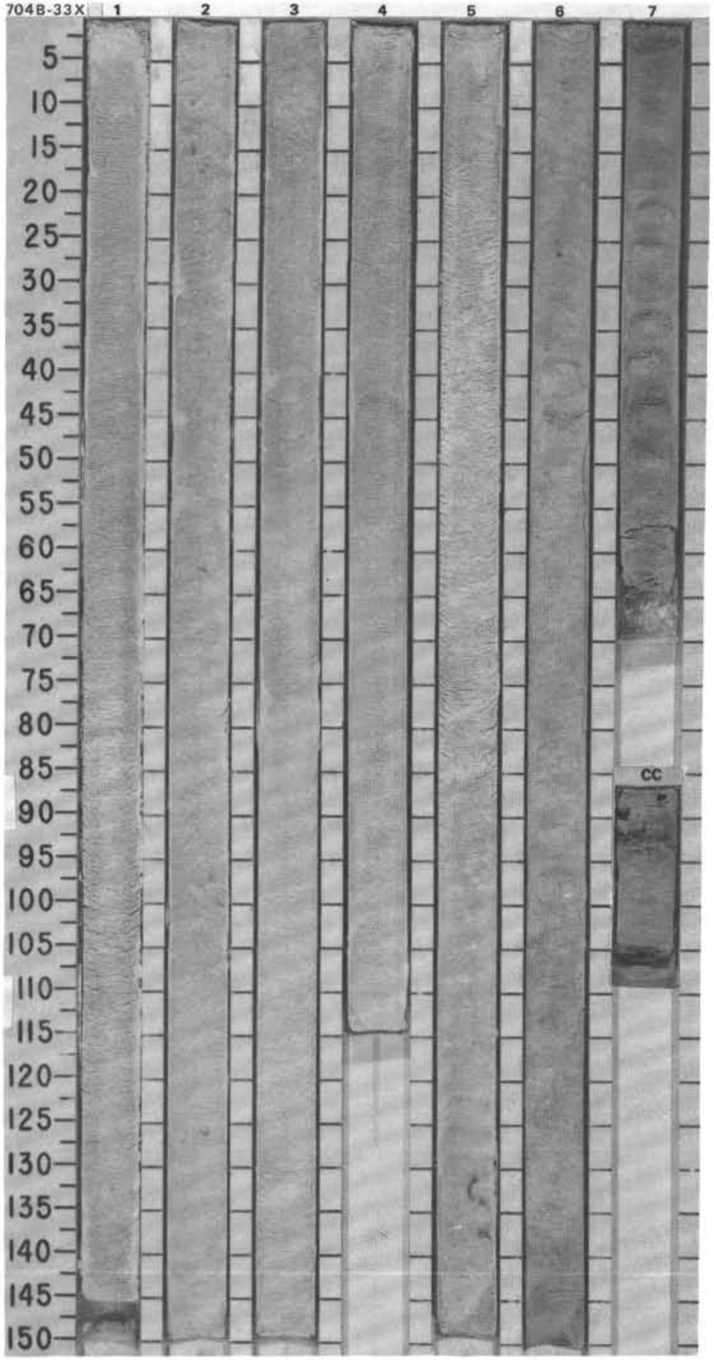

SITE 704 HOLE B CORE 34X CORED INTERVAL 2829.0-2838.5 mbsl; 308.7-318.2 mbsf

TIME-ROCK UNIT	BIOSTRAT. ZONE/ FOSSIL CHARACTER					PALEOMAGNETICS	PHYS. PROPERTIES	CHEMISTRY	SECTION	METERS	GRAPHIC LITHOLOGY	DRILLING DISTURB.	SED. STRUCTURES	SAMPLES	LITHOLOGIC DESCRIPTION
	FORAMINIFERS	NANNOFOSSILS	RADIOLARIANS	DIATOMS	SILICO-FLAGELLATES										
UPPER MIOCENE	MIDDLE MIOCENE - LOWER UPPER MIOCENE	NN 7? - 14	UPPER MIOCENE	*Denticulopsis hustedtii-D. lauta*	*Mesocena circulus/M. diodon* (UPPER MIOCENE)		$\phi=55.48$ $\rho_g=2.95$		1 2 3 4 5 6 7 CC	0.5 1.0					NANNOFOSSIL OOZE Drilling disturbance: Biscuits. Major lithology: Nannofossil ooze, white (no color code to 7.5YR 8/0), with opaque staining in Section 1, 130-150 cm, and Section 2, 0-89 cm; spots at Section 2, 21, 26, and 69 cm. Opaque (pyrite?) bleb in Section 6, 84 cm.

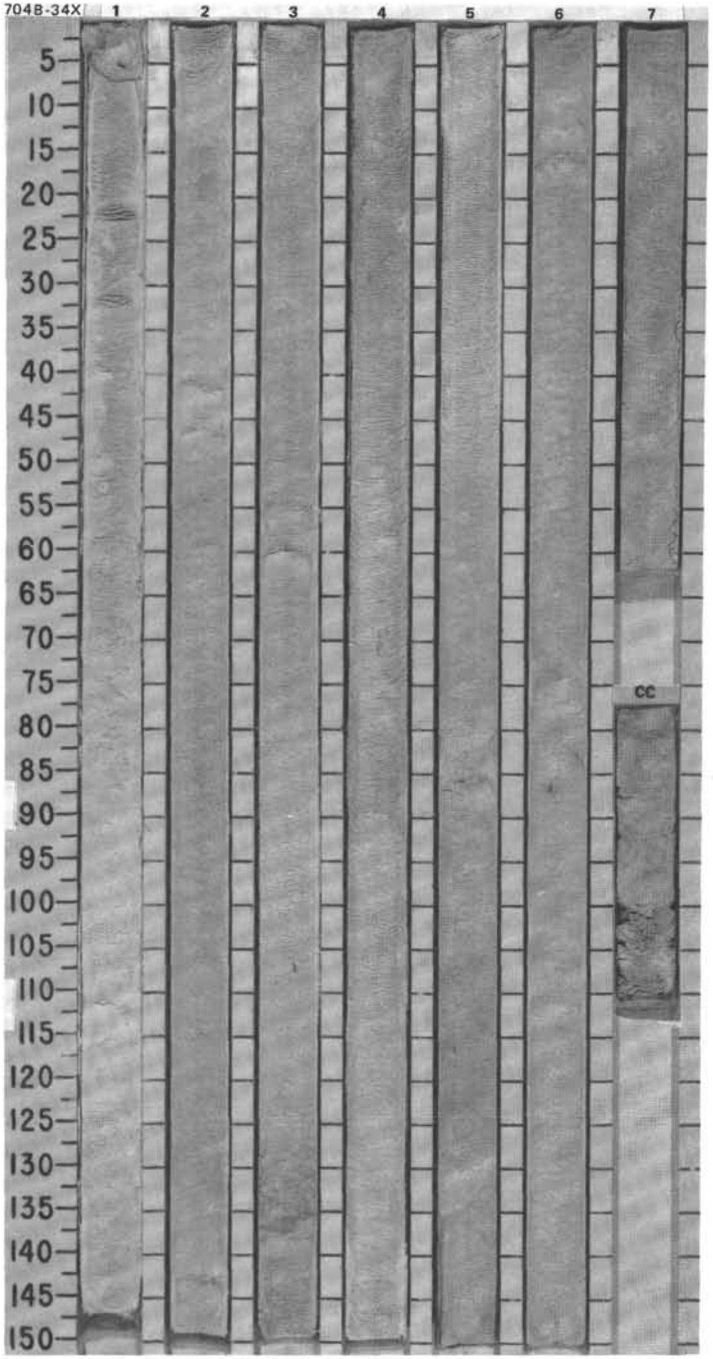

SITE 704 HOLE B CORE 35X CORED INTERVAL 2838.5-2848.0 mbsl; 318.2-327.7 mbsf

TIME-ROCK UNIT	BIOSTRAT. ZONE/ FOSSIL CHARACTER FORAMINIFERS	NANNOFOSSILS	RADIOLARIANS	DIATOMS	SILICO-FLAGELLATES	PALEOMAGNETICS	PHYS. PROPERTIES	CHEMISTRY	SECTION	METERS	GRAPHIC LITHOLOGY	DRILLING DISTURB.	SED. STRUCTURES	SAMPLES
UPPER MIOCENE	MIDDLE MIOCENE - LOWER UPPER MIOCENE	NN 7?-14	unzoned (UPPER MIOCENE)	*Denticulopsis hustedtii-D. lauta*	*Mesocena circulus/M. diodon* (UPPER MIOCENE)		$\phi=68.79$ $\rho_g=2.52$		1 2 3 4 5 6 7 CC	0.5 1.0				* *

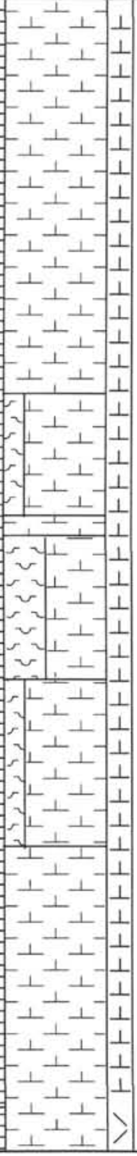

NANNOFOSSIL OOZE and DIATOM-BEARING NANNOFOSSIL OOZE

Drilling disturbance: Biscuits throughout the core.

Major lithology: Nannofossil ooze, white (no color code) to light greenish gray (5GY 7/1), and diatom-bearing nannofossil ooze, light greenish gray (5GY 7/1). Opaque horizons and spots at Section 2, 18, 25, 32, 58, and 69 cm; Section 3, 37-42 cm; Section 4, 10-15 cm; and Section 5, 139-144 cm.

Minor lithology: Diatom nannofossil ooze, light greenish gray (5GY 7/1), with yellowish spots of higher diatom accumulation.

SMEAR SLIDE SUMMARY (%):

	4, 89 D	5, 50 D
COMPOSITION:		
Micrite	Tr	Tr
Foraminifers	5	5
Nannofossils	55	85
Diatoms	40	10

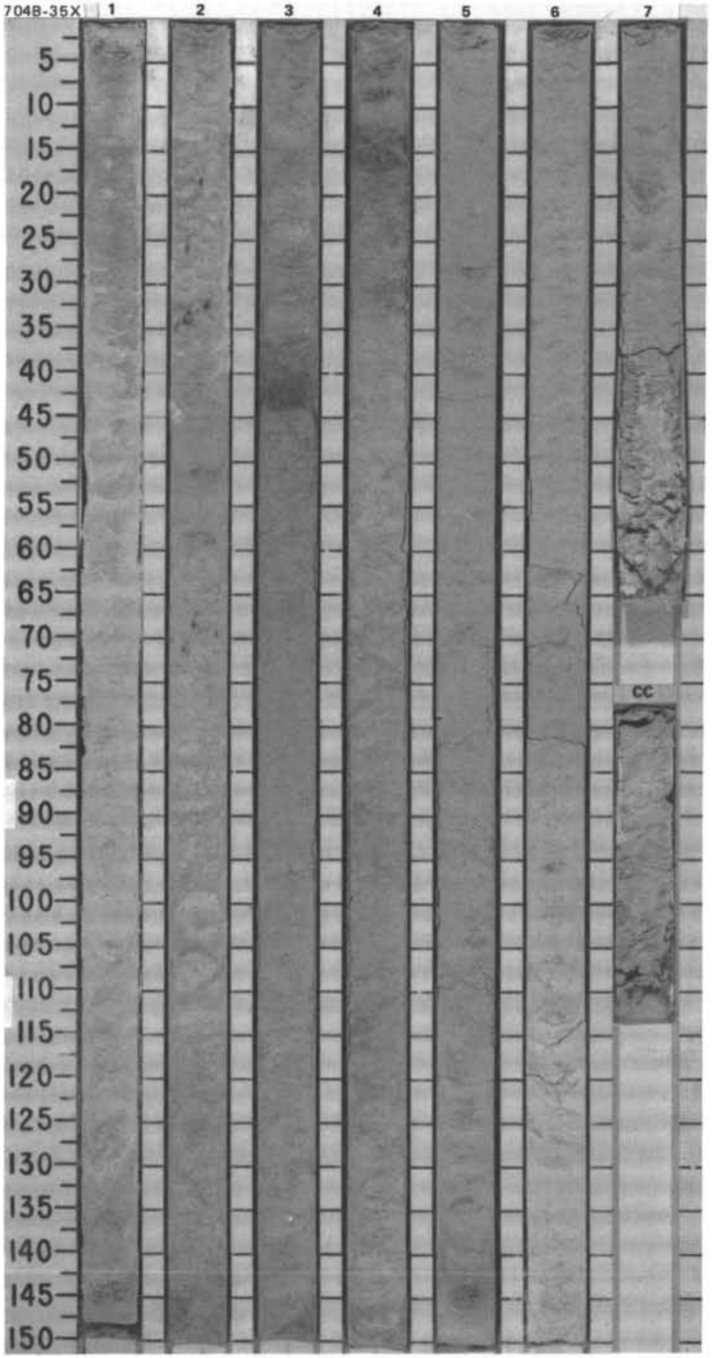

SITE 704 HOLE B CORE 36X CORED INTERVAL 2848.0-2857.5 mbsl; 327.7-337.2 mbsf

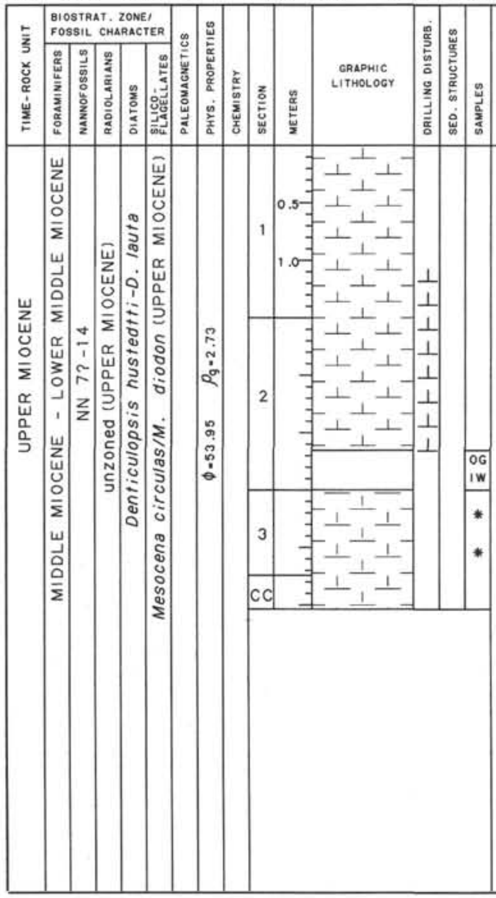

LITHOLOGIC DESCRIPTION

NANNOFOSSIL OOZE

Drilling disturbance: Biscuits.

Major lithology: Nannofossil ooze, white (no color code to 2.5YR 8/0). Opaque staining in Section 1, 4, 97, 105, and 116 cm; Section 2, 4, 6, 65, and 70 cm; and Section 3, 15 and 23 cm.

SMEAR SLIDE SUMMARY (%):

	3, 16 D	3, 55 D
COMPOSITION:		
Accessory minerals:		
Mn-micronodules	10	—
Micrite	1	Tr
Foraminifers	Tr	5
Nannofossils	89	94
Diatoms	Tr	1

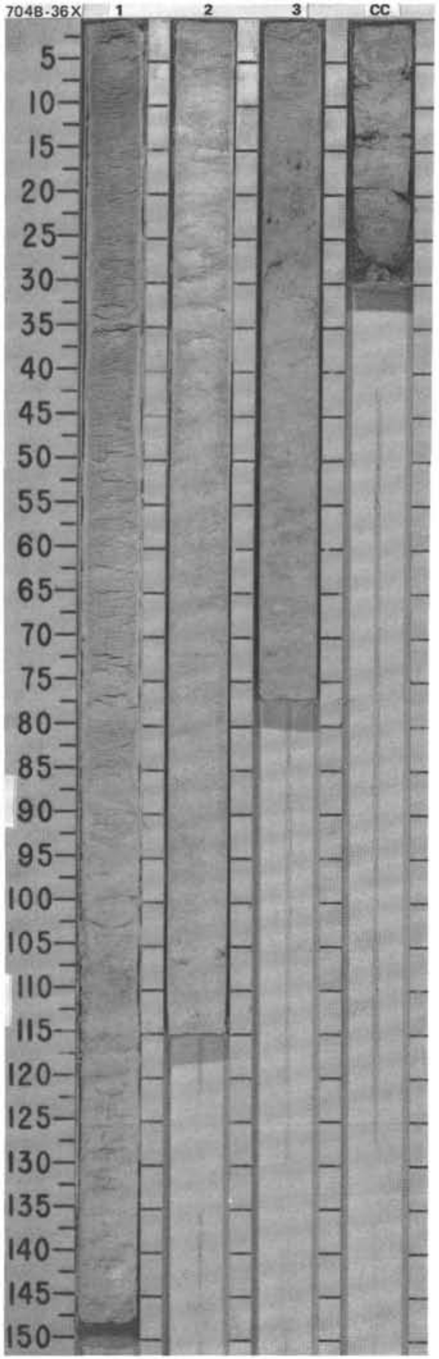

SITE 704 HOLE B CORE 37X CORED INTERVAL 2857.5-2867.0 mbsl; 337.2-346.7 mbsf

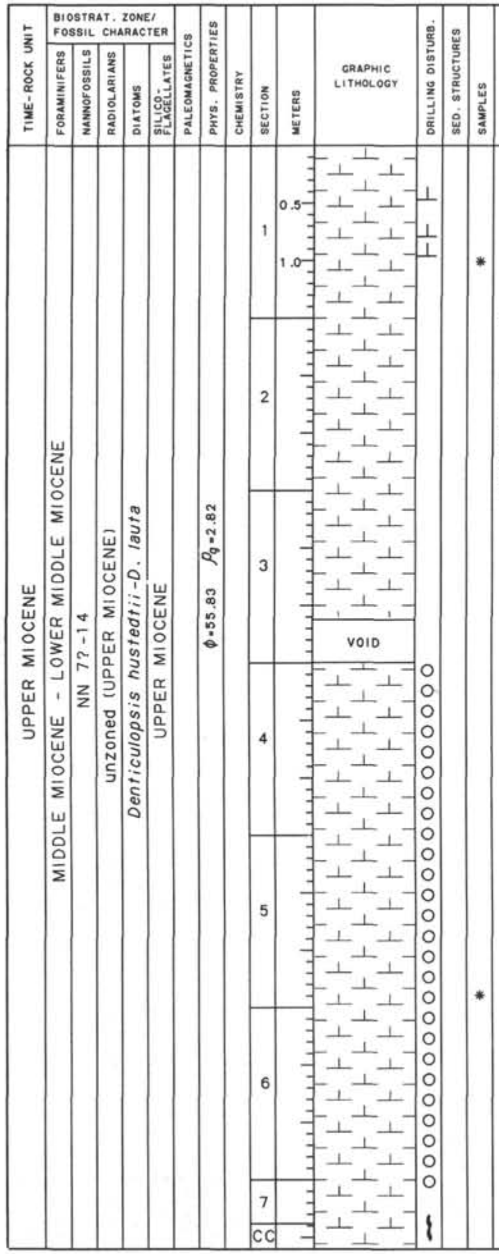

LITHOLOGIC DESCRIPTION

NANNOFOSSIL OOZE

Drilling disturbance: Soupy in Sections 4, 5, 6, and 7; biscuits in Section 1.

Major lithology: Nannofossil ooze, white (no color code) to light gray (5Y 7/1). Opaque (pyrite?) staining in Section 1, 17-19 and 96 cm; Section 2, 63-66 cm; and Section 3, 55-59 and 97-101 cm.

SMEAR SLIDE SUMMARY (%):

	1, 100 D	5, 140 D
COMPOSITION:		
Micrite	—	5
Foraminifers	3	2
Nannofossils	89	88
Diatoms	5	5
Radiolarians	Tr	Tr
Fragmented carbonate	3	—

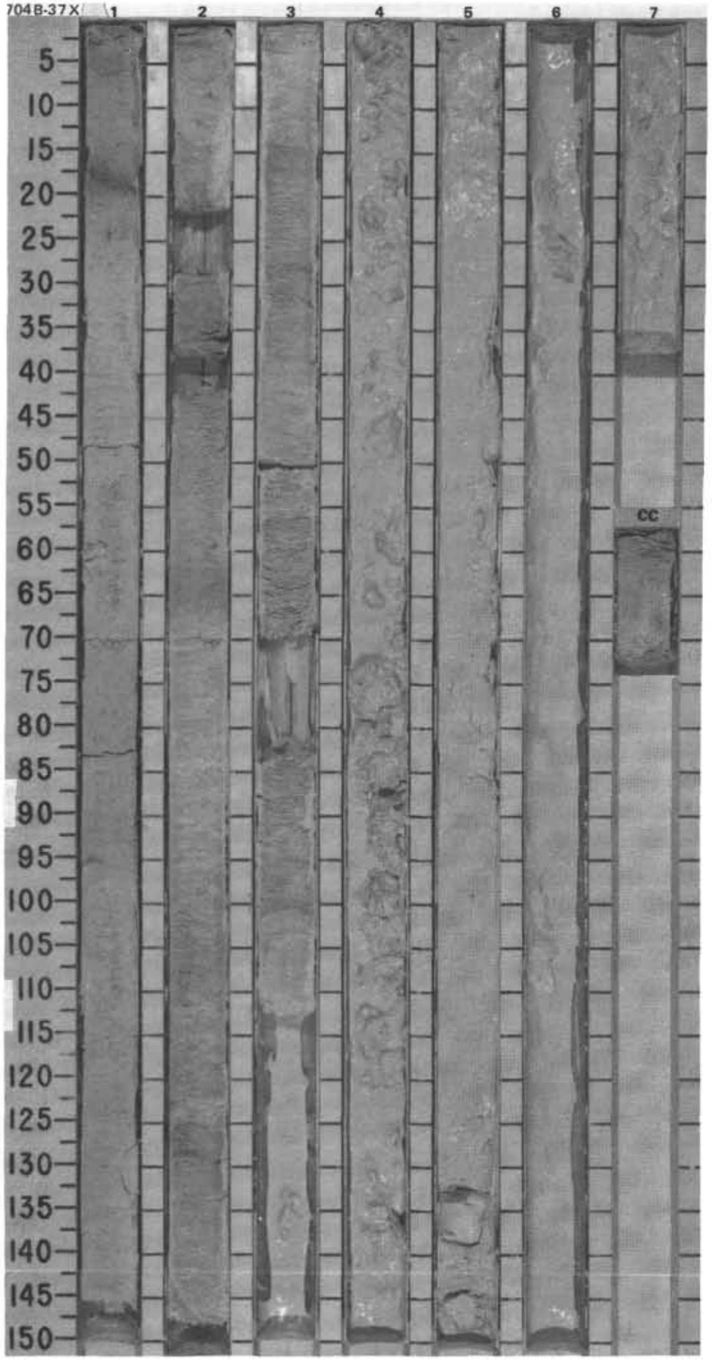

SITE 704 HOLE B CORE 38X CORED INTERVAL 2867.0-2876.5 mbsl; 346.7-356.2 mbsf

TIME-ROCK UNIT	BIOSTRAT. ZONE/ FOSSIL CHARACTER					PALEOMAGNETICS	PHYS. PROPERTIES	CHEMISTRY	SECTION	METERS	GRAPHIC LITHOLOGY	DRILLING DISTURB.	SED. STRUCTURES	SAMPLES	LITHOLOGIC DESCRIPTION
	FORAMINIFERS	NANNOFOSSILS	RADIOLARIANS	DIATOMS	SILICO-FLAGELLATES										
UPPER MIOCENE	MIDDLE MIOCENE - LOWER MIDDLE MIOCENE	NN 7?-14	unzoned (UPPER MIOCENE)	*Denticulopsis hustedtii-D. lauta*	UPPER MIOCENE				1						NANNOFOSSIL OOZE Major lithology: Nannofossil ooze, white (no color code).

SITE 704 HOLE B CORE 39X CORED INTERVAL 2876.5-2886.0 mbsl; 356.2-365.7 mbsf

TIME-ROCK UNIT	BIOSTRAT. ZONE/ FOSSIL CHARACTER					PALEOMAGNETICS	PHYS. PROPERTIES	CHEMISTRY	SECTION	METERS	GRAPHIC LITHOLOGY	DRILLING DISTURB.	SED. STRUCTURES	SAMPLES	LITHOLOGIC DESCRIPTION
	FORAMINIFERS	NANNOFOSSILS	RADIOLARIANS	DIATOMS	SILICO-FLAGELLATES										
UPPER MIOCENE	MIDDLE MIOCENE - LOWER MIDDLE MIOCENE	NN 7?-14	unzoned (UPPER MIOCENE)	*Denticulopsis hustedtii-D. lauta*	UPPER MIOCENE (UPPER MIOCENE)		ϕ=53.42 ρ_g=2.85		1 2 3 4 5 6 7 CC	0.5 1.0	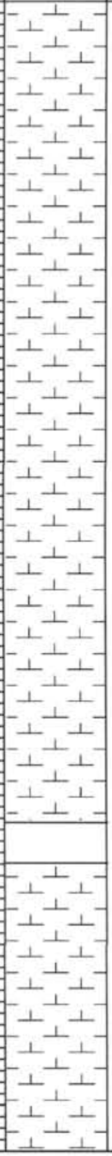			* * OG IW	see below

NANNOFOSSIL OOZE

Major lithology: Nannofossil ooze, white (no color code). Opaque staining in Section 4, 122 cm; Section 5, 29 cm; and Section 6, 98-107 cm. Pumice pebble in Section 6, 102 cm.

Bioturbation, causing very faint pale brown mottling in Section 4.

SMEAR SLIDE SUMMARY (%):

	2, 100 D	4, 60 D
COMPOSITION:		
Foraminifers	1	Tr
Nannofossils	98	99
Diatoms	1	1

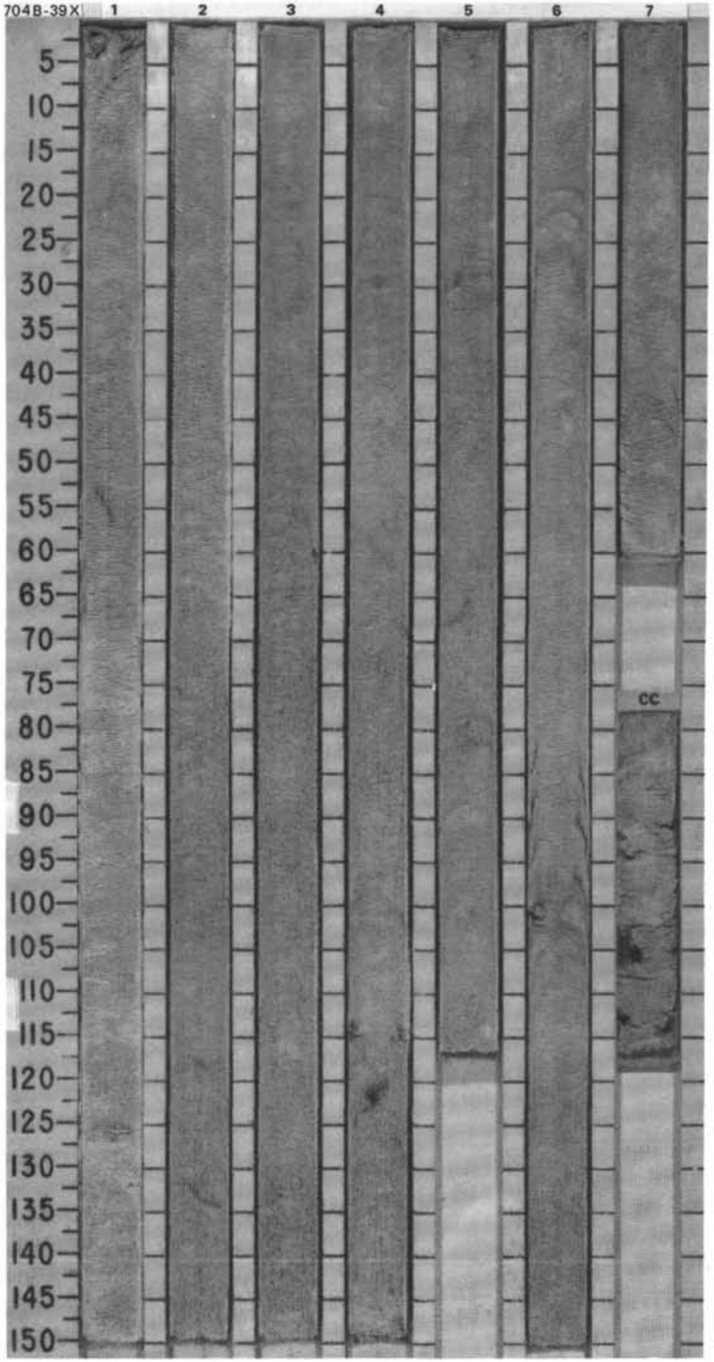

SITE 704 HOLE B CORE 40X CORED INTERVAL 2886.0-2895.5 mbsl; 365.7-375.2 mbsf

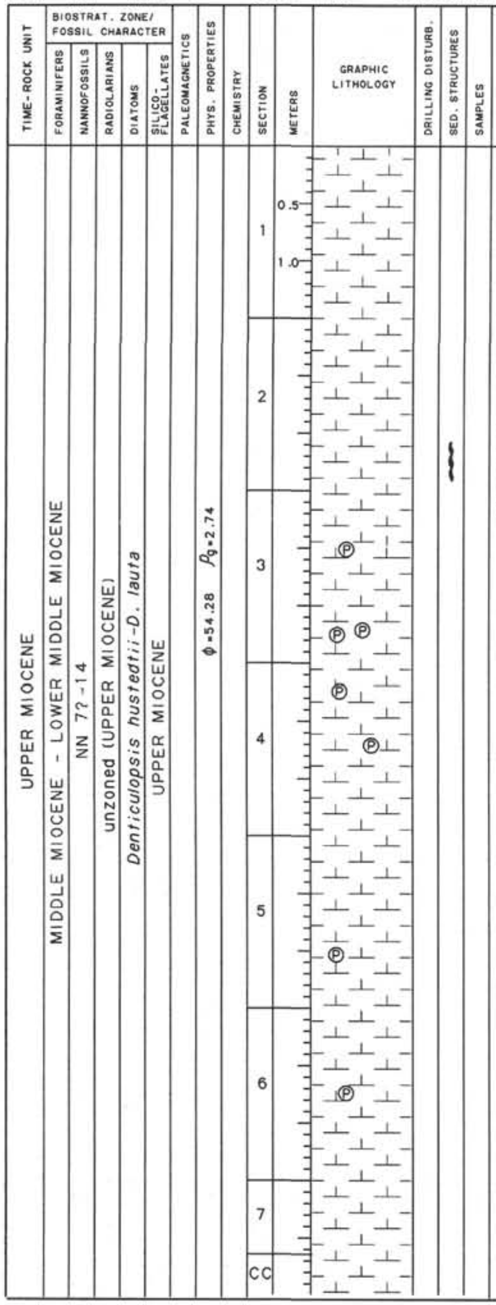

LITHOLOGIC DESCRIPTION

NANNOFOSSIL OOZE

Major lithology: Nannofossil ooze, white (7.5YR 8/0), with pyrite-bearing spots in Section 3, 53, 128, and 150 cm; Section 4, 1, 80, and 109 cm; and Section 5, 110 cm. Pyritized burrow, filled with nannofossil ooze in Section 4, 28 cm.

Bioturbation: Faint, causing mottling in Section 2, 116–150 cm.

SMEAR SLIDE SUMMARY (%):

	1, 90 D
COMPOSITION:	
Volcanic glass	Tr
Micrite	2
Foraminifers	5
Nannofossils	85
Diatoms	7
Radiolarians	1
Sponge spicules	Tr

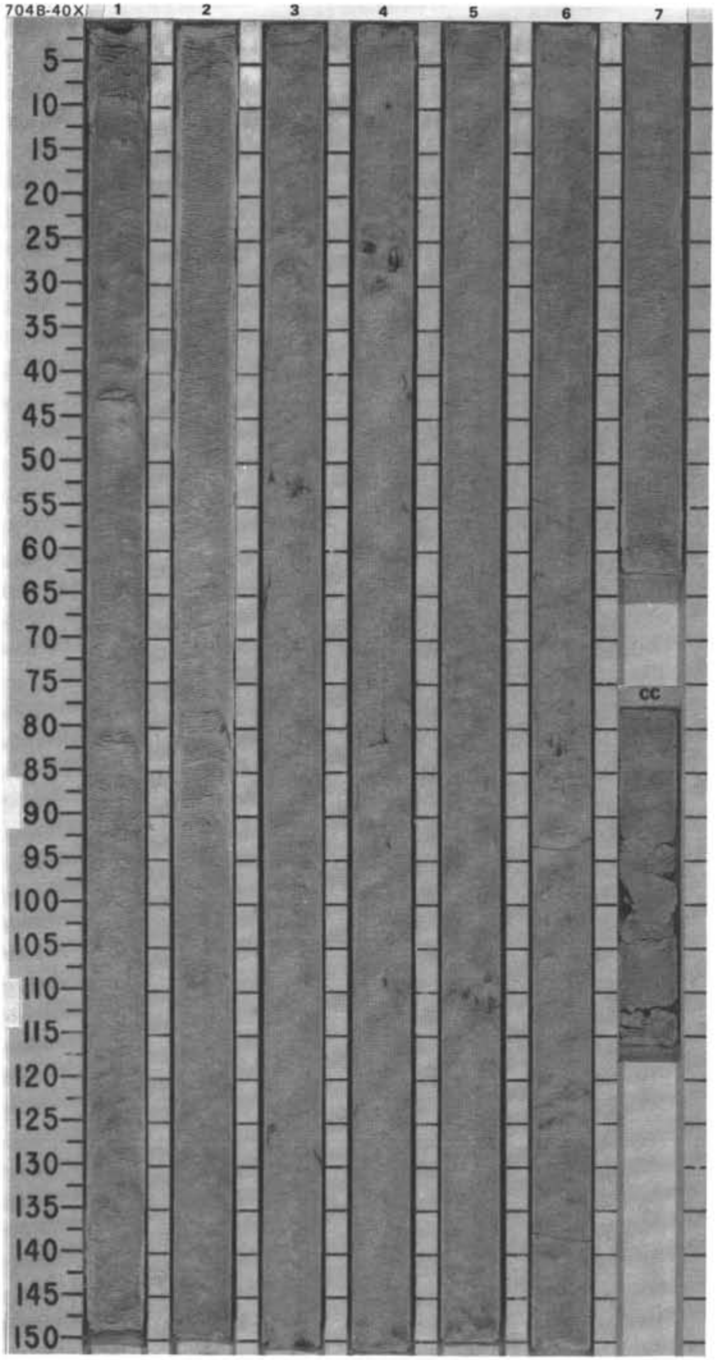

SITE 704 HOLE B CORE 41X CORED INTERVAL 2895.5-2905.0 mbsl; 375.2-384.7 mbsf

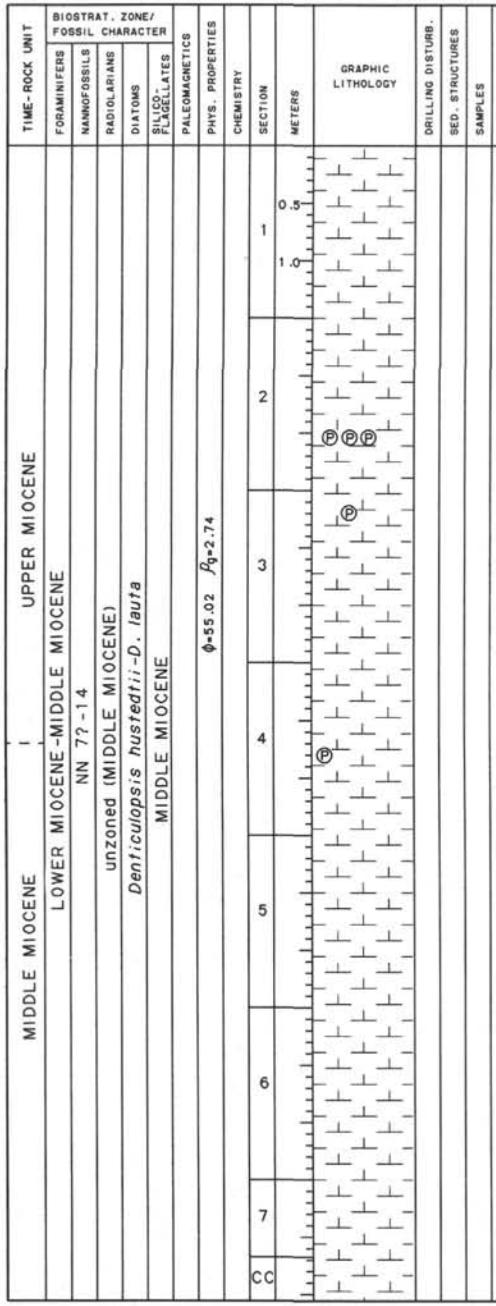

LITHOLOGIC DESCRIPTION

NANNOFOSSIL OOZE

Drilling disturbance: Slight in Section 1, 0-65 cm.

Major lithology: Nannofossil ooze, white (7.5YR 8/0) to light greenish gray (5GY 7/1). Pyrite-bearing spots in Section 2, 100-116, 120-125, and 145 cm, and Section 4, 25 and 85 cm.

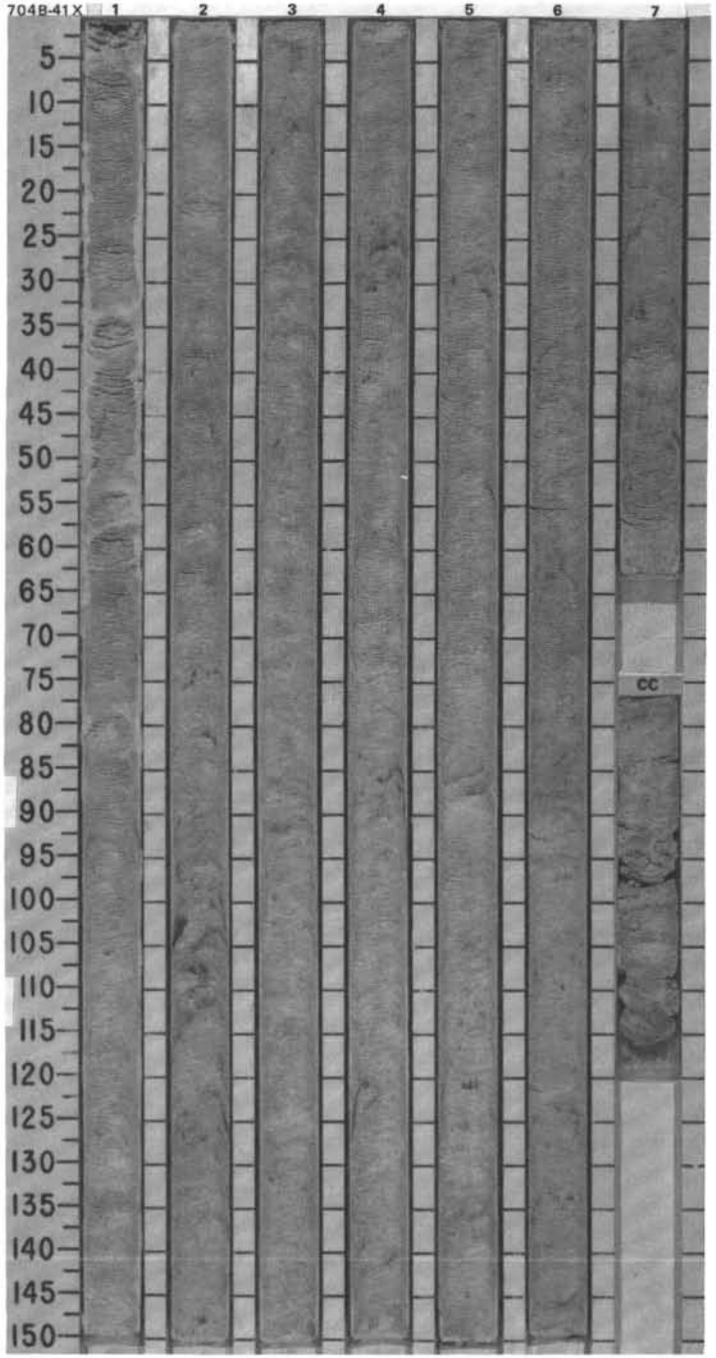

SITE 704 HOLE B CORE 42X CORED INTERVAL 2905.0-2914.5 mbsl; 384.7-394.2 mbsf

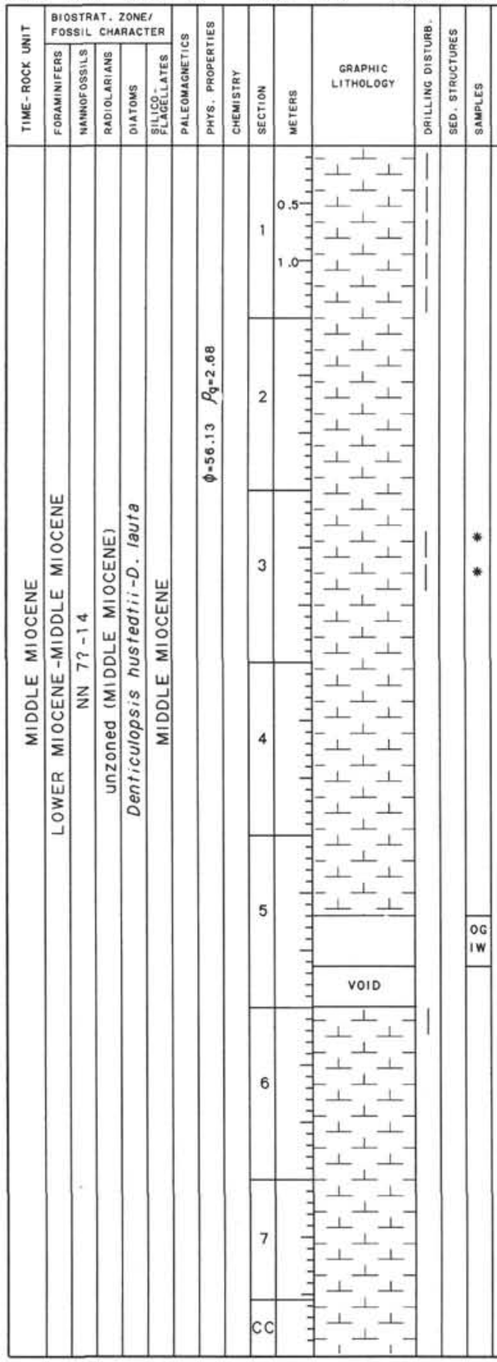

LITHOLOGIC DESCRIPTION

NANNOFOSSIL OOZE

Drilling disturbance: Slight, in Section 1 and Section 3, 40-90 cm.

Major lithology: Nannofossil ooze, white (5Y 8/1). Pyrite(?)-bearing spots in Section 2, 15 and 136 cm; Section 4, 45 cm; Section 5, 45 cm; and Section 6, 115 cm.

SMEAR SLIDE SUMMARY (%):

	3, 38 D	3, 70 D
COMPOSITION:		
Volcanic glass	—	Tr
Accessory minerals	Tr	Tr
Opaques (pyrite)	Tr	—
Foraminifers	2	3
Nannofossils	76	92
Diatoms	12	3
Radiolarians	4	Tr
Sponge spicules	1	—
Silicoflagellates	Tr	—
Micrite	4	2

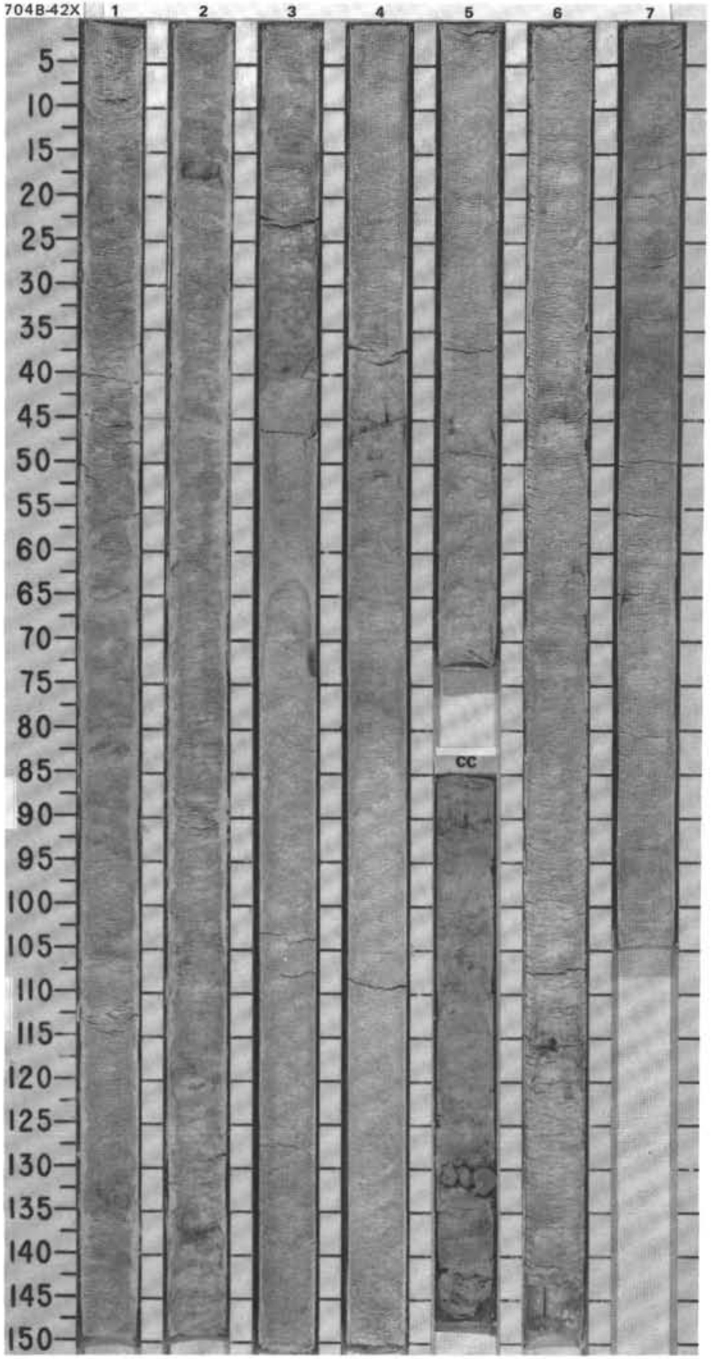

SITE 704 HOLE B CORE 43X CORED INTERVAL 2914.5-2924.0 mbsl; 394.2-403.7 mbsf

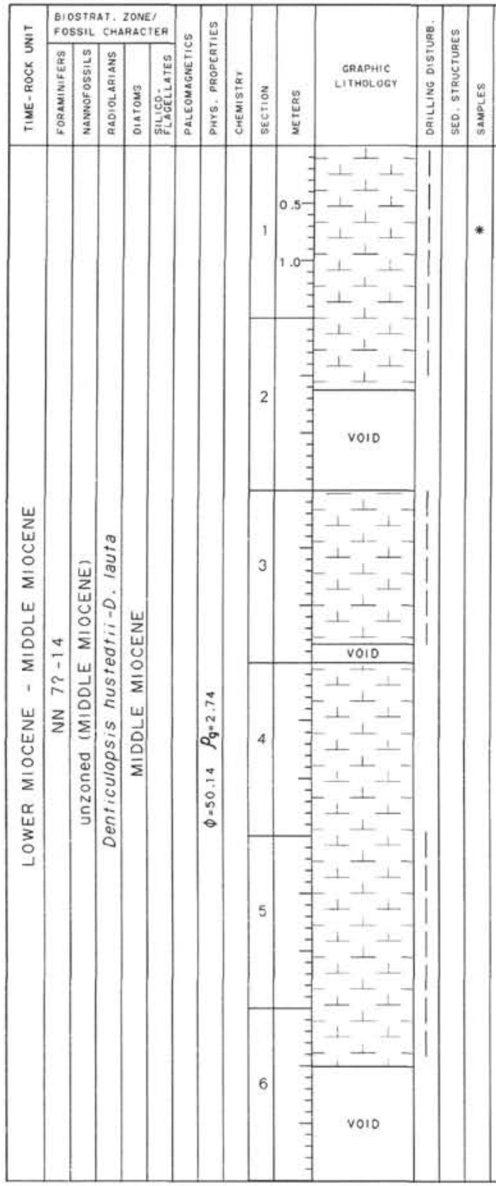

LITHOLOGIC DESCRIPTION

NANNOFOSSIL OOZE

Drilling disturbance: Slight.

Major lithology: Nannofossil ooze, white (2.5Y 8/0) to light gray (2.5Y 7/0). The latter color is concentrated on small horizons, dispersed throughout the core.

SMEAR SLIDE SUMMARY (%):

	1, 75 D
COMPOSITION:	
Nannofossils	87
Diatoms	5
Radiolarians	Tr
Micrite	8

Cont.

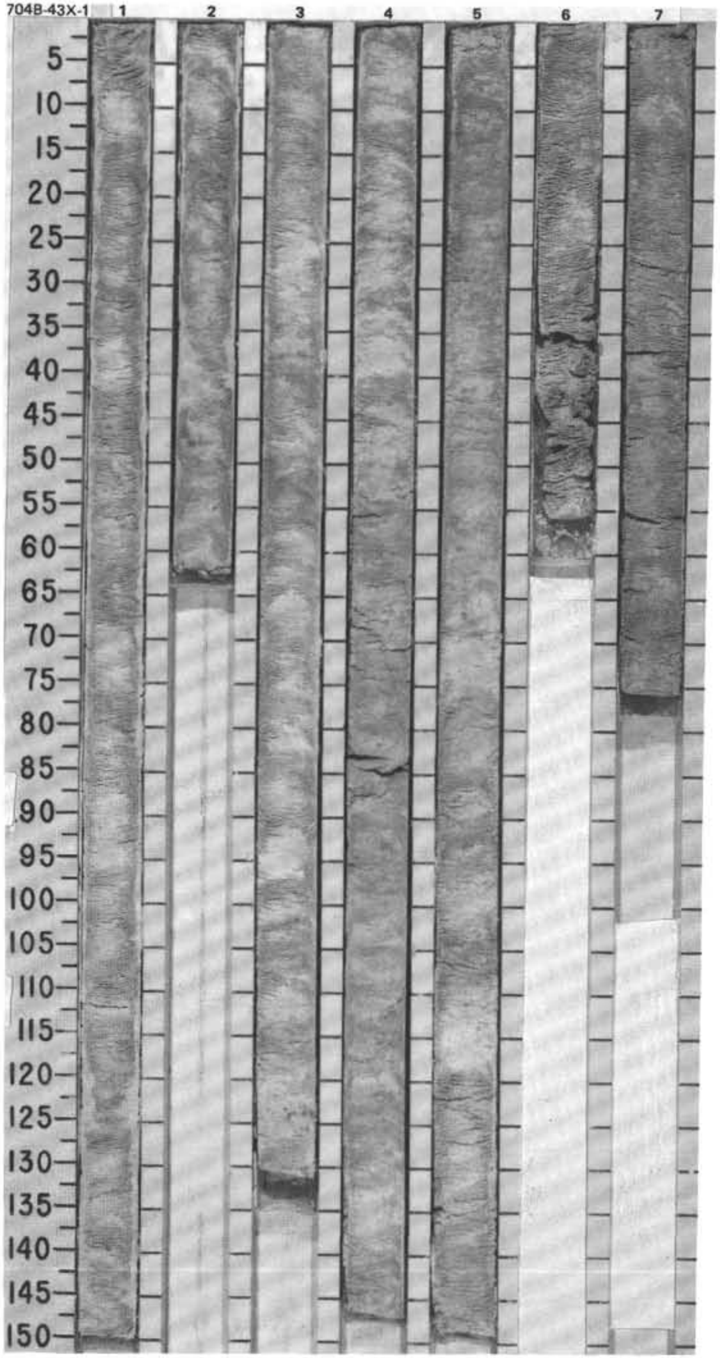

SITE 704 HOLE B CORE 43X CORED INTERVAL 2914.5-2924.0 mbsl; 394.2-403.7 mbsf

TIME-ROCK UNIT	BIOSTRAT. ZONE/ FOSSIL CHARACTER					PALEOMAGNETICS	PHYS. PROPERTIES	CHEMISTRY	SECTION	METERS	GRAPHIC LITHOLOGY	DRILLING DISTURB.	SED. STRUCTURES	SAMPLES	LITHOLOGIC DESCRIPTION
	FORAMINIFERS	NANNOFOSSILS	RADIOLARIANS	DIATOMS	SILICO-FLAGELLATES										
									7 8 CC		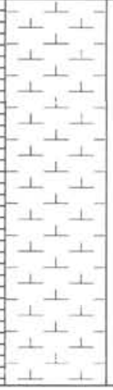				Cont.

SITE 704 HOLE B CORE 44X CORED INTERVAL 2924.0-2933.5 mbsl; 403.7-413.2 mbsf

TIME-ROCK UNIT	BIOSTRAT. ZONE/ FOSSIL CHARACTER					PALEOMAGNETICS	PHYS. PROPERTIES	CHEMISTRY	SECTION	METERS	GRAPHIC LITHOLOGY	DRILLING DISTURB.	SED. STRUCTURES	SAMPLES	LITHOLOGIC DESCRIPTION
	FORAMINIFERS	NANNOFOSSILS	RADIOLARIANS	DIATOMS	SILICO-FLAGELLATES										
MIDDLE MIOCENE	LOWER MIOCENE-MIDDLE MIOCENE	NN 7?-14	unzoned (MIDDLE MIOCENE)	*Denticulopsis hustedtii-D. lauta*	MIDDLE MIOCENE		ϕ=58.92 ρ_g=2.78		1 2 CC	0.5 1.0	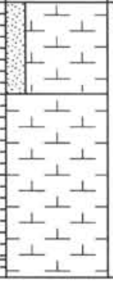				NANNOFOSSIL OOZE Drilling disturbance: Soupy to moderate in Section 1, 0-80 cm. Major lithology: Nannofossil ooze, light greenish gray (5GY 7/1), with pyrite(?)-bearing horizons in Section 2, 20 and 38 cm. Minor lithology: Sand-bearing nannofossil ooze, light greenish gray (5GY 7/1), in Section 1, 0-80 cm. Sand components are pumice, quartz, benthic foraminifers, and pyrite. Probable contamination during heat flow measurement(?).

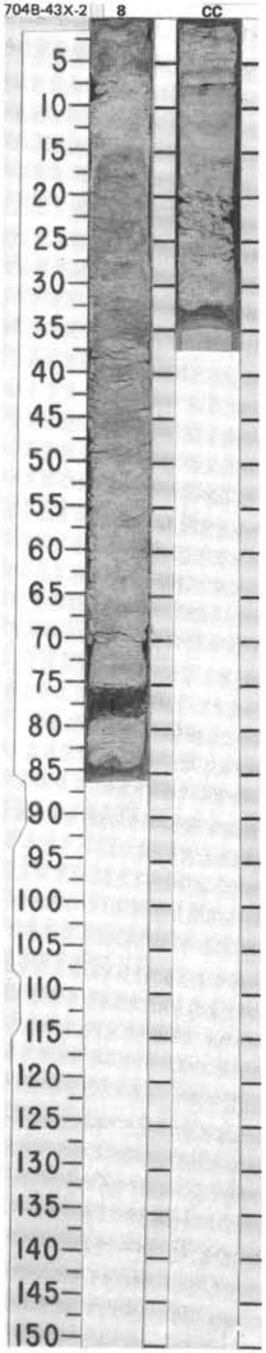

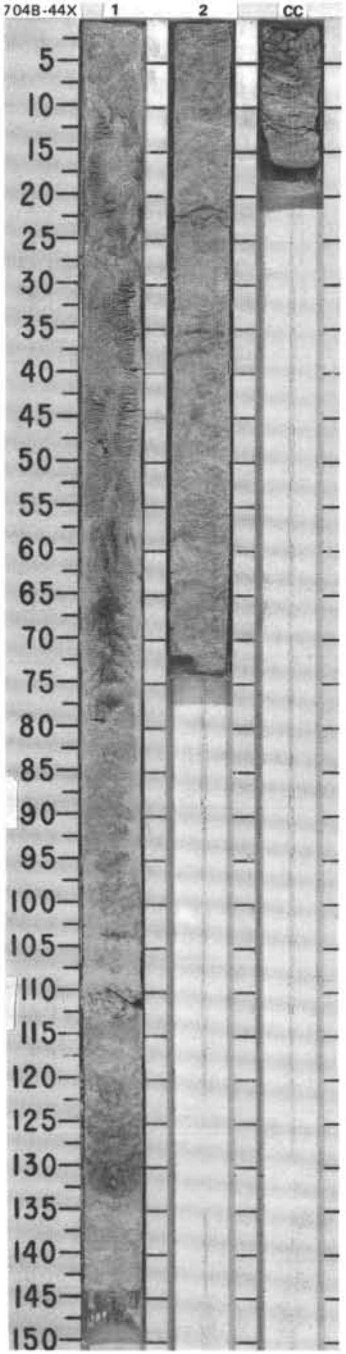

SITE 704 HOLE B CORE 45X CORED INTERVAL 2933.5-2943.0 mbsl; 413.2-422.7 mbsf

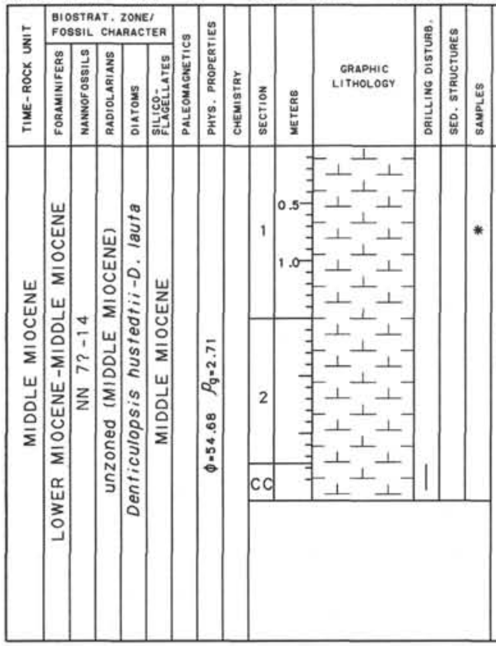

LITHOLOGIC DESCRIPTION

NANNOFOSSIL OOZE

Major lithology: Nannofossil ooze, white (7.5YR 8/0).

SMEAR SLIDE SUMMARY (%):

	1, 75 D
COMPOSITION:	
Nannofossils	84
Diatoms	8
Micrite	8

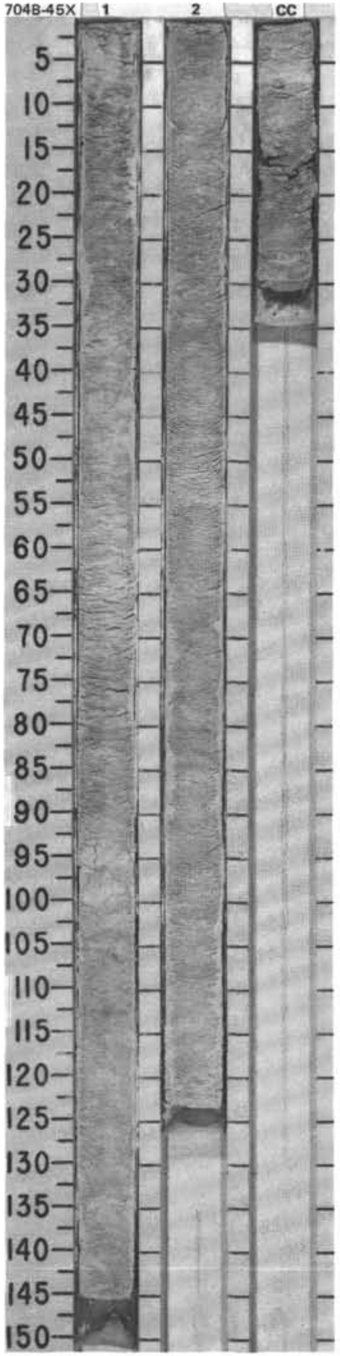

SITE 704 HOLE B CORE 46X CORED INTERVAL 2943.0-2952.5 mbsl; 422.7-432.2 mbsf

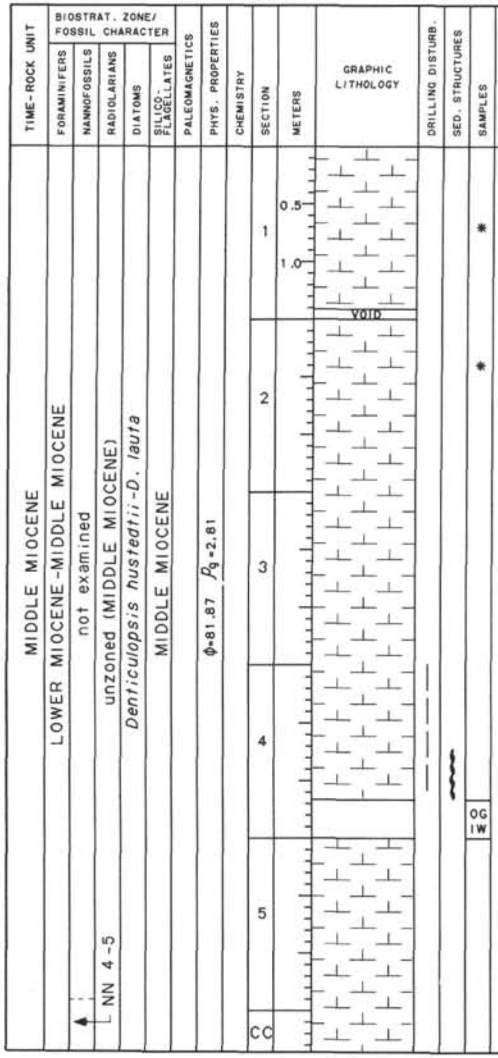

LITHOLOGIC DESCRIPTION

NANNOFOSSIL OOZE

Drilling disturbance: Slight in Section 4.

Major lithology: Nannofossil ooze, white (7.5YR 8/0) to light gray (7.5YR 7/0). Indurated chalk occurs in Section 2, 38-41 cm, and Section 4, 85-105 cm.

Minor bioturbation in Section 4.

SMEAR SLIDE SUMMARY (%):

	1, 75 D	2, 40 M
COMPOSITION:		
Feldspar	—	Tr
Volcanic glass	—	1
Accessory minerals	—	Tr
Nannofossils	92	83
Diatoms	3	4
Radiolarians	—	Tr
Micrite	5	12

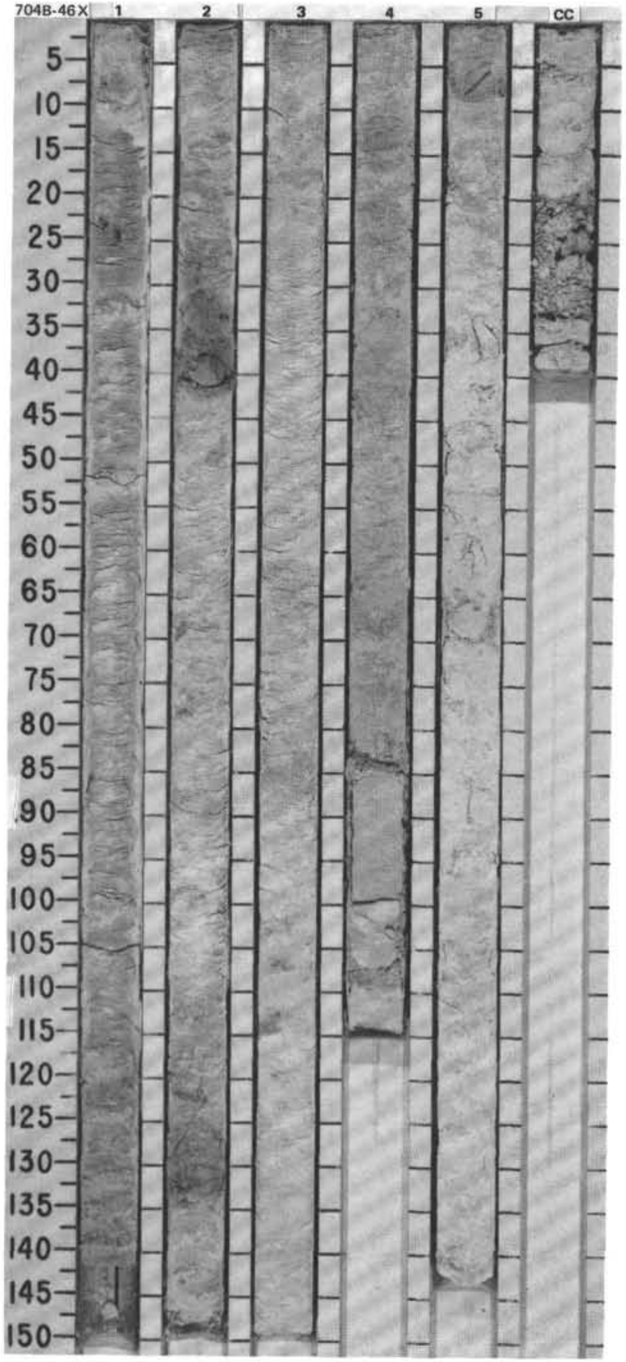

SITE 704 HOLE B CORE 47X CORED INTERVAL 2952.5-2962.0 mbsl; 432.2-441.7

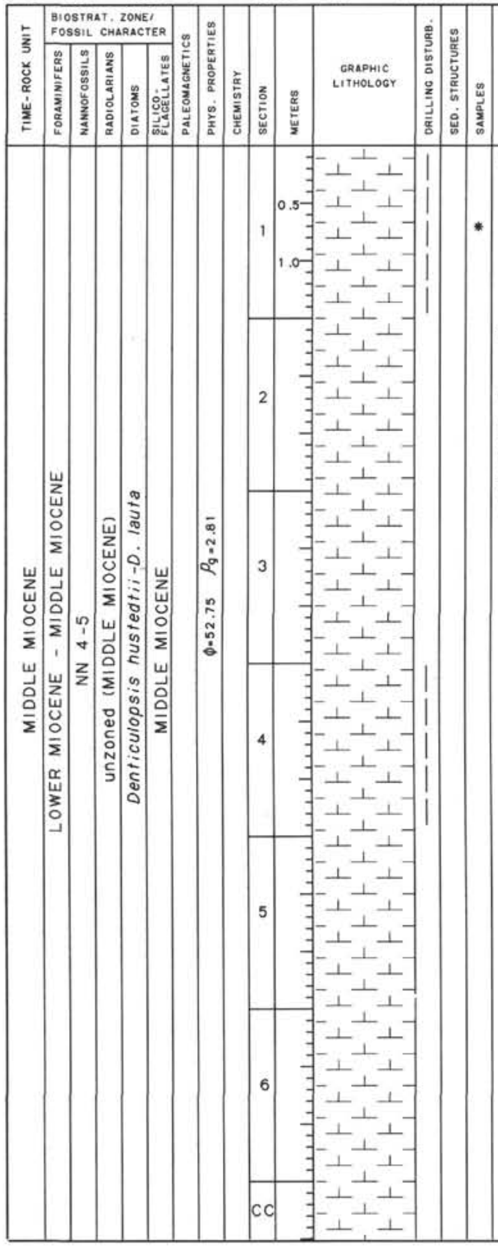

LITHOLOGIC DESCRIPTION

NANNOFOSSIL OOZE

Drilling disturbance: Slight in Section 1, and in Section 4.

Major lithology: Nannofossil ooze, white (no color code to 5Y 8/1), light greenish gray (5GY 7/1), with indurated clasts in Section 2, 100 and 130 cm; and Section 3, 50-55, 67, 77, and 108-114 cm; light yellowish brown (2.5Y 6/4) in Section 4, 137 cm, and Section 5, 124-126 cm.

SMEAR SLIDE SUMMARY (%):

	1, 70 D
COMPOSITION:	
Volcanic glass	Tr
Foraminifers	7
Nannofossils	15
Diatoms	3
Radiolarians	Tr
Micrite	15

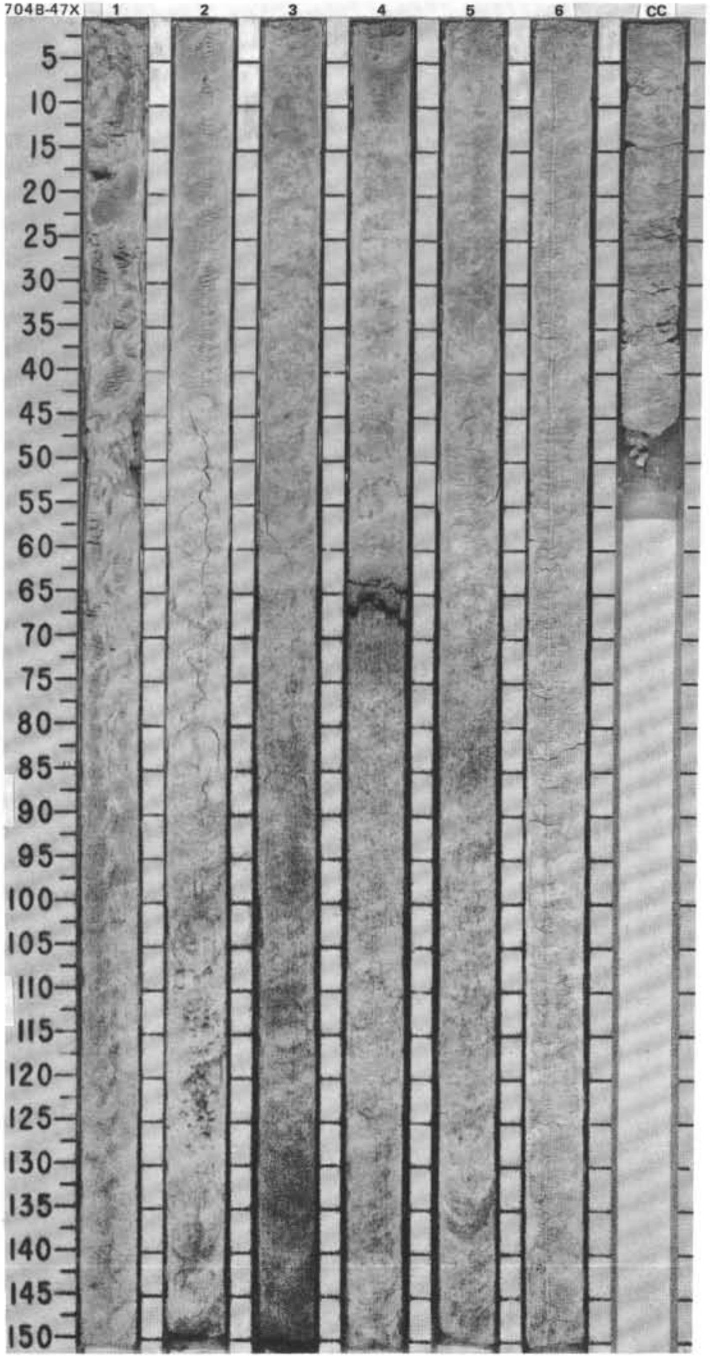

SITE 704 HOLE B CORE 48X CORED INTERVAL 2962.0-2971.5 mbsl; 441.7-451.2 mbsf

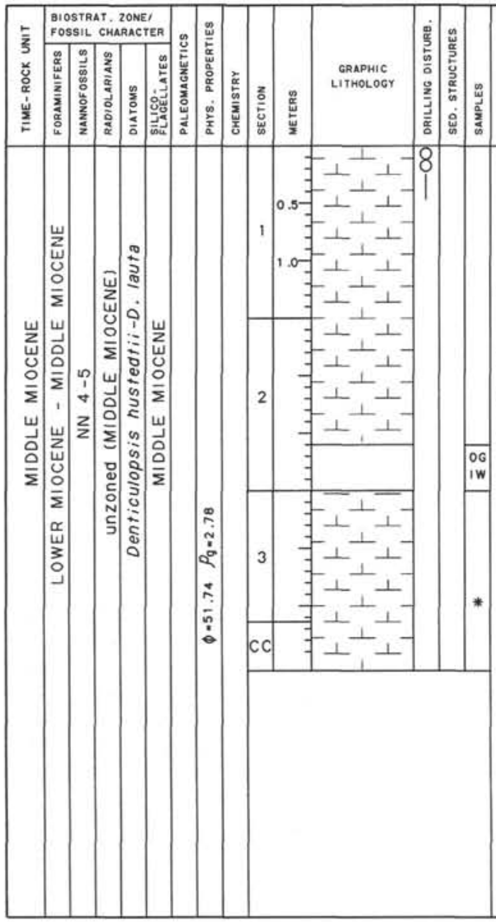

LITHOLOGIC DESCRIPTION

NANNOFOSSIL OOZE

Drilling disturbance: Soupy in Section 1, 0-15 cm; slight in Section 1, 15-30 cm, and Section 3, 0-20 cm.

Major lithology: Nannofossil ooze, light greenish gray (5GY 7/1) to white (no color code). Pyrite(?)-bearing spot in CC, 15 cm.

SMEAR SLIDE SUMMARY (%):

	3, 98 D
COMPOSITION:	
Foraminifers	7
Nannofossils	81
Diatoms	Tr
Micrite	—

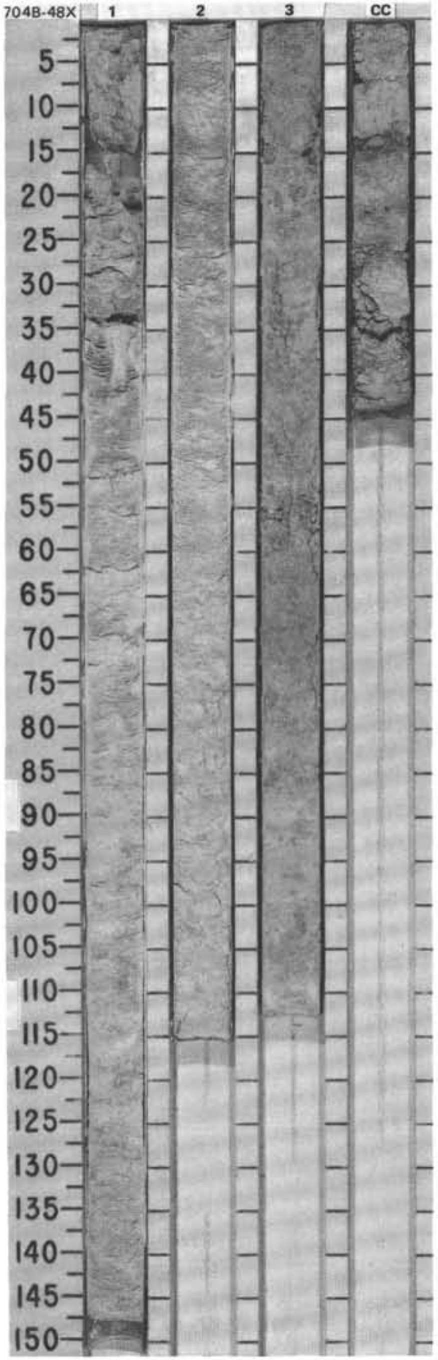

SITE 704 HOLE B CORE 49X CORED INTERVAL 2971.5-2981.0 mbsl; 451.2-460.7 mbsf

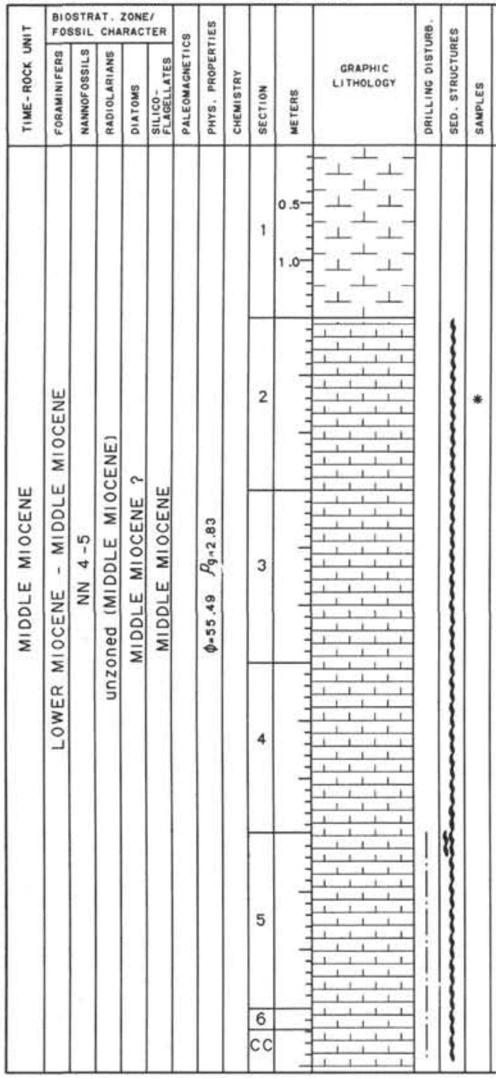

LITHOLOGIC DESCRIPTION

NANNOFOSSIL CHALK

Drilling disturbance: Moderate in Section 5.

Major lithology: Nannofossil chalk, light greenish gray (5GY 7/1). Dark gray (N4) bioturbated laminae in Section 4, 105-150 cm, and Section 5, 140-150 cm.

Minor lithology: Nannofossil ooze, white (5Y 8/1), with indurated chalk clasts in Section 1, 42-44 and 122-124 cm.

Bioturbation: Minor in the chalk. *Zoophycos* in Section 2, 98 and 116 cm; and *Chondrites* in Section 4, 105-150 cm, and Section 5, 140-150 cm.

SMEAR SLIDE SUMMARY (%):

	2, 70 D
COMPOSITION:	
Volcanic glass	1
Accessory minerals	Tr
Foraminifers	8
Nannofossils	76
Diatoms	5
Micrite	—

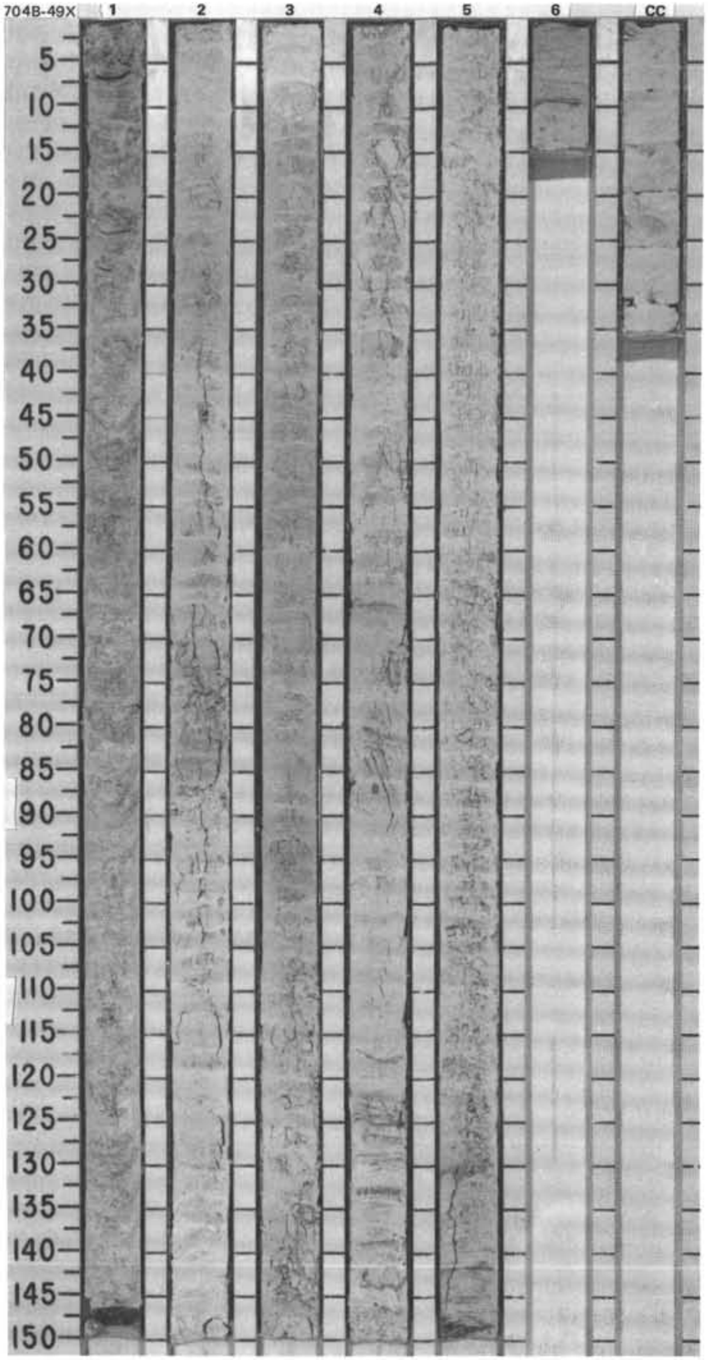

SITE 704 HOLE B CORE 50X CORED INTERVAL 2981.0-2983.0 mbsl; 460.7-462.7 mbsf

TIME-ROCK UNIT	BIOSTRAT. ZONE/ FOSSIL CHARACTER					PALEOMAGNETICS	PHYS. PROPERTIES	CHEMISTRY	SECTION	METERS	GRAPHIC LITHOLOGY	DRILLING DISTURB.	SED. STRUCTURES	SAMPLES
	FORAMINIFERS	NANNOFOSSILS	RADIOLARIANS	DIATOMS	SILICO-FLAGELLATES									
MIDDLE MIOCENE	LOWER MIOCENE-MIDDLE MIOCENE	*C. abisectus* Zone - NN 4	unzoned (MIDDLE MIOCENE)	MIDDLE MIOCENE ?	MIDDLE MIOCENE		ϕ=54.74 ρ_g=2.99		1 CC	0.5 1.0	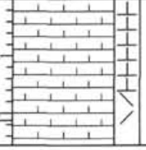			*

LITHOLOGIC DESCRIPTION

MICRITE-BEARING NANNOFOSSIL CHALK

Drilling disturbance: Biscuits.

Major lithology: Micrite-bearing nannofossil chalk, white (no color code).

SMEAR SLIDE SUMMARY (%):

	1, 30 D
COMPOSITION:	
Nannofossils	75
Diatoms	TR
Radiolarians	Tr
Sponge spicules	2
Micrite	20
Fragmented carbonate	3

SITE 704 HOLE B CORE 51X CORED INTERVAL 2983.0-2992.5 mbsl; 462.7-472.2 mbsf

TIME-ROCK UNIT	BIOSTRAT. ZONE/ FOSSIL CHARACTER					PALEOMAGNETICS	PHYS. PROPERTIES	CHEMISTRY	SECTION	METERS	GRAPHIC LITHOLOGY	DRILLING DISTURB.	SED. STRUCTURES	SAMPLES
	FORAMINIFERS	NANNOFOSSILS	RADIOLARIANS	DIATOMS	SILICO-FLAGELLATES									
MIDDLE MIOCENE	LOWER MIOCENE-MIDDLE MIOCENE	*C. abisectus* Zone - NN 4	unzoned (MIDDLE MIOCENE)	MIDDLE MIOCENE ?	MIDDLE MIOCENE				1 CC	0.5 1.0	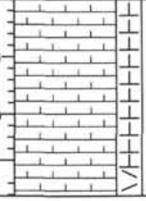			*

LITHOLOGIC DESCRIPTION

MICRITE-BEARING NANNOFOSSIL CHALK

Drilling disturbance: Drilling biscuits.

Major lithology: Micrite-bearing nannofossil chalk, white (no color code).

SMEAR SLIDE SUMMARY (%):

	1, 74 D
COMPOSITION:	
Volcanic glass	Tr
Foraminifers	5
Nannofossils	60
Sponge spicules	Tr
Micrite	20
Fragmented carbonate	15

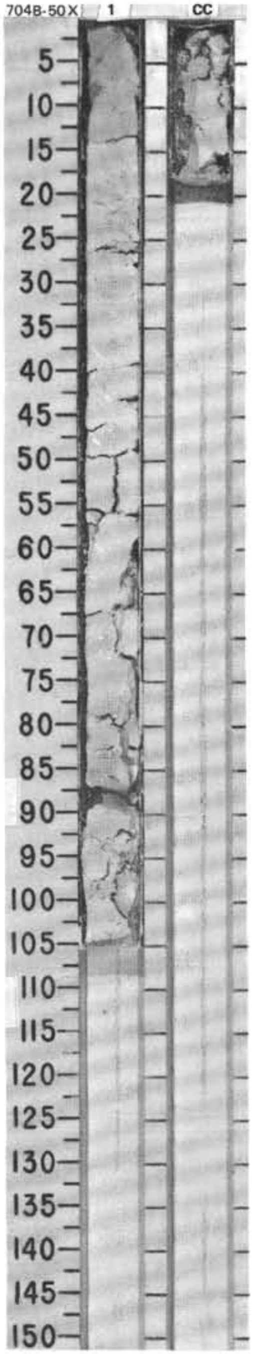

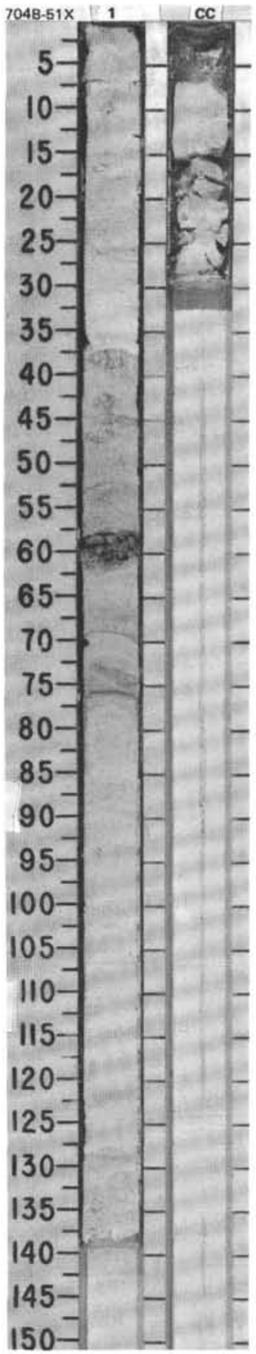

SITE 704 HOLE B CORE 52X CORED INTERVAL 2992.5-3002.0 mbsl; 472.2-481.7 mbsf

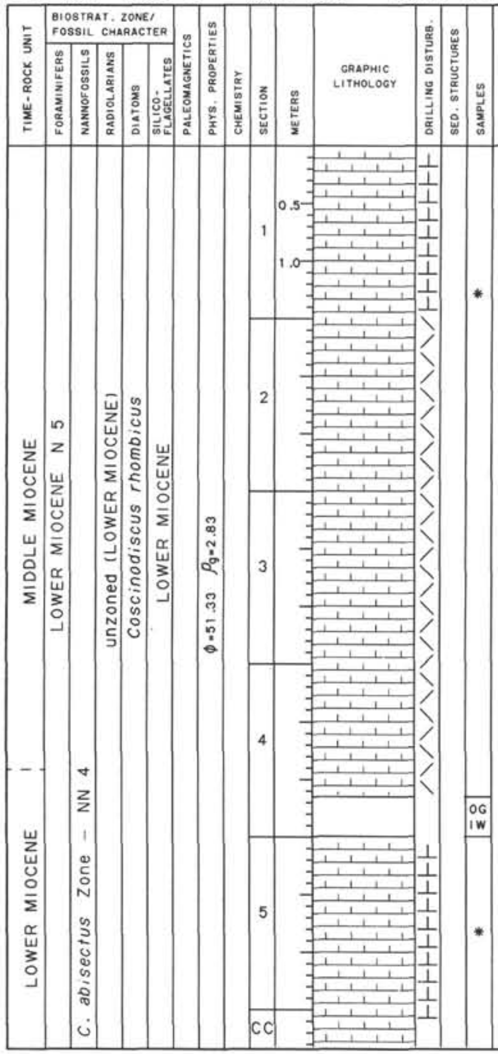

LITHOLOGIC DESCRIPTION

MICRITE-BEARING NANNOFOSSIL CHALK

Drilling disturbance: Biscuiting throughout.

Major lithology: Micrite-bearing nannofossil chalk, white (no color code).

Minor lithology: Pumice in Section 2, 20 cm.

SMEAR SLIDE SUMMARY (%):

	1, 125 D	5, 80 D
COMPOSITION:		
Foraminifers	Tr	Tr
Nannofossils	77	80
Diatoms	Tr	—
Radiolarians	Tr	Tr
Sponge spicules	Tr	Tr
Micrite	20	20
Fragmented carbonate	3	—

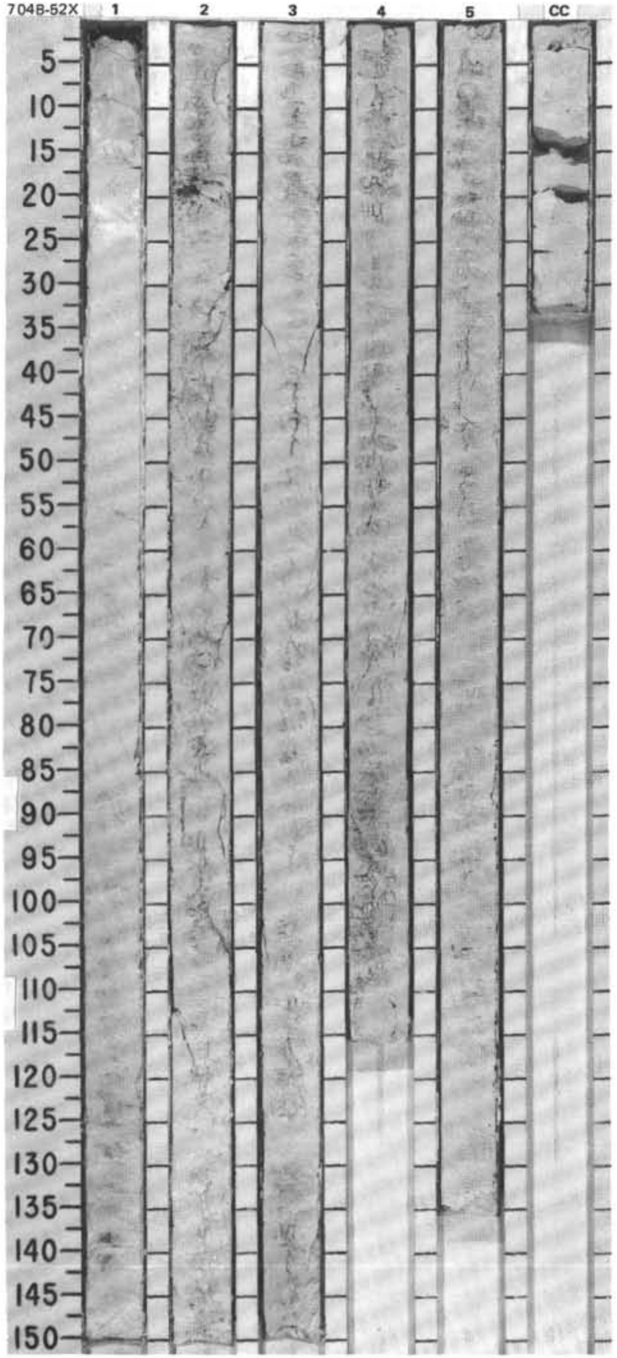

SITE 704 HOLE B CORE 53X CORED INTERVAL 3002.0-3011.5 mbsl; 481.7-491.2 mbsf

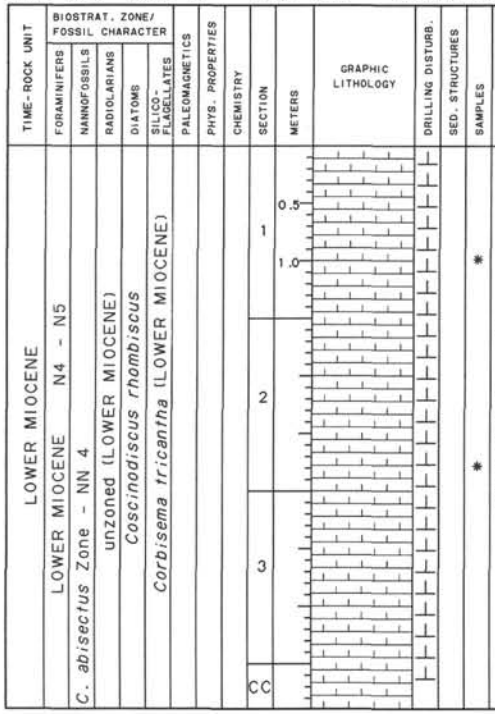

LITHOLOGIC DESCRIPTION

MICRITE-BEARING NANNOFOSSIL CHALK

Drilling disturbance: Biscuiting throughout.

Major lithology: Micrite-bearing nannofossil chalk, white (no color code) and light gray (5Y 7/1).

Minor lithology: Schist pebble (downhole contamination?) in Section 1, 8-9 cm.

SMEAR SLIDE SUMMARY (%):

	1, 100 M	3, 120 D
COMPOSITION:		
Volcanic glass	3	—
Foraminifers	2	5
Nannofossils	58	60
Radiolarians	—	Tr
Sponge spicules	2	Tr
Micrite	30	30
Fragmented carbonate	5	5

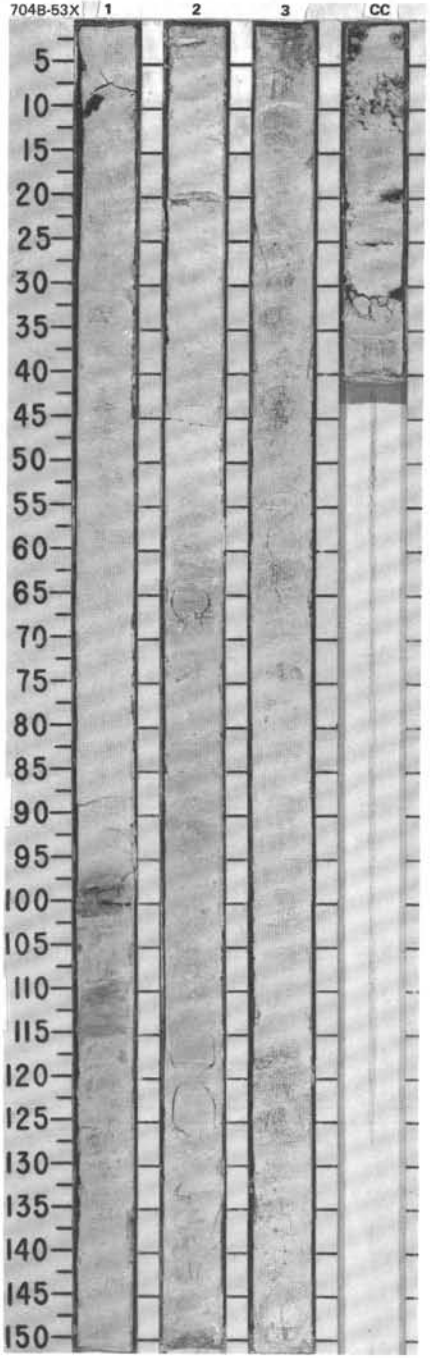

SITE 704 HOLE B CORE 54X CORED INTERVAL 3011.5-3021.0 mbsl; 491.2-500.7 mbsf

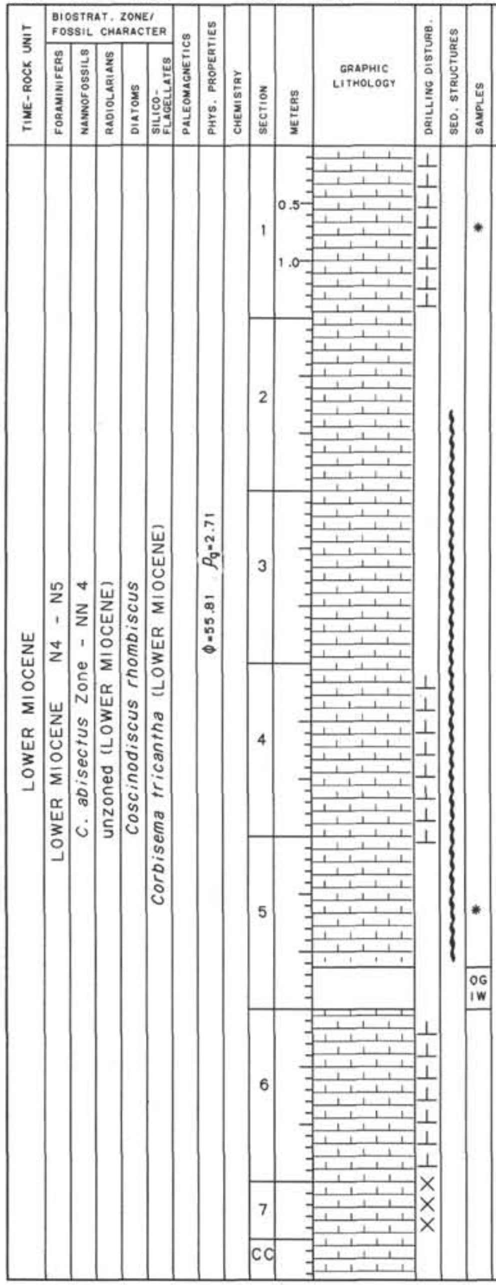

LITHOLOGIC DESCRIPTION

MICRITIC NANNOFOSSIL CHALK (INDURATED)

Drilling disturbance: Biscuiting in Sections 1, 4, 6, and 7.

Major lithology: Micritic nannofossil chalk, white (no color code and 5Y 8/1), gray (N6), light gray (N7); minor bioturbation, mainly *Zoophycos*.

SMEAR SLIDE SUMMARY (%):

	1, 70 D	5, 70 D
COMPOSITION:		
Foraminifers	2	3
Nannofossils	65	61
Diatoms	1	Tr
Radiolarians	Tr	Tr
Sponge spicules	2	1
Micrite	30	30
Fragmented carbonate	—	5

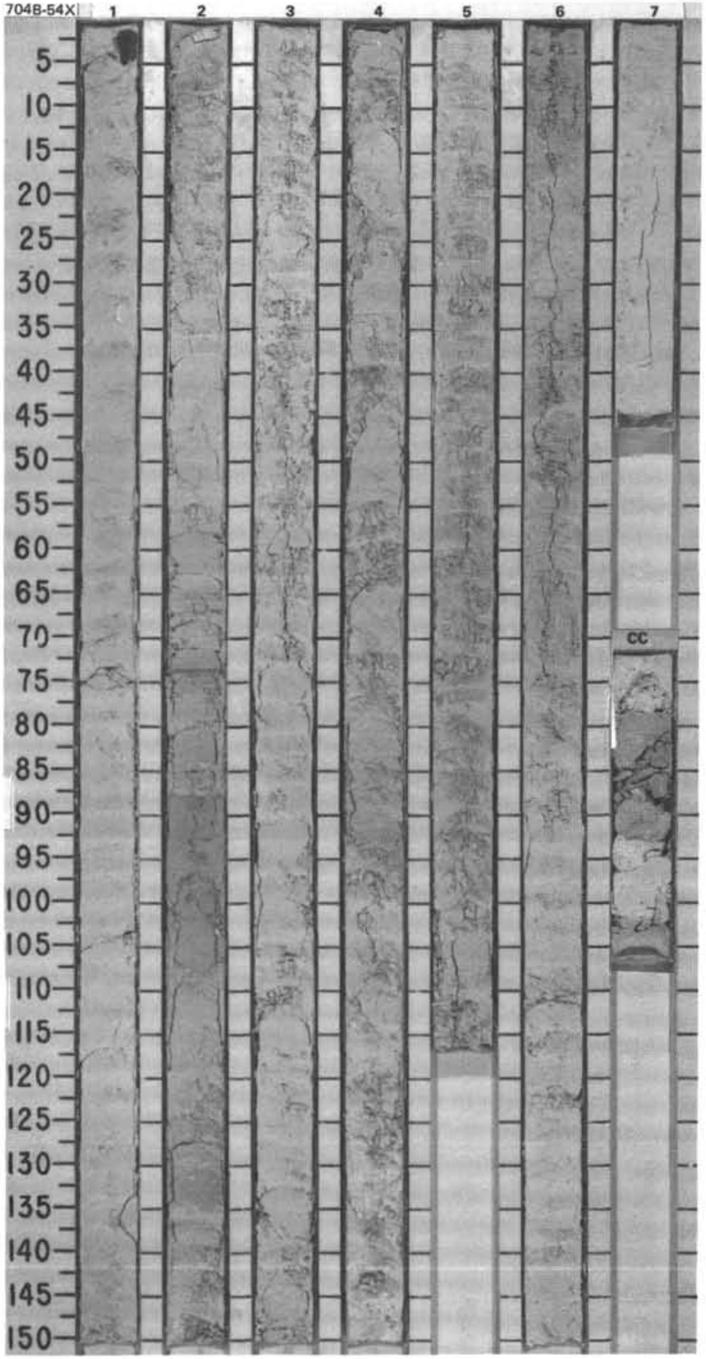

SITE 704 HOLE B CORE 55X CORED INTERVAL 3021.0-3030.5 mbsl; 500.7-510.2 mbsf

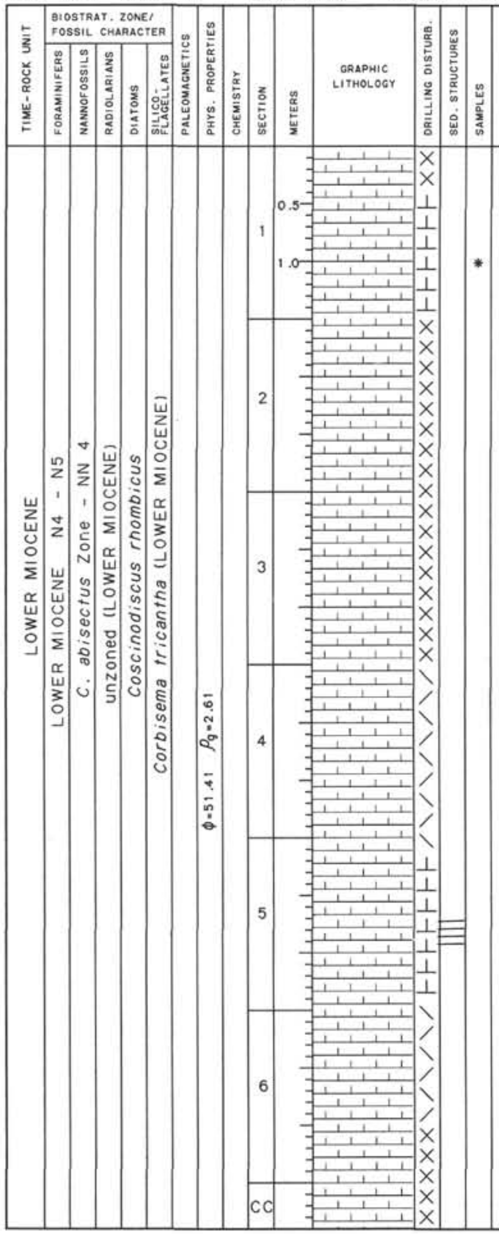

LITHOLOGIC DESCRIPTION

MICRITIC NANNOFOSSIL CHALK (INDURATED)

Drilling disturbance: Fracturing and biscuiting throughout.

Major lithology: Micritic nannofossil chalk, white (no color code) and light gray (5Y 7/1).

SMEAR SLIDE SUMMARY (%):

	1, 105 D
COMPOSITION:	
Clay	5
Volcanic glass	Tr
Accessory minerals	Tr
Nannofossils	65
Diatoms	Tr
Radiolarians	Tr
Sponge spicules	Tr
Micrite	—

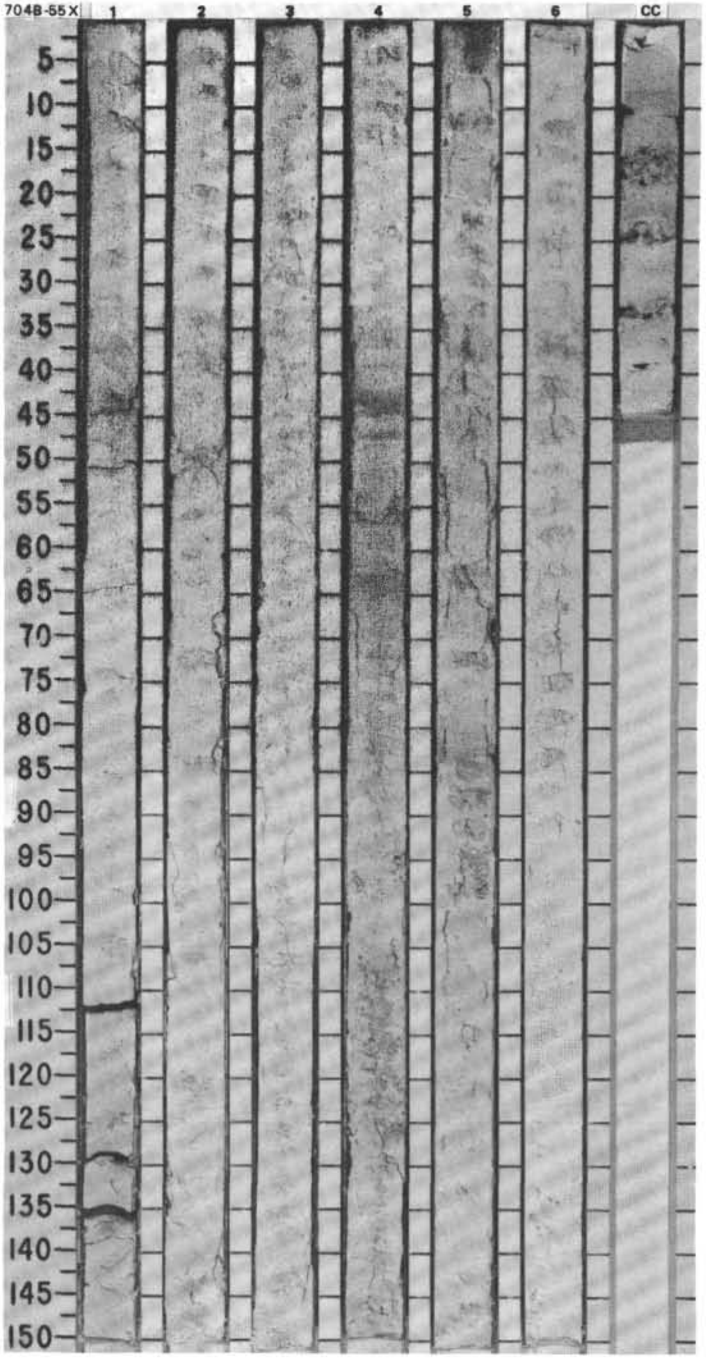

SITE 704 HOLE B CORE 56X CORED INTERVAL 3030.5-3040.0 mbsl; 510.2-519.7 mbsf

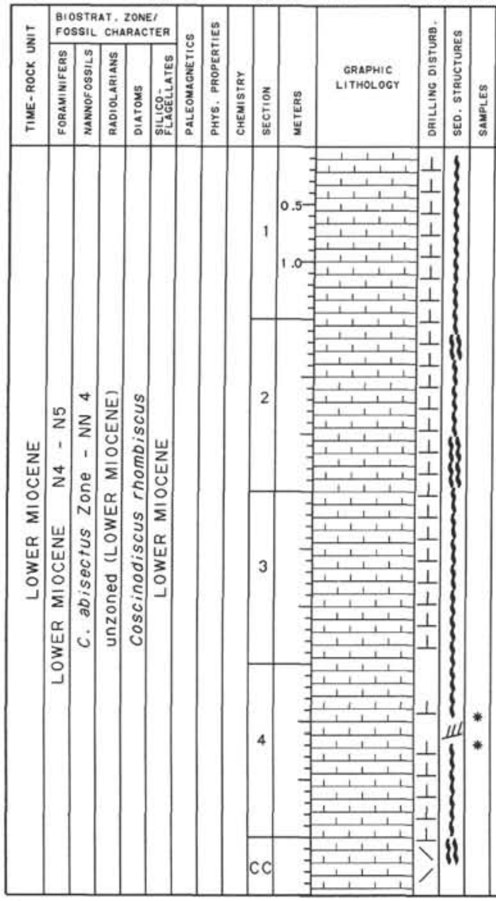

LITHOLOGIC DESCRIPTION

MICRITIC NANNOFOSSIL CHALK (INDURATED)

Drilling disturbance: Fracturing and biscuiting throughout.

Major lithology: Micritic nannofossil chalk, white (5Y 8/1, 10YR 8/1) and light gray (5Y 7/1). Micro-cross-laminae in Section 4, 37-68 cm, indicating turbidite. Bioturbated throughout, mainly *Zoophycos* and *Planolites*.

SMEAR SLIDE SUMMARY (%):

	4, 55 M	4, 73 D
COMPOSITION:		
Feldspar	Tr	—
Clay	11	5
Volcanic glass	2	1
Foraminifers	5	—
Nannofossils	42	54
Diatoms	Tr	—
Micrite	40	40

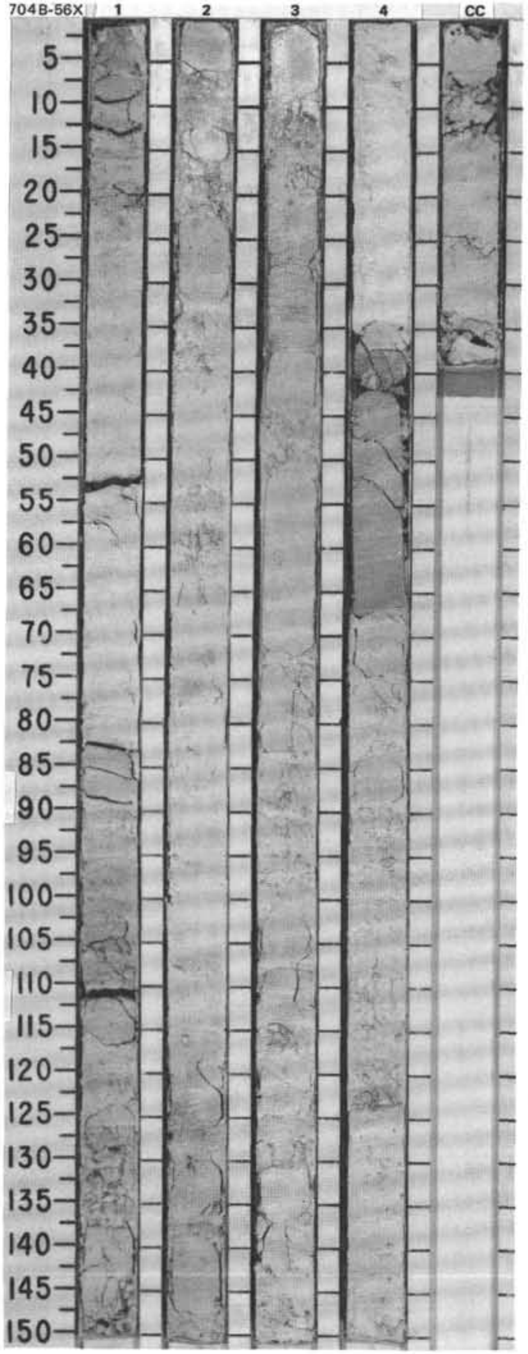

SITE 704 HOLE B CORE 57X CORED INTERVAL 3040.0-3049.5 mbsl; 519.7-529.2 mbsf

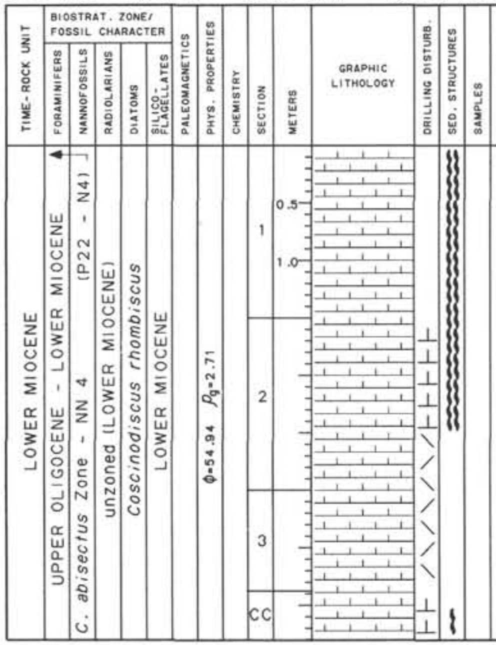

LITHOLOGIC DESCRIPTION

MICRITIC NANNOFOSSIL CHALK (INDURATED)

Drilling disturbance: Biscuiting and fracturing throughout.

Major lithology: Micritic nannofossil chalk, white (no color code and 5Y 8/1) and light gray (5Y 7/1). Moderately bioturbated, Section 1 and Section 2, 0-100 cm.

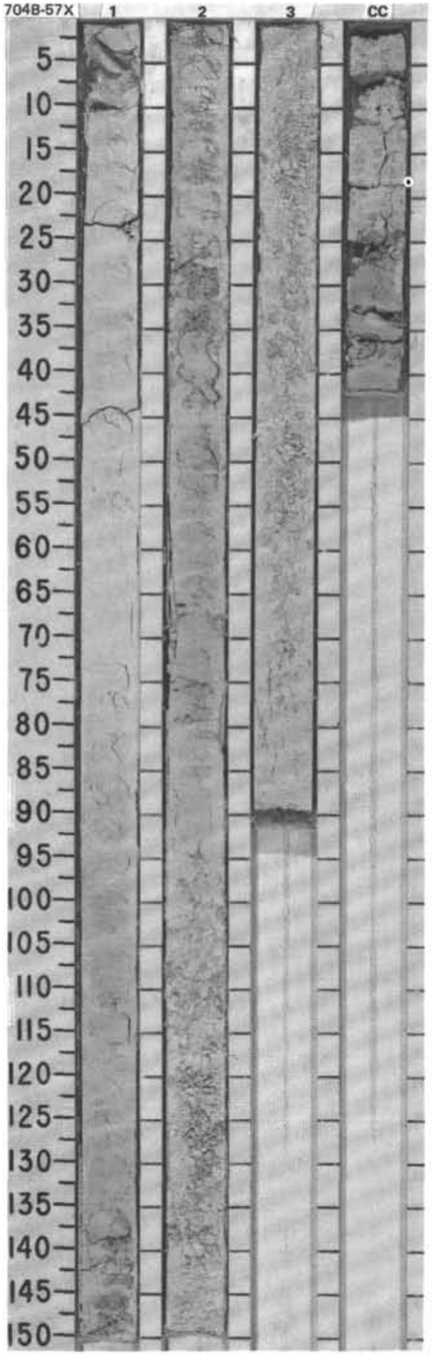

SITE 704 HOLE B CORE 58X CORED INTERVAL 3049.5-3059.0 mbsl; 529.2-538.7 mbsf

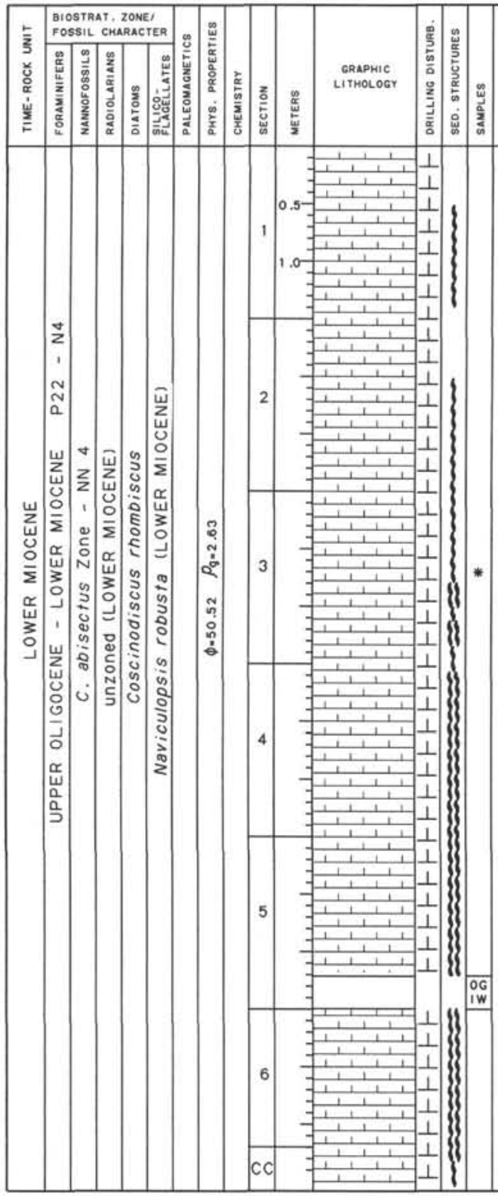

LITHOLOGIC DESCRIPTION

MICRITIC NANNOFOSSIL CHALK (INDURATED)

Drilling disturbance: Biscuited and fractured throughout.

Major lithology: Micritic nannofossil chalk, white (10YR 8/1), bioturbated throughout.

SMEAR SLIDE SUMMARY (%):

	3, 75 D
COMPOSITION:	
Clay	5
Volcanic glass	Tr
Micrite	30
Nannofossils	65
Diatoms	Tr

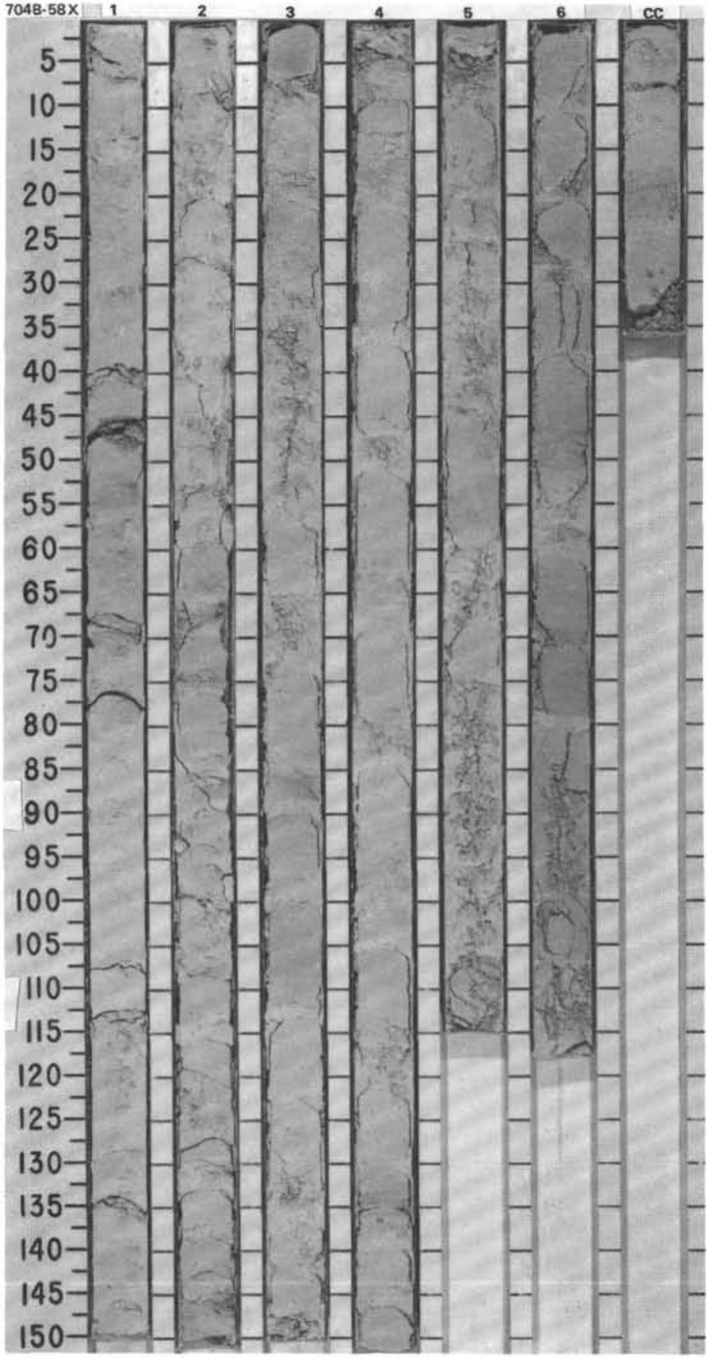

SITE 704 HOLE B CORE 59X CORED INTERVAL 3059.0-3068.5 mbsl; 538.7-548.2 mbsf

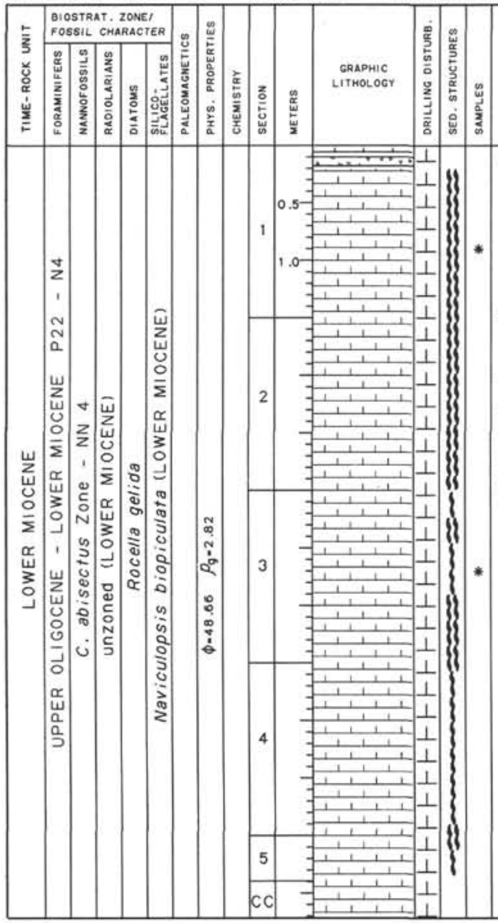

LITHOLOGIC DESCRIPTION

MICRITIC NANNOFOSSIL CHALK (INDURATED)

Drilling disturbance: Biscuited and fractured throughout.

Major lithology: Micritic nannofossil chalk, white (10YR 8/1), bioturbated throughout.

Minor lithology: Volcanic breccia in Section 1, 10-15 cm.

SMEAR SLIDE SUMMARY (%):

	1, 141 M	3, 70 D
COMPOSITION:		
Clay	15	5
Volcanic glass	4	Tr
Foraminifers	Tr	—
Nannofossils	41	55
Diatoms	Tr	—
Sponge spicules	Tr	—
Micrite	40	40

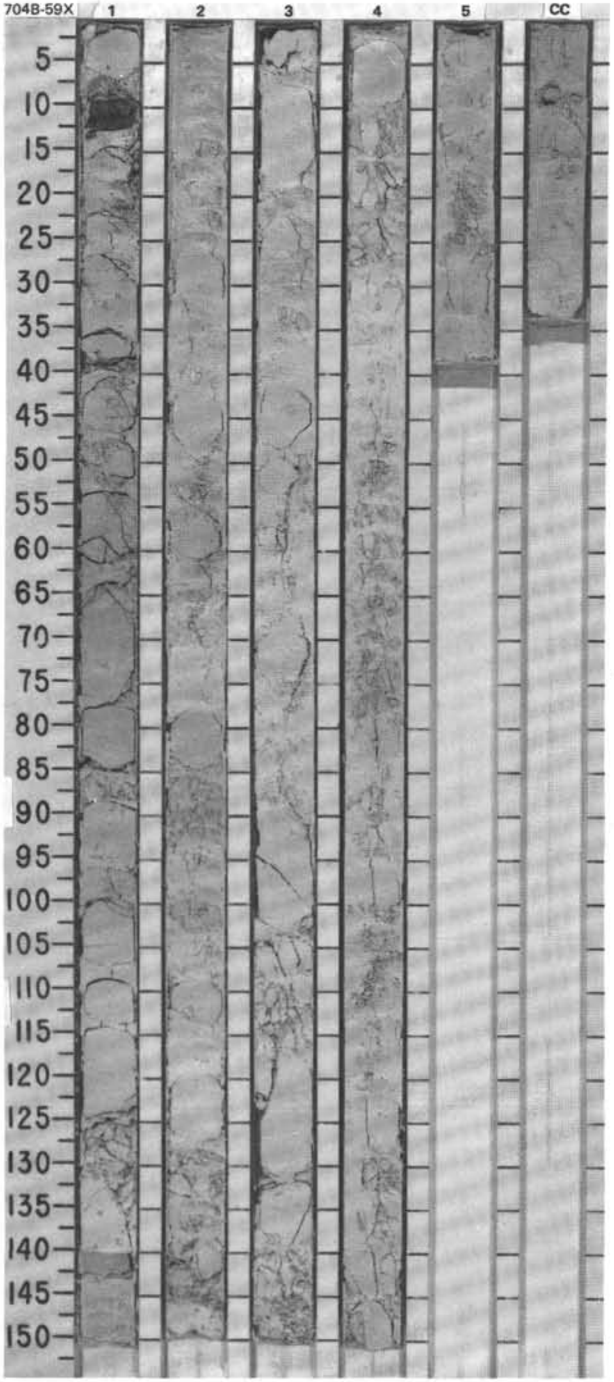

SITE 704 HOLE B CORE 60X CORED INTERVAL 3068.5-3078.0 mbsl; 548.2-557.7 mbsf

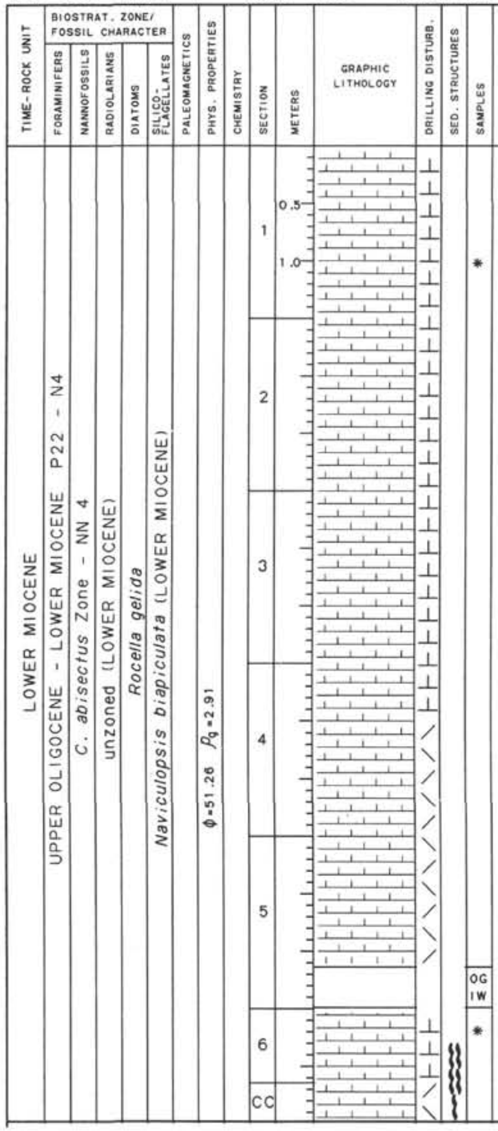

LITHOLOGIC DESCRIPTION

MICRITIC NANNOFOSSIL CHALK (INDURATED)

Drilling disturbance: Biscuited and fractured throughout.

Major lithology: Micritic nannofossil chalk, white (10YR 8/1) and light gray (5Y 7/1).

SMEAR SLIDE SUMMARY (%):

	1, 106 D	6, 20 M
COMPOSITION:		
Clay	5	15
Volcanic glass	Tr	1
Accessory minerals:		
Opaques	—	Tr
Foraminifers	Tr	1
Nannofossils	50	48
Diatoms	Tr	Tr
Micrite	45	35

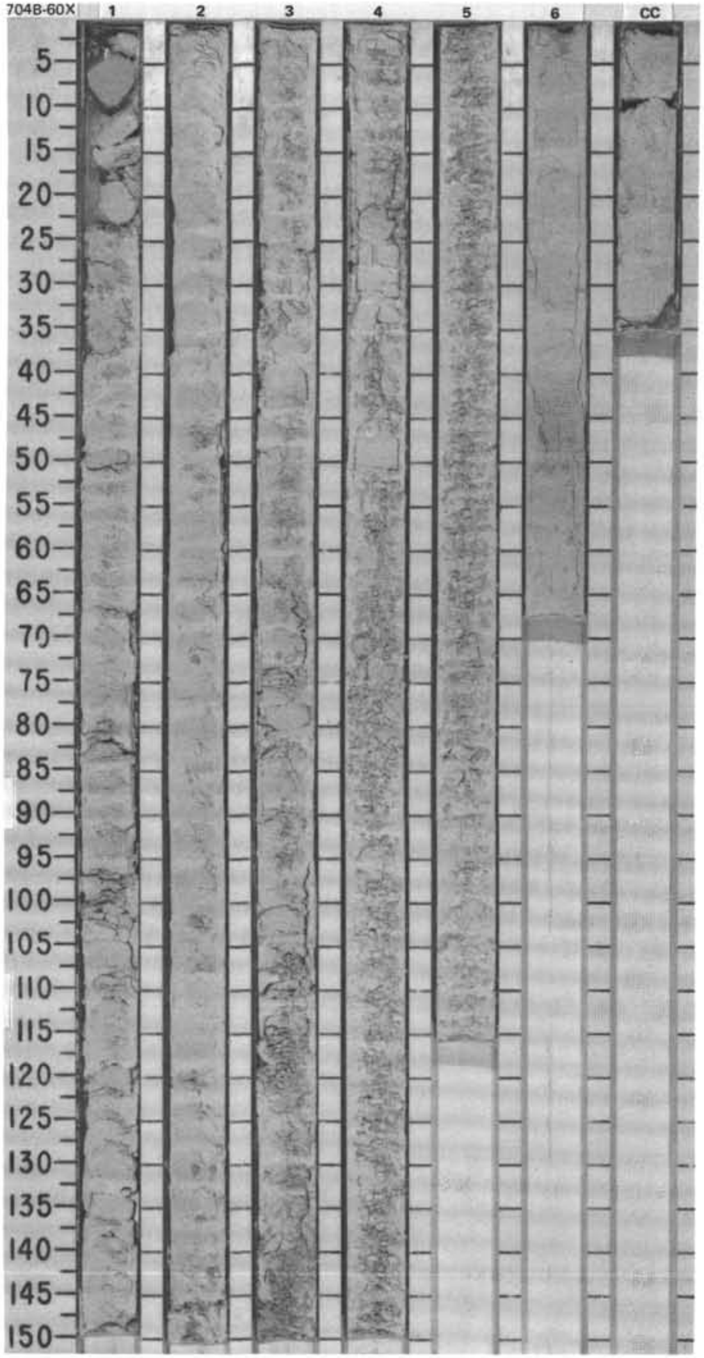

SITE 704 HOLE B CORE 61X CORED INTERVAL 3078.0-3087.5 mbsl; 557.7-567.2 mbsf

TIME-ROCK UNIT	BIOSTRAT. ZONE/ FOSSIL CHARACTER					PALEOMAGNETICS	PHYS. PROPERTIES	CHEMISTRY	SECTION	METERS	GRAPHIC LITHOLOGY	DRILLING DISTURB.	SED. STRUCTURES	SAMPLES	LITHOLOGIC DESCRIPTION
	FORAMINIFERS	NANNOFOSSILS	RADIOLARIANS	DIATOMS	SILICO-FLAGELLATES										
LOWER MIOCENE	UPPER OLIGOCENE - LOWER MIOCENE P22 - N4	*C. abisectus* Zone - NN 4	unzoned (LOWER MIOCENE)	*Rocella gelida*	*Naviculopsis biapiculata* (LOWER MIOCENE)		ϕ=49.29 ρ_g=2.85		1 2 CC	0.5 1.0	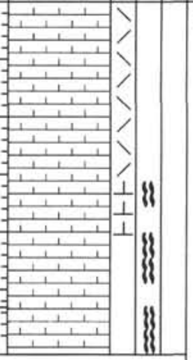				MICRITIC NANNOFOSSIL CHALK (INDURATED) Drilling disturbance: Biscuited and fractured throughout. Major lithology: Micritic nannofossil chalk, white (10YR 8/1) to light gray (10YR 7/1). *Zoophycos* and *Planolites* burrows.

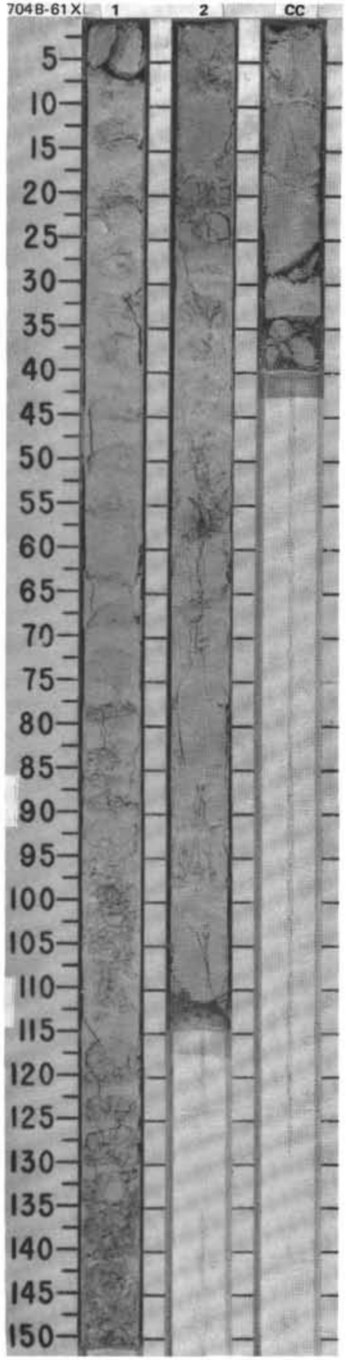

SITE 704 HOLE B CORE 62X CORED INTERVAL 3087.5-3097.0 mbsl; 567.2-576.7 mbsf

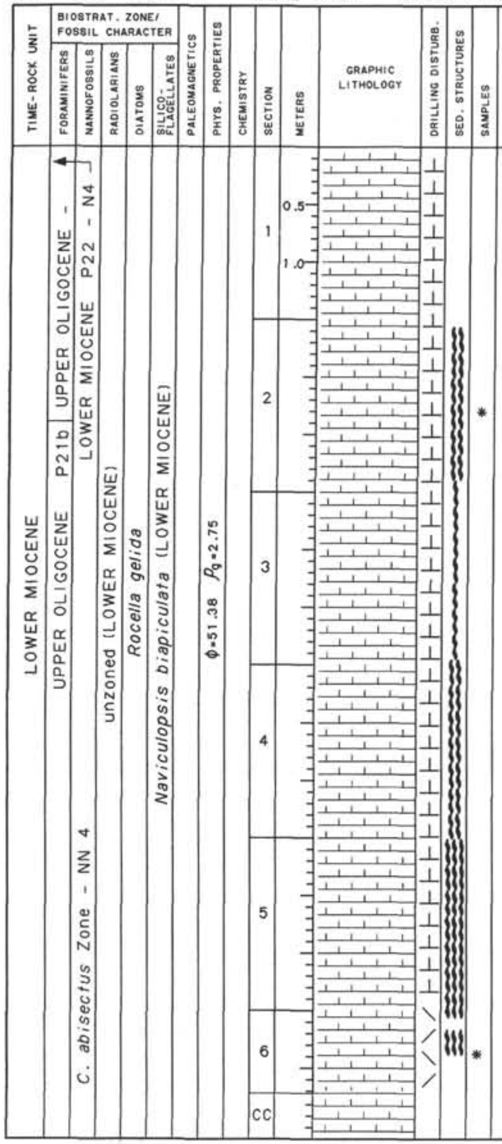

LITHOLOGIC DESCRIPTION

MICRITIC NANNOFOSSIL CHALK (INDURATED)

Drilling disturbance: Biscuited and fractured throughout.

Major lithology: Micritic nannofossil chalk, white (10YR 8/1) and gray (10YR 7/1). Moderately to highly bioturbated by *Planolites*, *Chondrites*, and *Zoophycos*.

SMEAR SLIDE SUMMARY (%):

	2, 80 D	6, 40 D
COMPOSITION:		
Volcanic glass	1	1
Foraminifers	3	10
Nannofossils	64	53
Diatoms	5	2
Radiolarians	Tr	2
Sponge spicules	6	2
Micrite	20	30

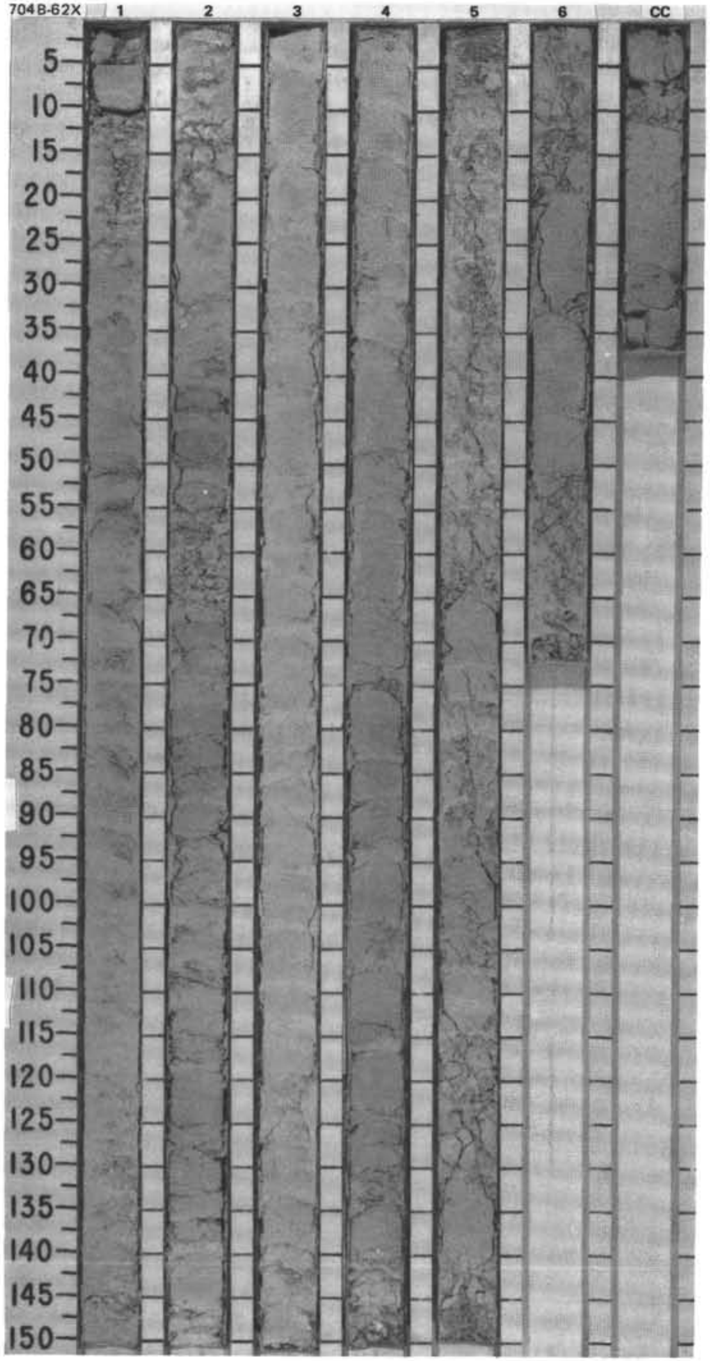

SITE 704 HOLE B CORE 63X CORED INTERVAL 3097.0-3106.5 mbsl; 576.7-586.2 mbsf

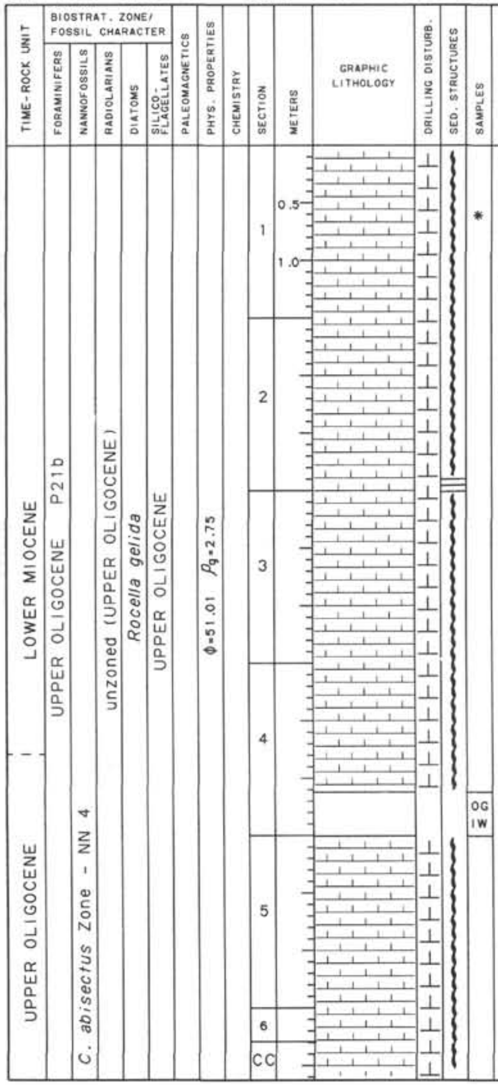

LITHOLOGIC DESCRIPTION

MICRITIC NANNOFOSSIL CHALK (INDURATED)

Drilling disturbance: Biscuited and fractured throughout.

Major lithology: Micritic nannofossil chalk, white (10YR 8/1). Bioturbated throughout by *Planolites* and *Zoophycos*.

SMEAR SLIDE SUMMARY (%):

COMPOSITION:

	1, 70 D
Volcanic glass	Tr
Foraminifers	6
Nannofossils	63
Diatoms	1
Micrite	—

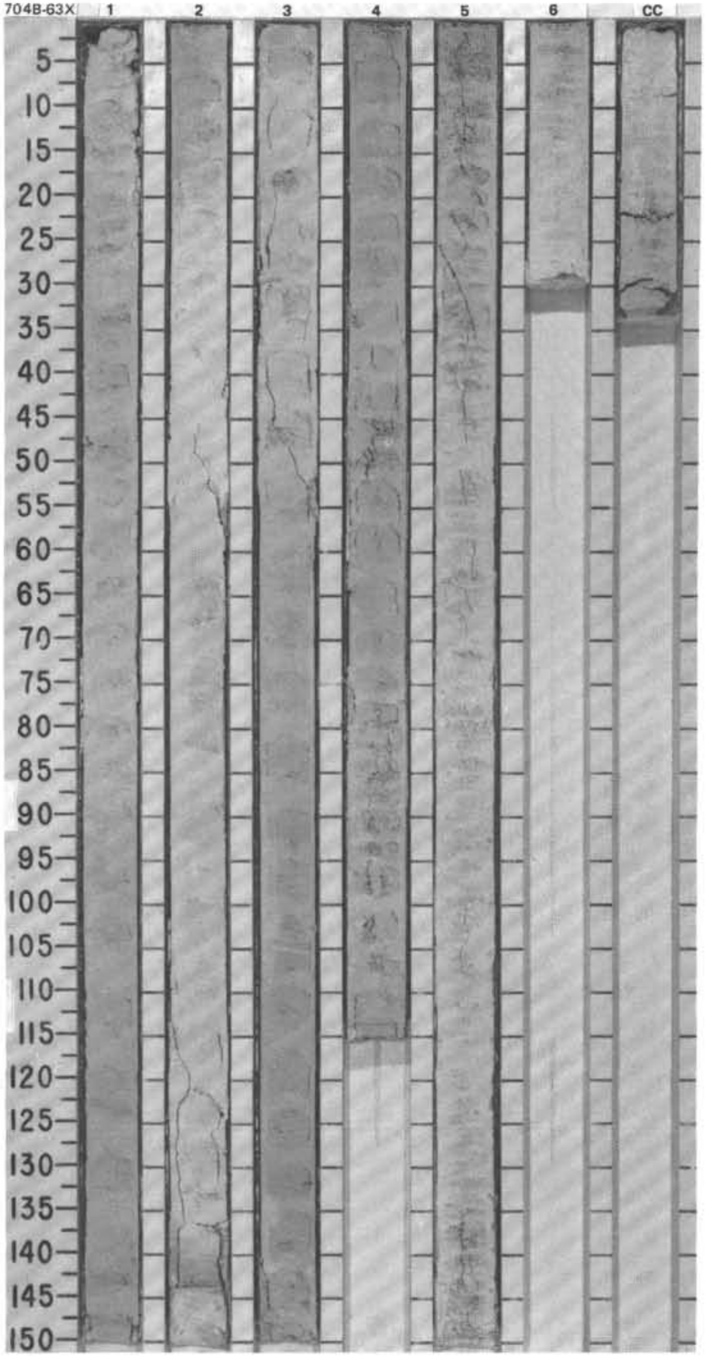

SITE 704 HOLE B CORE 64X CORED INTERVAL 3106.5-3116.0 mbsl; 586.2-595.7 mbsf

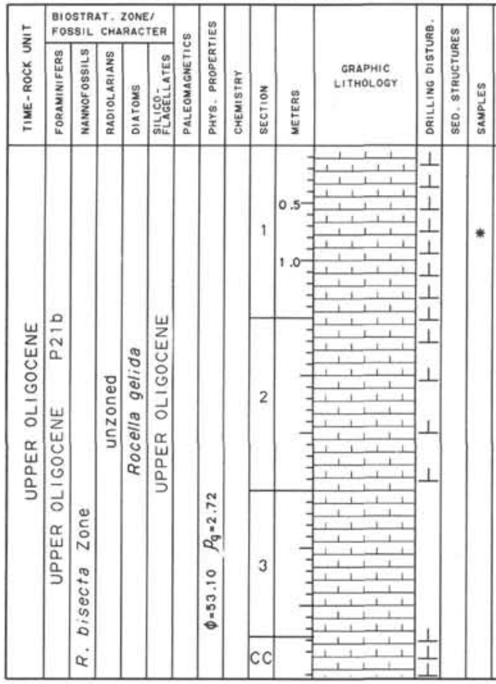

LITHOLOGIC DESCRIPTION

MICRITIC NANNOFOSSIL CHALK (INDURATED)

Drilling disturbance: Biscuited and fractured in Sections 1, 2, and CC.

Major lithology: Micritic nannofossil chalk, white (10YR 8/1).

SMEAR SLIDE SUMMARY (%):

COMPOSITION:	1, 79 D
Quartz/feldspar	Tr
Foraminifers	5
Nannofossils	75
Diatoms	5
Micrite	15

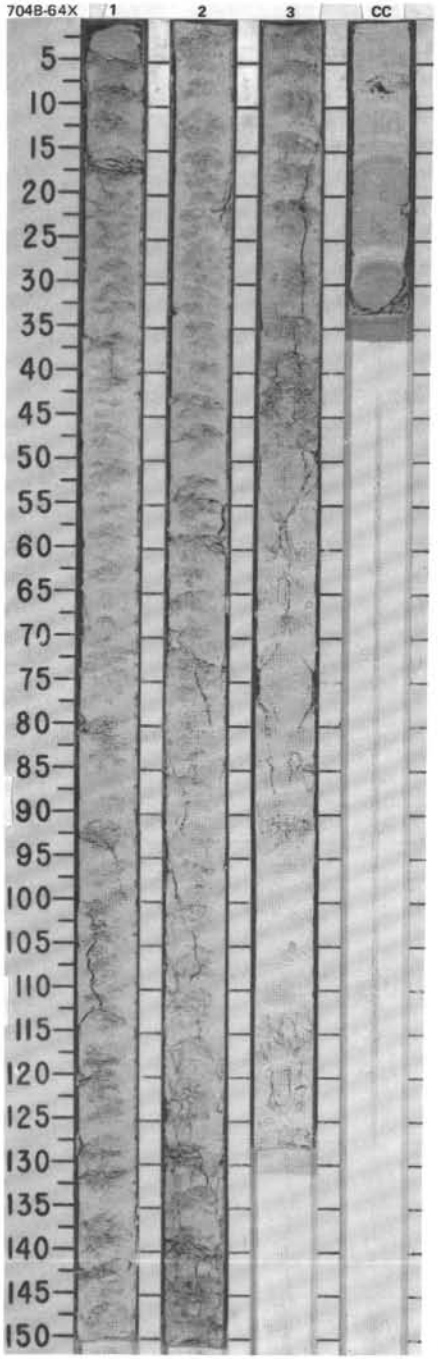

SITE 704 HOLE B CORE 65X CORED INTERVAL 3116.0-3125.5 mbsl; 595.7-605.2 mbsf

TIME-ROCK UNIT	BIOSTRAT. ZONE/ FOSSIL CHARACTER					PALEOMAGNETICS	PHYS. PROPERTIES	CHEMISTRY	SECTION	METERS	GRAPHIC LITHOLOGY	DRILLING DISTURB.	SED. STRUCTURES	SAMPLES	LITHOLOGIC DESCRIPTION
	FORAMINIFERS	NANNOFOSSILS	RADIOLARIANS	DIATOMS	SILICO-FLAGELLATES										
UPPER OLIGOCENE	UPPER OLIGOCENE P21b	*C. altus* Zone not examined	unzoned (UPPER OLIGOCENE)	*Rocella gelida*	UPPER OLIGOCENE		ϕ=52.10 ρ_g=2.61		1 2 3 CC	0.5 1.0	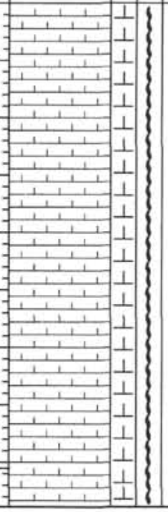				MICRITIC NANNOFOSSIL CHALK (INDURATED) Drilling disturbance: Biscuited and fractured throughout. Major lithology: Micritic nannofossil chalk, white (10YR 8/1). *Planolites* and *Zoophycos* burrows.

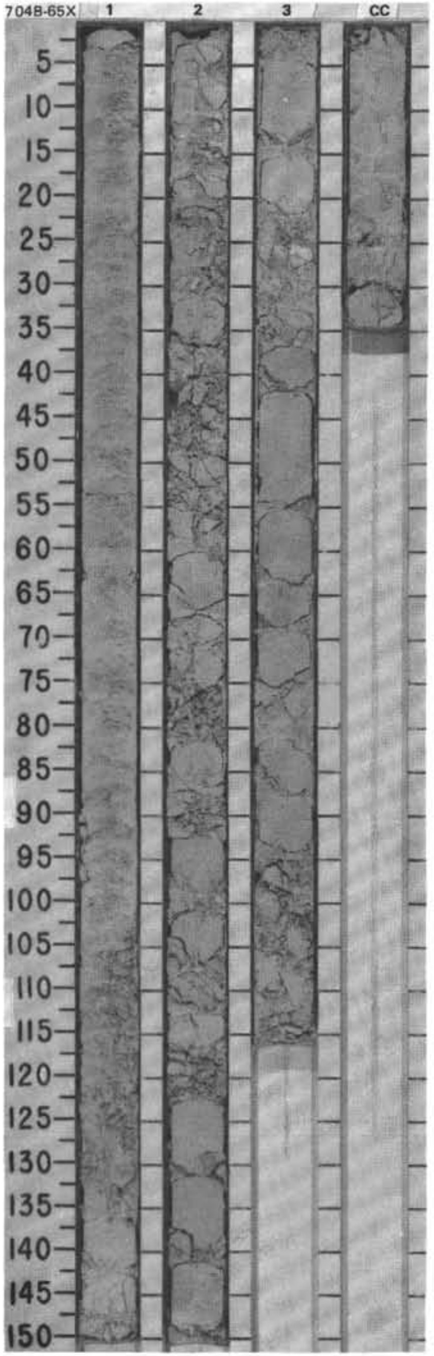

SITE 704 HOLE B CORE 66X CORED INTERVAL 3125.5-3135.0 mbsl; 605.2-614.7

TIME-ROCK UNIT	BIOSTRAT. ZONE/ FOSSIL CHARACTER					PALEOMAGNETICS	PHYS. PROPERTIES	CHEMISTRY	SECTION	METERS	GRAPHIC LITHOLOGY	DRILLING DISTURB.	SED. STRUCTURES	SAMPLES
	FORAMINIFERS	NANNOFOSSILS	RADIOLARIANS	DIATOMS	SILICO-FLAGELLATES									
UPPER OLIGOCENE	UPPER OLIGOCENE P21b	*C. altus* Zone	unzoned (UPPER OLIGOCENE)	*Rocella gelida*	*Corbisema archangelskiana* (UPPER OLIGOCENE)		$\phi = 52.35$ $\rho_g = 2.76$		1 CC	0.5	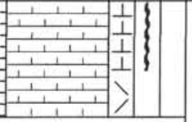			

LITHOLOGIC DESCRIPTION

MICRITIC NANNOFOSSIL CHALK (INDURATED)

Drilling disturbance: Biscuited and fractured throughout.

Major lithology: Micritic nannofossil chalk, white (10YR 8/1). *Planolites* and *Zoophycos* burrows.

SITE 704 HOLE B CORE 67X CORED INTERVAL 3135.0-3144.5 mbsl; 614.7-624.2 mbsf

TIME-ROCK UNIT	BIOSTRAT. ZONE/ FOSSIL CHARACTER					PALEOMAGNETICS	PHYS. PROPERTIES	CHEMISTRY	SECTION	METERS	GRAPHIC LITHOLOGY	DRILLING DISTURB.	SED. STRUCTURES	SAMPLES
	FORAMINIFERS	NANNOFOSSILS	RADIOLARIANS	DIATOMS	SILICO-FLAGELLATES									
UPPER OLIGOCENE	UPPER OLIGOCENE P21b	*C. altus* Zone	unzoned (UPPER OLIGOCENE)	*Rocella gelida*	*Corbisema archangelskiana* (UPPER OLIGOCENE)		$\phi = 49.62$ $\rho_g = 2.75$		1 CC	0.5 1.0	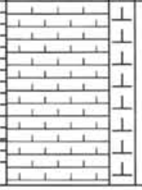			*

LITHOLOGIC DESCRIPTION

MICRITIC NANNOFOSSIL CHALK (INDURATED)

Drilling disturbance: Biscuited and fractured throughout.

Major lithology: Micritic nannofossil chalk, white (10YR 8/1).

SMEAR SLIDE SUMMARY (%):

	1, 65 D
COMPOSITION:	
Foraminifers	8
Nannofossils	69
Diatoms	8
Micrite	15

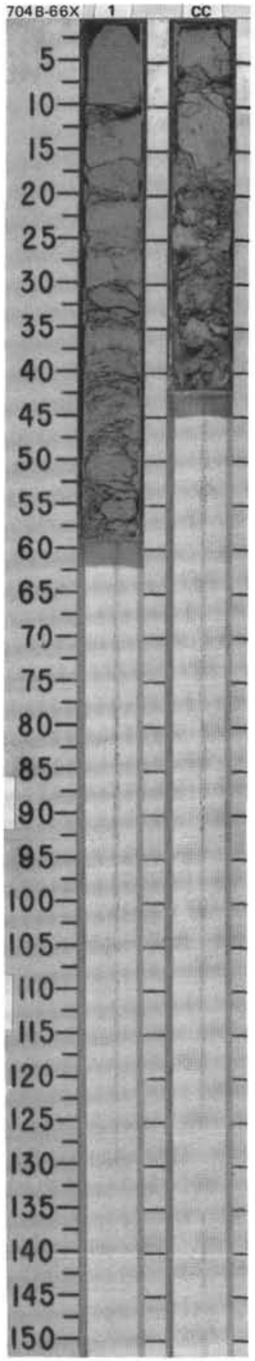

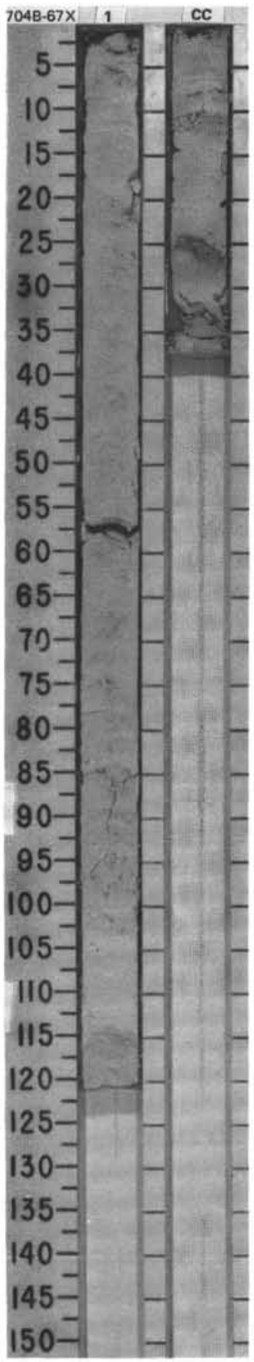

SITE 704 HOLE B CORE 68X CORED INTERVAL 3144.5-3154.0 mbsl; 624.2-633.7 mbsf

TIME-ROCK UNIT	BIOSTRAT. ZONE/ FOSSIL CHARACTER FORAMINIFERS	NANNOFOSSILS	RADIOLARIANS	DIATOMS	SILICO-FLAGELLATES	PALEOMAGNETICS	PHYS. PROPERTIES	CHEMISTRY	SECTION	METERS	GRAPHIC LITHOLOGY	DRILLING DISTURB.	SED. STRUCTURES	SAMPLES	LITHOLOGIC DESCRIPTION
UPPER OLIGOCENE	UPPER OLIGOCENE P21b	*C. altus* Zone	unzoned (UPPER OLIGOCENE)	*Rocella vigilans*	UPPER OLIGOCENE		$\phi=50.12$ $\rho_g=2.77$		1 2 3 CC	0.5 1.0					MICRITIC NANNOFOSSIL CHALK (INDURATED) Drilling disturbance: Biscuited and fractured throughout. Major lithology: Micritic nannofossil chalk, white (10YR 8/1).

SITE 704 HOLE B CORE 69X CORED INTERVAL 3154.0-3163.5 mbsl; 633.7-643.2 mbsf

TIME-ROCK UNIT	BIOSTRAT. ZONE/ FOSSIL CHARACTER FORAMINIFERS	NANNOFOSSILS	RADIOLARIANS	DIATOMS	SILICO-FLAGELLATES	PALEOMAGNETICS	PHYS. PROPERTIES	CHEMISTRY	SECTION	METERS	GRAPHIC LITHOLOGY	DRILLING DISTURB.	SED. STRUCTURES	SAMPLES	LITHOLOGIC DESCRIPTION
UPPER OLIGOCENE	UPPER OLIGOCENE P21b	*C. altus* Zone	unzoned (UPPER OLIGOCENE)	*Rocella vigilans*	UPPER OLIGOCENE		$\phi=48.36$ $\rho_g=2.75$		1 CC	0.5 1.0					MICRITIC NANNOFOSSIL CHALK (INDURATED) Drilling disturbance: Biscuited and fractured throughout. Major lithology: Micritic nannofossil chalk, white (no color code and 10YR 8/1). Minor lithology: Lithic fragment (downhole contaminant?) in Section 1, 0-5 cm.

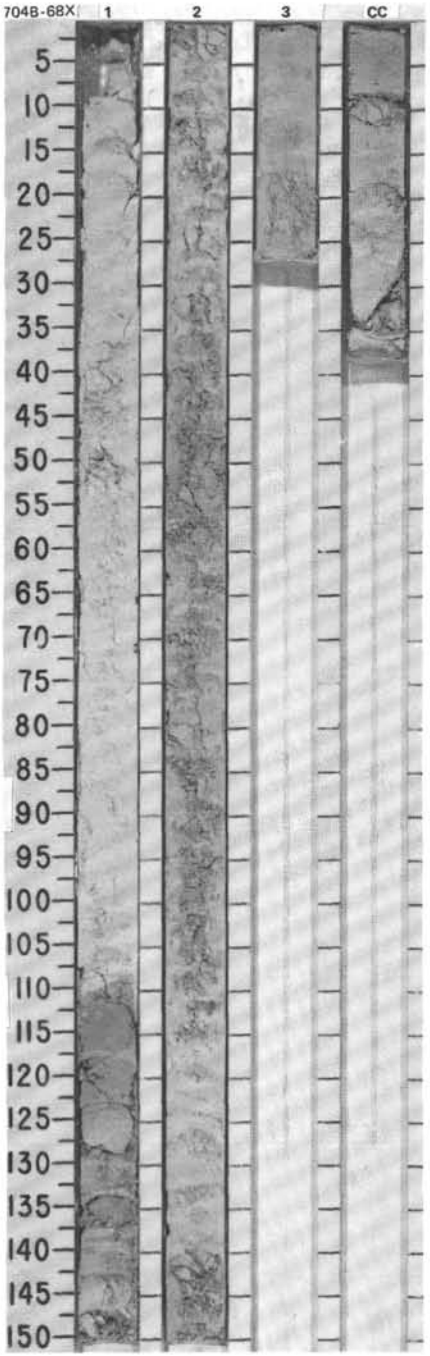

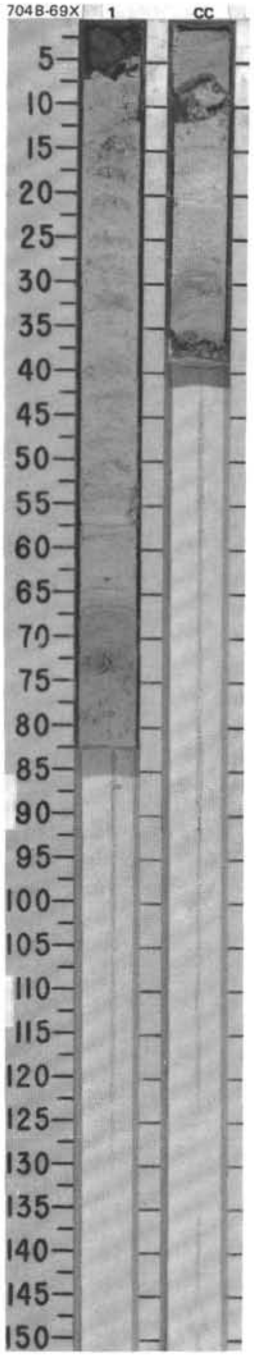

SITE 704 HOLE B CORE 70X CORED INTERVAL 3163.5-3173.5 mbsl; 643.2-652.7 mbsf

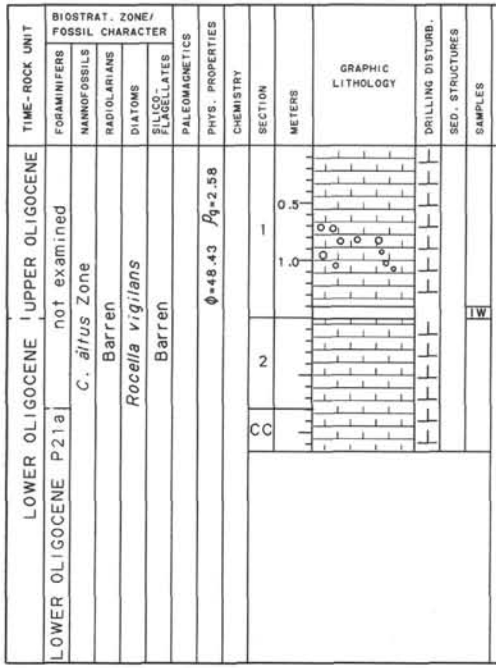

LITHOLOGIC DESCRIPTION

MICRITIC NANNOFOSSIL CHALK (INDURATED)

Drilling disturbance: Biscuited and fractured throughout.

Major lithology: Micritic nannofossil chalk, white (10YR 8/1).

Minor lithology: Pebbles mixed with nannofossil ooze in Section 1, 70-112 cm.

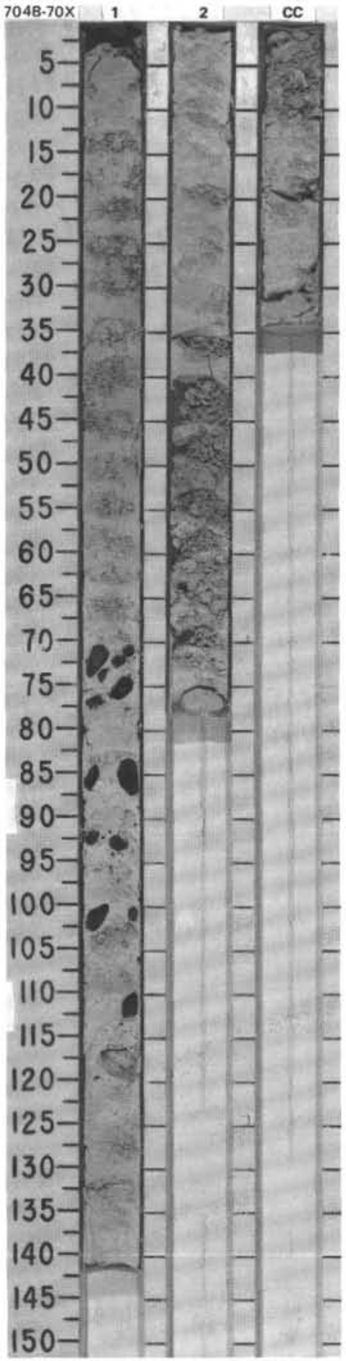

SITE 704 HOLE B CORE 71X CORED INTERVAL 3173.5-3182.5 mbsl; 652.7-662.2 mbsf

TIME-ROCK UNIT	BIOSTRAT. ZONE/ FOSSIL CHARACTER					PALEOMAGNETICS	PHYS. PROPERTIES	CHEMISTRY	SECTION	METERS	GRAPHIC LITHOLOGY	DRILLING DISTURB.	SED. STRUCTURES	SAMPLES	LITHOLOGIC DESCRIPTION
	FORAMINIFERS	NANNOFOSSILS	RADIOLARIANS	DIATOMS	SILICO-FLAGELLATES										
LOWER OLIGOCENE	LOWER OLIGOCENE P20 - P21a	*C. altus* Zone	Barren	*Rocella vigilans*	Barren				1	0.5 1.0	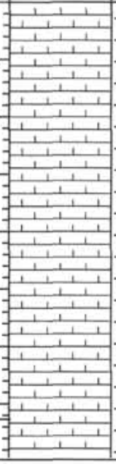	⊥			MICRITIC NANNOFOSSIL CHALK (INDURATED) Drilling disturbance: Biscuited and fractured throughout. Major lithology: Micritic nannofossil chalk, white (10YR 8/1) to light gray (10YR 7/1).
									2			⊥			
							ϕ=45.41 ρ_g=2.79		3			⊥			
									CC			⊥			

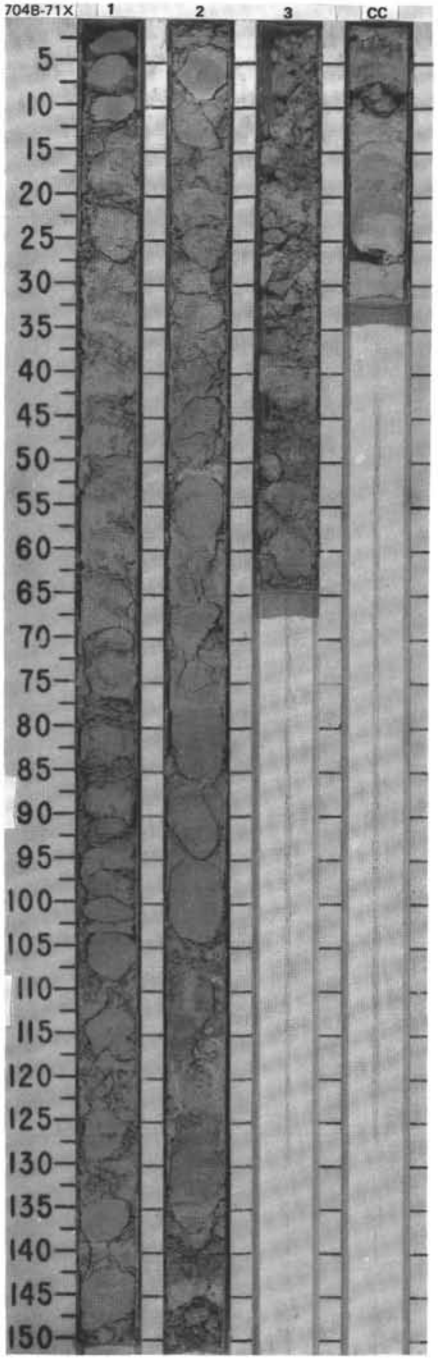

SITE 704 HOLE B CORE 72X CORED INTERVAL 3182.5-3192.0, mbsl; 662.2-671.7 mbsf

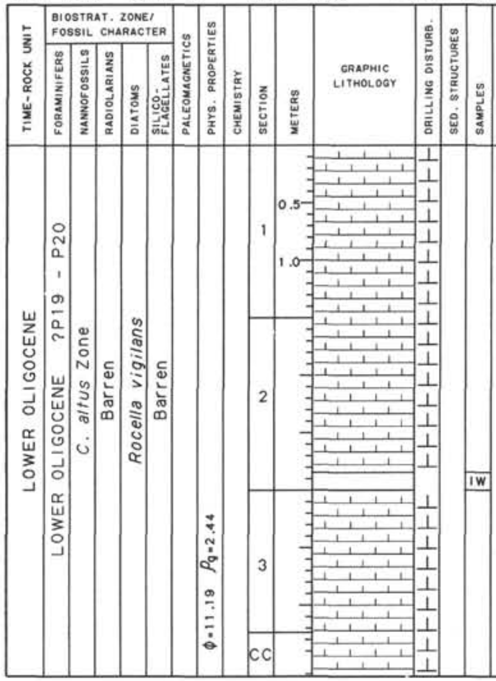

LITHOLOGIC DESCRIPTION

MICRITIC NANNOFOSSIL CHALK (INDURATED)

Drilling disturbance: Biscuited and fractured throughout.

Major lithology: Micritic nannofossil chalk, white (10YR 8/1) and light gray (10YR 7/1)

Minor lithology: Pebbles in Section 1, 0-5 cm.